Activities at Flixton Island: Integrating Scientific Approaches for the Study of Early Mesolithic Living at Ephemeral Sites

Volume one of two

Charlotte Catherine Aneliese Rowley

PhD

University of York

Archaeology

November 2017

Abstract

This thesis presents the novel analysis of the extensive lithic assemblage at the Early Mesolithic site of Flixton Island 2, Flixton, Yorkshire, and the geochemical analysis program carried out alongside that. The research project aimed to evaluate whether the use of several methods of analysis on sediments and lithics could produce a better understanding of activity areas and spatial patterning than had previously been achieved for Mesolithic dryland sites. A complementary case study was undertaken at Star Carr.

More than 20,000 lithic artefacts were typologically analysed to define the nature of the Long Blade and Early Mesolithic lithics assemblages from Flixton Island 2. Sediment samples associated with the Mesolithic lithics assemblage were analysed using general geochemical tests (colour and texture assessment, pH, calcium carbonate presence, and phosphate presence) alongside elemental characterisation using inductively-coupled plasma atomic-emission spectroscopy (ICP-AES) and portable x-ray fluorescence (pXRF). Spatial statistical methods were applied to explore and analyse the data.

At the more ephemeral of the two sites, Flixton Island 2, the use of both artefact analysis and geochemical analysis suggested that spatial patterning on site could be drawn out and mutually supported by the two avenues of evidence. At Star Carr, similar multi-elemental analysis on an occupation area that had archaeologically identified structural features strongly supported the case for the structure's proposed limits as well as providing new information about potential activity in the general vicinity. The two sites yielded results that indicated that geochemical testing, particularly multi-elemental characterisation, and combining that information with artefactual and structural evidence was a useful approach for future researchers to consider using to identify activity areas at both ephemeral and more significant Mesolithic sites.

List of Contents

Abstract 2

List of Contents 3

List of Tables 10

List of Figures 16

List of Accompanying Material 27

Acknowledgements 28

Author's declaration 29

Chapter 1 Introduction 30

1.1 Project aims and objectives 30

1.1.1 Project Rationale 30

1.1.2 Research aim 31

1.1.3 Objectives 31

1.2 Flixton Island 2 as a persistent place and palimpsest 31

1.2.1 Persistent places and palimpsests in theory 31

1.2.2 Activity areas and multi-elemental soil analysis 32

1.3 The excavations and previous research at Flixton Island 2 35

1.3.1 History of research 35

1.3.2 Recent investigations 38

1.3.3 Postglacial Lake Flixton's formation and the geology of the Vale 40

1.3.4 Soils of the Vale 43

1.3.5 Contexts of the dryland site 44

1.4 Structure of this thesis 45

Chapter 2 The Founding Research into Early Mesolithic Lithics 46

2.1 Introduction 46

2.2 Theoretical approaches to studying lithic artefacts 46

2.2.1 The three main approaches in lithic studies 46
2.2.2 Typology and classification systems 48
2.2.3 Functional studies 49
2.2.4 Technological studies 50
2.3 Considering British Mesolithic lithic assemblages 52
2.3.1 The role of microliths in identifying Mesolithic assemblages 52
2.3.2 Developing typologies and the earliest identification of a British Mesolithic microlithic culture (basally modified Horsham) 55
2.3.3 Defining further microlithic cultures (Star Carr and Deepcar) 59
2.4 Starting to contextualise the Early Mesolithic cultures 64
2.4.1 Branching out from typology 64
2.4.2 Functional approaches to assemblages 65
2.4.3 Early dating of Mesolithic cultures and exploring seasonality 72
2.4.4 Clarke's challenge to oversimplification 81
2.5 Summary 84
Chapter 3 The Dating and Chronology of Early Mesolithic assemblages 86
3.1 Introduction 86
3.2 Roger Jacobi's work on Early Mesolithic Chronologies 86
3.3 Michael Reynier's work on the definitions and chronology of Early Mesolithic cultural groups 90
3.3.1 Background 90
3.3.2 Typological work 90
3.3.3 Chronological work 97
3.4 Recent research on Early Mesolithic Chronologies 104
3.5 Summary 110
Chapter 4 The Lithics Assemblage from Flixton Island 2 112
4.1 Introduction 112
4.2 Methods 113
4.2.1 General methodology 113

4.2.2 Recorded attributes 114
4.2.3 Categories 116
4.2.4 Phasing 117
4.2.5 Issues 119
4.3 The Long Blade Assemblage 121
4.3.1 A possible Federmesser find 125
4.4 The Mesolithic Assemblage 125
4.4.1 Overview 125
4.4.2 Overall Spatial Patterning 130
4.4.3 Burnt and Heated Material 133
4.4.4 Raw materials 135
4.4.5 Technology 142
4.4.6 Knapped tools 153
4.4.7 Core Tools 173
4.4.8 Tool preparation debitage 181
4.5 Summary and discussion 182
Chapter 5 Geoarchaeological and Geochemical Research Methods 184
5.1 Introduction 184
5.2 Micromorphology 185
5.3 Sampling for geoarchaeological testing and elemental analyses in 2012 185
5.4 Basic geoarchaeological assessment 186
5.4.1 Soil colour and texture 187
5.4.2 Estimated carbonate presence 187
5.4.3 pH 187
5.4.4 Estimated phosphorus presence 188
5.4.5 Summary 188
5.5 Portable Energy-Dispersive X-ray Fluorescence (pXRF) 189
5.5.1 Introduction to pXRF 189
5.5.2 pXRF Equipment 189

5.5.3 pXRF analysis strategy in the field at Flixton Island 2 190
5.5.4 Accuracy, precision, quality assurance and controls conducted in the field for pXRF 191
5.5.5 Complementary sampling strategy for supplementary pXRF analysis in the lab at Flixton Island 2 and Star Carr 206
5.5.6 Procedure for pXRF analysis in the laboratory 206
5.5.7 Quality assurance and control readings for lab-based pXRF 207
5.5.8 pXRF results utilised for spatial mapping 210
5.6 Inductively Coupled Plasma Atomic Emission Spectroscopy (ICP-AES) 211
5.6.1 ICP-AES sampling strategy 211
5.6.2 ICP-AES sample preparation 211
5.6.3 ICP-AES analysis 212
5.6.4 ICP-AES outputs 213
5.6.5 Quality assurance and control readings for ICP-AES work 215
5.6.6 ICP-AES results used in spatial mapping 216
5.7 Statistical Analysis Methods 216
5.7.1 Handling data below the limit of detection 217
5.7.2 Descriptive statistics and basic plots 219
5.7.3 Hot Spot Analysis 220
5.7.4 Cluster and Outlier Analysis 221
5.7.5 Grouping Analysis 221
5.7.6 Principal Component Analysis 223
5.8 Summary 223
Chapter 6 Results of Geochemical Analyses on Flixton Island 2 soil samples 224
6.1 Introduction 224
6.2 General physical characterisation of the dryland soils 225
6.3 General elemental characterisation of sediments on site 229
6.4 Results from Trench 4 (2012 excavation) 233
6.4.1 Trench 4 Descriptive and Exploratory Statistics 234

6.4.2 Spatial visualisation of Trench 4 elemental concentrations measured by ICP-AES 252
6.5 Results from pXRF on Trenches 11, 12, and 15 (2014 excavation) 262
6.5.1 Descriptive and exploratory statistics on the dryland trenches excavated in 2014 267
6.5.2 Spatial visualisation of 2014 dryland trench field pXRF results 271
6.6 Summary of the dryland soils at Flixton Island 2 285
Chapter 7 Comparing Patterning in the Flixton Lithics and Soils 311
7.1 Introduction 311
7.2 A deeper exploration of spatial patterning in the Mesolithic lithics 311
7.2.1 Establishing the significance of the clusters 311
7.2.2 Establishing the extent of the clusters using Density Analysis on 3D located lithics data 313
7.2.3 Display of the sieve lithics data 316
7.2.4 Profiles of the lithic scatters 317
7.2.5 Discussion about the scatter profiles 323
7.3 A deeper exploration of spatial patterning in the soils 325
7.3.1 Integrating the elements into one model 325
7.3.2 Results of the Grouping Analysis of Trench 4 ICP-AES Results (from 2012 excavations) 326
7.3.3 Grouping Analysis for Trenches 11, 12 (north), and 15 field pXRF Results (from 2014 excavations) 335
7.4 Discussion 348
Chapter 8 Geochemistry on Structures at Star Carr 349
8.1 Introduction 349
8.2 Introduction to the structures 350
8.3 Potential complications 353
8.4 Individual Elemental Results 354
8.5 Grouping Analysis at Star Carr 359

8.5.1 Grouping analysis on the upper ICP-AES dataset from Star Carr based on major and key element results 359
8.5.2 Ruling out patterning due to proximity alone 362
8.6 Principal Component Analysis 363
8.6.1 Results of PCA on the Star Carr upper dataset 363
8.7 Summary and Comparison with Flixton Island 2 365
Chapter 9 Discussion and Conclusions 366
9.1 The question of activity at Flixton Island 2 366
9.2 Chronology, persistence and palimpsests 368
9.3 The people and activities at Flixton Island 2 372
9.4 Conclusions 375
Appendix 1 Deepcar-type assemblages, as outlined by Radley and Mellars (1964) 377
Appendix 2 Lithics Cataloguing, Definitions, and Typological Classification Notes 382
Categories used on catalogue spreadsheets 382
Appendix 3 Micromorphology notes 395
Taking the sample 395
Thin section processing 396
Microscopic analysis 398
Appendix 4 Field pXRF Quality Assurance and Control 400
Calibration Check Record for Flixton Island 2, 2014 field season 400
Beam Runtime Evaluation 400
Repeat readings from “control” areas 406
Overview 406
Elemental classifications by trench 407
Full data for Flixton Field pXRF 408
Star Carr 425
Appendix 5 Lab-based pXRF Quality Assurance and Control 439
Calibration Check Record 439
Control Readings 439

Systematic experimentation confirming polythene bags interfered with pXRF readings 440
General experiment premise 440
Equipment setup and blank readings 441
Control Sample Analyses 443
Appendix 6 Supplementary Statistical Tables and Graphs for Flixton Island 2 Geochemical Analyses 453
Introduction 453
VP12 ICP-AES Full Dataset 453
VP12 ICP-AES Individual Element Histograms (batches 1 and 4, Trench 4) 453
VP12 ICP-AES Individual Element Spatial Analysis Results (Trench 4) 463
Major 463
Minor 464
Trace 467
IUPAC Trace 473
VP14 FpXRF Full Dataset 490
VP14 FpXRF Individual Element Histograms 490
VP14 FpXRF Individual Element Spatial Analysis Results for Trenches 11, 12 and 15 .506
Major 506
Minor 507
Trace 509
IUPAC Trace 512
Appendix 7 Development of the Grouping Analysis model 521
Abbreviations 522
Glossary 523
Bibliography 527

List of Tables

Table 1. Early Mesolithic radiocarbon dates from Jacobi 1973, p.261. *Site codes obtained from Jacobi 1978. 86

Table 2. Early Mesolithic radiocarbon dates extracted from Jacobi 1976, pp.67–69. 88

Table 3. Early Mesolithic radiocarbon dates from Jacobi 1978, pp.297–301, with various Upper Palaeolithic dates discussed for comparison. 89

Table 4. The frequencies of microliths (blue in chart) and standard tools (orange) included in the study of sites suggested to be characteristically 'Deepcar' by Reynier (2005, 20).... 92

Table 5. Summary of Reynier's proposed typological characteristics for Star Carr, Deepcar and Horsham type assemblages (summarized from Reynier 2005, 18–22). 93

Table 6. Reynier's dates, information, and the calibrated values (dates sourced from Reynier 2005; calibration by C. Rowley) 102

Table 7. Lithic artefact categories employed during this study 116

Table 8. Summary of Long Blade assemblage finds by context groups 118

Table 9. Summary of the Mesolithic assemblage by context groups 119

Table 10. Proportion of burnt material in the Long Blade assemblage 123

Table 11. The Flixton Island 2 Mesolithic assemblage, overall breakdown 127

Table 12. The 'essential' assemblages for Flixton Island 2 and various example sites drawn from Mellars (1976), with the exception of the recent data for Star Carr drawn from Conneller et al. (2018) which she categorises as a Type B site. All Type B sites described by Mellars are provided. The Type A and B1 examples were chosen as being the sites summarised in Mellars with the lowest proportion of microliths (their defining aspect being that their assemblages show a high proportion of microliths), while the Type C example was chosen, similarly, for it being that with the lowest proportion of scrapers (high proportions of scrapers being the defining characteristic of that group). *saws = terminology Mellars uses meaning microdenticulates. 129

Table 13. The burnt and unburnt proportions of the assemblage 133

Table 14. Relative percentages of the source of cores deposited at Flixton Island 2 139

Table 15. Summary of the raw materials used to manufacture different tool categories.. 140

Table 16. Summary of the raw materials used to manufacture key tool types at Flixton Island 2 and Star Carr (data for the former from Conneller et al. 2018) 140

Table 17. Core types in the Mesolithic assemblage....143

Table 18. Comparison of core type assemblages from different Star Carr, Deepcar, and Horsham type sites (Star Carr data reproduced from Conneller et al. (2018) and southern sites derived from Reynier 2005, pp. 32 - 40, with type C cores associated with Reynier's "3 platforms, continuous" category and D and E cores associated with his "other" category 144

Table 19. Complete cores retrieved from sieving....146

Table 20. Summary of the core dimensions....148

Table 21. Summary of the core preparation debitage....149

Table 22. Raw materials of the core preparation debitage artefacts....149

Table 23. Primary and secondary debitage....151

Table 24. Core reduction and general debitage in the Mesolithic assemblage, including tested nodules of raw material ("complete" referring to complete flakes, blades or bladelets) 152

Table 25. Dimensions of measured complete flakes, blades, and bladelets (primary, secondary, or tertiary) in millimetres. 152

Table 26. The microlith assemblage by form. *Pieces described as "interrupted" in the table are those that have generally been retouched into a shape but where the apex of the arc or peak of the triangle is not retouched itself, thus leaving a small shoulder 154

Table 27. Summary of microliths retrieved from sieving, by trench 159

Table 28. Summary of scraper types....165

Table 29. Summary of the frequencies of scrapers retrieved from sieving, by trench....167

Table 30. The burin assemblage....168

Table 31. Relative proportions of the Mesolithic core tool assemblage....173

Table 32. Estimating calcium carbonate....187

Table 33. Eidt and Woods' (1974) phosphate spot test ratings....188

Table 34. Criteria utilised for assessing major, minor, and trace element contributors to samples/readings. *The International Union of Pure and Applied Chemistry (IUPAC) Gold Book defines trace elements as "any element having an average concentration of less than about 100 parts per million atoms (ppma) or less than 100 μg / g" (IUPAC 2009)....192

Table 35. Elements analysed through ICP-AES conducted by ALS Chemex (ME-ICP41), the units results are provided in, and the upper and lower detection limits for specific elements

(modified from Minerals 2009 with amendment received from Louise Clarke, ALS Minerals, pers. comm.) 213

Table 36. Basic geochemical assessment of samples from trench 4 226

Table 37. The results of the readings on topsoil and till controls from Flixton Island 2 by ICP-AES (ordered by highest content in the till sample) 230

Table 38. Descriptive statistics for some of the major and key minor elements analysed in local tills (in ppm). The table includes the results from the seven 'till' controls from Star Carr (values in parts per million), the Flixton Island 2 'till' control results for comparison (all analysed as part of this project by ICP-AES), along with C. Boston's readings in parts per million for tills at Skipsea and Filey on the east coast in Yorkshire, analysed by ICP-MS analysis (reproduced with permission from Boston 2007). All values were rounded to the nearest integer where appropriate 232

Table 39. Descriptive statistics including the number of valid readings (N) and the mean, median, standard deviation, range and maximum and minimum values in ppm from ICP-AES Batch 1 (main trench 4 results). a. Multiple modes exist. The smallest value is shown 235

Table 40. Descriptive statistics including the number of valid readings (N) and the mean, median, standard deviation, range and maximum and minimum values in ppm from ICP-AES Batch 4 (trench 4 expansion). a. Multiple modes exist. The smallest value is shown 237

Table 41. Number of valid readings (N), the mean, median, standard deviation, coefficient of variance, range, maximum and minimum values from lab pXRF analyses on subsample of 10 from trench 4 (units: ppm, where not dimensionless). a. Multiple modes exist. The smallest value is shown 239

Table 42. Statistics relating to skewness and kurtosis of ICP-AES results from trench 4..250

Table 43. Dates of pXRF analysis in the field at Flixton Island 2 as well as notes on conditions made in the field and highlights from the Met Office report for August 2014 (The Met Office 2015) (The Met Office 2015) 264

Table 44. Descriptive statistics for all the elements as measured in the field by pXRF, sorted by descending mean value. a. Multiple modes exist. The smallest value is shown 269

Table 45. Descriptive statistics for the major and key minor elements measured from samples recorded as till at Star Carr (values in parts per million). (Table reproduced from Table 21.2 in Rowley et al. 2018.) 354

Table 46. Ranges of values (ppm) from Star Carr tills compared with Boston's readings on till samples from Skipsea and Filey (reproduced with permission from Boston 2007) 355

Table 47. Plots of the central structure readings for each of the key elements, displayed by Jenks natural breaks in the non-normalized readings (in parts per million). (Reproduced from Rowley et al 2018.) 355

Table 48. ArcMap generated R2 values for each variable from the four different models for nine groupings at Star Carr. They are colour coded from highest values (red) to lowest (blue), with the highest and lowest values in bold font 360

Table 49. Detail of attributes recorded in lithics catalogue 384

Table 50. Calibration checks in the field at Flixton Island 2. *Time settings for analyser had been reset, this is the timestamp as embedded in the datafile. **It is unknown why these times were not recorded by the analyser 400

Table 51. Run time experiment details 401

Table 52. Run time experiment results 401

Table 53. A record of the readings taken in the field at Flixton in August 2014, both for repeats and for new readings, as well as notes on conditions made in the field and highlights from the Met Office report for August 2014 (The Met Office 2015). 406

Table 54. Summary of Field pXRF control reading results for trench 11 407

Table 55. Summary of Field pXRF control reading results for trench 12 408

Table 56. Summary of Field pXRF control reading results for trench 15. There were four different control spots read from the same grid square for Trench 15. This gives an estimation of the variability from within one grid square as well as providing the daily repeats for field conditions 408

Table 57. Trench 11 Field pXRF control readings data (rounded to 2 d.p.) 410

Table 58. Trench 11 Field pXRF control readings descriptive statistics (to 2 d.p.) 412

Table 59. Trench 12 Field pXRF control readings data (to 2 d.p.) 413

Table 60. Trench 12 Field pXRF control readings descriptive statistics (to 2 d.p.) 415

Table 61. Trench 15 Field pXRF control readings data (to 2 d.p.). *n/a = element in another category for this sample 416

Table 62. Trench 15, sample location 1 Field pXRF control readings descriptive statistics (to 2 d.p.) 419

Table 63. Trench 15, sample location 2 Field pXRF control readings descriptive statistics (to 2 d.p.) 420

Table 64. Trench 15, sample location 3 Field pXRF control readings descriptive statistics (to 2 d.p.) 421

Table 65. Trench 15, sample location 4 Field pXRF control readings descriptive statistics (to 2 d.p.) 422

Table 66. Trench 15 Field pXRF control readings descriptive statistics for all four reading locations considered as one set of data (to 2 d.p.) 423

Table 67. Descriptive statistics for all repeat readings across all trenches at Flixton using field pXRF (to 2 d.p.) 424

Table 68. Summary of control field pXRF results for Star Carr's western structure area 425

Table 69. Data for the field pXRF control repeats at Star Carr 425

Table 70. Descriptive statistics for the control field pXRF repeats at Star Carr (2 d.p.) 429

Table 71. Details of standard control repeats taken during the field season at Star Carr 430

Table 72. Standard control repeat results, taken while in the field at Star Carr 431

Table 73. Percent deviation of readings from the expected value of control samples 2710a and 2711a in the field at Star Carr (green: less than +/- 5 % out; light blue 5-20 % low, dark blue more than 20 % below expected values; light red 5-20 % high, dark red greater than 20 % high) 435

Table 74. Descriptive statistics for readings of control samples 2711a in the field at Star Carr, taken 2015 (ppm) 437

Table 75. Descriptive statistics for readings of control samples 2710a in the field at Star Carr, taken 2015 (ppm) 438

Table 76. Calibration check record for lab-based pXRF 439

Table 77. Readings for the five major elements in parts per million (ppm) in the bags. <LOD means below the limit of detection for that element in Geochem mode on this machine. 441

Table 78. Readings for the seven lesser important elements in ppm in the bags. <LOD means below the limit of detection. 442

Table 79. Readings for the five major elements in ppm for single layers of cling film. <LOD means below the limit of detection. 442

Table 80. Readings for the seven lesser important elements in ppm in a single layer of cling film. <LOD means below the limit of detection. 442

Table 81. Values in ppm for control sample of soil NIST 2710a. The certified values are in the top row while readings taken on the departmental pXRF are in subsequent rows and have a reading number. <LOD = below limit of detection. 445

Table 82. Values in ppm for control sample of soil NIST 2711a. The certified values are in the top row while readings taken on the departmental pXRF are in subsequent rows and have a reading number. <LOD = below limit of detection. 446

Table 83. Values in ppm for control sample of silicon dioxide. The certified values are in the top row while readings taken on the departmental pXRF are in subsequent rows and have a reading number. <LOD = below limit of detection. 448

Table 84. NIM-GBW07408 certified values of oxides for major elements and ppm for minor elements, all converted to estimate ppm for each central atom of an element plus its bonded oxygen atoms in the oxide form. Numbers in bold and dark red are those provided on the original certification. 450

Table 85. Values in ppm for the major elements in the control sample of NIM-GBW07408, as read by the departmental pXRF 450

Table 86. Values in estimated oxide wt % for the major elements. All except titanium were converted to the oxides listed. Titanium, having been provided in ppm as a minor element in the certified values, was not converted to an oxide but its ppm simply converted 451

List of Figures

Figure 1. Moore's shouldered point (as published as Plate XVI in Clark 1954, p.136, not to scale) 36

Figure 2. Previous excavations at Flixton Island, image reproduced from an internal report by Barry Taylor (POSTGLACIAL Project). Grey trenches indicate Moore's investigation, red trenches were carried out by the VPRT. Site 1 is on the southern part of the island in the vicinity of Moore's large grey trench and site 2 is on the more northerly, dual peaked, part of the island, with the two parts nearly connected by a gravelly ridge. 37

Figure 3. The POSTGLACIAL Excavations, relative to previous excavations in the vicinity (the area delineated in the inset map shows the excavations relative to Figure 2). Contour data was created by Barry Taylor for the POSTGLACIAL project during the environmental coring project that formed his PhD (Taylor 2012) 39

Figure 4. The general areas discussed throughout the text 40

Figure 5. The location of (a) the Vale of Pickering, (b) the uplands enclosing the vale, (c) the underlying geological deposits in the vale, with the orange being lacustrine deposits suggesting the edges of glacial palaeolakes Pickering and Flixton (reproduced from Evans et al. 2017, p.296) 41

Figure 6. The location of the archaeological sites around Palaeolake Flixton, with (a) showing the margins of the British-Irish Ice Sheet and (b) showing the important Palaeolithic and Mesolithic sites on the lake edges (reproduced from Candy et al. 2015, 61) 42

Figure 7. Photomicrograph of aggregated mixture of amorphous iron replaced organic material, humic fine-medium quartz sand and humic clay, sample Flixton VP12/1 (4.5mm = frame width; plane polarized light) (reproduced from internal report by French 2015) ... 44

Figure 8. Callender's Scottish microliths (1927, p. 319) (not to scale) 53

Figure 9. Clark's microlith classifications, showing examples of all major types (A - G). For the geometric forms i.e. type D microliths, subtype 1 are triangles, 2 crescent, 3 lozenge, 4 lanceolate, 5 sub-triangular, 6 trapezoid, 7 rhomboid, 8 trapeze (after Clark 1933, 56–60). Not to scale. 57

Figure 10. Clark's Microlithic 'spectra' (reproduced from Clark 1933, p.64) 58

Figure 11. The microlithic industry from Deepcar, Yorkshire (reproduced from Radley and Mellars 1964, p.10, not to scale) 61

Figure 12. Awls from Deepcar (reproduced from Radley and Mellars 1964, p.17, not to scale)..... 62

Figure 13. Warcock Hill South's awls (reproduced from Radley and Mellars 1964, p.17, not to scale). 64

Figure 14. The Loshult arrow (photograph by Arne Sjöström, reproduced from Larsson and Sjöström 2011a). 67

Figure 15. Microliths and microburins from Thatcham (reproduced from Wymer & King 1962, p.342)..... 71

Figure 16. Jacobi's microlith classification system here based on examples from Mesolithic Wealden. (1-4) Broad blade microliths; (5-9) Narrow Blade microliths; (10) Hollow-based points; (11-13) Inversely retouched points (reproduced from Jacobi 1978b, 16)..... 74

Figure 17. Clarke's examples of hafted microliths as reproduced by Butler (2005, 89)..... 84

Figure 18. Reynier's comparative microlith typology clustered bar chart (2005, p.25). The typologies are: 1 – oblique points; 2 -partially backed points; 3 – triangles; 4 – rhomboids; 5 – trapezoids; 6 – backed points; 7 – transversely based points; 8 – obliquely based points; 9 – hollow based points; 10 – tanged points (2005, p.25) 95

Figure 19. Reynier's box and tail diagram of British Early Mesolithic radiocarbon dates. The dates are uncalibrated, arranged in their chronological order with the tails set at 2 standard deviations (s.d.). The dashed vertical lines indicate the dating plateaux (2005, p.69)..... 99

Figure 20. The dates utilised by Reynier having been calibrated in OxCal v4.2.4, using the IntCal13 atmospheric curve. The site, date identification code, and site types are appended as the labels..... 101

Figure 21. Probability distributions of radiocarbon dates associated with Star Carr-type microlith assemblages (Reproduced from Conneller et al. 2016, p.6.)..... 107

Figure 22. Probability distributions of radiocarbon dates associated with Deepcar-type microliths assemblages (reproduced from Conneller et al. 2016, p.7)..... 108

Figure 23. Probability distributions of radiocarbon dates associated with Basally Modified microliths (reproduced from Conneller et al. 2016, p.8)..... 109

Figure 24. Summary of the use of Early Mesolithic assemblage types as proposed by Conneller et al. The shading reflects the probability that an assemblage type was in use at a particular time (reproduced from Conneller et al. 2016, p.10). 110

Figure 25. All 3D located lithics across the site, symbolised by classification as Long Blade/Federmesser or Mesolithic..... 113

Figure 26. Examples of patinated flint (the centre piece is also burnt). Find numbers, from left to right: <100735>, <107356>, and <100242>. 120

Figure 27. The Long Blade assemblage 121

Figure 28. 3D located Long Blade and Federmesser material 122

Figure 29. Raw materials of the Long Blade assemblage 122

Figure 30. Find <110501> (Photo taken by N. Gevaux) 124

Figure 31. <100213> (Photo taken by N. Gevaux) 124

Figure 32. <106967> (left) and Figure 33. <100242> (photos taken by N. Gevaux) 124

Figure 34. <106591> (Photo taken by N. Gevaux) 125

Figure 35. Overview of the Flixton Island 2 Mesolithic assemblage 126

Figure 36.The complete 3D located Mesolithic assemblage, with finds from categorically gully contexts symbolised separately 130

Figure 37. The 3D located Mesolithic assemblage from the main dryland trenches 131

Figure 38. Zoom on the gully and bar 132

Figure 39. The Mesolithic assemblage from the wetland trenches 132

Figure 40. Examples of burnt or heated material. 133

Figure 41. The burnt Mesolithic material from Flixton highlighted against the unburnt material 134

Figure 42. The burnt Mesolithic tools compared with other burnt material 135

Figure 43. The Flixton Island 2 Mesolithic assemblage in terms of raw material used 137

Figure 44. Photograph of the chert artefacts (photography by N. Gevaux). Find numbers, from left to right: sl/191 and sl/15. 137

Figure 45. Photograph of the possibly limestone artefacts. Find numbers, from left to right: sl/194, sl/192, and sl/193....137

Figure 46. Red-tipped material (photography by N. Gevaux). Find numbers, from left to right: <101285>, <103931>, and <105663>. 138

Figure 47. Raw materials of the Mesolithic cores 139

Figure 48. The Mesolithic core technology, with proportion of the core technology assemblage and artefact count (total count: 192 artefacts) 143

Figure 49. Examples of cores (photography by N. Gevaux). From left to right, top row then bottom: <100617> A2 type in Wolds flint; <101357> B1/irregular core in till flint; and <106899> B1 core in Wolds flint. 145

Figure 50. Distribution of the 3D located complete cores 145

Figure 51. 3D located cores by type (N.B. there was one additional A1 type core in the wetland, not illustrated here) 146

Figure 52. Cores displayed by maximum length as a crude proxy for size 147

Figure 53. The distribution of core preparation debitage and core fragments, alongside the complete core assemblage 150

Figure 54. Photographs of a selection of microlith types from the site (photography by N. Gevaux) 155

Figure 55. Distribution of the microliths and microburins across the site 158

Figure 56. Distributions of the different microlith types across the dryland 159

Figure 57. Examples of the awls/piercers and mèches de foret (photography by N. Gevaux) 162

Figure 58. Distribution of the 3D located awls, piercers and mèches de foret 164

Figure 59. Examples of scrapers (photography by N. Gevaux) 165

Figure 60. The distribution of scrapers and partial scrapers 166

Figure 61. Scrapers by type 167

Figure 62. Examples of the burins (photography by N. Gevaux). 1 is a dihedral burin, 2 is a double angle break burin, and 3 is a possible dihedral burin. 169

Figure 63. Distribution of burins and partial burins 170

Figure 64. The microdenticulates (photography by N. Gevaux) 171

Figure 65. Distribution of the 3D located microdenticulates 172

Figure 66. Distribution of the 3D located core tools across the site 174

Figure 67. Tranchet axe/adze <101854> (photography by N. Gevaux) 175

Figure 68. Preform / broken adze <101636> (photography by N. Gevaux) 176

Figure 69. Photo of small roughout / near complete adze <106735> (photography by N. Gevaux) 177

Figure 70. Roughout <100813> (photography by N. Gevaux) 179

Figure 71. Roughout <104850> (photography by N. Gevaux) 180

Figure 72. Example of a strike-a-light (photography by N. Gevaux).....181

Figure 73. Mesolithic tool preparation debitage assemblage 182

Figure 74. The sampling strategy for trench 4 (VP12): black dots indicate the full array of samples taken; red triangles are those analysed by ICP-AES to provide general coverage; those in yellow were analysed by ICP-AES, pXRF in the laboratory, and general testing such a pH measurement for more detailed understanding.....186

Figure 75. Sampling in the field in trench 4 (photograph by the POSTGLACIAL project) .186

Figure 76. A reading being taken in trench 11 using the soil foot setup (photograph courtesy of the POSTGLACIAL project).....191

Figure 77. Plan of grid pXRF readings were taken on (one reading per square), in the field at Flixton in 2014 191

Figure 78 A - C. Dot plots of the major element values read from the repeat readings in the same location on different days in the field by pXRF. Note, trench 15's plot depicts 4 pairs of repeats at 4 different 'sample' locations (S1 - 4) in the trench, from within the same grid square.....195

Figure 79 A - C. Minor element values read from repeats on different days in the field by pXRF.....198

Figure 80 A-C. Dot plots of the trace element values read from repeats on different days in the field by pXRF.....200

Figure 81 A-C. Dot plots of the IUPAC trace element values read from repeats on different days in the field by pXRF. If a sample had a successful reading of an element in one repeat but not the other, the reading below the limit of detection is displayed as a point at 1 ppm. If an element was not read at all in any sample, it is not included in any plot 202

Figure 82 A - C. Dot plots of the IUPAC trace element values read from repeats on different days in the field by pXRF: the same results as in Figure 8 but with error bars.....203

Figure 83. Vertical setup for the Olympus Flex Stand, looking down on the stand, with the lid of the chamber lifted to show inside the chamber and the analysis window.....207

Figure 84. The ten samples used in the basic geochemical assessment.....227

Figure 85. Excavations in trench 4 during the 2012 excavation season: this is at the base of the soil, with the yellowish till exposed and only shallow lenses of the mixed soil-till interface (1119) remaining except behind the excavators (photography by the POSTGLACIAL project).....227

Figure 86. A plot of the pH readings from trench 4, ranging from pH 6.83 (slightly acidic) to 7.37 (neutral) 228

Figure 87. Samples analysed from trench 4, labels denoting grid square and with location points symbolised by submission batch (triangle for batch 1 ICP-AES, circle for expansion batch 2 ICP-AES, blue for samples use for the basic assessment and analysed by pXRF). The plans of potential features are also shown (at the western end of the trench) 233

Figure 88 A-E. Comparison of the means for each element as read by ICP-AES (batches 1 and 4) and pXRF in the trench 4 samples. All values in ppm 244

Figure 89. ICP-AES results from all samples in trench 4 (from batches 1 and 4), alongside the results from just batch 1. Visualised using Jenks natural breaks 253

Figure 90. The basic visualisation (Jenks Natural Breaks; top), Hot Spot Analysis (centre), and Cluster-Outlier Analysis (bottom) for iron results (Fixed Band Neighbourhood = 1.85m) 254

Figure 91. The basic visualisation (Jenks; top), Hot Spot Analysis (centre), and Cluster-Outlier Analysis (bottom) for aluminium results (Fixed Band Neighbourhood = 1.85m). 255

Figure 92. The basic visualisation (Jenks; top), Hot Spot Analysis (centre), and Cluster-Outlier Analysis (bottom) for calcium results (Fixed Band Neighbourhood = 1.85m) 256

Figure 93. The basic visualisation (Jenks; top), Hot Spot Analysis (centre), and Cluster-Outlier Analysis (bottom) for magnesium results (Fixed Band Neighbourhood = 1.85m). 257

Figure 94. The basic (Jenks Natural Breaks) visualisation of the results for all detected trace elements. 260

Figure 95. The analysis strategy for field pXRF carried out on the Flixton Island dryland trenches in 2014, with south circular feature illustrated (other two potential features too indistinct and not planned). 262

Figure 96. pXRF analysis grid colour coded by date of analysis 263

Figure 97. An aerial view from the east of the site, with trench 11 in the foreground and the long, thin trench 12 to the south, starting to run down into the lake area to the south (with trench 15 to the northwest of 12 and the wetland trenches to the north of all of these). North is to the left of the picture. Cropped from photograph taken by Paul Howden 265

Figure 98. An elevated photograph facing southeast from the northwest of trench 11, where the slight dip into the southeastern (far) corner can be made out, along with plough marks in the centre-south area of the trench. (Photo taken by the POSTGLACIAL Project.) 265

Figure 99. An elevated side view from the western side of trench 15 (with the northern end of trench 12 to the southeast and trench 11 to the north in the background). (Photo taken by the POSTGLACIAL project.) 266

Figure 100. Simple, HSA and C-OA (left to right) plots of readings from pXRF for silicon 271

Figure 101. Simple, HSA and C-OA plots of readings from pXRF for aluminium 272

Figure 102. Simple, HSA and C-OA plots of readings from FpXRF for iron 274

Figure 103. Simple, HSA and C-OA plots of readings from FpXRF for calcium 275

Figure 104. Simple, HSA and C-OA plots of readings from FpXRF for potassium 276

Figure 105. Simple, HSA and C-OA plots of readings from FpXRF for titanium 277

Figure 106. Simple, HSA and C-OA plots of readings from FpXRF for chlorine 277

Figure 107 A-W. Basic plots of the values read in ppm from pXRF for the trace elements 283

Figure 108. Results of the Average Nearest Neighbour analysis on the main dryland area, which suggests statistically significant clustering based on the 3D located assemblage (autogenerated by the ANN tool, ArcMap). 313

Figure 109. Kernel Density plot of the 3D located Mesolithic assemblage 314

Figure 110. Kernel Density plot of the 3D located Mesolithic assemblage, with the general area polygons superimposed 315

Figure 111. Overlaying the weighted centroids for sieve lithics over the density analysis of the 3D lithics (only sieve material from trenches 4, 9 and 12 could be reliably visualised by grid square as 11 and 15 were impacted by post-excavation errors as discussed in section 4.2.5 317

Figure 112. The density raster across the main dryland area. The outer edge of the layer highlighted red in the density raster was used to define the outer bounds for the three main scatters (southwest, central, and southeast dryland) 318

Figure 113. The 3D located lithics falling within the grid squares identified as the main scatter squares 318

Figure 114. The artefact counts for different lithic categories in the central dryland scatter 320

Figure 115. The artefact proportions for different lithic categories in the central dryland scatter, 3D located data only 320

Figure 116. The artefact proportions for different lithic categories in the central dryland scatter, 3D and sieve data combined....321

Figure 117. The artefact counts for different lithic categories in the southwest dryland scatter, 3D located data only....321

Figure 118. The artefact proportions for different lithic categories in the southwest dryland scatter, 3D located data only....322

Figure 119. The artefact counts for different lithic categories in the southeast dryland scatter, 3D located data only....322

Figure 120. The artefact proportions for different lithic categories in the southeast dryland scatter, 3D located data only....323

Figure 121. The 3D located microlith and scraper distributions superimposed over the density raster....324

Figure 122. Example of a two group run incorporating all major/minor elements....327

Figure 123. The parallel box plot associated with the two group run in the previous figure....327

Figure 124. Example of a five group run incorporating all major/minor elements....328

Figure 125. The parallel box plot associated with the five group run in the previous figure....328

Figure 126. Example of a seven group run incorporating all major/minor elements, with the potential activity areas highlighted. The red outlined areas are those lower in calcium; the blue is those moderately higher in calcium and moderately lower in magnesium....329

Figure 127. The parallel box plot accompanying the seven group analysis in the previous figure....329

Figure 128. An example of the seven group runs incorporating manganese and phosphorus....331

Figure 129. The parallel box plot accompanying the seven group analysis in the previous figure....331

Figure 130. The lithic density raster superimposed on the grouping analysis results (seven-group run example, with key areas highlighted)....332

Figure 131. The ephemeral features plotted in trench 4....333

Figure 132. The features plotted in trench 4, compared with the lithics density raster and the areas of interest identified from the geochemical grouping analysis....334

Figure 133. The features compared with the specific locations of finds and the geochemically identified areas of interest.....334

Figure 134.The reading grid for pXRF analysis in the field (light grey), with the excavated trench outlines illustrated to show the overlap of the northern end of trench 15 excavated and analysed by pXRF in 2014 (teal outline), with trench 4 excavated and sampled.....335

Figure 135. An example two-group run on the combined key elements as measured by pXRF 337

Figure 136. The parallel box plot describing the groups in the previous figure.....337

Figure 137. An example five-group run on the combined key elements as measured by pXRF 338

Figure 138. The parallel box plot describing the groups in the previous figure.....338

Figure 139. An example nine-group run on the combined key elements as measured by pXRF 340

Figure 140. The parallel box plot describing the groups in the previous figure.....340

Figure 141. An example of the five-group runs with key areas discussed in text highlighted. The dark blue outlined areas are characterised by lower silicon and moderately higher calcium. The dark red area has higher silicon while all other elements are slightly or moderately low. The yellow area has moderately higher potassium and aluminium as well as slightly higher iron and titanium in some of the runs. The purple area was tentatively drawn out as an area with slightly higher calcium/higher phosphorus samples in the nine-group runs. The green area was frequently a little different to the rest of trench 12, with values near the global averages. The black area is an area that was often isolated in the nine-group runs but with an inconsistent profile. 341

Figure 142. The grouping analysis model for the pXRF results overlain with the lithics from the associated trenches.....342

Figure 143. The lithics and soils analysis results from trench 11, with A) the five-group soils grouping analysis underlying on the left, and B) the nine-group analysis on the right.....344

Figure 144. The lithics and soils analysis results from trench 15, with the five-group soils grouping analysis underlying on the left, and the nine-group analysis on the right.....345

Figure 145. The lithics and soils analysis results around the plotted feature in K-3, trench 15 346

Figure 146. The lithics (black data points) and five-group soils analysis results from trench 12 347

Figure 147. The general sampling grid across the western structure and the central occupation area, superimposed with plans of the features and symbolised to illustrate the main context variations across the area 351

Figure 148. Sampling over the central structure: the eastern trench edge is at the top of the photo, which is the edge that cuts through the central structure. The structure is in the vicinity, and to the southwest, of the white sample boxes seen near that trench edge. Sampling was taking place across the darker occupation spread areas at the time of the photo. (Kite photograph taken by Sue Storey, reproduced from Rowley et al. 2018.) 351

Figure 149. The grid of soil samples processed for ICP-AES analysis (dark grey). The western structure is the 6 x 4m grid to the west, the rest of the samples are considered to be from the central area. Most of the samples cover the occupation spread and structure (reproduced from Rowley et al. 2018) 352

Figure 150. Ironpan seen at Star Carr, 2015 excavations 354

Figure 151. The western structure and central structure areas, with 9 groupings specified for the complete dataset. (Reproduced from Figure 21.5 in Rowley et al. 2018.) 361

Figure 152. The parallel box plot generated on ArcGIS of the compositions of the different groups identified in Run 1 of the nine group analyses 361

Figure 153. (left) a biplot illustrating the relationships between 1) the five elements (depicted as variable vectors) and their contribution to the components, 2) the individually projected data points for each sample and therefore 3) the relationship between the variable loadings on the components and the elements as shown by their proximity on the graph. Data points are symbolised by area; (right) a plot of the same individually projected sample data points, highlighting the relationship of samples from different areas to the components (made by connecting the most dispersed points of each spread). (Reproduced from Figure 21.6 in Rowley et al. 2018.) 364

Figure 154. The microlithic industry from Deepcar, Yorkshire (reproduced from Radley and Mellars 1964, p.10, not to scale) 378

Figure 155. Awls from Deepcar (reproduced from Radley and Mellars 1964, p.17, not to scale) 380

Figure 156. Acetone vapour exchange setup for drying micromorphology tins from Flixton Island 2 and Star Carr, with a pot of anhydrous calcium chloride as desiccant on right end of the bottom row in the photograph 397

Figure 157. Anhydrous calcium chloride as desiccant, with the fresh powder shown on the left, and the expanded exhausted powder shown on the right 397

Figure 158. The histograms for the data as measured in batch 1 and 4 of the ICP-AES analysis on trench 4 462

Figure 159. The histograms for the data as measured during the field pXRF analysis of trenches 11, 12, and 15 505

List of Accompanying Material

- CD with supplementary data

Further Open Access records of the data will be available through the Archaeology Data Service.

Acknowledgements

I very much wish to thank the following family, friends and colleagues for their guidance, help and support over the past four years. I could not have done it without these people:

The whole POSTGLACIAL team (my academic family) but particularly Becky Knight, Mike Bamforth, Shannon Croft, Emma Tong, Anita Radini, Neil Gevaux, Andy Needham, Don Henson, Chantal Conneller, Charly French, and huge thanks to my supervisor Nicky Milner for her enthusiasm, inspiration and support.

Barry Taylor, Amy Gray Jones, and all the excavators and post-excavation volunteers for Flixton Island 2 and Star Carr (especially the ones who took the soil samples, I hope you like what I did with them). This project would never have been possible without your hard grafting.

Those who offered me specialist advice, training, assistance, and laughs along the way: Michelle Alexander, Penny Bickle, Ed Blinkhorn, Clare Boston, Annika Burns, Oliver Craig, Gianni Gallello, Helen Goodchild, Carl Heron, Roland Kröger, Carol Lang, Beth Nash, Steve Roskams, Hayley Saul, Matthew von Tersch, Haylee Widdall and Helen Williams.

My examiners, Geoff Bailey and Clare Wilson, for their very useful advice and encouragement during my viva.

The departmental administrators: Claire McNamara, Claire Watkins, Janine Lyon, Vicky Moore and Andrea Dugdale.

The AHRC and ERC for funding this PhD and for funds to go to a conference, and the Department of Archaeology at York for granting me a Departmental Research Fund award to attend an international conference.

Lastly, none of it would have been possible without the support and encouragement of my family and other friends, particularly Ian, Mum, Dad, Mackie, Nanny Fifi, Cinzia, Cristina, Mike, Lucy, Liz, Niamh, Joe, Sophie, Izzy, Trumerz (your turn), Camille, Hope, Amy, Charlie, George and Chloë, but many others too. You might not think you did anything but, at various points in time, you made a big difference.

This work is dedicated to my grandmothers, Catherine Joan, Euphemia and Avis, all incredibly smart, inspiring women; and my cat, Duchess, for just being her lovely, little self.

Author's declaration

A modified version of chapter eight on the geochemical analyses at Star Carr was published between thesis submission and viva voce examination in Milner, N., Conneller, C. and Taylor, B. (Eds.) (2018) Star Carr, Volume 2: studies in technology, subsistence and environment. White Rose University Press: York. The other results presented in this thesis are not yet under review or formally published.

I declare that this thesis is a presentation of original work and I am the sole author. This work has not previously been presented for an award at this, or any other, university. All sources are acknowledged as references.

Chapter 1 Introduction

1.1 Project aims and objectives

1.1.1 Project Rationale

Our understanding of the Mesolithic has been dominated by sites such as Star Carr, where large quantities of organic remains have been found and features in the ground have been excavated, suggesting the use of structures. However, the majority of Mesolithic sites across the British Isles are made up of lithic assemblages of wildly varying sizes, from as many as hundreds of thousands of stone artefacts, right down to small, sporadic finds discovered by keen amateurs. Often, these lithics are found without any significant assemblage of organic remains due to preservation conditions. They also often lack significant structures or features. However, these lithic scatters also have the potential to provide information on activity areas and the lifeways of people inhabiting the site. Although there appears to be a lack of evidence, in some cases it is there but just not visible to the naked eye, but by using a range of scientific techniques it may be possible for new insights to be gained.

Looking for the 'invisible' archaeology was an approach used on the POSTGLACIAL project, which examined the Early Mesolithic sites of Star Carr and Flixton Island 2, both found on a palaeolake (Lake Flixton) in the Vale of Pickering. One of the other types of material available at nearly all sites, particularly those formally excavated, are the soils and sediments in which the lithics are found. Usually, these contexts are very broadly visually described and evaluated in the field, and bulk and micromorphological samples may be taken to develop better understandings of the natural, use, abandonment, and post-abandonment processes that occurred on the site generally or to understand specific features. However, as both spatial recording and elemental analysis techniques have developed, so too have the capabilities for making more of this ever-present resource to investigate archaeologically-associated geochemical spatial patterning at higher resolution.

Whilst Flixton Island 2 has been known for over 60 years for the discovery of a Late Upper Palaeolithic horse butchery site (Moore 1954), new excavations from 2012-2014 discovered a completely new Early Mesolithic lithic assemblage on the top of the island with a little over 20,000 pieces. Unfortunately, as this was found on the dryland, it lacked directly associated organic finds, though there was a small assemblage from an adjacent gully infilled with peat which is assumed to be associated with the lithic scatter. In addition, this site had no clear structural remains. Therefore, it is more typically in keeping with the usual, more ephemeral, British Mesolithic sites. The huge quantities of lithics found at Flixton

Island needed analysis, but it was also important to attempt to identify activity areas on the dryland by incorporating a much more detailed analysis of the sediments than is usually conducted and integrating the two datasets, lithics and sediments, through statistical spatial analysis.

1.1.2 Research aim

The research project aimed to evaluate whether the use of several methods of analysis on sediments and lithics, could produce a better understanding of activity areas and spatial patterning than had previously been achieved for Mesolithic dryland sites.

1.1.3 Objectives

1. To typologically catalogue the Flixton Island 2 lithic assemblage
2. To examine the spatial patterning of the lithics using GIS
3. To analyse the soil geochemistry from Flixton Island 2 using multi-elemental soils analyses
4. To plot the geochemical results spatially to identify patterning using GIS and statistical methods
5. To consider the spatial patterning of the lithics and geochemistry as an integrated dataset, in order to map potential 'invisible' activity areas and consider the entire body of evidence from the site holistically
6. To analyse and plot soil geochemistry samples from Star Carr using multi-elemental soils analyses, as a comparative study

1.2 Flixton Island 2 as a persistent place and palimpsest

1.2.1 Persistent places and palimpsests in theory

In considering settlement patterns on British Mesolithic sites, Mellars (1976) argues that as organic remains are usually absent from British Mesolithic sites then definitions of settlements have to rely mainly on two forms of evidence: traces of structural features such as post-holes and the spatial distribution of lithic artefacts and knapping debris. Notably, he also comments that soil geochemistry is also an option that at that point had not been deployed on British Mesolithic sites (p.377). Lithic analysis itself has, in the past, dehumanised assemblages into inaccessible records with little to suggest about the people behind them. McFadyen (2007) raised the idea that depositions of material could be seen not as discarded refuse solely, but an active part of people making themselves at home at a site. Bailey and Galanidou (2009) raised the complementary concept that palimpsests could illustrate people's deeper connections with a site, and as different users arrive or return to

a site they would be connecting with dwellers that had been there in the past and also perhaps anticipating dwellers in the future.

The number of lithic artefacts and their density at Flixton Island, immediately suggested that the assemblage could be a palimpsest of material. If we consider this in the light suggested by McFadyen (2007) and Bailey and Galanidou (2009), then there is immediately a sense of community through time and space, and perhaps even home building here, even if more temporary than some other sites in the Vale of Pickering. While the lithics are what initially signal the presence of this palimpsest, a significant occupation of and/or repeated return to a site also has the potential to leave invisible traces of activity in the form of geochemical signatures. As such, Flixton Island 2 was an opportunity to test the application of multi-elemental analysis in identifying activity area markers at an Early Mesolithic site, that in turn would benefit from information about the complex palimpsest being drawn out.

1.2.2 Activity areas and multi-elemental soil analysis

Various methods and approaches have been used in studying soils and sediments associated with archaeological sites and assemblages in the past, but rarely when considering Mesolithic sites and the relationship to lithic assemblages in particular. Multi-element soils analysis is a well-established avenue of research within archaeological projects (cf. Entwistle & Abrahams 1997; Wilson et al. 2008; Dore & López Varela 2010; Pastor et al. 2016). However, comprehensive horizontal surveys of sites have most often been applied to sites with clear structures or limits; either natural (such as cave floors, as in Homsey and Capo 2006) or anthropogenic (such as buildings, e.g. Middleton and Price 1996; Vyncke et al. 2011). These confine the potential zones of activity and, also, often provide a degree of protection by sheltering the sediments. In contrast, perhaps because Mesolithic sites do not tend to have clear structures, there has been very little multi-elemental analysis carried out on sites of this period, though there has been more work using other proxies such as single-element analysis and magnetic susceptibility (e.g. Linderholm 2010; Johansson 2014). However, where remnants of buried soils are present, either in situ or redeposited in shallow features, there is the possibility that ephemeral geochemical signatures of past activities could be identified.

The basis of the concept is that as people repeatedly use areas of the site or landscape for specific purposes, i.e. persistent places, a proxy signature can build up that can represent the activity and behaviours if it can be identified and interpreted appropriately. In response to the most recent interest in identifying 'anthropic activity markers' (AAMs), an entire volume of the journal *Environmental Archaeology* was recently dedicated to papers stemming from a symposium dedicated to the topic (Lancelotti,Pecci and Zurro 2017). The

appeal of identifying these markers, either through consideration of ethnoarchaeological and experimental archaeological observation or from the study of sites with known histories, is that as knowledge builds about the nature of microscopic proxies for behaviours then activities that do not necessarily leave macroscopic evidence can start to be identified. This is naturally highly pertinent for research into ephemeral sites such as those from Mesolithic Britain. However, the approach taken must be considerate of the fact that it is not just anthropogenic activities from the specific period of interest that will leave or influence markers. The nature of the underlying geology and substrates, and also natural and anthropogenic processes that have occurred in the locality since the archaeological occupation of interest will all have a potential bearing on the signature detected. As a result, interdisciplinary and multi-proxy approaches are being pushed to address this issue of equifinality and the careful consideration of spatial distribution is a crucial element in this process (*ibid*.).

Work identifying anthropic activity markers has been developing over a long time, although that specific term was only recently formalised (Rondelli et al. 2014; Lancelotti,Pecci and Zurro 2017). Much of the early work in identifying activity areas on archaeological sites developed from understanding spatial relationships using single-element methods. In particular, phosphate analysis was particularly popular as being both a reliable and long-established indicator of human occupation first utilised by Olaf Arrhenius in the 1920s (Arrhenius 1929 as cited in Middleton 2004). However, there are issues that can arise from using only one element for activity area identification; for example, phosphorus has been found to be enhanced by so many different activities and modern (particularly agricultural) practices that it almost too readily indicates human occupation. As such, multi-elemental approaches are often stronger as the combined consideration of elements can add weight or nuance to the arguments for specific activity, essentially operating as multiple strands of evidence as well as allowing better consideration of the influence of natural processes (Middleton 2004).

Many of the earliest works considering multiple elements (and other proxies such as carbohydrates) were geared around defining activity areas within known archaeological residential areas, such as the study of plazas (Wells 2004), or embedded in clearly defined floor surfaces, such as lime-plastered floors (as reviewed in Barba 2007). Middleton and Price (1996) produced one of the seminal works, considering multi-elemental signatures from earthen house floors at both modern and archaeological sites in Mexico and Canada using ICP-AES. They found that the activity in the modern houses could be identified based on the chemical residues in the soils, and that the archaeological features could be both distinguished from the natural soils and that specific types could be distinguished from each other. The use of modern or historically known comparisons to generate an

ethnoarchaeological understanding of how activities would influence chemical signatures has itself been an important aspect of the development of the field and the body of knowledge generated this way is still in constant development (e.g. Knudson et al. 2004; Terry et al. 2004; Friesem and Lavi 2017; Pecci,Barba and Ortiz 2017; Lancelotti et al. 2017).

Having become a more established method with very promising potential, researchers looked to evaluate the consistency of signatures between sites further as it was acknowledged how site histories, pre- and post-depositional soil processes such as leaching, and underlying geology would potentially influence the results. Wilson et al. (2008) compared results from known contexts on various abandoned farms from across the UK. They specifically chose sites that were as similar in nature as possible (encompassing similar agricultural practices, being from a similar period, and so on) so as to be comparable. They confirmed that in these contexts, too, there were significant differences in the soil chemistry of contrasting functional areas and that despite the site-specific effects on the soils, there was enough similarity in the elemental enhancement profiles that, using statistical modelling, functional interpretations could be successfully made. They did draw out more nuances though, finding that materials such as charcoal and bone would influence retention of certain elements such as calcium and strontium, and also that specific input materials such as these did not have distinct enough elemental profiles as to be identified or that they were often too mixed in the soils to be able to tell. As such, functional areas could be differentiated, and the specific activities had generally recognisable signatures that the overall activity could be suggested, but the balance of what materials had produced that signature could not be predicted.

These are just a few examples of the work that has been conducted over the past few decades on using multi-elemental analysis to differentiate and/or understand activity areas. Despite the potential for building up such depths of information about how people were living on different kinds of site and within many different landscapes, there has been a lack of this kind of work applied to Mesolithic, and particularly British Mesolithic, contexts. Mikołajczyk and Schofield (2017) presented the results of portable x-ray fluorescence analysis on peat samples from the intertidal Early Mesolithic site of Clachan Harbour, on the island of Raasay, Scotland. The study was based on samples retrieved by augering every 5 m along a 55 m transect, with two samples taken from each core at the base and top of the peat unit that contained and overlaid the lithic assemblage which had been used to relatively date the site. As such, the analysis was designed to get a sense of the occupation area of the site in relation to the ancient coastline, rather than to build up a picture of regions of activity across the full area of the site. The sample at the top of the unit was taken as a control for the post-depositional period signature to compare with the samples from the base that had the potential for being enriched geochemically through Mesolithic activity.

Studying the results using principal component analysis (PCA), they isolated a grouping of elements associated with Principal Component 1 made up of phosphorus, sulfur, chlorine, calcium, vanadium, bromine, and strontium. They raise the point that while these are all generally abundant in marine environments, phosphorus, sulfur, calcium, and bromine are biophilic and therefore can reflect the amount of organic matter in a deposit and so be indicative of anthropogenic enrichment via organic waste deposition as had been found in previous studies in Iceland (Mikołajczyk and Milek 2016) and elsewhere. This was coupled with the fact that there was a sharp decline in the presence of these elements around 20-25 m along the transect in the basal peat towards the sea, which may indicate the truncation of the area of human activity at the edge of the water. This is a well-argued paper with a consideration for the local environmental context while at the same time establishing the potential extent of the Mesolithic site. While it does not explore the potential variable zones of activity there, as research on sites from other periods has successfully achieved, it provides this different variant of new information that can be gleaned from the application of multi-elemental analyses.

As such, the question of whether and how multi-elemental geochemical signatures could be used as activity area markers on Mesolithic sites has not been explored. This is not to say that people have not been working on establishing activity areas, however, but that this has usually been done through extensive lithic studies looking at refitting, microwear, and residues analysis such as the work by Chantal Conneller, Aimée Little and Shannon Croft as part of the POSTGLACIAL project on Star Carr. It was decided to utilise multi-elemental analysis at Flixton Island 2 as a potential additional method that could be applied to other sites in the future if successful, as well as directly comparing it to similar analysis carried out on potential structures at Star Carr.

1.3 The excavations and previous research at Flixton Island 2

1.3.1 History of research

In the summer of 1947, a local archaeologist named John Moore examined some exposed gravels in a ditch and identified a humanly-worked flint blade (Moore 1950). Further examination of the ditch developed into the excavation of Flixton Island site 1. Flixton Island site 2 was initially identified on the slopes of a bipartite hillock, located along a peat covered gravel ridge less than 500 m to the north from Flixton Island 1. The hillock would have originally protruded from the palaeolake Flixton's waters, whereas now the area is entirely peaty agricultural land. Site 2 was similarly found by Moore rootling through some of the basal peats in a ditch on the northernmost periphery of the area, towards the end of the

excavations at site 1, in which he found preserved animal remains that would later prove to be from the Palaeolithic occupation of the site in what he aptly termed the 'Horse Layer'.

Moore excavated Flixton Island 2 in late summer 1948 and also in March and July 1949 (Moore 1954), finding a "scatter of Mesolithic flints, charcoals and traces of animal remains, including red deer" at the base of a layer of peaty detrital mud (Moore 1954, 192). Then below further layers of gravel (that contained some resorted bones) and sand, and at the base of a layer of peaty nekron mud (gyttja, mud formed from the decay of peat in wetland contexts) he rediscovered the Horse Layer which contained bones belonging to at least three horses, a fragment of bird bone, a small flint blade, and a distinctive microlithic shouldered point with "steep, almost vertical secondary working" (*ibid*., and see Figure 1). Moore would go on to locate up to nine other sites around the Vale in short succession including site 4, which would come to be known as Star Carr (Moore 1950).

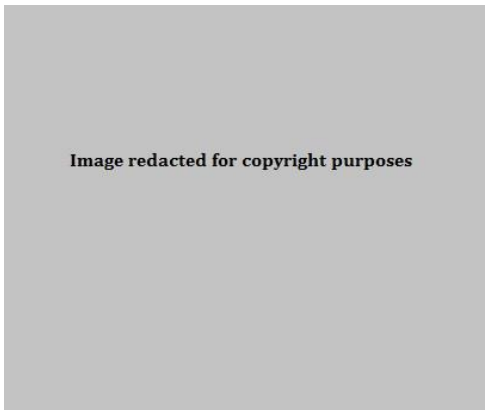

Figure 1. Moore's shouldered point (as published as Plate XVI in Clark 1954, p.136, not to scale)

Further test pits were excavated before 2012 by the Vale of Pickering Research Trust. These excavations recovered 17 artefacts from Flixton Island 2 that were evaluated by Chantal Conneller. Amongst these was one microlith, a possibly unfinished obliquely blunted point which is a very typical tool in Early Mesolithic assemblages, accompanied by 16 pieces of various kinds of debitage. Conneller thought the debitage suggested these finds may have been on the edge of a larger scatter where knapping took place (Conneller, pers. comm.).

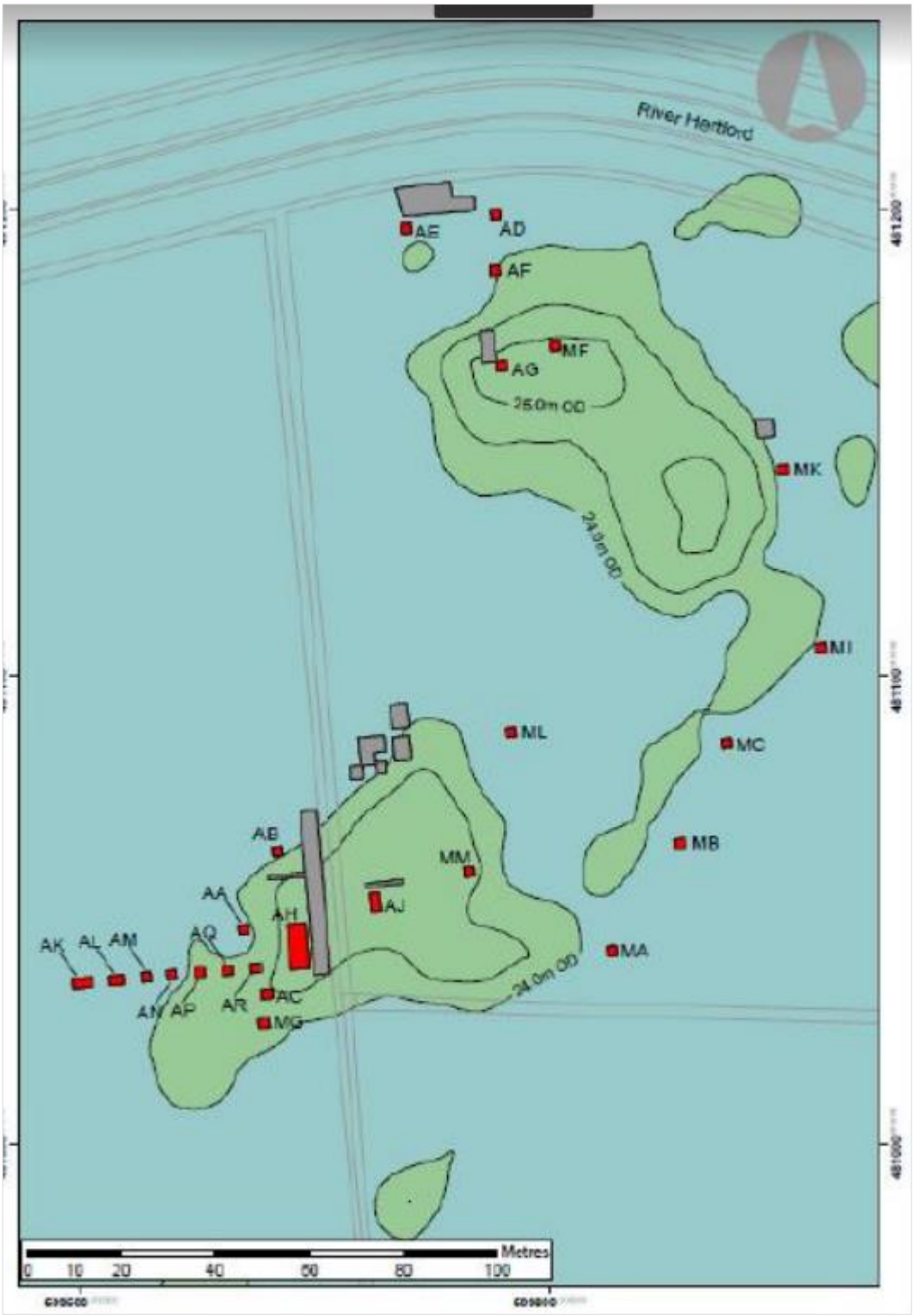

Figure 2. Previous excavations at Flixton Island, image reproduced from an internal report by Barry Taylor (POSTGLACIAL Project). Grey trenches indicate Moore's investigation, red trenches were carried out by the VPRT. Site 1 is on the southern part of the island in the vicinity of Moore's large grey trench and site 2 is on the more northerly, dual peaked, part of the island, with the two parts nearly connected by a gravelly ridge.

1.3.2 Recent investigations

In 2012, as part of the ERC funded POSTGLACIAL Project, the most recent investigations of the site of Flixton Island 2 commenced with an aim to re-excavate Moore's trench and obtain palaeoenvironmental data. An extensive geophysical survey, augering for environmental analyses, and small-scale excavation in the northern wetland area of the island near Moore's previous trench and two small areas on the dryland was initiated to achieve this. However, the site looked so promising that the trenches were extended, and further excavation was carried out on the dryland of the larger of the two peaks, which immediately resulted in the discovery of the Mesolithic site that was much more extensive than initially anticipated. As a result, two further seasons of excavation were carried out in August 2013 and August 2014 (see Figure 3). The trenches covered the apex of the dryland that to the north trailed down to a gully, then rose again to a second, but lower, bar of dryland, before falling off into the lake proper. To the south, the island falls off into the lake area bordered to the east by the spit that joins Flixton Island 2 and 1. Further trenches covered a large area of what would have been on the edge of the lake and into the lake itself. These were surrounding the location of Moore's trench. These general areas, that will be referred to throughout the text, are illustrated in Figure 4.

As expected from Moore's excavations, the wetland area consisted of two phases of Mesolithic and Palaeolithic material, the latter associated with predominantly horse remains. The dryland area was much shallower with only three stratigraphic units across depths of no more than 20 cm, often as shallow as 10 cm, at the apex, and no preservation of associated organic remains. It is in this area, and surroundings, that soil sampling and analysis was conducted. The general lithic assemblage there is accompanied by a significant assemblage of Early Mesolithic microliths, so it is assumed to be attributable to that phase. However, there were a handful of Palaeolithic lithic artefacts identified from the same trenches as will be discussed in chapter four. Dates on organic material from the gully have not yet been published but they correspond very broadly to the period when Star Carr was occupied.

Figure 3. The POSTGLACIAL Excavations, relative to previous excavations in the vicinity (the area delineated in the inset map shows the excavations relative to Figure 2). Contour data was created by Barry Taylor for the POSTGLACIAL project during the environmental coring project that formed his PhD (Taylor 2012)

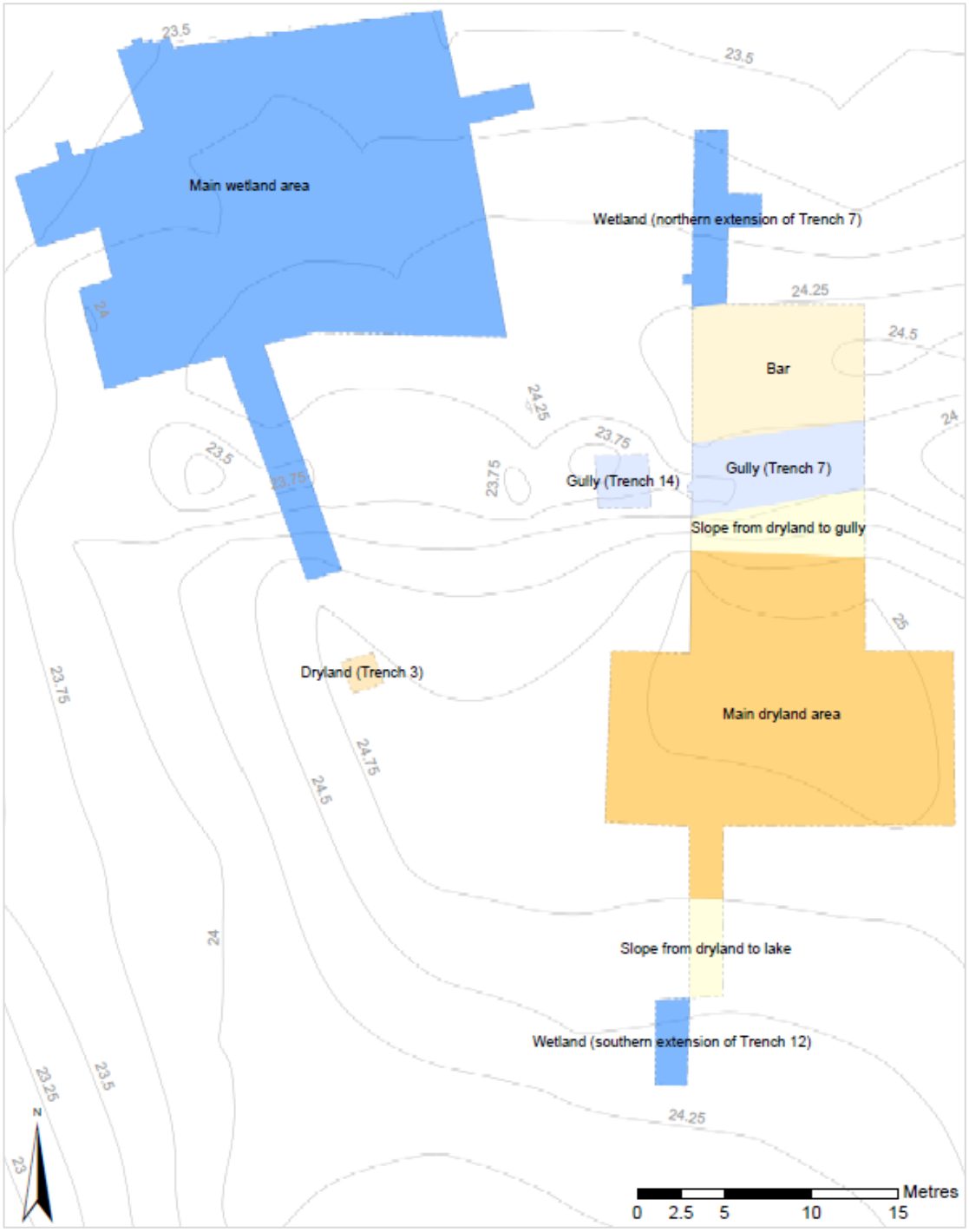

Figure 4. The general areas discussed throughout the text

1.3.3 Postglacial Lake Flixton's formation and the geology of the Vale

Flixton Island 2 and Star Carr are situated within the broad lowland forming the base of the Vale of Pickering which stretches for approximately 50km east to west. Many researchers have worked on reconstructing the environment in the Vale of Pickering in the name of both archaeological interest and as a region of interest for the study of glaciation/deglaciation processes at the end of the last ice age. The Vale is roughly bordered by three upland formations. To the north, the limestone and gritstone North York Moors rise to c. 250-430

m above sea level, in particular the southern range of these being called the Tabular Hills that feature flat summits composed of Corallian limestone ("nabs"). To the west, the Howardian Hills, a southernmost extension of the rocks of the Moors and therefore also on Corallian limestone rise to 174 m maximum at Yearsley Cross. To the south, the vale is bordered by the chalk derived Yorkshire Wolds rising to 150-240 m (Mellars & Dark 1998; Evans et al. 2017; and see Figure 5 and Figure 6).

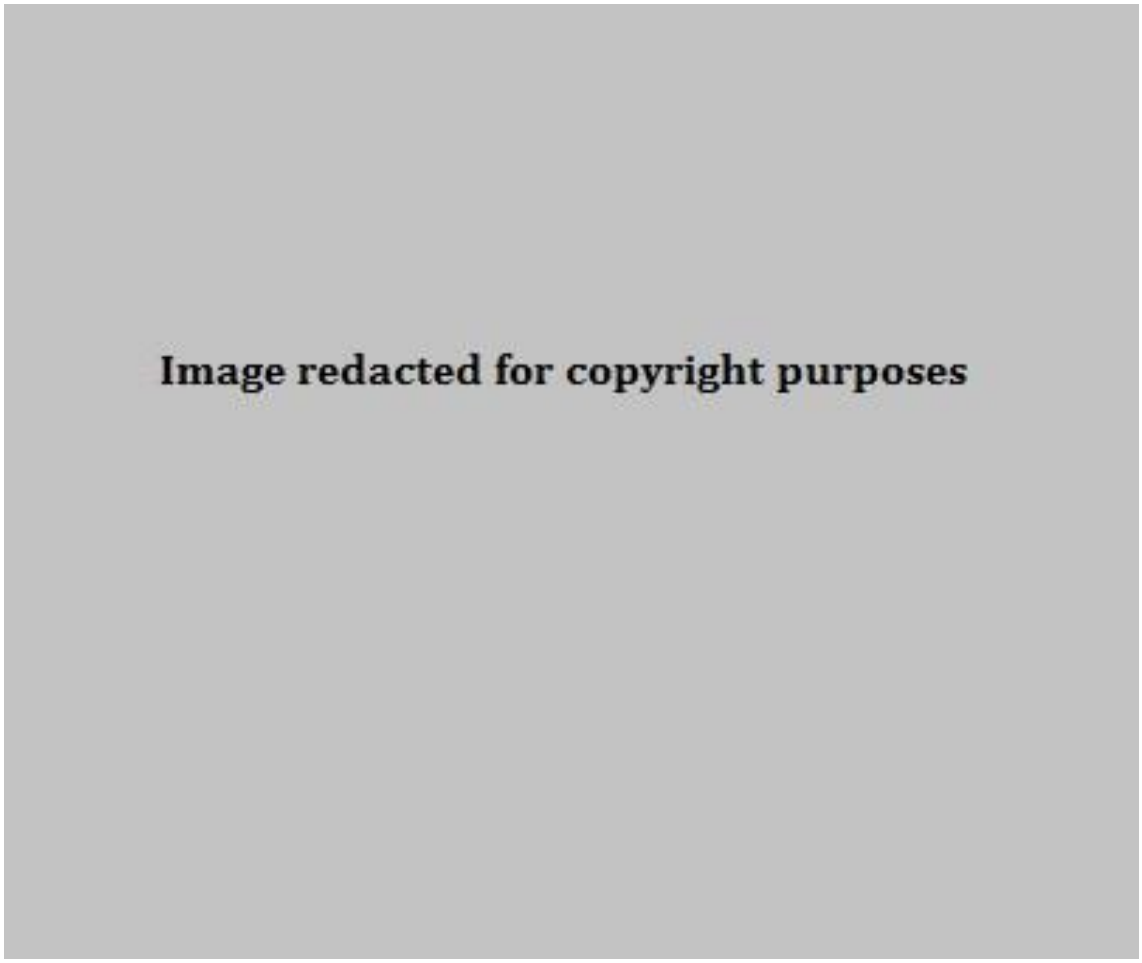

Figure 5. The location of (a) the Vale of Pickering, (b) the uplands enclosing the vale, (c) the underlying geological deposits in the vale, with the orange being lacustrine deposits suggesting the edges of glacial palaeolakes Pickering and Flixton (reproduced from Evans et al. 2017, p.296)

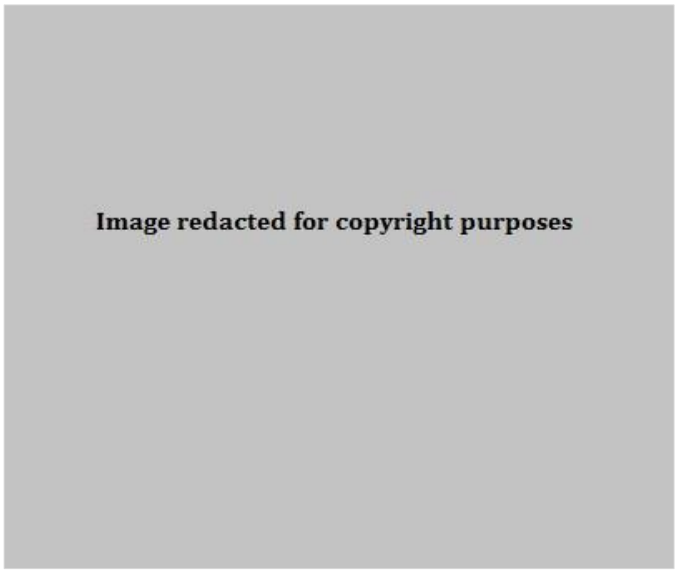

Figure 6. The location of the archaeological sites around Palaeolake Flixton, with (a) showing the margins of the British-Irish Ice Sheet and (b) showing the important Palaeolithic and Mesolithic sites on the lake edges (reproduced from Candy et al. 2015, 61)

The underlying geology was deposited over a succession of emergences from and submergences under the North Sea, including layers of shales, limestones and sandstones which are exposed and therefore accessible for gathering, past and present, along the coast. Flixton Island 2 and Star Carr are situated on top of superficial deposits that overlay bedrocks of the Speeton Clay Formation (BGS GB 1:50000 Rock Unit Map). The Speeton Clay Formation comprises of mudstones (sedimentary rocks formed from clays or muds), cementstones (a limestone consisting predominantly of fine grained carbonate) and sporadic bentonites (kinds of clay) (British Geological Survey). However, much of the geological topography physically exposed in the Vale is the superficial deposits, the nature of which were dictated by the expansion and contraction of the British-Irish Ice Sheet at the end of the last ice age, the Devensian.

With the Vale of Pickering being located on the edge of the extent of the ice sheet, the North Sea glacier prevented flow of the river Derwent into the North Sea itself (Evans et al. 2017). This dammed the eastern end of the Vale. The western end later became dammed by the Vale of York ice lobe at the Coxwold-Gilling Gap and the Kirkham Priory Gap, cutting off that drainage route as well and forcing it to eventually overflow towards the southwest between the Howardian Hills and the Wolds at Kirkham Priory between Malton and Stamford Bridge to continue the river's new course. Between these dams, a series of proglacial lakes formed in the Vale of Pickering due to the diversion of the river route, eventually forming Glacial Lake Pickering (in the west of the vale). As the glacial ice retreated, a series of hollows (kettle holes) and ridges (kames and moraines) were formed. Water accumulated in these hollows as well and eventually joined into one water body which was dammed in by the Flamborough Moraine at Filey to create Lake Flixton in the eastern end of the Vale at around

14.6 ka BP (12,600 BC) (Palmer et al. 2015; Taylor et al. 2018). It is palaeolake Flixton that contained Flixton Island, with the hillocks featuring sites 1 and 2 being separated by shallow water over a narrow spit of gravels (and therefore areas of reedswamp) during the Early Mesolithic. Star Carr was positioned 500 m eastwards from the island along the nearby northwestern shore of the lake, across deeper waters. Lake Flixton persisted through various periods of growth and shrinkage until c. 7250 cal BP (5300 cal BC), by which time it was replaced by fen, swamp, and carr deposits (Taylor 2012, 191).

In terms of the geology, this process resulted in superficial Quaternary deposits of sand and gravel and lacustrine deposits of silt and clays in the lake area, as well as the depositions of the formal Devensian till along with the moraines and boulder clays to the east of the Vale (which according to the British Geological Survey maps, does not extend as far as the sites themselves). Flixton Island and Star Carr lie on the edge of the two areas mapped as being Quaternary sands and gravels and lacustrine deposits. Cloutman (1988) found Flixton Island to be on a high in the gravel deposits. Generally, when these surfaces have been discussed at Star Carr and Flixton Island in the past, these hard and clayey superficial gravel deposits have been referred to generically as "till" (in distinction from the sediments and soils forming the site contexts). That convention is continued here for simplicity but it is technically likely a misnomer.

1.3.4 Soils of the Vale

The areas immediately around Flixton Island and Star Carr generally consist of fenland peat soils, that can be quite acidic, and freely draining slightly acidic loamy and sandy soils (data obtained from the LandIS Soilscapes Map Viewer, DEFRA/Cranfield Soil and AgriFood Institute, Anon, accessed November 2017). During the warm interstadials at the end of the ice age, and then with the initial warming of the Holocene, aquatic and emergent vegetation colonised the lake which resulted in marl (carbonate precipitate) formation in the lake itself (Mellars and Dark 1998). The peat soils started forming on the lake edges and gradually infilling the lake through deposition of layers of waterlogged vegetation which started occurring shortly after the start of the Mesolithic. The peat soils formed around the edges of the island, going into the lake. The peat soils in the Vale of Pickering, which have been drained in the past, can be extremely acidic as a side effect of the drainage of peat containing sulphides. During research into the decay of organic remains at the sites, High (2014) found that the peaty soils across Star Carr could be highly variable in pH, and extremely acidic, while those around Flixton Island 2 were generally more consistently neutral.

There would have been an area of reedswamp around the island, particularly off the northern side (Taylor 2012) and potentially areas of carr woodlands. The soil here would

have been naturally wet for extended periods of time and subject to fluctuations in groundwater when not submerged. The loamy and sandy soils, as up on the dryland in contrast, being free draining would be open to leaching to groundwater and if there was plant matter growing on the slopes of the island, they would have been subject to erosion (leading to sand at the base, which is potentially seen in the gully).

1.3.5 Contexts of the dryland site

There were three major contexts of relevance to the geochemical analysis at Flixton Island 2. Context (1000) refers to the topsoil. This was recorded as a medium grey-brown soft, desiccated peat with sandy inclusions. Charles French conducted micromorphological analysis on a sample taken from the topsoil in section described the slide as being "composed of an aggregated mixture of amorphous iron replaced organic material, humic fine-medium quartz sand and humic clay… This is indicative of a mixture of desiccated peat, clayey alluvium and sandy soil material" (French 2015, p.2, and see Figure 7).

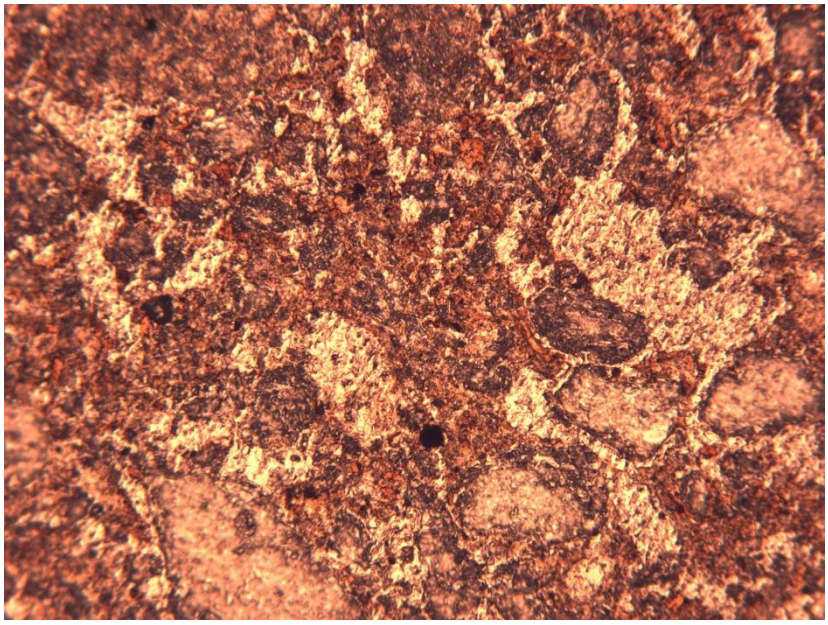

Figure 7. Photomicrograph of aggregated mixture of amorphous iron replaced organic material, humic fine-medium quartz sand and humic clay, sample Flixton VP12/1 (4.5mm = frame width; plane polarized light) (reproduced from internal report by French 2015)

Context (1119) is the interface of the topsoil and the till, formed of a mix between the two, and was thought to be bioturbated. It was medium brown with yellow/orange blotches, dry and crumbly. The material from this layer is assumed to be as close to the original deposition as possible, and it is proposed to be the Mesolithic soil horizon, but it will still certainly have moved to some degree due to bioturbation and light ploughing. It is this layer that was sampled and/or analysed. Context (1059) is the natural 'till'. It is a dense, orange/yellow clayey deposit with silt, sands and gravels mixed in. When dry it was very hard to trowel.

1.4 Structure of this thesis

As such, there were two assemblages (or sample sets) from the POSTGLACIAL excavations that were available for analysis from Flixton Island 2: the lithics and the soils. Past Mesolithic research has, quite logically, largely been focused on developing lithic typologies and attempting to make sense of developments in lithic types over time and space, as will be discussed in chapters two and three. For this thesis, typological lithics analysis was undertaken to determine the overall nature of the lithics assemblage and consider it in the light of current canon, which is reported in chapter four. This will establish the presence and balance of stone tools (both formal and expediently made on flakes or blades of lithic material), knapping technology (cores from which flakes and blades were initially knapped from), and waste products ("debitage") in the assemblage. This incorporates discussion of the spatial distributions of specific categories of tools and any noticeable patterning based solely on the lithics assemblage alone.

In addition, two elemental characterisation techniques were employed to investigate the patterns in soil composition: Inductively-Coupled Plasma Atomic-Emission Spectroscopy (ICP-AES) and Portable Energy Dispersive X-Ray Fluorescence (pXRF). The former is conducted in the laboratory (in this case by a commercial service provider) on samples carefully dried, sieved, and then redissolved in base solution for analysis. The latter can be conducted directly in the field or on samples prepared to varying extents in the laboratory. These methods and how they were applied at Flixton Island 2, both in the field and during post-excavation, is explained in chapter five, and the results are presented in chapter six.

The outputs of these two aspects of the project at Flixton Island 2 were married together through deeper exploration with spatial statistical analysis (predominantly in ArcMap). With these being the two dominant materials available on the dryland site, this avenue of research was specifically chosen to see what further information could be drawn out of the site than when the analyses were run independently. The results of this work are presented in chapter seven.

Finally, multi-elemental analysis on soils associated with structures and occupation areas at Star Carr is reviewed in chapter eight and compared with the results from Flixton Island 2. This gives a sense of the potential of this approach for a variety of Mesolithic sites.

Chapter nine concludes the thesis with a discussion of the key findings and their implications for activities that might have been occurring at Flixton Island 2, as well as suggestions for future work. There is a glossary available at the end of Volume Two.

Chapter 2 The Founding Research into Early Mesolithic Lithics

2.1 Introduction

Despite being our most common and reliable form of evidence for Mesolithic sites, lithic analysis has become largely the purview of specialists only. There are many aspects to lithic research which, when applied to an assemblage cumulatively, can give us the semblance of the form of the way groups and individuals were living. The more methods of analysis that are applied, the more detail of understanding is gained and hopefully the more reliable the interpretation becomes with each iteration. Problems arise, however, when the technological jargon becomes heavy and inaccessible and lengthy debates ensue about terminology and classification. This detracts from the ultimate desired outcome of lithic studies: to learn about the *people* of the past.

The Mesolithic site of Flixton Island 2 mainly consists of a significant lithic scatter on the dryland with little else preserved of other artefactual remains or features. The lithic analysis element of this thesis aims to establish the physical nature of this lithic scatter as well as trends in its spatial distribution and potential chronology to see what it can tell us about how people were living on and using the island. This information will then be considered alongside the results of the geochemical analyses undertaken as the second strand of research reported within this thesis.

As a preliminary to this, this chapter will first critically evaluate current understanding concerning lithic artefact analysis and particularly the received knowledge concerning Early Mesolithic microlithic cultures as presented through the academic literature. It is structured to cover the historical development of research into the Mesolithic and, seated within this context, the development of understanding regarding the classification, chronology, procurement, technology, functionality and behavioural implications of early Mesolithic assemblages.

2.2 Theoretical approaches to studying lithic artefacts

2.2.1 The three main approaches in lithic studies

Lithic research generally takes three practical routes focusing on subtly different aspects of the properties of the worked stone artefacts: typological, i.e. classification based on morphology of the artefact; technological, i.e. studies of how an artefact, either tool or waste

debitage, is produced and within which raw material studies can be included; and functional, i.e. studying the use of the artefact. Social interpretations as well as chronological development are touched on through all three approaches and researchers commonly need to combine different aspects to develop understanding in these areas. Finally, perhaps obviously but importantly, it must be considered that all interpretations are taking place within the modern social sphere and are subject to the personal influences of the individual interpreter(s). Considering various aspects of an assemblage is crucial if there is an aim to extrapolate deeper interpretations of social practice relating to the material culture preserved.

This has been illustrated well with the debates between François and Denise Bordes, the Binfords, and then Rolland and Dibble on Mousterian (Middle Palaeolithic) lithic assemblages. Bordes was the first to seriously and comprehensively attempt to characterise lithic assemblages by their typology and technology combined with statistical analysis, which can be symbolised by one of his many major publications in "*Typologie du Paléolithique ancient et moyen*" (1961). It was with the method provided by Bordes that assemblages started to be considered in terms of the frequency of key characteristic artefact types, those called 'type fossils' or '*fossiles directeurs*' (Pettitt 2009). Summarised very simply, Bordes, and later with his wife, argued that based on his typological analysis there were subgroups of cultural material reflected in the assemblage and equated these with different socio-cultural groups of people whose technologies barely intermixed, even if they personally did (e.g. Bordes and Sonneville-Bordes 1970).

Lewis and Sally Binford, on the other hand, argued that the subtypes in fact represented different types of activity occurring at different sites, in keeping with the seasonal round, not different social groups (e.g. Binford and Binford 1966). As such, they emphasised the functional aspect.

More recently, Rolland and Dibble posited that the tools being considered were subject to resharpening episodes and as such this accounted for some of the variability in the assemblages (e.g. Rolland and Dibble 1990; Dibble 1991). This further brings into the foreground the technological processes in action, relating to a more "people-centred", anthropological approach.

These interpretations are not entirely mutually exclusive. Certainly, the number of resharpening episodes depends on the task being undertaken (perhaps there is a minimum size required for a tool to be effective on a certain material for example), the availability of raw materials locally (wealth or dearth), a multitude of cultural preferences may be in play, and so on. These researchers all make strong cases for their focused approaches, they all advanced knowledge of the Mousterian generally, and their work will provide a foundation

for consideration of how these aspects of the assemblages interplay. However, all three providing valid outcomes means that they must be deconstructed, considered together and challenged to develop the closest interpretation of the past that we as archaeological observers can establish. As such, all three practical aspects of lithic analysis will be applied to some degree to the Flixton Island 2 assemblage. The separation of research addressing the three different aspects is convenient from a research point of view: clear goals and objectives can be applied in the implementation of methodologies. However, relating them together is a necessary challenge to get at the real workings of a site and therefore to develop understanding of the people who lived there.

2.2.2 Typology and classification systems

The first stage of large-scale lithic assemblage analyses is often the formulation of a catalogue of the finds based on their attributes. This usually includes their classification into type categories and may include further information about modifications (whether deliberate, accidental or natural) and visual properties of the raw material. Traditionally there is much emphasis on the typological classifications which first developed during the antiquarian and later culture-historical theoretical paradigms, with J. G. D Clark's early work on Mesolithic typologies being an example of this (Clark 1932, and see discussion below). These approaches had placed an emphasis on the collection of artefacts and distinguishing patterns in their attributes in the early stages of archaeology as a discipline, so naturally typology had an important role to play. A significant problem with these early approaches is the interpretation of variable material culture as representing variation in human socio-cultural groupings. In other words, sites were different because the people using them were from different societies. Material culture is not, however, solely a product of social groupings and this ignores site-specific contexts and influences such as the function of a particular site.

Typological classification aims to develop objectivity in lithic analysis, in that it provides a means of recording material in a standardised manner which should then be accessible, replicable, and understandable by multiple researchers. However, in practice it must be kept in mind that it will always be a subjective oversimplification of the data with the research interests and experience of the analyst coming into play. Not only are there often various options for recording systems available but the attributes they notice or are able to perceive will depend on their own research background and experience. Archaeologists actively make selection of what attributes to record, which influences the long term record and of course the interpretations based on that catalogue. As such, paradigmatic emphases come into play in an apparently objective methodology and over time different assets get emphasised or de-emphasised. This is not necessarily a problem, as long as the context of

past research is carefully considered. Implementing typological classification alone on an assemblage ignores site function considerations, technological influences, and social influences which make every site unique.

Yet, the usefulness of these categorisation systems is often underplayed. Lithic specialists apply such systems to help us simplify the highly variable masses of archaeological data and ultimately begin to glean knowledge about how people lived in the past not just on one site but across landscapes and even continents. It is a foundational starting point for the analysis of any significant assemblage and facilitates interpretation. Common terminology also naturally facilitates broad comparison and eases communication of complex ideas, as even if multiple recording glossaries are utilised they are usually comparable.

2.2.3 Functional studies

When considering lithic artefacts, it is useful to attempt to consider the perspective of any general tool producer and user as doing so highlights that classical typological classification alone is poor practice. An individual does not usually set out to make a particular tool for the sake of making the tool, but sets out to make a tool for its purpose or to practice the manufacturing process itself. Individuals also do not automatically reject an 'imperfectly' made tool if it is still adequate for the task intended. The amount of care and attention put into the manufacture and maintenance of the tool is likely to be the combined product of an appropriate level of expediency for the task, the personal pride and experience of the producer, and socio-cultural influences relating to its intended use.

If we accept these assumptions, then it must be acknowledged that the typology presented by an assemblage will be influenced by the intended function and outcomes of the tool's production and use. Functional analysis of tools is still partially based on the form, as with typological classification. Early typological classification often categorised tools into types named after their *assumed* function, for example the classification of "scrapers". These types were then frequently associated with working particular materials, for example scrapers being associated with hideworking. These are usually logical assumptions to make based on the shape of the tools, their bluntness or sharpness, their ability to be handled easily and other attributes. However, these assumptions were not tested rigorously and returning to the perspective of a tool user, there is likely to be occasion that a tool more obviously intended for a different job or perhaps even a waste product may be utilised if it fits purpose. Functional analysis, therefore, has emerged out of the need to test these assumptions.

Functional understanding of lithics can operate on two different scales: on the artefact level or on the whole assemblage (Conneller 2000, 111). Usewear and residue analyses are deployed to interrogate what individual artefacts were utilised for. The materials they were

used on, the way they were handled and manipulated, and the duration of their use can all potentially be investigated depending on the deposition conditions. Refitting programs also elucidate details about episodes of resharpening for reuse or the reworking of individual artefacts into different tools. However, microwear, residue analysis, and refitting are all highly time consuming, painstaking research processes and it is rare to be able to implement these analyses on a large scale.

At the broader site level, functional interpretations are then considered utilising statistical analyses of the proportions of different tool types and their spatial distributions when interpreting a whole assemblage, particularly in comparison with contemporary sites. As such, this facilitates researchers getting into the function of sites as well as how several sites may operate as part of a broader network of different kinds of site. This can be seen as a necessary complement to typological cultural differentiation. This was borne out of the functional-processual approaches that became increasingly popular from the 1950s but particularly in the 1970s and arose as part of a growing awareness of the issues with the more traditional culture-historical approach. Later these approaches loaned themselves to interrogating more about individual behaviours as well though, as post-processual critiques arose that required addressing.

2.2.4 Technological studies

Technological approaches consider not only the functional use of the object but the full life-history of an artefact from raw material procurement through usage to final deposition. As such, it considers an artefact potentially across a longer timescale and broader landscapes than a merely functional approach. Technological study of material culture was largely instigated by French researchers from the 1970s onwards, in the very active, emergent academic climate where the social sciences and particularly sociology and then psychology were becoming established as serious disciplines, complemented by developments in the already established discipline of philosophy, as seen through the works of Durkheim, Mauss and Leroi-Gourhan. The French body of theoretical technological study is distilled in concept of the *chaîne opératoire* (see discussions in Sellet 1993 and Conneller 2000). Literally translating as 'operational chain / sequence', this approach looks at the full life-history of different artefacts or the processual sequence that produces different artefacts.

Leroi-Gourhan identified between three stages of knowledge acting on the universal *chaîne opératoire*: 'automatic', 'mechanical', and 'lucid' (as discussed in Conneller 2000). The automatic element is the interplay of innate behaviours and genetic factors which influence technological production. The mechanical element is the knowledge implemented to conduct routine tasks, which may be socially transmitted or individually developed through

experience and may be unconscious or slightly modified. The lucid stage is where a query or problem is reasoned out consciously. How much bearing these three elements have depends on the novelty of the operation being enacted. Specifically considering lithic artefact production and use, Conneller argued that some of the key factors that affect the bearing of these three elements will be standardisation of cultural practices concerning how material is worked, who it is worked by, learning and communication, and raw material availability (2000, p.123).

Pelegrin (1990) identified between two stages of knowledge affecting the *chaîne opératoire* as an alternative/complementary approach to Leroi-Gourhan: '*connaissances*', i.e. conceptual knowledge, knowing ideal forms to be aimed at or ideal sequences which would be enacted to achieve those forms, and *'savoir-faire'*, i.e. know-how developed from memory and practice. This was developed largely based on experimental knapping research. On the one hand, knappers know what form they are aiming to produce and the general physical process they need to enact on a flint nodule to produce that form, but then their own experience (or lack of) will come into play, as will the actual nature of the nodule, for instance perhaps it is of poor quality or with many large inclusions. As such, sequences must be adapted in real time but also the mental knowledge of these sequences must also include a degree of flexibility and understanding of how to manage certain common issues (Pelegrin 1990; Schlanger 1994). As such, knappers do not simply act on the material, but the material itself can be considered to have a bearing on the active process decided upon by the knapper (Conneller 2000, p. 125). This is a techno-psychological approach to the *chaîne opératoire* concept; it considers the interplay between technology and the psychology of the participant implementing the technology (Karlin and Julien 1994). While these approaches open up new avenues to explore, it has been raised that much of this theory is based on modern experiences and notions of technology, by researchers who are not living with the technology day-to-day (Conneller 2000, p. 125), from heavily industrialised societies with mechanisation formulated on the concept of 'ideal' forms mass produced on a standard pattern (Ingold 2000, 321).

While researchers have developed typological, functional, and technological approaches to lithic assemblages, not all three can be applied to every site. In the case of Flixton Island 2, microwear and residue studies was piloted but proved largely fruitless considering the heavy patination, iron staining, and weathering inflicted on much of the assemblage (see discussion in chapter four). The following sections will now move on to consider how these approaches to artefacts have been deployed specifically to the study of Mesolithic assemblages from Britain, to introduce the debates over key cultural terms that the work at Flixton Island 2 will be seen to contribute to.

2.3 Considering British Mesolithic lithic assemblages

2.3.1 The role of microliths in identifying Mesolithic assemblages

The British Mesolithic is generally chronologically defined as spanning across approximately 5600 years from 9600 cal BC to 4000 cal BC (Milner et al. 2013). It is slightly more clearly defined here than elsewhere in Europe due to the limitations that glaciation had imposed during the last Ice Age on where could be inhabited within the current British Isles: climatic amelioration at the start of the Holocene allowed for relative proliferation of people and, therefore, sites at this time.

Relative to the Palaeolithic, it covers a short time frame and lacks the extensive body of evocative parietal art seen in those earlier sites both in Britain at Creswell Crags and particularly in France in contrast to the spectacular works at Lascaux, Pech Merle, Chauvet and so on. As such, there was a degree of resistance to recognising the Mesolithic as sufficiently different period to warrant terminological distinction. In 1870, the young but up-and-coming French archaeologist Cartailhac went so far as to propose that in fact there had been a depopulation of central Europe between the Palaeolithic and Neolithic as Magdalenian populations migrated northwards with the reindeer herds, known as his 'hiatus theory' (Valdeyron 2008). Eventually Piette's excavations at Mas D'Azil in 1887 along with de Mortillet's reconsiderations of various assemblages from the Paris Basin and excavations at La Tourasse in 1885 were key challenges to Cartailhac's hiatus theory. They provided a significant body of evidence for cultural material stratigraphically placed between Palaeolithic and Neolithic material and were therefore posited within the proposed hiatus period (*ibid*.). These sites yielded significant lithic assemblages, with the material from Mas D'Azil becoming the type fossil for the Epipalaeolithic lithic culture called the "Azilian", while de Mortillet proposed the "Tardenoisian" culture after the site of Fère-en-Tardenois. This illustrates how lithic assemblages have been key from the outset in even establishing academic acceptance of the Mesolithic, and these cultures would be compared to the British material in later years (e.g. Clark 1932). In the discussions of this 'hiatus-filling' material, lithics were categorised by their morphology, grouped into cultures by relative attributes, and their potential chronology or cultural associations were debated following suit of other culture-historical, contemporary research. As such, the development of lithic typology became a crucial and important part of the Mesolithic debate and research in this field was taken up with vigour.

At a similar time within Britain, the nature of similarly intermediate assemblages was being outlined for the first time through the literature. Honywood (1877), an antiquarian lithic specialist, who took the care to examine his assemblages with a hand lens, would identify a

"very curious" set of small artefacts from the forests around Horsham, in Sussex, that displayed blunting retouch on one side and a sharp cutting edge on the other which would turn out to be an early recognition of the interesting element and type fossil of the Mesolithic, the microlith) as well as other interesting small tools (such as microdenticulates). Gatty (1901) noted that in his collections from the northeast of England, similarly minute flint implements dominated some assemblages, and were not found with Neolithic axe heads or polished stone artefacts and yet they were distinct from the Palaeolithic material. Paterson (1913) comments that similar assemblages also lacked Neolithic arrowheads and questioned what they might be using instead.

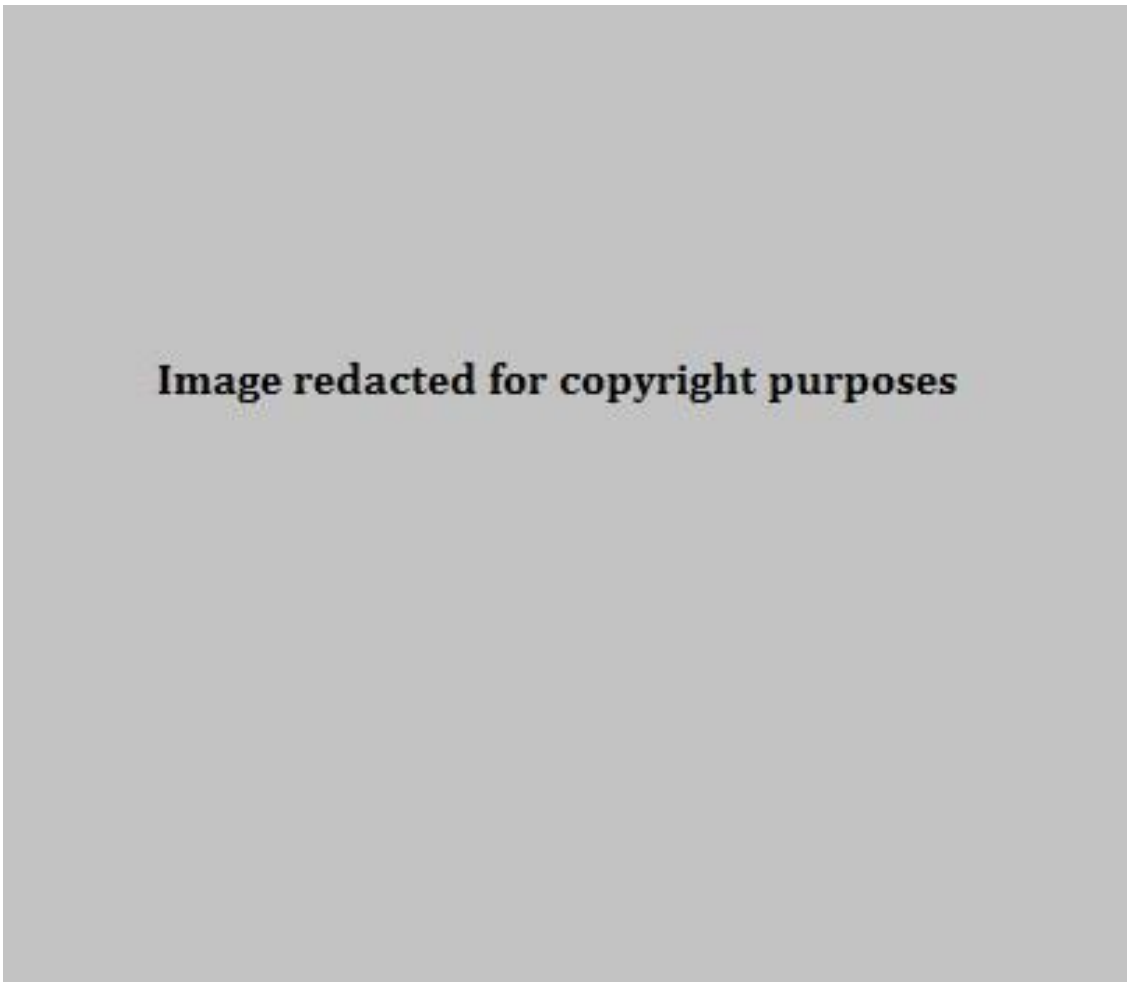

Figure 8. Callender's Scottish microliths (1927, p. 319) (not to scale)

The publication on the excavations lead by Crawford and Peake at Thatcham in 1922 was among the first to attempt to categorise and place a British microlithic assemblage within the broader culture-historical dialogues concerning cultural classification across Europe, drawing on comparisons with Svaerdbord, a Maglemosian type site from Zealand, Denmark (Crawford 1922). While comparing the lithic industry overall with Svaerdborg, they also noted the smallest lithics (microliths) were similar to those from sites under peat in the Yorkshire Moors, while the axes were similar to those recovered from Danish shell middens.

Callander published a paper concerning the "first comprehensive collection of Scottish microlithic implements" (1927, 318), and associated these artefacts with the European Tardenoisian culture. The microliths are described as being "triangles, crescents, small blades with battered backs and point tools" (Callander 1927, p.319 and see Figure 8), illustrating the emerging standardised descriptions of these pieces coming out; many of these terms, or similar, are utilised in descriptions of microlith classifications today and usually directly reflect the morphological characteristics of that piece.

By the time of J. G. D. Clark's *The Mesolithic Age in Britain* published in 1932, a comprehensive survey of the known British Mesolithic industries and sites, microliths are firmly associated with the debate concerning the status of the period. Clark defines the 'microlith' in his glossary as:

> *"… a narrow flake blunted on one or both edges by steep secondary chipping, but devoid of secondary work on either face…"* (1932, xx)

Clark argues strongly for the separation of the Mesolithic distinctly from the Palaeolithic, partly on the basis of climatic and environmental change at the end of the Ice Age but also because the "industries of the new age show a distinctive individuality" compared with earlier material (Clark 1932, 2). Later in the same text he goes a stage further in arguing that, along with migration, humanity "reacted" to the environmental changes in modifying existing or developing novel technologies which in turn altered the nature of the economy from hunter-gathering to production (1932, 6). This exemplifies the emerging dialogue emphasising the influence of the environmental context on societies and material culture that Clark later explores during his excavations at Star Carr and which would later be a common attribute of the more general New Archaeology and then functional-processual archaeological movements. The modification Clark refers to is the production of microlithic industries:

> *"…consisting of small points, triangles and crescents… [which] imply by their diminutive size the use of bone and wooden hafts into which several pieces were inset"* (1932, 7)

However, Clark seats the development of these industries in the rest of the 1932 publication within a more traditional cultural diffusion model, with material culture changing through external influences diffusing across Europe from different regions.

De Mortillet's Tardenoisian is better defined by the time of Clark's 1932 survey. Tardenoisian industries were now considered to characteristically feature 'microburins', the resulting debitage from the formation of a notch on a complete bladelet using fine retouch, at which point the bladelet is snapped off at the notch to shorten it for production

into a microlith through further retouching (a process known as the microburin technique). The tip or the base of the bladelet can be removed in this way, although most commonly of the two it will be the base with the bulb of percussion of the original blank that is removed. Other characteristic features of the Tardenoisian outlined by Clark included both blunted-backed microliths and then later-date trapeze-shaped microliths, while he described the Azilian as featuring triangular microliths as well as small, round scrapers (flakes or blades blunted to form a thick edge face) and burins (flakes or blades with removals perpendicular to the flat axis of the piece, thus forming a sharp corner on the piece).

Clark also acknowledges the relevance of *tranchet* axes, adzes and picks in Mesolithic assemblage identification. These are tools made on cores, which are shaped and then finished off with a removal transversely across the width to produce a sharp edge at one or both ends. Sarauw had excavated the site of Maglemose, western Zealand, Denmark in 1900 (Sarauw 1903 as cited in Clark 1932). This would become the type site for another Mesolithic cultural classification, the Maglemosian, which Clark claimed exhibits influence in British classifications where tranchet tools featured in the blade industry in combination with a microlith and bone tool tradition. Clark claims influences from this culture likely originated as derivative from eastern European Upper Palaeolithic trends and reached the east and south-east British coast where the tranchet axe is common (Clark 1932, 9). Based on this, he considered south-east England culturally distinct from the rest of Britain where tranchet tools were rare. As such, we start to see the earliest attempts to tease apart the microlithic cultures into further subgroups, in association with other tool types.

2.3.2 Developing typologies and the earliest identification of a British Mesolithic microlithic culture (basally modified Horsham)

After the 1932 survey publication, Clark's focus was then drawn to Honywood's collections from Horsham, whose work had been continued by local enthusiasts Attree and Piffard in the intervening years, and from whom Clark took over (Clark 1933). He places these microlithic assemblages within the Tardenoisian tradition but also designates them as being part of a "Horsham" microlithic culture, after the market town around which most of the sites had been identified (1933, 52). Clark discusses the distribution geographically of the culture and goes into detail about the relevant typological details, seemingly very much a product of the culture-historical approach (1933, 71). Clark further refines his definition of a microlith here to include both retouch and removal of the original bulb of percussion from the blade on which the microlith is formed.

One of the pivotal concepts to come out of this work was Clark's standardised classification of microlith forms which was the first to be developed for this material. Although designed

to facilitate recording of the Horsham sites "accurately and objectively" (1933, p.55), he widened his system to include all common British microlith types known at the time. He acknowledges that the system is incomplete and explicitly argues for other researchers to use this classification system as a foundation to build further detail on, "as by this means alone can we have an objective basis for comparison" (*ibid*.). This classification system is illustrated in Figure 9. On the one hand, the classification system produced a standardised system to be applied to lithic assemblages which would theoretically facilitate easier comparison between sites (and indeed researchers that later adopted the system were able to do this). The classifications are effectively a shorthand based on the morphological description of the pieces which should make the definitions clear, objective and simple to apply.

However, there are issues with this system. First and foremost, while many of these classifications can be drawn, there would not seemingly be a practical difference in the skill required for their manufacture or application in a composite tool except perhaps in terms of the handedness of individual users. For example, a type A1a microlith would probably not be hafted significantly differently to a type A1c microlith: These are obliquely blunted forms, the former with the left edge blunted, the latter with the right edge blunted. This creates an artificial sense of separation between similar types of artefact. Even artefact forms in different primary categories (type A, B, C etc.) can physically be very similar and in fact sometimes the category to place an artefact into is sometimes unclear (consider the similarity of types C2b and F2a). In these cases, there may be artificial over or under counting of certain artefact types in comparing the work by researchers who may be internally consistent in their own classifications but varying from other researchers. As a result, the interpreted cultural groupings based on the proportions of different artefact types will also be affected. Also, if we treat the classification system merely as a shorthand method of describing lithics then it introduces the problem that it will be much more easily accessible for lithic specialists than general archaeologists if used heavily in publications. To be accessible for the non-lithic specialist reader, the shorthand transcription has to be explained and decoded again.

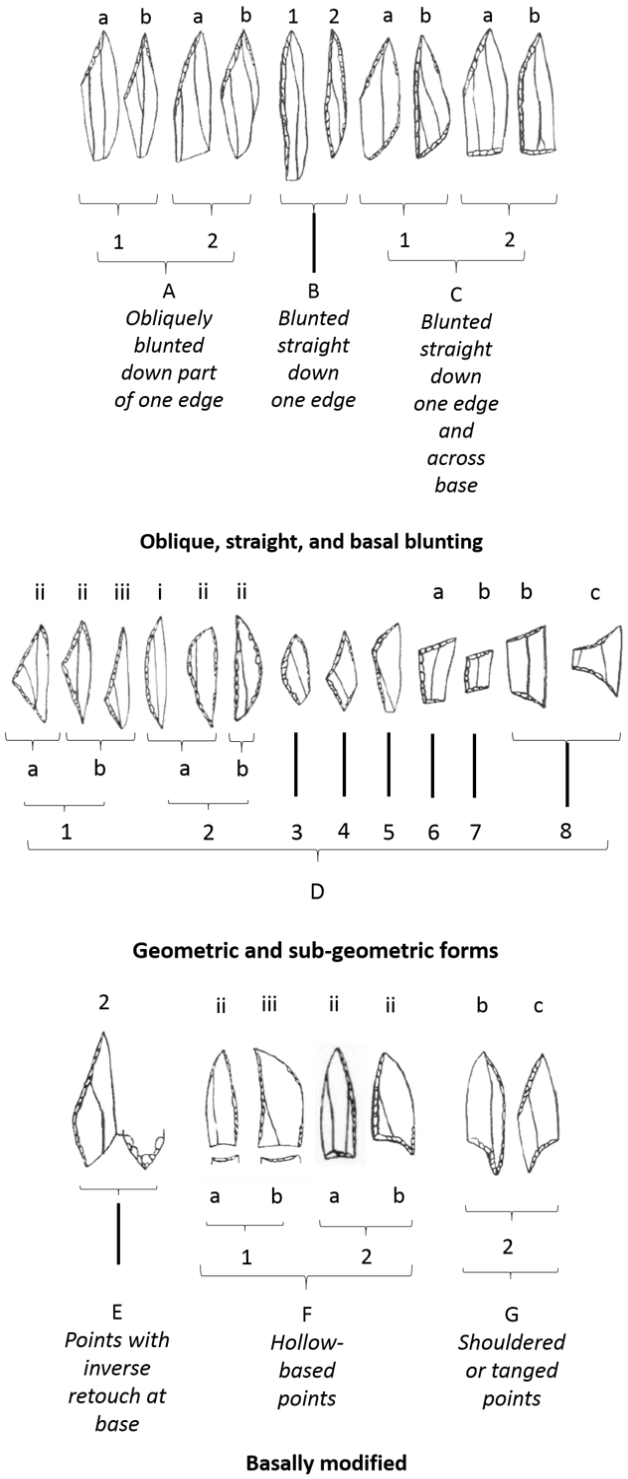

Figure 9. Clark's microlith classifications, showing examples of all major types (A - G). For the geometric forms i.e. type D microliths, subtype 1 are triangles, 2 crescent, 3 lozenge, 4 lanceolate, 5 sub-triangular, 6 trapezoid, 7 rhomboid, 8 trapeze (after Clark 1933, 56–60). Not to scale.

Setting these issues aside, in applying his standardised classification system, Clark produces tallies, percentages and illustrated "spectra" for individual sites or collective averages (see Figure 10). From this, he suggests the microlithic composition of the general typical composition of Horsham Tardenoisian assemblages. While still utilising typology to identify

cultural distinction, in employing a standardised classification system and basic statistical analyses, Clark made steps towards a more objective methodology with an emphasis on empirical evidence to formally support his arguments. This methodology would set the precedent for much lithics work in future decades.

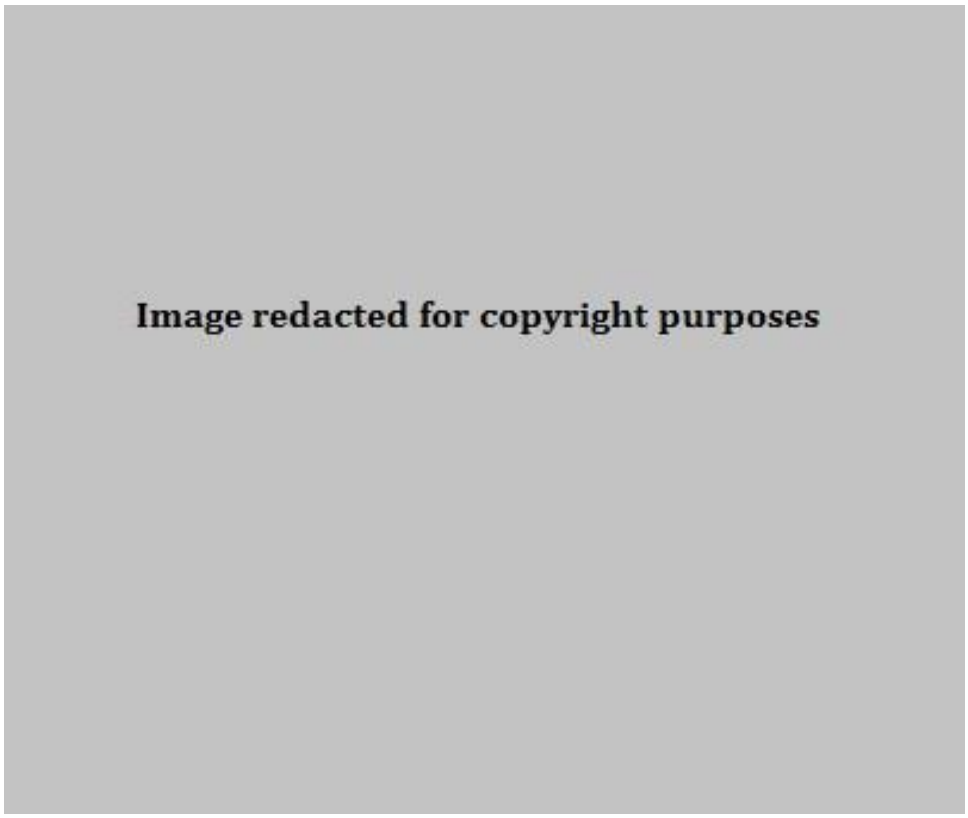

Figure 10. Clark's Microlithic 'spectra' (reproduced from Clark 1933, p.64)

This methodological approach also emphasises the importance of microliths in the definition of cultural distinctions. It also places their analysis largely in isolation from their context both geographically and within the broader technological assemblage they are part of: Sites are characterised by the proportion of different microlith types and classified into a culture type, there is no consideration of the variability of why certain tools were being made on different sites. It is implicitly assumed that cultural variation between social groups will override inter-site, contextually-induced variation. Clark's definition of the Horsham Tardenoisian in this paper is therefore dependent on his identification of a pattern in these sites without considering the context of deposition. As such, his proportional representations are objectively outlined and from this he assumes separate cultural groupings. Clark's classification system shows signs of being founded on the implicit assumption that the more complex forms are evolved from, and therefore later than, the simpler forms. This is a product of its time, when ideas of biological and then social evolution were coming into play on all interpretative levels in academic disciplines. Setting these issues aside, Clark characterises the Horsham culture as being identifiable by: large numbers of the simplest forms of microliths, namely his type A (obliquely blunted), type B

(blunted straight down one edge), and type C (blunted down one edge and across the base); high proportions of triangular microliths which are usually large and irregular; a degree of usually large, irregular crescents; and, most importantly for the Horsham assemblages, a unique and therefore characteristically high proportion of hollow-based (type F) microliths, the majority of which were of asymmetrical form, as well as tanged or shouldered points (type G). This was therefore the first definition of a British Early Mesolithic microlithic culture.

Clark also again refers back to the relevance of microburins and tranchet tools in assemblage classification, and considers the relatively small and unstratified selection retrieved in areas presenting the Tardenoisian Horsham culture. He draws on stratified finds from elsewhere which are not associated with the Horsham-characteristic hollow-based points but where tranchet axes or adzes are found in higher frequencies, suggesting that the "Horsham axes may be due to culture fusion or borrowing" from these other areas and that they are likely contemporary all the same (1933, p.76).

2.3.3 Defining further microlithic cultures (Star Carr and Deepcar)

In Clark's 1932 survey, a number of the sites featured in the North of England had been excavated by Francis Buckley, a well-known local landowner with a passion for archaeology and notably prehistoric lithic artefacts. Despite being self-taught, he became an established, reliable source on the area known for methodical excavation and good stratigraphic recording techniques. During the 1910s and 20s, he had excavated a number of sites in the Marsden area in the Pennine region (Buckley 1921, 1924). These sites were beneath peat, high on the moors, and were often small and well-defined spatially (Buckley 1924). One of these sites, Warcock Hill, was excavated in 1923 and 1924 and yielded some particularly interesting archaeological material. Two flint scatters were excavated here, with one grouping on the southern flank of the hill (usually now termed Warcock Hill North) and the other on a smaller hillock slightly further south still (Warcock Hill South). Buckley retrieved 5240 lithic artefacts from Warcock Hill North in four roughly circular groupings, one of which was filled with burnt flint and a high proportion of charcoal. He retrieved 619 pieces from Warcock Hill South, mainly within an area of 4 sq. yards but with smaller concentrations scattered around. Both assemblages were what he termed "Broad Blade" industries, that were generally larger and often obliquely blunted in some form, in contrast with "Narrow Blade" assemblages which featured small, geometric forms of microliths. However, he made a distinction between the Warcock Hill assemblages based on two attributes. Firstly, leading edge retouch, that is to say retouch down one side of a microlith and then along the edge of the opposite side at the tip, was comparatively rare on the microliths from the southern site. Secondly, the flint appeared to him to be from a different

raw material source being unpatinated, clear, brown or grey flint on the south site, while the north side inhabitants had utilised a generally patinated, grey Lincolnshire flint.

Although Clark (1932) considered these sites, he did not mention the distinction Buckley had drawn between the two areas of Warcock Hill. In 1964, however, Radley and Mellars (1964) recovered the information in their research to establish the typology of their assemblage from Deepcar, Yorkshire. Deepcar is on the edge of the Pennines, at the junction of upland and lowland zones (p.21) and significant reference to this context would be made in their interpretations.

The Deepcar assemblage itself was distinct from most Pennine lithic industries, homogeneous and extensive. In their analysis they found it completely lacked the small, geometric microlith forms such as crescents and trapezoids that characterised those assemblages Buckley had called 'Narrow Blade' industries, and most other known Pennine assemblages. As such, they thought it would prove interesting and useful for typological comparison (Radley and Mellars 1964, 13). Having identified how poorly much work in the Pennines had been carried out, although significant material had been collected, they looked at collections which had been an exception this: Buckley's work in Marsden, located only 17 miles north-west of Deepcar. They re-examined four of Buckley's more abundant, 'Broad Blade' industries for comparison with Deepcar: Warcock Hill South, Warcock Hill North, Lominot 2 and 3 (considered together), and Windy Hill site 3 (*ibid*.).

The Warcock Hill North, Lominot and Windy Hill assemblages were all similarly constituted to Radley and Mellars' Deepcar assemblage and predominantly made of the opaque grey or white flint that Buckley had noted as well. The Lominot sites excavated in 1924 and interpreted to be one collective site divided into two round emplacements were on high ground immediately to the south of an important geometric/Narrow Blade site, March Hill. Windy Hill site 3 is located to the north of the main hill, in a densely distributed assemblage at the summit of a shale spur, and had been excavated by Buckley in 1922.

Radley and Mellars outlined the character of these assemblages utilising Clark's classification system. In terms of the microliths (Radley and Mellars 1964, 9–10 & 15), the industries at Warcock Hill North, Lominot and Windy Hill were dominated by obliquely blunted points, with the retouch usually featuring on the left-hand side. Sometimes these featured additional leading edge retouch and of these a relatively large number of pieces had been initially blunted down the right-hand side instead. Alternatively, fairly frequently, pieces showed blunting down the whole of one side (what would later come to be termed "backed") which were mostly still relatively broad although a few were narrower and more rod like. Rare but still present are also several examples of large isosceles triangles. Figure 11 illustrates the different forms found at Deepcar.

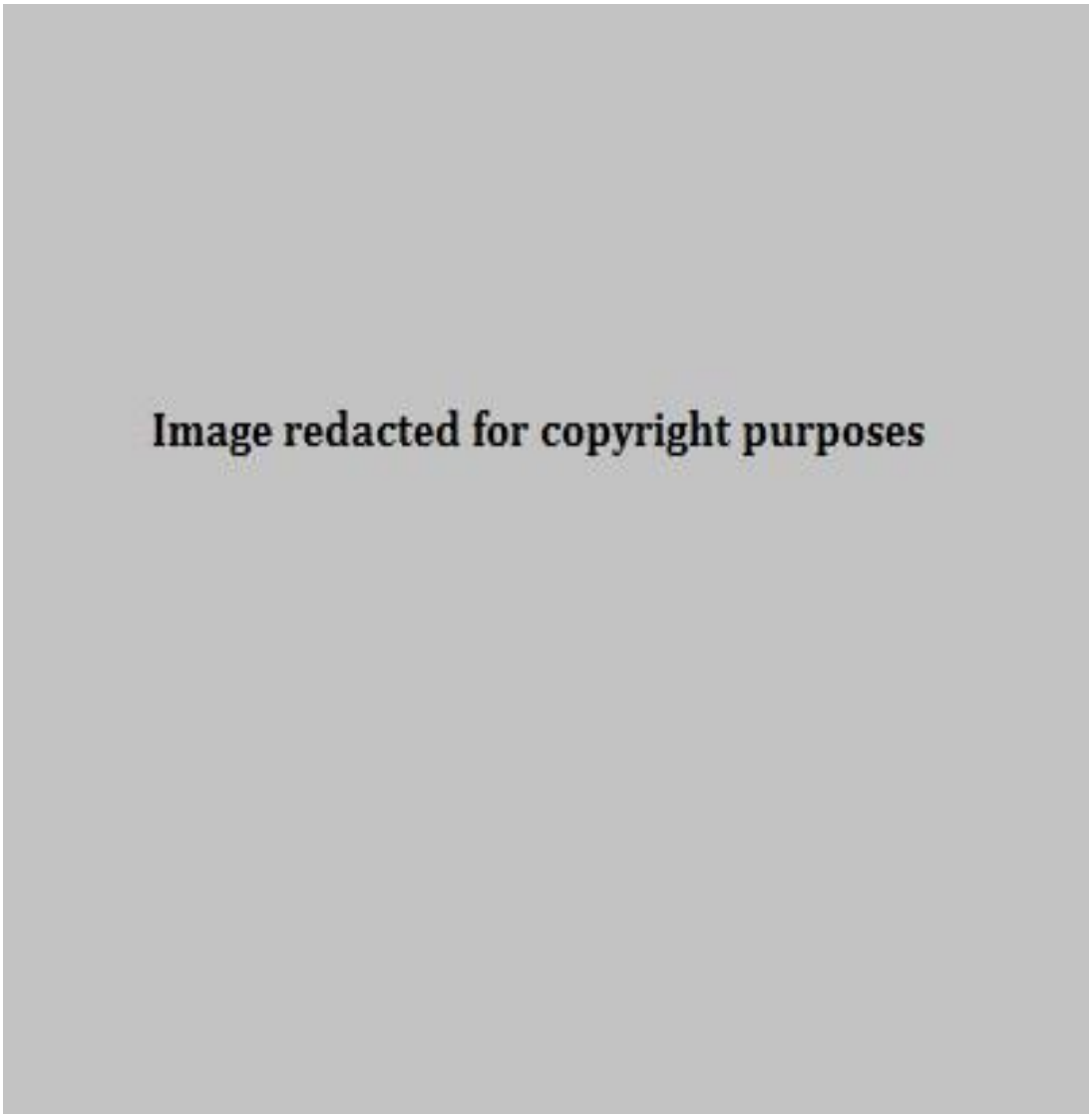

Figure 11. The microlithic industry from Deepcar, Yorkshire (reproduced from Radley and Mellars 1964, p.10, not to scale)

There was a range of similarities in the non-microlithic elements in the assemblages too. The types and balance of microburins, scrapers, burins, cores, truncations, microdenticulates, and utilised debitage at the sites all bore similarities (detailed further in Appendix 1 for reference, and also see glossary for terminology).

Two pieces were categorised by Radley and Mellars as awls although they are quite different from each other (Radley & Mellars 1964, pp.11–12 and see Figure 12). This classification was based on their function rather than morphological similarity, the only commonality being that they had been retouched to produce a point. In this case it can be seen that one artefact is steeply retouched all along its edges so that it comes to a fairly thick point at the tip. The other is neatly retouched with two small, adjacent (opposed) notches to produce a slightly protruding point off the side of the piece. This reflects the important issue with any nomenclature being based on an implicit assumption about use: Objects will not always be categorised separately even if they are significantly different physically and therefore potentially would have a different methodology in the practice of using them.

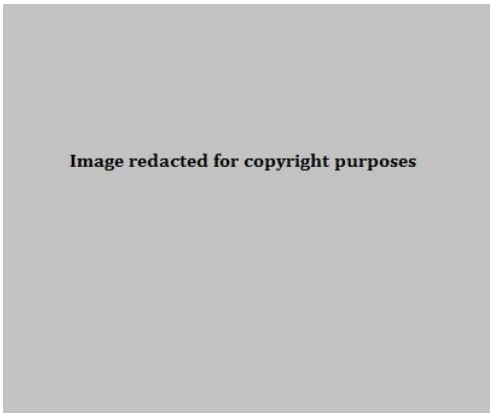

Figure 12. Awls from Deepcar (reproduced from Radley and Mellars 1964, p.17, not to scale).

Deepcar also produced one small possible tranchet axe which had been badly damaged by fire but no resharpening flakes were located implying that axes may not even have been used in the area except in material reuse and no axes or resharpening flakes were found in the other locations (Radley and Mellars 1964, 12 & 18). The main difference between Deepcar and the other sites is that the Marsden sites all feature a very small number of the minute geometric forms heavily utilised in the 'Narrow Blade' industries elsewhere in the Pennines. However, Radley and Mellars do also comment that all of these sites are near true 'Narrow Blade' sites or the geometric microliths in question were found in very discrete areas or higher up in the stratigraphy than the 'Broad Blade' assemblage elements (Radley & Mellars 1964, p.18). This, however, might be taken to suggest that Deepcar and similar sites are perhaps related to Narrow Blade assemblages chronologically and/or typologically; an idea which takes root more firmly in later research on Early Mesolithic typologies.

Through these comparisons, Radley and Mellars would outline the 'Deepcar' assemblage type based on these Pennine assemblages. They expanded their discussion to include excavations in south and east England at Shapwick, Middlezoy, Dozmare Pool, Broxbourne, Colne Valley and Thatcham; all sites considered to be within the similar Maglemosian

tradition (Radley & Mellars 1964, p.19 & 20). Despite the limited size of these assemblages, Radley and Mellars deemed them to also be very similar to the Pennine assemblages with two differences. Firstly, they note that the microlith form with blunting down the full length of both edges is absent on the northern sites but present on most in the south, for which there is no obvious explanation. Secondly, they note that the non-Pennine sites are characterised by tranchet axes, unlike those in the Pennines (*ibid*.). In addition to this, there is the presence of a single Horsham-style (basally modified) point at Thatcham although this was located during fieldwalking of the site and as such was technically unstratified (Wymer & King 1962 as cited in Radley & Mellars 1964). However, Mellars and Radley discuss that this may be an attribute of being a difference between upland and lowland sites, with the latter likely being more heavily wooded and, if an axe/adze is interpreted as being for tree felling then it would be needed more in such a context (1964, 20). They bring in the example of Pike Low as being a Pennine site which also has the markers of a Deepcar-type site but also has a clearly identifiable axe-resharpening flake, as well as two tranchet axes/adzes found through fieldwalking on the moors (Radley and Mellars 1964, 20; but also cf. Davies and Rankine 1960; Radley and Marshall 1963).

Radley and Mellars agreed with Buckley that Warcock Hill South is, however, quite different to Deepcar, Warcock Hill North and the other Pennine 'Broad Blade' sites discussed above. It too lacks the small geometric types, but aside from that "it possesses a number of original features which suggest comparisons with the Star Carr industry… rather than with the southern Maglemosian industries discussed" (Radley and Mellars 1964, 21). From Warcock Hill South, they characterised the microlith industry as being composed almost entirely of broad, obliquely blunted points which are never retouched on the leading edge; no points blunted down the whole of one edge; Warcock Hill South also featured a broad isosceles triangle and a trapeze. In terms of the macrolithic assemblage from Warcock Hill South, Radley and Mellars also drew attention to two "elongated steeply worked awls" (see Figure 13) which in one case in particular is strongly reminiscent of Star Carr's *mèches de foret*. In addition, the grey-white flint characteristically heavily employed at the other Pennine sites is only utilised for 10% of the pieces at Warcock Hill South and the assemblage is mostly made on mottled yellow to black translucent flint or chert. As such, they outlined the Star Carr type assemblage, a second major broad blade type that would be utilised by future researchers.

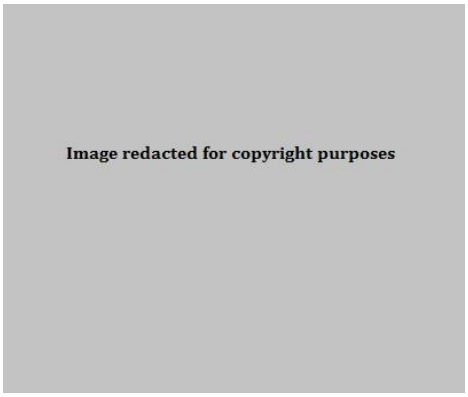

Figure 13. Warcock Hill South's awls (reproduced from Radley and Mellars 1964, p.17, not to scale).

Finally, they go on to tentatively suggest that both of these Broad Blade industries may be of an earlier date than the Narrow Blade industries with geometric microliths from the Pennines. This is based on the connections of the former with Thatcham and Star Carr that at this point had been dated to the Early Mesolithic although, note, this is before calibration was common practice, before there were more stringent sampling criteria expected to be met by dating samples, and they do not quote the dates they base this on. Later consideration by Clark, the radiocarbon date had been exceptionally high and difficult to reconcile with the anticipated forest history of England with the presence of pine at Thatcham (Clark 1972, 10). Despite this, based on more recent dating and Bayesian modelling from other sites, the Broad Blade sites do seem to be of an older date (as discussed below).

2.4 Starting to contextualise the Early Mesolithic cultures

2.4.1 Branching out from typology

As such, the three major assemblage types for the Early Mesolithic were first characterised largely based on differences in the microlithic components of assemblages, and later literature would name these groupings after their type sites of Star Carr, Deepcar, and Horsham. These typological definitions were developed during a time in archaeology where seriation was starting to be married with not only more traditional stratigraphic relative dating but also utilising pollen and the earliest radiocarbon dating, as Radley and Mellars did in the Deepcar discussion (1964). However, there was an apparent scarcity of viable preserved material and funding available for these forms of dating and by the time of Roger Jacobi's paper *Aspects of the "Mesolithic Age" in Great Britain* (1973), which would effectively be an update to Clark's *Mesolithic Age in Britain* (1932) and compile the known dates, few additional sites had been dated by these new means and in fact the main sources of dating on the Mesolithic had actually continued to be the classification of the stone industries and consideration of their distributions (Jacobi 1973, 237). However, more nuanced approaches

to lithics did develop in terms of an early consideration of their functionality and research developing the understanding of different types of sites based on both the cultures and the balance of the artefact types present.

2.4.2 Functional approaches to assemblages

Clark would go on to become best known for his work at Star Carr. He was approached through a museum contact by John Moore, who had by this time identified (through fieldwalking, excavations and augering) many sites around the Vale of Pickering and delineated the shores of the extensive palaeolake Flixton. The peat formation promised good conditions for organic preservation and Moore's Site 4 (Star Carr) had already yielded faunal remains from an exploratory cut. Clark took over the excavations of Star Carr and several sites in the Vale, while Moore continued in charge of others including Flixton Island 1 and 2. The first monograph published on Star Carr also included the short report of Moore's findings from his excavations at Flixton Island 2, but little detail was recorded except that "a scatter of Mesolithic flints" and then from the Long Blade layers "a small blade of flint without secondary working, and a shouldered point of microlithic size with steep, almost vertical secondary working" were found (Moore 1954, 192).

Clark's preliminary examination of the flint industry at Star Carr suggested it was related to the Maglemosian-type cultures, complete with tranchet adzes and their characteristic resharpening flakes (Clark 1954, xviii). Looking in further detail at the lithic industry comprising of 16,937 artefacts, he provides the now-usual summary statistics of the different artefact types represented, using his classification system. Instead of only separating them by type, he separates them into "waste", "utilized" and "finished" forms as well as discussing aspects of techniques of manufacture represented (pp.96–97). This reflects a concern for the technological understanding of assemblages, the basic *chaîne opératoire*, which would develop within British lithic studies in later decades. As part of this, he considers the inter-relatedness of certain artefacts (p.97). He identifies that the microburin technique was deployed at least to some extent in the production of microlith blanks which were then given final modifications and shaping with very steep, blunting retouch. This form of retouch was also utilised on other tool types to produce awls or for backing or truncating larger tools, while some of the flakes and blades were also burinated to provide fresh, sharp edges (p.98). In terms of the axe and adze type core tools identified, these were sharpened with transversely struck flakes in the tranchet style (p.98).

When discussing individual tool types, Clark also considers how they may fit into the broader technological scheme for the site. He identifies microburins, axe/adze resharpening flakes and also potential "core-rejuvenation" flakes (1954, 100). Yet again,

Clark demonstrates thinking through the processes of knapping and the methods of maximising the use of raw materials in identifying these knapping by-product artefacts. He also discusses primary flakes without secondary working or use wear as potentially having uses but he goes on to say that it is likely that they mostly represent knapping debitage within the whole assemblage (p.98). This is an interpretation that would later be challenged by microwear studies at Star Carr and elsewhere (Conneller et al. 2018). Gero (1991) would also argue more broadly that such an attitude is part of a reflection of an academic fixation on the formal, literally considered to be 'man' made tools over expedient ones that were considered to be in the realm of women's use and making (she also quotes, p.163, a rebuttal from a reviewer in 1988 saying that there was little evidence to suggest that lithic production was anything but a male activity). Regardless of the reasons, it reflects a dismissal of these, admittedly more difficult to identify and therefore more subjectively defined, tools that can make up significant proportions of an assemblage.

During the excavation season of 1950, Clark's team retrieved an elongated trapeze type microlith with "resin mounting" still adhering to the retouched edge (Clark 1954, 102). He compares this with two Star Carr barbed points with traces of a similar substance adhering to their tangs, an earlier find from Danish Klosterlund similar to the Star Carr microlith, and Swedish bog site of Lilla Loshult where a wooden shaft suitable for use for an arrow with microliths mounted in series utilising a similarly resinous substance had been found (pp.103 & 167, see also Figure 14). Along with the retrieval of several thin flat cakes of a similarly resinous substance which was visually identified as a likely wood-pitch or natural resin during the 1951 excavations, Clark touches on the potential for composite technologies on the site utilising the lithic assemblage (p.167).

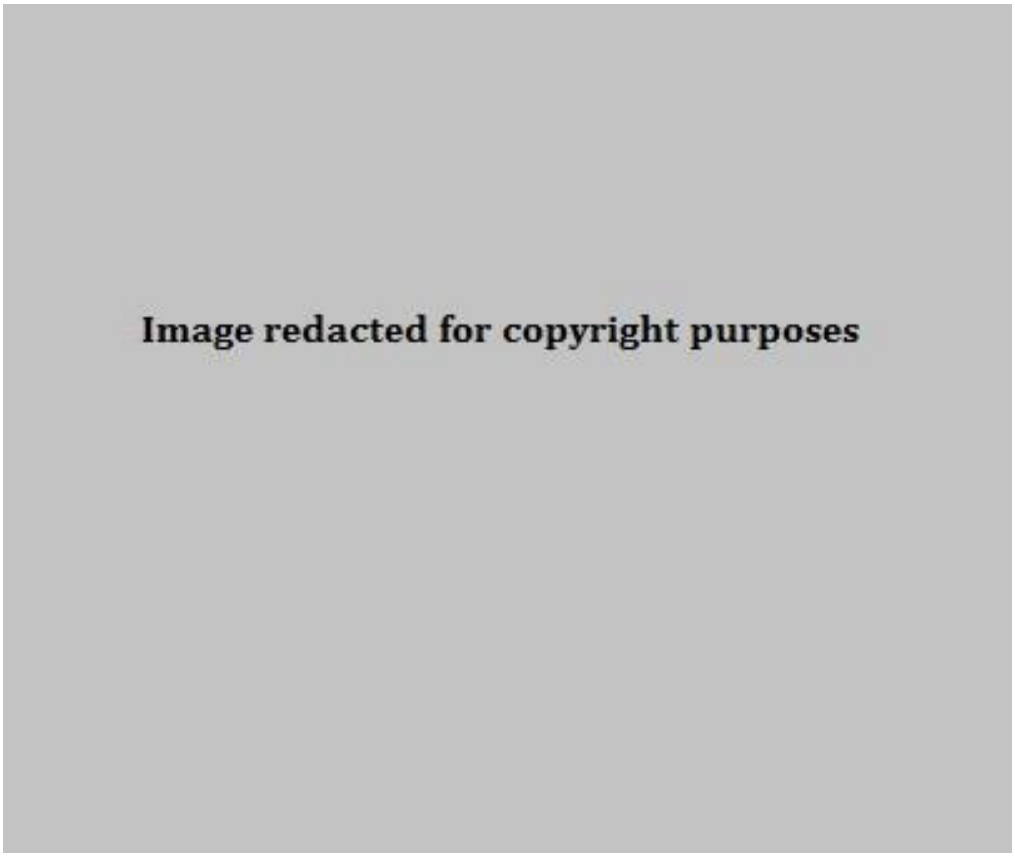

Figure 14. The Loshult arrow (photograph by Arne Sjöström, reproduced from Larsson and Sjöström 2011a).

Taking this technological analysis further, it is also evident that Clark starts to bring in functional interpretations of the lithic assemblage as well, particularly for the 'finished' tool types. Considering the Star Carr assemblage and other Maglemosian-type collections in the light of the Loshult find, which had exhibited a microlith hafted as a piercing tip and another acting as a barb on the side, Clark argues that microlith types could be divided into two groups: tips for which triangles, elongated trapezes, rhomboids and tanged microliths were most suited based on their morphology, and barbs made out of the obliquely blunted pieces which made up just over half of the Star Carr microlith collection (Clark 1954, pp.102 – 103). In considering the use of the microliths in a hunting technology, Clark is effectively making a functional interpretation as well as a technological one. However, in a microwear study of Mesolithic microliths from the site of Verrebroek in Belgium compared with experimental materials, Crombé et al. (2001) suggested the opposite: non-geometric (which would include obliquely blunted) microliths were likely used as tips and geometric microliths mainly used as barbs if the microwear was correctly interpreted. This really illustrates the risk of assuming use based on modern logic: it is not always possible to do deeper scientific analyses, but it is a trap to fall into making assumptions about use that have not been tested. Clark discusses the use-wear on certain pieces although he is not explicit about the methods used for this such as details of magnification and so on. He considers what uses the tools exhibiting use-wear may have been put to, in terms of what materials they may have been

used on, though this is again largely speculative. There are exceptions, however, such as the identification of a form of polish resulting from working bone which had been seen in experimental reconstructions by another researcher, one Dr. Curwen (Clark 1954, 114).

Clark also looks into functional interpretation at the site level, which he derived from the assemblage. He considers what technology is being produced on site or likely brought onto site by considering the debitage his team retrieved. For example, he discusses the scarcity of microburins perhaps suggesting that microliths on site are knapped elsewhere (Clark 1954, 103). He also illustrates that they had been able to identify some example series of refitting spalls and flakes with their original core which he interpreted to suggest flint knapping was being carried out on site (p.97).

Clark goes into description of the colour, patination and possible sourcing of the raw lithic materials, including discussion of underlying geology and the influence of deposition soils on patination (Clark 1954, p.97). This reflects a growing awareness of situating artefacts within their extra-site context of the wider landscape and environment, in keeping with Clark's general objectives for the site and his research at the time.

Between Star Carr's outstanding preservation for a British Mesolithic site and Clark's implementation of these new approaches to the material, the work here would set an enigmatic precedent for much future work on the British Mesolithic generally. Regardless of these innovative approaches to lithic analysis, analysis of the rarely abundant elsewhere faunal remains, including the curious red deer frontlets, was what really attracted the attention of researchers and as a result over the following few decades, much research centred around these elements both on the Star Carr assemblage and on work at other sites (cf. Noe-Nygaard 1975, 1977; Wheeler 1978; Pitts 1979; Noe-Nygaard 1983; Legge and Rowley-Conwy 1988). Lithic analysis, being entrenched in typology, was readily associated with culture-historical methods which were to be heavily critiqued under the New Archaeology and then Processual schools of thought. Lithic typological analysis was shifting from being the highlight of Mesolithic research to being a necessary but, in general perceptions, less inspiring or attractive aspect of research.

In 1962, Wymer and King published their report on recent excavations of further Maglemosian sites at Thatcham, building on Crawford and Peake's work in the 1920s (Peake 1922; Crawford 1922; Wymer and King 1962). This site forms an interesting comparison from the south of England to Flixton Island 2 and 1, Deepcar and Star Carr. Wymer mentions at least 10 sites previously known in the local area between Thatcham and the adjacent town of Newbury producing Maglemosian flint assemblages and establishing the region as another key area yielding Mesolithic sites. Being within a river valley, the area was also protected with deposits of peat that would potentially yield preserved organic material. The

sites were under risk of destruction by gravel-working, several being on a utilised gravel terrace north-east of the Moor Brook, with the intervening area being peaty reed swamp. Wymer excavated for four full-time seasons of excavation from 1958 to 1961 uncovering a sequence of five sites, Thatcham I to V.

Wymer had been awarded a grant to build a coffer dam which would facilitate excavating into the adjacent wetland deposits in 1961 (Wymer and King 1962, 332). The result was the uncovering of Thatcham site III in a depression between Wymer's sites I and II which were located on rises in the gravel terrace. The depression had been assumed to be a swamp in Mesolithic times and therefore not considered for excavation initially, but which actually emerged as the most productive area in the sequence excavated. Wymer considered the flintwork to reflect one industry although the stratigraphic sequence was unclear. The land surface they were mostly located on was operative from the Pre-Boreal to the beginning of the Atlantic according to pollen analyses from the silted-up lake marls and as such could date from any point within that time. Unfortunately the radiocarbon dating program needed to resolve the sequencing clearly was beyond the funds of the project (pp.335 & 337). They did however obtain some radiocarbon dates on charcoal which would suggest general contemporaneity with Star Carr at 9950 uncalibrated years BP (8000 uncal. BC) (p.337) and comparisons between the two sites would feature heavily throughout Wymer's publication. However, it should be noted that pine was well preserved on the site, and in Clark's 1972 publication which would revisit Star Carr and draw comparisons with new Maglemosian finds in England, he comments on the fact that the early date does not sit well with the understanding of how forest types had developed in postglacial Britain (1972, 10). With further dates, appropriately calibrated and modelled, it would later be considered that the Thatcham sites were occupied over a longer duration (Conneller et al. 2016) than Wymer and King anticipated.

Wymer considers the raw materials utilised on the site, commenting that a wide variety of flint colours and qualities were utilised which he assumes to be most likely gathered from the gravel beach of what had been the adjacent lake in Mesolithic times around which the reed swamp had by this time formed (Wymer and King 1962, 336 & 338). Typical of gravel flint, Wymer notes it was frequently internally cracked by movement or frost and several of the cores found had been abandoned because of these issues (p.338). Other flint had been sourced as nodules in chalk deposits, likely outcrops on the Hampshire Downs that were only six miles from the site (p.338). In addition to flint, one artefact knapped from quartzite was identified (p.338). For the most part the flint was unpatinated with the exception of the material from site III which was, in contrast, mostly patinated although Wymer could not suggest a reason for this. As this site was clearly too densely packed with lithic finds for it to be a single occupation, with one square yard yielding up to 764 flint artefacts, Wymer

could not use this for chronological distinction across the scatter of sites (Wymer and King 1962, 333, 335 & 338). This concern with the processes of material sourcing and abandonment demonstrates the growing awareness of the life cycle of lithic artefacts which came with the contextualisation needed for functional-processual interpretations. Wymer also discusses the site's evidence for other possible knapping techniques as well as the potential for refitting research to be conducted as numerous sequences had already managed to be reconstructed (p.338).

In terms of considering the balance between 'waste' and 'finished' forms, Thatcham's proportions are similar to those of Star Carr with 96.5% of the assemblage being waste compared with Star Carr's 92.8%. Waste here includes primary flakes (those first removed from a core so that one side is entirely covered in the nodule cortex), blade-like longer inner flakes, cores, core rejuvenation flakes, microburins and axe sharpening flakes, as with Clark's statistics. However, Wymer does go on to discuss the fact that at Thatcham the primary and blade-like flakes frequently show use wear in the form of "minute chipping or serration along an edge, or a faint lustre" and should not be regarded as "mere waste" (Wymer and King 1962, 339), as well as other specimens that look as though the edges have been ground smooth that were possibly used for scraping bone (p.350). He notes that many of these could have been hafted as knives without additional retouch, while the standard classification of formal 'knives' involved their being retouched into the appropriate form, highlighting again this issue with the interpretative terminology. In addition, at the end of his summary of the lithic industry he tallies up backed and trimmed flaked and blades into categories of the tools they resemble, such as 23 with a "scraper-like edge" (p.351). One flake has a possible adhesive attached to it which Wymer lists as a possible resin although he does not go into as much detail about the potential for composite technologies as Clark.

Wymer utilises Clark's typological classification system in his analysis. In terms of the microlithic typology of the site, the majority were obliquely blunted points forming 187 out of the 285 microlith assemblage (Wymer and King 1962, 342). Figure 15 illustrates the Thatcham microlith assemblage. Interestingly, he also comments on the influence of the shape of the initial blade on the final microliths and argues that the blank forms must have been selected accordingly which is an aspect of microlith assemblages that is rarely considered (p.342). There are not significant numbers of other microlith types, with a maximum number of ten oblique points with "retouch on the opposite side with a trimmed base" (p.342). There are also six sub-triangles, 6 sub-crescents, 4 tanged points, 4 rod-like, 3 isosceles triangles, 4 crescents, 2 elongated trapezes, 1 lozenge, 1 possible trapezoid, and 1 Horsham point that was raised earlier. There are also 69 microburins and an additional three unsnapped bladelets with notches in ready for burination, including one that has been notched at the distal end rather than the usual proximal.

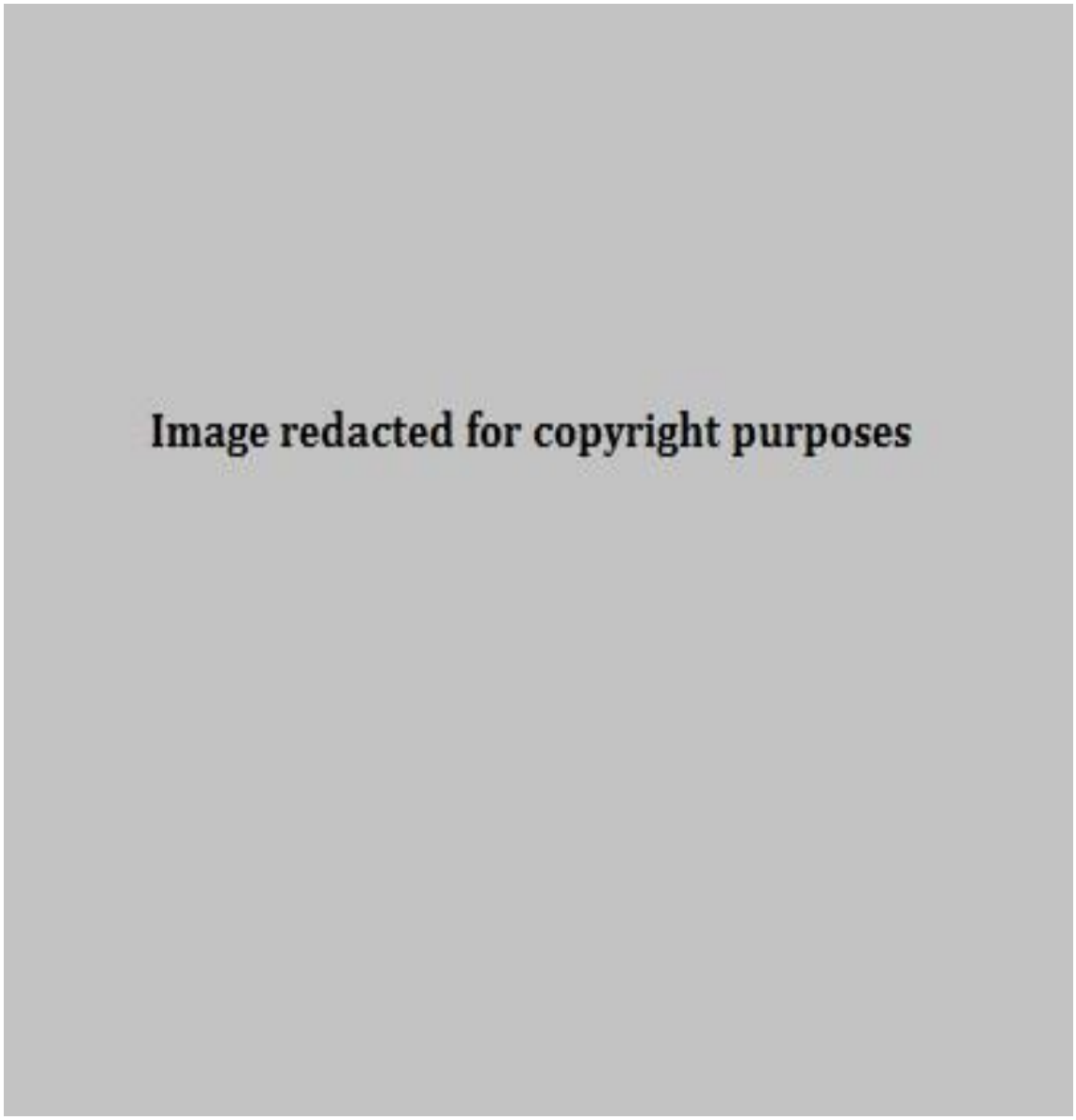

Figure 15. Microliths and microburins from Thatcham (reproduced from Wymer & King 1962, p.342)

In terms of the macrolithic nature of the site, cores were usually two platformed (155 examples retrieved) or, less frequently, single-platformed (n = 100) (Wymer and King 1962, 340). The Thatcham occupants had abandoned several cores without apparent reason fairly early on in their use life, yet excavators also found 129 rejuvenation flakes some of which belong to cores which are not discarded on-site but do refit with each other and therefore were off the same original core (p.340). Wymer uses this to discuss mobility of material to or from the site and the fact that this probably reflects partially on the ready proximity of the flint source that was the local beach, illustrating the inception of ideas of movement across the landscape which would be taken on much further by later researchers such as Chantal Conneller.

Wymer takes the consideration of the life cycle of lithic artefacts even further. Some cores looked to be retouched into scrapers and one was also used as a hammerstone, as deduced from the usewear on the apex (Wymer and King 1962, 340). In addition, five of the rejuvenation flakes showed general secondary working while several were made into burins (under 'gravers') (p.340). Of the gravers, most are transverse angle gravers (totalling 25) but there are also relatively high numbers of both simple (13) and oblique angle burins (19) with an additional 4 core burins, as well as eight of the spalls (Wymer and King 1962, 346 & 348). The fact that one burin spall refit was found and that burin had been further modified after the original burin modification, which was interpreted as suggesting the piece was fabricated and then used on site (p.348). There are 10 core tranchet axes or adzes from the site including one with a cutting edge showing characteristic bruising of use and one with two refitting sharpening flakes out of the sixteen of those found (p.344). Of the scrapers, the majority were retouched into curved end scrapers, with straight end scrapers and side scrapers being uncommon as well as very few hollow scrapers and again Wymer comments on how several unretouched implements could perform the functions envisaged for these scrapers however (p.348). Of the rarer forms found on site, there were 15 awls and piercers, with no *mèches de foret,* present along with 19 microdenticulates and 8 punches (p.350). In addition, the excavators retrieved two sarson stone hammerstones as well as three pieces of flint showing flaking and battering consistent with being used as a hammerstone (*ibid*.). As such, Wymer pays a significant attention to the detail of cataloguing and classification of the lithic artefacts as well as the consideration of their interrelatedness and potential functional interpretations throughout the publication on Thatcham.

2.4.3 Early dating of Mesolithic cultures and exploring seasonality

Roger Jacobi would come to the forefront of the debates concerning Mesolithic research. In the early 1970s, he started to bring in cluster analysis to test the strengths of lithic type classifications as well as publishing the first full synthesis of radiocarbon dates associated with those different classifications. He published prolifically and was a phenomenal synthesist of data so it is not possible to cover all of his work here or bring out all the nuances he draws upon, but a series of seminal papers in the early to mid-seventies would build upon key ideas from Radley and Mellars' discussions at Deepcar as well as much of Clark's work.

Jacobi's 1973 text produced the first complete list of all British Mesolithic industries that had been dated either by pollen analysis or radiocarbon dating (Jacobi 1973, 238 & 261). Jacobi argues that the sites can be divided into two categories dividing at around 6500 uncal. bc (Jacobi 1973, 238). While Jacobi provides the radiocarbon dates' errors (to 1 s.d.), he does not present calibrated dates; Suess had only published the first calibration curve in

1967 and regular calibration was not a common feature of publications. The earlier sites are characterised by a more restricted range of microliths forms, namely: obliquely blunted points; points with convex blunting all along one edge or both; either the aforementioned were occasionally found with with leading edge retouch; the only supplementary geometric forms being isosceles triangles or trapezes in very small numbers (1973, 238 & 239). They were 8-12mm wide and 50mm at fullest length in the sites he surveyed. These summarised the earlier dated assemblages, which he would therefore label them 'Early Mesolithic' assemblages. In his 1973 paper, Jacobi associates these very generally with the European 'Maglemose' culture, but in his 1976 paper he goes into this in much greater detail and specifically associates Star Carr, Warcock Hill South, Flixton Island 1 and other British sites which also fits into the Star Carr assemblage type mould, with the European 'Duvensee' industries. In a paper in 1978, focusing on British Mesolithic sites from the eighth millennium bc (i.e. still using uncalibrated dates) he would acknowledge Radley and Mellars' work to date and that he had confirmed the stylistic clusters using statistical analysis, and he would then go on to place both Star Carr and Deepcar type assemblages within this grouping (Jacobi 1978a). The definition between the two Early Mesolithic groups would be how Star Carr type sites never featured leading edge retouch, the only geometrics present there were large isosceles triangles and trapezes, and the mix of better quality translucent flint (Jacobi 1978a, 305).

The Early Mesolithic microlith forms are not exclusive to these earlier assemblages but would also feature in the post-6500 uncal. bc assemblages, heavily supplemented with narrow geometric forms with a mean width of 6 mm (Jacobi 1973, 239). As such, the radiocarbon dates, albeit uncalibrated, broadly supported Buckley's divisions of Early British Mesolithic lithic assemblages into Broad Blade and Narrow Blade industries. These were points with straight retouch along one or, less commonly, two sides; small scalene triangles (micro-triangles, ranging up to 7 mm wide, as he would later define them in 1978); rhomboids; occasional rectangles; occasional micro-crescents; and an appearance of points with bases retouched into a point, curve or hollow using inverse retouch, such as the Horsham point. Stratigraphy at the sites of Broxbourne, Wawcott, Fawke Common, Lackford Heath, Colne Valley sites also supported this sequential ordering (Jacobi 1973, 238). Despite putting the basally modified microliths into this category, he mentions that Horsham, in particular, may actually represent the bridge between the Early and Later Mesolithic (Jacobi 1978a, 239). He also defines a slightly separate Latest Mesolithic group, based on a dominance of rhomboids in much later assemblages (Jacobi 1976, 75). He adds strength to all of these arguments by successfully drawing parallels with many of the European sites throughout his texts as well as drawing in new data over time. As such, his sample size is more convincing than Radley and Mellars and he does build a convincing case. In his 1978

paper, he also considers the role of the broader tool set and argues that sites such as Pointed Stone 2 and 3 are the upland, hunting site equivalents of the Star Carr type sites as they have similar microliths but in contrast their assemblages are mostly made up of these, while the Star Carr base camps have a dominance of scrapers and burins assumed to be for hideworking (Jacobi 1978a, 315).

He also developed an updated classification system for microlith analysis during his PhD research which he did not formally publish until 1976. This typology is a simpler system, with 13 classes of individual artefacts divided amongst four groups for microliths and bladelets. This classification system is summarised in Figure 16. The four groups are partially based on Buckley in that the first two are 'Broad Blade' and 'Narrow Blade' microliths. Then the last additional two groups are 'Hollow Based' microliths and then 'Inversely Retouched' bladelets.

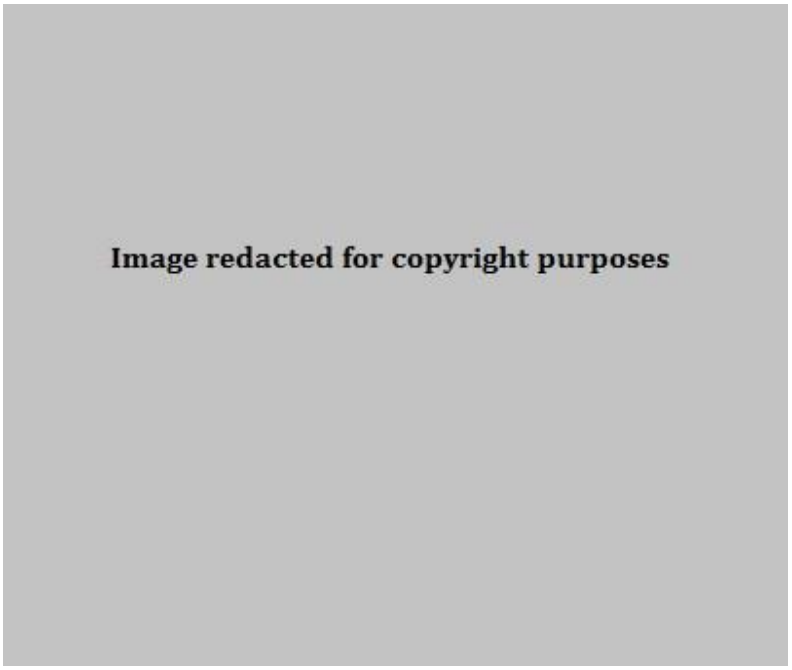

Figure 16. Jacobi's microlith classification system here based on examples from Mesolithic Wealden. (1-4) Broad blade microliths; (5-9) Narrow Blade microliths; (10) Hollow-based points; (11-13) Inversely retouched points (reproduced from Jacobi 1978b, 16)

It is evident that Jacobi's classifications stemmed out of a functional-processual approach to Mesolithic lithics, such as his association of scrapers with hideworking. While logical, there are certainly some major implicit assumptions in this potential interpretation. However, the very fact that Jacobi was willing to consider these alternatives is quite significant as it had often been implicitly assumed that the typological groupings of Star Carr, Deepcar and Horsham assemblages reflected socio-cultural groupings, with the cultural identity overruling fluctuations in site function or other aspects of a site that may influence the typology presented. That is not to say that the cultural typological groupings do not necessarily play the dominant role in a culture presented on sites but rather that it is problematic if they are assumed to do so without deeper consideration.

Environmental context and economic interpretations are heavily emphasised in archaeological functional-processual research. This suited the broader aims of the movement as a source of furthering archaeological information within a clear scientific framework, for example considering the construction of pollen diagrams, and contextualising artefacts within a functional framework as opposed to considering them in isolation. This was largely following the precedent set by Clark at Star Carr in both the original 1954 publication and a later monograph reconsidering the bioarchaeological information available for economic interpretation at the site published in 1972 (Clark 1972). This latter monograph had placed greater emphasis on the organic (particularly faunal) remains with barely a mention of the lithic assemblage except for spatial extent but within this, his interpretations turned further to the themes listed above. Sites are considered to be in lowland or upland contexts, seasonal base camps or hunting camps, set within territories of resource catchment exploitation and representing groups of a certain population or unit size. This is also reflected in Jacobi's works (e.g. 1973, 242–243). This would have appealed to the functional-processual movement fully underway by this time in archaeology in its utilisation of new scientific and computing methods, drawing on ethnographic analogy and attempting to explain the site in relation to its environmental context. However, generally this approach to Mesolithic sites de-emphasised the role lithic assemblages could play in developing deeper interpretations.

Mellars would continue the functional-processual trend in an active reinterpretation of British Mesolithic assemblages "not from the view-point of 'cultural' or chronological variations but rather in terms of the varying activities undertaken at the different sites" (1976, 375). His aim in this paper was to generate explicit models which could be tested and modified with new evidence over time, very much in keeping with the attempted integration of scientific method into archaeology and the social sciences more broadly. One refreshing novelty about Mellars' approach here is that he acknowledges the research overemphasis on use of land fauna and brings back into consideration the role of plant and coastal resources in hunter-gatherer diets, utilising ethnography for inspiration (*ibid*.). However, he points out that organic remains are usually absent from British Mesolithic sites and while interpreting artefact distributions can be more difficult than interpreting defined living areas, they are certainly viable sources of information from which social inferences can be drawn if the recording of the scatters is accurate, citing Flixton Island 1, Deepcar and Star Carr amongst good examples of this (Mellars 1976, 377).

Mellars starts his evaluation by comparing the area of distribution of retouched tools with the distributions of knapping debris, and found the distributions to be similar (Mellars 1976, 377). From this, Mellars argues that the overall distribution of artefacts in fact represents the usually inhabited base domestic living area. In addition, he compares artefact

scatters with understood structural feature plans where possible, such as Star Carr, and argues there is close agreement between the two (Mellars 1976, 377). Therefore, he argues, artefact scatters may well reflect unidentified structural arrangements on a site that are not reflected in the preservation by other means.

In order to proceed, Mellars also has to consider the occupation frequency of the site: whether it was used once or on repeated occasions. Some British Mesolithic sites, such as Oakhangar VII, had been interpreted as being palimpsests of reoccupation on more than one occasion and as such rather than representing the deposits from one large social group it actually could potentially reflect multiple smaller units (Mellars 1976, 378). Mellars argues that a more sharply defined spatial distribution should be considered, logically, more likely indicative of a single episode of occupation while more diffuse patterning would suggest repeated reoccupation. While logical, this does seem an oversimplified assumption to make and even considering Mellars' warnings to proceed with caution, he does not cite ethnographic or other analogies to support his argument, let alone archaeological examples from better defined archaeological sites.

Based on the combined lithic spatial distributions and structural features on a subgroup of the sites, Mellars estimated the total surface areas of the occupied sites. From this he divided them into three types of site which would provide an alternative differentiation between sites to the typological classifications still predominantly based on the lithic assemblages: type 1 sites occupy a very restricted area (10 – 15m^2 maximum) and Mellars suggests that these were inhabited by very small numbers of people for short periods of time; type 2 were settlements significantly bigger than type 1 sites (44 – 210m^2) with artefacts distributed uniformly over a regular, well-defined area and he therefore suggests occupation by significantly larger residential groups; type 3 were sites covering an area similarly sized or much larger than type 2 sites with a tendency to concentrate at several points within that area and at some sites, such as Farnham, comparable with a series of type 1 sites and appearing to be "multi-focus" (Mellars 1976, 379). In the three examples of type 3 sites, Mellars highlights that the remains of structures and from these suggests occupation of small social units although it is unclear how many of the small dwellings would be occupied at a single time. The issue with these distinctions is the assumption that the excavations have uncovered the full extent of sites and that there are no further sites in the local area; for example, in the case of classifying a type 1 site, in fact it may be within the more disperse type 3 site. An example of this is the site of Star Carr which Mellars categorises based on Clark's excavations as a type 2 site. However, later excavations have shown that Clark had not excavated the full extent of the site, and in fact much more of it remains to be uncovered (cf. Conneller et al. 2012) which means it is of a slightly different nature to any of Mellars' site categories.

Mellars goes on to present more detailed typological data for 46 British Mesolithic sites with a conscious aim of "focus[ing] attention on those features… of most obvious significance from a 'functional' point of view" (1976, 386–387). Mellars selects data from these sites about what he terms are the "essential" tool forms: microliths, scrapers, burins, axes/adzes, saws (microdenticulates), cores and microburins (p.386). He excludes from his list, and therefore his analysis, classifications of tool that are effectively more ambiguously classified including awls (and piercers), truncated pieces and miscellaneously retouched pieces because these are less consistently classified in the literature. Likewise, Mellars removes atypical specimens of scrapers and burins not manufactured on flakes and blades from his analysis. The advantage of this approach is that the resulting comparisons are drawn on the more standardised data from which Mellars could produce a generalised, coherent model; again, very much in keeping with the functional-processual approaches of the time. In fact, Mellars argues that consistency in the data record is necessarily the "primary consideration" for comparative studies (1976, 386). The disadvantage of this approach is that he is essentially ignoring a set of data which could theoretically completely change site function for individual sites, by ignoring the tools of potentially specific tasks/crafts such as beadworking. Similarly, if knapping occurs more heavily on one site, such as a base camp, but less so on another, like a hunting hide, then expedient tools on debitage will likely be more relevant and heavily used in the former. In turn, this actually runs the risk of downplaying the archaeology of a demographic who only uses the base camp, for example, perhaps children (an idea discussed in Gero 1991).

Mellars presents the frequency of cores as the numbers of cores per 100 'essential' tools and microburins per 100 microliths; a novel and simple way of presenting the 'waste' products in relative proportions to the tools (1976, 386–387). He does not include general waste flakes though as they are heavily impacted by the excavation protocols regarding the size of flakes to be retained and therefore unrepresentatively variable (p.386). He also chooses to disregard core-rejuvenation flake statistics because only a small number of sites have reliably identified these (*ibid*.).

On the basis of the essential tools and waste, Mellars argues for the division of the sites into three different groupings: type A, microlith dominated assemblages with particularly low proportions of blade and flake end-scrapers; B, assemblages with a balance of scrapers and microliths; C, scraper dominated assemblages (Mellars 1976, 386). He does not relate these back to his and Radley's classifications of Star Carr and Deepcar type sites but seems to see the three site typologies as parallel classifications.

Within the 14 Type A sites, Mellars notes that in addition to microliths dominating the assemblage, there is a notable bias in favour of one microlith type at over half of the sites

(Mellars 1976, 388). Iping Common, a lowland site, is the only site among these that is dominated by non-geometric microliths and it is estimated by Mellars as a significantly larger site area than the other sites in this type category with higher proportions of cores and scrapers than other sites in this class as well (p.388) so it does not seem to quite fit the model. Of the other 13 sites in this type category, two upland and one lowland emphasise small scalene triangles, three upland sites favour narrow, rod-like forms, and at the upland site of White Hill, small trapezoidal forms are favoured. Mellars interpretation of these sites is that they reflect industrial specialisation which in turn reflects a bias towards primary subsistence strategies such as hunting as opposed to the alternative of general maintenance or domestic categories such as hide working (*ibid*.). Note that this interpretation only presents a functional explanation for the bias in the assemblage and neither attempts to consider the cultural classifications of these sites or other non-functional interpretations.

There is little attempt to explain why certain microlith forms may have been particularly emphasised on a particular site, not even within a functional-processual framework where it could have been considered if there was a correlation between the emphasised type and varying environmental zones. Mellars does consider that these type A sites are found in both lowland and upland contexts but does not consider them in a more detailed environmental context than that. Of this, he argues it reflects that these sites are found in a variety of environmental locations. In the case of the upland sites, he suggests they would more likely have been used in the summer months on "climatic and economic" grounds due to the lack of evidence for substantial structures (Mellars 1976, 389). He also argues if the interpretation of scrapers as hideworking tools is accepted then their absence on these types of sites supports summer occupation where there may be less need for hide production (p.389). However, this does neglect the potential influence of both hide curation behaviours, seasonal availability of usefully-sized hide-yielding species, hide preparation times and simply the fact that in such exposed locations, summer nights are still potentially likely to be dangerously cold in such exposed locations. While Mellars' interpretation is based on logical assumptions about seasonal movements, they remain only assumptions and are quite often easily argued against with other logical arguments in keeping with straight-forward, functional motivations let alone considerations of other non-survivalist motivations.

Mellars' 31 Type B sites, with 'balanced' assemblages, include the sites of Deepcar, Star Carr, Flixton Island 1 and Thatcham (Mellars 1976, 390). Mellars acknowledges this is a very broad grouping and as such breaks the group into two divisions, a true Type B and a Type B1 which he suggests is an intermediary between type A and B sites. This B1 type is proposed on the basis that these sites present higher proportions of microliths than most Type B sites (ranging from 71–84.5% microlith) but lower proportions than the Type A sites

(which range from 88–97% microlith) (pp.390–391). However, for the three 'intermediate' sites Mellars successfully estimates the occupation area for, two of the sites utilise significantly larger areas than all Type A and B sites in two of the cases, and in the third case the only similarly sized site is the anomalous Iping Common (p.390). These B1 sites are all either pit-dwelling settlements or coastally-orientated settlements and therefore perhaps should be considered separately as they would potentially be functioning in a different manner to discrete, inland sites.

Within these sites, the nature of the microlithic subtypes represented is again variable, as are the proportions of the other macrolithic elements under consideration by Mellars. An example of the latter is the case of burins at Star Carr, Low Clone and Sandbeds which are all categorised by Mellars as Type B sites but their proportions of burins are considerably higher than other sites in both the Type A and B categories (1976, 391). There are several instances of deviation like this which again perhaps suggests that this is an over-generalised system of division.

In terms of the microlith variability, Mellars refers to Jacobi's 1973 review and acknowledges that chronological variation has a role to play (Mellars 1976, 391) but does not prioritise it over functional interpretation. He comments that if earlier British Mesolithic sites are categorised as having a more limited range of types represented, lacking geometric or narrow blade forms, then Star Carr type assemblages fall "clearly" into this chronological category and Deepcar type assemblages "probably" fall into it too (p.391). In comparing the assemblages present on his Type A and Type B sites, many of the former exhibit the bias towards particular microliths as discussed above which are usually geometric forms and therefore may be Later Mesolithic. Type B sites *overall* present a range of geometric and non-geometric forms which Mellars emphasises (*ibid*.), but what he does not comment on is the fact that many of these sites such as Star Carr, Deepcar, Flixton 1, Thatcham and so on do not exhibit geometric forms at all, as Jacobi had highlighted in his 1973 paper. Mellars' interpretation based on the overall profile of these sites is that they are generalised and therefore in functional terms likely representing "'domestically' oriented tasks" (*ibid*.). However, this does not take into consideration the subtler nuances within this large group of sites, many of which conflict with the overall profile, nor does he deeply consider the influence of potential chronological change or even the considerations of size that Mellars himself had highlighted earlier in the paper with his formulation of Type 1, 2 and 3 sites.

Equally so, the locations and sizes of Type B sites are highly variable, being found geographically across England and in upland, lowland and coastal contexts. Mellars notes this is a broader range of environments than Type A sites are found in, and particularly notes a high number of Type B sites in coastal environments in contrast to none of the Type

A sites found there (1976, 392). In addition to coastal locations in northern and western Britain, Mellars also highlights groupings in central and southern Pennine contexts and southern and eastern English lowland contexts (in which he includes the Yorkshire sites of Flixton 1 and Star Carr). However, as Jacobi discusses, while Mesolithic site distributions are impacted by Mesolithic relationships with the landscape and decision making, there are vast areas of the country, such as Cambridgeshire and Humberside, that appear to be lacking sites but they have simply been obscured, in those cases buried deep under the later fen formations (Jacobi 1973). Mellars does cursorily acknowledge this at the end of his paper, however (1976, 397). In addition, the sample sizes, particularly for Type A sites, are small and therefore run the chance of not being representative, especially as such sites will be easily missed even if the area is surveyed systematically.

Very much in keeping with the functional-processual nature of the rest of the paper, Mellars' social interpretations of the sites involve estimating the population of the inhabitants on the site and how many 'families' may be involved in the production of assemblages of this size and dispersal (in tandem with structural evidence). As such, for Type A sites Mellars proposes that the size of the social unit utilising the site approximates to the size of a single nuclear family (1976, 389), while Type B sites are interpreted as probably representing two or three family groups (p.392). The term 'family' is not explored except in mentioning the term nuclear in the Type A discussion, which is the imposition of a social structure not directly evidenced.

Mellars again returns to seasonal interpretations for Type B sites too, drawing on various forms of evidence including the nature of the lithic assemblage (1976, 393). He also considers Clark's interpretation of upland sites such as Deepcar as being summer encampments working in conjunction with lowland winter encampments such as Star Carr, in keeping with deer migrations and the general environment of the site (Clark 1972, 33–37). In terms of interpreting the lithics themselves, Mellars argues that the assemblages reflect a broader range of activities occurring on site with less specialisation (Mellars 1976, 393) and that the increased number of scrapers which he argues could be a response to an increased need for hides during a winter occupation. Similar arguments against this latter interpretation apply as for Mellars' arguments for summer occupation of Type A sites. Mellars also draws reference to Clark's suggestion that relatively high numbers of burins at Star Carr relates to the working of red deer antler and are therefore most required in late autumn and winter months when the antler is in the best condition for manufacture (Clark 1972, 34–35).

Finally, Mellars classifies three sites into a Type C category, that characteristically show a proportional dominance of scrapers (81.8–90.5%) in their assemblages. Aside from this,

they are highly variable in nature: Kettlebury I has 22 essential tools (by Mellars' definition) and an estimated area of 8.5m^2 set on inland lowland; Blubberhouses Moor in the Pennine uplands has 63 essential tools and yet an estimated area of 3.5m^2; the last, Freshwater West is a lowland coastal site with a significantly larger assemblage with 243 essential tools, an estimated area of 20m^2, and was likely repeatedly occupied (Mellars 1976, 394–395). His interpretation is based on the assumption that scrapers were used for hide-working and in combination with hazelnut as a seasonal indicator at *one* of the sites is that these are sites where skins "played an important – and possibly dominating – role… in anticipation of the increased need for skin clothing, tent covers etc. during the approaching winter months" (Mellars 1976, 395).

Finally, Mellars moves onto a third consideration of the sites, contrasting function as derived from their type A, B or C classification between those sites from the earlier or later Mesolithic. Mellars argues that a fine resolution consideration is not feasible given the lack of accurately dated sites, in significant contrast to Jacobi's approach (Mellars 1976, 395). Lowland and upland sites dated to the Early Mesolithic by typology or palynology, including Star Carr, Deepcar, and Warcock Hill North and South, primarily fall into the balanced Type B sites and being so, are interpreted as being occupied throughout long periods of the year. Mellars acknowledges the exception to this is Iping Common, the relatively very large Type A site that is possibly a summer occupation (*ibid*.). Unfortunately, he does not make a distinction between Star Carr, Deepcar and Horsham type sites.

Mellars ends acknowledging that the record we do have represents mainly hunting equipment as most of the distinctive lithic tools recovered are for the hunting or processing of land animals by his interpretation (Mellars 1976, p.397). He dismisses plant processing tools as unrecognisable, despite his assumptions about tools for hunting being largely speculative, drawing only loosely on ethnographic analogies. As such, at this stage there were four methods of categorising Early Mesolithic sites utilising the lithic assemblages which no-one successfully draws together or can truly clearly delineate site differences from based on typological, chronological, spatial, and presumed functional attributes.

2.4.4 Clarke's challenge to oversimplification

In the same volume as Mellars' publication, David Clarke published another important paper for Mesolithic studies: "Mesolithic Europe: the economic basis" (1976). This is a clear manifesto as well as a reconsideration of some of the data from across Mesolithic Europe in keeping with Clarke's other more theoretical work as the New Archaeology matured with application (cf. Clarke 1973). Clarke critiques many issues not simply with culture-historical approaches but also addresses many problems emergent in functional-processual

interpretations. In addition to general points such as effectively calling for the application of a hypothetico-deductive methodology and an awareness of the misapplication of Darwinian theory to social elements (Clarke 1976, 449), he makes several points relating directly to the interpretation of lithics.

In addition to a consistent implicit assumption that meat was the dominant proportion of the diet underlying interpretations (Clarke 1976, 450) and a bias in preservation of faunal over floral remains (p.451), there are a number of artefact biases in play. Firstly, he proposes there is an implicit assumption in some research that higher numbers of certain artefacts correlated with a higher dependence and importance of those artefacts and their interpreted uses (p.451). This is not always the case as large numbers may be produced for short duration, less important activities purely depending on the nature of the technology or on the other hand important activities may only require a low number of unspecialised artefacts (and all variations thereupon). Mellars' interpretations into Type A, B, and C sites based on microlith and scraper proportions within the assemblages is an apparent example of this assumption in action. Clarke also argues more persuasively for the biased preservation of meat processing equipment, as plant matter is simpler to process and "...often need[s] little more than dextrous hands and specialised teeth with the addition of a few wooden sticks and points…" in comparison with animal hunting and butchery processing that require specialist stone tools (1976, 451).

However, thirdly, the above two biases introduce interpretative bias in guiding towards a greater emphasis on hunting activities in the interpretation both of the assemblage itself and the general economic model developed (Clarke 1976, 452). Tools used for plant gathering and processing may be misinterpreted as hunting equipment and Clarke suggests that a significant proportion of lithic tools as well as organic tools used on plant materials are assumed to be used on animal material because of this. One functional issue Clarke does not comment on is the potential for reuse of tools on a variety of materials, perhaps despite the original use or quite deliberately.

In addition to biases, Clarke explores the detrimental effect of traditional, particularly unsupported, stereotypes built upon these. He passionately argues that the Mesolithic being characterised by the presence of microliths which are interpreted primarily as featuring in bow hunting composite technologies and therefore part of a meat-based dietary economy is one of the most accepted and problematic assumptions (Clarke 1976, 452). Firstly, he argues, microliths are not always even present in European postglacial assemblages and are "rarely" the most numerous artefact (p.452). Secondly, Clarke summarises the growing body of evidence for utilising composite tools in plant gathering and processing as well as other underexplored technologies such as snares, nets, and shell openers for exploiting non-

mammalian resources. He suggests that where microliths may have been used as Loshult-like arrow barbs, the bow poundage and arrows were light with low penetration capacity, with the lack of additional barbs on this simple arrow type supporting this argument, and therefore implies they were likely used for fish or bird hunting (p.452). In addition, knife hafts embedded with microliths which would be suitable for gathering different forms of plant material had been found at various Mesolithic and Upper Palaeolithic sites across the world and Clarke suggests these composite tools were early forms that would logically lead into the development of Neolithic (plant gathering) sickles (pp.453–455). He calls particular attention to a knife recovered from Columnata, North Africa, in the Capsian levels (a Mesolithic culture from the Maghreb) dated to around 6000 BC which demonstrates different types of microlith (two broken 'lunates', or crescents, and one broken triangle) usually interpreted as arrow barbs being used for the same purpose in being hafted as knife teeth (p.454).

Clarke also illustrates numerous ethnographic examples which are microlith hafting configurations not represented in the archaeological record (1976, 454–455). The precedent for this had been set by Clark in his 1954 Star Carr monograph and had been continued, fitting neatly with those such as Binford's applications of ethnoarchaeology to produce middle-range theories (cf. Binford 1978, 1980, 1983). This provides inspiration, however, in Clarke's publication the archaeological evidence is presented along with the ethnographic examples and it is unclear without detailed consultation of the text which pieces are those archaeologically evidenced and to what degree, as partial pieces are illustrated as reconstructed wholes (see Figure 17).

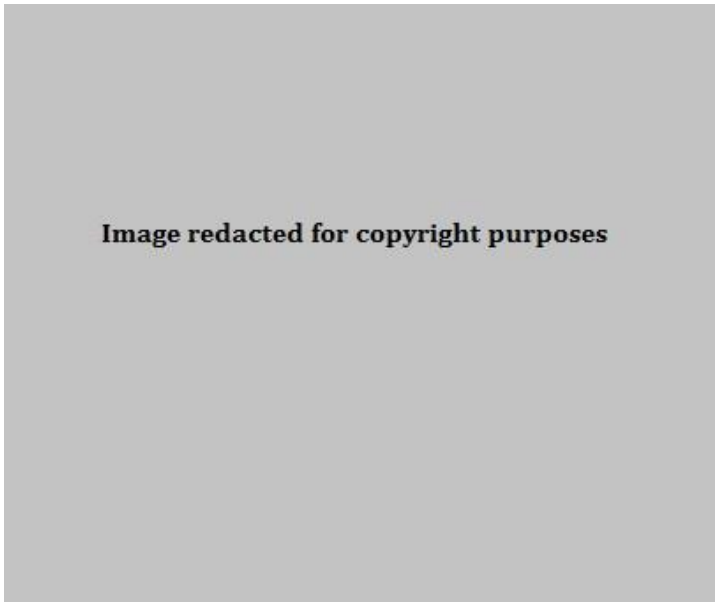

Figure 17. Clarke's examples of hafted microliths as reproduced by Butler (2005, 89)

Drawing these strands together, Clarke develops a simple theoretical example of a site's interpretation in which he describes "a family unit" and the different scenarios of different tools they may possess for various activities (1976, 456). From this he calculates the numbers of microliths required for those scenarios and from there the estimated ratios of vegetal to animal processing related microliths, which vary from 2:1 to 40:1 in the scenarios he proposes. This illustrates his point about plant processing well, though Clarke's family unit is clearly modelled on the Western (nuclear and extended) family model and entrenched in ideas of the males being the hunters and main gatherers, while women are the processors of plant material at camp:

> *"… we can visualise an industry in which, within a family unit, each hunter possesses half a dozen Løshult-type arrows (12 microliths in all), three or four bird and fish arrows (12-30 microliths)… he and four other family members carry varieties of harvesting knives (12 – 30 microliths) and two women hold slicing knives (2-6 microliths) and a grater board (100-2,700 microliths)…"(Clarke 1976, p.456)*

However, while this is highly speculative and riddled with these implicit assumptions, it did highlight the need for considering the multitude of applications of microlith-based composite tools in considering Mesolithic lithic assemblages.

2.5 Summary

As such, the British Early Mesolithic microlithic culture classifications of Star Carr, Deepcar, and Horsham type assemblages and sites had been established, and their relationship to the

functional and processual workings and occupational interpretations of a site were being explored. Mellars also developed two other methods based on attributes of site shape and features, as well as the balance of the composition based on classic formal tools. However, no single classification system came out of this work as the clear option for categorisation and there were a number of issues with all the categories developed. They generally seem to oversimplify the picture and while simplification is the aim of a model, the models developed as a result often had many anomalies and exceptions that highlight the instability of these schemes. As this work was heavily rooted in the broader developments occurring in archaeology as a discipline, it often reflected the many of the issues raised with later archaeologists concerning New Archaeology and later functional and processual archaeology such as emphasising the economic and functional interpretations over the experiential, more individualistic approaches that post-processualists including Chantal Conneller would later employ. However, regardless of how the interpretations were drawn, the general methods developed by these researchers provided a foundation for all later lithics researchers to build on and these are the frameworks still used by many British Mesolithic researchers today. One aspect that Roger Jacobi raised is the fact there are very few Early Mesolithic sites from the midlands (Jacobi 1973). He does not know if this is a genuine trend or simply that sites haven't been identified but any sites in these regions could perhaps go some way to explaining the obvious clash of the

The next chapter will consider in further detail how recent researchers have built on this earlier work, particularly Jacobi's work, to marry the Star Carr, Deepcar, and basally modified assemblage/site type categories into more recent radiocarbon data that has become available, and therefore how there are further problems separating these site types out.

Chapter 3 The Dating and Chronology of Early Mesolithic assemblages

3.1 Introduction

Radiocarbon dating was part of the scientific revolution in archaeology, but the dating of lithics by their inherent nature of not being datable themselves was dependent on a building up of a collection of dates stratigraphically associated with lithic assemblages where the means were available. As a result, it took a longer time for a corpus of dates to build up to consider how sites interpreted based on their lithics, with Jacobi's work to be the first to start to collate these.

3.2 Roger Jacobi's work on Early Mesolithic Chronologies

As mentioned in the previous chapter, Jacobi (1973) gathered the dates or date ranges for various Mesolithic assemblages as part of his review of Mesolithic Britain (reproduced in Table 1). However, they are uncalibrated and he does not consider any sampling biases that may have been introduced. This is something that became apparent as radiocarbon dating methods developed but was not often a consideration at the time of this paper. As such, while he notes the closeness of these dates, without calibration they could potentially be significantly different to their actual dates. From this uncalibrated data, the Deepcar type sites seem to appear earlier in the archaeological record but with an overlapping range to Star Carr sites.

Table 1. Early Mesolithic radiocarbon dates from Jacobi 1973, p.261. *Site codes obtained from Jacobi 1978.

Site	**Lab no.**	**Uncal. year bc**	**Uncal. year bp**	**Error ±**	**Pollen**	**Site Type**
Thatcham III	Q-659*	8415	10365	170	IV	Deepcar
Thatcham III	Q-658*	8080	10030	170	IV	Deepcar
Thatcham I / V	Q-651*	7890	9840	160	IV-VI	Deepcar
Thatcham I / V	?	7830	9780	200	IV-VI	Deepcar
Thatcham I / V	?	7530	9480	160	IV-VI	Deepcar
Star Carr	?	7607	9557	210	IV - V	Star Carr
Star Carr	?	7538	9488	350	IV - V	Star Carr

In his 1976 paper, Jacobi readdresses the issue of the emerging proliferation of regional terms for stone assemblage typologies which were in fact closely related on a techno-complex level from Britain and across Europe and proposes a more standardised terminology. The Broad Blade industries had originally been proposed by Buckley, as discussed above, from Pennine industries that by Jacobi's 1976 paper had been radiocarbon dated to the 8th millennium BC (Switsur and Jacobi 1975). The key point of the 1976 article is to acknowledge Britain's link to continental Europe in the light of recognition of the lost land link between the two by the inundation of the North Sea plain (which had been well established by the time of Childe's 1947 chapter on the Forest Period) and as such we see Jacobi readdressing how British assemblages fit with identified continental cultural groupings. Considering Thatcham III and Greenham Dairy Farm, both sites are classed as Broad Blade industries by the now accepted definition as having obliquely-blunted microlith points accompanied by much rarer isosceles triangle, elongated trapeze and rhombic microliths (Jacobi 1976, 67). Jacobi argues similar industries can be found across continental Northern Europe, in particular comparable to Maglemosian stages evidenced in Scandinavia which also mainly consist of obliquely blunted points supplemented by triangular but also convex backed microliths, industries from Duvensee which are contemporary but with higher proportions of isosceles triangles and trapezoids that mean these are specifically more similar to the Star Carr and Flixton 1 assemblages, and finally a selection of sites from the Low Countries (Ter Horst, Geldrop III2 and III3, Zonhoven, Stegerveld, and Hulhorsterzand VIII a/b) (see Table 2).

Jacobi's 1978 paper focuses specifically on Northern England in the eighth millennium BC. He adopts the interpretation of the characteristic elements of Early Mesolithic assemblages (broad obliquely blunted points; isosceles triangles; short or elongated bitruncated blades; convex backed points) as "archery equipment" (Jacobi 1978a, p.295) supplemented with core-axes, end-scrapers, burins, and truncated blades supposedly utilised for the exploitation of the emergent early postglacial environment of birch and later pine-hazel woodland with associated new flora and fauna availability. He situates these types of assemblages and resource exploitation in the broader European scheme as belonging to the north European Maglemosian "technocomplex" (*ibid*.). From this, Jacobi draws not only on the lithic assemblage typological classifications but also ties in the pollen spectra, faunal evidence and the radiocarbon dates available at the time to start to build a detailed chronology for Mesolithic northern England. While he mentions the typological classification of a selection of radiocarbon dated northern English sites that are Deepcar type (Lominot Site III, Money Howe I, and Waystone Edge) or Star Carr type (the type site and also Warcock Hill South), he comments this is a small number of dates to work with, the

Star Carr measurements at that time were 20 years old, and the other dates had large standard deviations to make anything more than general comments (see Table 3) (Jacobi 1978a, 297). The radiocarbon dates for the classified assemblages are used uncalibrated by Jacobi too. The uncalibrated dates themselves show significant overlap between the two typological groupings however and Jacobi does not emphasise their distinction at this stage but rather situates them either against radiocarbon dated or tundra pollen or Upper Palaeolithic sites such as Anston Cave that have associated faunal remains (Jacobi 1978a, 298–299).

Table 2. Early Mesolithic radiocarbon dates extracted from Jacobi 1976, pp.67–69.

Site	**Lab no.**	**Uncal. year bc**	**Uncal. year bp**	**Error +-**	**Site Type**
Greenham Dairy Farm	Q973	6829	8779	110	Broad Blade (British)
Rhuddlan E	?	6789	8739	86	Broad Blade (British)
Aberffraw	Har 1194	6640	8590	90	Broad Blade (British)
Draved 604 Syd	K1466	7440	9390	120	Maglemosian 0 and I (European, Jacobi associates with Broad Blade)
Draved 604 Syd	K1794	6840	8790	140	Maglemosian 0 and I (European, Jacobi associates with Broad Blade)
Stegerveld (terminus post quem)	GrN2461	7410	9360	110	*Similar to Broad Blade (between these dates)*
Stegerveld (terminus anti quem)	GrN2413	6550	8500	100	
Hulhorsterzand VIII a/b (terminus post quem)	GrN6086	7230	9180	80	*Similar to Broad Blade (between these dates)*
Hulhorsterzand VIII a/b (terminus ante quem)	GrN6075	6840	8790	100	

Table 3. Early Mesolithic radiocarbon dates from Jacobi 1978, pp.297–301, with various Upper Palaeolithic dates discussed for comparison.

Site	**Lab no.**	**Uncal. year bc**	**Uncal. year bp**	**Error +-**	**Site Type**
Lominot III	Q-1187	7615	9565	470	Deepcar
Money Howe I	Q-1560	7480	9430	390	Deepcar
Waystone Edge	Q-1300	7446	9396	210	Deepcar
Star Carr	Q-14	7607	9557	210	Star Carr
Star Carr	C-353	7538	9488	350	Star Carr
Warcock Hill South	Q-1185	7260	9210	340	Star Carr
Robin Hood's Cave	BM-603	8440	10390	90	Assumed Upper Pal.
Anston Cave	*BM-440A*	*7990*	*9940*	*115*	*Creswellian (Later Upper Pal.)*
Anston Cave	*BM-439*	*7900*	*9850*	*115*	*Creswellian (Later Upper Pal.)*
Anston Cave	*BM-440B*	*7800*	*9750*	*110*	*Creswellian (Later Upper Pal.)*

His discussion of Thatcham is interesting as although he utilises dates from this site, he does not classify it as being Star Carr or Deepcar type but rather simply utilises it as the south-eastern equivalent of Star Carr in having radiocarbon dates and good faunal preservation which seemingly reflects a slightly earlier colonisation in southern England of woodland flora and fauna of the postglacial Preboreal (Jacobi 1978a, 298). He notes that the (uncalibrated) dates for this site overlap with the northern site of Robin Hood's Cave at Creswell which yielded Upper Palaeolithic lithic assemblage as well as evidence for on-site butchery of horse and giant deer, *Megaloceros sp.* (p.298). If we accept Radley and Mellars' earlier grouping of Thatcham into a Deepcar (or even something similar) typology (1964) then here is a southern Deepcar site overlapping chronologically with an Upper Palaeolithic Horse Butchery site from Northern England. As sites later than Thatcham from south and north England then feature Broad Blade industries, this fits well into the general transition that Jacobi posits, being that with the transition to Preboreal and Boreal woodland across England with the warming climate, then Mesolithic peoples adopted Broad Blade Maglemosian technologies (Jacobi 1978: 301). This could be seen as environmentally deterministic: a criticism levelled frequently at functional-processual work from this period. Later considerations of the dating have further brought into question the linearity of Star Carr and Deepcar chronological sequencing, with Deepcar material perhaps appearing earlier in the record than originally anticipated, overlapping with Star Carr.

3.3 Michael Reynier's work on the definitions and chronology of Early Mesolithic cultural groups

3.3.1 Background

Michael Reynier, supervised by Roger Jacobi, produced work of particular significance in drawing together earlier research defining assemblage typologies and attempting to order these chronologically. In his British Archaeological Report dedicated to Early Mesolithic Britain, he aimed to decentralise the importance of Star Carr in the modelling of other Early Mesolithic sites and address the chasm that had emerged between cultural and behavioural models which had been largely influenced by Clark's economic work in the Vale (Reynier 2005). Typological and chronological research questions had often been sidelined in the fixation on interpreting resource utilisation on the many sites aiming to emulate Clark and follow the archaeological zeitgeist of Functionalism. Reynier proposed to draw on the older culture-historical approach to identify cultural, chronologically grouped entities while at the same time using behavioural studies to attempt to determine how those entities functioned (p.4).

3.3.2 Typological work

Reynier employs Clarke's general criteria for defining cultural 'assemblage-types' to Mesolithic lithic typologies and, by extrapolation, for exploring their relative chronological sequencing: Consistently re-occurring, polythetic (shared typical, though not strictly essential, common artefact types for each group that often appear together), and geographically restricted artefact groupings (cf. Clarke 1968; Reynier 2005, 5). As such, building on Switsur and Jacobi's data (1975) and introducing his own, Reynier argues that these criteria are met by the three previously defined lithic assemblage types from Britain (Star Carr, Deepcar, and Horsham). Reynier assessed the cultural groupings mainly based on his own detailed site data from a restricted geographical region, namely south-east England. The advantage of this approach is that it enables control for regional variation. On the other hand, it means that British assemblage types that are not strongly evident in this region perhaps are overlooked, de-emphasised or completely absent. Reynier selected this region in particular because it contained the highest concentration of Early Mesolithic sites in Britain and he had a good source of unpublished but well-excavated data from here (2005, 6). His study expands to consider the rest of England and Wales for his consideration of chronology, environment, settlement and cultural entity affinities but this builds on his previous regional-based identification of assemblage types. As such, to apply this as a model

nationally is problematic, although this model could theoretically be advantageously built upon by consideration of, and comparison with, other geographically defined regions.

Reynier is selective in the study assemblages he utilises in his own analysis, with the exception of the settlement analysis which he expands his sample for. He terms his selection scheme "RID criteria": Reliability, of collection and association; Integrity, avoiding contamination or mixing; Dating, with reliable methods. As such, while this guarantees that the data he relies on is robust, which is important, this is not a random sample. There is an inherent bias, even if justified, towards sampling recently excavated and dated sites with clear stratigraphy and means a body of data are immediately invalid for this portion of the study. Only nine sites are ultimately considered for the resultant detailed analysis, which is a very small sample size. This is a matter of concern considering Reynier then uses a model constructed from these data to discuss the whole of Britain. On the other hand, any statistical patterns in Reynier's analysis can at least be considered with a fair degree of trust with regards to those specific nine sites at least. It would be inappropriate to build a model without these criteria in place too: the problem is that more appropriate sites should have incorporated, or the argument as a national model should have been proposed more tentatively or even abandoned for not having enough data.

Of the nine sites, three fall into each of the three traditional typological divisions of Star Carr, Deepcar, and Horsham type sites (Reynier 2005, 15). Reynier moves on to consider the typology, technology, and comparative absolute chronologies of these sites. Table 4 shows the numbers of microliths and tools assessed for each of the three 'Deepcar' sites, including a simple representation as a pie chart of their proportional representations, as an example. The assemblages themselves are highly variable in size, and microliths and tools are represented in variable proportions (Reynier 2005, 20). This, in itself, potentially suggests a different functional nature to the sites. You would expect not only different proportions but also different kinds of tools and even perhaps different kinds of microlith presented relating to the function they were intended for, without starting to consider psychological and social factors influencing past associations with those site locations. Reynier does not discuss how the sites may be interpreted in terms of human action, he only considers their classification based on his RID criteria. If his data supports the division of Early Mesolithic assemblages into the three types, then it does not necessarily mean these are reflecting different cultural groupings with different chronological periods of use, Reynier's inherent assumption, but each grouping could be representing sites with a common function or meaning to the people who utilised them. In establishing the nature of the sites, Reynier found that the data he gathered for 'standard' tools (in this case meaning worked tools excluding microliths) on area of primary retouch ('lateralisation'), additional retouch and length categories was statistically "uninformative" regarding the typological distinction of

an assemblage (p.18). This may suggest that several site types are being represented within the typological distinctions, as such there may be several subtypes of Star Carr site, Deepcar site and so on.

Table 4. The frequencies of microliths (blue in chart) and standard tools (orange) included in the study of sites suggested to be characteristically 'Deepcar' by Reynier (2005, 20).

	Iping Common	**Marsh Benham**	**Thatcham III**
Total microliths	386	24	127
Total standard tools	131	86	124
Total lithics	517	110	251
Simple proportional representation		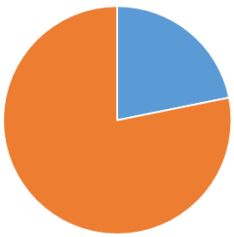	

As such, Reynier's methodology does not facilitate explanation of the toolset but uses it as a passive indicator as a chronological marker. In deliberately aiming to define types which he can associate chronologically, however, he ignores the functional influences which would potentially have encouraged knappers to emphasise particular tools or produce less of others. If there are genuinely Deepcar type sites reflecting a socio-cultural entity but then within them there are different kinds of Deepcar type sites with different activities occurring then they will have a differently balanced assemblage.

Knowing whether actual change over time or the function, the fact that different people may be using the site either contemporaneously or sequentially, the amount material is transported to and from or reused at a site, post-depositional disturbances or perhaps other factors is what predominantly defines the assemblage present at a site is therefore a crucial issue ignored by Reynier. Where Reynier does discuss the potential for interpretation of assemblages, it is after he has categorised them, when he considers and then rejects the idea of extrapolating socio-cultural meaning based on the three assemblage types on the grounds that he does not feel there is enough archaeological data available as yet (2005, p.30). It is fair to be cautious as even with the wealth of data he collected from those nine sites in great detail, this is a small sample size, and even including summary data he collected from other sites, the patterns he draws are not always clear.

Of the nine sites selected from south-east England, three represented each assemblage type: Broxbourne 104, Pointed Stone 3 and the patinated series from Thatcham III represented

Star Carr type sites; Iping Common, Marsh Benham and the unpatinated series at Thatcham III represented Deepcar type sites; Kettlebury 103, Longmoor 1 and St. Catherine's Hill represented the Horsham type (Reynier 2005, 15). Table 5 summarises the compositional characteristics that Reynier proposes are supported for Star Carr, Deepcar and Horsham type assemblages following his analysis of the nine sites.

Table 5. Summary of Reynier's proposed typological characteristics for Star Carr, Deepcar and Horsham type assemblages (summarized from Reynier 2005, 18–22).

	Star Carr	**Deepcar**	**Horsham**
Microlith assemblage attributes	• Restricted typological range • Dominated by obliquely blunted points (26% - 63%) • Moderate frequencies of isoceles triangles and trapezoids (5 - 15% each) • No partially-backed points • Convex backed points occasionally recorded • Left hand side primary retouch low • Leading edge additional retouch absent or rare • Small mean length (18-34mm) • Generally angular in outline and broad, feathered distal terminations	• Dominated or with high frequencies of obliquely truncated points (20 - 40%), similar to Star Carr type assemblages • Marked frequency of partially-backed points (15 - 20%) • 'Moderate' frequencies of trapezoids (<10%) • Low frequencies of triangles, rhomboids and backed points (1 - 5%) • May be basally modified points • Bias to left hand side primary retouch (>70%) • Notable incidence of additional leading edge retouch (20%) • Generally, the mean length of the microliths is longer (33 - 38mm), with slender outlines and narrow, pointed basal terminations.	• Characteristic presence of hollow-based points (5-15%) and other basally worked forms (<2%) • 'Notable' frequency of geometric forms: Triangles (5-25%), rhomboids (5-10%) • Absence of trapezoids • Bias to left hand side leading edge retouch (>95%) • High proportion of additional leading edge retouch • Small mean length (22-26mm) • Generally small, highly angular and pointed basal terminations
Balance of standard formal tools	• Also restricted in typological range • Scrapers: most dominant tool class (26 - 68%); almost exclusively short end forms • Burins: rare (11 - 48%); Well characterised • Piercers (11 - 26%): mèches de foret are characteristic • Truncated pieces (7-30%) • Microdenticulates, chamfered pieces and backed pieces are rare or absent (<5%)	• Scrapers: dominant tool form; mostly short end form (30 - 45%); small number of long end scrapers (no statistics generated) • Burins: poorly characterised (0 - 30%); high frequencies of 'corbiac' or 'pseudo' burins (no statistics) • Piercers variable frequency (0 - 13%) • Core tools variable (usually flake axes) (3-7%) • Microdenticulates (1 - 23%) • Truncated pieces (8 - 52%) are usually present though in variable frequencies • Chamfered and backed pieces are rare and poorly characterised (< 2%)	• Dominated or with high frequencies of obliquely truncated points (20 - 40%), similar to Star Carr type assemblages • Scrapers: dominant tool form; mostly short end form; increased frequency of nosed form (no statistics generated) • Burins: rare and poorly characterised (<10%) • Truncated pieces in moderate frequencies (4-14%) • Core tools rare (<2%) • Microdenticulates rare (c. 1%) • Chamfered pieces variable but distinctively higher presence (6 – 35%)

Reynier separates Thatcham III into two microlith assemblage types and it happens that the Star Carr type is patinated and Deepcar is the unpatinated series (Reynier 2005, 20). At Warcock Hill South, the flint lacking patination was deemed to be Star Carr type, not solely based on non-patination though but in tandem with the lack of leading edge retouch, as discussed above. Patination was suggested as criteria by Mellars and Radley but patination occurs for a number of chemical reasons in the soil and can suggest that the material was deposited at different time, used on different materials, or has been subject to different processes after post-deposition so it should not be used as a typological indicator. It can also be influenced by the raw material source and therefore variations in material inclusions within the flint. Compounding this, quite often 'patination' is used to encompass post-depositional cortification as well (i.e. redevelopment of cortex) which is a different process (Henson 1982). Environmental factors on patination were not considered for their influence on assemblage-type attribution by Reynier or others.

As such, the spatial distribution on site needs to be considered, as well as the nature of both the surrounding sediments and the raw lithic material source. In the case of Thatcham III, both scatters lie within a shallow basin but they are spatially distinct, supporting their separate identification (with the patinated from the north-east corner separate to a larger scatter to the south-west). They both lie within clayey or clayey silt layers, although the lower clay layer which contained most of the patinated flint assemblage in the Eastern scatter is not recorded for the Western sections which do not feature patinated material. As such, the heightened patination is potentially a product of the heightened clayey nature of the sediment. Patination may be a sign of an assemblage type being utilised in a particular locale, how long it has been exposed on the surface, or being from a particular type of flint prone to patination, but how legitimate it is to use that as an actual attribute of a site typology is more ambiguous. It is healthier to approach it as an indicator of an environmental factor, as one might consider the underlying geology or geographical location more. Again, this also raises the question of whether locales are chosen for a specific functional reason relating to intention over cultural factors.

Reynier utilises Jacobi's typological classification system in his analysis and considers the proportional representation of different attributes (2005, p.11). As such he looks at the common microlith typologies represented, the main edge that features retouch (left tip, right tip and so on), sides featuring additional retouch, and microlith length. He then averages the values for differentiated Star Carr, Deepcar, and Horsham type sites (pp.18-22). Reynier argues his data supports that there are three different types of assemblage, reflecting the three Early Mesolithic site types as traditionally defined by past research. This form of analysis seems inappropriate for such a small sample size as it overgeneralises and glosses easily over any significant variation evidenced, which in this case, if it were

evidenced, would be at a minimum affecting one third of the sample data (there being only three sites per assemblage type).

Consider the results of Reynier's comparative microlith typology clustered bar chart (Figure 18). Reynier argues that his data reflects a dominance of obliquely blunted points (1) complemented by triangles (3) and trapezoids (5) in the Star Carr type assemblages, obliquely blunted points (1) complemented by partially-backed points (2) with a small number of mixed other microlith forms in the Deepcar type assemblages, and finally hollow-based points (9) as being characteristic, supplemented with geometric forms (3 and 4 although traditionally 5 also fall into this category) for Horsham type sites (Reynier 2005, 24).

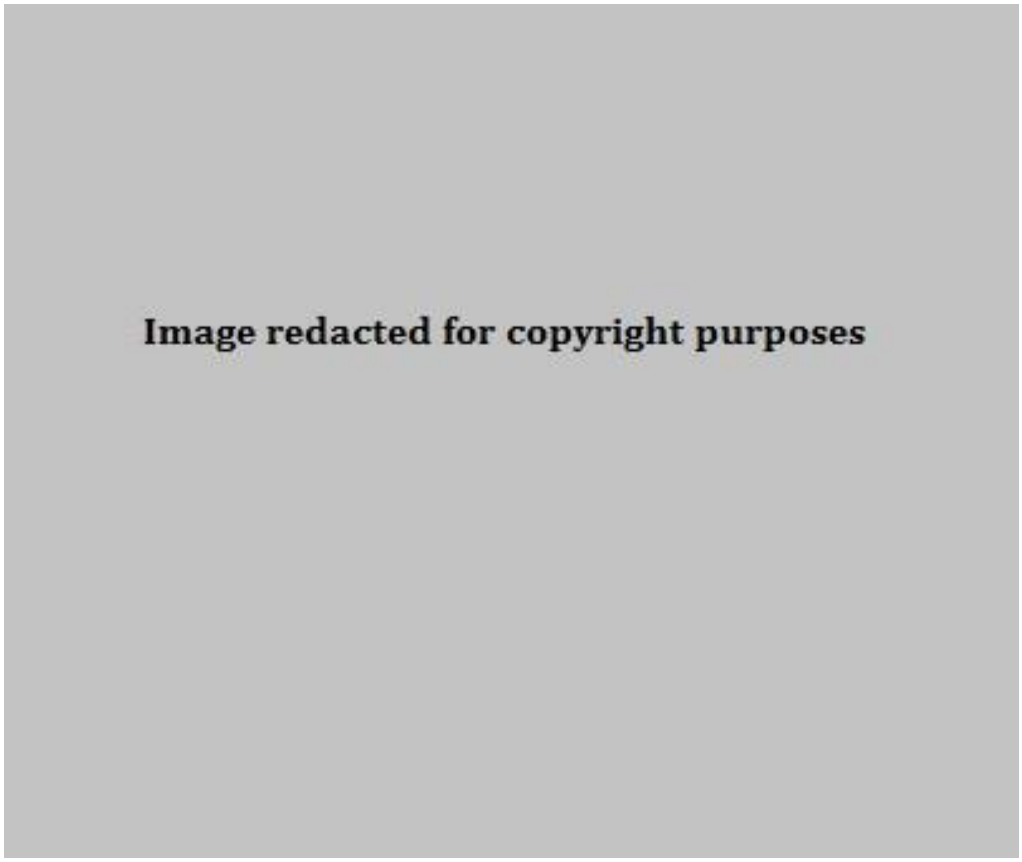

Figure 18. Reynier's comparative microlith typology clustered bar chart (2005, p.25). The typologies are: 1 – oblique points; 2 -partially backed points; 3 – triangles; 4 – rhomboids; 5 – trapezoids; 6 – backed points; 7 – transversely based points; 8 – obliquely based points; 9 – hollow based points; 10 – tanged points (2005, p.25)

While the clustered bar chart does reflect these points, these descriptions do not hold up as well comparing the individual site data. Of the three Star Carr type sites, oblique points represent a majority of 62.5% in the Thatcham III patinated series, consisting of 15 of the microliths; but 34.8% from Broxbourne 104 (n=8 microliths); and 26.2% from the site of Pointed Stone 3 (n=11 microliths) (Reynier 2005, p.25). While at Thatcham (patinated) and Broxbourne, the next highest percentages of any other microlith type are triangles at 8.3% and 13.0% respectively, at Pointed Stone 3 the second highest category consists of 7 trapezoid microliths making up 16.7% of the assemblage which is a slightly higher

percentage comparatively. Note, the total numbers of microliths at each site means that one microlith represents a significant percentage. These figures do support the overall picture of the Star Carr type assemblage as summarised above, but they also show there is a lot of variability in how these ratios are acted out which suggests any generalization needs cautious consideration. Compounding this, all three sites but particularly Broxbourne and Pointed Stone have very high proportions of the microlith assemblage categorised simply as 'fragments' which cannot be identified. In addition, theoretically, the different make up at Thatcham could relate to the fact that there is a Deepcar type site nearby: these sites or the other Thatcham microsites could have been dynamically related, as even if not contemporaneous, the potential for reuse of materials may have impacted the dynamics.

One particular point to note is that Reynier comments that "[c]ore tools usually include flake axes (not represented in the study assemblages)" (Reynier 2005, 22). This is a reminder of how utilising a small sample of sites from a specific geographical region and without consideration of site function is not an adequate sample for characterisation, as these samples are lacking a common tool type. As a result, Reynier is not as much questioning whether the type is a valid category with his research but more adding to the evidence already established in support of the distinction (and the same applies to his Deepcar and Horsham evaluations). This is not an invalid contribution to make to archaeological discourse: On the contrary, it is building the evidence for a particular theory and the detail he entered into is both necessary and time consuming so applying it more broadly would have taken longer than one PhD project (which is what the publication covers). Yet it is not the re-evaluation he implies in the introduction to the report. Instead he is categorising his sample of sites to fit with the traditional categories already posited by other researchers as discussed above and starting to tease out further nuances and a deeper look at them. However, these sites cannot be considered without the other historically studied sites which validates their being labelled as a particular type in the first place.

Reynier does draw on the range of different proportions of certain lithic forms in his definitions but in fact again this highlights the weakness of the small sample size he is drawing on. For example, for his Deepcar assemblages, truncated pieces make up 8 to 52% of the assemblage they come from (2005, pp.18 & 22). This is a very broad range, especially considering this is only across three sites. In fact the percentages are 51.9% (Iping Common), 8.1% (Marsh Benham), and 11.3% (Thatcham III) (p.20). There is no strong pattern or correlation. Then, if we consider the values for Star Carr type assemblages in contrast we get 6.9% (Broxbourne 104), 10.5% (Thatcham III patinated) and 30.4% (Pointed Stone 3). While these values are generally slightly lower, the ranges overlap significantly and the fact that the data is only from three sites per assemblage type means

that the trend is very weakly supported and is misrepresentative. Reynier's bar charts depicting the mean values do not show any representation for error or range either.

The final cautionary tale Reynier's typological data illustrates is that assemblages need to be evaluated for how complete they are i.e. whether the complete assemblage has been retrieved, whether the site was protected or disturbed, whether excavation technique would have omitted retrieval of certain finds. This may not always be able to be accurately estimated, but it should at least be taken into consideration. While there are occasionally 'characteristic' indicators of assemblage type, such as Horsham points, many of the attributes of the three assemblage types overlap, and the overlap does not just occur between, say, Star Carr and Deepcar and then Deepcar and Horsham but there is also overlap between Star Carr and Horsham. As such, the assemblage types are not as clear cut as Reynier's report and earlier research seems to suggest; the categories seem much more fluid. Great care needs to be taken in considering whether it is statistically justifiable to genuinely classify a site in this way and should probably be conducted on an individual site-by-site basis relating to the nature of activities that are suggested may be occurring on that site.

3.3.3 Chronological work

In addition to reviewing the Early Mesolithic assemblage types, Reynier created a catalogue of radiocarbon dates from sites across Britain which fulfil a set of preliminary criteria in terms of sampling standards, which ensures a certain degree of reliability (Reynier 2005, 65). These include pre-treatment to reduce the modern carbon signature; not being sampled in bulk (i.e. after the advent of Accelerator Mass Spectrometry methods); sampled from species with a short life-span (<20 years); being a discrete sample (single context, and "closely associated" with the stone assemblage); and finally, being humanly accumulated or "otherwise modified" sample to ensure the sample is not the result of a natural event. These criteria are thorough and promise improved measurements and more secure dating (cf. Bayliss 2015).

As a result, only dates on the following materials were included in his synthesis: modified bone, modified antler, modified wood, charred hazelnuts (which he acknowledges can be a natural occurrence) and mastics. Pre-treatment to negate the effect of exogenous carbon-14 that entered the sample from the burial environment, storage or conservation is considered a requirement of most modern procedures, and although the treatments themselves are variable the aim is for an uncontaminated sample as a common outcome (Bayliss 2015). Bulk samples pose problems because the larger the sample, the more likely you are to obtain a range of mixed dates (consider, for example, a sample of charred

hazelnut shells) and similarly with longer-lived species which can theoretically give you a range of readings if they lived their full expected lifespan before death. As lithics cannot be directly dated themselves, absolute dating can only be conducted on reliably associated organic material so setting a standard for this association is wise, as natural accumulations can occur independent of site activity and therefore within a different timeframe so they must be avoided.

However, there are certain issues with Reynier's selection. There are only 15 sites with radiocarbon dates fulfilling Reynier's strict criteria, and two of these are either 'Long Blade' or Later Mesolithic assemblage types utilised for comparison only. Again, as with the assemblage studies, this is a small sample size for extrapolating theory across Britain. This is, of course, but the nature of archaeological data availability. It must still be taken into consideration as an issue, however.

Unfortunately, the dates are presented as uncalibrated in the monograph. Calibration is something now expected from publications as a necessary stage of the interpretative process but it was not routine practice when Reynier produced his publication. The production rate of radiocarbon in the atmosphere varies through time. To get a representative calendar date from the radiocarbon measurements, the measured age has to be compared to measured ages of samples for which the actual age is known. Such samples may be available from tree rings, plant macrofossils, speleothems, corals and foraminifera (Reimer et al. 2013). For this purpose, several internationally agreed calibration curves have been produced from this natural record and are constantly being updated with new data (*ibid*.). Bayliss (2015) strongly recommends that both the uncalibrated and calibrated dates are published, as well as the error values and the unique laboratory identifier code for the sample as this would give both the means for a reader to update the calibrated dates as new curves are released but also gives the most realistic interpreted actual date for the time, as calibration can alter the date by several hundred years.

Reynier does not ignore the issue completely, however, and makes reference to work on calibration curves by Becker, Kromer and Trimborn (cf. Becker,Kromer and Trimborn 1991; Becker 1993; Kromer and Becker 1993). Through oak and pine tree ring analysis, these researchers identified a series of date plateaux taking effect in the Early Mesolithic, i.e. where the uncalibrated dates of samples read closely together but are in fact potentially separated by several centuries. These occurred at 10,000, 9600, 9200, 8750, and 8200 ^{14}C year BP, where radiocarbon dates of these values can represent a range of dates spanning up to 450 dendro (absolute) years (Becker,Kromer and Trimborn 1991, 648; Kromer and Becker 1993). These plateaux impact the interpretation of dates falling between them as well, for example the interval between the 10,000 and 9600 ^{14}C year BP plateaux could

represent a timespan a minimum of 90 to a maximum of 860 dendro years long (Becker,Kromer and Trimborn 1991, 648).

Reynier notes these four plateaux, or in his terminology 'compressions' (Reynier 2005, 66), but rather than calibrating individual dates, he attempts to use the plateaux as benchmarks for grouping the dates clustered between them and to discuss the potential for skewing. To facilitate this, he plots the radiocarbon (uncalibrated) dates on a timeline as a box and tail diagram (with the tails set at 2 standard deviations representing the probability error range) depicting the compression events with vertical lines (Figure 19). He then discusses how the data falls in relation to those plateaux lines, which is deceptive. Without calibrating the dates, which would take into consideration known plateaux within the curves utilised, the data points plotted are not actually representative of realistic dates which could be much closer together or further apart from each other. As such examining data groupings within this is not very meaningful. This is amplified by the fact that some of the dates' standard deviation tails cross the plateaux values (which would change their calibrated probability curve considerably).

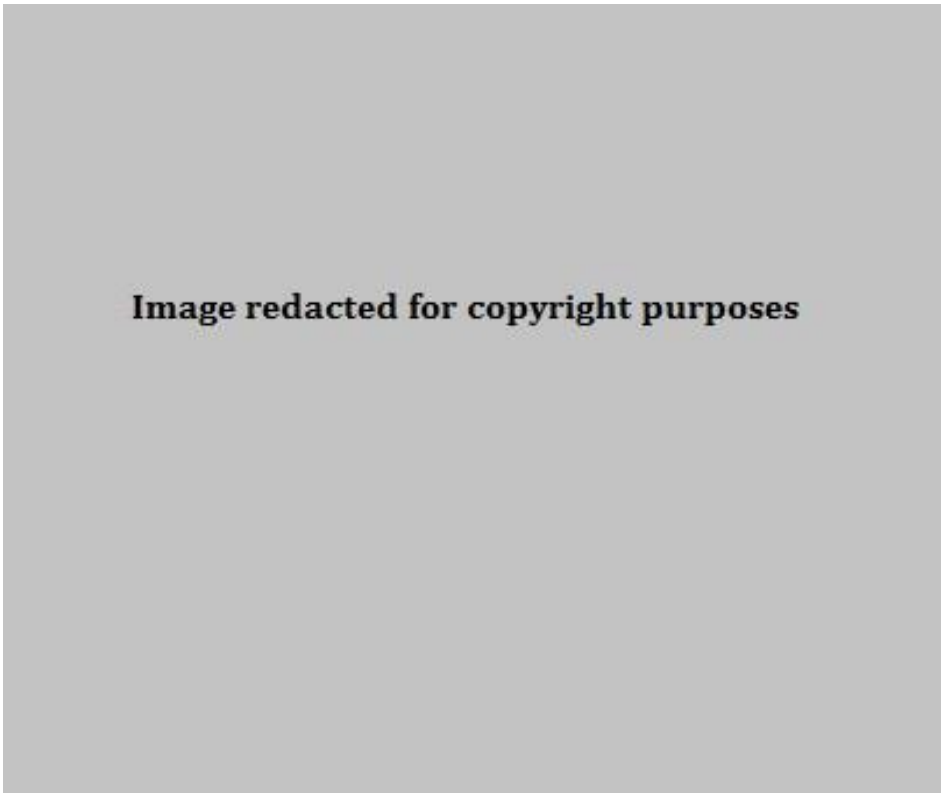

Figure 19. Reynier's box and tail diagram of British Early Mesolithic radiocarbon dates. The dates are uncalibrated, arranged in their chronological order with the tails set at 2 standard deviations (s.d.). The dashed vertical lines indicate the dating plateaux (2005, p.69)

Furthermore, these specific methodological issues are compounded by more general ones. Reynier discusses some data fitting the general trend shown better than others and therefore the trend fitting dates possibly being a 'better indication' of that portion of the Early Mesolithic (p.66). Any trend seen here though is only based on 27 data points, and

while as archaeologists we often accept that a larger sample size is simply not available, this does impact the reliability of the analysis (N.B. one of these points, labelled OxA-1135, is also from an unknown site as this lab code is actually assigned to a date from Upper Palaeolithic German site, checked against Baales 2006). Some of these dates also relate to the same site and therefore lithic assemblage overall, so the question arises as to whether it is acceptable to compare these as individual data points as they come from a specific context, in terms of both society and environment, which might influence the type of lithic assemblage produced. Their inclusion as separate data points will skew the overall interpretation to reinforce a *chronological* pattern to lithic assemblage production which may in fact be more of a *contextual* one.

There is also the issue that the size of a site is not consistently considered so one value is a single date taken from an anthropogenic deposit on a site that could have been occupied anywhere from a few hours to several generations. Reynier does include multiple dates from some sites, such as Star Carr, but he does not discuss an active method of engaging with this factor where multiple dates are not available. Consideration of this is most crucial during calibrations because the shorter lived a site is, the proportionately greater the scatter of probability surrounding the actual date and duration of the original event (Bayliss 2015). For the most realistic interpretation of a site's date range, when there are multiple dates from individual sites, these need to be considered together to also take into account the relationships between samples which is typically conducted using Bayesian chronological modelling. The association of those particular dates to a particular typology still stands.

Finally, Reynier does not discuss $\delta^{13}C$ values for the radiocarbon dates he accepts for his study, or whether he accepts samples where this value could not be taken (due to sample size or lab facilities). This value allows correction for fractionation which can enhance or deplete heavier carbon isotopes i.e. ^{13}C and ^{14}C relative to the lighter ^{12}C isotope which can skew the measured date, a quality check on the radiocarbon age which needs to be qualified against consideration of the method used to obtain the $\delta^{13}C$ value, and a check for potential reservoir effects influencing the sample, although all the data Reynier utilises are from terrestrial plants or animals that consume terrestrial sources so this data will not be impacted heavily by this factor if at all (for further discussion see Bayliss 2015).

Setting these methodological issues aside, calibrating the dates raises the most problematic issue of all. Figure 20 shows the dates having been calibrated in OxCal v4.2.4, using the IntCal13 atmospheric curve. Table 6 provides the data.

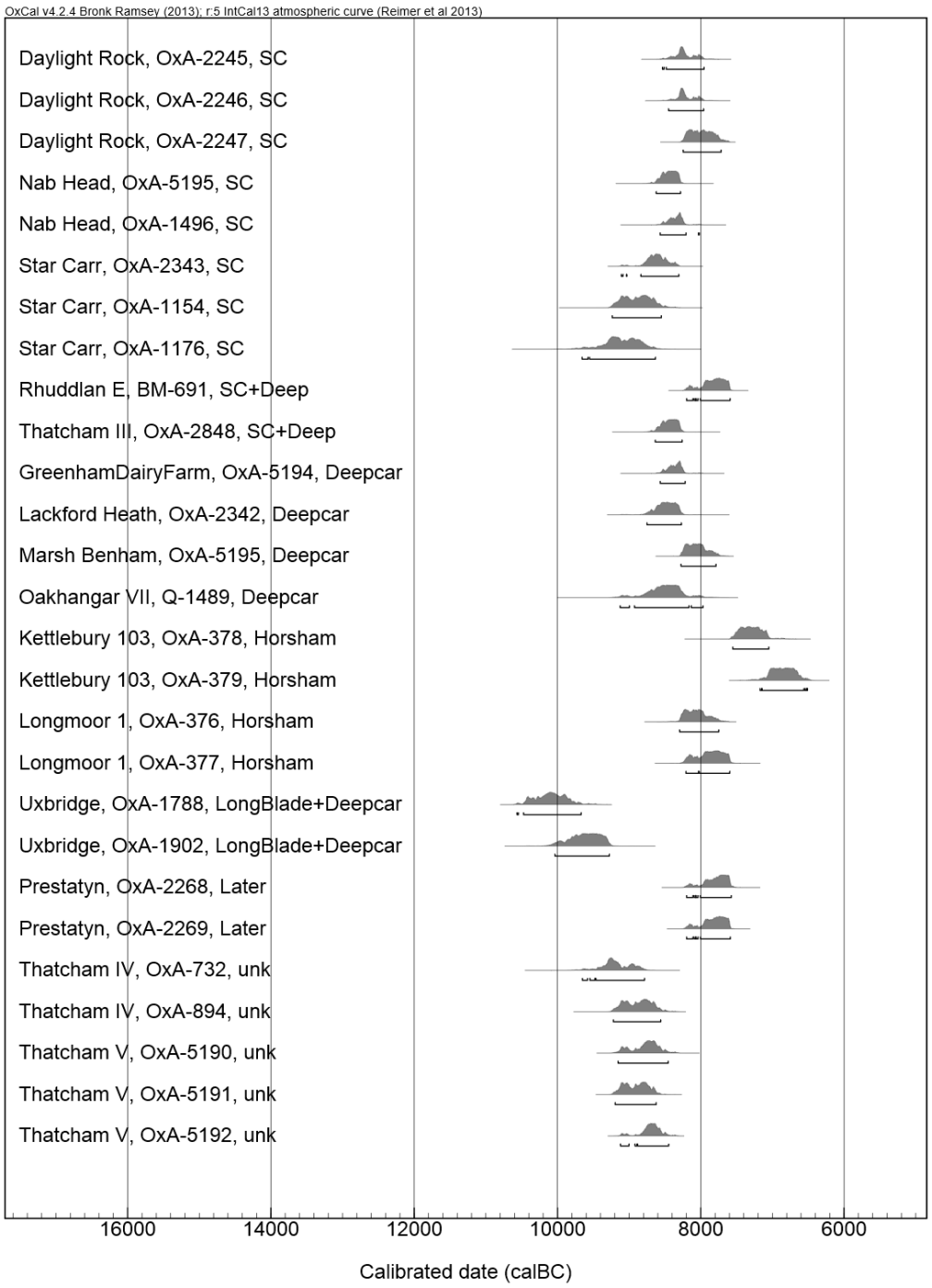

Figure 20. The dates utilised by Reynier having been calibrated in OxCal v4.2.4, using the IntCal13 atmospheric curve. The site, date identification code, and site types are appended as the labels.

Table 6. Reynier's dates, information, and the calibrated values (dates sourced from Reynier 2005; calibration by C. Rowley)

Site	Lab no.	Sample	Uncal. year bp	Error +-	from cal BP	to cal BP	%	from cal BC	to cal BC	%	Lab
Daylight Rock	OxA-2245	Charred hazelnut	9040	90	10410	9910	100	8460	7960	100	Oxford RCAU
Daylight Rock	OxA-2246	Charred hazelnut	9030	80	10370	9910	100	8420	7960	100	Oxford RCAU
Daylight Rock	OxA-2247	Charred hazelnut	8850	80	10210	9600	100	8260	7650	100	Oxford RCAU
Greenham Dairy Farm	OxA-5194	Charred hazelnut	9120	80	10510	10170	100	8560	8220	100	Oxford RCAU
Kettlebury 103	OxA-378	Charred hazelnut	8270	120	9530	8990	100	7580	7040	100	Oxford RCAU
Kettlebury 103	OxA-379	Charred hazelnut	7940	120	9130	8450	100	7180	6500	100	Oxford RCAU
Lackford Heath	OxA-2342	Resin block	9240	110	10710	10200	100	8760	8250	100	Oxford RCAU
Longmoor 1	OxA-376	Charred hazelnut	8930	100	10250	9680	100	8300	7730	100	Oxford RCAU
Longmoor 1	OxA-377	Charred hazelnut	8760	110	10200	9530	100	8250	7580	100	Oxford RCAU
Marsh Benham	OxA-5195	Charred hazelnut	8905	80	10240	9690	100	8290	7740	100	Oxford RCAU
Nab Head	OxA-1495	Charred hazelnut	9210	80	10590	10220	100	8640	8270	100	Oxford RCAU
Nab Head	OxA-1496	Charred hazelnut	9110	80	10500	10170	100	8550	8220	100	Oxford RCAU
Oakhangar VII	Q-1489	Charred hazelnut	9225	170	11070	9940	100	9120	7990	100	Cambridge
Rhuddlan E	BM-691	Charred hazelnut	8739	86	10160	9530	100	8210	7580	100	British Museum
Star Carr	OxA-2343	Resin 'cake'	9350	90	10770	10260	100	8820	8310	100	Oxford RCAU
Star Carr	OxA-1154	Antler frontlet	9500	120	11200	10430	100	9250	8480	100	Oxford RCAU
Star Carr	OxA-1176	Worked antler	9700	160	11610	10580	100	9660	8630	100	Oxford RCAU
Thatcham III	OxA-2848	Resin on flake	9200	90	10590	10200	100	8640	8250	100	Oxford RCAU

Site	Lab no.	Sample	Uncal. year bp	Error +-	from cal BP	to cal BP	%	from cal BC	to cal BC	%	Lab
Thatcham IV	OxA-732	Worked antler beam	9760	120	11410	10750	100	9460	8800	100	Oxford RCAU
Thatcham IV	OxA-894	Burnt elk antler	9490	110	11190	10440	100	9240	8490	100	Oxford RCAU
Thatcham V	OxA-5190	Cut-marked bone	9430	100	11100	10410	100	9150	8460	100	Oxford RCAU
Thatcham V	OxA-5191	Cut-marked bone	9510	90	11180	10550	100	9230	8600	100	Oxford RCAU
Thatcham V	OxA-5192	Cut-marked bone	9400	80	11070	10410	100	9120	8460	100	Oxford RCAU
Prestatyn	OxA-2268	Charred hazelnut	8700	100	10160	9520	100	8210	7570	100	Oxford RCAU
Prestatyn	OxA-2269	Charred hazelnut	8730	90	10160	9530	100	8210	7580	100	Oxford RCAU
Uxbridge	OxA-1788	Horse molar	10270	100	12420	11620	100	10470	9670	100	Oxford RCAU
Uxbridge	OxA-1902	Horse mandible	10010	120	12040	11200	100	10090	9250	100	Oxford RCAU

Based on the calibrated data for the sites Reynier considers in his chronological model, withstanding the fact that this is not a fully specified Bayesian model, the date ranges for the Star Carr and Deepcar type sites overlap significantly, although the Deepcar dates tend to range slightly later and some overlap Later Mesolithic sites. The Horsham sites overlap Deepcar and Later Mesolithic.

Regardless, Reynier did propose a relative chronology of types of assemblages based on the uncalibrated, but plateaux grouped, dates. His work illustrates how troublesome categorising lithic assemblages truly is. Lithic analysis is so time consuming that it cannot easily be applied by one researcher consistently across a decent sample of sites, across different geographical regions. Reynier went to significant and admirable lengths to characterise his sites in detail and also to collate data from other sites, but it was not enough for an adequate sample to truly test the groupings. The other issue is whether approaching lithic assemblages with an emphasis on distinguishing their cultural groupings is an appropriate method: If Deepcar reflects a culture in its traditional sense, a body of people with shared traditions using those sites, is a Deepcar hunting camp similar enough to a Deepcar base camp (assuming those activity interpretations are valid in the first place) that it is clear enough to distinguish those sites from Star Carr comparisons? This major issue was compounded in Reynier's work by building a chronology based on uncalibrated dates. Conneller et al. (2016) stepped up to address this last issue in a more recent paper that will lastly be addressed.

3.4 Recent research on Early Mesolithic Chronologies

Conneller (2000) addressed the question of chronology within her doctoral thesis specifically relating to the Vale of Pickering. She drew on the radiocarbon dating and environmental evidence as Reynier would in his later work utilising the southern assemblages. The same dating plateaux/compressions affect the Vale of Pickering Early Mesolithic dates as much as anywhere else. In addition, many of the radiocarbon dates for Northern England produced large standard deviations (Conneller 2000, 106). In terms of sample selection, submerged aquatic plants from palaeolake Flixton will have been affected by a reservoir effect caused by their taking on carbon from the carbonate-rich deposits that formed the lake basin (Day 1996; Mellars and Dark 1998). As of 2000, a number of radiocarbon dates had been determined for sites in the Vale linked reasonably securely to human activity. As such, originally Conneller argued that for the north of England, the combination of large standard deviations, the dating plateaux, and the lack of well-associated material meant the chronology of lithic variations (between Deepcar and Star

Carr material) was undeterminable (2000, p.110). This was further compounded by the even smaller sample size within the constraints of the Vale of Pickering itself.

As part of the response to this, the POSTGLACIAL project, working with Alex Bayliss of Historic England, incorporated a thorough program of dating sites across the Vale to build a more extensive corpus of dates, including dates from both Star Carr and Flixton Island 2. A refined typochronological Bayesian model, published in 2016, was then developed incorporating the new calibrated dates, along with dates from other sites including some of those considered by Reynier and Jacobi (Conneller et al. 2016). The dates covered Long Blade, Star Carr, Deepcar, basally modified and small scalene triangle (start of the Late Mesolithic) assemblages. Bayesian modelling allows for a more detailed consideration of the probability of calibrated dates to be accurate, in incorporating probability curves and degrees of confidence into the model (Conneller et al. 2016, 4). Replicated measurements of some dates were incorporated into the model as weighted means as well, theoretically improving the precision of the date (*ibid*.). 305 measurements were included in the modelling, and although 200 of these were from the model for Star Carr, the outstanding 105 samples alone is a much larger sample than Reynier's had been and is a much stronger starting point (*ibid*.).

Stringent criteria for accepting dates for incorporation into the model, which covered the caveats outlined by Reynier, were applied (Conneller et al. 2016, 4): samples of short-lived material (whether single-entity or bulk) that can be clearly associated with a particular microlith form were fully included in the model; samples that might include a component of material that could have had an age-at-death offset (most commonly unidentified charcoal) were included as termini post quos for the associated lithics; samples of peat that probably contained a component of aquatic plant macrofossils that might have incorporated hard-water error were included as termini post quos; samples that are not directly associated with particular lithic forms but which stratigraphically underlie them were included as termini post quos constraints on the calibration of dates that are directly associated with the lithics; samples of short-lived material that are not directly associated with particular lithic forms but which stratigraphically overlie them are included as termini ante quos constraints on the calibration of dates that are directly associated with the lithics; a number of the dates were omitted as potentially inaccurate as well, e.g. if they were considered accidental modern intrusions.

Overall, this provides the best model to date of the chronologies. The models for the currency of Star Carr, Deepcar, and basally modified type assemblages are reproduced in Figure 22, Figure 21 and Figure 23. Each distribution represents the relative probability that an event occurs at a particular time. Two distributions per date were plotted by

Conneller at al.: one in outline, which is the result of simple radiocarbon calibration, and a solid one, based on the chronological model used. Distributions other than those relating to samples correspond to aspects of the model. For example, the distribution 'start long blades' is the estimated date when long blades were first used in Britain. Measurements followed by a '?' have been excluded from the model for reasons described in the text. The large square brackets down the left-hand side along with the OxCal keywords define the overall model exactly (red: excluded from model; grey: TPQ possible old-wood effect or hard-water error; blue: TPQ/TAQ stratigraphic constraint; red: excluded from model). As summarised by Conneller et al. (2016), the model suggests that:

> "Star Carr-type assemblages first appeared in *9805–9265 cal BC (95% probability; start Star Carr-type…*), probably in *9495–9290 cal BC (68% probability)*. Star Carr-type assemblages disappeared in *8230–7520 cal BC (95% probability; end Star Carr-type…),* probably in *8165–7835 cal BC (67% probability)* or *7830–7815 cal BC (1% probability)*" (Conneller et al. 2016, 6).
>
> "Deepcar type assemblages first appeared in *9460–8705 cal BC (95% probability; start Deepcar-type…),* probably in *9090–8775 cal BC (68% probability)*. Deepcar-type assemblages disappeared in *8200–7240 cal BC (95% probability; end Deepcar-type…),* probably in *8075–7620 cal BC (68% probability)*" (Conneller et al. 2016, 7).
>
> "[B]asally modified microlith-type assemblages first appeared in *9280–8305 cal BC (95% probability; start basal modified…*), probably in *8690–8335 cal BC (68% probability)*. Basally modified microlith-type assemblages disappeared in *7030–5845 cal BC (95% probability; end basal modified…*), probably in *6960–6460 cal BC (68% probability)"* (Conneller et al. 2016, 8).

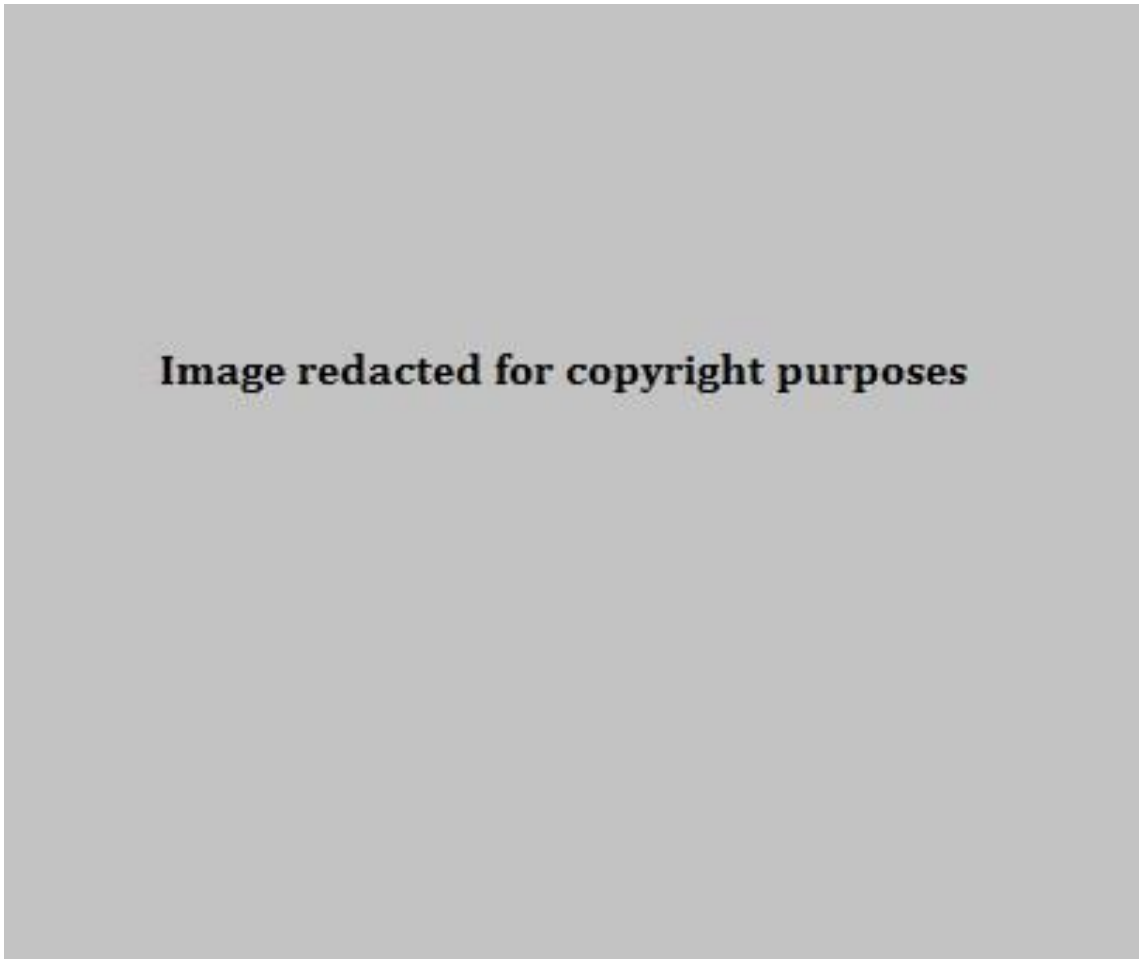

Figure 21. Probability distributions of radiocarbon dates associated with Star Carr-type microlith assemblages (Reproduced from Conneller et al. 2016, p.6.)

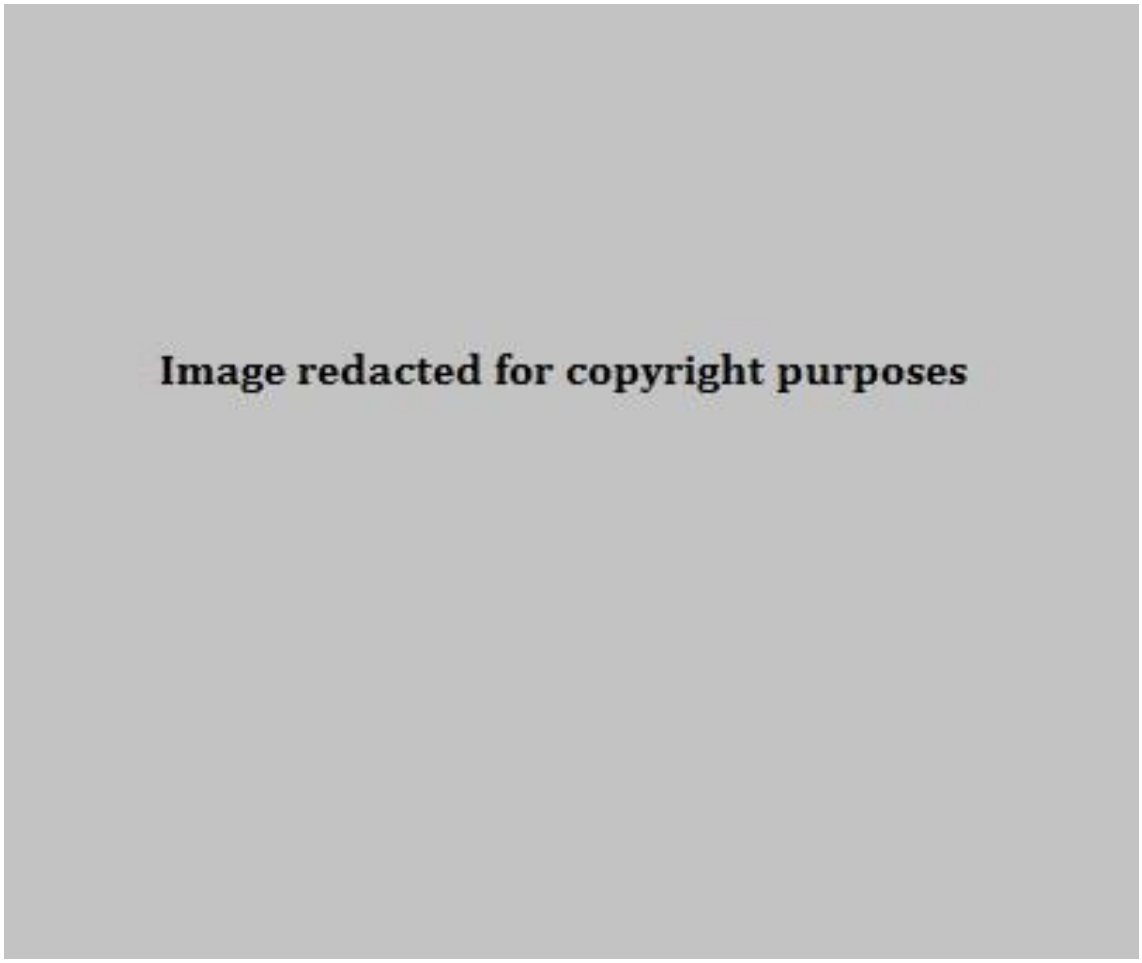

Figure 22. Probability distributions of radiocarbon dates associated with Deepcar-type microliths assemblages (reproduced from Conneller et al. 2016, p.7).

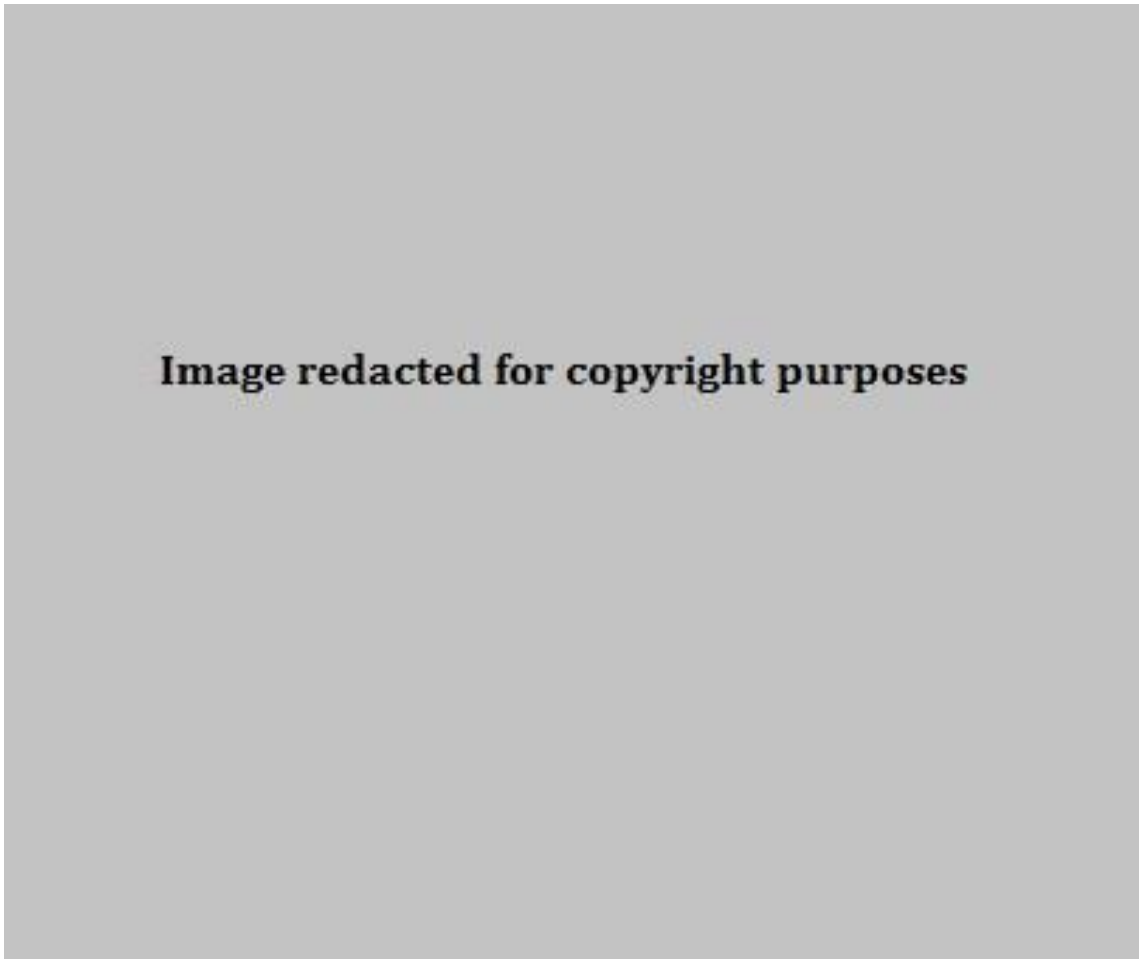

Figure 23. Probability distributions of radiocarbon dates associated with Basally Modified microliths (reproduced from Conneller et al. 2016, p.8).

Considering these dates, there is a significant overlap between the probabilities of the usage of Long Blade, Star Carr and Deepcar type assemblages. Conneller and Higham (2015) had previously proposed a gap between Long Blade and early Mesolithic cultures, but this more recent model allowed for better quantification of uncertainties. Figure 24 summarises the results of the model (Conneller et al. 2016, 10). On the basis of the recent model, Long Blades are highly likely to have appeared earliest, Star Carr material next earliest, and "it is *80% probable* that [Long Blades] continued in use after the first appearance of Star Carr type assemblages" (their italics), if only for a relatively short period of several centuries. However, this is only based on the dates from two Long Blade sites, Flixton Island 2 (Flixton II) and Three Ways Wharf, Uxbridge. If they reconfigure the model to incorporate the Long Blade dates from Flixton Island 2 as being from one hunting event, the gap is reestablished, with only a 39% probability that there is an overlap between them. This illustrates how the lack of dates available from sites and how the scant few dates available are integrated into models can have a significant bearing on modelling the relationships between cultural

groupings, and Conneller et al. (2016) acknowledge that the interpretation here remains open.

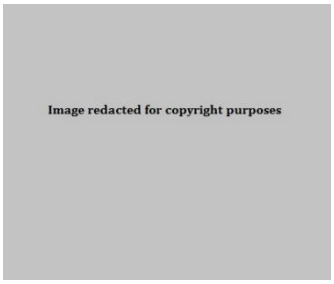

Figure 24. Summary of the use of Early Mesolithic assemblage types as proposed by Conneller et al. The shading reflects the probability that an assemblage type was in use at a particular time (reproduced from Conneller et al. 2016, p.10).

As such, Conneller et al. (2016) consider the potential of a gap between Long Blade and Star Carr type material specifically, and the best specified model presented suggests that there is an overlap between the two cultural groupings. They then go on to consider how it is 95% probable based on their model that Deepcar type assemblages appeared later than Star Carr type assemblages, but 100% probable that Star Carr and Deepcar type assemblages overlapped in use. This does fit with Reynier's generally proposed patterning. However, of specific interest to Flixton Island 2 and this project, is the potential for overlap of Long Blade and Deepcar type assemblages. It is not impossible that the relationship between Long Blade and Star Carr, and Long Blade and Deepcar type assemblages was subtly different. Star Carr type assemblages may have been developed by a different group of people, or for fulfilling a particular niche or function, that came into use and ran parallel to Long Blade sites; however, if there is a more significant gap or at least smaller overlap between Long Blade and Deepcar sites, there is a possibility that Deepcar sites were what replaced or took over from Long Blade sites. As such, then Star Carr and Deepcar run parallel to each other instead, as they appear to do based on the Conneller et al model. This is not to suggest that Deepcar sites would have the same functionality as Long Blade sites, but rather that there is a possibility that whatever made Long Blade technology go out of production may have equally driven the innovation of Deepcar type assemblages, with Star Carr type assemblages being produced for separate but still potentially related reasons of their own.

Finally, there is a significant overlap of basally modified sites with the later Star Carr and Deepcar dates, which shows that these were potentially appearing quite early. They also appear to last a longer time than the other two kinds of Early Mesolithic sites, based on the dates in this model.

3.5 Summary

This chapter has demonstrated how both the typologies and the chronologies of Early Mesolithic microlithic cultures are not clear cut but still ambiguous, even given the rigorous

modelling demonstrated by Conneller et al. Far from laying the sequencing to rest, this model incorporating a large sample of dates on well-sampled material has confirmed the significant overlap of these types of assemblage. This again raises the issue of how well sites fit into these categories and ultimately of how these assemblages should be interpreted. The next chapter will report the findings of the lithics analysis at Flixton and consider how well they sit within this framework as well.

Chapter 4 The Lithics Assemblage from Flixton Island 2

4.1 Introduction

The POSTGLACIAL excavations were conducted with an emphasis on 3D recording of the spatial distribution of the lithic assemblage. This methodology follows on from previous work at the site and in the Vale of Pickering (Moore 1950, 1954; Conneller,Little and Birchenall 2018; Conneller et al. 2018) but also fits particularly with this project's aim to identify potential activity areas. This was facilitated by EDM-based 3D locating of the in situ finds, thorough sieving by grid square so as not to lose resolution completely on ex situ finds, and retaining spall material smaller than 'fingernail size' as advocated by Conneller for Star Carr. This approach proved highly fruitful at Flixton in yielding a much larger assemblage of microliths and microburins, as well as smaller contributions of other finds, than would otherwise have been obtained. In addition, this yielded high-quality data for spatial analyses. This chapter presents the results of the typological and basic technological analysis of the lithics assemblage.

During the most recent excavations, Flixton Island 2 yielded 20,191 knapped lithic artefacts generally from two traditionally defined cultural groupings: Long Blade Late Palaeolithic and Early Mesolithic material. Within this, there is one identified possible Federmesser backed/shouldered point. This total does not include the coarse stone assemblage, which was not studied as part of this project. In contrast, the excavations at Star Carr by both Clark and the POSTGLACIAL Project retrieved a combined total of 41,820 lithic artefacts, however this was over a much larger area (Clark 1954, Conneller et al. 2018). Most of the Early Mesolithic material was very densely deposited on the dryland areas of the island which seems to have been a hot spot for activity within the landscape, considering the size of the assemblage across such a small space. This also makes it more likely for scatters from different times to overlap. The lithic assemblage excavated during the POSTGLACIAL project, including the material from both time periods, was analysed as part of this thesis. The Long Blade material and the Federmesser point will be summarised here but explored in more detail in a separate publication (Conneller & Rowley, in prep). The Early Mesolithic assemblage will be the main focus of this chapter because this is the material that overlaps with the geochemical soil sampling on the dryland.

It was clear during excavation (and can be seen on the plots in Figure 25) that the full extent of the dryland occupation of the site had not been excavated, as is often the case with Mesolithic sites. This area yielded such a large number of finds that potential activity areas can be discussed but this will not necessarily represent all of the activities that took place on the island.

Figure 25. All 3D located lithics across the site, symbolised by classification as Long Blade/Federmesser or Mesolithic.

4.2 Methods

4.2.1 General methodology

The full lithic dataset is provided in digital format on the associated media. Lithics were catalogued largely following the method employed by Conneller at Star Carr and other Vale

of Pickering sites (Conneller 2000; Conneller et al. 2018). This was carried out in order to facilitate easier comparison of the sites in the Vale for purposes of contextualization. Conneller's original method had been based on the typological system proposed by Healy (Healy 1988), Jacobi's microlith types (Jacobi 1981 as cited in Conneller, Little, Garcia-Diaz, et al. n.d.; and as described in Butler 2005), and burin types by Inizan et al. (Inizan et al. 1992 as cited in Conneller, Little, Garcia-Diaz, et al. n.d.). The recording for Flixton incorporated additional attributes about the condition of the material given the specific patination and staining seen on the assemblage. "Prehistoric Flintwork" by Butler (2005), "Technology and terminology of Knapped Stone" by Inizan et al. (1999), "Stone Age Reference Collection (SARC)", and the accompanying website, by Grace (2012), and Reynier (2005) were used as general references throughout.

Attributes were initially recorded in Excel, then integrated as point data in ArcGIS using the 3D locations where known, or incorporated into weighted point centroids where known by grid square. The EDM used was a Leica TC705 which records 2mm + 2 ppm on the Infrared Fine setting, though this does not allow for human error introduced by utilising a reflective staff (e.g. if the reflector staff was at a slight angle). Pieces which did not have 3D locations because they had been found in the sieve or unstratified, were largely from known grid squares and contexts and included in tallies accordingly.

4.2.2 Recorded attributes

The following attributes were recorded for every 3D located artefact (also see Appendix Two for a full listing and the glossary for quick definitions):

- Find number as a unique identifier: Find numbers are six-digit numbers for individual finds recovered during trowelling, while any non-debitage sieve or spall lithic finds were assigned a unique identifier prefixed with "sl/" and the numbered sequentially starting at 1. Occasionally trowelled finds were bagged together: In those cases, the find was designated a new six-digit number during post-excavation, though the original number was recorded in the catalogue in the notes section, and the 3D location data was duplicated for that new entry.
- Known location information including site, trench, context, x, y, and z coordinates, any notes from the field including orientation, and also storage location during post-excavation.
- Quantity in the bag (refitting finds located together were treated as one find but the quantity here showed how many refitting pieces were associated with that find number).

- Completion of the piece (i.e. proximal, proximal-medial, medial and so on; tip, medial and base were used for microlith recording).
- Typology (each piece was assigned a general type classification and where appropriate a subtype).
- Whether manufactured on primary or secondary removal debitage.
- Whether modified (e.g. crested).
- Macroscopic wear, damage, and residues.
- Whether burnt or heated.
- Length and width for complete pieces, plus thickness for cores and unusual tools (if noticeably thick).
- Cortical extent (rated from one to five on basis of how many fifths of the piece's surfaces were covered by the cortex).
- Raw material details including material (e.g. flint, quartz) and source (e.g. Wolds, where it was possible to suggest).
- Colour, inclusions and translucency.
- Notable patination or staining (the entire assemblage was stained orange or brown to varying degrees, only notably different patination or none was noted).
- Refit information (only sporadically attained through my own project, supplemented by the undergraduate dissertation work by Bethany Nash at the University of York).
- Additional notes (including a record of whether pieces had been examined by Chantal Conneller, Aimée Little, or Shannon Croft to check attribution of tool types, peculiarities, microwear, and potential residues).

For 8534 of the sieve lithics, a more compact form of recording was used to ensure all could be examined within the timeframe of the PhD. In these cases, the colour, inclusions and translucency were not included and only very notable, non-modern, potential macrowear and very notable patination were recorded, while modern damage and weathering would not be recorded as it was present on many of the pieces. For these sieve lithics, the dimensions of complete debitage pieces were not measured. However, complete tools were still measured, being in much smaller numbers in the assemblage overall. The other attributes were still recorded.

It should be noted that it was challenging to categorise the flint due to the weathering and patination and therefore much of the time the material could not be attributed to till flint, Wolds flint, or flint from other sources. Don Henson's raw materials reference collection was utilised for comparison (cf. Henson 1982). Where raw material type was assigned, this was usually based on the opacity and inclusions in the flint with some consideration of the cortex type.

4.2.3 Categories

Table 7 summarises how catalogued lithic finds, having been typologically and technologically catalogued, were subsequently grouped into categories for analysis and visualisation. Categories were prioritised from top to bottom of the table (i.e. if an artefact might have fallen into two categories then it was placed in the category higher up in the table). Each category was paired up with an associated "possible" category that was for pieces that potentially fell into that category but there was ambiguity in their identification e.g. a piece catalogued as "nodule chunk / possible core fragment" was catalogued as "possible core technology". This acknowledged these pieces were potentially more than they seemed but allowed them to be clearly segregated.

Table 7. Lithic artefact categories employed during this study

Category	**Finds Included**
Microliths	Complete and partial microliths, and backed bladelets.
Microburins	Successful and attempted microburins.
Removed tools	All non-core tools (burins, scrapers, piercers etc.) and partials thereof that are not microliths, supplemented with denticulated, truncated, backed, notched, and otherwise retouched debitage that did not fall into a classical tool category. Possible tools included possibly denticulated, retouched, notched, backed pieces.
Core tools	Axes/adzes, preforms, core tools, strike-a-lights.
Tool debitage	Burin spalls, re/sharpening flakes (all tools).
Core technology	Cores, core fragments.
Core preparation	Platform rejuvenation debitage, core tablets, flancs de nucléus. Plunging debitage was included in the "possible core preparation" category.
Crested / possibly crested	Isolated, as cresting could be to facilitate a longer debitage piece either for the benefit of knapping, with the aim of producing a longer piece, or with the aim of rejuvenating a platform.
Possibly utilised debitage	Any debitage possibly utilised but not modified into tools specifically.

Category	Finds Included
Core initiation debitage	Primary (one face >95% covered in cortex) and secondary core reduction debitage (with one face partially but <95% covered in cortex) not obviously utilised. Pieces that could have been secondary or tertiary pieces, catalogued as "2 - 3" for reduction stage in the catalogue, were placed into the "possible core initiation" category. This classification was usually because they were small pieces with a little cortex so while formally secondary pieces they were evidently not for removing significant swathes of cortex, or perhaps were fragments and therefore it was unclear whether they were secondary removals or not.
Possibly burinated	These are pieces with removals creating a full or partial cross-section through the piece from dorsal to ventral (usually) in some way, which were not obviously burins or utilised but had the potential to be irregular burins, unsuccessful burins, or simply burinated through use or otherwise accidentally.
Core reduction	Tertiary debitage not obviously utilised but appear humanly knapped. Tertiary / unknown ("3 / unknown" reduction stage) debitage was included in the "possible core reduction" category. As such, this could contain not just intentional core reduction debitage flakes, blades and bladelets but also incidental debitage chunks and chips.
General debitage	Debitage with an unknown reduction stage and not obviously utilised but shows signs of being humanly worked.
Possible debitage	Nodule chunks with no clear further working, lithics that were possibly natural or possibly debitage, and heat spalls.

4.2.4 Phasing

4.2.4.1 Overview of phasing

In order to tease out generic debitage that may be Long Blade rather than Mesolithic, the contexts were used as a starting point, particularly in the wetland areas of site where stratigraphy was better differentiated. Trench contexts were phased into four main categories by the POSTGLACIAL team: Long Blade (LB), Redeposited Long Blade (RLB), Mesolithic (M), and post-Mesolithic. Some contexts were unassigned as they potentially contained mixed Palaeolithic, Mesolithic and/or more modern material. Others were unknown as they could have been redeposited material from any other context (e.g. molehill finds).

4.2.4.2 Long Blade phase

This phase occurs mainly in the wetland area of the site. The Long Blade contexts are very distinctive. At the base, there is a lower layer of organic mud which contained significant quantities of bone, mainly horse but some red deer (Knight, in prep.), and which correlates with Moore's 'Horse Layer'. A little under a third of the Long Blade assemblage was located in this layer (see Table 8). On the surface, horse hoof prints were identified in the muds, having been filled in by sands and gravels from an overlying sediment. A flake fragment was found when removing sediment (context 1248), from the cut of a hoof print. Moore found a flint blade and a shouldered point in this Long Blade layer (see chapter one).

Bands of the sands and gravels appear to have been washed over the muds. Within them, samples of redeposited bone and lithics were found, similar to the scenario found by Moore. The interpretation is that these have been washed down with the sands and gravels too and, although they are not in situ, they would have been deposited during the Long Blade occupation of the site. The majority of the Long Blade lithic material came from these redeposited contexts.

One further piece from the wetland, a distinctive Long Blade, was found on the spoil heap from trench 1 with sands and gravel adhering to it. Finally, there was also a small number of identifiably Long Blade or possible Long Blade finds, based on technological features, from the dryland and Mesolithic or unassignable wetland contexts. The Long Blade assemblage was supplemented by one possible Federmesser (i.e. Upper Palaeolithic; slightly earlier than Long Blade chronology) piece found in the topsoil in dryland trench 9.

Table 8. Summary of Long Blade assemblage finds by context groups

Context	Long Blade Finds
Long Blade contexts	17
Redeposited Long Blade contexts	35
Dryland till	3
Dryland topsoil	1 (+ 1 Federmesser)
Total	**56 (+ 1 Federmesser)**

4.2.4.3 Early Mesolithic phase

There are Mesolithic contexts in all trenches across the site, but the dryland contexts were largely dominated by technology usually associated with the Mesolithic (see Table 9). The dryland trenches were relatively shallow with the dominant contexts being: (1000) topsoil; (1119), a very thin "interface", an indistinct boundary layer of mixed lower topsoil and till,

which was not always easily distinguishable from the topsoil as the colour and texture change was so gradual; and the clayey till itself (1059). It is in the mixed interface layer that the lithic finds were considered to be closest to their original deposition, based on the finding of several axe/adzes or preforms here which do not usually travel far. However, all the finds are assumed to have moved around to some degree, particularly vertically given the presence of fine plant roots, animal burrows and high worm counts. The degree of homogenisation of the patterning of the lithics and geochemical signatures will later be used to discuss the potential degree of disturbance. These main contexts were supplemented by various 'feature' fills thought to be either Mesolithic or natural.

Above the sands and gravels in the wetland trenches, peat has formed and within this is Mesolithic lithic material. This was a much smaller quantity of artefacts than those from the dryland contexts. In addition, a small number of lithic artefacts were found in gully contexts. Bone which was found in the gully deposits has been dated and is Early Mesolithic in date. The material from the gully is likely to be material from the dryland site that had rolled downslope. It will be compared to the Mesolithic phase material.

The debitage pieces from the dryland contexts were assumed to be Mesolithic rather than Long Blade, although with further refitting and more detailed technological analysis it is possible that more of the material could be assigned to the Long Blade occupation. Where in doubt, lithic artefacts were treated as belonging to the Mesolithic phase, rather than the Long Blade phase. There was no suggestion of Neolithic or later lithic artefacts except for one flake fragment from the topsoil in trench 11, <sl/331>, that looked like a gunflint (similar to others that have been previously found elsewhere in the Vale according to Chantal Conneller (pers. comm, 2017).

Table 9. Summary of the Mesolithic assemblage by context groups

Contexts	Mesolithic finds
Dryland contexts	19827
Wetland contexts	337
Dedicated gully contexts	31
Unknown contexts	139
Total	**20334**

4.2.5 Issues

Unlike at Star Carr, microwear analysis conducted by Aimée Little was unfortunately largely unsuccessful in the pilot study on dryland lithics due to the heavy patination, weathering,

and iron staining of the assemblage which masked or removed the relevant attributes, had they ever been there initially (see Figure 26). Shannon Croft's pilot study of 12 pieces for residue analysis at Flixton yielded information on the natural processes occurring on site but no supplementary evidence for anthropogenic processes (Croft 2017). The staining and patination also made identification of the raw material difficult for Flixton Island. Chantal Conneller and Don Henson were consulted, having greater experience with the materials used in the Vale and North East of England, and after looking at a sample of the 2012 cores they similarly agreed that many of the pieces could not be confidently attributed as till, Wolds, or otherwise sourced flint. They were able to suggest additional minor signs to look for, in terms of the size of the inclusions being much larger in the Wolds flint and different kinds of cortex usually encountered on till versus Wolds flint, which improved the subsequent attributions of the 2013 and 2014 material and therefore more of this material was able to be classified.

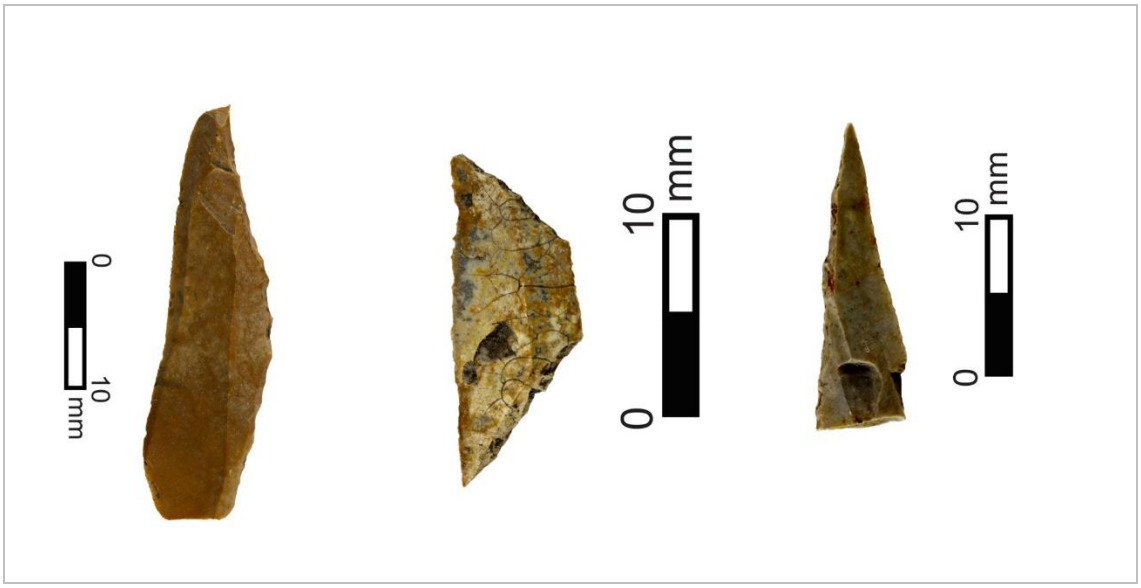

Figure 26. Examples of patinated flint (the centre piece is also burnt). Find numbers, from left to right: <100735>, <107356>, and <100242>.

Negative grid square numbers were utilised as trenches were expanded. Unfortunately, this caused some confusion in the field and led to erroneous recording on finds bags: Some excavators had assumed the minus sign was a hyphen so it was subsequently ignored when writing out negative grid numbers or added when writing out positive ones depending on the individual excavator. This was particularly problematic in 2014, where dryland trenches 11 and 15 both ranged across row numbers +4 to -5. This was not identified by the trench supervisor until late in the excavation and was further compounded during post-excavation processing when some of the sieve and spall bags with numbers which could be negative or positive were combined. As all in situ finds were 3D located, this material was still locatable and therefore spatial data remained viable. However, for the sieve and spall material from trenches 11 and 15, the material could be from the positive or negative grid

square. As such, sieve material from these two trenches is treated as if from an unknown grid square. This impacted 6030 pieces. The remaining dryland trenches from 2013 and 2014 did not feature mixed positive/negative grid numbering so this did not impact the spatial resolution of the find locations as long as the trench was known.

4.3 The Long Blade Assemblage

The small Long Blade assemblage of only 56 finds, as shown and summarised in Figure 27, Figure 28, and Figure 29, includes those from contexts phased as being Long Blade or Redeposited Long Blade as well as finds characteristically Long Blade stylistically from elsewhere on site. The assemblage consists mainly of tertiary debitage or debitage fragments, with a small amount of primary and secondary core initiation debitage. There is one core fragment. Much of this material was heavily patinated and water rolled, so while it appears to be a more balanced mix between till and Wolds flint than seen in the Early Mesolithic assemblage, it is possible this is partly down to misidentification, compounded by material lost to poorly stratified contexts that is then assumed to be Mesolithic when not diagnostic. A very small number of these artefacts were burnt (see Table 10).

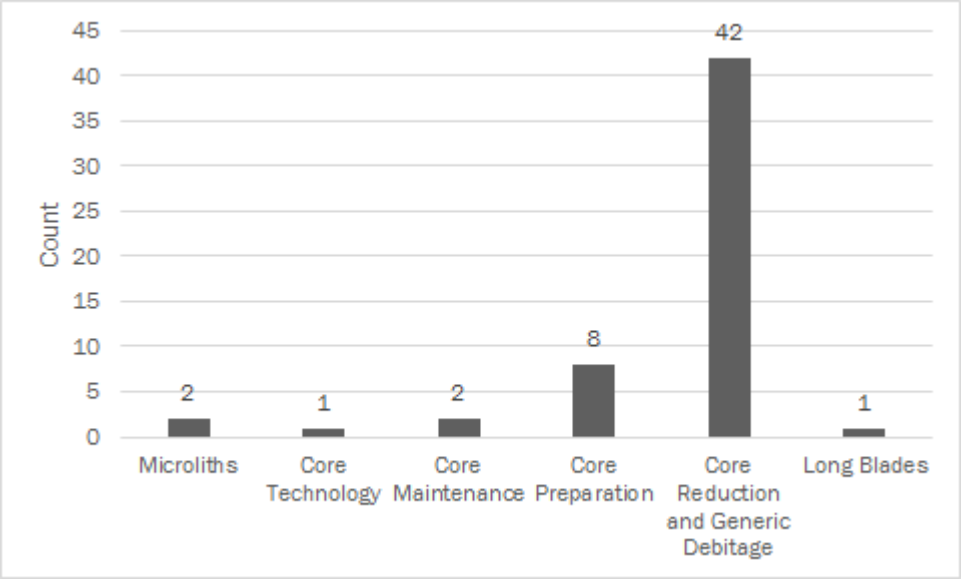

Figure 27. The Long Blade assemblage

Figure 28. 3D located Long Blade and Federmesser material

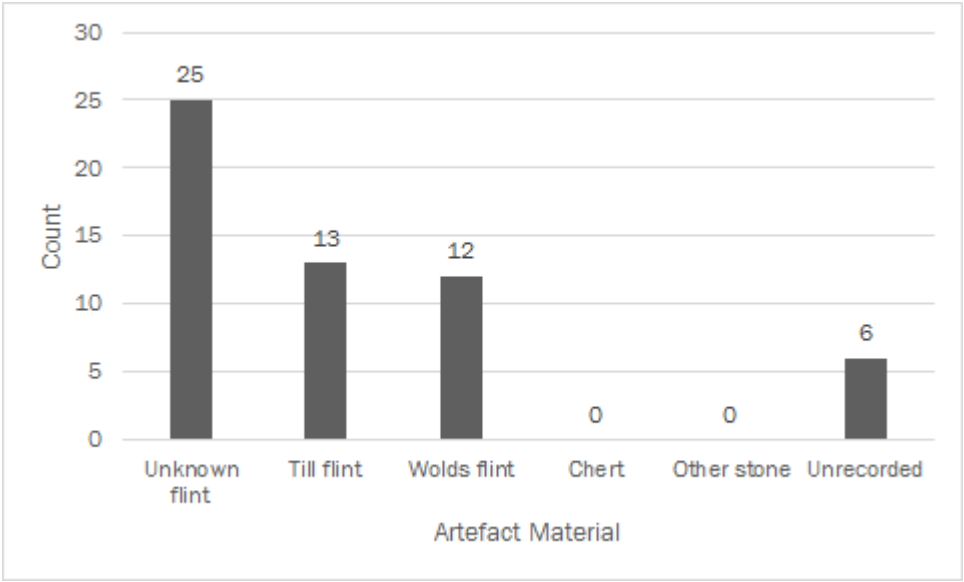

Figure 29. Raw materials of the Long Blade assemblage

Table 10. Proportion of burnt material in the Long Blade assemblage

Long Blade Artefacts	Count	Percent
Burnt	2	4%
Not Burnt	54	96%
TOTAL	**56**	**100%**

There were four particular finds of note. <110501> was unfortunately found on the spoil heap for Trench 1 but is a classic long blade (Figure 30). It would fall into the traditional 'grossklingen' category, being 14.7 mm long (following Reynier 2005). <100213> is a blade segment that was found in association with horse remains (see Figure 32) and preliminary evaluation by Aimée Little suggested that there was possible butchery microwear on this blade segment (Little 2014, pers. comm.).

Find <106967> is a tanged/hollow based asymmetrical point with concave inverse basal truncation of similar dimensions to the tanged/shouldered point found by Moore; however, the tang is less pronounced on the POSTGLACIAL piece (Figure 32). It was found in an upper peat context (1002) which is a later deposit, not associated with either the Long Blade material or the Mesolithic phase. It is most likely to be Long Blade given its typology therefore the context is problematic. It was found during sieving in grid square R19 in trench 10, but was actually found very close to the edge of Moore's trench and one possibility is that it was perhaps found out of situ. If, for instance, Moore's spoil had been piled up in this vicinity it may have derived from the spoil heap. Equally, the edges of Moore's trenches were very hard to locate and there is a slight possibility that it might have been present in Moore's backfill.

Find <100242> is a partial narrow backed bladelet very similar to others found at Long Blade assemblage yielding sites elsewhere in the Vale, and with similarities to the tip of Moore's shouldered point as well (Chantal Conneller 2015, pers. comm.; see (left) and Figure 33). This was found in wetland trench 10. There are a number of similar partial microliths with very linear fine retouch at an acute angle from the axis, one of which has a similar basal breakage to the wetland example, from the dryland (<100664>, <111898>, <sl/117>, <sl/177>, <sl/380>) which, for now, are recorded as "acute straight backed" as part of the Mesolithic assemblage. As such, while only a small assemblage, this preliminary evaluation of the Flixton Island 2 Long Blade material still yielded interesting results.

Figure 30. Find <110501> (Photo taken by N. Gevaux)

Figure 31. <100213> (Photo taken by N. Gevaux)

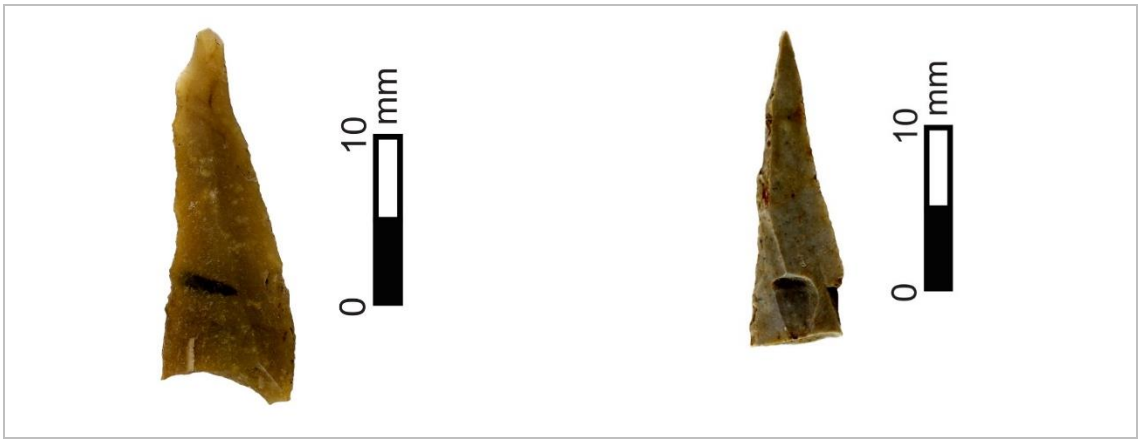

Figure 32. <106967> (left) and Figure 33. <100242> (photos taken by N. Gevaux)

4.3.1 A possible Federmesser find

Find <106591> from the topsoil in trench 9 was distinctive both in its style as a tanged point, and in being heavily patinated suggesting it was exposed on the surface for a longer time than much of the other material (i.e. before peat formation; Figure 34). Conneller has suggested that this is actually a possible Federmesser find, akin to some of those found elsewhere in the Vale (2017, pers. comm.).

Figure 34. <106591> (Photo taken by N. Gevaux)

4.4 The Mesolithic Assemblage

4.4.1 Overview

A total of 20,191 artefacts were excavated and assigned to the Mesolithic assemblage from the site (summarised in Figure 35 and Table 11). Artefacts from contexts that are potentially mixed Palaeolithic / Mesolithic material, including the lithics from the gully contexts, are assumed to be Mesolithic unless technologically clearly otherwise.

The majority of the Mesolithic assemblage (71% based on count), consisted of tertiary core reduction pieces (flakes, blades, and bladelets all lacking cortex) and generic tertiary debitage pieces (debitage chips, chunks, and spalls). The second most dominant category was core initiation pieces i.e. primary and secondary removal flakes produced when preparing a core for knapping by removing the cortex. These were complemented by 1% of the assemblage consisting of cores and core fragments (core technology) and a further 1% resulting from core preparation/initiation practices (i.e. core tablets to rejuvenate previously utilised platforms and so on). This is supportive of knapping occurring on site which is interesting given the location of the site in the landscape and will be explored further below when considering the raw materials.

The tools assemblage (microliths, other knapped types, and core) make up around 5% of the assemblage artefact count, totalling a little under 1000 artefacts. Table 12 summarises the breakdown of the "essential" tools assemblage as defined by Mellars (1976; as discussed in detail in chapter one). While the full extent of the lithics was not excavated, the lithics

were present in some quantities over a broad, contiguous area and therefore falls into a Mellars Type II settlement which he suggests would represent a substantial grouping of people. Combining this and the lithics assemblage composition we can suggest Flixton Island 2 to be closest to a type B or 'balanced' assemblage type in Mellars' site typology. Other Type B sites include Flixton Island 1, Star Carr, Thatcham, and Deepcar though, i.e. a broad range of other large Early Mesolithic sites with both Star Carr and Deepcar microlithic type assemblages and in some cases potential palimpsests. While this does give a starting point for comparing the site to others, and covers the two dominant formal tools on the site (microliths and scrapers), it is not possible to compare the possibly utilised debitage pieces which at Flixton Island 2 would be a further 209 informal tools in addition to the 510 considered in this comparison, and nor does it consider the small awl/piercer contingent at Flixton which is much greater at other type B sites such as Star Carr and as such an aspect of the functionality of the sites is lost.

The tools are supplemented by a small assemblage of identified tool sharpening and resharpening spalls. This latter category count would potentially be increased by a more extensive refitting program that would allow assignment of more ambiguous debitage into this category but this provisionally shows that tools are being prepared and refreshed for reuse on site.

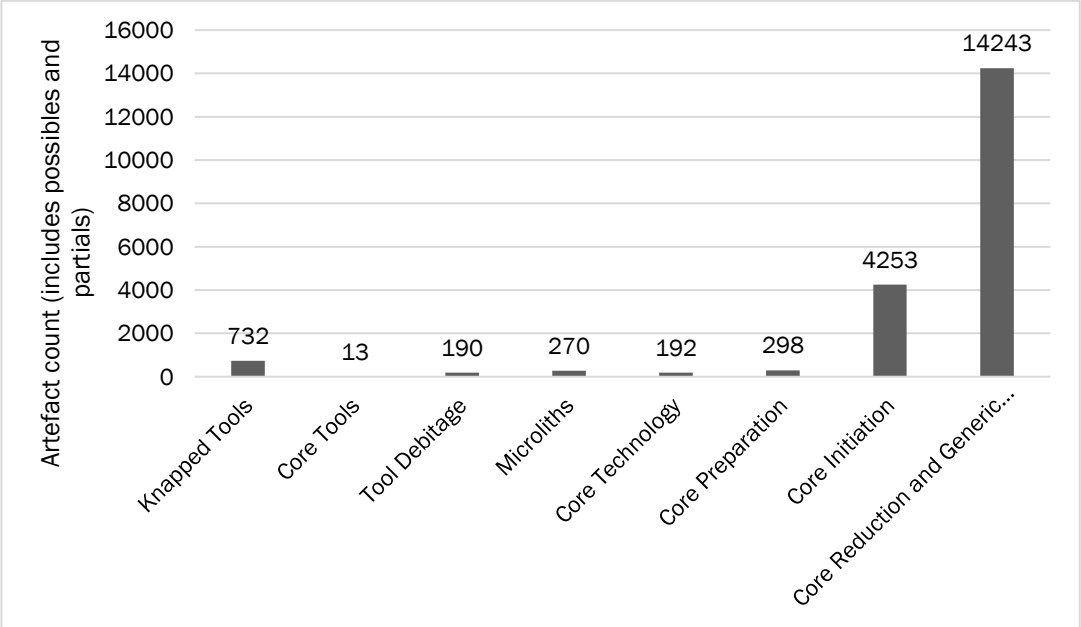

Figure 35. Overview of the Flixton Island 2 Mesolithic assemblage

Table 11. The Flixton Island 2 Mesolithic assemblage, overall breakdown

Category	Count (includes partials)	Percent of Flixton Assemblage
Microliths	**270**	**1%**
Knapped Tools	**732**	**4%**
Awl / Piercer	17	0%
Backed pieces	12	0%
Burin	35	0%
Combination	8	0%
Denticulate	3	0%
Mèche de foret	5	0%
Microdenticulate	8	0%
Notched pieces	9	0%
Scrapers	196	1%
Truncated pieces	9	0%
Otherwise retouched	26	0%
Possibly modified	195	1%
Possibly utilised	209	1%
Core Tools	**13**	**0%**
Axe / Adze	1	0%
Axe / Adze Roughout or Preform	4	0%
Possible Large Core Scraper / Planer	1	0%
Possible Wedge / Splitter	1	0%
Core Scraper	2	0%
Strike-a-light	2	0%
Potentially utilised cores	2	0%
Tool Debitage	**190**	**1%**
Microburins	84	0%
Microburins / notched bladelets	5	0%
Partial microburins	2	0%
Partial microburins / notched bladelet segments	3	0%
Possible microburins or fragments thereof	30	0%
Burin spall	9	0%
Burin spall segment	1	0%
Other tool resharpening debitage	1	0%
Possible tool debitage	55	0%
Core Technology	**192**	**1%**
Core	112	1%
Core fragment / possible irregular core	6	0%
Core fragment	61	0%
Possible core technology	13	0%
Core Preparation	**298**	**1%**
Core tablet	30	0%
Flanc de nucléus	11	0%
Other platform rejuvenation debitage	49	0%
Plunging debitage	13	0%
Crested / possibly crested debitage	31	0%
Possible core preparation debitage	164	1%
Core Initiation	**4253**	**21%**
Complete primary debitage	86	0%
Complete secondary debitage	537	3%
Primary or secondary (uncertain) debitage	1710	8%

Category	Count (includes partials)	Percent of Flixton Assemblage
Possible core initiation debitage	1920	10%
Core Reduction and Generic Debitage	**13190**	**65%**
Complete tertiary bladelet	681	3%
Complete tertiary blade	462	2%
Complete tertiary flake	1056	5%
Fragments and segments (tertiary / unknown)	7755	38%
Debitage chips and spalls	2783	14%
Debitage chunks	411	2%
Tested nodules	3	0%
Nodule chunks	39	0%
Possibly humanly worked debitage	**1053**	**5%**
TOTAL	**20191**	**100%**

Table 12. The 'essential' assemblages for Flixton Island 2 and various example sites drawn from Mellars (1976), with the exception of the recent data for Star Carr drawn from Conneller et al. (2018) which she categorises as a Type B site. All Type B sites described by Mellars are provided. The Type A and B1 examples were chosen as being the sites summarised in Mellars with the lowest proportion of microliths (their defining aspect being that their assemblages show a high proportion of microliths), while the Type C example was chosen, similarly, for it being that with the lowest proportion of scrapers (high proportions of scrapers being the defining characteristic of that group). *saws = terminology Mellars uses meaning microdenticulates.

			Flixton Island 2	**Type A**	**Type B1**	**Type B Upland**	**Type B Lowland**				**Type C**
Category	**Artefact**	**Unit**	(n=510)	Farndale (n=66)	Selmeston (n=183)	Deepcar (n=144)	Flixton Island 1 (n=264)	Thatcham (n=500)	Star Carr, Clark (n=920)	Star Carr, Conneller (n=952)	Kettlebury I (n = 22)
'Essential' Tools	Microliths	Percent of 'Essential' Tool Assemblage	52%	88%	71%	59.6%	29.5%	57%	27%	33%	18.2%
	Scrapers		38%	3%	21.80%	32.5%	62.5%	25.8%	35.4%	36%	81.8%
	Burins		7%	5%	1.10%	7%	7.2%	11.4%	36.3%	24%	0%
	Microdenticulates*		2%	4.5%	6%	0.90%	0%	3.8%	0.4%	5%	0%
	Axe/adzes		1%	0%	0%	0%	0.8%	2%	0.8%	2%	0%
Waste Products	Cores	Count per 100 'essential' tools	21.9	37.9	90.1	14.9	49.6	53	31.8	33.8	36.3
	Microburins	Count per 100 microliths	45.2	5.2	20.8	150	41	25.3	10.9	28.5	50

4.4.2 Overall Spatial Patterning

The distribution plot of the Mesolithic assemblage shown in Figure 36 demonstrates how there is Mesolithic material from across the wetland and dryland contexts of the site. As can be seen, the majority of the lithics are on the main dryland area but there are artefacts and clusters in other areas of the site as well.

Figure 36.The complete 3D located Mesolithic assemblage, with finds from categorically gully contexts symbolised separately

The dryland area was found to be very densely covered with lithic material, although initial closer inspection of the 3D located data (Figure 37) shows there are definite areas of greater lithic density which are potential clusters either reflecting deposition or accumulation due to post-depositional processes. 3D locations were not taken for lithic material from the highest topsoil. However, it is thought that lower (1000) and more so (1119) were less

disturbed by post-depositional processes due to the presence of larger artefacts here, such as axes/adzes, which tend to be less easily moved. Therefore, it is hoped that these reflect something closer to the genuine deposition patterns despite there being some assumed movement of the material through bio- and hydroturbation processes as well as occasional ploughing. The clustering into roughly circular scatters supports that this is the case, in that the material does not appear to have been dragged out linearly. The statistical significance of these potential clusters, and the composition of the artefacts within them, is discussed in depth in chapter seven.

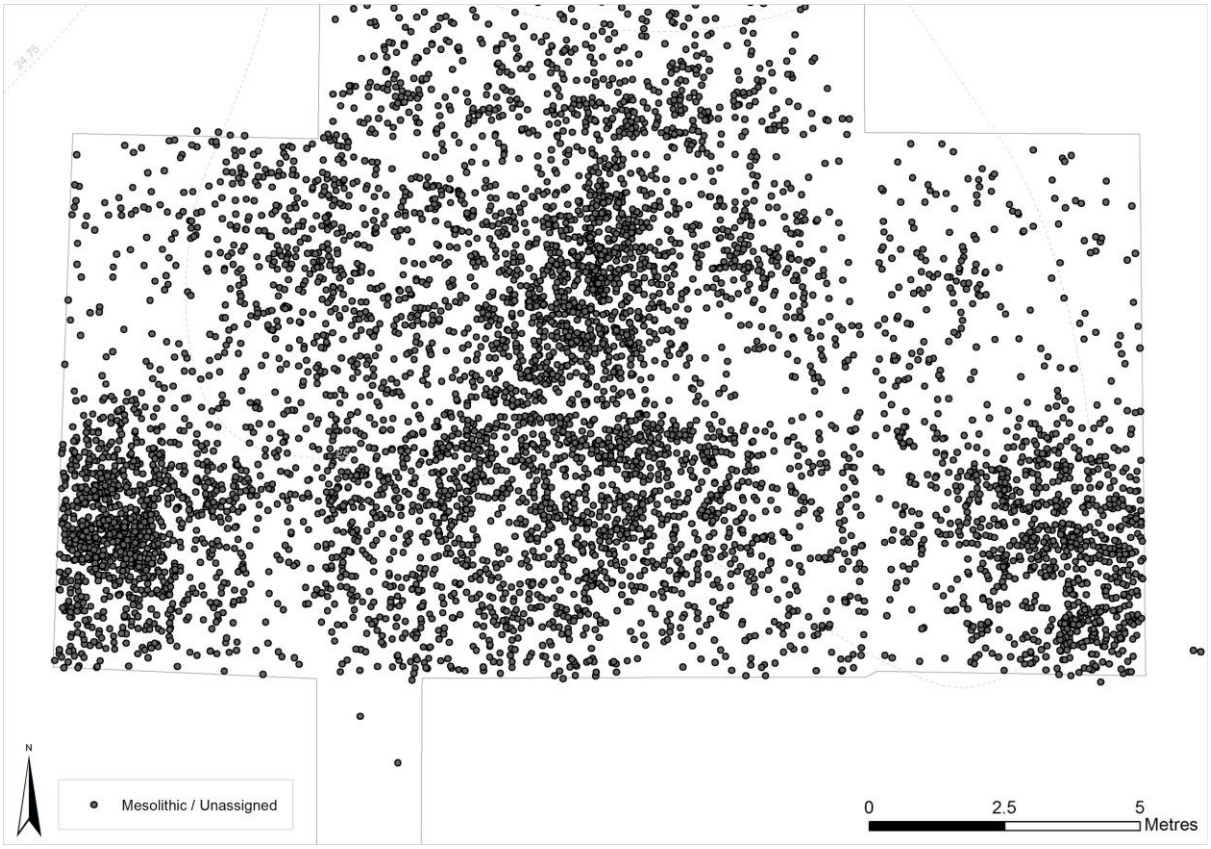

Figure 37. The 3D located Mesolithic assemblage from the main dryland trenches

There was further material from trench 3 (the westernmost dryland trench), the gully, and the slightly raised bar of land to the north of the gully (see Figure 38). The gully itself contained a spread of lithics in no particular concentration, three of which were cores and one of which exhibits signs of crushing or impact suggesting it may have been used as a pick. The rest of the material found here was for core initiation, core reduction, and a plunging blade potentially used to rejuvenate and therefore extend a core's use life. On the raised bar, the small cluster to the west contained two microliths accompanied by several bladelets and some general debitage including a possibly crested blade. The small cluster to the east contained core reduction and initiation artefacts as well as general debitage.

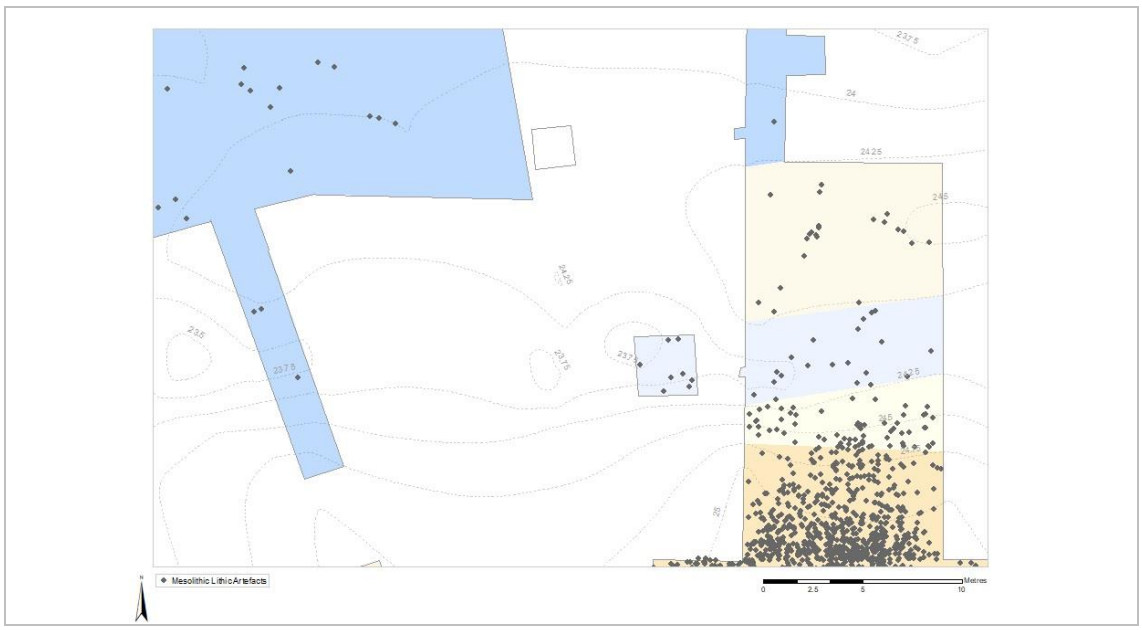

Figure 38. Zoom on the gully and bar

In the wetland, there was a focus of material in the west of the major excavation area in the Mesolithic peat deposits (see Figure 39). This scatter contained a variety of tools including a denticulate, a combination dihedral and truncation burin (with a potential scraper section), another scraper or attempted truncation burin, a large microburin or small notched blade, and a partial of the same. The rest of the scatter was mostly core reduction debitage but also core initiation material, a core tablet, and a partial core tablet indicating there may have been in-situ knapping here.

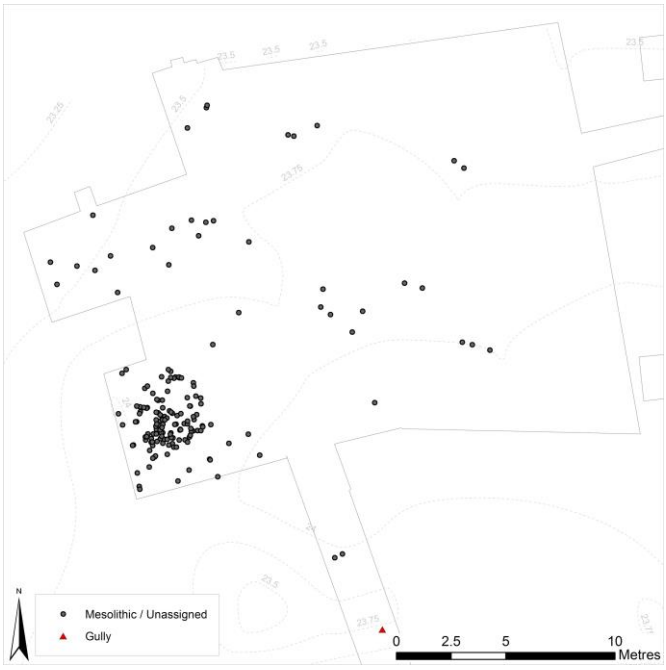

Figure 39. The Mesolithic assemblage from the wetland trenches

4.4.3 Burnt and Heated Material

Table 13 summarises the proportion of pieces that show burning or intentional heat modification (with examples shown in Figure 40). This was identified from discolouration, crazed microcracking, or glossy lustre on removal or retouch faces. As can be seen, a notable proportion of the assemblage is burnt or heated, but this is much less than the proportion of material seen burnt at Star Carr which was 16.54% (Conneller et al. 2018).

Table 13. The burnt and unburnt proportions of the assemblage

Effect	Count	Percent
Burnt or heated	1662	8%
Possibly burnt	24	0%
Unburnt	18447	92%
	20133	**100%**

Figure 40. Examples of burnt or heated material.

Figure 41 shows the distribution of heated or burnt material (excluding possibly burnt material) and it can be seen that there are scatters of burnt material on the wet and dryland. The areas of concentration are the same as for the unburnt material. The scatter in the southwest of the main dryland area (in trench 15) was noted during excavation for having a slightly darker context and some burnt microdebitage, though not enough to be a clear hearth However, the other dryland focal areas in trenches 4 and 11 were not identified during excavation from the other areas as finds were generally so omnipresent. Visualising

the burnt tools isolated from the burnt debitage (Figure 42) suggested that burnt tools did not seem to cluster particularly.

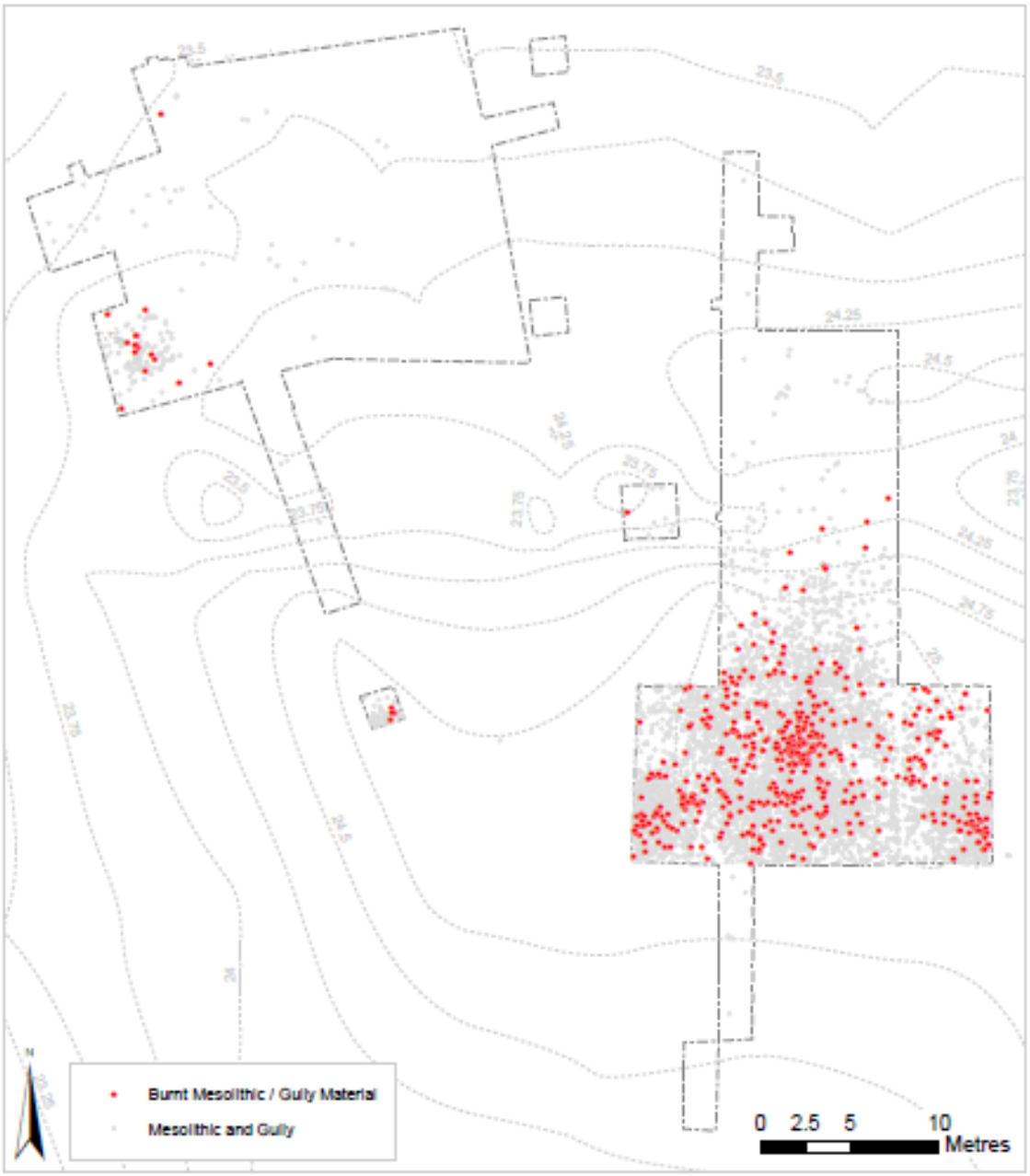

Figure 41. The burnt Mesolithic material from Flixton highlighted against the unburnt material

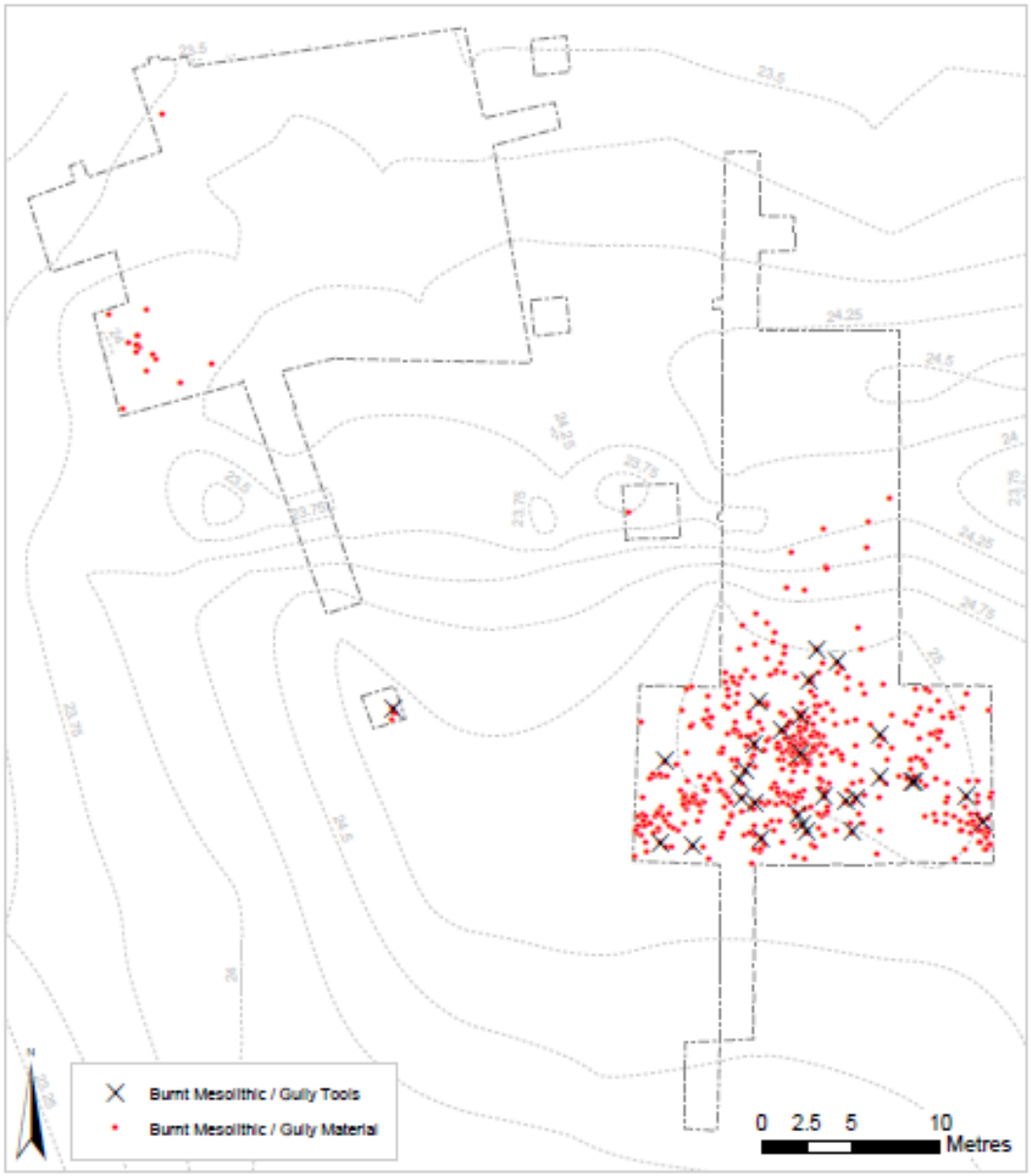

Figure 42. The burnt Mesolithic tools compared with other burnt material

4.4.4 Raw materials

Any raw material used on the site would have had to be sourced and transported to the site as there are no natural source exposures on the island itself, but it is interesting that there does seem to be a high proportion of knapping material (cores, core preparation, core initiation and reduction debitage) in the assemblage in absolute terms of raw count. The three tested nodules from Flixton measured as roughly a clenched fist's size (averaging length 73.4 mm, width 56.3 mm), so would have been easily transported, if still heavy. In conflict with this, there were no clearly isolated cache deposits identified during the excavations as found at other Vale sites (Conneller and Schadla-Hall 2003), perhaps surprisingly given the isolated location. However, the other three caches from the Vale have been on sites on the lakeshore, not on any of the island sites, so this is consistent. This may

indicate a more limited or more sporadic use of the island as it may indicate they did not anticipate returning to the location but this seems unlikely given the amount of material present. Alternatively, it may have been that they knew from previous occupations there would be material left over and they only ported what extra they needed both to and from site. It could also be simply that any caches were in an unexcavated area of the island or that they were not identified amongst the general density of the dryland finds.

Figure 43 provides the assemblage-wide total counts of artefacts made from each material, with over 7000 pieces being uncategorizable, despite consideration, due to the general weathering and patination of the assemblage and 7000 pieces unrecorded (this applied to some of the sieve material that was recorded in less depth, but if it was unrecorded then it was flint as all other materials were noted). However, of the material that could be identified, over 4500 artefacts were thought to be made of flint sourced from the till, and therefore likely the coast, while only a little over 1000 were made from the slightly more local Wolds flint (a ratio of approximately 4.5:1). This echoes the preference for till-sourced flint seen at Star Carr, where till outnumbered Wolds flint at a ratio of 4.84:1 (Conneller et al. 2018). At Deepcar and other sites high up in the Pennines, the preference was for Wolds flint (Radley and Mellars 1964). Wolds flint is generally considered the harder to knap of the two as it contains more inclusions and is coarser grained, also making it opaque or semi-opaque as a result which may impact aesthetics, but it is a more local source than the coastal till flint for sites in the Pennines. The coast is not particularly far from Flixton, however, and it would only take around an hour or two to walk to the nearest beaches even given the different coastline (Weninger et al. 2008).

A very small number of artefacts were identified as being made of a much darker chert, including two microliths and one partial microlith, but there were no cores in the assemblage suggesting these were brought to the site in their final state or, less likely given the lack of debitage too, the cores were carefully curated before and after the site was occupied (Figure 44). In addition to these, a small number of blades were retrieved that initially could easily have been taken for natural stone material; however, the pieces refit and do look to have been humanly knapped off the same core. It is tentatively suggested these may have been made of a form of limestone (Figure 45). It is possible that more of this latter material, particularly if there had been a core of it, would have been missed during excavation as it was unconvincing until considering it once refitted.

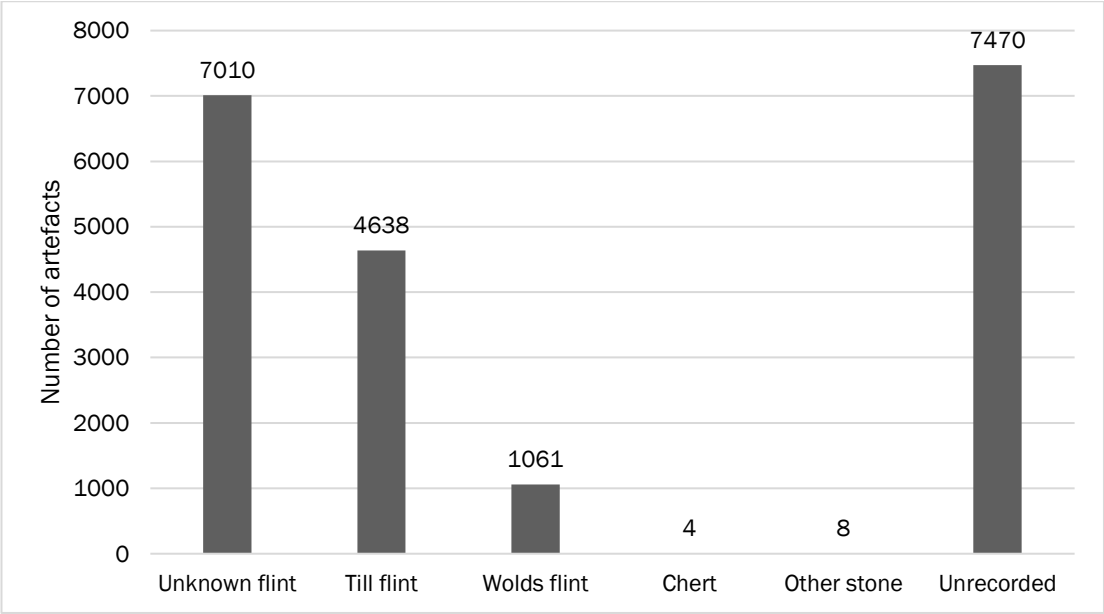

Figure 43. The Flixton Island 2 Mesolithic assemblage in terms of raw material used

Figure 44. Photograph of the chert artefacts (photography by N. Gevaux). Find numbers, from left to right: sl/191 and sl/15.

Figure 45. Photograph of the possibly limestone artefacts. Find numbers, from left to right: sl/194, sl/192, and sl/193.

The flint from both the till and the Wolds is highly variable, from translucent material of clear brown or honey colour through to more speckled and opaque pieces. Colour was recorded but the iron staining made it very difficult to gauge any original redness over stained red-orange colouration, though some pieces appear to have been red speckled flint. In addition, a small number of flints appeared to have deeper red tips or edges from an unknown process but these were checked by Shannon Croft and did not appear to be a residue under magnification but instead were inherent in the material (Figure 46).

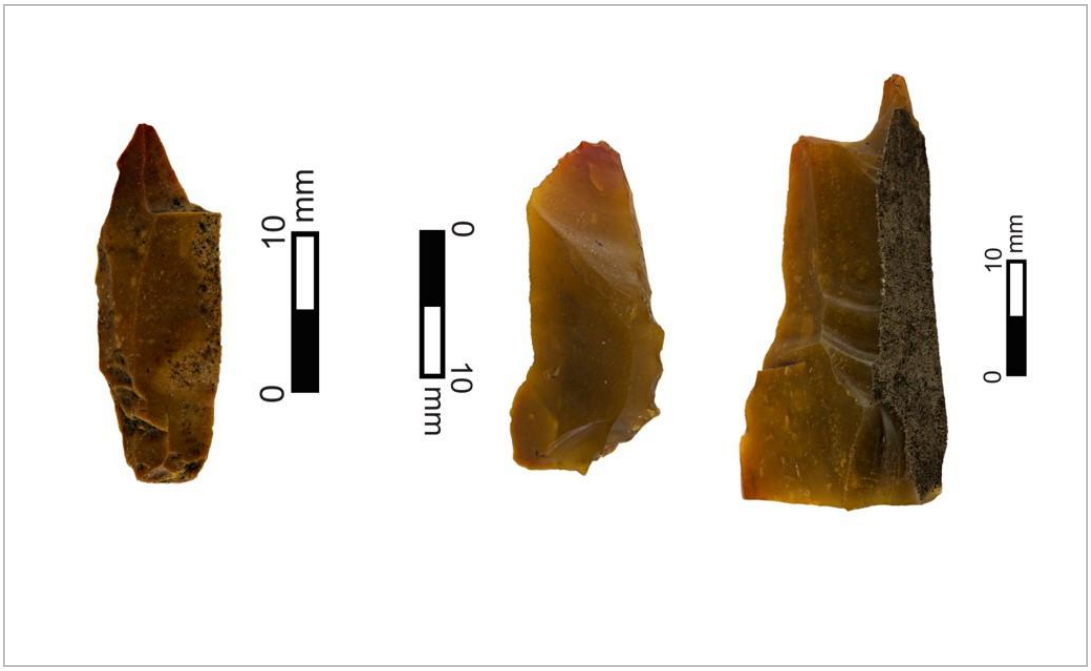

Figure 46. Red-tipped material (photography by N. Gevaux). Find numbers, from left to right: <101285>, <103931>, and <105663>.

Figure 47, Table 14 and Table 15 summarise the raw materials used to manufacture tools. Both till flint cores and tools are more common than Wolds ones but, in general, a slightly lower proportion of tools are made of the till flint than represented by the core assemblage. This could be because a higher proportion of the cores were able to be identified to source than tools, but there is a large difference in those positively identified in favour of manufacturing on till flint. As such, this suggests either that these Wolds tools were being manufactured elsewhere and brought into the site, or that those cores were being used here too but carried away more frequently afterwards. As the Wolds flint is the more local flint, it would make more sense that if any material were going to be curated for longer use it would be the till flint; this shifts the interpretation in favour of those tools being brought in ready-made instead.

Table 16 presents the raw materials used to manufacture the major tool types from the site (microliths, scrapers, burins, awls/piercers, axes/adzes, and partials thereof). Aside from three chert tools (microliths or partials), all other tools were flint. Fairly high proportions of all tool types could not be assigned to their source which skews the data somewhat.

However, if the successfully recorded data can be considered to be adequate samples (which for microliths and scrapers there is a better sample of successfully assigned flint than the other tool types) then some approximate comparisons can be drawn. There was a slightly higher preference for microliths to be manufactured on till flint than all other tool types. A similar pattern, although much more extreme in till flint preference, is seen at Star Carr. However, while at Star Carr there was a similar preference reflected in the awls, at Flixton there was not and the remaining key knapped tools all showed a slightly weaker preference for till with one Wolds flint artefact for every 3.6 till flint artefact of those tool types.

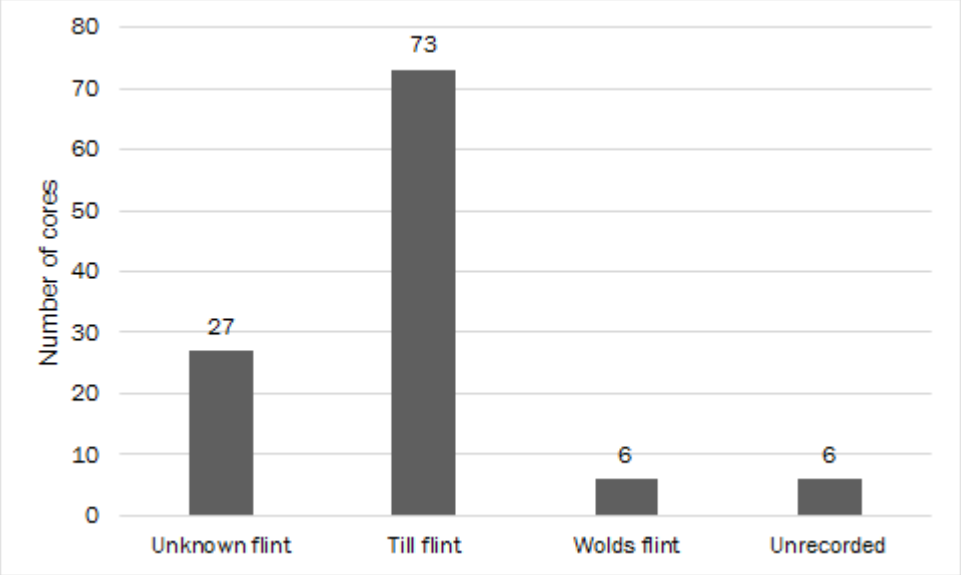

Figure 47. Raw materials of the Mesolithic cores

Table 14. Relative percentages of the source of cores deposited at Flixton Island 2

Core materials	**Total**	**Percent**
Unknown flint	27	24%
Till flint	73	65%
Wolds flint	6	5%
Unrecorded	6	5%
TOTAL	**112**	**100%**

Table 15. Summary of the raw materials used to manufacture different tool categories

TOOL CATEGORY	**Unknown flint**	**Till flint**	**Wolds flint**	**Chert**	**Other**	**Unrecorded**	**TOTAL**
Microliths	40	181	46	3	0	0	**270**
Percent of microliths	*15%*	*68%*	*17%*	*1%*	*0%*	*0%*	***100%***
Knapped Tools	329	285	70	0	0	41	**725**
Percent of knapped tools	*45%*	*39%*	*10%*	*0%*	*0%*	*6%*	***100%***
Core Tools	1	7	5	0	0	0	**13**
Percent of core tools	*8%*	*54%*	*38%*	*0%*	*0%*	*0%*	***100%***
ALL TOOLS	**370**	**473**	**121**	**3**	**0**	**41**	**1006**
PERCENT	**37%**	**47%**	**12%**	**0%**	**0%**	**4%**	**100%**

Table 16. Summary of the raw materials used to manufacture key tool types at Flixton Island 2 and Star Carr (data for the former from Conneller et al. 2018)

Overview of raw materials of key tool types	**Unknown flint**	**Till flint**	**Wolds flint**	**% Unknown flint**	**% Till flint**	**% Wolds flint**	**Flixton Ratio Wolds to Till**	**Star Carr Ratio Wolds to Till**
Microliths (and partials)	40	181	46	15%	68%	17%	1:3.9	1:16.2
Scrapers (and partials)	68	97	27	35%	50%	14%	1:3.6	1:7
Burins (and partials)	11	18	5	31%	51%	14%	1:3.6	1:2.5
Awl / Piercer (and partials)	3	11	3	18%	65%	18%	1:3.6	1:9

Patination and material selection is also often used in assigning the assemblage to a classic Early Mesolithic type (i.e. Star Carr, Deepcar, Honey Hill). This can relate to certain types of flint used being variably prone to patination as the kind of patination seen often relates to the flint's microstructure, permeability, and impurities. It will also be impacted by deposition conditions as it is caused by general weathering and influenced by other environmental factors so such an indicator should be treated with a high degree of caution (Schmalz 1960; Hurst and Kelly 1961). Recortification can also present as patination. It made sense to take patination into consideration concerning the Pennine site at Warcock Hill where two typologically distinct assemblages from the crown of the hill were made on

different types of flint and exhibited different patination: Buckley (1924 as cited in Reynier 2005) distinguished between the brown and grey flint scatter lacking patina and the scatter of grey Lincolnshire flint patinated white. The scatters were later assigned by Radley and Mellars (1964) as being a Star Carr type assemblage made of the former, joined by a Deepcar type one made on the latter. However, applying these criteria to sites and landscapes where the raw material availability is subtly different is not necessarily appropriate.

The Flixton Island 2 assemblage is generally stained, presumably with iron as much of it is brown or orange, and iron panning is known to occur in local soils. There are also sometimes physical deposits of what appear to be iron oxides on the surface of some artefacts. While this has not been confirmed chemically on the Flixton flint, samples were visually examined under the microscope by Shannon Croft and compared with very likely natural iron depositions confirmed by Raman spectroscopy on artefacts from Star Carr (Croft 2017). Where there was modern breakage, the flint often showed through its "true" matrix colour of lighter brown, grey, or white (with varying degrees of translucency).

In addition to this, many of the pieces at Flixton were white patinated. Some of these were only lightly patinated with a semiopaque white patina, while others were completely masked with an opaque white patina frequently accompanied by fine lines of orange deposition. In addition to white patina, thought to be caused by desilication, there are possibilities for gloss patina, desert patina, and stain patina (Howard 2002). Several pieces showed potential glossing or residues but often in the centre of facies where such glossing did not logically extend from use, so this is thought to be from weathering processes though this has yet to be confirmed by microscopic analysis. Even finely worked microliths varied from clear translucent brown till flint through to opaque flint stained mid brown or orange with signs of white patina and further iron depositions on top.

Burnt or heated lithics were often less susceptible to stain patination, seemingly retaining a colour closer to their original if they were not oxidised white, or burnt brown or black. The heating of these pieces was identified from glossiness on later retouch scars or breaks, heat spalling, or microcracking.

4.4.5 Technology

With a little over 100 cores being retrieved during excavation, people were certainly bringing material here with an intention to knap. The core technology assemblage is summarised in Figure 48 and Table 17. In terms of core types, cores with a single platform with part of the circumference worked (A2) or two opposed platforms (B1) were dominant (see Figure 49 for examples), followed by two platforms at right angle (B3) and multi-platform (C) types, and lastly with 10 or fewer examples of A1, B2, D and E type cores.

Conneller's assemblage at Star Carr was similarly dominated by A2 and B1 types as were the Pointed Stone (Star Carr type site) and Longmoor 1 (Horsham type) sites as evaluated in Reynier (2005, 32–40), and summarized in Table 18. Reynier's evaluation of ten southern sites showed that A2 cores are often the dominant type in Early Mesolithic assemblages, if this sample is representative of broader trends. Both the Flixton Island 2 and Star Carr assemblages were most similar to both Pointed Stone and Longmoor I generally, but they also both show a greater variability than the southern sites with 25% and 24% of their core assemblages respectively being C, D, or E type (the only site similar in that respect is Kettlebury 103, Horsham type, but that has much higher proportions of B3 cores than all other sites). It must be kept in mind that the cores that we retrieve as archaeologists are the product at the end of its use life (with added post-depositional damage) and, at various stages, a core could have had other platforms that have been overwritten, potentially over several periods of use and in different locations. Given the lack of consistency in the assemblages studied by Reynier, even between those of a similar type, core types do not seem to be a reliable indicator of the type of site. Overall, Flixton Island 2 is more variable in core types represented than all the other assemblages it is compared to, even Star Carr; this is perhaps because they are experimenting with exploiting the material to best advantage considering they have had to port it to the site, or perhaps because it is of quite mixed quality.

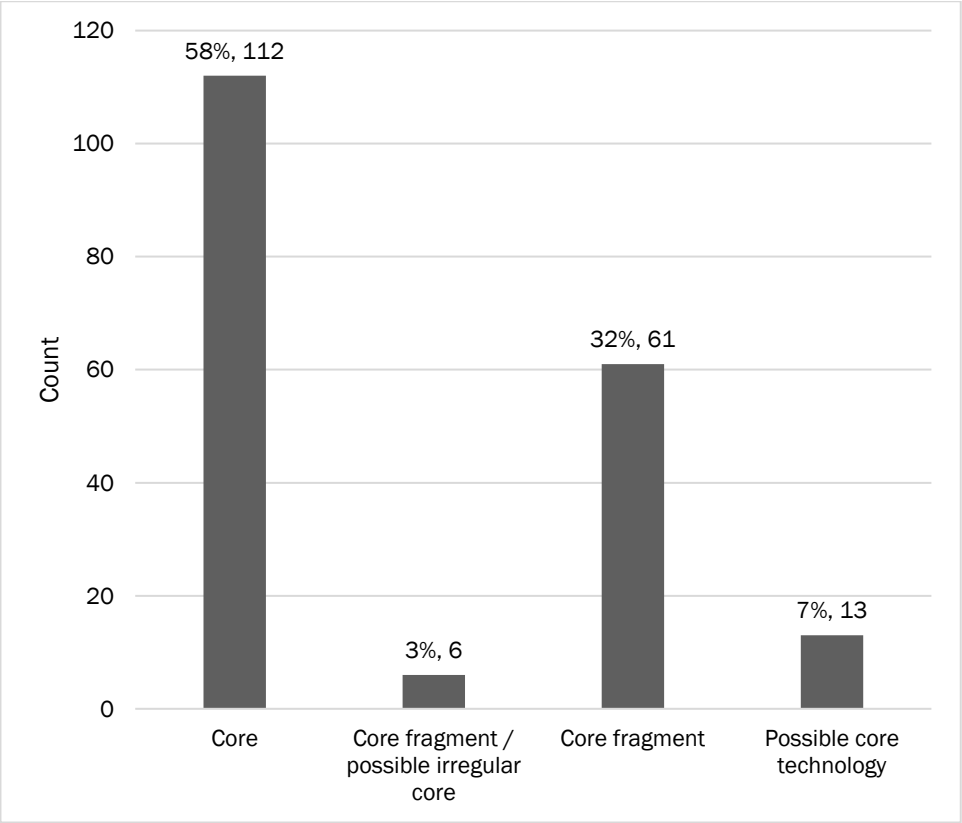

Figure 48. The Mesolithic core technology, with proportion of the core technology assemblage and artefact count (total count: 192 artefacts)

Table 17. Core types in the Mesolithic assemblage

Core types	**Count**	**Percent**
A1: Single platform, removals from entire circumference	9	8%
A2: Single platform, removals from partial circumference	31	28%
B1: Opposed platform core	22	20%
B2: Two platforms, one at an oblique angle	10	9%
B3: Two platforms, one at right angle	11	10%
C: Multi-platform core	18	16%
D: Core reduced either side of a ridge	2	2%
E: As D, but multi-platform	8	7%
TOTAL	**112**	**100%**

Table 18. Comparison of core type assemblages from different Star Carr, Deepcar, and Horsham type sites (Star Carr data reproduced from Conneller et al. (2018) and southern sites derived from Reynier 2005, pp. 32 - 40, with type C cores associated with Reynier's "3 platforms, continuous" category and D and E cores associated with his "other" category

	Flixton Island 2		**Star Carr Type**				**Deepcar Type**			**Horsham Type**		
Core types	***Count***	**Percent**	**Conneller's Star Carr**	**Pointed Stone**	**Broxbourne**	**Thatcham II SC**	**Iping Common**	**Marsh Benham**	**Thatcham III Dc**	**Kettlebury 103**	**Longmoor 1**	**St Catherine's Hill**
A1	*9*	8%	4%	0%	0%	0%	2%	0%	0%	0%	7%	0%
A2	*31*	**28%**	**34%**	**47%**	**38%**	6%	**47%**	**47%**	**48%**	19%	**36%**	**63%**
B1	*22*	**20%**	**28%**	**40%**	0%	17%	16%	18%	15%	6%	**39%**	0%
B2	*10*	9%	7%	7%	**54%**	**72%**	**31%**	18%	**23%**	**25%**	2%	**25%**
B3	*11*	10%	4%	0%	0%	0%	0%	2%	4%	**25%**	9%	13%
C	*18*	16%	11%	7%	0%	6%	1%	16%	8%	19%	2%	0%
D	*2*	2%	6%	0%	8%	0%	2%	0%	2%	6%	5%	0%
E	*8*	7%	7%									
Total	***112***	**100%**	**100%**	**100%**	**100%**	**100%**	**100%**	**100%**	**100%**	**100%**	**100%**	**100%**

Figure 49. Examples of cores (photography by N. Gevaux). From left to right, top row then bottom: <100617> A2 type in Wolds flint; <101357> B1/irregular core in till flint; and <106899> B1 core in Wolds flint.

As shown in Figure 50, 3D located cores were found generally spread across the dryland, with one isolated example (an A1 type, of not particularly large dimensions nor being opposed platform which might have suggested it was disturbed Long Blade) in the Mesolithic contexts from the wetland trench. There is one area of core concentration in the southwest of the main dryland area (in what would have been trench 15, in the vicinity of the possible feature in K-3). Most of the complete cores retrieved from sieving were from trench 4 (see Table 19). Plotting the cores by type did not reveal any particular types to be grouped as all are found dispersed across the dryland (see Figure 51). As such, there does seem to be a cluster in the vicinity of the southwest scatter but not connected to a particular style of knapping.

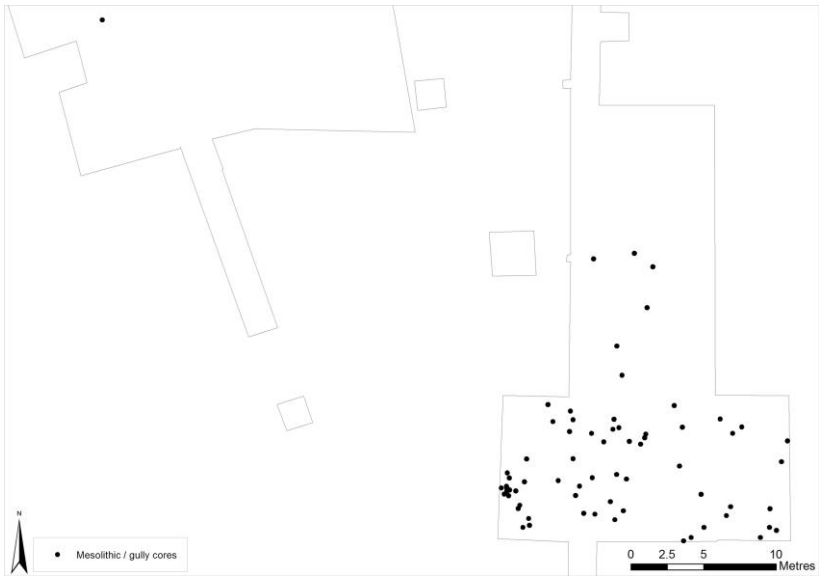

Figure 50. Distribution of the 3D located complete cores

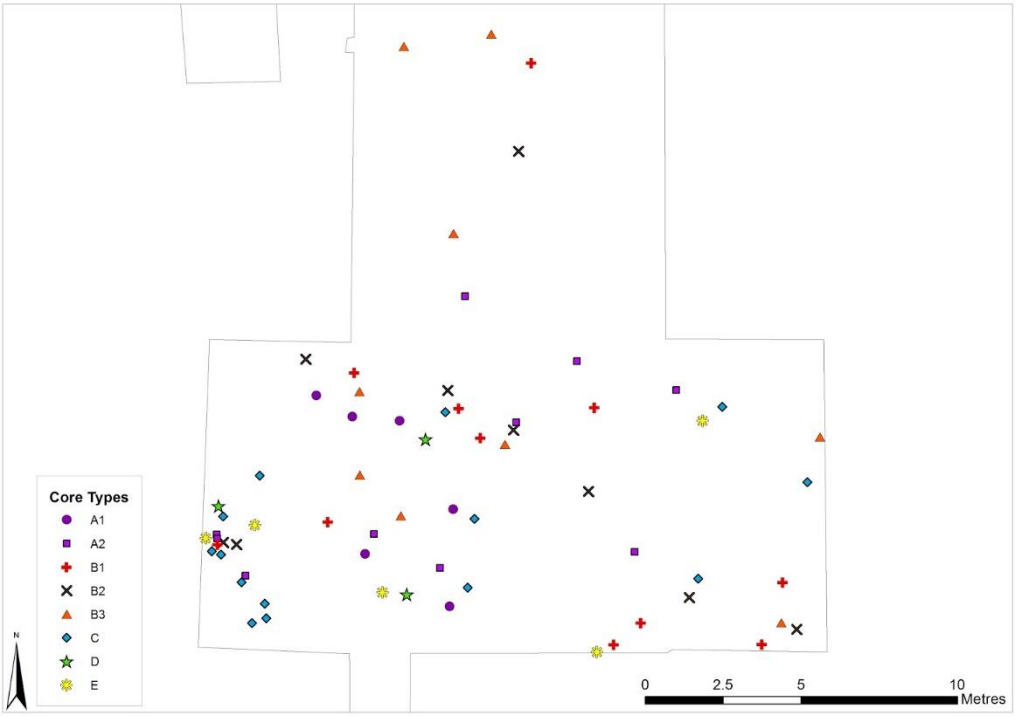

Figure 51. 3D located cores by type (N.B. there was one additional A1 type core in the wetland, not illustrated here)

Table 19. Complete cores retrieved from sieving

Trench	Complete cores retrieved from sieving
4	22
7	5
9	3
11	5
12	3
15	6
Unknown	1
TOTAL	**45**

Core sizes vary somewhat, with length being particularly variable (min: 22.5 mm, max: 82.37 mm, and see Table 20 for further detail). The longest cores (greater than 60 mm long) were all found in the topsoil on the dryland (in trenches 4, 11, and 15) and not in any single location but in different grid squares (Figure 52). Four out of five of these were opposed platform cores (B1) which suggests they may be part of the Long Blade assemblage instead. Two had natural handholds based on the cortex and one had a seemingly attempted core tablet removal to rejuvenate the platform, which appeared to have been disrupted by undulations in the cortical surface. There are feather and hinge terminations present on these large examples, as occurs throughout the core assemblage more generally, implying

either inexperienced knappers or expedient working. The smallest cores (less than 20 mm long) were similarly found in sieve material from across the dryland (in trenches 4 and 15 again as well as 9 and the northern end of 12), so there does not seem to be a spatial differentiation in deposition or post-depositional sorting of cores based on size.

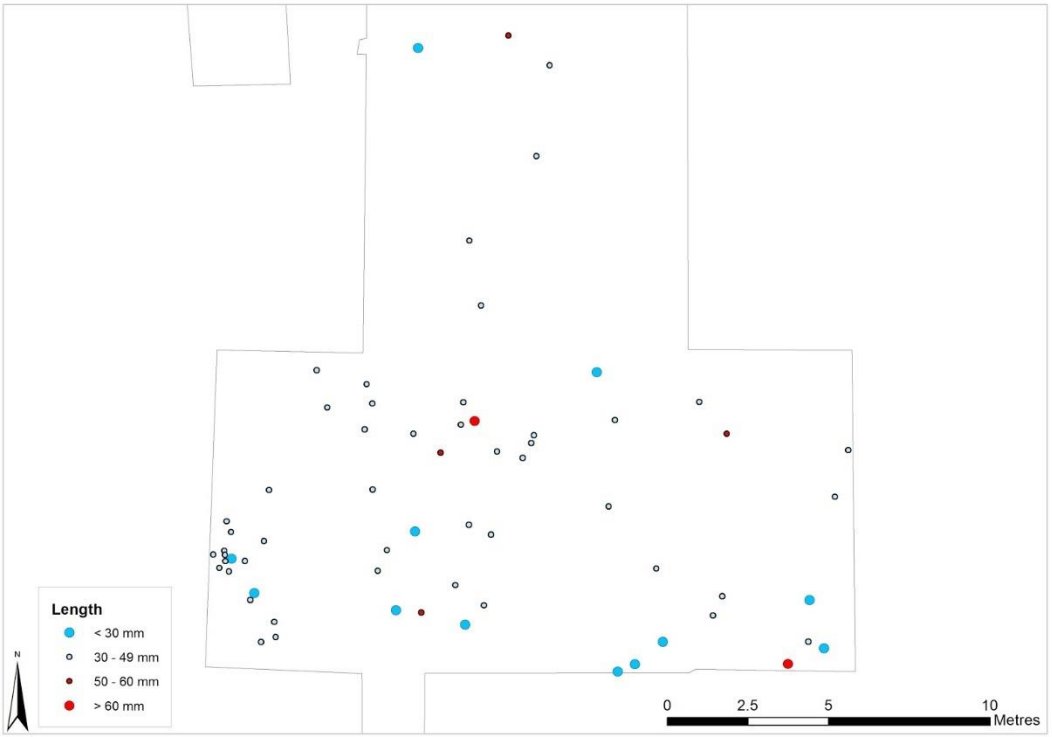

Figure 52. Cores displayed by maximum length as a crude proxy for size

With 50% of the cores measuring between 33 and 46.9 mm, many cores were well utilised but not thoroughly exhausted (see Table 20). The smallest cores were all till flint, with mostly small feathered bladelet removal scars although some hinge terminations were also evidenced, perhaps as evidence of trying to really exploit these cores to their limits. One of these small cores showed a plunging removal to perhaps allow further extension of the use life of the piece. The smallest was at the limit of being viable for knapping in the hand, the platform being a thumb's width. However, only one was of the translucent till flint, which is often considered the best quality as its lack of inclusions means it is more predictable to knap (and perhaps considered more aesthetically pleasing too) but most were opaque or semi-opaque varieties. Three of them were single platform but three had two platforms, at least at the time of discard and deposition.

Table 20. Summary of the core dimensions

Core Dimensions (mm)	**Length**	**Width**	**Height**
Average	40.94697248	33.97894737	21.92
Minimum	22.5	17.8	11.6
Maximum	82.37	65.9	32.3
Median	40.7	32.5	21.35
Quartile 1	33	27.7	18.875
Quartile 3	46.9	38.95	24.275
Std Dev	10.73	9.25	5.14

The suggestion of knapping activity is supported by the presence of 134 artefacts resulting from attempts at core rejuvenation (Table 21): there are a number of core tablets (which are removed to rejuvenate entire platform surfaces), flancs de nucléus (wide flakes assumed to be taken to rejuvenate the side faces of cores, though these may just be wide general flakes), other platform rejuvenation debitage, plunging flakes (that may have been to remove large areas of cortex or expose more of the nodule's inner surface for longer removals to be made), and crested flakes (again to remove longer debitage pieces). Some of these pieces may have been removed with other intentions in mind but in combination with the core count and island location, it is considered likely that a good proportion were for core rejuvenation purposes, at least initially as they could have been used afterwards regardless (and core tablets from Star Carr showed ephemeral traces of use as discussed in Conneller et al. 2018). There is a higher proportion of core preparation pieces of Wolds flint (52% till, 14% Wolds) than there were proportionally in the core assemblage (which was 65% till and 5% Wolds flint as detailed above), which is potentially because working Wolds cores could well have required more modifications to rejuvenate and therefore extend their use life due to inclusions and areas of inconsistent coarseness (see Table 22).

Table 21. Summary of the core preparation debitage

Core preparation artefact	**Count**
Core tablet	19
Core tablet segment	11
Flanc de nucléus	10
Partial flanc de nucléus	1
Core tablet / flanc de nucléus	2
Other platform rejuvenation debitage	47
Plunging debitage	13
Crested / possibly crested debitage	31
Subtotal	**134**
Possible core preparation debitage	164
TOTAL	**298**

Table 22. Raw materials of the core preparation debitage artefacts

Material of core preparation artefact	**Count**	**Percent**
Unknown flint	79	27%
Till flint	156	52%
Wolds flint	43	14%
Chert	0	0%
Other	0	0%
Unrecorded	20	7%
TOTAL	**298**	**100%**

Adding in the core preparation artefacts and core fragments to the distribution plot of the cores (Figure 53) suggests that knapping and ongoing rejuvenation processes are occurring mainly on the dryland but knapping could also have occurred in the wetland too, with either the cores being removed from the vicinity after the activity there has finished or the core preparation artefacts were utilised as tools in their own right in that latter area in some way as there are no cores discarded there despite this. Adding in this data also amplifies the idea of the cluster that was suggested from the cores in the southwest corner of the main dryland area.

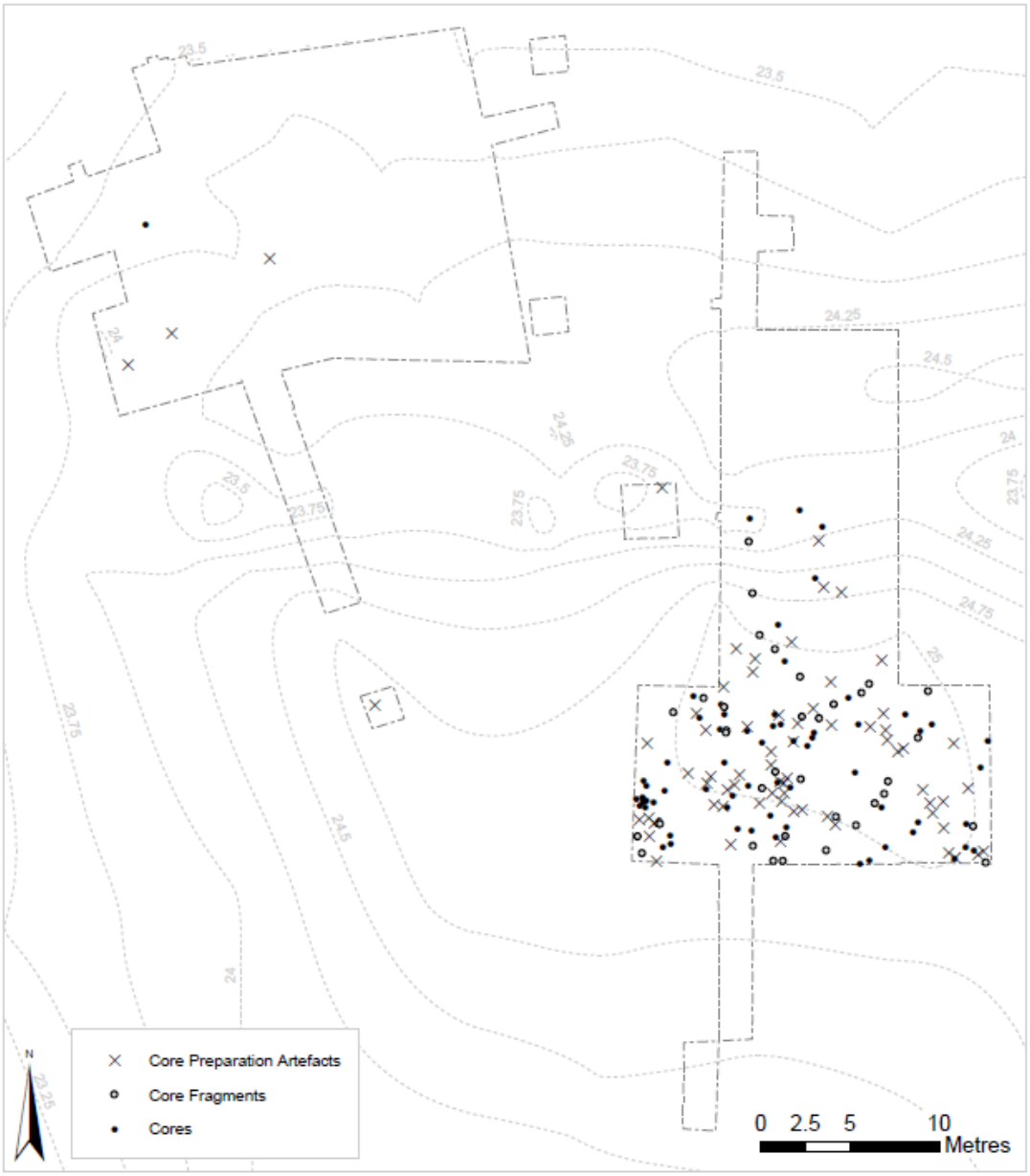

Figure 53. The distribution of core preparation debitage and core fragments, alongside the complete core assemblage

The presence of primary, secondary and tertiary debitage, further supports the argument that there was intentional transportation of material to site for in-situ knapping (Table 23). Occasionally nodules were tested and seemingly discarded after only one or two removals, with one nodule and its single primary removal being successfully refitted, however most of the material was worked down further, even the material with more inclusions and sometimes challenging cortical faces which were worked around. Flakes and then blades dominated the secondary and primary debitage types, unsurprisingly as this removes more cortex in one removal than bladelets.

Table 23. Primary and secondary debitage

Core Initiation Debitage	**Count**
Complete primary debitage,	86
of which:	
Bladelet	2
Blade	13
Flake	71
Complete or partial secondary debitage,	537
of which:	
Bladelet	40
Blade	137
Flake	340
Bladelet segment	1
Blade segment	5
Flake fragment	14
Primary or secondary (uncertain) debitage,	1710
of which:	
Bladelet segment	152
Blade segment	322
Flake fragment	522
Indeterminate	714
Possible core initiation debitage	1920
TOTAL	**4253**

The tertiary debitage produced was mostly flakes, then bladelets, then blades (see Table 24). This changes to flakes, blades, then bladelets when considering the segments and fragments, although the indeterminate fragments could have been parts of 'flakes or blades', 'flakes or bladelets', or 'blades or bladelets'. Complete blades (primary, secondary, or tertiary) went up to 135.1 mm in length (see Table 25 for summaries of dimensions). These were longer than the maximum at Star Carr and overlapping with the lengths of Vale Long Blade assemblages according to Conneller et al. (2018). The average blade length, however, was 41.5 mm and the standard deviation from this was only 11.32 mm.

Table 24. Core reduction and general debitage in the Mesolithic assemblage, including tested nodules of raw material ("complete" referring to complete flakes, blades or bladelets)

Core Reduction / General Debitage	**Count**
Complete tertiary bladelet	681
Complete tertiary blade	462
Complete tertiary flake	1056
Fragments and segments (tertiary / unknown), of which: Bladelet Blade Flake Indeterminate	7755: 1707 1011 1022 3989
Debitage chips and spalls	2783
Debitage chunks	411
Nodule chunks	39
Tested nodules	3
Possibly humanly worked debitage	1053
TOTAL	**14243**

Table 25. Dimensions of measured complete flakes, blades, and bladelets (primary, secondary, or tertiary) in millimetres.

Dimensions (mm)	**Blades (n = 499)**		**Bladelets (n = 444)**		**Flakes (n = 1027)**	
	Length	**Width**	**Length**	**Width**	**Length**	**Width**
Average	41.516	16.108	26.03964	8.9655405	25.040059	19.758187
Minimum	12.2	12	8.3	1.4	5.2	3.6
Maximum	135.1	50.8	57	11.9	92	62.4
Median	40	15	24.75	9.2	22.85	17.5
Q1	33.7	13.3	20.275	7.575	16.9	13.325
Q3	47.45	17.65	30.65	10.5	30.2	24
Std Dev	11.32	3.95	8.57	1.9	11.44	9.03

4.4.6 Knapped tools

4.4.6.1 Overview

The formal tools and associated debitage such as resharpening spalls make up 6% of the Mesolithic assemblage. Of the tools themselves, 270 are microliths, 302 are other formal tool forms (e.g. scrapers), 221 are retouched or possibly modified fragments, while 209 are possibly utilised debitage flakes and blades. Till flint is again the dominant material, with all formal tools being flint except for two microliths and one partial microlith of dark chert. Most of the formal tools are single type tools, although there is also a small number of combination tools. The general debitage showing potential use macrowear is a significant proportion of the complete tool assemblage, though this is treated as a provisional number as usage was unable to be confirmed using microwear or residue analyses at this time. However, it seems highly likely that at least some of this debitage would have been utilised and therefore would be a significant feature of the toolkit represented here.

4.4.6.2 Microliths

The microlith forms were generally those associated with the Early Mesolithic and seemed to be in keeping with Broad Blade assemblages supplemented with some artefacts that were alike to some Later Mesolithic microliths in form but usually larger in size. The assemblage consisted of 141 complete microliths and 129 partials or fragments thereof. Two of these artefacts were retouched, fine bladelet tools and as such grouped with microliths but may have been used, as other tools are generally assumed to have been, for example as piercers. Finally, there were two exceptionally small fragments recovered that appeared to have fine enough retouch to be parts of microliths but were so small they could also have been from microburins or other finely worked tools. The breakdown by microlith type is provided in Table 26 and a selection are photographed in Figure 54.

The assemblage yielded a wide variety of types of microlith, dominated by obliquely truncated forms (n = 88) that are very typically dominant in Early Mesolithic “Star Carr”, “Deepcar” and “Honey Hill” type assemblages (and indeed in the form of ‘zonhoven points’ in Long Blade assemblages) (Reynier 2005). A large majority of the microliths are of Early Mesolithic types with a few exceptions of Late Mesolithic forms and some irregular variations. It must be remembered that Reynier’s work was based on the analysis of only nine sites and other studies, such as Saville’s (Saville 1981b) work which included three sites and lithic scatters, to define Honey Hill type assemblages were also based on small sample sizes.

Table 26. The microlith assemblage by form. *Pieces described as "interrupted" in the table are those that have generally been retouched into a shape but where the apex of the arc or peak of the triangle is not retouched itself, thus leaving a small shoulder

Type	**Count**	**Percent**
Obliquely truncated	89	34%
Backed (convex) points	10	4%
Partially backed (convex)	45	17%
Partially backed (concave)	5	2%
Partially narrow backed (acute straight)	5	2%
Isosceles	16	6%
Regular isosceles	*11*	*4%*
Extra large isosceles (>30 mm length)	*2*	*1%*
*"Interrupted" isosceles**	*3*	*1%*
Scalene	22	8%
Regular scalene	*14*	*5%*
Extra large scalene (>30 mm length)	*4*	*2%*
Small scalene (<10 mm length)	*1*	*0%*
*"Interrupted" scalene**	*3*	*1%*
Lunate	5	2%
Regular lunate	*3*	*1%*
*"Interrupted" lunate**	*2*	*1%*
Straight backed (lunate blade)	1	0%
Partially straight backed (lunate blade)	1	0%
Bitruncated trapezoidal	4	2%
Bitruncated rhombic	1	0%
Rod/boat-shaped	1	0%
Irregular	22	8%
Fragments	36	14%
TOTAL	**262**	**100%**
To be confirmed	8	3%

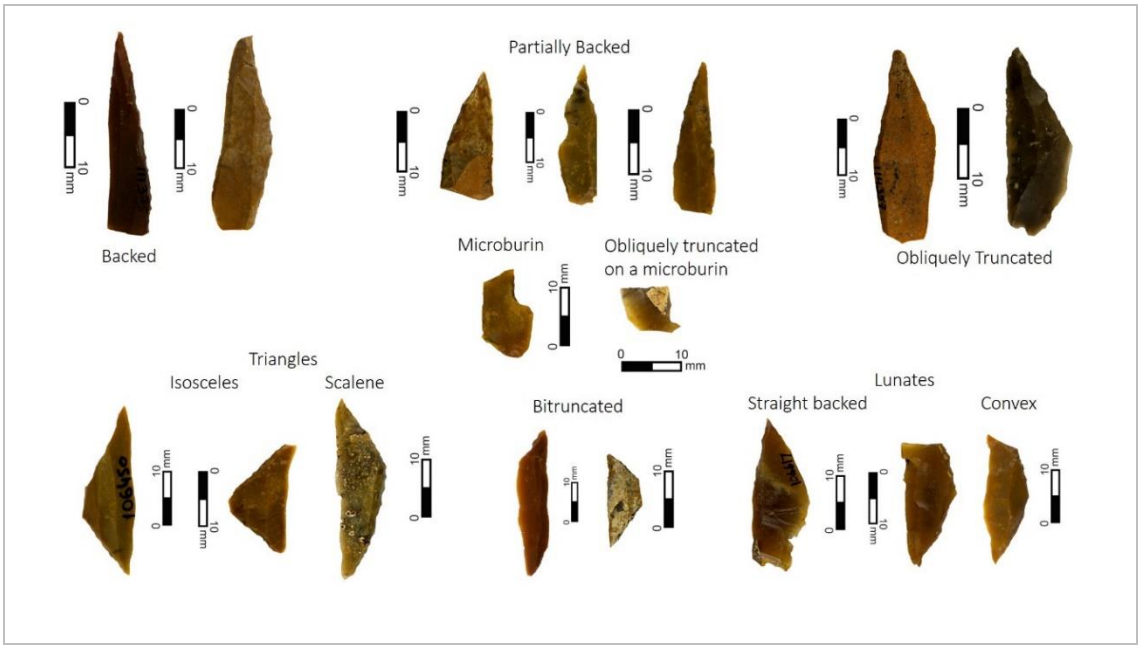

Figure 54. Photographs of a selection of microlith types from the site (photography by N. Gevaux)

The obliquely truncated points are followed by half as many partially backed pieces, followed by scalene and then isosceles triangles. These are joined by ten backed points with the more classic convex retouch. As defined by Radley and Mellars (1964) and later supported by Reynier (2005), Star Carr type assemblages tend to be more restricted in the types represented, being dominated by obliquely truncated points (Reynier's sites: c.26% to 63%) and lacking backed points and partially backed points (completely in Reynier's sites). They also tend to have more trapezoids than Flixton Island 2, and no rhomboids (Reynier's sites: 1–7 trapezoids and 0 rhomboids). As such, the profile does not comfortably fit as a Star Carr type assemblage.

Deepcar type assemblages tend to have more variety, with quite a high proportion of partially backed points (Reynier: 15-20%), a small number of backed points, rhomboids and triangles (Reynier: c. 1-5% each), and generally fewer trapezoids (Reynier: <10%) than Star Carr type assemblages. While the partially backed points, backed points and trapezoid figures from FI2 are in keeping with Reynier's percentile ranges, there is only one rhomboid from FI2 but also a very high proportion of triangles (14%, of which 8% are scalene) which is not in keeping with this assemblage type.

Saville's Honey Hill type assemblages, on the other hand, do tend to have more similar proportions of triangles, with his sites yielding approximately 5-15% isosceles triangles, 2-30% scalene triangles, as well as significant numbers of partially backed points (1981). However, Saville's sites did have higher proportions of completely backed points (15-30%) and rhomboids (5-15%) than seen in the FI2 assemblage. These tool types were both present, however, and the rhomboid count may have been underestimated: 12 artefacts (5%) show retouch on one or both of the edges at the basal end but did not fall into a classic

rhomboidal or trapezoid shape. With a more relaxed definition of these microlith types, their numbers would be bolstered (though even if all were assigned to one of these formally bitruncated types, they would still only potentially match isosceles and not surpass the scalene triangle contributions).

A small number of the microliths (n = 7, 2% of the microlith assemblage) show basal modification, in addition to the 12 showing retouch on one or occasionally both of the edges at the basal end. However, this is not the classic inverse basal retouch that is semi-invasive, as seen characteristically on Honey Hill sites, such as the recently published Ashfordby, Leicestershire (Cooper et al. 2017). One of the FI2 basally modified pieces could possibly be considered hollow based but it was only slightly concave, unlike more classic hollow based points that typify Horsham type assemblages from the south of England, and as Horsham assemblages are a southern phenomenon this is not surprising. Finally, an additional eight pieces showed possible basal (n = 3) or basal edge (n = 5) retouch but it was either too lightly done or interrupted by modern damage to be entirely confident. As such, 2% of the microlith assemblage was basally modified, increasing to 7% of the assemblage if including all those with basal or basal edge modification and this figure increases to 10% if the possibly modified pieces are incorporated. When considering the Honey Hill type assemblages, Saville's descriptions of a small sample of four sites from the Midlands and East Anglia fell between 5 and 20 % basally modified (Alan Saville 1981b; Alan Saville 1981a, the latter as cited in Reynier 2005). Nor is there an emphasis on inverse retouch to modify the base at Flixton, the dominant basal retouch type at those sites. As such, Flixton has a small basally-modified element to its assemblage unlike the typical Star Carr and Deepcar type sites that would not be expected to have any, but not as significantly as the classic basally modified assemblage types either or with the characteristic types classically associated with Honey Hill or Horsham assemblages.

Radley and Mellars (1964, 9) and Reynier (2005, 22) found left lateralization tends to be preferred but more common in Deepcar (Reynier: c. 80% of microliths left lateralized) and basally modified assemblages (Reynier: >95% in Horsham assemblages studied) than Star Carr ones (Reynier: c.65%). Of the 88 obliquely truncated points, only 58 were lateralized to the left (66%). Of the 55 partially backed pieces, 48 were lateralized to the left (87%). Of the ten convex backed points, four were left lateralized (and one was unclear) (36%). As such, for all these artefact types combined, 71% are left lateralized. Adding in the other backed pieces and fragments where a side could be identified with reasonable confidence (n = 192), only 63% (n = 120) could be attributed as left lateralized, compared with 26% that were right lateralized, and 12% that could not be identified. So, while left lateralized generally, the lack of high proportions is more in keeping with Star Carr type assemblages.

In addition, only 11of the pieces from the assemblage showed leading edge retouch (4%). In both Radley and Mellars' work (1964, 15) defining Deepcar type assemblages and Reynier's on Deepcar and basally modified Horsham and Honey Hill, higher proportions were recorded for those assemblage types (Reynier's figures being between 15-25% in 2005, 22). Flixton again sits between assemblage types.

Finally, the average length of complete or near complete microliths was 26.6 mm and width was 9.6 mm. This sits in the centre of the range of means for Reynier's Star Carr assemblages (18-34 mm), short of the minimum mean of his Deepcar assemblages (33 mm), and at the upper end for his basally modified Horsham assemblages (maximum mean being 26 mm, 2005, pp.18 & 22). Saville's Honey Hill assemblages had mean lengths between 21-26 mm as well (Reynier 2005, 29; Saville 1981b, 55).

Considering all these aspects, Flixton Island 2 is not comfortably consistent with any of the classic assemblage types. Based on the microliths in terms of types present, it seems to fit best with Deepcar, though with a higher proportion of scalene triangles than expected, or Honey Hill, though with the lack of the decently sized, and crucially characteristic, basally modified component. In terms of dimensions and lateralization, it seems to fit more with Star Carr type assemblages. The applicability of these tool assemblage types, at least regarding Flixton Island 2, is called into question. This could be due to its nature as an insular location, perhaps relating to different activities occurring here, as well as different raw material availabilities than the other sites compared. The nature of the people who used the site could be different or another complementary site part of a network utilised throughout the landscape: This could easily be an insular version of a site used by people who used Star Carr, or other sites around the Vale, or seasonally used by people who also used the upland sites in Yorkshire (though to be clear there is no specific, categorical, link such as cross-site material refits between Flixton Island 2 and any other Vale sites at present).

However, perhaps most likely, the non-conforming composition could also be due to a palimpsest of Early Mesolithic occupations of potentially different assemblage types (indicated by the high presence of a variety of large geometric microliths), with some Long Blade materials being incorporated (in the form of the narrow backed bladelets) as well as Later Mesolithic artefacts (the small scalene, rod/boat-shaped pieces, and one irregular geometric microlith that was between a microscalene and a subrectangular shape) activity. The shallow stratigraphy does not aid interpretation; however, spatial horizontal distributions do suggest some grouping. The 3D located microliths do generally tend to cluster in the three scatters within the main dryland area (Figure 55 and Figure 56). The sieve-retrieved microliths are summarised by trench in Table 27 as well. Most of these were

retrieved from dryland trenches, notably trench 4 from which 56 were retrieved, joined by one example from wetland trench 6 and four pieces whose original locations were unrecorded.

Figure 55. Distribution of the microliths and microburins across the site

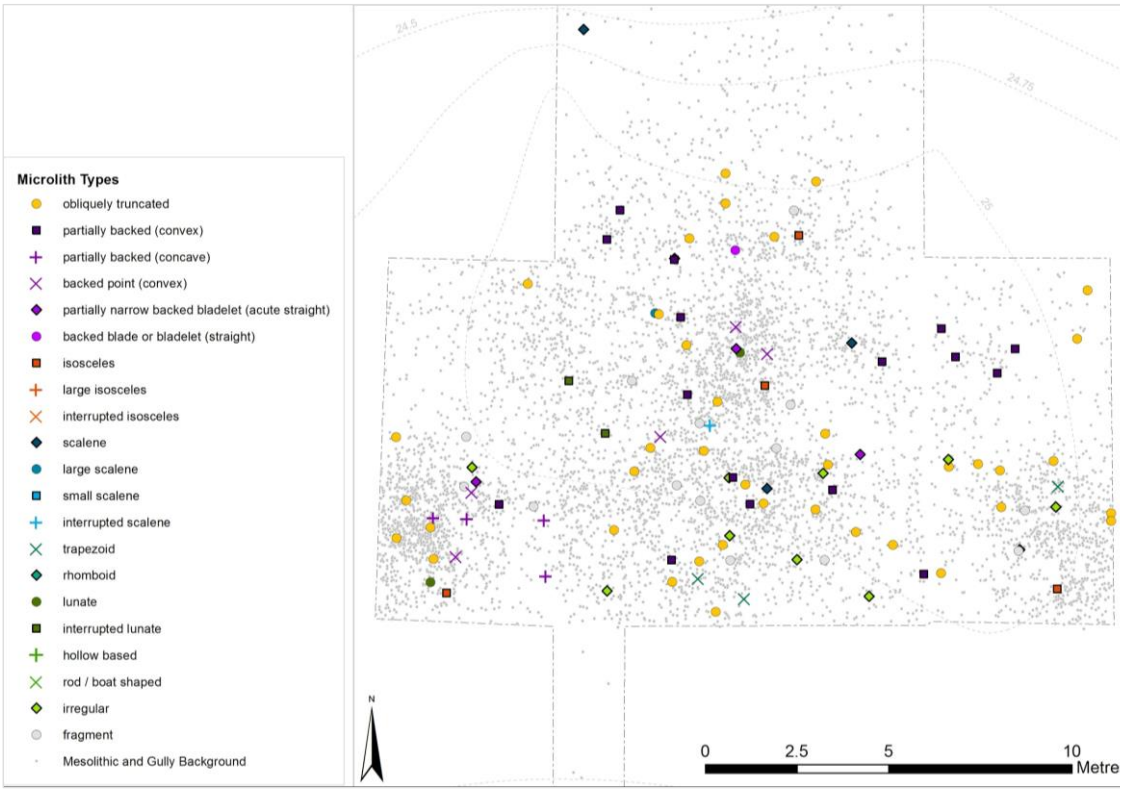

Figure 56. Distributions of the different microlith types across the dryland

Table 27. Summary of microliths retrieved from sieving, by trench

Area of site	Trench	Count
Dryland	4	56
	9	25
	11	30
	12	2
	15	24
Dryland / gully / bar	7	9
Wetland	6	1
Unknown trench / not applicable	-	4

The one 3D located lithic in the wetland trenches is an obliquely truncated fragmentary tip and is not near the wetland Mesolithic cluster. This is joined by one sieved microlith from trench 6 near the Mesolithic scatter, that was a complete obliquely truncated point. These being common Early Mesolithic types, these do not suggest any reason to consider the scatter as part of a separate occupation to the dryland.

A complete obliquely truncated point was retrieved from trench 14 in the base of the gully and there is a partial scalene triangle on the slope down from the main dryland area into

the gully in trench 7. This supports the interpretation of the gully deposits being associated with the Mesolithic phase. Scalenes are generally more common later in the Early Mesolithic, but they are also in the earlier assemblages occasionally. There are two complete obliquely truncated points together up on the northern bar which again is not particularly suggestive of chronology. There were no sieve lithics identified from north of the gully in trench 7 to accompany these pieces.

There are three pieces from trench 3, further to the west on the dryland, all 3D located. These included one complete and one partial obliquely truncated point but also a partially convex backed piece with inverse basal retouch. The basally-modified piece might suggest a slightly later (still Early Mesolithic) occupation period of the site is reflected in trench 3 but it is not a lot of data to base this on.

The microburins, as microlith manufacture debitage (and indeed one microlith <sl/465> was manufactured directly onto a notched and snapped proximal microburin, see Figure 54), are generally associated with the microliths in the main dryland area in those clusters, although they are a little more generally dispersed across the area. In addition, there are two microburins from the area of the wetland Mesolithic cluster.

Moore had retrieved 78 microliths from Flixton Island 1, while 313 microliths or their fragments were recovered during the POSTGLACIAL excavations at Star Carr. In addition to the microliths presented here, Moore had retrieved no Mesolithic microliths from Flixton Island 2 as far as he reported (Moore 1954), while the VPRT excavations yielded one obliquely blunted point (Conneller and Schadla-Hall 2003; Chantal Conneller pers. comm.). As such, for the location and relative to these neighbours in the landscape, this seems a moderately high number. However, in terms of use, if multiples were being hafted onto one tool, such as the arrows found at various sites across England including Star Carr and elsewhere in Europe like Loshult (cf. discussions in Myers 1987, 1989; Kuhn and Stiner 2001; Larsson 1990; Larsson and Sjöström 2011b), then the total number may represent only a quarter or less of this number in terms of composite tools being prepared. The sizeable microburin assemblage suggests that microlith manufacturing was occurring on site.

Crombé et al. (2001) found that microwear on an assemblage of over 400 microliths from an Early Mesolithic site in Belgium indicated damage consistent with being used as tips or barbs on projectiles and that, of these, obliquely truncated points, basally retouched points, and backed points all had damage consistent with being usually used as tips while triangles and crescents (lunates) had damage more usually consistent with being used as barbs when compared to an experimental collection. If the microliths at Flixton Island 2 were similarly used for projectile point manufacture, then there is a mixture of tips and barbs available but

with an emphasis on tips. The preliminary work by Aimée Little suggested one microlith did show damage consistent with an impact, which would imply post-usage deposition, and many of pieces show tip macrowear and possible use retouch (Aimée Little, pers. comm.). This is supported by the fact that a high proportion of the pieces are fragments, but this could have been breakage during other processes. It must be remembered that microliths could well have been used to manufacture a whole plethora of tools and do not necessarily indicate hunting but have been argued to be used on plant material at other sites in fact, and being portable have been used elsewhere in the world as finely worked prestige objects for trading and gifting (cf. Clarke 1976; Kuhn and Stiner 2001; Torrence 2002 and other papers in ; Elston et al. 2002; Larsson and Sjöström 2011b; Cooper et al. 2017). Unfortunately, none of the pieces from our excavations seem to retain any signs of hafting mastics or other substances for residue analysis.

4.4.6.3 Awls or Piercers and Mèches de Foret

These are blades or flakes with retouch along one or both edges leading to the tip or an artificial point, that form usually sturdy points or apices. As the name implies, these have traditionally been assumed to be for piercing or drilling. The distinction between the two types is often made based on the wear indicating the direction of usage, so they are recorded as one category here. Furthermore, there is a distinctive type of piercer called a *mèche de foret*, which have been retouched fully or nearly fully along both edges and around the base, coming to a converging to a blunt-sided point at both ends, often in an elongated teardrop shape. Clark (1975, 108) suggests these were used specifically as drill bits. As such, these artefacts can sometimes look similar to certain microliths, for example those partially backed with leading edge retouch or even lanceolate shaped, and some artefacts in both categories may have been used for the same or similar purposes (whether that is piercing or otherwise). For the purposes of this thesis, classification was based on awls/piercers exhibiting cruder retouch and the pieces being generally slightly more chunky and larger (see Figure 57).

Figure 57. Examples of the awls/piercers and mèches de foret (photography by N. Gevaux)

There were 17 awls/piercers and five mèches de foret, or partials thereof, recorded at Flixton (excluding possibles). Where there was only the tip of the piece, the piece was recorded an awl/piercer tip (as the more general category). This is a much smaller assemblage than that at Star Carr, where 69 of these artefacts were retrieved during the POSTGLACIAL excavations, to supplement Clark's previously retrieved piercer assemblage of more than 100 examples, and some of these were located in the vicinity of several beads (Milner et al. 2016; Conneller et al. 2018).

Seven of these were complete or near-complete awls/piercers, three of which were identified as being made from till flint and two from Wolds (the other two being unidentifiable). Five were bilaterally worked, while two were unilaterally worked up to the tip. The tip had been broken off the near complete example. The average length of these was 36.7 mm, ranging from 24.0 mm to 49.8 mm, and the average width was 18.75 mm, ranging from 11.7 mm to 29.0 mm. Two of these were recorded as being notably thick pieces, having maximum thicknesses of 11.5 mm and 14.8 mm. Two of these pieces also retained some cortex on the ventral side.

Four complete mèches de foret were recorded. These averaged out at slightly longer at 38.26 mm (with a range between 26.6-60.2 mm), but also narrower at 15.8 mm (between 12.7-18.8 mm) than the general piercers. Three were on till flint, one was made of flint from

an unknown source. Two examples noted as being more chunky than the other two, with thicknesses of 7.3 mm and 9.2 mm, also retained a small amount of cortex, possibly intended to provide grip, but both were retouched around the base and either completely or very near to their full circumference. One of these, <107354>, was a slightly more unusual example in that it did not form the parallel sided, lanceolate / teardrop outline but has some retouch at the tip on the right hand side that cut into the piece concavely, forming a slight asymmetrical hook to the tip of the piece on that side.

Mèches de foret are very often associated with Star Carr type assemblages specifically, following Radley and Mellars' (1964, 21) and Reynier's (2005, 22) analyses. However, awls/piercers are more generally present in greater levels in Star Carr assemblages anyway, with Reynier recording them as between 11-48% of the assemblages he analysed, while they are generally present in more variable, but lower levels in Deepcar (0-13%) and basally modified assemblages (5-25%). Altogether, they form less than 1% of the Flixton assemblage but the presence of mèches de foret means the site is closest to Reynier's Deepcar ranges.

Ten pieces were recorded as partial awls or piercers. Eight of the partials were tips, two of which had a small amount of cortex remaining on the ventral side. Eight of the piercer/awl partials, seven of which were tips, were bilaterally blunted, while the remaining two were unilaterally blunted. Two were made of patinated Wolds flint. One further patinated Wolds artefact was the basal end of a mèche de foret.

All the 3D located awls, piercers and mèches de foret were excavated from the southern end of the main dryland area (see Figure 58). There is no further particular clustering of the group as a whole, as while there are some of the complete awls/piercers in close proximity, the numbers are too low whether or not to say this is a true grouping. Of the ten that were retrieved during sieving, all were found in dryland trenches as well. Four were from trench 4, one from trench 9, four from trench 11, and one from trench 15. None were recorded as being from the same or even an adjacent square to each other or the 3D located pieces; however, two pieces (from trench 4 grid A1 and trench 9 grid C-3) fell within the area of the central dryland cluster.

Figure 58. Distribution of the 3D located awls, piercers and mèches de foret

4.4.6.4 Scrapers

Scrapers were by far the most prominent formal tool type, joined by microliths and possibly utilised debitage, with 196 scrapers or partial scrapers being retrieved (excluding the possible scraper count). The majority (n = 112) were end or end and side scrapers, along with 48 fragments that were parts of scrapers with end retouch, though lacking the rest of the piece they could have been parts of other scrapers that included end retouch (see Table 28). This is typical for an Early Mesolithic site (Butler 2005, 105). As at Star Carr, short end scrapers are better represented than long ones which Conneller argues may have prevented breakage during use (Conneller et al. 2018). All double ended scrapers were short too. 95 of the scrapers had between one-fifth to three-fifths cortex coverage on the dorsal side, 77

of which were end scrapers. Six of the hollow scrapers were end scrapers, the remaining one was an end and side scraper.

Figure 59. Examples of scrapers (photography by N. Gevaux)

Table 28. Summary of scraper types

Scrapers and partial scrapers types	**Count**
End, long	25
End, short	77
End, fragment	48
End and side	10
Double (all short)	9
Side	6
Round	2
Nosed	3
Irregular	12
Fragment	4
TOTAL	**196**
Of these:	
Hollow	*7*
Spurs	*4*
Micro (<20 mm dia.)	*15*

All 3D located scrapers were found on the dryland, with a small number on the slope going down into the gully, but none were found in the wetland areas or gully itself (see Figure 60). There are two clusters which are in the areas of lithic clustering in the centre (trench 4) and the southwest (trench 15) of the main dryland area. There are also quite a few in the southeastern dryland general cluster but they are not as closely spaced. Considering the distribution by type, the cluster areas were mainly made up of end scrapers but at the same time end scrapers were distributed across all the other areas, and there was no clustering obvious for any of the other scraper types (see Figure 61). There were 86 scrapers

additionally retrieved from sieving which mainly came from trench 4 and trench 11 (see Table 29). Seven of these were from the central dryland cluster (and it must be remembered that the grid squares being unreliable in trenches 11 and 15 means that those tools from the southeastern and southwestern dryland clusters retrieved by sieve cannot be assigned to grid square and therefore finds from these clusters will potentially be underestimated).

Figure 60. The distribution of scrapers and partial scrapers

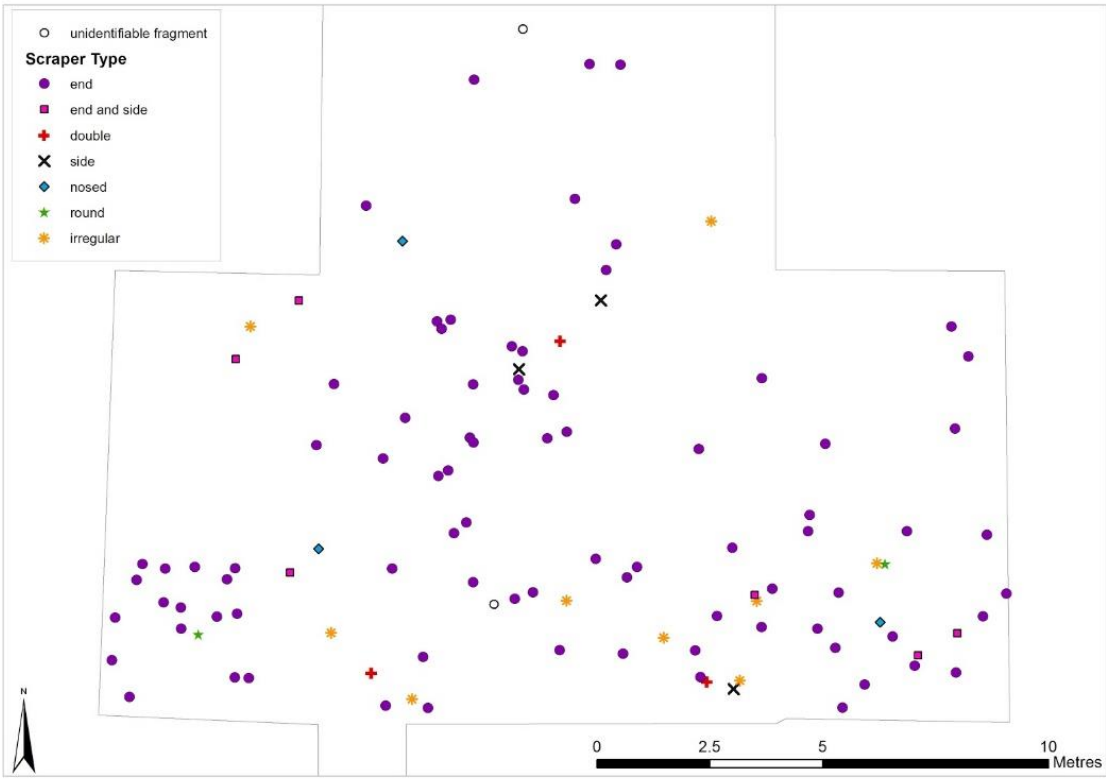

Figure 61. Scrapers by type

Table 29. Summary of the frequencies of scrapers retrieved from sieving, by trench

Trench	Count of Scrapers and Partial Scrapers
4	41
7	5
9	3
11	25
15	6
Unknown	6
TOTAL	**86**

A small spur or two were present on four of the scrapers (<106265>, <112683>, <114260>, and <sl/364>), which is a feature flagged by Conneller as being on some of the scrapers from Star Carr and Seamer C as well. This was usually at the end of a row of normal retouch, where a deeper removal was made to leave a spur protruding at the end. This was interesting as it would have a bearing on any material being worked on, potentially leaving a groove in the material if the scraper was being drawn along the material with the blunted edge in contact as is usually assumed. One of these scrapers was also a possible attempted burin combination as well, <110991>. In addition, irregular scraper <sl/331> was potentially a gun flint rather than an actual Mesolithic scraper. <105606> was

manufactured on a core tablet or platform rejuvenation flake, while <110883> was manufactured on a crested blade. One fragment was suggestive of being part of a scraper but it was lacking ripples indicating directionality.

The morphology of scrapers is generally that the retouch produces a sturdy edge which is not apparently for slicing material, but more likely useful for scraping or forming wide grooves depending on the pressure and depth it is worked to. Wear and residue analyses on the tools from other sites has often suggested they have been used for hide or leatherworking, or use on similarly soft materials, but also on bone, wood and minerals for ochre (cf. papers in Marreiros,Bicho and Gibaja 2014). As such, as with the other two main types of tools, these are a versatile tool suited to many different activities.

4.4.6.5 Burins

Burins were the second most common non-microlith knapped tool type, with 35 complete or partials identified of this tool type. Of these, there were 33 complete examples while two were partial (representing 0% of the global assemblage, and see Figure 62). This is a much lower number than recovered from Star Carr during the POSTGLACIAL excavations (n=232) though proportionally this is still only c.1% of the assemblage there, while proportionally at Reynier's Star Carr sites they were between 11-49% of the assemblages (though this was only two to 14 artefacts, as reported in Reynier 2005 p.19; Conneller et al. 2018). This does raise the question, again, of the validity of the groupings, especially when comparing assemblages of such different sizes. Reynier's Deepcar sites yielded 0-27% (zero to 34 artefacts), while his Horsham sites yielded 1-13% (one to five artefacts, as reported in Reynier 2005, p.20). Regardless, various burin types are represented, as recorded in Table 30. Break and truncation angle burins are the most common types, followed by dihedral burins, which is typical for Mesolithic sites in the Vale in contrast to Long Blade sites that tend of have more dihedral burins (Conneller and Schadla-Hall 2003; Conneller et al. 2018). Slightly unusual pieces were burin <sl/204> that was manufactured on what had been an axe or adze resharpening flake, and <111677> with a plunging removal that formed it into a dihedral burin.

Table 30. The burin assemblage

	Single angle	**Double angle**	**Unknown**	**3 or more burin removals**	**Total**
Attempted break	0	0	1	0	**1**
Attempted truncation	0	0	1	0	**1**
Break	4	4	2	0	**10**

	Single angle	Double angle	Unknown	3 or more burin removals	Total
Concave truncation	0	1	1	0	**2**
Dihedral	0	0	6	0	**6**
Irregular	0	0	2	0	**2**
Truncation	1	3	6	0	**10**
Unknown	0	0	3	0	**3**
				TOTAL	**35**

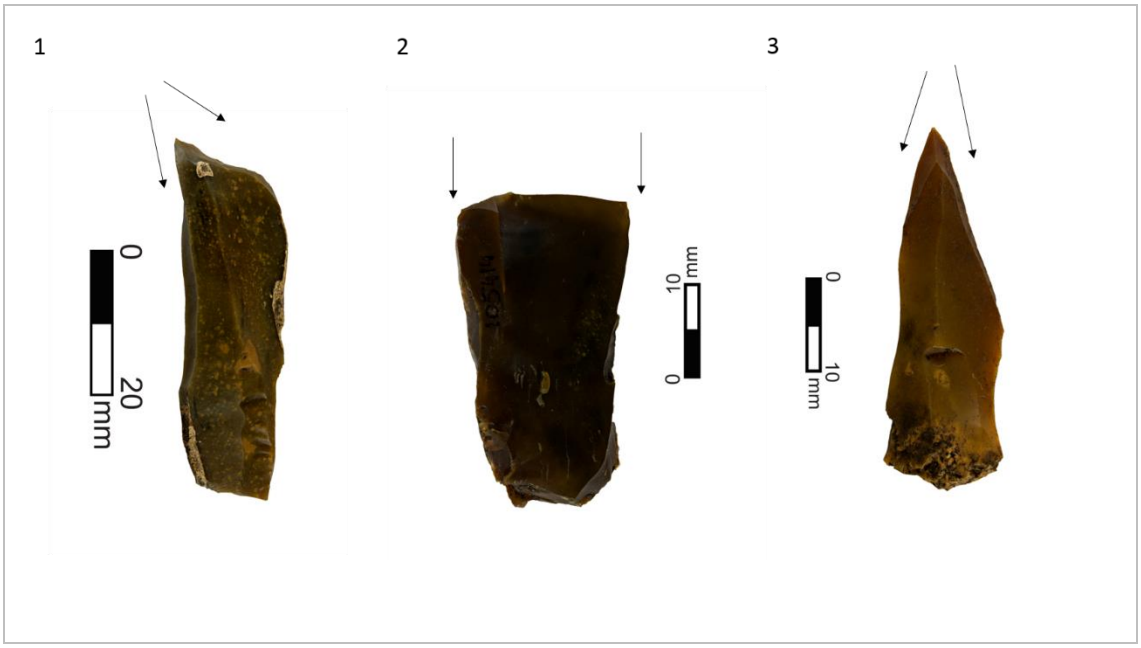

Figure 62. Examples of the burins (photography by N. Gevaux). 1 is a dihedral burin, 2 is a double angle break burin, and 3 is a possible dihedral burin.

The burins were challenging to identify, so if any tool type is underestimated it is likely to have been these. During recording a "possibly burinated" category was utilised to record pieces that were not obviously classical burins but may have been expediently burinated or not identified as a classic burin type accidentally. These pieces totalled 135, which would still bring burins in, albeit at a much closer, second place and it is very unlikely most of these possibly burinated pieces are actually burins as recording "erred on the side of caution".

Many of the 3D located burins and partial burins were in the general vicinity of the central dryland cluster or the southeast dryland cluster, though they were found generally throughout the main dryland area (Figure 63). One was also found in trench 14 in the gully. None were found in the main wetland trenches. Displaying the burins by type did not reveal any particularly strong type clustering, although one (unusual) concave truncation burin and an irregular burin were found in very close proximity in the western end of the main

dryland area. Two truncation burins and a break burin were also very close to each other in the vicinity of the southeastern cluster. 14 burins and partials were retrieved during sieving from the dryland: five in trench 4, three in trench 9, two in trench 11, two in trench 12, two in trench 15. Very few lithics were retrieved from trench 12, the trench that extended down the southern slope off the dryland, so the presence of two burins there in diagonally adjacent grid squares (grid squares E-6 and F-7) is notable. One was a double angle break burin and the other a double angle concave truncation burin, neither of which are particularly common on site which is also interesting, though no particular interpretation can be proposed based on the presence of these two finds alone. One single angle break burin was found in A3, putting it in the central cluster area. One additional burin, <110704>, had no location data recorded, unfortunately.

Figure 63. Distribution of burins and partial burins

4.4.6.6 Microdenticulates

Microdenticulates are more common in Early Mesolithic assemblages generally, becoming rarer later in the period (Butler 2005, 109), but according to Reynier (2005, 22), they were rarer on the Star Carr and Horsham type sites but formed 1–23% of the assemblage at Deepcar sites. Only eight microdenticulates or partials thereof were found on site, two in situ and six from sieving, in comparison to 23 recorded by Conneller for Star Carr. Four complete examples were found in trench 4, supplemented by four partial examples from trench 15 so all were retrieved from dryland contexts. They were generally characterised by very carefully executed denticulations, even by general standards (see Figure 64). These tools have been associated with working fine plant or other soft material (cf. Högberg 1994; Barton 1992; Conneller et al. 2018), although microwear and residue analysis needs to be conducted further before confirming this on a specific site and to more generally establish or refute this idea as canon for the Mesolithic.

Figure 64. The microdenticulates (photography by N. Gevaux)

Two of them had further retouch blunting the opposite edge, presumably to allow pressure to be applied during use or for hafting, which is rare according to Butler (2005, 109) but more common in later periods according to Högberg (1994, 19). All were on tertiary blade/lets so there was no 'natural' backing of cortex on any piece. In the case of find <101685>, the fine retouch produced a finely denticulated concave edge which is more usual for this tool type according to Butler, but the others here were straight or slightly convex where it was possible to tell. Two of the artefacts were patinated.

Only two of the identified microdenticulates (or partials) were found during trowelling and 3D located. They are both found in the vicinity of the central dryland cluster (Figure 65). Of the six recovered from sieving, two were also from trench 4, one in the central cluster area (in grid square A1). The other four were from dryland trench 15, in the west of the main dryland area (unfortunately where the grid square provenancing was impacted by the issues with numbering so cannot be reliably attributed to a location within it).

Figure 65. Distribution of the 3D located microdenticulates

4.4.7 Core Tools

4.4.7.1 Overview

The core tool assemblage was small which is not unusual for an Early Mesolithic site, but quite varied in nature and yielding some interesting pieces for consideration (Table 31). However, one thing to note is that axes/adzes in the Vale have only been found at Star Carr, No Name Hill (another island that was a short way away from Flixton), and in Moore's excavations of Flixton Island 1 (Conneller and Schadla-Hall 2003, 102). Following Inizan et al. (1999, 44 & 51), bifacial or multifacial shaping that is used to create axes, adzes and picks, falls into two general phases with one optional subphase in the middle: Roughing out is when the main bifacial surfaces are fashioned initially; the preform is an optional subphase where the roughout is more carefully prepared into something much closer to its final shape; finally the finishing phase is when the contour is cleaned up into its final form with finer working and retouch, particularly on the lateral edges. According to Inizan et al. (1999, 51), heat treating can occur during any of these stages as well.

One axe/adze was found (the nature of its use unable to be confirmed at this stage), which was quite different in nature to some of the roughouts and preforms found as discussed below. In addition, there were various axe roughouts and preforms of different sizes, one of which had been extensively burnt. Other core tools included some very large tools as well as smaller pieces manufactured on worked down cores, and strike-a-lights. There were also two cores with potential, but unconfirmed, microwear.

Table 31. Relative proportions of the Mesolithic core tool assemblage

Core Tools	**Count**	**Percent**
Axe/Adze	1	8%
Axe/Adze Roughout or Preform	4	31%
Possible Large Scraper or Planer	1	8%
Possible Wedge or Splitter	1	8%
Core Scraper	2	15%
Strike-a-light	2	15%
Potentially utilised cores	2	15%
TOTAL	**13**	**100%**

The 3D located core tools were distributed on the dryland of the site and on the slope going north from there into the gully (Figure 66). The axe/adze and preforms were not grouped at all but spread across the area. Two core tools were close together in the centre-south of the dryland area. One core tool was in the area of the southeast dryland cluster. All three of the core tools retrieved from sieving were found in trench 4, on the peak of the main dryland area, though none fell within the area of the central dryland cluster.

Figure 66. Distribution of the 3D located core tools across the site

4.4.7.2 Flixton Island 2's axe/adze

One complete tranchet axe or, more likely, adze was identified, find <101854>. It is 98.1 mm in length, 40.2 mm in width, and 18.7 mm thick (Figure 67). The flint is a mid brown with light orange appearing inclusions. It has a large chalky cortex dimple on opposite ends on

both sides, possibly providing areas for gripping as it naturally fits in the hand. One side is generally flatter though not through extensive sequential inverse retouch removing large flakes but seemingly more sporadic large removals to get it broadly into the appropriate shape, including some blade removals to narrow the piece along one edge. On the other side, the face is overall more convex, especially at the end without the cortex which has been shaped with more systematic large invasive retouch into a smoother dome and as such the piece has a curved, broadly subtriangular cross-section. On this face, there are two tranchet removals (transverse removals obliquely cutting through the adze body to produce a sharp edge at one end) at either end of the piece, both struck from the same side of the piece. The rest of that edge is generally blunted with smaller invasive and semi-abrupt retouch. One section of the opposite edge is also blunted, but there are also large removals and even an irregular chunk taken out of it which produces a sharper edge (the opposite side retains the scars of invasive retouch there but the bulb scars have been removed when the chunks came away). One of the tranchet edges is undamaged, but the other has some invasive removals jutting into it from the edge which could be from use and there is some possible gloss or other polish along that edge. This likely adze was checked by Shannon Croft for residues and Aimée Little for microwear but there were no positive results.

Figure 67. Tranchet axe/adze <101854> (photography by N. Gevaux)

4.4.7.3 Preforms and roughouts

Find <101636> is an interesting piece as it appears to be an irregular but small axe/adze, seemingly near complete, but then burnt with perhaps an attempt at a tranchet removal after it has been heated (Figure 68). There are, however, large heat spall scars on one surface and this removal at the end may also have been a heat spall event rather than a deliberate attempt to rejuvenate the piece. As it does not appear to have been used or finished, it is recorded as a preform. It is made on Wolds flint that has subsequently patinated orange and then opaque white, with glossy lustre inside the post-heating scars. The piece has large invasive flake and blade removals stemming from one side of the piece. The natural distal end of the original flake or nodule chunk has been honed to a thin, sharp edge by some of these removals that only shows occasional damage not particularly suggestive of use (the original platform those removals stemmed from has been obliterated by one large removal across their original end, perpendicular to their direction, which is then used as a platform for working the opposite face). It measures as 53.4 mm long, 34.0 mm wide, and 18.8 mm in thickness. It is not well finished or shaped and it is possible it was intentionally discarded into a fire as it was realised it was not fit for purpose.

Figure 68. Preform / broken adze <101636> (photography by N. Gevaux)

Smaller piece <106735> is only 42.8 mm long by 35.7 mm wide by 13.3 mm thick (Figure 69). This appears to be a small roughout, that has perhaps been abandoned after shaping and cortex removal proved difficult, or it may have been a completed but more expedient and very simple axe/adze. Roughouts are not usually present around Lake Flixton according to Conneller et al. (2018), which they argue is because initial roughing out possibly took place at the source: this is such a small piece, that it may have been a spontaneous attempt at producing a small axe or adze on a piece that was not initially intended for this purpose or that was considered light enough to transport as it was. Being so small, it was not identified as such a find in the field or packaged for microwear and residue analysis (which required a different collection procedure that avoided handling the flint).

Figure 69. Photo of small roughout / near complete adze <106735> (photography by N. Gevaux)

It is a similar flint to the axe, a very slightly darker brown with light orange and black inclusions and chalky cortex on either side. It looks like it could be from a tabular piece as the cortex is flat and 'sandwiches' the piece in the centre on both sides with the knapped outer areas tapering to an edge, so the piece is only slightly biconvex overall and flattened lenticular in cross-section. This is more in keeping with an axe than an adze profile (Butler 2005, 55). It has invasive retouch on one or the other of the sides around most of its circumference, cutting into the areas that retain cortex. One end is thicker and retains a crushed platform on one side, while the other side has a large invasive flake removal emanating from it that could have been an attempted tranchet blow although the angle would be irregular. The other end tapers down to a ridge that may have been formed with a tranchet blow but has large removals scarring across the tranchet surface if so. Some of the removals are stepped, where they have been struck at an angle that forces them too deep into the surface for a removal to flake off cleanly, and frequently stop abruptly in the cortified area. It is hard to imagine this find being intended or used for the same kind of task as the other adze, as it is so much smaller and therefore lighter.

It could have been hafted but, if not, in the hand it would need to be used quite differently as well, assuming both were used by an adult (which is not necessarily the case). It could have been used on the same but thinner pieces of the same material though, for example comparing working on a trunk to working on thin branches of wood, but this would need to be supported by microwear and residues to be able to comment on this and as yet there is no suggestion as to what either artefact might have been used to work. For now, this piece is classified as a roughout as it shows no signs of extensive shaping or finishing retouch.

Find <100813> is a large roughout or preform that has two potentially attempted tranchet blows at one end that have been either quite shallow and therefore not permeating through the entire cross section to produce the sharp edge, or unsuccessfully ending in a step termination as it has cut in too deep (Figure 70). Further tranchet removals have not been attempted though they could have been. It does not show any crushing or apparent macrowear from use or being hammered, supporting the definition as an unfinished preform. It is manufactured on opaque and quite patinated Wolds flint. It is technically biconvex but flatter on one side, so it is subtriangular in cross-section at one end, where there is still some adhering cortex as well, while more lenticular at the end with the attempted tranchet removals. There are large invasive removals on both sides of the piece, many terminating with steps, some of which go into the cortex: It is not particularly finely worked even for the fact that this material is poorer quality in terms of it being larger grained with more inclusions and therefore more difficult to knap. One edge is a largely continuous, if roughly worked, ridge. The opposite edge, however, has two large blades removed from it that extend two-thirds down the piece, cutting through the side

perpendicularly (like burinations). The new edges formed by these removals have been used as the platforms for the invasive retouch to shape the two main faces of the piece. This could have been to give the piece a very crude backing and holding the piece righthanded or lefthanded is comfortable with the index finger extended along this ridge and gives a great deal of control over the piece. The remaining third, at the end with the attempted truncations, is the more standard ridge edge. There is a large flake removal which disrupts the curve of one face significantly. No edges are sharp.

Figure 70. Roughout <100813> (photography by N. Gevaux)

Find <104850> is considered to be an attempted roughout that has been abandoned in the early stages of shaping (Figure 71). There are large invasive flake removals along some areas of edge and the ends, but many of these end in step terminations. It is manufactured on a chunk of Wolds flint with many inclusions and rough cortex that would have made it

difficult to work. It could have been used as a core in itself, but the flaking does imply an early attempt at shaping.

Figure 71. Roughout <104850> (photography by N. Gevaux)

As such, the roughouts on the worst material were attempted but abandoned early in their roughing out, perhaps after realising just how difficult the flint would be to knap. They do feature many step terminations though and it is possible that these chunks of poor material were merely being practised on. It was perhaps considered worth the effort of bringing the nodules of these to the island regardless as it is the more local flint. It is possible they were brought to the island pre-dressed to these extents: More extensive refitting would be needed to explore this further. There were pieces of material that looked as if they should refit with the burnt preform, but none of these were successful.

4.4.7.4 Strike-a-lights

The two strike-a-lights are both made on recycled till flint microcores (see Figure 72). These are roughly round outlined, with a nosed section with larger removals either side of the

nose to make it protrude. They were similarly proportioned, with <sl/154> measuring 29.4 mm from nose to base, 23.7 mm wide, and 13.7 mm thick, while <sl/145> was similarly proportioned at 21.4 mm by 31 mm by 13.4 mm respectively. Both were located on the dryland in trench 4, within a few metres of each other. As Andrefski (1998, 73) points out, while strike-a-lights may well be for producing sparks for setting fires, this is another functional interpretation that should be tested.

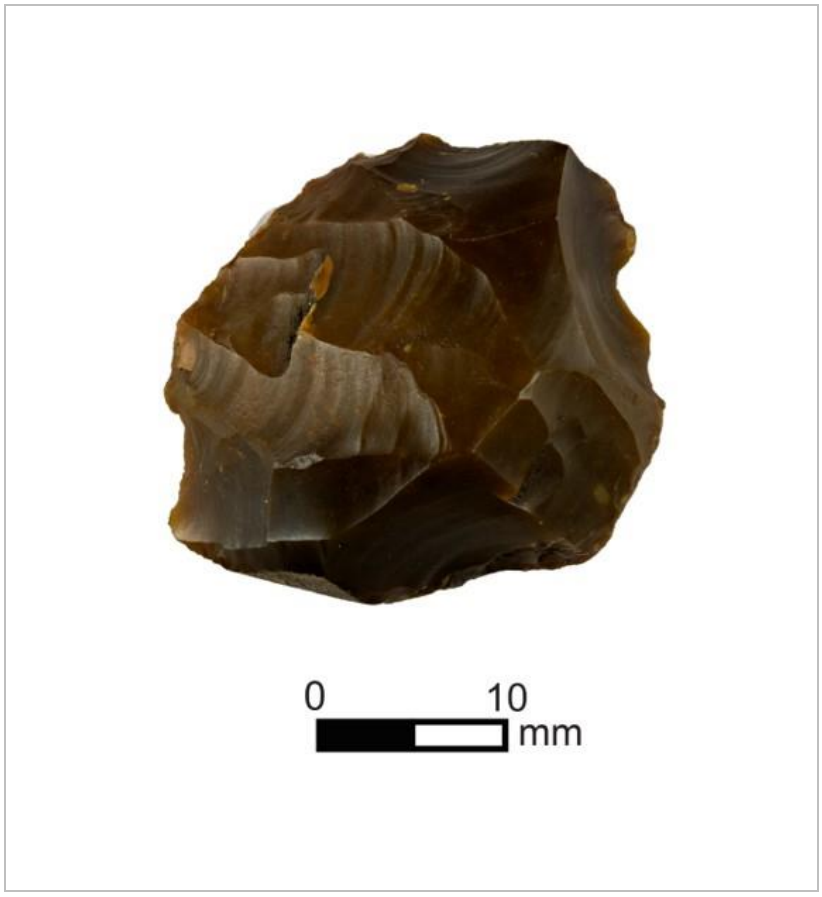

Figure 72. Example of a strike-a-light (photography by N. Gevaux)

4.4.8 Tool preparation debitage

Finally, the tool assemblages were complemented by an assemblage of 'tool preparation' debitage including microburins, assumed to be a byproduct from microlith production, and both primary and resharpening burin spalls (Figure 73). A more detailed refitting study would potentially identify more of such debitage, particularly within the debitage classified as 'potential tools' that show signs of modification, but regardless, this small collection again suggests both production processes on site as well as the presence or at least rejuvenation of tools after their use. Microwear and residue analyses may also illustrate some of these pieces being tools in themselves.

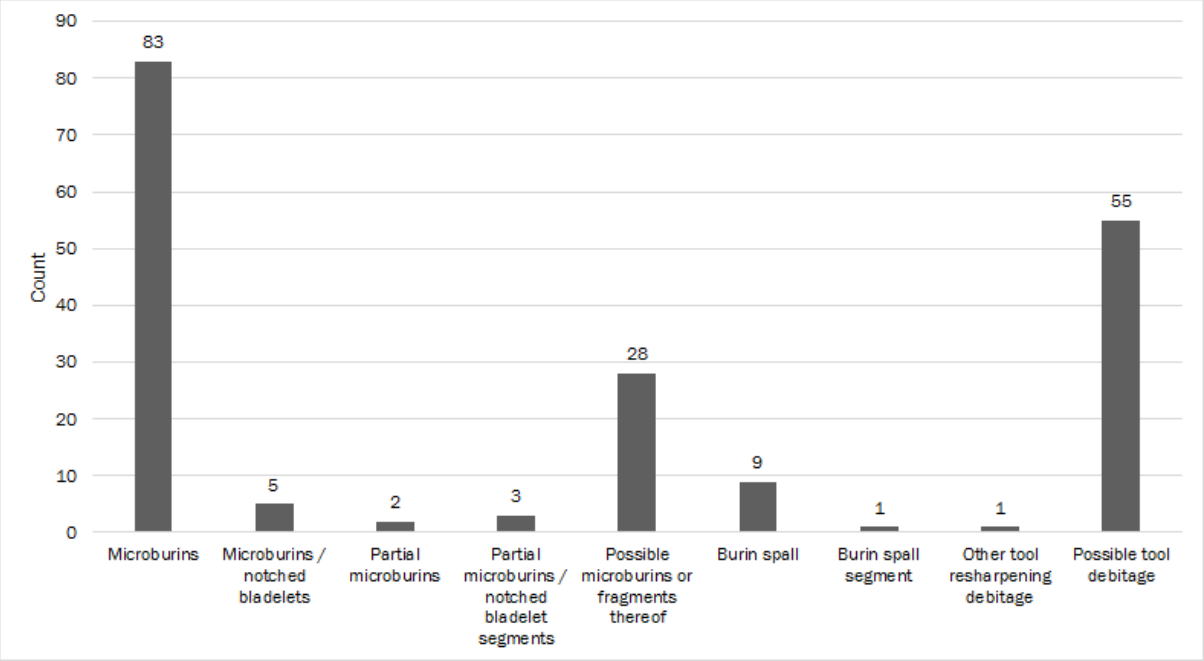

Figure 73. Mesolithic tool preparation debitage assemblage

4.5 Summary and discussion

The lithics assemblage illustrates the palimpsest of at least two occupations of the island, one Late Upper Palaeolithic with the Long Blade material and the other the Early Mesolithic material. While the majority of the Long Blade material was found in wetland contexts, in association with faunal remains, there are occasional pieces up on the dryland. This may mean more of the dryland and gully material could be attributable to the Long Blade phase but without clear stratigraphy or a more detailed consideration of the technological attributes, at present only material confidently Long Blade is included in this phase.

The Mesolithic assemblage is an assortment of knapping and tool production debitage and a variety of both core and knapped tools in various stages of their life cycles. Tools vary from finely worked to potentially expedient, quickly manufactured pieces. Being mostly manufactured on the finer-grained till flint, it seems this material was brought here and worked preferentially, but there are fine microliths manufactured on some of the coarsest material with more inclusions, including the three chert examples. Terminations on some cores seem to have mostly neat feather terminations, potentially suggesting skilled working, while others show a lot more hinges and step terminations which could indicate a poorer degree of control on the part of the knapper and does not always correlate with poorer quality flint being worked.

Flixton Island 2 does not seem to fall into any of the 'classic' assemblage types. However, the previous definitions of these assemblage types are not based on large samples of hundreds of sites but instead tens of sites from across the country and often grouped in certain areas,

such as Reynier's sites from the south. What Flixton illustrates well is a need for consideration of the site-specific context for all assemblages. These 'types' can be a good starting point for comparing sites but they should not be considered rigid or even robust classifications. It is not alarming that Flixton does not neatly conform: It is entirely predictable.

It is possible the complicated picture at Flixton relates to how the site was being used and interacted with, being at an insular location and presumably being travelled to for a specific reason that may well exploit or depend upon that attribute in some way. It is also possibly connected to the length of time it was used over; the dryland, in particular, could be a palimpsest of multiple occupations. Unfortunately, the lack of stratigraphy at Flixton does not assist with detangling this issue. While areas of horizontal clustering are generally identified, those on the dryland do not seem to very clearly correlate with any particular tool types. As such, the clusters may be areas of site used for similar activities, but these could be contemporaneously in use or used on different occasions. However, the Mesolithic cluster on the wetland does seem to have a slightly different composition to those clusters on the dryland. The relationship between the Long Blade and Mesolithic material at Flixton is not clear on the dryland. The dryland cluster compositions are further explored in the next chapter, when the results of the lithics are considered in comparison to the soils results.

Conneller et al. (2016) discuss the dating of the Early Mesolithic assemblage types and suggest that Star Carr, Deepcar and basally-modified assemblages appear in the record in that order but overlapped in time (as discussed in detail in Chapter 3). What these cultural groupings mean is still uncertain: It is not assumed, anymore, to imply different peoples moving in or being forced out of an area, though it could reflect different preferences over a variety of social scales. It could relate to cultural material drift over time. It could reflect changes in resources or site use which would be grounded in functional, socio-cultural and personal decision making. It could be related to personal preferences and aesthetic choices. The composition of a site's lithic assemblage is likely a combination of all these influences and others. As such, again, a deep consideration of the site-specific context is critical for understanding any lithic assemblage, perhaps more so than attempting to force the site into an oversimplified schema of assemblage types.

Given this situation, the Flixton assemblage is a new piece of the puzzle towards understanding how the sites in the Vale may have operated together as a network over space and time. This will be further considered in the Discussion chapter.

Chapter 5 Geoarchaeological and Geochemical Research Methods

5.1 Introduction

Soil and sediment samples from Flixton Island and Star Carr were subjected to an array of geochemical analyses in the lab or in situ. Some of these were conducted with an aim to characterise the nature of the soils and sediments: Munsell colour and texture rating, calcium carbonate presence, phosphate presence, pH, and micromorphology. Other methods were employed to identify spatial variation in the geochemical signatures of the soils on site: chemical characterisation using inductively coupled plasma atomic emission spectroscopy (ICP-AES) and portable x-ray fluorescence (pXRF), both in the field and in the laboratory.

While Flixton Island 2 was the main focus, work conducted on the Star Carr soils had the potential to provide a useful comparison point being a Mesolithic site in the local landscape but with clearer features and activity areas evident on the ground than Flixton Island. The specific methods deployed during particular field seasons and to particular areas of the sites were adapted to the research questions being asked at the time and the practical limitations of the live project. Samples for general testing and ICP-AES were taken throughout the 2012 and 2013 field seasons for Flixton Island and in the 2013 and 2014 field seasons for Star Carr. The University of York departmental portable XRF machine was purchased in August 2014 in time for the Flixton Island 2014 field season and then the final Star Carr field season in 2015 so in-situ testing was rolled out as well as continuing the other physical sampling.

Time pressures often limited where or to what extent sampling could be conducted or what methods were specifically rolled out in certain trenches, given that some of the work was being conducted in the final seasons of the project and also given the safety cordon required for conducting pXRF that suspended excavation in the near vicinity. Physical samples were taken from across the main dryland trench 4 at Flixton Island 2. The other dryland trenches were not fully sampled, but in 2014 trenches 11, 12 and 15 were extensively analysed in-situ using pXRF and selective physical samples taken for further lab-based analysis. For Star Carr, the Central Structure and surrounding area excavated in 2014 was physically sampled and analysed by both ICP-AES and, later, pXRF in the lab on processed samples. Then the Western Structure was analysed in-situ using pXRF and also sampled for ICP-AES during 2015. The pXRF results for Star Carr are still being processed and not presented within this thesis.

5.2 Micromorphology

Micromorphology facilitates the analysis of samples that are undisturbed by the excavation process. The samples are processed into resin blocks in a manner to preserve their structure and composition as they were in-situ in the soil so that the formation, disturbance and modification processes that have affected those deposits can be assessed as thin sections with transmitted light microscopy. This was not an avenue of research that could be fully explored within the time frame of this PhD project, although one sample from the dryland topsoil at Flixton Island (the results of which are summarised in the introduction) and several samples from Star Carr (the results of which are summarised in Chapter Eight) were processed by myself, Emma Tong and Carol Lang at the University of York. Sampling was originally undertaken by Helen Williams in 2012 and 2013. Micromorphology samples were taken from Flixton in 2012 to characterise the degree of bioturbation in the dryland trenches. Samples from Star Carr in 2013, 2014 and 2015 were to develop an understanding of the dryland contexts as well as specific structures. The slide production process used is detailed in Appendix Three. The slides were analysed by Charles French at the University of Cambridge and these results are utilised in this thesis to help inform the results from the geochemical analyses.

5.3 Sampling for geoarchaeological testing and elemental analyses in 2012

Geoarchaeological prospection for the dryland site on Flixton Island 2 in 2012 was conducted by sampling on a 0.25 m^2 grid across trench 4 covering an area of 10 x 5 m (see Figure 74 and Figure 75). These were taken from the layer considered to be the in-situ Mesolithic soil horizon below the topsoil, context (1119), which centred on the extensive dryland lithic scatter. A total of 800 bulk soil/sediment samples were collected, though not all were eventually analysed (discussed below). The trench had been yielding significant amounts of lithic artefacts early on so following advice from Charles French and Lisa-Marie Shillito, this fine-resolution sampling was conducted to enable a detailed characterisation of the associated sediments. The sampling team wore powder-free nitrile and vinyl gloves to deposit samples excavated using trowels in aluminium foil wraps which were in turn sealed in individual resealable plastic bags. The samples were stored at room temperature from August 2012 when they were taken until the dates they were set out for drying between January – April 2014, at the start of this PhD project.

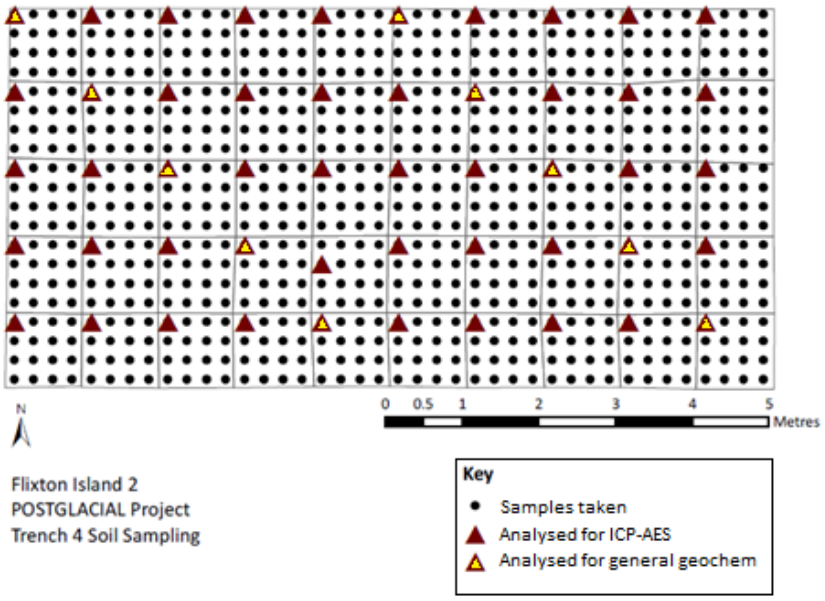

Figure 74. The sampling strategy for trench 4 (VP12): black dots indicate the full array of samples taken; red triangles are those analysed by ICP-AES to provide general coverage; those in yellow were analysed by ICP-AES, pXRF in the laboratory, and general testing such a pH measurement for more detailed understanding.

Figure 75. Sampling in the field in trench 4 (photograph by the POSTGLACIAL project)

5.4 Basic geoarchaeological assessment

With an aim of generally characterising the trench 4 sampled sediments, a sub-sample of ten of the 800 samples, on two diagonal transects going across trench 4 north-west to south-east, were subjected to a barrage of general geochemical assessment techniques (denoted by the yellow triangle symbols in Figure 75, above). The samples were air dried for two

weeks at room temperature and then assessed for colour, texture, calcium carbonate content, pH, and ring test for phosphate content.

5.4.1 Soil colour and texture

Soil colour is the result of the historic and ongoing palaeoenvironmental conditions the soil is exposed to and is determined by factors such as organic matter, iron and moisture content (Holliday 2004, 193–196). Munsell codes, the standard usually utilised for soil colour assessment, can be broken down into grade (degree of blending), colour (the underlying colour or colours if blended), value (amount of light reflected i.e. darkness) and chroma (saturation) of the overall hue. The air-dried samples were remoistened on a white background for the evaluation. During excavation, this context was interpreted as the mixed interface of the topsoil (the A horizon) and the 'till'. As discussed in section 1.3.3 the further underlying bedrock formation is mudstone but the superficial, mixed deposits (largely clayey and silty at this locale but with some sands and gravels) are very deep here and so essentially seem to serve as a heterogeneous parent material.

5.4.2 Estimated carbonate presence

This is a very simple, relative indicator test, rather than an accurate absolute measurement, as it is judged on naked eye observation of the sample's reaction with dilute hydrochloric acid (10% acid with distilled water mixture). Commonly known as the "acid test", hydrochloric acid (HCl) is added one drop at a time to a small sample of dried soil (approximately 2g weight) and the audible and visible reaction is noted to provide the estimation (see Table 32).

Table 32. Estimating calcium carbonate

Audible Indicators	**Visible Indicators**	**% $CaCO_3$**
None	None	< 0.1
Faint spitting	None	0.1 – 0.5
Spitting	Specks of bubbles on grains	0.5 – 1.0
Spitting audible away from ear	Slight reaction visible	1.0 – 2.0
Easily audible	Obvious reaction	2.0 – 5.0
Very audible	Vigorous effervescence	5.0 – 10.0+

5.4.3 pH

10 g of the air-dried sample was mixed with 25 ml distilled water, stirred and left for 15 minutes. Then the mixture was restirred before the pH was measured on a calibrated Jenway 3510 model meter.

5.4.4 Estimated phosphorus presence

This is a standard relative indication spot test rather than an accurate measurement of phosphorus, and by extension the phosphates, in the soils. Similar to the calcium carbonate test, it is conducted by observing and visually assessing the results of an ongoing reaction involving the soil after a set length of time. Following the method developed by Eidt and Woods (1974), 2 drops of a reagent made up of 35 ml (6 mol) hydrochloric acid and 5 g ammonium molybdate dissolved into 100 ml cold distilled water are added using a pipette to 50 mg of dried soil which has been placed in the centre of a circle of filter paper. After 30 seconds, using a fresh pipette, 2 drops of a second reagent consisting of 0.5 g ascorbic acid dissolved in 100 ml distilled water is also added to the soil. Phosphorus in the soil reacts with the molybdate to form a blue compound which is visible in the rays of liquid spreading out on the filter paper around the soil after the dilute ascorbic acid is added. The visual characteristics of the blue compound on the filter paper, including the colour intensity, length of rays, estimated percentage ring around the sample, and timings of appearance are noted within the two minute window after the addition of the second reagent (see Table 33). To ensure the reagents were working properly, the same mixtures were tested on a sample of soiled cat litter, with high phosphate presence, and it came up with a clear indication of phosphate (value 5).

Table 33. Eidt and Woods' (1974) phosphate spot test ratings

Phosphate Rating	**1**	**2**	**3**	**4**	**5**
Time of appearance of rays (seconds)	120+	90 - 120	50 - 100	20 - 60	50 – 30
Percent ring around sample	0	0 - 50	50	75	100
Length of rays (mm)	0	0 - 2	2 - 3	3 - 5	5 – 8+
Intensity of blue colouration	None	Very pale	Pale	Medium dark	Dark

5.4.5 Summary

The methods described above were utilised to assess the general nature of the soil across the dryland site at Flixton Island 2 on ten samples taken in 2012. Further geochemical analysis to evaluate the elemental composition of specific areas and therefore potential activity foci on site was also conducted on an expanded range of samples from 2012 as well as on samples from later excavation seasons at both Flixton Island 2 and Star Carr. Elemental variation needed to be measured in various areas across the sites, at high resolution. Two methods were explored to fulfil this requirement: portable x-ray fluorescence (pXRF), both in the field and on prepared samples in the laboratory, and

inductively coupled plasma atomic emission spectroscopy (ICP-AES), a laboratory technique.

5.5 Portable Energy-Dispersive X-ray Fluorescence (pXRF)

5.5.1 Introduction to pXRF

Summarizing from Shackley (2011), XRF spectrometry apparatus contains an X-ray source, which it directs at the material being analysed, and an X-ray detector. X-rays are a form of electromagnetic radiation with a short wavelength and high energy. When atoms are excited with short wavelength, high energy radiation, if the energy is high enough then one or more electrons may be ejected from the atom (ionization). Within atoms, electrons exist in various orbitals which have different energy levels related to how strongly they experience the positive (attractive) nuclear charge, with those lowest in energy being more strongly attracted by the nucleus. X-rays can have a high enough energy to match the additional (potential) energy needed to expel core (low energy) electrons from the targeted atom. From this energetic, excited state, an electron within the same atom but higher in energy than the one that was ejected, drops into the vacant orbital releasing the difference between its original energy state and the new one as a photon. This photon (the fluorescent radiation, which is an X-ray) is detected and its energy level measured by the XRF apparatus. The energy level of the emitted photon is characteristic and known for different atoms' orbitals allowing the apparatus to quantify which atoms and in what proportion are present at the surface of the material being analysed. The caveat to this is that any given atom may appear as several peaks in the spectrum and these peaks may sometimes overlap with those of other elements. Therefore, the limit of detection depends not only on the sensitivity of the instrument itself but also on the composition of the specific sample, and the peaks it produces, and as such there are no absolute detection limits available for reference.

5.5.2 pXRF Equipment

The readings were taken on the departmental Olympus DELTA Portable ED-XRF (energy-dispersive x-ray fluorescence) Analyzer, Professional Alloy model, operating in a preset Geochem mode, equipped with a rhodium 40kV/4W tube anode and Silicon Drift Detector. The range of elements detected is restricted to magnesium through to uranium. Each reading incorporated 1 minute at low energy (10kV) for lower atomic weight elements (Mg, Al, Si, P, S, Cl, K, Ca, Ti, Mn) and 1 minute at high energy (40kV) for higher atomic weight elements (V, Cr, Fe, Co, Ni, Cu, Zn, Ta, W, Hg, As, Se, Pb, Bi, Rb, U, Sr, Y, Zr, Th, Nb, Mo, Ag, Cd, Sn, Sb, Ti, Mn). Optimal beam runtimes, which can be manually configured by the user, were established through a small experiment conducted in the field (see Appendix Four). The beam integrates a 25 x 28 mm area through a Prolene® (polypropylene) window. Spectra

were loaded into proprietary Olympus Delta XRF calibration software and counts in parts per million were obtained as a comma separated value file.

As mentioned above, unlike with ICP-AES, the limits of detection (LODs) vary dynamically with the sample being analysed (Olympus 2014a). The machine is set up for the kind of sample material (e.g. soil, alloy, ore) and also to interpret peaks within an expected framework of elements. You can never analyse all elements with any one setup as the spectral peaks interfere and cannot be distinguished. This guides the analysis mode selected by the user on the machine. Each sample will give a different array of peaks even within the constraints of that framework, especially when dealing with a material as complex as soil. The limits of the detection vary depending on the peaks the machine records for that specific sample as certain high peaks will mask the signals from other elements. The results are corrected for inter-elemental spectral inferences automatically by the machine's software when using the Olympus Delta, here for 38 elements analysed. The software does this automatically as part of its output algorithms but it will never be guaranteed to be perfect as it is essentially a model and depends on how well the elements present in the sample have been pre-empted in the mode selection.

The software is able to provide estimates of the limits of detection for those elements that should be read in the selected mode but are recorded below the limit of detection (or absent) in the results. Elements not listed above however would have the potential to interfere with readings without the software being able to distinguish the issue and as the machine is not configured to detect them even if they were in the sample they would not be recognised as such.

5.5.3 pXRF analysis strategy in the field at Flixton Island 2

Readings in the field were taken *in-situ* on deposits in context 1119, the mixed layer of topsoil and till that has the potential to contain signatures of the weathered Mesolithic land surface. Readings were taken utilising the Olympus 'Soil Foot' attachment (see Figure 76), so the window of the analyser was directly in contact with the trowelled back sediment.

Readings were taken on a 0.5 m^2 grid (four readings per 1m^2) at the interface layer. The whole of Trench 11 was tested on this grid. As more than half the field season had passed when analysing Trench 15, a full north-south transect (on the same grid) and then the last three east-west rows (which had also been flagged as containing a high amount of burnt material and a possible feature) were analysed to cover as much area as possible and to get the best possible sense of changes across the area whilst still allowing time to finish excavating the trench afterwards. Similarly, Trench 12 was analysed in a pattern with the same goals, so readings were taken at the northern end, centre, and southern end. The reading grid is illustrated in Figure 77.

Figure 76. A reading being taken in trench 11 using the soil foot setup (photograph courtesy of the POSTGLACIAL project)

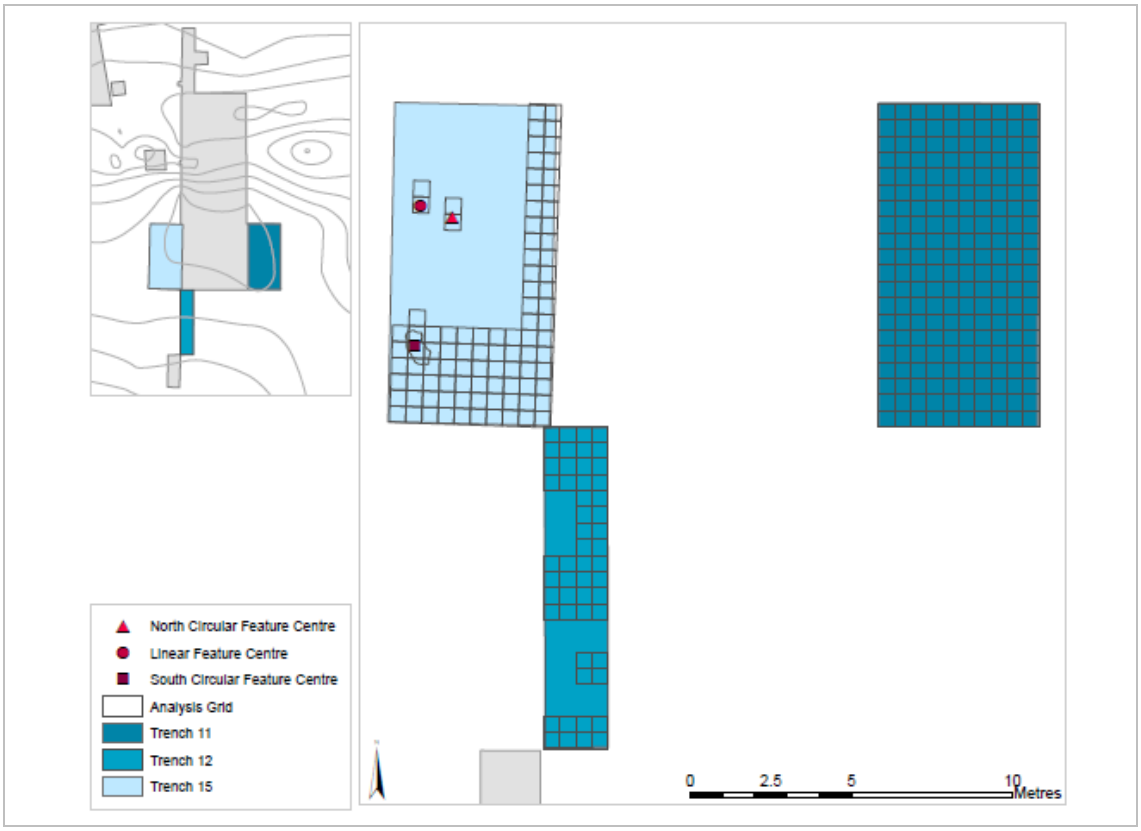

Figure 77. Plan of grid pXRF readings were taken on (one reading per square), in the field at Flixton in 2014

5.5.4 Accuracy, precision, quality assurance and controls conducted in the field for pXRF

Calibration checks were routinely run daily as a minimum and more frequently as deemed necessary on days with changeable weather (which potentially affects readings, see below).

Standardised controls, with the exception of the alloy utilised for calibration, were not available during the 2014 Flixton excavation season for analysis in the field but were used for the pXRF on samples in the laboratory.

However, trenches would frequently take more than one day to complete testing and as such, repeat readings were taken at designated points within the trenches to provide a comparison between the different days' data. The results give a sense of the degree of variability between daily readings and permit the assessment of the impact of changeable field conditions on the *precision* of the data (i.e. how tightly the results group). Wetness of the soils can impact pXRF as water molecules can interfere with the readings (Olympus 2014b, 134). It is possible this would interfere with different elemental readings to different extents as well. Physical samples from locations analysed in the field were later analysed by pXRF and ICP-AES as prepared samples in the laboratory, which would allow for an assessment of the method's *accuracy* as well as precision (i.e. how close to the 'real' values these readings may be).

The record of daily calibration checks, full details of the repeat readings, weather conditions where noted, the raw data results from these readings, and basic descriptive statistical assessment (mean, range, min and max values, and standard deviation) are all provided in Appendix Four. Table 34 details how elements were divided into categories as part of the assessment per trench.

Table 34. Criteria utilised for assessing major, minor, and trace element contributors to samples/readings. *The International Union of Pure and Applied Chemistry (IUPAC) Gold Book defines trace elements as "any element having an average concentration of less than about 100 parts per million atoms (ppma) or less than 100 µg / g" (IUPAC 2009)

Categories	**Parts per million (ppm) atoms**
Major	>10000
Minor	1000 - 10000
Trace	100 - 1000
IUPAC* Trace	<100
Below limit of detection	Unmeasurable
If any readings higher, then bumped up into next category (if some readings <LOD, then those are displayed as measurements of 1.00 ppm artificially)	
Light elements excluded from charts as such a high proportion of all samples (as to be expected)	

The instrument also calculates an estimation of its own measurement error, associated with every successful reading of an element, that is provided with the output data. It was initially planned to display the error values on all the dot plots, i.e. demonstrating the calculated instrumental precision on the same plot as these daily variances in precision. However, for

the major elements, the daily variances were so much greater in scale than the machine's measurement errors that the error bars would not display clearly so the error bars are not plotted on the major element charts. In contrast, the error bars were much wider than the daily variances when considering the IUPAC category trace elements, so in those cases plots with and without the error bars are provided for clarity. The error values are provided in the data tables in the appendix for reference.

In addition to these, the instrument can provide estimated limits of detection for the elements it was unable to read, as discussed above. This is seemingly, however, a generously calculated estimate as instances in the repeats where the element has been measured some of the time but not others has suggested much lower levels of the element are actually present than the suggested limits of detection. As such, initially it was thought to display these as errors on the plots, but the values are so high they render the scale of the plots ineffective for considering the successful reading values. The values are provided in the data tables, however, for comparison.

The estimated light element contribution (such as oxygen) in samples is also provided as part of the outputs from the analyser. As these are grouped as simply "light elements" (LE in the tables) and consist of a large proportion of the samples (as to be expected, as they are bound up with the heavier elements as compounds such as oxides). These values were such a high proportion of each sample, these also are not plotted but provided in the tables as a raw value in ppm.

5.5.4.1 Results from repeat readings: notes

This section will summarize and evaluate the results from the repeat readings in the same locations at the start of every day there was analysis in the field, while the full data are provided in Appendix Four.

Repeat readings were taken in the southeasternmost sample location in trenches 11 and 12, and the northeasternmost sample location in trench 15. The sample locations were selected as being those most accessible when considering the position of the excavation team and the safety cordon in place around the machine (specified by university regulations), however those in trenches 11 and 12 were also the areas of the trench that were usually slightly damper than the rest of the trench so if they were going to be impacted by changing moisture levels, these repeats would flag that up.

There are two things to note. Firstly, it must be appreciated that the values that are generated by the analyser are the estimated proportion of the sample interacted with by the analyser. They are output as a percentage or in parts per million atoms, which is itself a proportion (count per 1,000,000 atoms). They are not absolute values, such as a

measurement in micrograms would be. Therefore, if one element is read to be a higher proportion (i.e. has a higher ppm), another will be read to be lower. The readings give you the proportions of the elements read as relative to each other and do not include elements that are not read in this setup.

Secondly, where readings were below the limit of detection, and with only very crude approximations of the limits of detection generated by the analyser, the points representing these visually were arbitrarily set at 1 ppm. It must be remembered these readings could have been higher or equally there could have been zero in the sample; however, it is very unlikely to have been a main constituent of the sample that has been missed.

5.5.4.2 Results from repeat readings: major elements

Of the major elements, aluminium (Al), iron (Fe), and (where present in such abundances) calcium (Ca) are all relatively well grouped on the plots (see Figure 78A-C) suggesting the precision of the measurements of these elements are not as strongly affected by field conditions. The differences between maximum and minimum readings seen within the repeats (statistical range of the readings) vary between 92 ppm up to 17,401 ppm but as major elements (i.e. with readings over 10,000 ppm), any variability in the field that is significantly more than this is likely to be of interest.

The results for silicon (Si) were much more broadly distributed in all three control areas on different dates, and therefore seem to be less precise. The range for the silicon readings from trench 11 is over 100,000 ppm and trench 12 over 70,000 ppm. The lowest readings were on the 25th and 27th August. Comparison with the field notes suggests that drier conditions on the 25th and 27th might have resulted in a lower reading of silicon than in wetter conditions on other dates (possibly because the proportions of other elements are being underestimated in wet conditions). Aluminium follows the same trend, albeit across a much tighter range. The highest readings for calcium and iron are on these days in contrast, though again with little range to their readings.

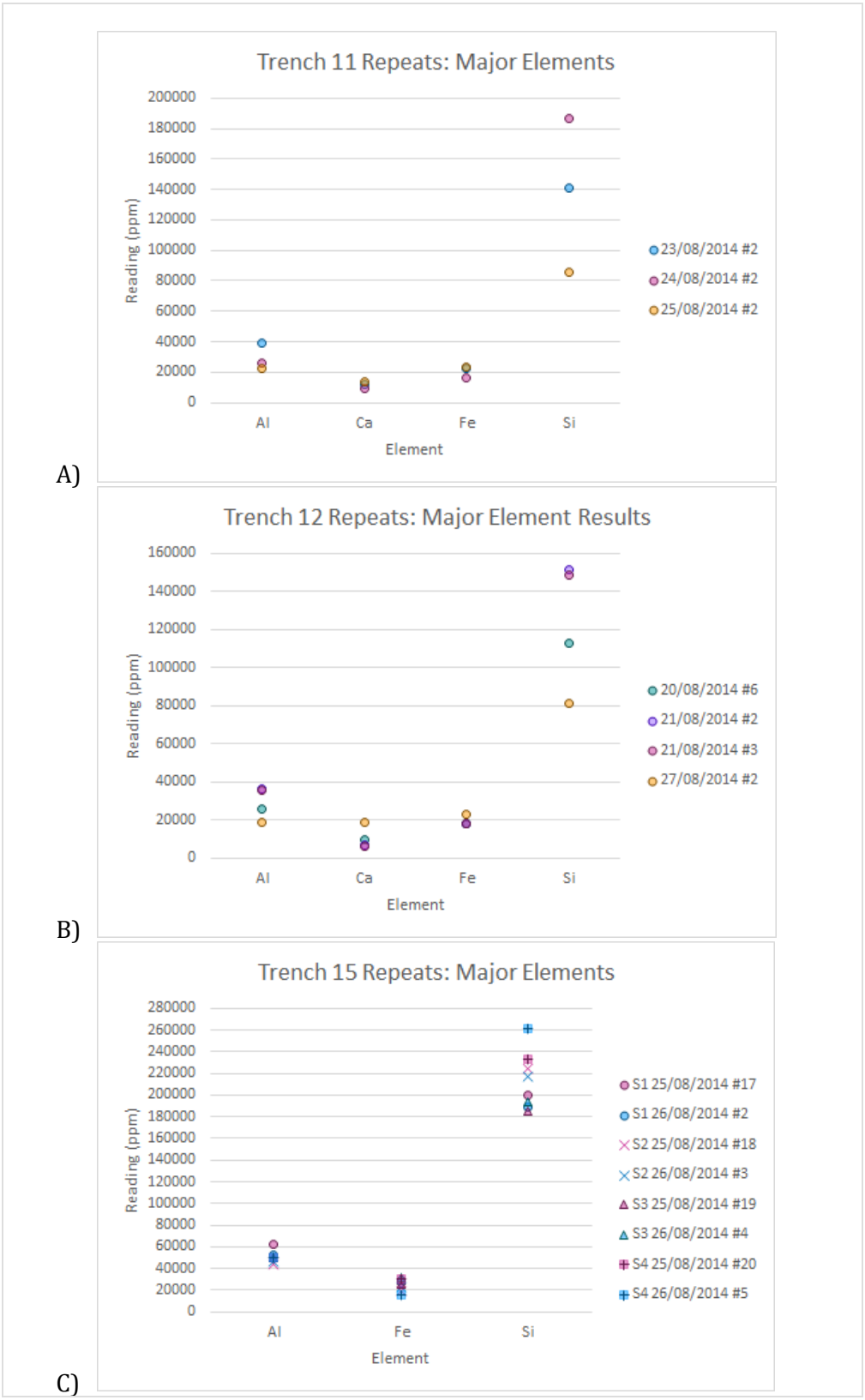

Figure 78 A - C. Dot plots of the major element values read from the repeat readings in the same location on different days in the field by pXRF. Note, trench 15's plot depicts 4 pairs of repeats at 4 different 'sample' locations (S1 - 4) in the trench, from within the same grid square.

Trench 15's silicon readings are higher than those from the other trenches in absolute terms, but less variable compared to each other across the two consecutive days they were

taken (with the maximum difference in repeats seen in sample 4 at 28,042 ppm). These two days were recorded as being likely dry in the northeast according to the Met Office report for August 2014 (The Met Office 2015), and while there were no condition notes taken for 26th this does fit with the notes for the 27th. As such, trench 15 may be genuinely higher in silicon as we might expect it to be a more accurate value with less wet conditions affecting readings, and for it to be lowest on these days following the trends in other trenches. For the four different reading locations in trench 15, all within the grid square G4, two of the readings increased and two of them decreased on the second day so the repeat readings were not consistently changing with general field conditions alone. Even the smallest difference in these readings (7713 ppm), from the first day to the second in one location, is not accounted for by the measurement errors suggested by the analyser (ranging between 650 - 850 ppm), however.

Repeat locations in trench 15 were also further towards the peak of the dryland hillock and therefore perhaps slightly better drained and therefore less affected by wetness; although in this case as they were being read on likely dry days, one would expect the readings to be lower anyway. It is worth noting that for the trench 15 repeat readings, of which the 4 different locations were within the same grid square, there is quite a large range of just over 75,000 ppm despite the proximity, with a minimum value of 184,987 against a maximum value of 260,691 ppm. In contrast, the highest reading from the other trenches is 186,381 ppm, so only just above the trench 15 minimum value (and the other three readings measured Si to be lower than the trench 15 minimum value). This could be due to natural variance, more localised field conditions, or differences in activity that have taken place by chance in those locations selected as control areas. As such, the picture for silicon readings seems complicated both across site even across short distances and reading precision is compounded with a potential effect by field conditions. As such, variability in silicon readings will have to be cautiously considered as whether due to field conditions or other reasons, the ranges reflect this element is noticeably less precisely measured than all the other elements.

5.5.4.3 Results from repeat readings: minor elements

Calcium (Ca) and sulfur (S) were less abundant in trench 15 readings than in trench 11 and 12 (Figure 79A–C), and therefore appear here as minor readings. Calcium appears here as a minor element for trench 15 (rather than a major one) and sulfur is a trace element for trench 15 (rather than a minor one). This reflects that the relative measured proportions of these elements are lower in trench 15 than trenches 11 and 12, based on these repeats. Calcium drops as low as 2093 ppm, compared to a minimum of 6330 ppm in the other trenches. This could have been attributable to genuine changes across the site or

relating to the days trench 15 was measured being drier; however, comparing to the results from the complete trenches (chapter six) the trench does genuinely seem to be lower in calcium. Sulfur only reads a maximum of 567 ppm in trench 15, but compared to a minimum of 564 ppm in the other trenches this is not so remarkable and simply highlights the variance in readings of this element across site.

Absolute measurements of abundance of potassium (K) and titanium (Ti) are relatively elevated in trench 15 compared with trenches 11 and 12. The titanium readings were the more precise of the two. Differences between repeats in potassium across site range between 328-1793 ppm. Differences between repeats in titanium across the three trenches range between 79-958 ppm. Within grid square G4 in trench 15, the four repeat samples K range by 1175 ppm and Ti by 1250 ppm across the 8 readings. As such, variation due to field condition changes as well as variability within small areas (as the machine may have in a slightly different position, by millimetres) is greatest at 1793 ppm for potassium and at 1250 ppm for titanium. While much less than the variances in the major elements, this can be quite a significant difference considering the values themselves generally range between 2000 - 6000 ppm. This would still not bump either element up into the major element category, but it needs to be considered. These elements read lower in drier conditions potentially.

As can be seen from the error bars, the estimated instrument error (as provided by the analyser with the outputs) is small compared to the variability in readings.

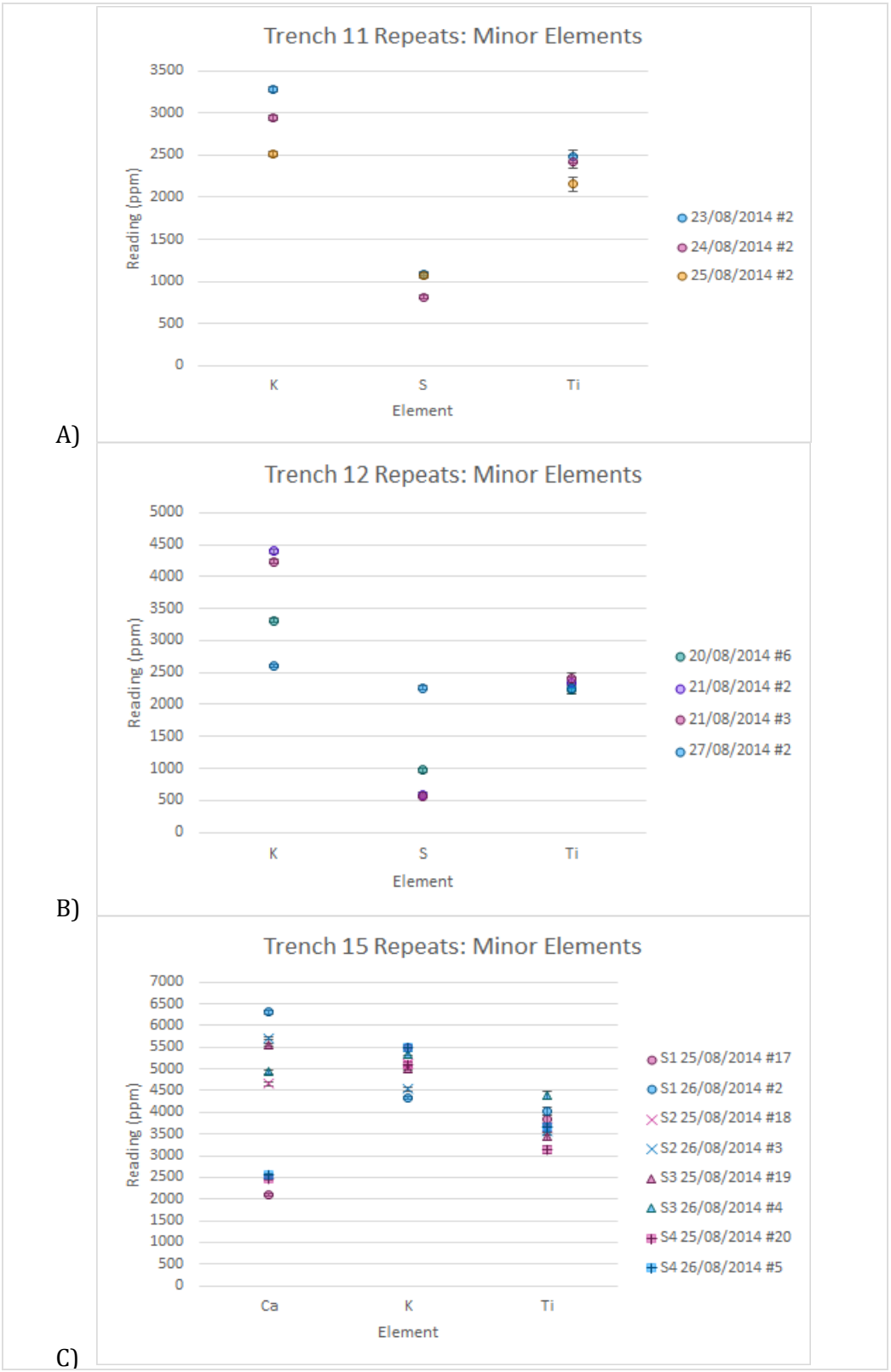

Figure 79 A - C. Minor element values read from repeats on different days in the field by pXRF

5.5.4.4 Results from repeat readings: trace elements

The results for the elements manganese (Mn), phosphorus (P), vanadium (V), zirconium (Zr) and, in the case of the trench 15 samples, sulfur (S) all have readings between 95 ppm and 589 ppm and statistical ranges (i.e. maximum differences) between 84 - 253 ppm. As such, they vary over much more limited ranges in proportional readings than the more dominant elements and are, in the grander picture, more precise (Figure 80 A-C).

Manganese and vanadium have readings broadly between 100 - 200 ppm. Both are well grouped across all the samples with ranges of 102 ppm and 78 ppm respectively yet, with means of 139 and 184 ppm readings respectively, this degree of day-to-day variability can significantly increase the reading. However, this gives a sense of what might be a genuine peak in these elements. Their higher readings in trenches 11 and 12 tended to be on the drier days so it is possible field conditions had an influence in this way. As seen before with silicon, the readings in trench 15 did not vary consistently despite being taken on the same consecutive dates and the proximity of the samples. Three of the four repeat readings for V went down while three of the four for Mn were higher (and the odd ones out were different locations, not one sample consistently out from the other three). The same was seen for zirconium (Zr) with three of the repeats in trench 15 being lower and one higher. When taking into consideration the measurement error of the machine as well, the ranges in which these repeat readings could fall give or take the error do overlap in most of the samples or come very close to each other. As such, the results from trench 15 were generally consistent with each other across the two dry days.

Zirconium tends to be of slightly higher proportions than manganese and vanadium (minimum reading: 253 ppm; maximum reading: 516 ppm). Zr readings from all trenches covered overlapping ranges of values, very broadly speaking, though readings were more disperse than for Mn and V. The trench 15 repeats tended to be quite close to one another with a minimum difference of 20 ppm up to a maximum difference of 71 ppm. This is also quite small compared to the size of the readings, and measurement errors which are all estimated to be <3 ppm. The lowest trench 11 reading was again on the 25th, the second lowest trench reading on the 27th for trench 12 (and it was similar to the lowest reading from the 20th which was a generally dry day with isolated showers). As such, this gives a good general sense of the precision of the machine and also that Zr may be slightly affected by field conditions but not greatly.

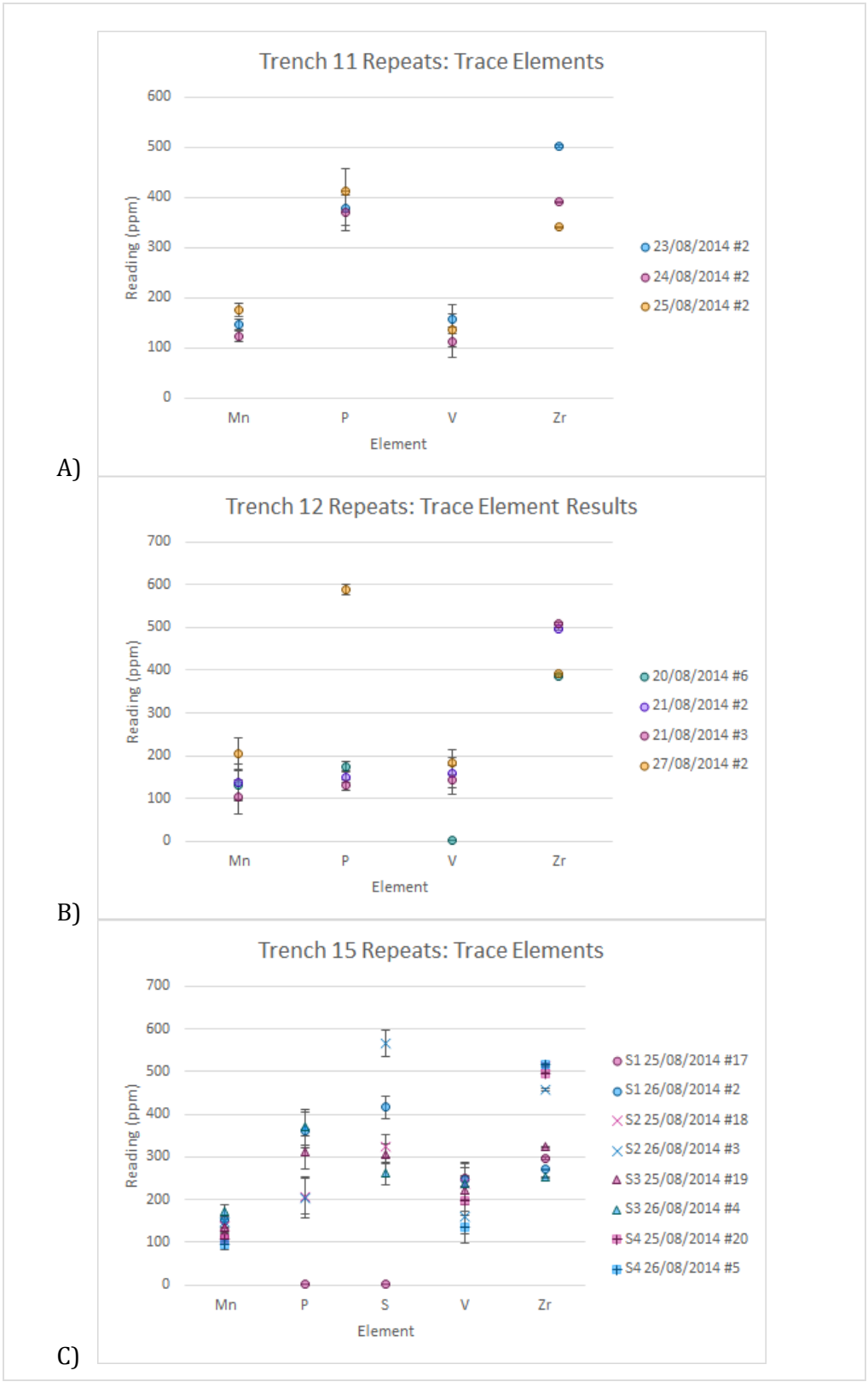

Figure 80 A-C. Dot plots of the trace element values read from repeats on different days in the field by pXRF

Phosphorus is an element often greatly enhanced by anthropogenic as well as other activity and deserves a thorough appraisal. Theoretically, pXRF will detect both fixed and "available" P in the soils, not just one or the other, as it looks at the sample area available within the analyser window as a whole and does not depend on an extraction, perhaps

putting it at an advantage compared with ICP-AES and certainly over the basic P soil tests often conducted for archaeological soil assessments. Phosphorus being a trace element at least in these repeated sample locations suggests it will be easier to identify peaks if there are enhancements on the level anticipated (not to say that it will be easy to interpret those as being modern contaminations or archaeological residuals).

Phosphorus is more variable than the other trace elements so far discussed, varying between 131 ppm minimum and 589 ppm maximum readings. P reads highest on the 25th for the trench 11 repeats and very obviously higher on the 27th for the trench 12 repeats; it is therefore possible that P estimations are enhanced in the drier conditions. The readings from trench 15 came out generally between the lowest and highest readings from the other two trenches, though there were three readings where the P was estimated to be below the limits of detection. Two of these were the repeats for sample location 4 and therefore consistent with each other. However, the other was taken on the 25th for sample location 1 and its repeat on the 26th yielded a reading of 363 ppm, showing a marked difference. The estimated limit of detection for this failed reading was 350.76 so it is possible that a similar reading could have been obtained and was just missed but as said above, the algorithm generating the limits of detection seems generous. The other successful readings were between 204 and 370 ppm. Overall, this gives a sense of P potentially being difficult to evaluate when it is a trace element but peaks from anthropogenic enhancement should be noticeably higher than this.

While phosphorus gets taken up by plants as a key nutrient, it also becomes fairly rapidly fixed in soils as insoluble and resistant inorganic phosphate compounds in acidic soils generally combining with Al, Fe, and to a lesser extent Ca and also adsorbing to soil particles, particularly in clayey conditions which are less inert (Gasser and Bloomfield 1955). These compounds are generally resistant to mineralisation by microorganisms as well and therefore tend to become fixed in soils for years: This was promising for detecting activity areas using this method, and also meant that consideration of ratios of P to Al, Fe and Ca would be of interest. The stability of the compounds may mean its extraction is more challenging for ICP-AES analysis and therefore pXRF will be a valuable method in assessment of this.

5.5.4.5 Results from repeat readings: IUPAC trace elements

These results include all elements with any viable readings at all, all of which are below 100 ppm (Figure 81 A-C). Elements that were detected at these levels in all 15 repeat readings from all trenches were arsenic (As), niobium (Nb), lead (Pb), rubidium (Rb), strontium (Sr), tantalum (Ta), yttrium (Y), and zinc (Zn). Cadmium (Cd), chromium (Cr), molybdenum (Mo), nickel (Ni), thorium (Th), uranium (U), silver (Ag), bismuth (Bi) and copper (Cu) were

detected in some of the samples. Some readings of sulfur (S) were also at these IUPAC trace levels or below the LOD (yet others were much higher as discussed previously).

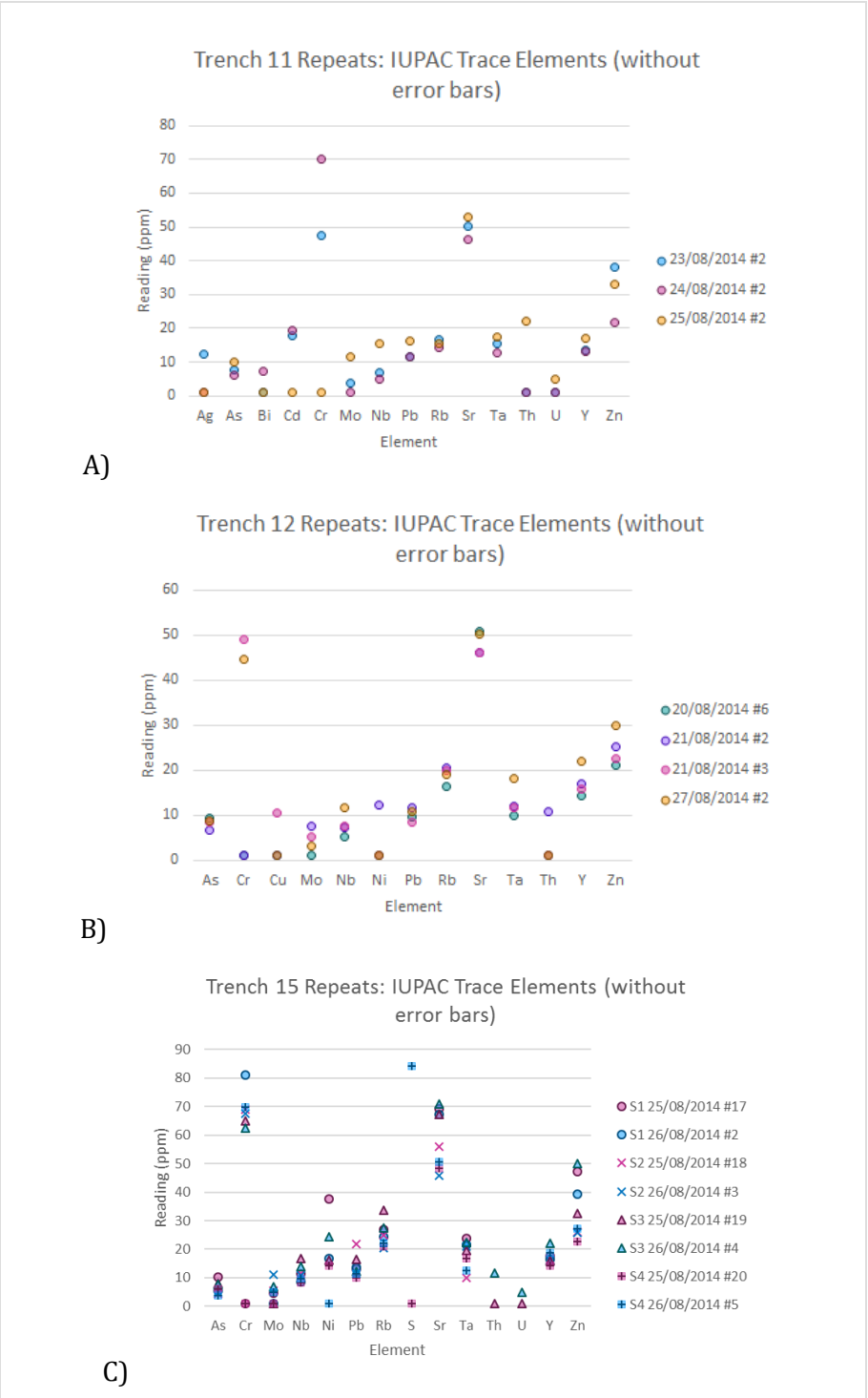

Figure 81 A-C. Dot plots of the IUPAC trace element values read from repeats on different days in the field by pXRF. If a sample had a successful reading of an element in one repeat but not the other, the reading below the limit of detection is displayed as a point at 1 ppm. If an element was not read at all in any sample, it is not included in any plot

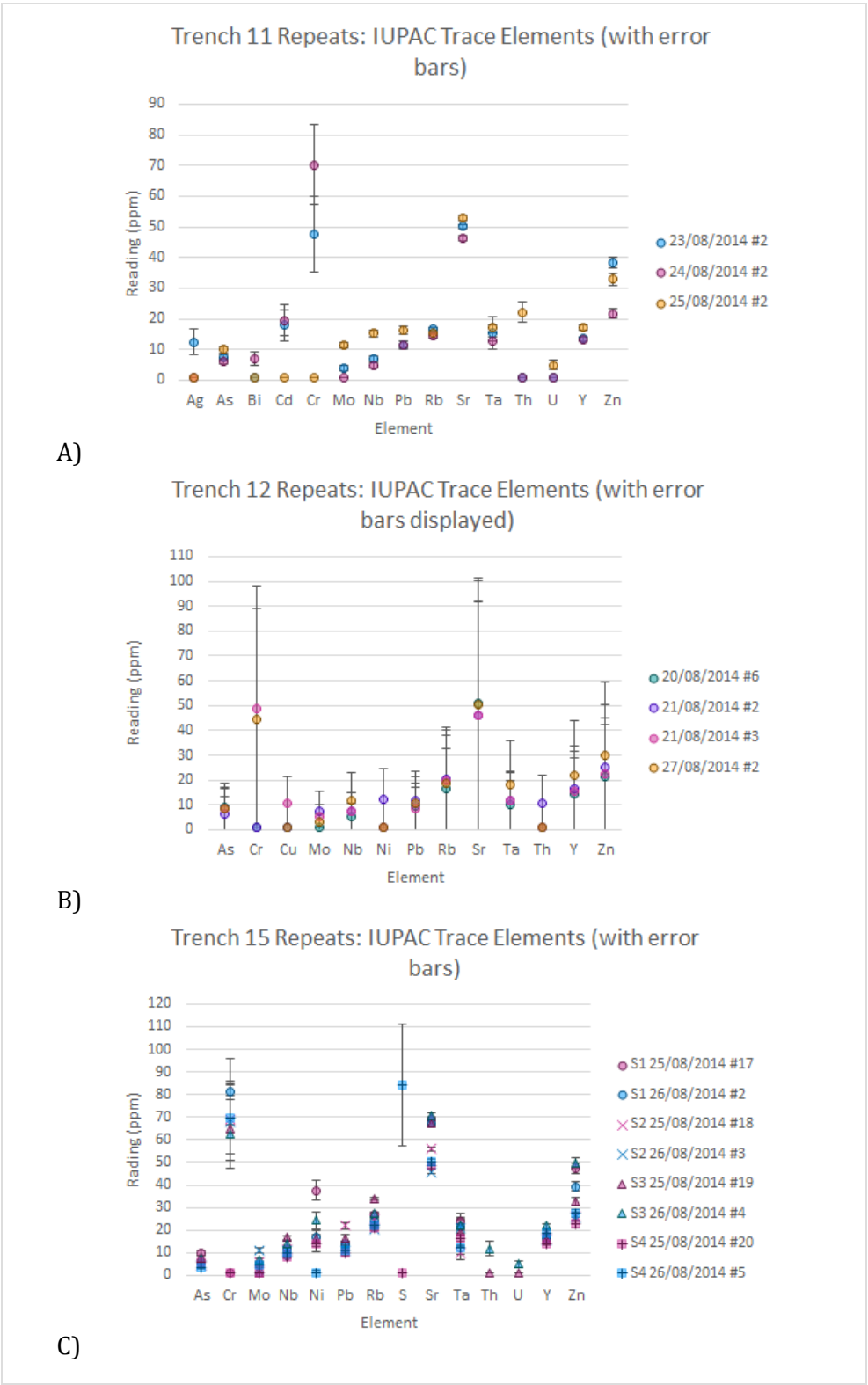

Figure 82 A - C. Dot plots of the IUPAC trace element values read from repeats on different days in the field by pXRF: the same results as in Figure 8 but with error bars

As such, these are very small concentrations of elements being evaluated here. Cr and Zn particularly but also Ni, Sr, and Ta all have slightly greater ranges than the other elements and therefore perhaps slightly lower precision, although when dealing with such small quantities of material it could also be due to random chance that these elements are being ionized and then detected at times or due to slightly different positioning of the instrument.

As can be seen for many of these elements, the measurement errors are very high relative to the levels of elements being dealt with and often error bars are significantly greater than the range shown by the elemental readings themselves (Figure 82). As such, it is to be expected these elements may be present in low concentrations in the soils and higher readings may indicate elemental enhancement in some form but the variances in precision particularly for Cr and Zn had to be considered. For many of these elements, the highest readings are on the drier days and suggesting the detection of these extra trace elements may be better facilitated given drier conditions, though this is not a consistent trend for all elements. Given the interplay of measurement error, it was decided this is something that needed to be evaluated specifically on a case-by-case basis if there appear to be peaks in these elements.

5.5.4.6 Results from repeat readings: non-detects

Chlorine (Cl), cobalt (Co), mercury (Hg), magnesium (Mg), antimony (Sb), selenium (Se), tin (Sn), and tungsten (W) were not detected in any of these samples. These were either below the limits of detection or genuinely absent from the soils. The estimated limits of detection were sometimes on the scale of several thousand ppm, however, so this is somewhat uninformative.

5.5.4.7 Assessment of precision based on the repeat results from Flixton

The locations for the repeat sample readings were selected by chance, as discussed previously, so they are not necessarily representative of the "background" levels. They may happen to be within areas heavily affected by contamination or previous activity. There was no way of isolating areas of non-activity from those of activity so this could not have been improved upon. However, their general consistency is encouraging and these readings give a sense of the day-to-day variations in readings of specific elements relative to the computed measurement errors and limits of detection. Certain elements seem to be more consistently detected to similar levels by the pXRF, others seem to be more dependent on field conditions or other unknown variables. These readings provide context for considering the outputs from the trenches as a whole.

5.5.4.8 pXRF on certified control samples in the field at Star Carr

During the field season at Star Carr in 2015, an area featuring a structure was analysed using pXRF and samples from the structure area were taken for ICP-AES. The pXRF results are not presented in this thesis (whereas the ICP-AES results are discussed in chapter eight). However, by 2015, in order to evaluate accuracy as well as precision of readings, a set of control samples of certified standards had been obtained. Readings on these were taken at

the start and end of every pXRF session, and they give a sense of how the machine's accuracy and precision varies independent of field conditions. These are potted controls of different materials that are either soils or materials of a similar nature that have been independently tested and their chemical composition verified. These samples are provided as sealed sample pots with Prolene® windows through which they are analysed. The control materials utilised at Star Carr were:

- NIST 2710a - internationally recognised control Montana soil with independently verified certified values utilising multiple methods (NIST Certificate issued: 7 April 2009), provided by Olympus

- NIST 2711a - internationally recognised control Montana soil with independently verified certified values utilising multiple methods (NIST Certificate issued: 22 May 2009), provided by Olympus

Olympus recommend that values from controls should be expected to be within 20% of the actual certified values of standards (Olympus 2014b, 101). This is a low degree of accuracy to expect for research purposes, but gives a rough ball park to start evaluations with. As such, control readings from the field were initially evaluated by highlighting all elements with readings out by more than +/-20%. Secondly, those that were out between +/-5 to +/-20% were highlighted along with readings below the limit of detection that should have been less than 10 ppm readings. This gives a sense of the accuracy of measurements for particular elements. The standard deviation and the range were also calculated to give a sense of the precision of the readings. The full results are provided in Appendix Four but in summary:

- Elements that tended to be greater than 20% too low in one or both samples: silver (2711a), arsenic (2711a), calcium (2710a), cadmium (2710a), cobalt, chromium, magnesium, nickel, phosphorus (2711a), silicon (2711a).
- Elements that tended to be either 20% too high or too low (mixed): antimony, selenium, uranium.
- Elements that tended to be greater than 20% too high in one or both samples: iron, mercury, molybdenum, niobium, sulfur, tantalum, thorium, vanadium, yttrium, zirconium (2711a).

Those elements that were usually only out so significantly in one sample (those with the sample code in brackets) are therefore perhaps those whose readings may be more affected by the overall composition factors of the soil. These readings were taken nine months after the original Flixton field readings so these can only give a tentative suggestion of the

accuracy of those earlier readings but it does suggest what elements the machine can be expected to be more or less precise for.

5.5.5 Complementary sampling strategy for supplementary pXRF analysis in the lab at Flixton Island 2 and Star Carr

Readings were evaluated on site mainly utilising the spectral display feature on the pXRF machine to compare multiple readings at a time. When different spectra obviously presented, then physical soil samples were taken to conduct lab based pXRF on prepared samples (and sometimes ICP-AES, detailed below) for further analysis. In two of the trenches, potential features were identified so pXRF readings were taken within and around the features. Regardless of the results from the pXRF, soil samples were taken for ICP-AES and/or lab based pXRF from these features for quality assessment.

5.5.6 Procedure for pXRF analysis in the laboratory

Samples to be analysed by pXRF were airdried in aluminium foil boats in a warm, dry room at the Department of Archaeology, York. The dried samples were lightly disaggregated by hand with a clean porcelain pestle and mortar, passed through a clean 2mm aperture brass-aluminium sieve, more heavily ground with the same pestle and mortar and finally sieved through a clean 1mm aperture sieve to separate fine fraction samples. All the samples were of a similar, fine density by the end of this process, varying only a little in sand content (between sandy loam and loamy sand), with occasional pebbles or small natural stones that were removed during the sieving. The apparatus was dry wiped with blue roll between samples. Fresh disposable, powder free, nitrile gloves were worn for processing each sample. The coarse fraction remaining from the sieving was retained in case of future analysis. This process took approximately 5-10 minutes per sample (including equipment cleaning time).

For analysis, samples were loaded into the Olympus pXRF Flex Stand, setup in a vertical position so that the sample window was positioned directly above the analyser window (see Figure 83). The fine fraction was loaded loose on top of a disposable sheet of Prolene® (polypropylene) film which was changed between each sample. It was loaded directly above the window, with enough sediment to cover the analysis window and a depth to the peak of the pile to a minimum of 2 cm. Samples were loaded wearing a fresh pair of powder-free nitrile gloves, though generally the soil did not come into contact with the hands as they were poured from their storage bag and then from the film sheet back into it when complete. The chamber was dusted down with lint-free tissues and a compressed air duster between samples. Initially, samples were to be analysed in polythene resealable bags, which is a standard method, but it was found that these interfered with the readings using the University of York setup and supplies (see section 5.5.7.2).

Figure 83. Vertical setup for the Olympus Flex Stand, looking down on the stand, with the lid of the chamber lifted to show inside the chamber and the analysis window.

5.5.7 Quality assurance and control readings for lab-based pXRF

5.5.7.1 Control sample tests

In addition to the usual daily calibration checks (detailed in Appendix Five), certified control sample readings were taken at the start of every lab-based session, every 20 readings, whenever there was a risk of significant contamination e.g. there had been a soil spillage, and at the end of every session where possible (occasionally the machine recorded as operating at too high a temperature and had to be allowed to cool overnight thus preventing further readings). The sample pots are designed to allow easy loading into the stand with good contact with the analyser window. The control materials utilised here were the same NIST 2710a (NIST Certificate issued: 7 April 2009) and NIST 2711a (NIST Certificate issued: 22 May 2009) samples as those used in the field at Star Carr. A silicon dioxide sample had been purchased and was also utilised:

- Silicon Dioxide (SiO_2) fine powder - sourced from Sigma Aldrich (certification date: 20th October 2014)

The results from the control sample analyses are provided in Appendix Five and on the supplementary digital media. The results from these analyses were inspected at the time, to ensure contamination was not interfering with sample readings. When any variance or contamination was detected, the sample chamber on the Flex Stand and the analyser itself (particularly the analyser window) were dusted down again with a lint-free tissue and controls were repeated. This cycle was repeated until contamination was no longer detected.

These results were initially evaluated as the repeats in the field were by first looking at results outside the 20% margin, then looking at how those within that fall into below 5% out from expected value and between 5 - 20% out from expected value. For the 2711a and 2710a readings, in summary:

- Elements that tended to be greater than 20% too low in one or both samples: **magnesium**, **phosphorus**, **calcium (2710a)**, **chromium**, **cobalt** (2711a), **arsenic**, selenium (2711a), **silver (2711a)**, cadmium (2710a), tantalum (2711a)
- Elements that tended to be either 20% too high or too low (mixed): **antimony**, thorium, **uranium**
- Elements that tended to be greater than 20% too high in one or both samples: **sulfur**, **vanadium**, **iron**, *nickel (2711a)*, copper, **yttrium**, **zirconium (2711a)**, **niobium**, **molybdenum** (2710a), tungsten, **mercury**, bismuth (2710a)

The results in bold are those that agree with the accuracy issues seen when the samples were run in the field at Star Carr (if the sample is listed but not highlighted then that element was out for both samples in the Star Carr run). The only conflicting result was nickel which had previously been flagged as reading too high in the samples and as such should perhaps be considered as a mixed result element but the certified value is less than 25 ppm in both samples so it could be the low levels of this element are causing it to be overestimated.

Specifically regarding the SiO2 controls, since this is as close to running a blank as possible (while the soil controls can be showing a complicated picture involving interference peaks), all the silicon readings were within the +-20% suggested limit. All readings were low, being in the -5 to - 20% category but on closer examination of these, 25 were in the -10% to -20% category but the majority of 84 were in the -5 to -10% category so generally only slightly low. The only two elements which repeatedly came up with erroneous readings were iron (usually in trace amounts, but quite frequently) and aluminium (not as often but as readings between 969.44 ppm up to 6150.33 ppm when it should not be present at all). However, the chamber was recleaned after these readings and this resolved the issue. Very occasionally there were readings for other elements, all as trace / IUPAC trace level readings (usually below 20 ppm) and never more than three times. Again, recleaning the chamber resolved

these issues and at such levels they could have simply been erroneous peaks rather than actual contamination.

5.5.7.2 Impact of pXRF analysis of prepared samples through polythene bags

Portable XRF analysis of soil samples in polythene bags is a standard technique (Olympus 2014b, 126 Appendix C), as the bags do not theoretically impact the readings. However, for three samples, the bags were analysed by pXRF before samples were put in them so that this could be tested: samples 1087, 1343, 1615 from 2012 were utilised for this and this raised some concerns about possible interference. The full details of this experiment are provided in Appendix Five.

A small experiment was devised with input from Dr. Gianni Gallello (MATRIX project, University of York) to fully explore the impact of the bags on readings using the University of York Flex Stand setup and also to consider alternative sample loading options (as a pellet press was unavailable at this time). The samples were scanned within the Flex Stand's test chamber, in the vertical position so the weight of the sample pressed down under its own weight against the analysis window which faced upwards.

We focused on investigating the impact of the bags on key elements making up soil compositions, i.e. aluminium, calcium, iron, silicon, and titanium. We also looked at a selection of other important elements in characterising soils: copper (Cu), manganese (Mn), nickel (Ni), potassium (K), strontium (Sr), zinc (Zn), and zirconium (Zr). As alternatives to bags, we investigated using supermarket-bought cling film and spare Prolene® (polypropylene) film discs as loose soil mounting substrates. NIST 2710a, NIST 2711a, the Sigma Aldrich Silicon Dioxide (SiO_2) fine powder were used as the controlled samples. In addition, the following reference soil sample was also incorporated into this study:

- NIM GBW07408 - internationally recognised control Chinese soil with independently verified certified values utilising alternative methods, provided by Gianni Gallello (certified values provided as pers. comm.)

In summary, the results showed that a signal from the empty bags and, to a lesser extent, the cling film was picked up inconsistently by the analyser even without samples and misinterpreted as peaks of elements that were unlikely constituents of the plastics. The Prolene® was not detected without a sample. In readings taken using the samples, the bags could cause elements to be detected up to 88% less than their known proportions. Cling film similarly reduced signals of some elements to up to 75% of what they should be. The bags and cling film generally underestimated the readings for most major elements (redistributing the values to minor element readings). In contrast, the readings from the

samples using the Prolene® as substrate were all within the Olympus-recommended 20% error margins for operation.

5.5.7.3 Machine error in iron readings

The experiments on the interference of bags also valuably highlighted that the iron readings from the machine were all reading consistently high regardless of the methodology employed: the machine was subsequently sent for recalibration to correct for this. Recalibration took place in February 2016, i.e. after all fieldwork was complete, but all lab based analyses on the pXRF were reconducted at this stage. This must be taken into consideration when viewing the iron results, particularly those from the field.

5.5.8 pXRF results utilised for spatial mapping

As there was no known feature or distinct activity context for Flixton Island 2, it was decided to keep consideration to a broad range of elements as much as possible. This would allow identification of spatial patterning whilst not biasing interpretation towards anthropogenic activity: While the goal was to identify possibly anthropogenic activity, any patterning identified would need to be evaluated for how likely it was to be ancient anthropogenic enhancement or natural processes or more recent anthropogenic enhancement.

However, there were a number of elements available using this method that are commonly considered to be those likely enhanced by a wide variety of anthropogenic activities, as identified from literature review. Sixteen elements of the thirty-six elements available to be analysed from the pXRF data fell into this category: aluminium (Al), calcium (Ca), cobalt (Co), chromium (Cr), copper (Cu), iron (Fe), potassium (K), magnesium (Mg), manganese (Mn), nickel (Ni), phosphorus (P), lead (Pb), sulfur (S), strontium (Sr), vanadium (V), and zinc (Zn). However, of these 16, only aluminium, iron, potassium, manganese, lead, strontium and zinc had all values (in both the field and lab readings) that were all above the machine LODs. Cobalt and magnesium were not detected (i.e. were below the LOD) in any readings by pXRF at Flixton Island 2, and the same went for antimony (Sn), selenium (Se), and tin (Sn). Results for calcium, chromium, copper, nickel, phosphorus, sulfur, and vanadium featured some values below the LODs and therefore would require substitution if they were to be integrated into certain analyses (see discussion below on how results below the LOD were handled).

Other elements available were not entirely discounted either, as they held the potential to reinforce spatial patterning witnessed, or indicate that enhancement was being caused by different processes or more recent anthropogenic activity. Of these, niobium (Nb), rubidium (Rb), silicon (Si), titanium (Ti), yttrium (Y), zirconium (Zr) all had values above the limits of detection. The remaining elements would require substitution for full integration. However,

many of these were trace elements being present in relatively tiny amounts and with higher chances of error and that was taken into consideration as well.

5.6 Inductively Coupled Plasma Atomic Emission Spectroscopy (ICP-AES)

Summarizing from Pollard and Heron (1996, 31–36), in order to analyse samples through ICP-AES, the processed sediments are reacted with an acid to form a soluble species and introduced as a mist to a plasma flame. A plasma is a state of matter which can be induced, in this case when argon gas is subjected to a strong, oscillating radio frequency, electromagnetic field, forcing electrons to separate from their atoms and therefore ionising the gas into a plasma. Ions and electrons in the plasma have very high velocity and their collisions with the analyte mist causes the analyte's molecules and atoms to break down into charged ions and electrons as well. The loss of electrons and then the ions' recombination with electrons in the plasma causes radiation to emit at wavelengths characteristic of the elements involved which is detected by the apparatus. The intensity of the different photons detected, also measured by the apparatus, corresponds to the proportion of the atoms they are characteristic of in the chamber. As such the elemental composition of the sample can be deduced by controlling for the readings that are contributed by the argon gas and aqua regia.

5.6.1 ICP-AES sampling strategy

From the 800 samples taken across Trench 4, the fine fraction material from the subsample of 65 out of the original 800 samples were submitted to a commercial laboratory for ICP-AES (see Figure 74). 10 of the subsamples were selected deliberately from the same samples used in the general characterisation analyses detailed in section 5.4 . In addition, two control samples from the topsoil and till were also submitted.

5.6.2 ICP-AES sample preparation

Based on the recommended method outlined by French (2015a, 92), both prepared and semi-prepared samples were submitted to ALS Minerals for ICP-AES. Preparation involved drying and separating out the coarse from fine fractions of each sample. The semi-prepared samples were provided as air-dried samples in resealable plastic bags, lightly disaggregated to remove the largest stones, and submitted to ALS Minerals without thorough sorting. The following sample preparation procedure was conducted by ALS Minerals prior to ICP-AES (method code: ME-ICP41): 1) Removal by dry sieving of >1mm coarse fraction (code: SCR-51); 2) Light disaggregation by hand using mortar (specially arranged instead of pulverisation in steel bowls which can cause contamination); 3) Removal by dry sieving of >180µm coarse fraction (code: PREP-41). For Flixton Island 2, this methodology was employed for the till and topsoil samples taken for comparison with the occupation layer

samples. All the samples from Star Carr submitted for analysis by ICP-AES were prepared by ALS Minerals in this manner also.

All other samples were prepared in house by the following method before submission to ALS Minerals for ICP-AES as a standalone procedure. To protect the samples from contamination in the lab, a drying system was devised. The samples were placed in disposable aluminium boats with perforated lids of the same, placed on moisture-indicating silica gel beads in sterile airtight boxes. The silica, as the desiccant, changes from orange to colourless as it absorbs moisture. In practice, this provided a useful visual check that the drying procedure was working, when it was slowing in rate and for when the desiccant needed to be replenished. The sample was considered dry when the weight of the sample did not fluctuate by more than 0.1% of its original weight over a 24-hour period. Samples were weighed in grams to two decimal places. For a 15g wet-weight sample, this process took about one week in the drying chambers. Gloves and acetone rinsed implements were used at all times.

The dried samples were lightly disaggregated by hand with a clean porcelain pestle and mortar, passed through a clean 1mm aperture brass-aluminium sieve, more heavily ground with the same pestle and mortar and finally sieved through a clean 180μm aperture sieve to separate fine fraction samples before submission to ALS Global Minerals in resealable polythene bags. The apparatus was thoroughly cleaned with soap and water and then rinsed with acetone between samples. Fresh disposable gloves were worn for processing each sample. The coarse fraction remaining from the sieving was retained in case of future analysis. This process took approximately 40 minutes per sample (including equipment washing time).

5.6.3 ICP-AES analysis

ICP-AES was conducted on the dried, sorted sample fine fractions by ALS Minerals (procedure code: ME-ICP41). ME-ICP41 involves sample decomposition in aqua regia in a graphite heating block (Minerals 2009). The resulting solution is diluted to 12.5ml with deionised water and then analysed. ALS Minerals Loughrea conducted the analyses on either a Varian 725 RD ICP-OES system or Agilent Technologies ICP-OES system (Louise Clarke, ALS Minerals, pers. comm.).

The digestion method can be varied and is usually selected based on the research question relating to the material, e.g. if soil samples are being specifically analysed for heavy metal contamination in an industrial setting, then a digestion method specifically designed to facilitate analysis of heavy metal content will be selected (Lajunen and Perämäki 2004, 292). Total digestion or partial extraction can be implemented using different extractants, leaching and dissolution methods. Total digestion of samples in aqua regia (a standard

mixture of concentrated nitric acid and hydrochloric acid) was recommended for the samples from Flixton Island and Star Carr as it had been successfully used by Charles French at other archaeological sites and would facilitate analysis of a wide array of elements (French, pers. comm.). Breadth of elemental analysis was important given the lack of previous work on Mesolithic activity areas meaning that it could not be predicted what elements might prove important in the study but also as the intention was to get a general sense of any patterning in the geochemistry, not only from Mesolithic signatures but also more recent processes, to better understand what the lithics assemblage and associated sediments may have been subjected to post-depositionally as well. Therefore, there was a conscious effort to select a method that avoided pre-empting any specific results, so a total digestion method was considered appropriate.

During comparison of the main results, it was evident that certain elements were reading lower from the ICP-AES results than anticipated in the light of the later pXRF results. Despite ICP-AES being widely regarded as a more accurate and precise method, aqua regia does not completely solubilise some elements, so readings using this digestion method are best only compared relative to each other. There are several reasons this can occur. Firstly, in fine ground soils and sediments, metals associated with larger particles of harder materials rather than being associated with softer clayey particles may be less efficiently transported into the plasma (Nomura and Oliveira 2007, 5). Secondly, while aqua regia is commonly considered an effective solvent for many materials, it is less effective on some rock-forming elements which form stable diatomic oxides known as "refractory species" (Lahr,Kahn and Morton 2007, 70). However, after consideration of the results in detail, aqua regia digestion was still considered to provide adequate results for comparison relative to each other, which fulfilled the needs of this project (see section 5.6.5.2 5.6.5 for further explanation). In retrospect, and if time and funding had permitted, a subselection of the samples would have been subjected to a panel of digestion methods to assess their relative advantages and sensitivities towards certain elements to refine this methodological decision.

5.6.4 ICP-AES outputs

The spectrometers use a method template containing 61 analytical lines and 28 interferent lines. The available elements and detection limits for this method are summarised in Table 35. The results are corrected for inter-elemental spectral inferences by ALS Global before return as both a comma separated values file and as spectra.

Table 35. Elements analysed through ICP-AES conducted by ALS Chemex (ME-ICP41), the units results are provided in, and the upper and lower detection limits for specific elements (modified from Minerals 2009 with amendment received from Louise Clarke, ALS Minerals, pers. comm.)

Element	Symbol	Units	Lower limit	Upper limit
Silver	Ag	ppm	0.2	100

Element	Symbol	Units	Lower limit	Upper limit
Aluminium	Al	%	0.01	25
Arsenic	As	ppm	2	10000
Boron	B	ppm	10	10000
Barium	Ba	ppm	10	10000
Beryllium	Be	ppm	0.5	1000
Bismuth	Bi	ppm	2	10000
Calcium	Ca	%	0.01	25
Cadmium	Cd	ppm	0.5	1000
Cobalt	Co	ppm	1	10000
Chromium	Cr	ppm	1	10000
Copper	Cu	ppm	1	10000
Iron	Fe	%	0.01	50
Gallium	Ga	ppm	10	10000
Mercury	Hg	ppm	1	10000
Potassium	K	%	0.01	10
Lanthanum	La	ppm	10	10000
Magnesium	Mg	%	0.01	25
Manganese	Mn	ppm	5	50000
Molybdenum	Mo	ppm	1	10000
Sodium	Na	%	0.01	10
Nickel	Ni	ppm	1	10000
Phosphorus	P	ppm	10	10000
Lead	Pb	ppm	2	10000
Sulfur	S	%	0.01	10
Antimony	Sb	ppm	2	10000
Scandium	Sc	ppm	1	10000
Strontium	Sr	ppm	1	10000
Thorium	Th	ppm	20	10000
Titanium	Ti	%	0.01	10
Thallium	Tl	ppm	10	10000
Uranium	U	ppm	10	10000
Vanadium	V	ppm	1	10000
Tungsten	W	ppm	10	10000
Zinc	Zn	ppm	2	10000

The results of the analysis are returned from ALS-Chemex in the form of a Microsoft Excel Comma Separated Values (csv) file. The results are supplied as a mixture of parts per million (ppm) or percentages of the sample, depending on the appropriate scale for that element (i.e. higher ppm readings get presented as percentages for ease of general viewing). While these essentially mean the same thing (they are both expressions of proportions of the material), they were standardised to ppm so that the results would be directly comparable and comparable with the pXRF results while being correlated on ArcGIS.

5.6.5 Quality assurance and control readings for ICP-AES work

ALS Chemex provide the results of several blank runs and several control sample runs with every batch of samples submitted to them. The samples for Flixton Island 2 and Star Carr were submitted in four batches. All batches passed ALS Chemex's quality tests and received a Quality Control certificate.

5.6.5.1 Blank runs

In Batch 1, three blanks yielded a trace reading of a single element (silver, boron, bismuth). In Batch 3, one blank yielded a 10 ppm reading for phosphorus. All other elements were measured as below the limits of detection in all blanks for all batches.

5.6.5.2 Control sample and duplicate sample tests

The ICP-AES values were quality assurance and control tested by ALS Minerals. The controls used were standard ones selected for ICP-AES and ICP mass spectrometry:

- GBM908-5, an oxide cap silver ore
- GBM908-10, an oxide copper and gold ore
- GEOMS-03, a multi-element reference material
- ICP-4, an in-house Certified Reference Material used by ALS Minerals
- MRGeo08, a mid-range multi-element reference material
- OGGeo08, an ore grade multi-element reference material

As can be seen, many of these controls are not soil controls but powdered metal ores. It was possible therefore that soils would not read as well. The repeats on the genuine samples informed on the precision in the measurements of samples, which seemed consistently tight.

However, accuracy could only be evaluated with cross-reference to results derived by other methodologies on the same samples. As introduced above in section 5.6.3 with the results from pXRF as a comparative methodology available, it was found that the accuracy of the ICP-AES readings of site samples had in fact been impacted by the selection of aqua regia

digestion: readings were consistent with each other (i.e. precise) but accuracy looked to have been negatively impacted, as some elements were lower than anticipated given the lab-based pXRF readings. This was considered unlikely to be highly detrimental to understanding anthropogenic enhancement in localised areas, as chemical enhancements that have managed to invade the soil are unlikely to be trapped within its rocky formations and, furthermore, the samples were prepared and treated consistently with larger silicate-based rocks filtered out. The general similarity of results derived by the same method on different samples from the same site suggested that they could be compared relatively to other samples from that site at least. This does explain some of the discrepancy with the pXRF readings, however, and intersite, absolute value comparisons were not drawn. In contrast, field pXRF was more likely to show greater discrepancies as the coarse stone and rock components had not been sieved out.

5.6.6 ICP-AES results used in spatial mapping

Similar to the pXRF analysis, of the 35 trace and heavy metal elements that can be measured through this method of ICP-AES (as listed above in Table 35), 19 elements commonly identified and associated with activity areas on archaeological deposits were available to be analysed from the ICP-AES analyses: aluminium (Al), barium (Ba), calcium (Ca), cobalt (Co), chromium (Cr), copper (Cu), iron (Fe), potassium (K), lanthanum (La), magnesium (Mg), manganese (Mn), sodium (Na), nickle (Ni), phosphorus (P), lead (Pb), sulfur (S), strontium (Sr), vanadium (V), and zinc (Zn). For all of these elements except sodium, all values were above the LOD. For sodium, all samples from the first batch submitted to ALS Chemex were above the LOD, but all the samples in the second batch (although from the same trench and even grid square as some of the first batch samples) were below the LOD. This immediately suggested a discrepancy might be seen between the results from the two batches (see chapter six) and also that these values for sodium would have to be substituted for in order to display the results as one integrated dataset (see discussion below for the handling of readings below the LOD and substitution methods).

In addition to these elements known to be of possible interest, values for arsenic (As), mercury (Hg), scandium (Sc), and titanium (Ti) were above the limit of detection in all readings, although for some only in trace amounts. Bismuth (Bi), cadmium (Cd), gallium (Ga), thorium (Th), thallium (Tl), uranium (U), and tungsten (T) were not detected in any samples by ICP-AES. All other elements measured had some values below the LOD and therefore would require substitution for integration.

5.7 Statistical Analysis Methods

The chemical characterisation data utilised in this study were initially collated into Excel as comma separated value (CSV) files and then Excel workbooks. The data were subsequently

imported into IBM SPSS Statistics 22 and Origin 2017 for statistical analyses and integrated into a geographical information system using ESRI ArcMap 10.2 through to 10.5 for complementary spatial and additional geostatistical analysis. Using ArcMap permitted spatially visualising single-data distributions, exploring the relationships within and between the datasets, as well as facilitating integration of not only both the pXRF and ICP-AES data but also with artefact distribution data, recorded plough scars, potential features and earlier geophysics work. Grouping Analysis, a cluster analysis method deploying a k-means++ algorithm, was conducted on ArcGIS 10.4.1 and 10.5 and Principal Component Analysis was conducted on SPSS 24 and OriginPro 2016.

5.7.1 Handling data below the limit of detection

There were readings below the limits of detection (LOD) for certain elements in the data generated both by pXRF and ICP-AES. There is a significant amount of literature on the handling of data below the limits of detection in statistical analyses. Some researchers have advocated developing methods to substitute statistically likely, or at least statistically reasonable, values for the absent data (cf. Helsel and Cohn 1988; Hewett and Ganser 2007; Antweiler and Taylor 2008; Flynn 2009; Helsel 2010). These can be simply direct substitution of the value zero, the LOD value itself, or values generated by very basic calculations such as half of the LOD value, right through to calculating more complex predicted estimates based on the distribution of the actually measured values in other samples. In a thorough review of the literature, Helsel (2010) called for journal editors to immediately reject papers submitted which integrated substitutions for readings below the LOD in all but one analytical circumstance. The editorial commentary on Helsel's paper in the same journal issue explained that their board decided to not to take that quite so far so long as the "key principal as with all measurements and data treatments is that the conclusions must be justified by the evidence, or, to put it another way, approximations in the data treatment must not be so gross as to undermine the validity of the conclusions" was maintained, whilst encouraging researchers to take heed of Helsel's very valid warnings of the errors that can potentially arise from substitution (Ogden 2010, 255).

It was decided that for the descriptive statistics, only actual measured values would be included in the calculation of mean, range etc. Substitution needed to be made for integration into ArcMap however, as even straightforward simple visualisations using statistical 'bins' (using natural breaks in the data or employing other statistical methods to group the dataset say into 5 groups - 'bins' - in colour coded ascending order) would not allow visualisation of attributes that were mixed entries of number and text e.g. if the LOD were 2 and the value was below the LOD then <2 could not be use as a meaningful numerical value.

In the case of ICP-AES, the LOD is a fixed value per element for the instrument as discussed above. For pXRF, the LOD varies from sample to sample and also with the selected operational mode on the machine at the time of analysis, due to the potential for interference between peaks from both readings and elements not being measured that are misinterpreted. As a result, the pXRF LODs for each element are mathematically estimated on a case by case basis through preprogrammed algorithms as part of the machine's software and provided as one of the outputs when a reading is categorised as below a statistically valid limit. This immediately introduced an issue of whether to handle the data consistently between the two methods.

The greatest challenge facing this is that the pXRF estimated LODs were much higher than the occasional actual value readings obtained in comparable samples from the same method, unlike the ICP-AES LODs which were all lower than any readings obtained. For example, from the field pXRF readings at Flixton, 329 out of 332 single readings (or 334 out of 338 including averaged readings from repeats) had a silver content reading below the LOD. The four measured silver readings were between 17.82 to 20.24 ppm. However, for the 335 samples with readings below the LOD, the estimated LOD values ranged between 593.55 to 1316.5 ppm. As such, any substitution for those values statistically based on the estimated LODs could result in those points appearing to have higher values than the actually measured values in samples where a reading was successful even if the substitution was calculated as half the LOD or similar. This seems unlikely, and it is possible that the algorithm estimating the LODs is 'overcautious' in estimating how high the absent value could potentially be, providing a potential absent maximum rather than a realistic LOD. These low actual readings also raised the validity of including the analysis of silver in the results, along with several other elements including cadmium, copper, mercury, bismuth and uranium. Indeed, actual readings in these elements were not considered indicative of areas of interest in isolation, however they were analysed to see if they would correspond with areas of enhancement (or depletion) for other elements.

Equally, the issue with substituting with 0 is that this ran the risk of enhancing peaks. For example, the single successfully measured value for magnesium taken in the field in 2014 at Flixton was 39977.15 ppm. However, all other values were below the LOD and estimated LODs in this case ranged between 6872.6 to 92624.76 ppm. As such, the difference between the actual value and substituted values of zero would be 39977.15 ppm. Whereas, substituting 0 for the readings below the LOD for silver, the highest actual reading for which was 20.24 ppm, the difference between this and the substitutes was on a much lower scale. This would be the benefit of substituting with half the LOD or similar, as the substituted value would be on a similar scale to the real values; however, that only works if the LOD given is confidently realistic and that was only the case with the ICP-AES values.

Substitution of estimate values based on the values above the LOD is another method often employed and has been argued to provide smaller error rates when tested on falsely censored datasets (Croghan and Egeghy 2003). As Croghan explains, this can be done with an extrapolation (i.e. regression) technique or a standard method known as maximum likelihood estimation. The risk with these methods is that the small sample sizes being worked with here could make the estimations less reliable. Essentially, this may misrepresent the data too.

On balance, it was decided to proceed with substitution with zero for the purposes of this project. Given the range of estimated LODs for pXRF, simple substitution of the LOD, half the LOD or the LOD divided by the square root of two were ruled out.

5.7.2 Descriptive statistics and basic plots

Descriptive statistical analyses, variance, and correlation analyses were performed on the elemental characterisation dataset using IBM SPSS Statistics software (versions 22 and 24) to test the variability in the samples as well as compare control samples from the topsoil and till to the archaeological layers. Flixton Island 2 has no distinguishing features to demarcate utilised areas so horizontally distributed controls could not usefully be taken as, given the ephemerality of many Mesolithic sites and the short-lived nature of some associated activities, any area could have been utilised in the past. As such, samples were considered in terms of their relative variation from each other rather than from an assumed known baseline signal. The risk with this is that anthropogenic influences on the soils need to be greater than natural variations in the soil to be identified. Given the ephemerality of some activities, this means some areas could be missed. However, on balance, it was decided that for this exploration of whether the detection of any Mesolithic activity areas was even viable or plausible, focusing on analysing stronger signatures of activities was acceptable.

In addition to the analyses in SPSS, elemental readings were visually plotted and statistically analysed in ArcMap. The results of the elemental analyses were integrated into ArcMap using layers of gridded square digital polygons generated using the Fishnet tool to represent the sampling grids employed in different years at Flixton Island and Star Carr. The sample or in-situ reading values were taken as representative of that grid square as a digital feature and therefore associated as an attributed value to that feature, to then be visualised or analysed. As such, the analysed sample grids defined the spatial resolution of the statistical analyses.

For the Flixton Trench 4 samples, the 50 analysed samples (of the 800 taken) were spaced out from each other by 1 m, with one from the north-western corner of each 1 m^2 of the broader site grid, as discussed above in section 5.3 In this case, the samples were not

visualised to show a continuous surface but just the 0.25 m^2 squares they were taken from, spaced out as separate features. The values could have been interpolated to represent a wider vicinity but as the samples were so widely spaced it was felt this would be misrepresentative. Formal statistical interpolation in ArcMap proved to be unconvincing with such a small number of samples and ruled out as a method.

In contrast, the readings from Flixton Trenches 11, 12 and 15 (section 5.5.3 and Star Carr (section 8.2 were taken at finer resolution, with a reading available from the approximate centre of every 0.5 m^2 of the sample grid, in some cases across a wider continuous area. As such, the reading values were attributed to every digital feature representing the 0.5 m^2 grid squares and visualised as a continuous surface, with the increase to four readings per 1 m^2 considered to justify this representation.

For the preliminary visualisation, the elemental readings were grouped into classes which were calculated using an algorithm based on Jenks Natural Breaks. This is a data clustering method which simply divides the dataset up into *N* groups by finding the top *N* groups that best minimise the group's average deviation from the group mean (Jenks 1967). The sample square was then symbolised by group (class) for a visual representation of the values in parts per million.

5.7.3 Hot Spot Analysis

While Natural Breaks visualisation is good for a preliminary consideration of the data, and for presenting the data without transforming from the original data in any way, any interpretation of that visualisation is highly subjective. As such, it is preferable to explore potential patterns through various supplementary statistical methods. The statistical tools in ArcGIS are designed to test the null hypothesis that the patterns in the data are the result of random processes. These statistical analyses were conducted using the same digital layers as used for the Natural Breaks visualisation.

The Hot Spot Analysis tool on ArcMap visualises each feature not only based on its own value (i.e. the element readings associated with that sample, its attributes as a feature) but also considering its immediate neighbourhood (which is optimised in coverage extent), in comparison to the global (entire) study area using an algorithm based on the Getis-Ord Gi* Statistic (Bennett and Vale 2014). These statistical Hot or Cold Spots are considered to be areas where there are significantly significant clusters of similar values. In other words, this tool identifies areas where high values are adjacent to other high values at a statistically significant level relative to the study area (and similarly low values are near other low values). This means that the highest probability Hot or Cold Spots are not necessarily in the same locations as the highest values. The criteria are stricter than just having one extreme

value for designating a location a Hot/Cold Spot, it requires there to be other high or low readings in the local neighbourhood. In fact, a high reading can be designated the centre of a Cold Spot if the surrounding readings are all sufficiently low. This tool, in essence, identifies the centre of clusters of high or low values.

5.7.4 Cluster and Outlier Analysis

The Cluster and Outlier Analysis tool again identifies clusters in high and low values, however it also identifies outliers by separating the consideration of feature values and neighbourhood values. It identifies statistically significant clusters and outliers by comparing features to features and neighbourhoods to neighbourhoods and categorising all features based on the result, utilising an algorithm based on the Anselin Local Moran's I statistic (Bennett and Vale 2014). As such, it divides all features into one of four classes: high value feature in a high value neighbourhood (a 'high-high potential cluster'); low value feature in a low value neighbourhood (a 'low-low potential cluster'); a high value feature, but surrounded by a low value neighbourhood (a 'high-low potential outlier'); a low value feature, high value neighbourhood (a 'low-high potential outlier'). This takes the form of a z-score which if statistically significant will be a Hot Spot (high-high cluster), a Cold Spot (low-low cluster), or statistically significant Outliers (low-high or high-low). Negative *z*-scores are outliers, positive *z*-scores are clusters. If the z-scores are not statistically significant, they are insignificant or otherwise random.

As such, this tool highlights different and theoretically complementary patterns to the Hot Spot Analysis tool. This tool specifically highlights where values are different from their neighbourhoods.

5.7.5 Grouping Analysis

Grouping Analysis, available in the Spatial Statistics toolbox, was selected as one of the methods to further explore the datasets. The output results from this tool are in the form of a visual plot of grouped samples based on multiple attributes as well as a breakdown of the groupings' traits. This provides an easy to understand means of exploring and visually examining the data. Like other algorithms for cluster and component analysis, it is a way of looking for trends in more complex datasets with higher numbers of variables that may correlate positively or negatively. However, the solution of a model from any cluster analysis algorithm is classed as computationally difficult ('NP-hard') so it is not possible to ensure the optimal solution has been found from one run or one tool. As such, results must be compared and interpreted judiciously but can inform about the underlying structures in the dataset (Bennett and Vale 2014; ESRI).

The ArcGIS Grouping Analysis tool clusters features based on trends in their attributes and symbolises features accordingly to produce a visual plot. In this case, sample locations were grouped by their elemental composition traits measured in parts per million. The values are automatically standardized by the tool, using a z-transform, to reduce over-influence of variables with naturally large variances. Groupings were purely based on elemental composition, not the spatial proximity of samples to each other. The groupings were not spatially constrained, i.e. samples did not need to be contiguous to be grouped. A k-means++ algorithm is utilised for calculating the clusters with this setup (Arthur and Vassilvitskii 2007).

The tool has to be told where to grow the analysis of groups from, called 'seed features'. Once seeds are identified, all data points are assigned to the most similar seed feature. A mean data centre is then computed for each group and the points are repeatedly assigned to the closest centre until the model is stable. The number of seeds that are used to grow the groups is the same as the number of groups being defined (e.g. specifying for six groups means six seeds will be employed). These seeds can be prespecified, completely randomised or selected by the tool to optimise group differentiation after random initialisation ("Find Seed Locations"). Here the latter (optimised) method was selected in order to avoid preempting any patterning. As such, there can still be slight variations in results from repeated runs of the tool due to the randomness in initialisation.

The Grouping Analysis tool can statistically suggest the optimal number of groups, based on the highest pseudo F-statistics. The results of this varied due to the randomised seed initialisation of each run. This is reported with the statistical models in chapters seven and eight.

As such, the tool was set up to: have no spatial constraints on the groupings (thus allowing non-adjacent samples to be grouped, therefore only grouping them only based on the input elemental variable/s); utilise euclidean distances; find the seed locations (i.e. not prespecifying the seed location or making it totally random, but basing it on the data itself); and, evaluate the optimal number of groups using that variable or combination of variables. The variables were the elements available through ICP-AES or pXRF. The values were the measurements of those variables in parts per million (ppm). The variables incorporated into the model had to be selected, rather than all simply input, as if the number of variables is greater than 15, then a detailed output report cannot be produced through the tool on ArcGIS and that is important in assessing the robustness of the model, so it is preferable to keep the input variables low. This was not a concern as many of the variables had either no variability at all, only had values below 15 ppm, or had values that were rounded up in the

output from ALS Minerals as to make the data difficult to compare with the other elements. As such these were the variables ruled out initially.

5.7.6 Principal Component Analysis

The results from Star Carr were also loaded into SPSS 24 and OriginPro 2016 as datasheets in order to run Principal Component Analysis (PCA). As the datasets from pXRF and ICP-AES could not be treated as one for Flixton Island 2, there were not enough samples to use this statistical analysis. K-means clustering, as employed for the grouping analysis, aims to group the samples themselves. PCA, on the other hand, aims to reduce the dimensions in the data by grouping variables into linear, uncorrelated variates (linear combinations called components) that capture as much of the variance as possible (Ding and He 2004; Field 2009). As such, if the scores on components identified using PCA group together and are consistent with the groupings identified from the k-means++ clustering then it would suggest support for the groupings based on the geochemistry.

5.8 Summary

The suite of techniques described above were implemented at both Flixton Island 2 and Star Carr as a means of investigating the signatures available in the soil. Chapter six will discuss the results of this work at Flixton Island 2 and then the thesis will go on to discuss what the ramifications of these results may be in terms of potential activity areas and how they integrate with both artefact distributions as well as the recorded ploughing and post-depositional interference. Then chapter eight will look at the results of this for Star Carr, as a comparative case study.

Chapter 6 Results of Geochemical Analyses on Flixton Island 2 soil samples

6.1 Introduction

This chapter is divided into two main sections. The first reports the results of analyses aimed to generally characterise the site soil's physical characteristics and elemental 'fingerprint' alongside summarising pertinent background information for reference. It is important to remember that while the two elemental analysis methods used, ICP-AES and pXRF, provide outputs of spectra and readings in percent or parts per million (ppm), they cannot be considered as absolutely comparable, neither provides perfect readings of any sample, and both have their strengths and weaknesses. One is a bulk technique (ICP), the other a surface technique (pXRF). One measures only the elements that have successfully been digested in an acidic solvent (ICP), the other measures elements present but only from a certain depth into the sample and including potential inclusions when done in-situ (pXRF). Both have limited ranges of elements available to be analysed and are based on initial assumptions about the general makeup of the samples. As such, even though their outputs are in the same units, sometimes measuring the same elements even, they produce different but equally valid patterning.

It is better to think of the two methods as two different but related techniques, similar to an application of two geophysics techniques like magnetometry and resistivity. They may pick up some of the same features, they may pick up different ones: neither set of results should be ignored, neither is better or worse compared to each other (given the specific accuracy and precision errors inherent to both), and they should be considered as complementary approaches. This is important as methods such as pXRF are often maligned for lower precision and accuracy while in fact they may be more suited to a given application and give a more accurate reading than another technique that is generally considered more precise or accurate overall. No set of results will ever be a perfect representation of a sample and as such even the absolute values should be considered with caution.

Comparing the patterning of values determined by one method, preferably within the same batch, is more likely to be meaningful than comparing entirely separate datasets to each other. The second section reports the results of the statistically based spatial analyses conducted on the geochemical data and therefore any spatial patterning identified which may suggest activity areas. At the start of a statistical analysis, it is crucial to be clear what research questions are being asked of the data. This will motivate what statistical analyses are conducted on the dataset. In the case of both the ICP-AES and the pXRF results, there

were two sets of questions applicable: one to the standalone datasets for each element and the other to the datasets as integrated with other data such as the lithic dataset.

The research questions that drove the statistical analysis workflow for the standalone soils datasets were in two general groups: (1) is it possible to produce an approximate baseline signal for the site in order to form a general picture of the site, as far as can be discerned? (2) is there any spatial patterning in the individual and combined elemental results i.e. are there any patterns to be explained? Is the patterning random? These can be resolved reasonably well with statistics, the null hypothesis being that the readings from the samples are randomly patterned. This is explored within this chapter.

An additional question is: (3) is there any correlation between different elements which might be indicative of Mesolithic anthropogenic activities? This is much more difficult to argue for. Spatial patterning in the soil geochemistry may be significant but it may relate to natural chemical processes, other post-depositional processes, post-Mesolithic anthropogenic processes, Palaeolithic processes (as we know we have Long Blade material on site) or genuine Mesolithic processes. The approach to this has been to see which elements group if any, which may support the interpretation of a specific activity, and to integrate the soils data with the lithics data and other datasets available from past research on the site. This starts to be explored at the end of this chapter and continues in the integration chapter (chapter seven).

6.2 General physical characterisation of the dryland soils

Flixton Island was an island within a low-lying basin that was infilled with a glacial-melt palaeolake. It is now a grassy field of drained farmland. Part of the drainage scheme across the landscape was the creation of the Hertford cut around 1820 which runs along the border of the field, approximately 20 m from the previous banks of the island. It was in the banks of the cut in the 1940s, and therefore relatively early in the drainage of the vicinity, that Moore located the site by finding horse bone in an exposed area. The modern field has mainly been used for sheep husbandry, rather than crop growing; while it has been ploughed, it is thought that this has only occurred once or twice in recorded history, according to the landowner. As such, there have been heavily fluctuating water levels affecting the soils over the millennia as well as some likely gradual bioturbation.

From the basic assessment conducted on 10 samples from across the island's dryland trench in 2012, the soils from the dryland consist of a loamy sand of very dark grey or brown (see Table 36, Figure 84 and Figure 85 below). During the excavations, visually-identified manganese compounds were frequently found in nodules (1-2 cm length) and occasionally mistaken for lumps of charcoal by those less familiar with it; it was checked in the field

through looking at the streak it produced which would be grey-black compared with the streak from charcoal which would be brown-black, though this was not geochemically tested. Iron is also a frequent component in compounds in the Vale of Pickering soils, as evidenced on the artefacts themselves in the degree of iron staining and iron precipitate deposits as well as notable iron panning in the soils at Star Carr though this last phenomenon was not seen extensively at Flixton Island 2.

Table 36. Basic geochemical assessment of samples from trench 4

Sample	**Munsell Colour**	**Texture**	**Estimated CaCo3**	**pH**	**Phosphate qualitative signal**
VP12 1087	10YR3/1	Loamy Sand	<0.1%	7.06	None
VP12 1151	10YR3/1	Loamy Sand	<0.1%	7.11	Weak
VP12 1215	10YR3/2	Loamy Sand	<0.1%	7.37	None
VP12 1279	10YR3/1	Loamy Sand	<0.1%	6.83	Weak
VP12 1343	10YR3/1	Sandy Loam	<0.1%	6.92	None
VP12 1487	10YR3/1	Loamy Sand	<0.1%	7.16	None
VP12 1551	10YR3/2	Loamy Sand	<0.1%	7.16	Weak
VP12 1615	10YR3/2	Loamy Sand	0.1-0.5%	7.12	Weak
VP12 1689	10YR3/1	Loamy Sand	0.1-0.5%	6.97	Weak
VP12 1753	10YR3/1	Loamy Sand	0.1-0.5%	7.02	Weak

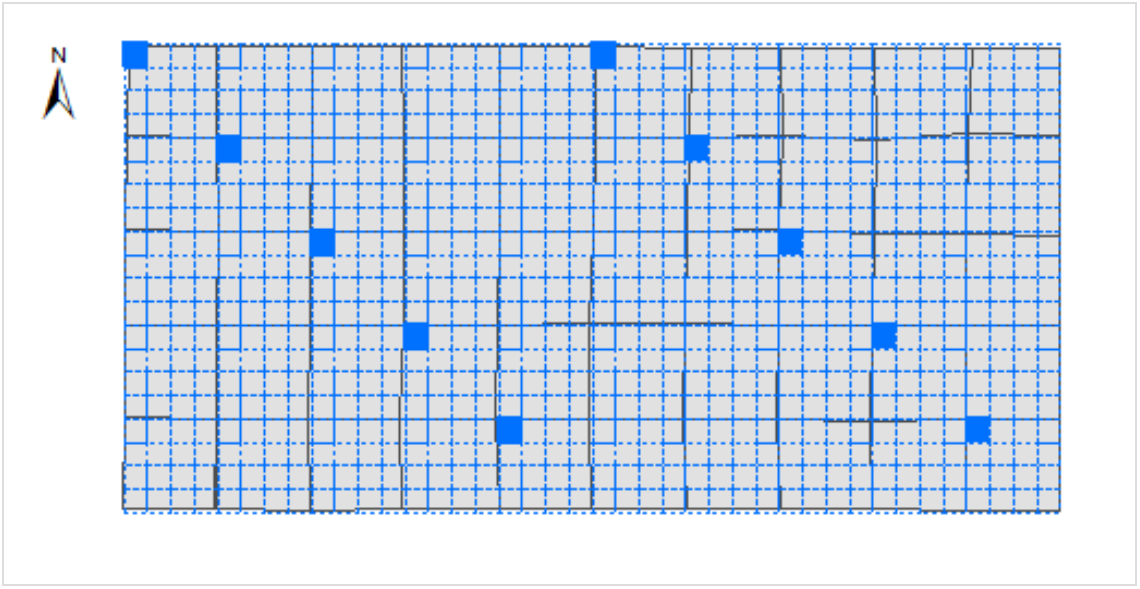

Figure 84. The ten samples used in the basic geochemical assessment

Figure 85. Excavations in trench 4 during the 2012 excavation season: this is at the base of the soil, with the yellowish till exposed and only shallow lenses of the mixed soil-till interface (1119) remaining except behind the excavators (photography by the POSTGLACIAL project)

These ten samples from trench 4 were mainly homogenous. The soil colour refers to the matrix colour as no mottling could be detected in the mixed excavated samples, but according to the context register there were yellow and orange blotches. The matrices are a yellowish-red blend (hue: 10YR) which are very dark (value: 3) and yet not very richly coloured (chroma: 1 or 2). Overall 10YR3/1 presents as a very dark grey brown while 10YR3/2 is a very dark greyish brown. The yellowish-red (with orange mottling) reaffirms the presence of iron compounds, as has been similarly found at Star Carr, which would have

formed under oxidised conditions (Sparrow,Peverill and Reuter 1999, 62). There were no pale grey colours indicating considerable gleying although the mottling might suggest there had been periods of waterlogging up on the dryland (*ibid*.).

Samples overall had a gritty feel and when moistened could hold a small ball shape when moulded and as such were categorised as loamy sand or sandy loam (i.e. predominantly sand with slightly varying proportions of clay), not a peat as seen further into the wetland zone both at Flixton Island and Star Carr. The dominance of sand would suggest that it would be fairly well draining. In addition, the superficial geological deposits below the site will have impacted water drainage, being composed of mixed size particulates but also being generally clayey. Overall the conditions would have been changeable and this would negatively impact preservation, lacking the anaerobic peaty conditions of the wetland, which accounts for the lack of organic remains from the dryland area and organic residues on the lithics.

The calcium carbonate test indicated that there was less than 0.1% or between 0.1 – 0.5% $CaCO_3$ in the samples and as such the readings were extremely low across the trench. This correlates with less alkaline soils and therefore is consistent with the expectation for this to be a neutral or acidic soil. It also suggests that the area has not been limed for agricultural purposes (which would increase drainage, certain elements in the soil, and plant nutrient uptake of other elements), at least not with marl, chalk or limestone.

The pH varied between 6.83 and 7.37 with a mean average for the ten samples of 7.07, as such presenting as neutral (see Figure 86). This was in keeping with Kirsty High's previous work on the site (High 2014).

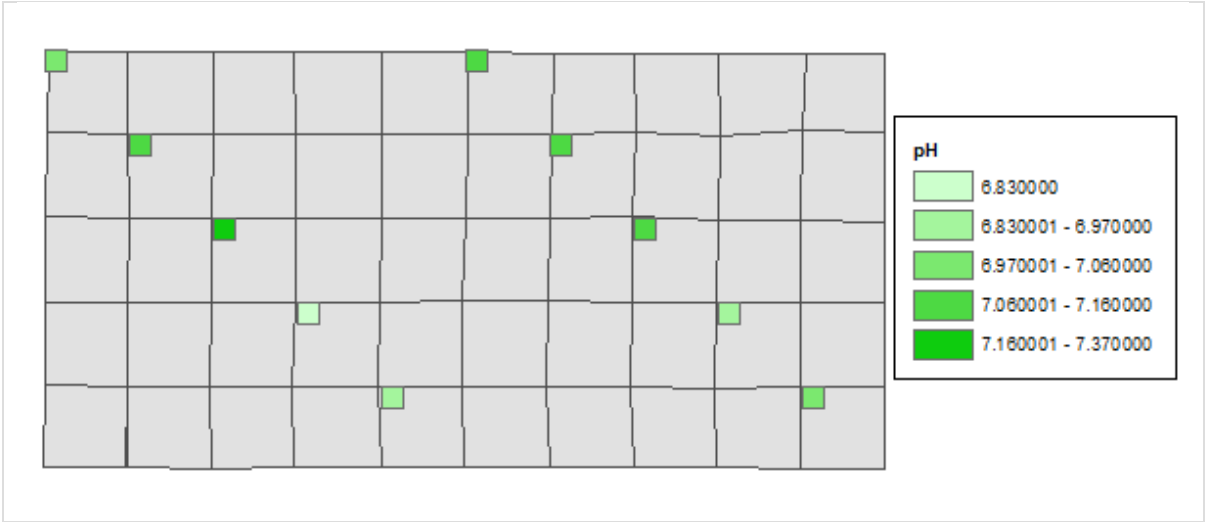

Figure 86. A plot of the pH readings from trench 4, ranging from pH 6.83 (slightly acidic) to 7.37 (neutral)

It was anticipated the phosphorus levels could be quite high in the soils because of the modern use of the field for low intensity sheep grazing some of the year. However, the values suggested by the indicator test were low, rated at 1 or 2 on a scale of increasing

phosphorus presence from 1 to 5. This suggests that the modern sheep grazing has not raised the soluble phosphate levels across the site recently or uniformly, and it is known from the landowners that the sheep kept here were a small flock and only in the field for part of the year. Isolated peaks in phosphorus from the pXRF or ICP-AES may still, however, be indicative of a single excretion incident from the modern sheep.

It should be noted that the spot test only assesses the amount of soluble phosphorus. As such, the test does not measure the amount of fixed inorganic phosphorus which can be tightly bound with minerals in both acidic and alkaline soils or the amount of organic phosphorus still incorporated in organic matter (Iyamuremye and Dick 1996). This can result in a degree of underrepresentation of the amount of phosphates in the soil from this test, although relative to each other the readings are still generally uniform. As a result of this, this test is not adequate alone for sampling to identify ancient activity areas.

If any activity in the Mesolithic caused peaks in phosphorus, it is very likely to have been taken up by plants at some point in the intervening period if it was unfixed and it is only if it had become fixed rapidly after deposition that we would see peaks resulting from it in a total digestion method. ICP-AES, involving total acid digestion, should be better placed to measure insoluble phosphorus bound up in more stable compounds in the soil.

6.3 General elemental characterisation of sediments on site

In order to consider the potential elemental anomalies indicating activity areas on site, establishing a sense of the "baseline" or background levels of elements was attempted. However, soils are undergoing constant, dynamic processes influenced by many factors so, as a result, they are very complex and can be quite variable even in close proximity. Any evaluation of background levels should always be considered as very generalised. As discussed in Chapter 1, the Vale of Pickering's geology is of mixed mudstone formations overlain with deep superficial deposits of Quaternary sands, gravels and till (with the superficial deposits hereafter referred to collectively as till when discussing the sites). Such deposits are inherently highly variable in composition, being largely composed of redeposited material from across potentially very long distances; therefore, we had to anticipate this being reflected to some extent in the samples from the site.

At Flixton, it was not possible to take a clear set of background controls horizontally adjacent stratigraphically to the occupied area contexts as activity could have taken place anywhere on the island and there were no clear features to delineate the boundaries of the site. This is valuable in a way in that regardless of the features of any site, activity can extend outside of features and into areas otherwise unmarked anyway, yet at Flixton we start off with a lack of any clear boundaries and therefore no preconceptions. None of the dryland

areas excavated were completely devoid of archaeological material. However, vertically differentiated controls were taken from the topsoil and the till in a location adjacent to the 2012 and 2013 trenches at Flixton, using a core taken by augering during a field visit in November 2013 with Dr. Barry Taylor, a reference comparison with the samples from the in-situ layers. These were analysed by ICP-AES and the results are provided in Table 37 below. The only element that seems to be on a different scale (i.e. in the 1000s rather than the 100s) is sulfur which read as 1000 ppm in the topsoil but only 400 ppm in the till. There are greater discrepancies between the more dominant element readings than between the trace elements. 12 elements detectable using this method were not detected in either sample while all other elements had readings in both samples. Elements have been divided in the table into major (<10,000 ppm), minor (1000 - 10,000 ppm), trace (100 - 999 ppm), and IUPAC trace (<100 ppm) which gives a more general sense of the significance of their contributions as components of the soils, as suggested by this method.

Table 37. The results of the readings on topsoil and till controls from Flixton Island 2 by ICP-AES (ordered by highest content in the till sample)

Classification	**Element**	**Till**	**Topsoil**
Major	Fe_ppm	20400	17500
	Al_ppm	10000	7300
Minor	Ca_ppm	4000	9300
	Mg_ppm	2200	1200
	S_ppm	400	1000
Trace	P_ppm	400	530
	K_ppm	300	200
	Ba_ppm	210	310
	Ti_ppm	200	100
	Mn_ppm	101	145
	Na_ppm	100	100
IUPAC Trace	Zn_ppm	49	39
	V_ppm	46	33
	Cr_ppm	25	17
	Ni_ppm	25	14
	Cu_ppm	19	13

Classification	Element	Till	Topsoil
	Pb_ppm	19	24
	Sr_ppm	16	30
	La_ppm	10	10
	As_ppm	9	9
	Co_ppm	8	5
	Sc_ppm	5	2
	Be_ppm	0.8	0.6
Non-Detects	Th_ppm	<20	<20
	Bi_ppm	<2	<2
	Sb_ppm	<2	<2
	B_ppm	<10	<10
	Ga_ppm	<10	<10
	Tl_ppm	<10	<10
	U_ppm	<10	<10
	W_ppm	<10	<10
	Hg_ppm	<1	<1
	Mo_ppm	<1	1
	Cd_ppm	<0.5	<0.5
	Ag_ppm	<0.2	<0.2
Sample Weights	*Coarse fraction weight (>1mm) g*	*2.9*	*0.5*
	Fine fraction weight (<1mm) g	*15.3*	*12.4*

Aluminium and iron are the only two elements with “major” readings in both samples. Calcium, magnesium and sulfur follow suit as “minor” contributors. The majority of the

remaining elements came out as trace, including phosphorus, which corresponded with the indicator test for low phosphate levels despite being a total digestion method.

In addition to the two Flixton controls, seven till samples were taken from the dryland at Star Carr in areas apparently outside of the apparent occupation zones, taken to be indicated by the scarcity of artefacts there (see chapter eight and Rowley, French and Milner 2018). These were also analysed by ICP-AES. The descriptive statistics for the seven key major and minor elements from the till samples more than 1 m from the recorded occupation spread contexts at Star Carr are provided in Table 38. Aluminium and iron were again the contributors with the highest readings, although calcium also had readings that would categorise it as a major contributor. Potassium, magnesium and phosphorus were also minor rather than trace contributors at Star Carr.

In comparison, Boston (2007) conducted a geochemical examination by ICP mass spectrometry of a sample of glacigenic sediments from eastern England, the closest sites being from Skipsea and Filey (also in Table 38). As expected, she found the till composition (and she looked at true geological tills) reflected complex deposition dynamics and a high degree of variation. Despite this, for many elements a general similarity of concentrations for certain elements in parts per million (ppm) could be seen to differentiate the different till samples from different sites she studied. Interestingly, however, Boston found that different tills from the same site could not be geochemically differentiated even when visually distinct (Clare Boston, pers. comm. 2016). Overall, Boston's work illustrates the variance in samples seen from tills across the east of the UK which can be compared with the geochemical readings from Flixton and Star Carr.

Table 38. Descriptive statistics for some of the major and key minor elements analysed in local tills (in ppm). The table includes the results from the seven 'till' controls from Star Carr (values in parts per million), the Flixton Island 2 'till' control results for comparison (all analysed as part of this project by ICP-AES), along with C. Boston's readings in parts per million for tills at Skipsea and Filey on the east coast in Yorkshire, analysed by ICP-MS analysis (reproduced with permission from Boston 2007). All values were rounded to the nearest integer where appropriate

Values in ppm		**Al**	**Ca**	**Fe**	**K**	**Mg**	**Mn**	**P**
Flixton Island 2 Till (1 sample)	**Reading**	10000	4000	20400	300	2200	101	400
Star Carr Till (7 samples)	**Mean**	11320	3990	18907	646	3180	125	735
	Minimum	3500	1300	7100	200	700	17	90
	Maximum	31200	20000	46500	1700	6100	703	4750
	Range	27700	18700	39400	1500	5400	686	4660
	Median	11500	3600	18000	500	3300	94	580

Values in ppm		Al	Ca	Fe	K	Mg	Mn	P
	Mode	11100	3500	17500	500	3500	88	550
	Std. deviation (popul.)	3978	1892	5665	363	965	98	622
Skipsea tills (Boston's results)	**Minimum**	4611	4323	6384	5689	517	114	1681
	Maximum	67988	134020	38636	21228	10612	966	12507
Filey tills (Boston's results)	**Minimum**	17257	5930	19372	9439	629	301	12
	Maximum	42022	88533	43319	23397	11535	570	1321

6.4 Results from Trench 4 (2012 excavation)

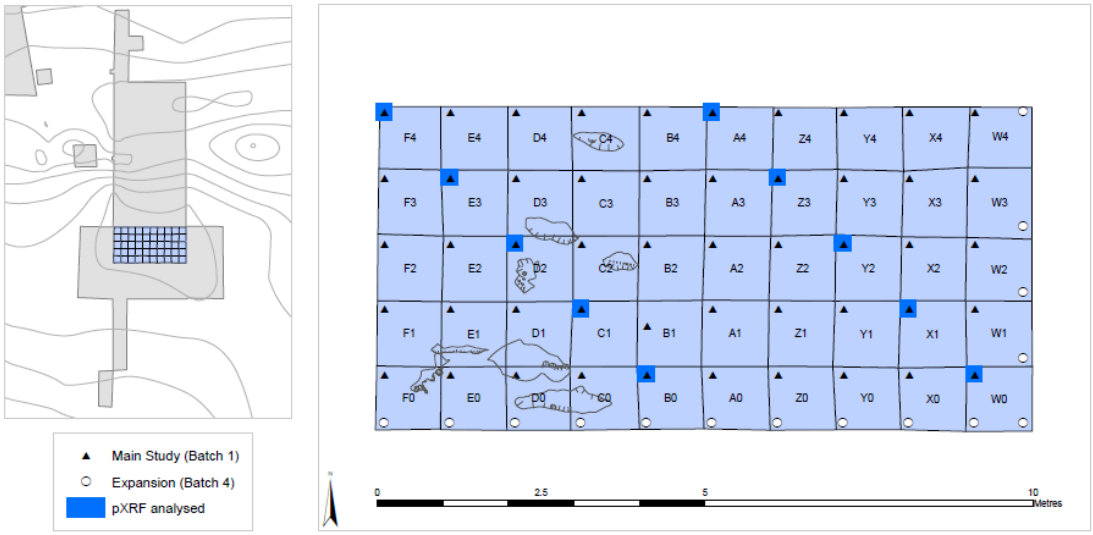

Figure 87. Samples analysed from trench 4, labels denoting grid square and with location points symbolised by submission batch (triangle for batch 1 ICP-AES, circle for expansion batch 2 ICP-AES, blue for samples use for the basic assessment and analysed by pXRF). The plans of potential features are also shown (at the western end of the trench)

Trench 4 was the main dryland trench excavated in 2012. Samples were taken in trench 4, as described in the methodology chapter and shown in Figure 87, and submitted as ICP-AES batches 1 and 4. The samples were taken systematically across the trench regardless of whether they were from within a potential feature (also displayed in Figure 87). ICP-AES batch 1 (submitted in 2014) consisted of the 50 samples taken from the northwesternmost sample on the 0.25 m^2 grid across each metre grid square. A further 15 samples from were analysed as part of ICP-AES batch 4 (submitted in 2016) which were aimed to be an expansion on the previous samples and consisted of the southwestern most sample from

the grid squares running along the southern edge of the trench (row 0), and the southeasternmost sample from the grid squares running along the eastern edge of the trench (column W). In addition, the two corner samples from W0 and W4 were taken. This was done so that samples from all four edges and corners of the trench were included. This meant that the outermost metre grid squares along the south and east edges had two samples from them analysed and the southeastern corner grid square (W0) had three samples from it analysed. W4, the northeasternmost corner square, should also have had three samples analysed but only two were viable (the ones from its northeastern and northwestern corners). As shall be seen, the expansion was not entirely successful as it seems there was a systematic methodological difference that impacted the results from the two batches, making them incomparable (despite being the same methodology implemented by the same commercial laboratory). Field pXRF was not available at this stage, but analysis by laboratory pXRF was conducted on 10 sample subset (highlighted in Figure 87) for comparison purposes as well, from the same samples the general geochemical characterisation was conducted.

6.4.1 Trench 4 Descriptive and Exploratory Statistics

The following results tables show the descriptive statistics for all the elements as measured by ICP-AES and pXRF, sorted by descending mean value. The statistics are calculated based on successful readings, and does not include substitution for those below the limits of detection so the descriptive statistics are entirely based on detected results. However, one thing to note is that on the values appear to have been rounded by ALS Chemex to different degrees. This is seemingly because the resolution of the measurements for certain elements is not as high as for other elements and this therefore impacts the precision of the technique for those elements.

Table 39, Table 40 and Table 41 detail the number of valid cases (N), range, maximum and minimum values for all elements that had at least one detected result and the mean, median, mode (or denoted if multimodal), standard deviation and coefficient of variance where appropriate for the ICP-AES results batches 1 and 2 and the lab pXRF results respectively.

Table 39. Descriptive statistics including the number of valid readings (N) and the mean, median, standard deviation, range and maximum and minimum values in ppm from ICP-AES Batch 1 (main trench 4 results). a. Multiple modes exist. The smallest value is shown

Batch 1 (main tr. 4)	N	Missing	Mean	Std. Error of Mean	Median	Mode	Std. Deviation	Coefficient of Variance	Variance	Skewness	Kurtosis	Range	Minimum	Maximum	25th percentile	50th percentile	75th percentile
Fe_ppm	50	0	22176	250.95	22150	20200.00[a]	1774.51	8%	3148902	0.21	0.1	8450	17650	26100	20775	22150	23225
Ca_ppm	50	0	9544	234.73	9700	9700.00[a]	1659.78	17%	2754861	-0.13	0.62	8500	5000	13500	8425	9700	10550
Al_ppm	50	0	8848	70.07	8900	8500	495.49	6%	245506.1	-0.1	0.96	2800	7400	10200	8500	8900	9200
Mg_ppm	50	0	1473	18.69	1500	1400	132.18	9%	17470.41	-0.03	0.44	700	1100	1800	1400	1500	1600
S_ppm	50	0	827	24.21	800	800	171.19	21%	29307.14	-0.33	0.12	800	400	1200	700	800	1000
P_ppm	50	0	558	25.64	510	500	181.34	32%	32882.65	2.05	5.58	940	320	1260	447.5	510	612.5
Ba_ppm	50	0	355.3	5.78	350	350	40.88	12%	1670.83	-0.06	-0.25	190	250	440	323.75	350	390
K_ppm	50	0	204	2.8	200	200	19.79	10%	391.84	4.84	22.33	100	200	300	200	200	200
Mn_ppm	50	0	158.94	3.86	159	137.00[a]	27.29	17%	744.9	-0.15	-0.76	109	101	210	138.5	159	182.5
Ti_ppm	50	0	120	5.71	100	100	40.41	34%	1632.65	1.55	0.41	100	100	200	100	100	100
Na_ppm	50	0	100	0	100	100	0	0%	0			0	100	100	100	100	100
Zn_ppm	50	0	39.56	1.21	38	35	8.55	22%	73.03	1.32	2.75	44.5	24.5	69	34	38	43.63
V_ppm	50	0	38.96	0.34	39	40	2.38	6%	5.65	-0.05	0.4	12.5	32.5	45	37	39	41
Sr_ppm	50	0	30.35	0.7	31	26	4.93	16%	24.26	-0.21	0.31	24	17	41	26.75	31	33.25
Pb_ppm	50	0	25.96	0.51	26	24.00[a]	3.62	14%	13.09	0.78	2.34	20	19	39	23.88	26	28
Cr_ppm	50	0	18.71	0.16	19	19	1.14	6%	1.31	-0.48	1.17	6	15	21	18	19	19
Ni_ppm	50	0	16.73	0.2	17	17	1.44	9%	2.08	0.21	-0.26	7	13.5	20.5	15.75	17	18
B_ppm	32	18	10.94	0.94	10	10	5.3	48%	28.13	5.66	32	30	10	40	10	10	10
As_ppm	50	0	10.87	0.21	11	10	1.49	14%	2.21	-0.17	-0.29	7	7	14	10	11	12

Batch 1 (main tr. 4)	N	Missing	Mean	Std. Error of Mean	Median	Mode	Std. Deviation	Coefficient of Variance	Variance	Skewness	Kurtosis	Range	Minimum	Maximum	25th percentile	50th percentile	75th percentile
La_ppm	50	0	10.2	0.2	10	10	1.41	14%	2	7.07	50	10	10	20	10	10	10
Cu_ppm	50	0	8.71	0.35	8	7	2.5	29%	6.25	1.32	1.88	12	5	17	7	8	10
Co_ppm	50	0	5.39	0.08	5	5	0.57	11%	0.32	-0.25	-0.71	2	4	6	5	5	6
Sc_ppm	50	0	2.98	0.02	3	3	0.14	5%	0.02	-7.07	50	1	2	3	3	3	3
Sb_ppm	5	45	2.2	0.2	2	2	0.45	20%	0.2	2.24	5	1	2	3	2	2	2.5
Mo_ppm	50	0	1.26	0.06	1	1	0.44	35%	0.2	1.13	-0.76	1	1	2	1	1	2
Hg_ppm	2	48	1	0	1	1	0	0%	0			0	1	1	1	1	1
Be_ppm	50	0	0.75	0.01	0.78	.700[a]	0.06	8%	0	0.23	-1.03	0.25	0.65	0.9	0.7	0.78	0.8
Ag_ppm	22	28	0.22	0.01	0.2	0.2	0.04	18%	0	1.77	1.25	0.1	0.2	0.3	0.2	0.2	0.2
Bi_ppm	0	50															
Cd_ppm	0	50															
Ga_ppm	0	50															
Th_ppm	0	50															
Tl_ppm	0	50															
U_ppm	0	50															
W_ppm	0	50															

Table 40. Descriptive statistics including the number of valid readings (N) and the mean, median, standard deviation, range and maximum and minimum values in ppm from ICP-AES Batch 4 (trench 4 expansion). a. Multiple modes exist. The smallest value is shown

Batch 4 (tr. 4 exp.)	N	Missing	Mean	Std. Error of Mean	Median	Mode	Std. Deviation	Coefficient of variance	Variance	Skewness	Kurtosis	Range	Minimum	Maximum	25th percentile	50th percentile	75th percentile
Fe_ppm	15	0	16420	499.92	16300	15500	1936.2	12%	3748857	0.1	-0.79	6200	13200	19400	15300	16300	17600
Ca_ppm	15	0	7416.67	311.21	7400	6800.00[a]	1205.3	16%	1452738	0.53	2.32	5350	5050	10400	6800	7400	8100
Al_ppm	15	0	7350	238.4	7100	6600.00[a]	923.31	13%	852500	0.59	-0.08	3400	5800	9200	6600	7100	7800
Mg_ppm	15	0	1130	49.23	1100	1100	190.68	17%	36357.14	0.27	-0.27	700	800	1500	1000	1100	1300
S_ppm	15	0	780	48.99	800	800	189.74	24%	36000	-0.18	0.43	700	400	1100	700	800	900
P_ppm	15	0	470.67	46.37	460	460	179.58	38%	32249.52	0.92	0.04	580	230	810	350	460	500
Ba_ppm	15	0	256	7.48	250	250	28.98	11%	840	0.66	0.54	110	210	320	240	250	270
K_ppm	15	0	180	10.69	200	200	41.4	23%	1714.29	-1.67	0.9	100	100	200	200	200	200
Mn_ppm	15	0	131.93	7.49	134	78.00[a]	29.02	22%	842.35	0.06	0.41	114	78	192	112	134	149
Ti_ppm	15	0	100	0	100	100	0	0%	0			0	100	100	100	100	100
Na_ppm	0	15															
Zn_ppm	15	0	39.1	3.29	37	34.00[a]	12.76	33%	162.72	0.68	-0.03	43.5	22.5	66	27	37	49
V_ppm	15	0	29.43	0.98	29	31	3.8	13%	14.46	0.21	-0.14	14	23	37	27	29	31
Sr_ppm	15	0	23.03	0.84	23	24.00[a]	3.24	14%	10.52	0.41	2.39	14.5	16.5	31	21	23	25
Pb_ppm	15	0	22.93	1.56	22	17.00[a]	6.03	26%	36.35	0.65	0.37	23	13	36	19	22	28
Cr_ppm	15	0	16.3	0.55	16	15.0[a]	2.14	13%	4.56	0.2	-0.99	7	13	20	15	16	18
Ni_ppm	15	0	12.77	0.5	13	13	1.94	15%	3.75	0.37	0.2	7	10	17	11	13	14
B_ppm	0	15															
As_ppm	15	0	7.87	0.4	8	6.00[a]	1.55	20%	2.41	0.39	-0.52	5	6	11	6	8	9
La_ppm	15	0	10	0	10	10	0	0%	0			0	10	10	10	10	10

Batch 4 (tr. 4 exp.)	N	Missing	Mean	Std. Error of Mean	Median	Mode	Std. Deviation	Coefficient of variance	Variance	Skewness	Kurtosis	Range	Minimum	Maximum	25th percentile	50th percentile	75th percentile
Cu_ppm	15	0	8.13	0.79	7	7	3.04	37%	9.27	0.47	-0.67	10	4	14	6	7	11
Co_ppm	15	0	4.4	0.13	4	4	0.51	12%	0.26	0.46	-2.09	1	4	5	4	4	5
Sc_ppm	15	0	2.13	0.09	2	2	0.35	16%	0.12	2.4	4.35	1	2	3	2	2	2
Sb_ppm	5	10	2.2	0.2	2	2	0.45	20%	0.2	2.24	5	1	2	3	2	2	2.5
Mo_ppm	15	0	1	0	1	1	0	0%	0			0	1	1	1	1	1
Hg_ppm	3	12	1	0	1	1	0	0%	0			0	1	1	1	1	1
Be_ppm	14	1	0.59	0.03	0.6	0.5	0.09	15%	0.01	0.95	0.34	0.3	0.5	0.8	0.5	0.6	0.63
Ag_ppm	1	14	0.2		0.2	0.2		0%				0	0.2	0.2	0.2	0.2	0.2
Bi_ppm	0	15															
Cd_ppm	0	15															
Ga_ppm	0	15															
Th_ppm	0	15															
Tl_ppm	0	15															
U_ppm	0	15															
W_ppm	0	15															

Table 41. Number of valid readings (N), the mean, median, standard deviation, coefficient of variance, range, maximum and minimum values from lab pXRF analyses on subsample of 10 from trench 4 (units: ppm, where not dimensionless). a. Multiple modes exist. The smallest value is shown

	N (Valid)	Range	Minimum	Maximum	Mean	Median	Mode	Std. Deviation	Coefficient of variance	Skewness	Kurtosis
Si	10	46567.2	199915	246482	222076	219938	199915.08[a]	16451.9	7%	0.24	-1.51
Al	10	10085.1	44273.6	54358.7	48037.3	47951.8	44273.64[a]	2806.21	6%	1.09	2.37
Fe	10	11600.8	37475.6	49076.3	42916.3	43132.9	37475.57[a]	4094.91	10%	0.03	-1.61
Ca	10	5288.01	7304.09	12592.1	9896.16	9881.9	7304.10[a]	1864.2	19%	0.02	-0.97
K	10	1194.36	3922.93	5117.29	4453.01	4396.2	3922.93[a]	343.99	8%	0.58	0.37
Ti	10	398.71	3758.26	4156.97	3904.65	3854.94	3758.26[a]	122.89	3%	0.98	0.41
S	10	799.49	433.4	1232.88	834.9	763.94	433.40[a]	260.39	31%	0.16	-1.02
Zr	10	88.8	399.18	487.98	434.54	433.05	399.18[a]	30.07	7%	0.41	-0.93
Mn	10	96.12	198.38	294.5	252.47	259.26	198.38[a]	32.32	13%	-0.34	-1.32
V	10	43.24	226.64	269.88	244.97	244.98	226.64[a]	12.13	5%	0.42	1.43
Cr	10	54.8	58.11	112.91	81.45	76.69	58.11[a]	16.29	20%	0.71	0.25
Sr	10	15.76	74.47	90.24	80.8	79.71	74.47[a]	5.32	7%	0.47	-1
Zn	10	29.4	39.99	69.39	55.12	56.92	39.99[a]	9.2	17%	-0.09	-0.65
Ni	10	7.54	30.94	38.47	33.76	33.31	30.94[a]	2.28	7%	0.89	0.54
Pb	10	9.35	24	33.35	29.32	30.96	24.00[a]	3.46	12%	-0.65	-1.39
Rb	10	3.53	24.65	28.17	26.44	26.45	24.65[a]	1.23	5%	-0.15	-1.29
Ta	10	4.26	19.46	23.72	21.78	22.12	19.46[a]	1.49	7%	-0.38	-1.08
Y	10	5.77	16.03	21.8	19.03	18.96	16.03[a]	1.97	10%	-0.21	-0.76
As	10	5.25	8.51	13.76	11.26	11.54	8.51[a]	1.68	15%	-0.19	-1.03
Cu	2	0.89	10.19	11.08	10.64	10.64	10[a]	0.63	6%		
Bi	8	4.62	8.55	13.17	9.87	9.39	9[a]	1.46	15%	1.96	4.36
Nb	10	2.11	6.53	8.64	7.14	6.88	6.53[a]	0.62	9%	1.9	3.57

	N (Valid)	Range	Minimum	Maximum	Mean	Median	Mode	Std. Deviation	Coefficient of variance	Skewness	Kurtosis
Hg	4	0.68	6.19	6.87	6.58	6.63	6[a]	0.29	4%	-0.98	1.7
U	2	0.3	4.9	5.2	5.05	5.05	5[a]	0.21	4%		
Ag	0										
Cd	0										
Cl	0										
Co	0										
Mg	0										
Mo	0										
P	0										
Sb	0										
Se	0										
Sn	0										
Th	0										
W	0										
LE	*10*	*42150.7*	*643308*	*685459*	*666580*	*671258*	*643307.91[a]*	*13006.3*		*-0.6*	*-0.3*

The *N* value tallies the number of cases (i.e. values) the statistics are calculated from, in this case therefore this is the number of readings for an element that were above the limit of detection out of 50 for batch 1 or 15 for batch 4. In the ICP-AES results, bismuth, cadmium, gallium, thorium, thallium, uranium, and tungsten were not detected in any samples in either batch. In the smaller set of batch 4 samples, boron and sodium were also undetected. Boron had been detected in 32 of the batch 1 samples (albeit at levels ranging between only 10 to 40 ppm), and sodium had been detected in all 50 (all measuring exactly 100 ppm, however, suggesting that this value had been rounded to this value by ALS Chemex). This was a clear mismatch between the batches and was unlikely to be due to actual differences in the soil considering the proximity of these samples to other samples. This suggested there was potentially a discrepancy in digestion method or some other aspect of the method for batch 4 that meant the samples were not as effectively dissolved in the aqua regia before analysis and therefore was a sign the batches may not be comparable. Antimony, mercury and silver are only read in a subset of the samples in both batches.

The mean is essentially a hypothetical model, if a simple one, created to summarise data. Based on the means from the ICP-AES, iron is the only major element (using the same definition of major as utilised previously, so > 10,000 ppm) from both datasets. Calcium, iron and magnesium are minor (1000 - 10,000 ppm) contributors. Sulfur, phosphorus, barium, potassium, manganese, and titanium have means between 100 - 1000 ppm in both batches, joined by sodium in batch 1 (undetected in batch 4), so are trace contributors. However, it should be noted that as all batch 1 samples were recorded as having a likely rounded value of 100 ppm exactly, the mean is simply 100 ppm. Zinc, vanadium, strontium, lead, chromium, nickel, arsenic, lanthanum, copper, cobalt, scandium, antimony, molybdenum, mercury, beryllium, and silver have mean values of <100 ppm based on the measurements above the LOD in both batches, joined by boron in batch 1 and these are therefore also trace contributors but with the lowest values (IUPAC trace classification).

Figure 88 (A-E) collates the means of all elements obtained from ICP-AES and lab-based pXRF in trench 4. The means of elemental readings from ICP-AES batch 4 are lower than those for the same elements in batch 1 for the major and minor elements, and for most of the trace elements as well (a few are equal). This suggests that a systematic methodological difference has caused the readings to be lower rather than them being different due to a genuine difference in the soils. The difference between the means is more pronounced the greater the absolute values are. For example, the difference between the mean values for iron from batch 1 to batch 4 is -5756 ppm, whereas for arsenic the difference is only -3.003 ppm. However, while the trace element values and means are less affected in absolute value differences, those differences can be just as significant proportionately given the more

limited values and ranges of those elements initially. As such, this again suggests that the batches should not be directly compared to each other on absolute values.

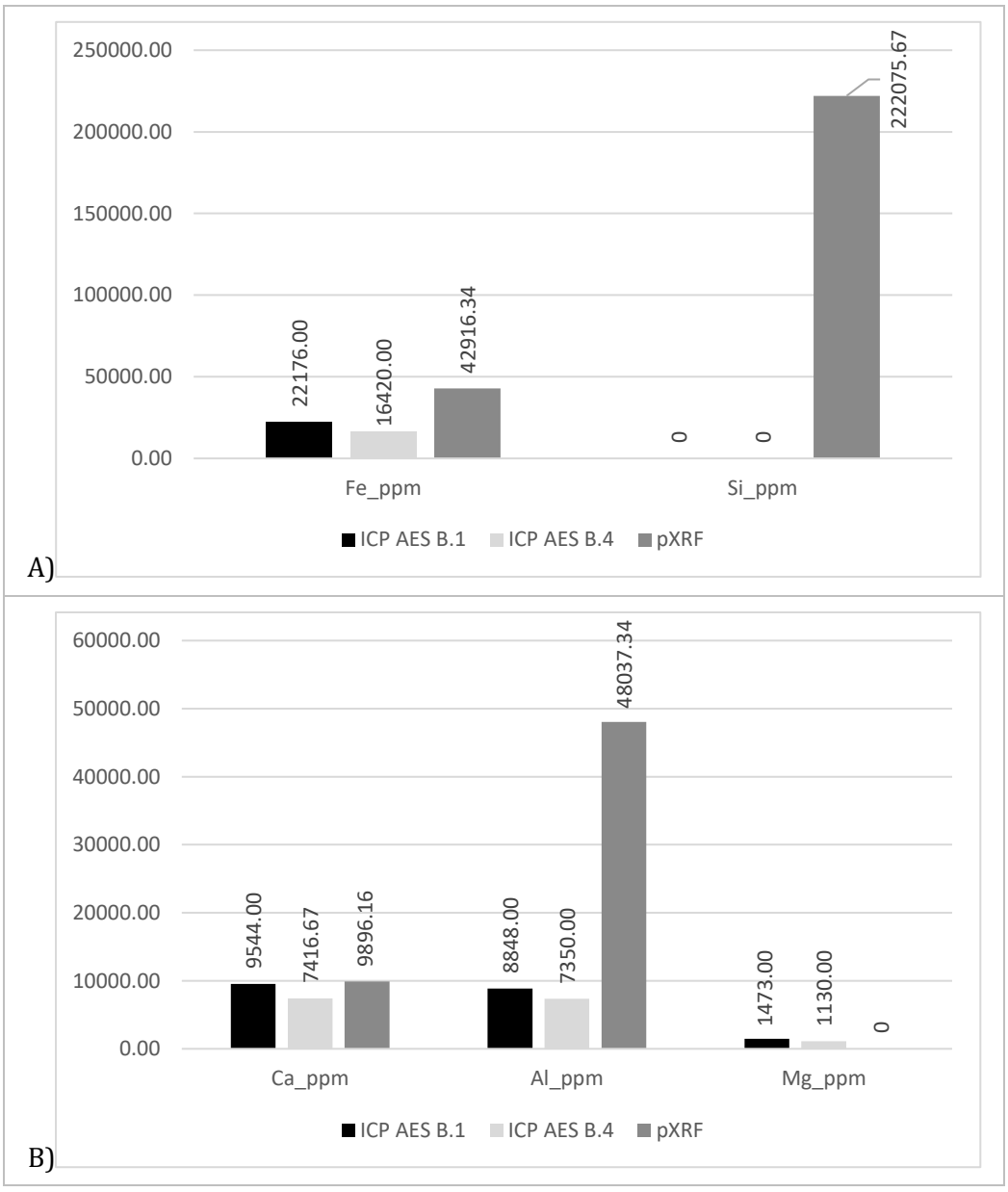

C)

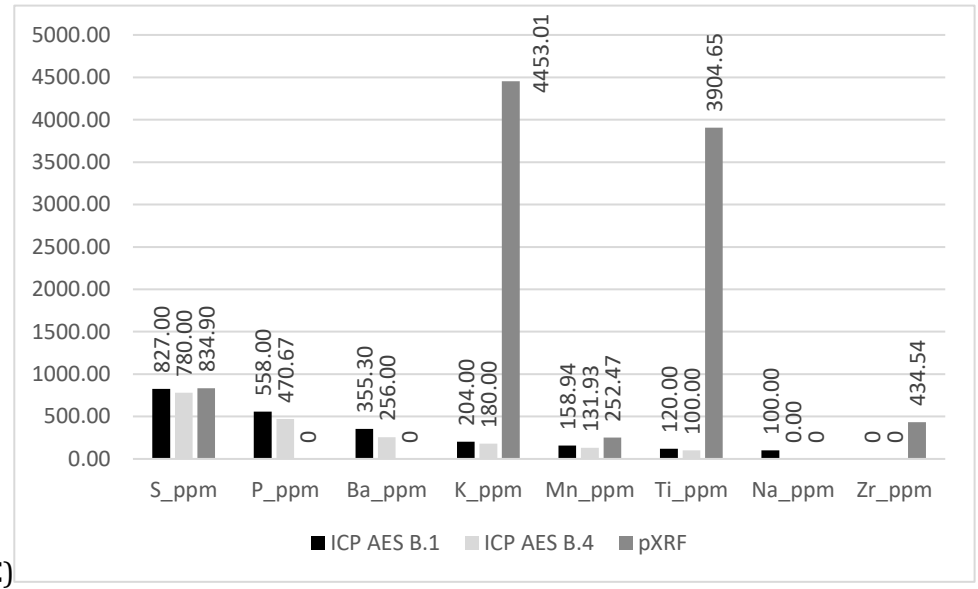
5000.00
4500.00
4000.00
3500.00
3000.00
2500.00
2000.00
1500.00
1000.00
500.00
0.00
827.00
780.00
834.90
558.00
470.67
0
355.30
256.00
0
204.00
180.00
4453.01
158.94
131.93
252.47
120.00
100.00
3904.65
100.00
0.00
0
0
0
434.54
S_ppm
P_ppm
Ba_ppm
K_ppm
Mn_ppm
Ti_ppm
Na_ppm
Zr_ppm
ICP AES B.1
ICP AES B.4
pXRF

D)

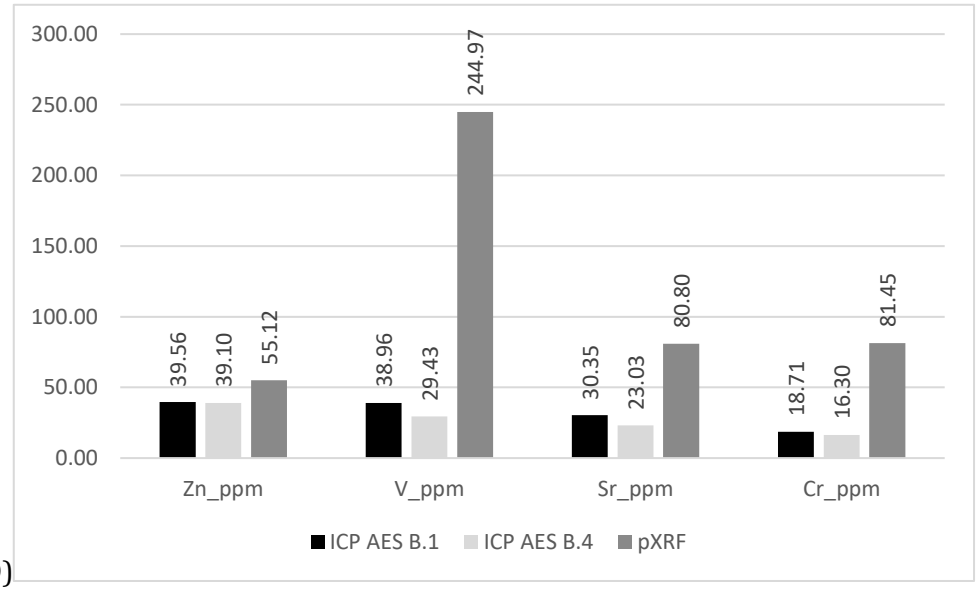
300.00
250.00
200.00
150.00
100.00
50.00
0.00
39.56
39.10
55.12
38.96
29.43
244.97
30.35
23.03
80.80
18.71
16.30
81.45
Zn_ppm
V_ppm
Sr_ppm
Cr_ppm
ICP AES B.1
ICP AES B.4
pXRF

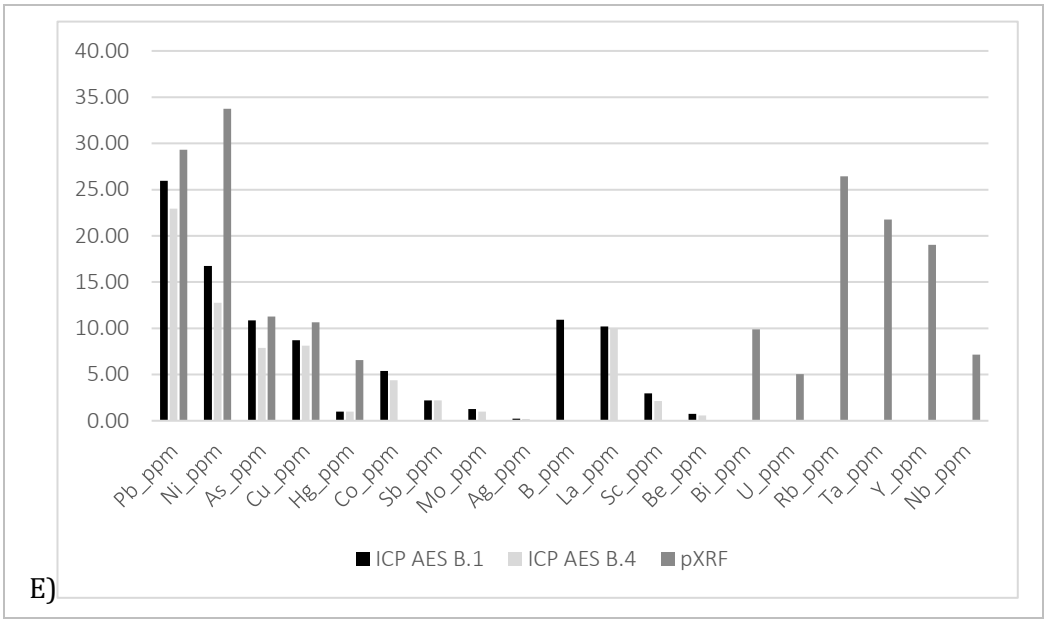

E)

Figure 88 A-E. Comparison of the means for each element as read by ICP-AES (batches 1 and 4) and pXRF in the trench 4 samples. All values in ppm

When comparing the results from ICP-AES against those from pXRF on lab prepared samples, the suggested contribution of different elements to the samples is broadly similar but has nuanced differences when considering the details. Many elements remain in the same classification (as major, minor, trace, IUPAC trace) based on the means, but many also shift into the next classification up or down. Two elements change classification more significantly: Magnesium and phosphorus. Magnesium was classified as a minor contributor with comfortably over 1000 ppm for both ICP-AES means, however the pXRF analysis was unable to detect the element despite theoretically being setup to do so (it was below the LOD). The estimated pXRF LOD for magnesium was well above these values, however, ranging between 13865 and 16183 ppm. Similarly, phosphorus readings were 471 - 558 ppm on average in the ICP-AES batches, classifying them as a minor contributor, and were also recorded as below LOD, estimated ranging between 555 and 615 ppm, by pXRF. As such, from the estimated LODs, this seems to be simply that for these specific elements, the machine is unable to read at these concentrations with this setup.

Basing classification on the lab pXRF means, two major contributors are silicon (which is not measured by ICP-AES) and iron (which agrees with the ICP-AES result). The iron values are different however, with the pXRF mean value being much higher than the ICP-AES mean. Aluminium is also a major contributor as based on mean pXRF, and in fact has a higher mean than iron, as opposed to a minor contributor as suggested by the ICP-AES means.

Calcium remains classified as a minor contributor and has a similar mean value to the batch 1 mean. Potassium and titanium, in contrast, have much higher values obtained from the pXRF averages, with pXRF means 21 and 32 times higher respectively than the greater of

the ICP-AES means obtained for those elements. This bumps those results up from being classified as trace to minor contributors.

Of the other elements classified as trace contributors based on the means of the ICP-AES results, sulfur and manganese remained in the same classification based on the pXRF means. The sulfur pXRF mean was similar to the batch 1 ICP-AES mean, though the manganese result was slightly higher. Barium and sodium were not available to be measured in this pXRF setup. The pXRF mean for Zirconium suggested it was a trace contributor, and this element could not be measured by ICP-AES. Vanadium measured out as being an IUPAC trace element with means of 29 and 40 ppm by ICP-AES, but the pXRF mean was 245 ppm, which would classify this as a more significant trace element as well.

Aside from vanadium, the elements classified as IUPAC trace elements based on the ICP-AES means were classified the same based on pXRF results where the results were available or detected. This includes zinc, strontium, lead, chromium, nickel, arsenic, copper, and mercury. All means from the pXRF were a little higher than the means by ICP-AES though.

Cobalt, antimony, molybdenum, and silver were recorded as being below the limits of detection for pXRF and the readings obtained from ICP-AES were indeed well below the estimated LODs for pXRF detection. Means of 5 ppm for uranium and 10 ppm for bismuth were obtained by pXRF, and were recorded as below the LOD for ICP-AES.

Boron, lanthanum, scandium, and beryllium are not available for measurement in this pXRF setup so could not be compared to the IUPAC trace classified ICP-AES values. Similarly, rubidium, tantalum, yttrium, and niobium were all measured as IUPAC trace elements by pXRF but were not available by ICP-AES for comparison. Cadmium, thorium, and tungsten were recorded as below the limits of detection for both methods and were therefore at least consistent. Chlorine, selenium, tin, gallium, and thallium were either not available or below the limits of detection for either method.

The variance is the sum of the squared errors divided by the number of observations minus 1, which in practical terms gives us the average error between mean and the observed values (Field 2009, 6). The standard deviation is the square root of the variance, to convert the variance into the same units as the original measure (here, parts per million). As such, the standard deviation can be calculated to provide checks for how well the mean represents the data. The lower the standard deviation, the closer data points are to the mean. In terms of the soils on site, this can suggest whether there are going to be significant variances from the mean in the measurements across the trench of a given element and also if there are possibly going to be notable 'hot spots' (or cold spots). However, while we are dealing with measurements of elements in the same units, the mean values of the different elements vary quite significantly from each other. The coefficient of variation (COV, the ratio

of the standard deviation to the mean) can provide a comparable measure of dispersion (because it is dimensionless) that takes into account that the means are different, which standard deviation cannot do.

Sodium and mercury in ICP-AES batch 1 and titanium, mercury, molybdenum, lanthanum in batch 4 had standard deviations of 0 ppm and COVs of 0% as all successful measurements were the same value (as they had been rounded up). This was not an issue in the pXRF results, where values were either below the LOD completely or not rounded up to such a degree. The batch 4 results had either 0 or 1 successful readings of silver, boron, and sodium and therefore a standard deviation and COV could not be calculated and these entries are blank.

The elements with the greatest standard deviations, i.e. with values clustering less closely around the mean, are those with correspondingly greater values and ranges between minimum and maximum values. However, the COV illustrates that when taking into account the difference in means, there is not as clear a trend. In ICP-AES batches 1 and 4 and the lab pXRF on 10 samples, the highest standard deviations were for iron, calcium and aluminium supplemented with silicon where it could be measured in the pXRF analyses. In the ICP-AES results, magnesium, sulfur and phosphorus all have standard deviations greater than 100 as well, again being some of the most abundant elements. However, the COVs for the batch 1 readings were only greater than 20% for sulfur (21%), zinc (22%), copper (29%), phosphorus (32%), titanium (34%), molybdenum (35%), and boron (48%), which suggests these elements were more notably disperse in the trench readings than iron (8%), calcium (17%) or magnesium (9%). For boron, only 32 of the 50 samples yielded values above the limit of detection, however. In batch 4, the COVs were greater than 20% for manganese (22%), potassium (23%), sulfur (again, 24%), lead (26%), zinc (again, 33%), copper (again, 37%), and phosphorus (again, 38%). Given the repeat between batches, this could suggest that sulfur, zinc, copper and phosphorus are particularly variable across the site.

In contrast to the trend with the mean values, the standard deviations are generally higher in ICP-AES batch 4 indicating the means here are not as good a model of the data as for batch 1, which is unsurprising given the smaller sample size in the former. Similarly, the standard deviations calculated for the even smaller pXRF sample set were generally higher still. Scores clustering less tightly around the mean (and the higher standard deviations) suggest the mean is a less accurate model of the data when discussing consistently greater contributors to samples. As this generally affects more major contributors, it seems that this may reflect a greater range of values produced when their relative contribution is higher rather than necessarily reflecting any hot spots / cold spots influencing the results at this stage. Boron and copper seem to be the only elements with anomalously high

standard deviations relative to the other elements with similar absolute values to them. This supports the alternative trend in the COVs. Boron could be due to the smaller number of successful readings, as mentioned above. Copper however is not immediately explainable and therefore may feature some significant hot or cold spots causing greater variance in the dataset.

This general trend is followed in the pXRF results as well, with the major contributors (silicon, iron, aluminium and calcium) having the greatest standard deviations. The standard deviations tend to be much larger for the pXRF values than their ICP-AES counterparts, especially so for the more significant contributors. This is likely at least partly caused by the very small sample size here as much as genuine significant variability in those elements. However, notably, sulfur appeared again as the only element with a COV greater than 20% (at 31%) which again indicates a potential for hot or cold spots in this element's spatial patterning.

The shape of the frequency distribution for the readings of each element needed to be considered through further descriptive statistics in order to select the most appropriate analytical tools. This is because the shape of the distribution will impact the probability curve for that distribution and therefore any interpolations based on the dataset. The pXRF results were purely taken for comparative purposes and are too few to interpolate between or subject to clustering analyses so they are not discussed in these terms. Histograms of the ICP-AES data are provided in Appendix Six and it can clearly be seen that even with the major contributors, with all 65 samples having successful readings, none of the results are normally distributed with several being multimodal (Fe, Ca, Mn, Pb, Be from batch 1; Ca, Al, Mn, Zn, Sr, Pb, Cr, As from batch 2). The major and minor elements sometimes approach normality but are still not certainly close to normal from basic visual inspection. The batch 4 histograms are less close to normal than batch 1 but this is again likely due to the small sample size.

In addition to visually examining the histograms, if a dataset is closer to an ideal normally distributed model then the mean and median will be more similar. In these data, the differences tend to be greater as the absolute values get larger. Titanium in batch 1 and potassium in batch 4 are noticeable as having slightly greater differences between the median and mean than the other elements with similar values, but not hugely so. Readings are recorded as being 100 or 200 ppm for titanium and 100, 200 or 300 ppm for potassium which suggests it is the precision issue causing the rounding of values arising again.

More formal measures of non-normality are available. Skewness, an assessment of the symmetricity of the distribution on either side of the mean, and kurtosis, which assesses the width of the peak relative to the distribution of values in the peak, shoulders or tails of the

curve, can be examined. Table 42 provides the results of the evaluation of skewness, kurtosis, the associated standard errors for those values, and the division of those values by their standard errors which allows a 'rule-of-thumb' assessment of whether the values are notably different from normality (if +/- 1.96 as per the method outlined by Rose et al. (2015). Skewness and kurtosis could not be calculated for sodium and mercury in either batch, nor titanium, boron, lanthanum, molybdenum, or silver in batch 4 alone. This is either due to the low number or entire lack of successful readings, or the lack of variability between readings or the rounding of readings. The rule of thumb illustrated some skewness and kurtosis was extreme where they had been successfully calculated, with the value divided by the standard error being greater than +/- 10 for both values for potassium, boron, lanthanum, and scandium in batch 1.

Skewness (asymmetry) is zero in a normal distribution. Skew was notable for phosphorus, potassium, titanium, zinc, lead, boron, lanthanum, copper, antimony, molybdenum, and silver in batch 1, and for scandium and antimony in batch 4. The lanthanum and scandium values were exceptionally high. This indicates the results for all these elements are positively skewed which indicates (counterintuitively) most readings are to the lower end of the full range of elemental values. This suggests there may be some statistically significant hot spots or high outliers. Skewness was -7 in scandium in batch 1 and -1.67 for potassium in batch 4 (both with the rule of thumb calculation output being < -1.96), suggesting a non-normal, significant negative skew with a few low readings but most scores falling high within the entire range of the elemental values, and therefore suggesting potential cold spots or outliers. However, there were only 5 successful readings of antimony and such a small sample size is not well suited to considering in terms of distribution shape as there is simply not enough data. Silver and boron had 22 and 32 readings respectively so were less susceptible but, relative to having the full set of 50 readings, these were not as good a sample size as the other elements.

Kurtosis (tailedness) indicates whether there are more scores clustering in the tails or the peak of the distributions. In SPSS, the mathematical definition of kurtosis is what is referred to as the "excess kurtosis", which means it is transformed so that kurtosis in a normal distribution measured on SPSS would measure as 0 (while straightforward kurtosis for a standard normal distribution technically falls at 3). Phosphorus, potassium, zinc, lead, boron, lanthanum, copper, scandium, and antimony in batch 1 and calcium, strontium, scandium and antimony in batch 4 all showed significant positive kurtosis. This indicates those data distributions have sharper peaks and heavier tails than normally distributed data.

Where data is not normally distributed or significantly varies from the normal distribution, then it would need to be transformed, detrended or declustered before applying any advanced interpolation techniques. However, it was decided it would be preferable to keep as close to the original dataset as possible and that methodology applied to all the data regardless of whether close to normal or otherwise should be consistent. As such, it was decided that interpolation would be a less appropriate method for visualising the data and other techniques would be explored as described in the chapter five. The results are presented in the next few sections.

Table 42. Statistics relating to skewness and kurtosis of ICP-AES results from trench 4

Batch:	1						4					
Tr 4 ICP-AES	Skewness	Std. Error of Skewness	Skew/Std .Error of Skew	Kurtosis	Std. Error of Kurtosis	Kurtosis/ Std. Error of Kurt.	Skewness	Std. Error of Skewness	Skew/Std .Error of Skew	Kurtosis	Std. Error of Kurtosis	Kurtosis/ Std. Error of Kurt.
Fe_ppm	0.21	0.34	0.62	0.10	0.66	0.16	0.10	0.58	0.18	-0.79	1.12	-0.71
Ca_ppm	-0.13	0.34	-0.38	0.62	0.66	0.93	0.53	0.58	0.92	2.32	1.12	2.07
Al_ppm	-0.10	0.34	-0.30	0.96	0.66	1.45	0.59	0.58	1.01	-0.08	1.12	-0.07
Mg_ppm	-0.03	0.34	-0.08	0.44	0.66	0.66	0.27	0.58	0.46	-0.27	1.12	-0.24
S_ppm	-0.33	0.34	-0.99	0.12	0.66	0.18	-0.18	0.58	-0.30	0.43	1.12	0.38
P_ppm	2.05	0.34	6.09	5.58	0.66	8.44	0.92	0.58	1.59	0.04	1.12	0.04
Ba_ppm	-0.06	0.34	-0.18	-0.25	0.66	-0.37	0.66	0.58	1.14	0.54	1.12	0.48
K_ppm	4.84	0.34	14.38	22.33	0.66	33.74	-1.67	0.58	-2.88	0.90	1.12	0.80
Mn_ppm	-0.15	0.34	-0.46	-0.76	0.66	-1.14	0.06	0.58	0.11	0.41	1.12	0.37
Ti_ppm	1.55	0.34	4.60	0.41	0.66	0.62		0.58	0.00		1.12	0.00
Na_ppm		0.34	0.00		0.66	0.00						
Zn_ppm	1.32	0.34	3.92	2.75	0.66	4.15	0.68	0.58	1.17	-0.03	1.12	-0.03
V_ppm	-0.05	0.34	-0.14	0.40	0.66	0.60	0.21	0.58	0.37	-0.14	1.12	-0.13
Sr_ppm	-0.21	0.34	-0.63	0.31	0.66	0.47	0.41	0.58	0.70	2.39	1.12	2.13
Pb_ppm	0.78	0.34	2.31	2.34	0.66	3.53	0.65	0.58	1.12	0.37	1.12	0.33
Cr_ppm	-0.48	0.34	-1.42	1.17	0.66	1.77	0.20	0.58	0.34	-0.99	1.12	-0.88
Ni_ppm	0.21	0.34	0.63	-0.26	0.66	-0.40	0.37	0.58	0.63	0.20	1.12	0.18
B_ppm	5.66	0.41	13.65	32.00	0.81	39.54						
As_ppm	-0.17	0.34	-0.50	-0.29	0.66	-0.44	0.39	0.58	0.67	-0.52	1.12	-0.46
La_ppm	7.07	0.34	21.01	50.00	0.66	75.54		0.58	0.00		1.12	0.00
Cu_ppm	1.32	0.34	3.91	1.88	0.66	2.85	0.47	0.58	0.81	-0.67	1.12	-0.60

Batch:	1						4					
Tr 4 ICP-AES	Skewness	Std. Error of Skewness	Skew/Std .Error of Skew	Kurtosis	Std. Error of Kurtosis	Kurtosis/ Std. Error of Kurt.	Skewness	Std. Error of Skewness	Skew/Std .Error of Skew	Kurtosis	Std. Error of Kurtosis	Kurtosis/ Std. Error of Kurt.
Co_ppm	-0.25	0.34	-0.75	-0.71	0.66	-1.07	0.46	0.58	0.78	-2.09	1.12	-1.87
Sc_ppm	-7.07	0.34	-21.01	50.00	0.66	75.54	2.40	0.58	4.15	4.35	1.12	3.88
Sb_ppm	2.24	0.91	2.45	5.00	2.00	2.50	2.24	0.91	2.45	5.00	2.00	2.50
Mo_ppm	1.13	0.34	3.35	-0.76	0.66	-1.15		0.58	0.00		1.12	0.00
Hg_ppm								1.22	0.00			
Be_ppm	0.23	0.34	0.68	-1.03	0.66	-1.56	0.95	0.60	1.59	0.34	1.15	0.29
Ag_ppm	1.77	0.49	3.61	1.25	0.95	1.31						

6.4.2 Spatial visualisation of Trench 4 elemental concentrations measured by ICP-AES

The basic plots are a straightforward visualisation (choropleth) of each point based on the reading for that element in parts per million (ppm). Elemental readings were grouped into 5 classes using Jenks Natural Breaks (see chapter five). The sample square was then symbolised by class, with red indicating higher values through to blue for lower values. Initially, the results from the combined ICP-AES batch data (from batches 1 and 4) were intended to be displayed on the same plot. However, it became clear that the systematic difference between the batches was masking the impact of any spatial patterning in the sample coverage from batch 1.

Figure 89 shows the results for aluminium levels in the soil samples from across the trench as both a combined dataset visualisation and just batch 1 visualised. As can be seen, when visualising the readings from batches 1 and 4 as if one dataset, the spatial patterning has different spots emphasised. As the batch 4 readings were lower on average than the batch 1 readings from the trench, as discussed above, this makes the higher values look more distinctly like hotspots and also masks the relative depletions in batch 1 when visualising. As such, it was decided to visualise the data only using the results from batch 1 which are guaranteed to be consistent with each other.

This result in itself is important as it suggests caution is advised, not just when comparing batches from the same site processed by the same commercial laboratory but even more so when comparing data from other sites processed by different methods and on different equipment. The discrepancy in the results may be from the slightly different preparation methods employed (with batch 1 being processed in house, the other batch being processed by ALS Chemex) but if anything it would be anticipated that the materials prepared in house at York might have been less well digested as a result of manual as opposed to mechanical processing producing less well pulverised fine fractions. However, the results suggest the opposite, with the higher readings indicating more thorough digestion of batch 1. This highlights the need for strict consistency and preferably sample submission in one complete batch where at all possible. As a result, the following plots (and statistical analyses after that) are only based on the results for batch 1. Regardless, there is a sample from every grid square in trench 4 so coverage is still good and a total of 50 samples allowed for a range of statistical analyses to be run on the data.

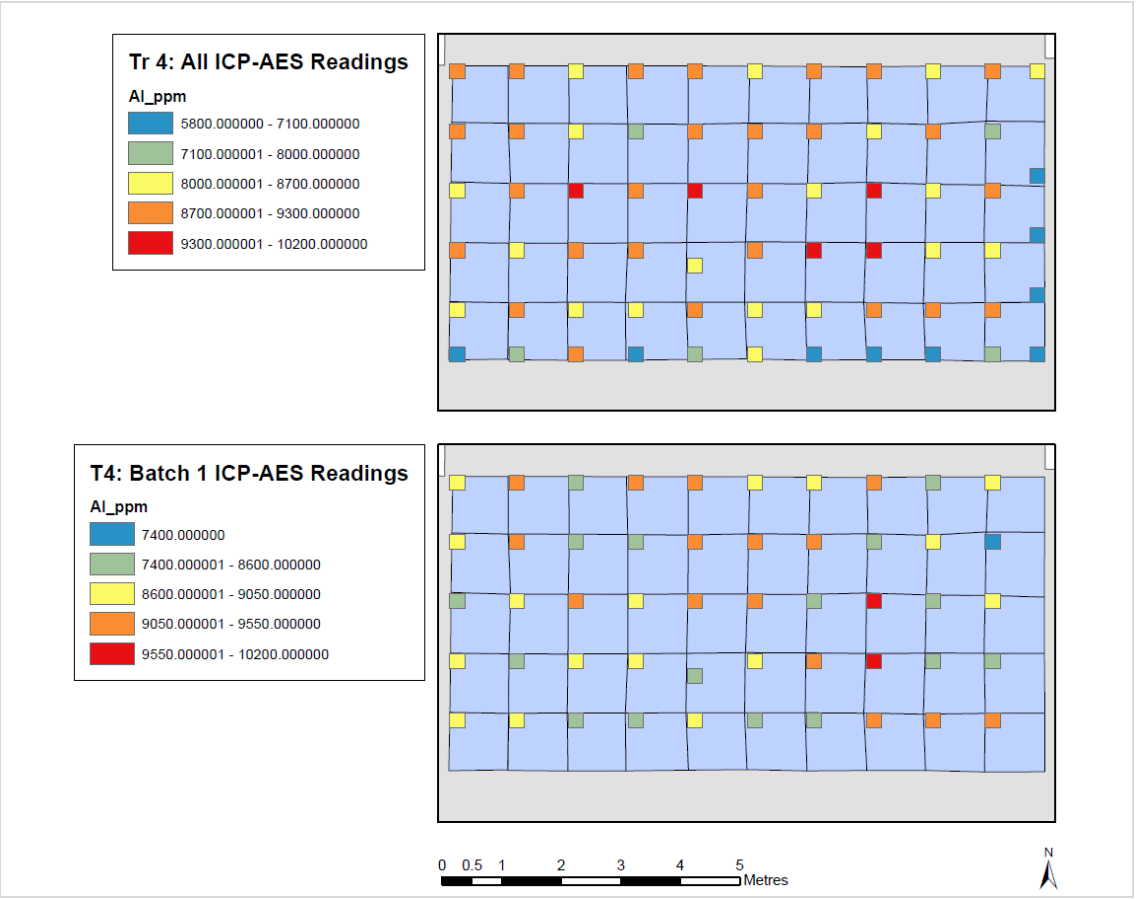

Figure 89. ICP-AES results from all samples in trench 4 (from batches 1 and 4), alongside the results from just batch 1. Visualised using Jenks natural breaks

In addition to the basic plots, a number of further spatial statistical analyses were conducted for each element. This allows a more nuanced, statistically-grounded assessment of any patterning identified from the basic plots. The Hot Spot Analysis (HSA) tool identifies areas where there are statistically significant clusters of similar values and the complementary Cluster-Outlier Analysis tool identifies areas where features and their neighbourhoods are high or low (hot spots or cold spots), and where high features are surrounded by low values or vice versa (outliers). The neighbourhood for these tools running on the VP12 ICP-AES dataset was set to including readings within a fixed distance band of 1.85 m, which would allow the inclusion of all of the immediately adjacent readings to a sample to be included (considering/comparing a minimum of 2 up to a maximum of 8 readings excluding the feature under study).

6.4.2.1 Iron, the major elemental contributor

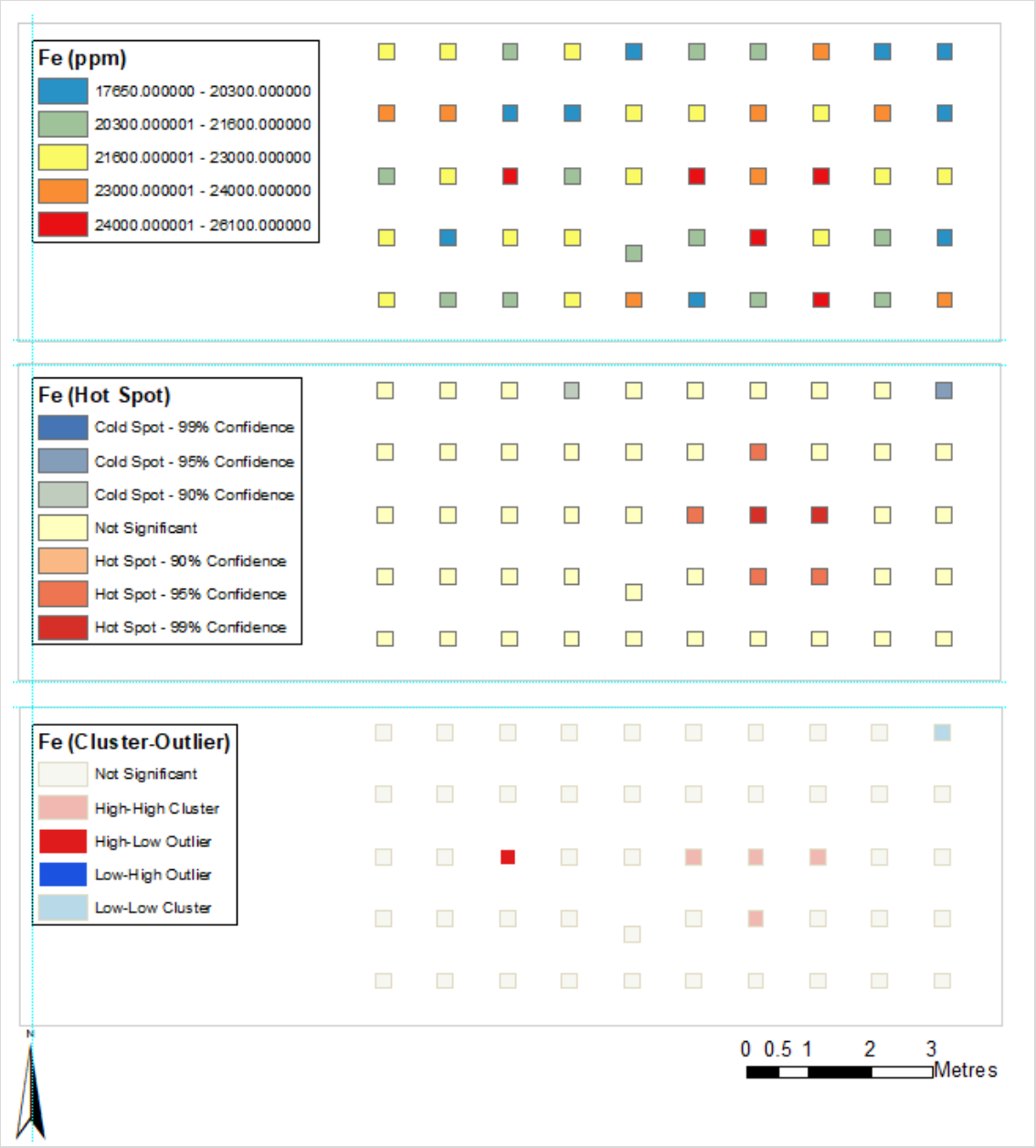

Figure 90. The basic visualisation (Jenks Natural Breaks; top), Hot Spot Analysis (centre), and Cluster-Outlier Analysis (bottom) for iron results (Fixed Band Neighbourhood = 1.85m)

Iron was the only element present in major concentrations in some of the samples. In the basic visualisation in Figure 90, the readings symbolised as falling within the highest band (red) in this case are a minimum of 3700 ppm greater than readings falling into the lowest band (blue). It can be seen there is a possible grouping of high (red) or reasonably high (orange) readings just east / southeast of the centre of the trench. This enhancement can be seen in the visualisations of other elements in the same samples, if we take this as a template for a potentially enhanced area (specifically the samples from Y2 to 0, Z2 to 1, and A2). The western end of the trench seems more variable in iron content.

The proposed hot spot is confirmed as being statistically significant by Hot Spot and Cluster-Outlier analyses (and as such by two separate statistical methods). HSA identifies two

statistical cold spots as well along the northern edge of the trench. C-O confirms the hot spot locale as well as seconding the easternmost of the two cold spots. It also identifies an outlier to the west of centre.

6.4.2.2 Minor contributors (aluminium, calcium, magnesium)

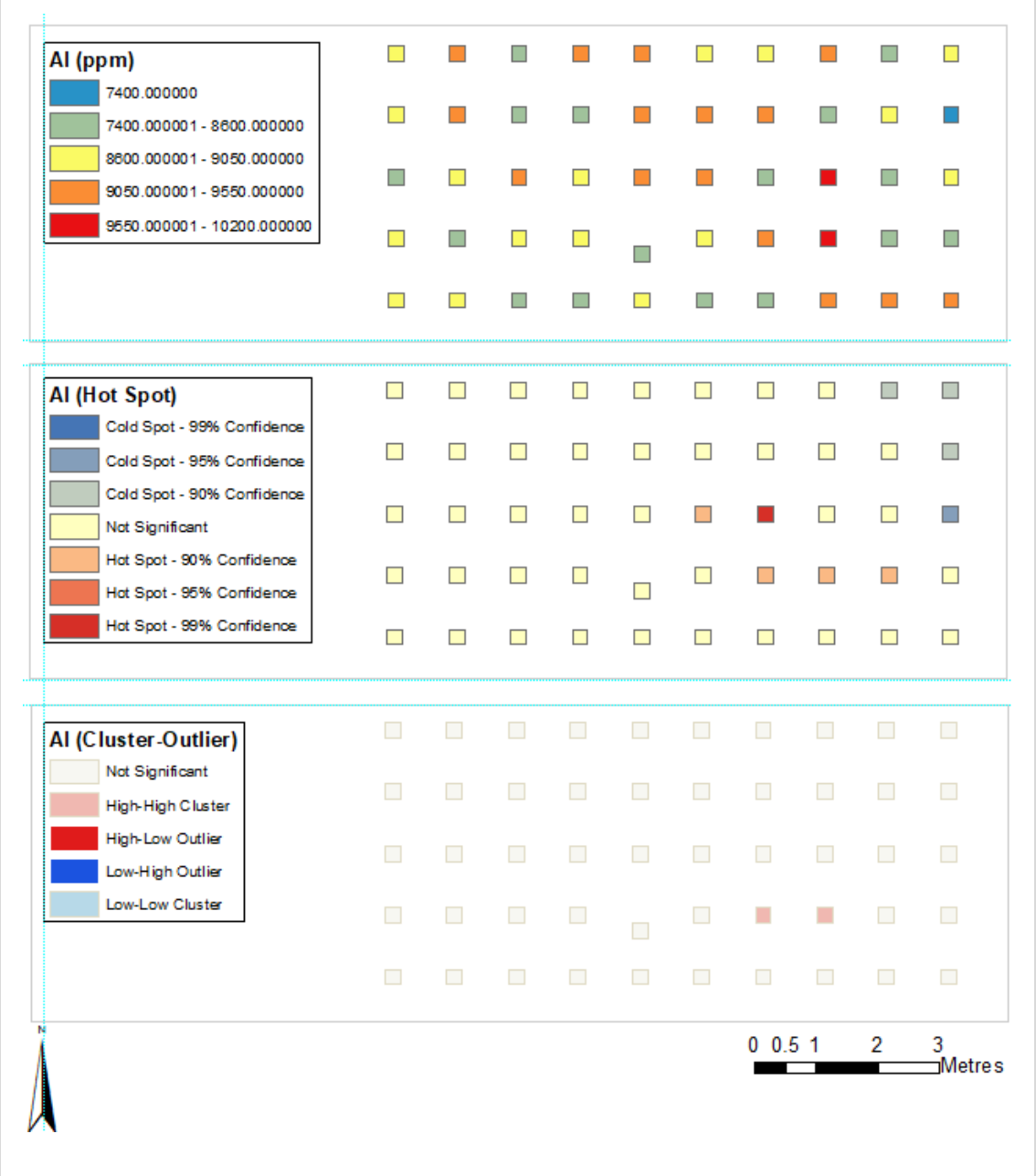

Figure 91. The basic visualisation (Jenks; top), Hot Spot Analysis (centre), and Cluster-Outlier Analysis (bottom) for aluminium results (Fixed Band Neighbourhood = 1.85m).

Similar to iron, aluminium read highest in the region east of centre, supported by identification of hot spots in the same region by HSA and C-OA (Figure 91). The other readings are less polarised than those seen in iron but generally follow a similar trend with dark / light blue or orange / red banded readings falling in similar locations to those in iron. No outliers were identified by C-OA.

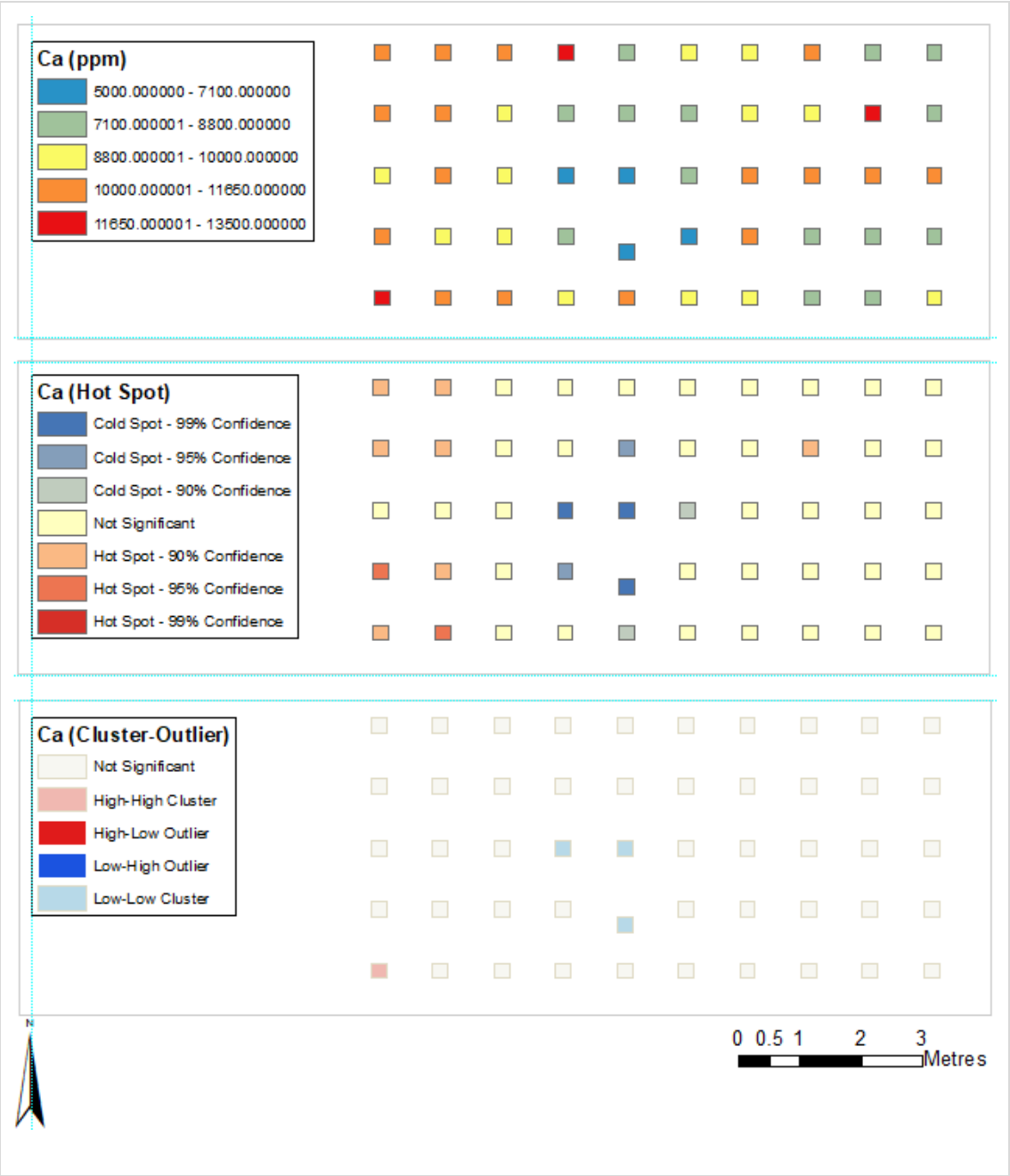

Figure 92. The basic visualisation (Jenks; top), Hot Spot Analysis (centre), and Cluster-Outlier Analysis (bottom) for calcium results (Fixed Band Neighbourhood = 1.85m)

Calcium showed a different patterning to the other two elements with a grouping of low readings to the west of centre (Figure 92). This was also seconded by the HSA and C-OA. In addition, both of the statistical analyses flagged regions where there were groupings of orange-level readings as being statistically significant hot spots which were not easily identified from the simple visualisation. Three hot spot regions were flagged by HSA, one of which seconded by C-OA.

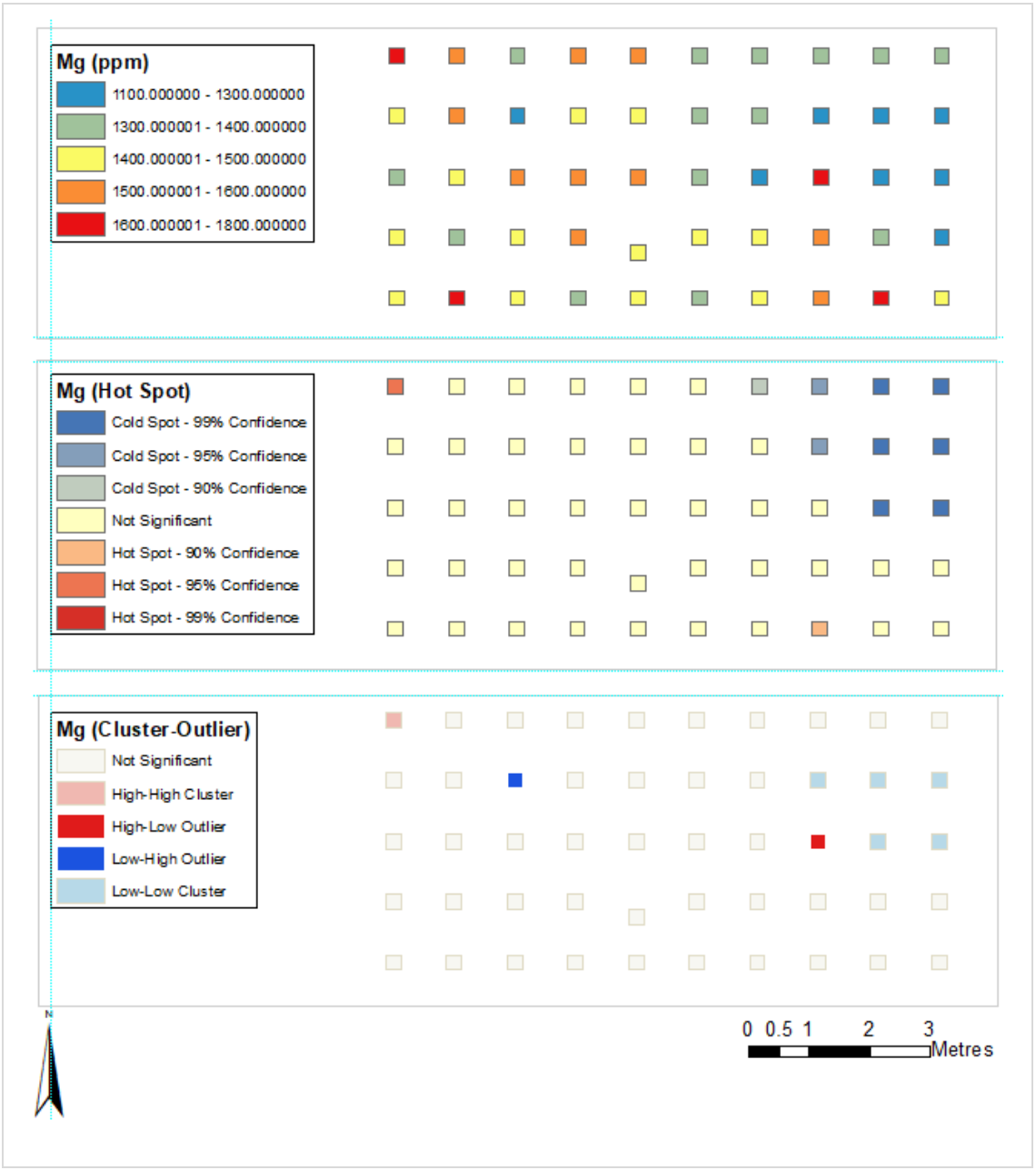

Figure 93. The basic visualisation (Jenks; top), Hot Spot Analysis (centre), and Cluster-Outlier Analysis (bottom) for magnesium results (Fixed Band Neighbourhood = 1.85m).

Magnesium gave a more mixed signature than the elements so far discussed (Figure 93). It again had some of its highest readings in the southeast-of-centre area, although more to the southeast in general coverage. However, north-east of this was a clear area of low readings, and in fact the northeast quadrant of the trench seemed to be generally low in magnesium aside from the one red-band reading that correlated with the highs in aluminium and calcium. The other end of the trench was variable.

Hot spot analysis supported a cold spot in the northeast of the trench, the more southeastern location of a hot spot and a hot spot in the very northwestern corner. The cluster-outlier analysis supported the northwestern hot spot and the northeastern cold spot but the southeastern hot spot did not meet the criteria for this test and instead there is a high-low outlier flagged for just a little north of that area instead. In addition, there is a low-

high outlier in the northeastern quadrant. As such, the magnesium results seem more variable generally across the trench and potentially more randomly patterned.

6.4.2.3 Trace contributors (both general and IUPAC, to include barium, potassium, manganese, sodium, phosphorus, sulfur, titanium as well as silver, arsenic, boron, beryllium, cobalt, chromium, copper, mercury, lanthanum, molybdenum, nickel, lead, antimony, scandium, strontium, vanadium, zinc)

The following plots are for the trace elements found in the Flixton samples (Figure 94). The aim of plotting these trace elements was to see if they supported any of the patterning in the more dominant elements and, later, in the lithics distributions. Even though an argument for an activity area based on these trace elements alone would likely be very weak, considering how these data may exhibit complementary patterning to other data would potentially allow for a more nuanced interpretation of that patterning as well.

As these are in trace amounts, the difference between symbolised high and low values can sometimes be a matter of only a few parts per million. As such, these results must be treated with care. Even so, certain trace elements did present patterning, with only these miniscule differences, which was similar to patterning in the major and minor elements. Only the basic visualisations (Jenks Natural Breaks) are provided here in text as, given the low ppm values and the fact the readings were below the LOD more commonly here, then this was considered the most straightforward representation of the data without being misleading (the statistical analyses are provided in Appendix Six for reference however). Readings that only have one to three bands visualised are derived from readings that had only one to three different values respectively. For example, the results for titanium were recorded as only being one of two values: 100 or 200 ppm. The results for these readings were provided from ALS Chemex in this presumably rounded up format and no greater resolution was available.

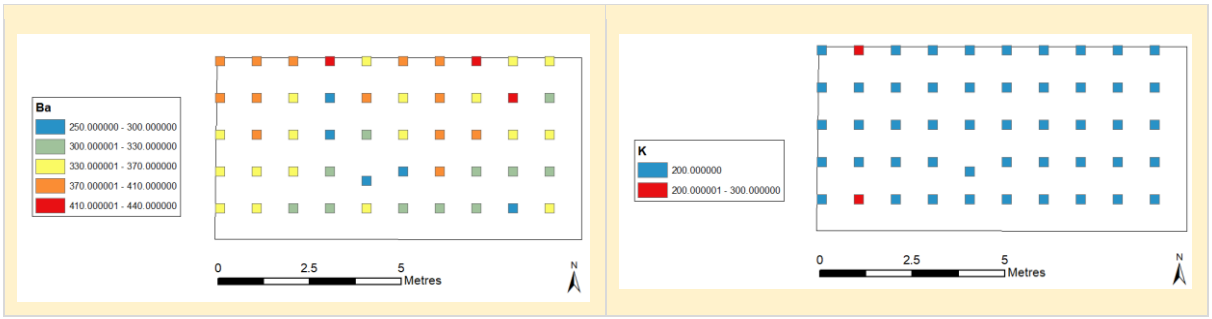

Mn
101.000000 - 124.000000
124.000001 - 150.000000
150.000001 - 171.000000
171.000001 - 191.000000
191.000001 - 210.000000
0 2.5 5 Metres
N
Na
100.000000
0 2.5 5 Metres
N
P
320.000000 - 420.000000
420.000001 - 540.000000
540.000001 - 660.000000
660.000001 - 910.000000
910.000001 - 1260.000000
0 2.5 5 Metres
N
S
400.000000
400.000001 - 700.000000
700.000001 - 900.000000
900.000001 - 1050.000000
1050.000001 - 1200.000000
0 2.5 5 Metres
N
Ti
100.000000
100.000001 - 200.000000
0 2.5 5 Metres
N
Ag
0.000000
0.000001 - 0.200000
0.200001 - 0.300000
0 2.5 5 Metres
N
As
7.000000 - 8.000000
8.000001 - 9.500000
9.500001 - 10.000000
10.000001 - 12.000000
12.000001 - 14.000000
0 2.5 5 Metres
N
B
0.000000
0.000001 - 10.000000
10.000001 - 40.000000
0 2.5 5 Metres
N
Be
0.650000
0.650001 - 0.700000
0.700001 - 0.750000
0.750001 - 0.800000
0.800001 - 0.900000
0 2.5 5 Metres
N
Co
4.000000
4.000001 - 5.000000
5.000001 - 5.500000
5.500001 - 6.000000
0 2.5 5 Metres
N
Cr
15.000000 - 17.000000
17.000001 - 18.000000
18.000001 - 19.000000
19.000001 - 20.000000
20.000001 - 21.000000
0 2.5 5 Metres
N
Cu
5.000000 - 6.000000
6.000001 - 8.000000
8.000001 - 10.000000
10.000001 - 13.000000
13.000001 - 17.000000
0 2.5 5 Metres
N

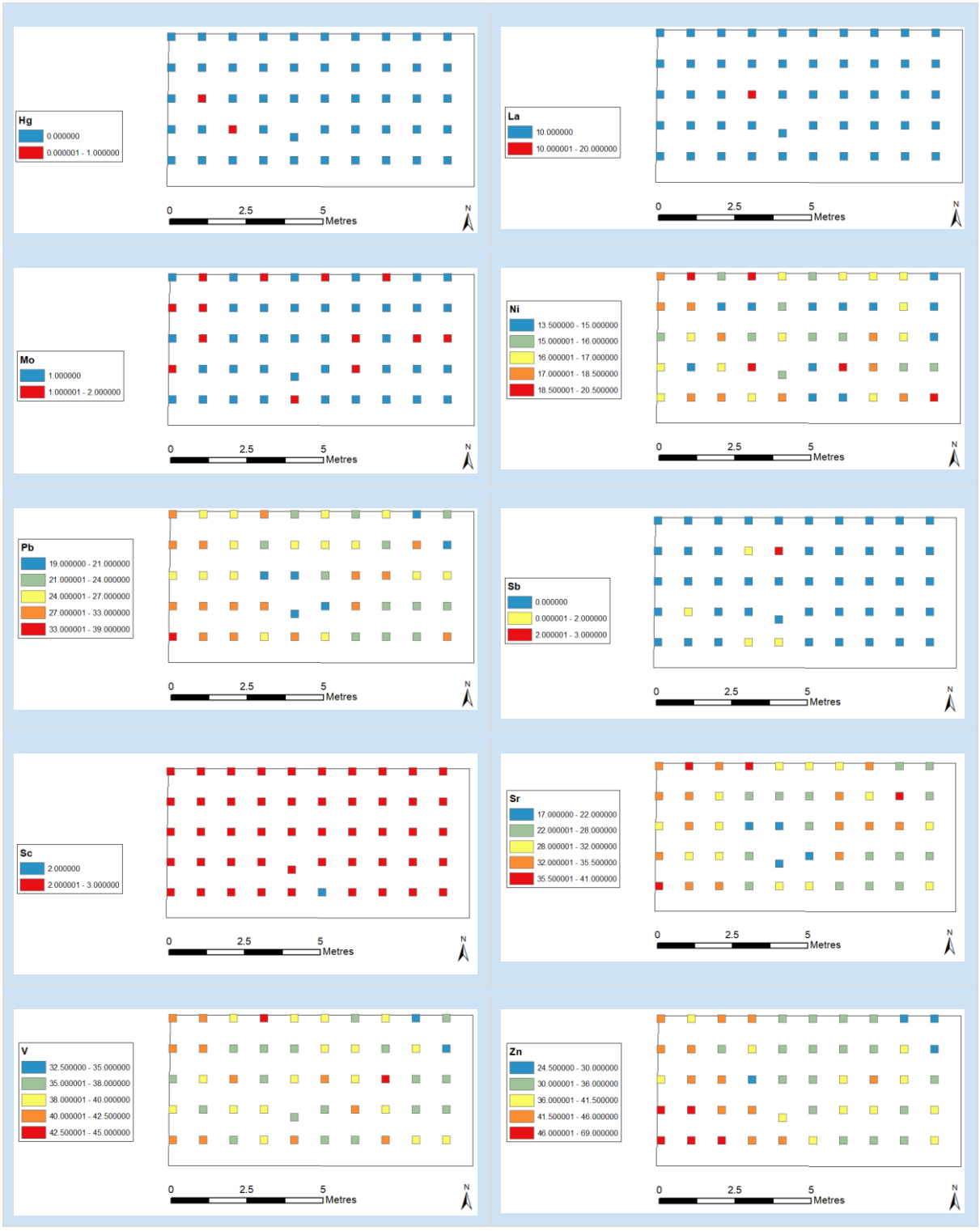

Figure 94. The basic (Jenks Natural Breaks) visualisation of the results for all detected trace elements.

Titanium, arsenic, cobalt, chromium and arguably manganese, beryllium, copper, nickel, vanadium all show high readings in that east-of-centre enhanced area. However, the hot spot is only statistically significant for titanium and arsenic (by HSA and C-OA), but not for cobalt, chromium, manganese, beryllium, vanadium (by either method), while there is a high-low outlier flagged for copper and nickel by C-OA.

Barium, manganese, phosphorus, sulfur, boron, lead, strontium and arguably zinc and copper all seemed to exhibit that west-of-centre depletion area fairly clearly. Arsenic and

nickel also have some low values here. A cold spot in that vicinity is statistically significant for barium (both methods), manganese (both), phosphorus (both), sulfur (both), boron (only by HSA), lead (both), strontium (both), copper (both), arsenic (HSA only), but not by either method for zinc or nickel. There is a high-low outlier reading directly south of the area for sulfur and arsenic, but not overlapping with the centre of the general vicinity of the cold spot. As such, this cold spot is statistically significant for quite a lot of the elements.

The readings for titanium, while only yielding values of either 100 or 200 ppm, so not at the best resolution, suggested there may be a third area of enhanced values. This seemed to fall in the west of the trench, running along the western edge of the proposed depletion area in samples from grid squares B0, C1, and D2. Taking these three high readings in the titanium plot in the western area as a template, manganese, sulfur, arsenic, cobalt, copper, nickel, and arguably chromium and molybdenum all reflect some similar enhancement in this area. This would include the outliers for sulfur and arsenic mentioned in the previous paragraph, along with a similar high-low outlier for molybdenum. However, the only element this is statistically significant for is mercury (both methods), not even titanium. In many of the statistical analysis plots however there is a hot spot identified further to the southwest though, covering that corner of the trench. This was statistically significant for manganese (both methods), phosphorus (both), sulfur (only HSA), silver (both, but with a low-high outlier from C-OA), cobalt (both but not extending as far as the western edge), copper (both), lead (both), strontium (both), zinc (both), and technically for potassium also (by HSA, but identified as a high-low outlier by C-OA and considering these results are apparently rounded, this is not as convincing).

Overall, there are areas of potential spatial patterning identified from these individual elemental plots. In chapter seven, the elemental results are combined into groupings and then this model is compared with the spatial data for the lithics assemblage (see section 7.3.2

6.5 Results from pXRF on Trenches 11, 12, and 15 (2014 excavation)

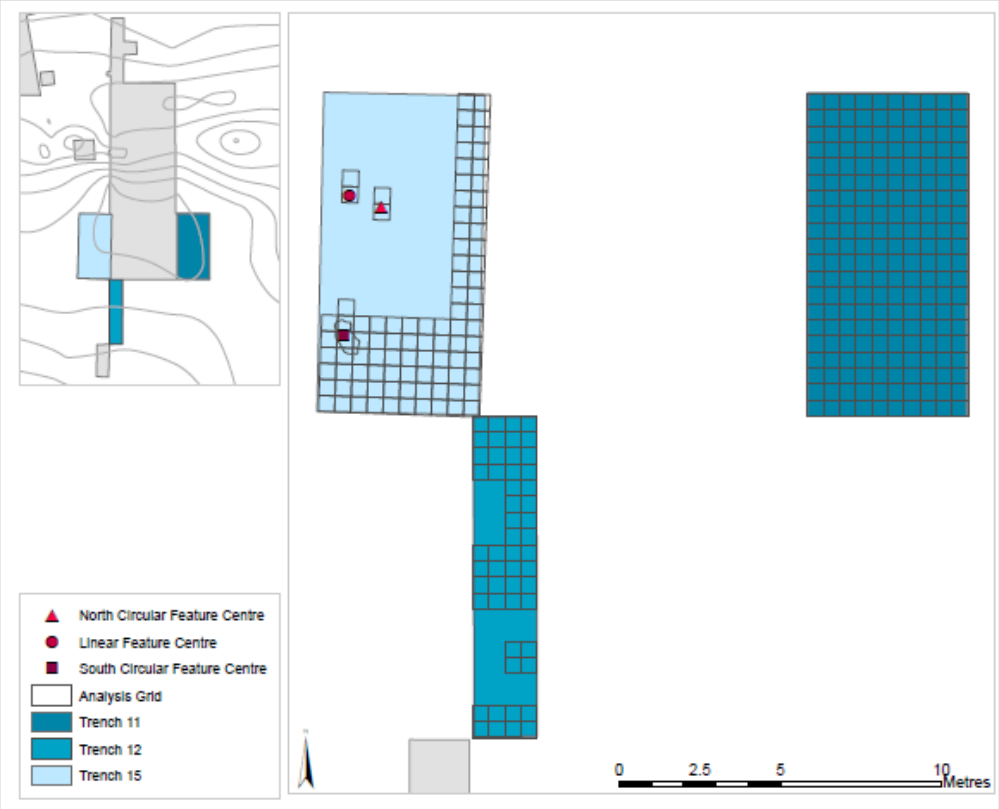

Figure 95. The analysis strategy for field pXRF carried out on the Flixton Island dryland trenches in 2014, with south circular feature illustrated (other two potential features too indistinct and not planned).

The dryland trenches excavated in 2014 were all at least partially analysed by pXRF in the field. The entirely of trench 11 was analysed while only subsamples of trenches 12 and 15 could be covered due to time demands, as shown in Figure 95. Analyses were conducted either to provide systematic coverage of a featureless area, to provide coverage of specific features, or for the daily repeat readings discussed in chapter five. Possible features were identified in Trench 11 based on crude examination of the pXRF results in the field only, there were no visible physical markers of features there. In Trench 12, there were no immediately distinguishable features by either method. However, in Trench 15 there were three visually identified possible features which were analysed in-situ by pXRF, one of which was in the middle of the area analysed as part of the general sweep of the trench. A reading was taken from the centre of each feature and that was used as the reading for that quadrant. Several readings were taken surrounding each feature and if they fell within a different quadrant then that was used as the reading for that quadrant too. This approach was consistent with the method applied to the ICP-AES sampling from 2012 where samples from features were taken as part of the general coverage of the trench and treated in the same way as the general coverage.

The field pXRF results for trenches 11, 12 and 15 were plotted using the same methods as for the trench 4 ICP-AES results. These results represent surface measurements taken in-situ from every quadrant of a grid square covered (including those from features as discussed above), and are therefore both subject to weather changes and, being unsieved, with inclusions potentially influencing the results also. As such, we might expect a higher proportion of outliers where inclusions have significantly impacted a result. We would expect if weather conditions were influencing the results then that would produce an obvious pattern correlating with days and times and with topography (if water is draining downslope for example). Figure 96 shows the quadrants analysed colour coded by date of analysis and Table 43 is a breakdown of how analyses were conducted along with weather notes.

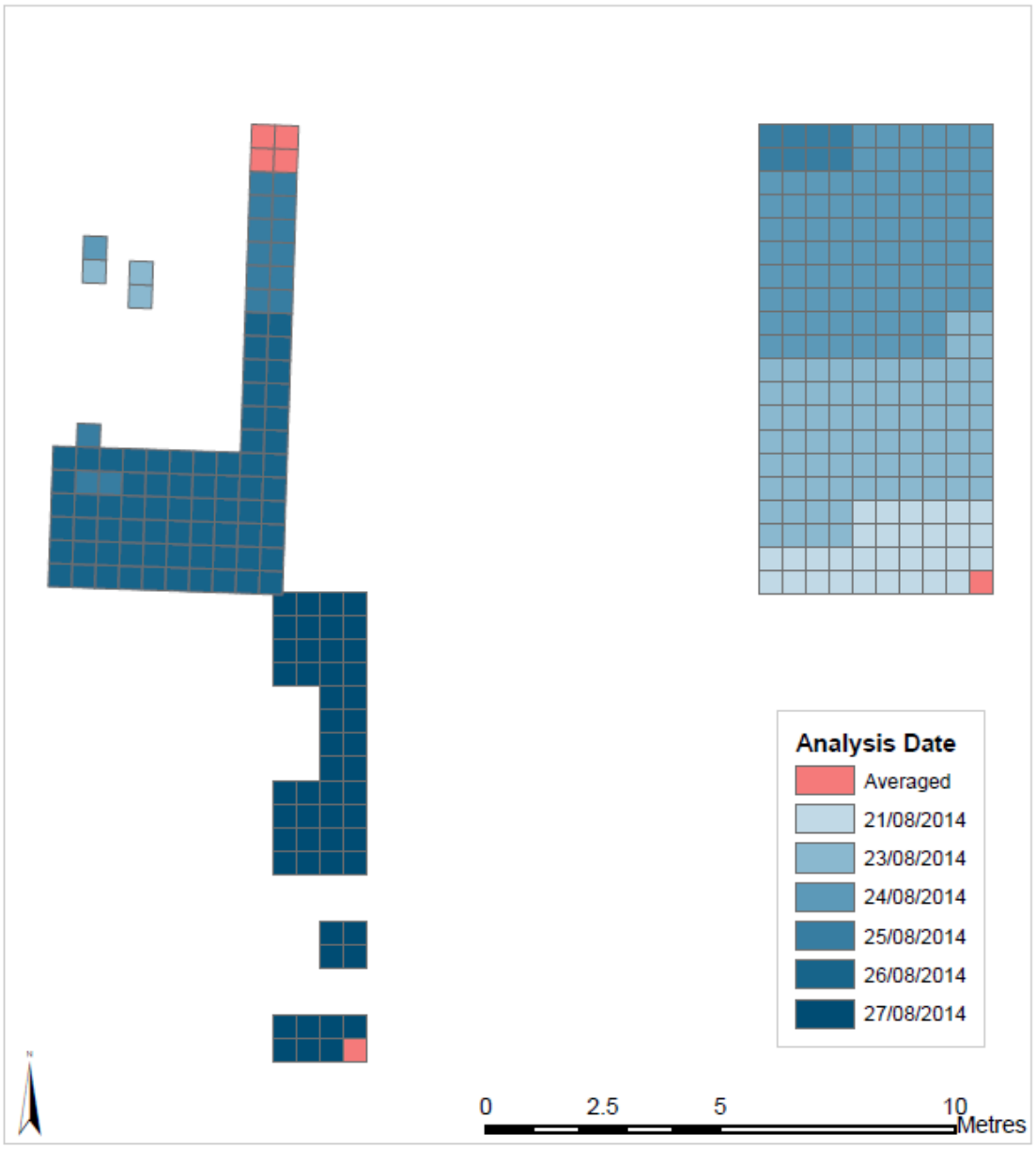

Figure 96. pXRF analysis grid colour coded by date of analysis

Table 43. Dates of pXRF analysis in the field at Flixton Island 2 as well as notes on conditions made in the field and highlights from the Met Office report for August 2014 (The Met Office 2015) (The Met Office 2015)

Date	Area analysed	Weather notes
21.8.14	Trench 11 commenced, starting with Row -5 and Row -4 up to and including grid sq. T-4.	The 21st started mainly bright with isolated showers but a band of rain spread from the northwest of England during the afternoon, reaching the southeast during the evening.
23.8.14	Remainder of Row -4, complete Row -3, - 2, - 1 and grid square R0. (In addition, readings from the Trench 15 northern circular and linear possible features were taken on this day.)	The showers were more widespread and frequent on the 23rd with the heaviest ones in the east of England.
24.8.14	Remainder of Row 0, complete Row +1, +2, +3, and Row +4 up to and including grid square T4. (Plus, additional readings from Trench 15's northern linear possible feature were taken on this day to improve the resolution in that area.)	A bright but chilly start on the 24th but it was a bright day for many.
25.8.14	Remainder of Row +4. Trench 11 complete. Trench 15 commenced, grid squares G4, +3, +2, +1. (In addition, readings for the southern circular feature were taken on this day.)	The country was split on the 25th with the northern half mainly dry and bright.
26.8.14	Grid squares G0, G-1, G-2, G-3, G-4, G-5 completed the north-south transect. Then outstanding grid squares to form east-west transects across Rows -3, -4 and -5 were then completed in that order.	Dry but mainly cloudy; remaining cool in a northwest wind.
27.8.14	Complete sample of Trench 12.	The 27th was generally dry and bright.

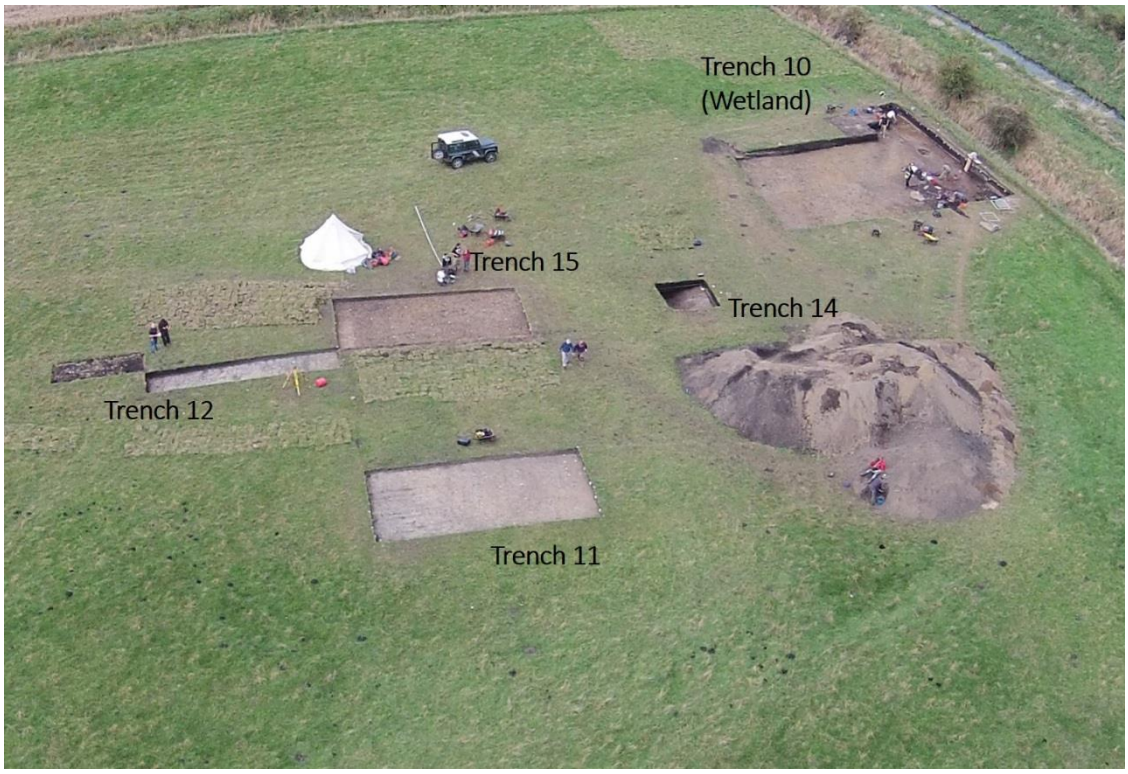

Figure 97. An aerial view from the east of the site, with trench 11 in the foreground and the long, thin trench 12 to the south, starting to run down into the lake area to the south (with trench 15 to the northwest of 12 and the wetland trenches to the north of all of these). North is to the left of the picture. Cropped from photograph taken by Paul Howden

Figure 98. An elevated photograph facing southeast from the northwest of trench 11, where the slight dip into the southeastern (far) corner can be made out, along with plough marks in the centre-south area of the trench. (Photo taken by the POSTGLACIAL Project.)

Figure 99. An elevated side view from the western side of trench 15 (with the northern end of trench 12 to the southeast and trench 11 to the north in the background). (Photo taken by the POSTGLACIAL project.)

Trenches 11 and 15 were on the top of the dryland with their southern ends slightly lower where the ground started to slope down the side of the hillock (Figure 97Figure 98Figure 99). Trench 12 ran southwards from the southeast corner of trench 15 with a slightly steeper slope going down into what would have been into the southern liminal zone on the edge of the lake (Figure 99). Trench 11 was analysed first, travelling from the southeast corner of the trench for the first readings to the northwest corner for the final readings overall. Readings were taken travelling from east to west across the trench in complete rows of grid squares, taking the four readings from each quadrant of the grid square before moving on to the grid square next to the west. When a row was completed, the machine was moved back to the eastern edge to start the next row. In other words, the first row analysed was the southernmost row -5, then -4, -3, and so on up to northernmost row +4. Starting in row -5, grid squares R-5 was analysed first then S-, T-, U- and V-5. The corners of nearly all squares were analysed in this order of quadrants: southeast, southwest, northeast, northwest. This last step provided unnecessary awkwardness when integrating into ArcGIS and it is recommended that instead the sampling is done in complete transects rather than keeping quadrant readings together (even if that is a subdivision of the main grid) if it is to be repeated on other sites, for greater ease in the digitising of the data. It can be seen that there are some plough scars in the centre-south area of this trench.

For trench 15, in addition to areas sampled around three specific potential features, general coverage readings were taken to do one complete grid square wide transect from north to south across the trench and three complete east-west transects. The east-west transects were adjacent to each other and covered the southern end of the trench, positioned to specifically cover the squares surrounding the southernmost of those features which consisted of an area of darker sediments surrounded by a significant amount of burnt flint

and also to facilitate the northern end of the trench to continue to be excavated while pXRF analysis in the trench could be completed with the appropriate safety distances at the southern end.

Finally, sampling was carried out for systematic coverage in trench 12. This trench had yielded noticeably less artefacts than the other trenches (see discussion in lithics results chapter), did not have any obvious features, and was not further excavated after pXRF. As the southern end of trench 15 would need to be further excavated however, the northern end needed to be sampled first. As this was in the final days of digging, the aim was to complete samples spanning the length and width of the trench as much as possible in the remaining time. As such the analyses followed a slightly irregular route which, regardless, provided good coverage of the trench. All of these readings were taken on the same date (27.8.14).

As such, if day-to-day weather variations were influencing results in an obvious manner, a crude test of this would be if the patterning simply matched up to the dates of weather changes and this will be discussed when considering the results below.

6.5.1 Descriptive and exploratory statistics on the dryland trenches excavated in 2014

Basic exploratory statistical analysis was initially conducted on the dataset including the general coverage, features and averages of readings taken on control areas. This meant there were 345 readings or averages of readings each representing a single analysis point taken into consideration. Table 44 shows the descriptive statistics for all the elements as measured in the field by pXRF, sorted by descending mean value. They were not rounded up from the outputs provided by the machine. The statistics are calculated based on successful readings, and does not include substitution for those below the limits of detection so the descriptive statistics are entirely based on detected results. Cobalt, magnesium, antimony, selenium, tin, and tungsten were all below the limit of detection in all field pXRF readings.

Based on the means from the field pXRF results, silicon, aluminium and iron are the major elemental contributors to the soils. Calcium, potassium, and titanium are all minor contributors supplemented by a single successful chlorine value that read at 1631.22 ppm (possibly an outlier, miscalculation of interference, or an inclusion reading). The other major and minor contributors were read in every single sample. Sulfur, zirconium, phosphorus, vanadium, and manganese are all trace contributors and based on a mean drawn from a minimum 224 successful readings. Lastly, various IUPAC trace elements were

identified though sometimes only in a small number of samples (noted in brackets here if less than 100 readings available): chromium, strontium, zinc, rubidium, tantalum, cadmium (only 15 samples), yttrium, silver (5), nickel, thorium, lead, niobium, copper (3), mercury (1), molybdenum, bismuth (5), arsenic, and uranium (67) (listed in order of descending mean value).

The distribution histograms are again provided for reference in Appendix Six. As can be predicted from the skewness and kurtosis values as well as the fact that some of the distributions have multiple modes, most of the results were non-normally distributed and the same statistical methods for spatial visualisation as for the VP12 data were deployed on these data.

Table 44. Descriptive statistics for all the elements as measured in the field by pXRF, sorted by descending mean value. a. Multiple modes exist. The smallest value is shown

Element	N (Valid)	N	Mean	Std. Error of Mean	Median	Mode	Std. Deviation	Skewness	Std. Error of Skewness	Kurtosis	Std. Error of Kurtosis	Range	Minimum	Maximum	25th Percentile	50th Percentile	75th Percentile
Si_ppm	345	0	234431.19	2106.29	237545.74	82090.92[a]	39122.55	-0.64	0.13	0.81	0.26	247701.02	82090.92	329791.94	213213.01	237545.74	260031.41
Al_ppm	345	0	40389.04	565.80	39391.28	33029.68	10509.29	0.26	0.13	0.19	0.26	71149.05	8772.43	79921.48	32732.63	39391.28	47480.20
Fe_ppm	345	0	23488.52	291.10	23320.37	10344.33[a]	5406.98	1.14	0.13	5.03	0.26	48021.80	10344.33	58366.13	19823.97	23320.37	26505.72
Ca_ppm	345	0	6201.94	126.24	5997.92	5077.28	2344.87	0.92	0.13	1.91	0.26	15816.48	1476.34	17292.82	4487.61	5997.92	7402.40
K_ppm	345	0	4212.21	57.94	4166.37	1462.27[a]	1076.26	1.22	0.13	5.25	0.26	9104.23	1462.27	10566.50	3592.37	4166.37	4719.86
Ti_ppm	345	0	3701.18	39.03	3701.39	2229.97	724.94	0.18	0.13	0.57	0.26	4417.10	1653.80	6070.90	3248.25	3701.39	4133.54
Cl_ppm	1	344	1631.22		1631.22	1631.22						0.00	1631.22	1631.22	1631.22	1631.22	1631.22
S_ppm	325	20	546.12	22.06	458.94	75[a]	397.64	3.47	0.14	22.49	0.27	4040.34	74.55	4114.89	315.84	458.94	680.44
Zr_ppm	345	0	522.46	8.47	501.57	170.61[a]	157.25	0.87	0.13	1.31	0.26	994.24	170.61	1164.85	416.03	501.57	607.75
P_ppm	224	121	305.57	10.25	265.19	128[a]	153.36	2.49	0.16	11.17	0.32	1216.83	127.65	1344.48	204.05	265.19	373.74
V_ppm	340	5	218.65	2.79	220.54	219.41[a]	51.42	0.04	0.13	-0.18	0.26	274.80	93.68	368.48	180.54	220.54	252.68
Mn_ppm	345	0	145.20	2.06	141.70	115.49[a]	38.27	1.75	0.13	10.21	0.26	385.37	56.84	442.21	120.59	141.70	165.95
Cr_ppm	221	124	75.75	1.78	69.85	51[a]	26.40	1.65	0.16	3.77	0.33	169.55	43.57	213.12	56.47	69.85	86.83
Sr_ppm	345	0	62.24	0.76	60.85	57.61	14.13	4.99	0.13	50.49	0.26	192.71	29.57	222.28	55.72	60.85	67.39
Zn_ppm	345	0	33.13	0.51	31.47	24.22[a]	9.49	1.21	0.13	3.96	0.26	71.64	14.12	85.76	26.49	31.47	39.06
Rb_ppm	345	0	23.97	0.27	23.67	22.63	5.01	2.16	0.13	13.28	0.26	54.38	8.57	62.95	21.63	23.67	25.94
Ta_ppm	342	3	21.41	0.32	21.11	15.83[a]	5.91	0.79	0.13	1.94	0.26	44.50	8.94	53.44	16.84	21.11	25.13
Cd_ppm	15	330	20.23	0.73	19.99	16[a]	2.81	0.93	0.58	0.73	1.12	9.73	16.47	26.20	18.34	19.99	21.34
Y_ppm	345	0	18.78	0.22	18.53	16.47	4.15	0.99	0.13	4.84	0.26	38.09	7.59	45.68	16.00	18.53	21.01
Ag_ppm	5	340	17.81	0.84	17.82	15[a]	1.88	0.00	0.91	-0.79	2.00	4.86	15.39	20.24	16.05	17.82	19.57
Ni_ppm	203	142	16.56	0.31	15.79	11[a]	4.39	1.01	0.17	1.05	0.34	23.09	9.74	32.83	13.12	15.79	19.26
Th_ppm	172	173	16.29	0.56	14.08	10.73	7.39	2.03	0.19	5.46	0.37	46.11	8.82	54.93	10.96	14.08	18.29

Element	N (Valid)	N	Mean	Std. Error of Mean	Median	Mode	Std. Deviation	Skewness	Std. Error of Skewness	Kurtosis	Std. Error of Kurtosis	Range	Minimum	Maximum	25th Percentile	50th Percentile	75th Percentile
Pb_ppm	345	0	15.77	0.19	15.44	13.54[a]	3.62	0.48	0.13	0.89	0.26	24.41	5.38	29.79	13.45	15.44	17.74
Nb_ppm	345	0	12.56	0.22	11.95	10.19[a]	4.05	1.60	0.13	7.35	0.26	37.60	3.86	41.46	9.96	11.95	14.37
Cu_ppm	3	342	11.20	0.55	10.72	11[a]	0.96	1.69	1.22			1.72	10.58	12.30	10.58	10.72	
Hg_ppm	1	344	9.84		9.84	9.84						0.00	9.84	9.84	9.84	9.84	9.84
Mo_ppm	294	51	9.07	0.28	7.97	9.40	4.79	1.57	0.14	3.33	0.28	31.44	2.91	34.35	5.70	7.97	10.79
Bi_ppm	5	340	8.48	0.43	8.35	7[a]	0.96	-0.47	0.91	-0.04	2.00	2.49	7.10	9.59	7.66	8.35	9.37
As_ppm	341	4	7.58	0.14	7.35	4.55[a]	2.62	2.92	0.13	20.09	0.26	27.59	3.13	30.72	5.88	7.35	8.71
U_ppm	67	278	6.29	0.18	5.97	5[a]	1.48	1.34	0.29	1.94	0.58	7.20	4.47	11.67	5.04	5.97	6.98
Co_ppm	0	345															
Mg_ppm	0	345															
Sb_ppm	0	345															
Se_ppm	0	345															
Sn_ppm	0	345															
W_ppm	0	345															

6.5.2 Spatial visualisation of 2014 dryland trench field pXRF results

6.5.2.1 Major elemental contributors (silicon, aluminium and iron)

Silicon was the highest present of the elements as measured by pXRF in the field. From the basic (Jenks Natural Breaks) plot of the values in ppm, a cold spot appears in the southeastern corner of the eastern trench (see Figure 100). The rest of Trench 11 initially appears quite mixed, with some high values. In the western trench, there is a possible hot spot in the southern end of the trench, around the centre-east area of the southern trench edge. Trench 12 (the southernmost trench) features a hot spot near its centre and just south. The areas containing features are slightly low in Si.

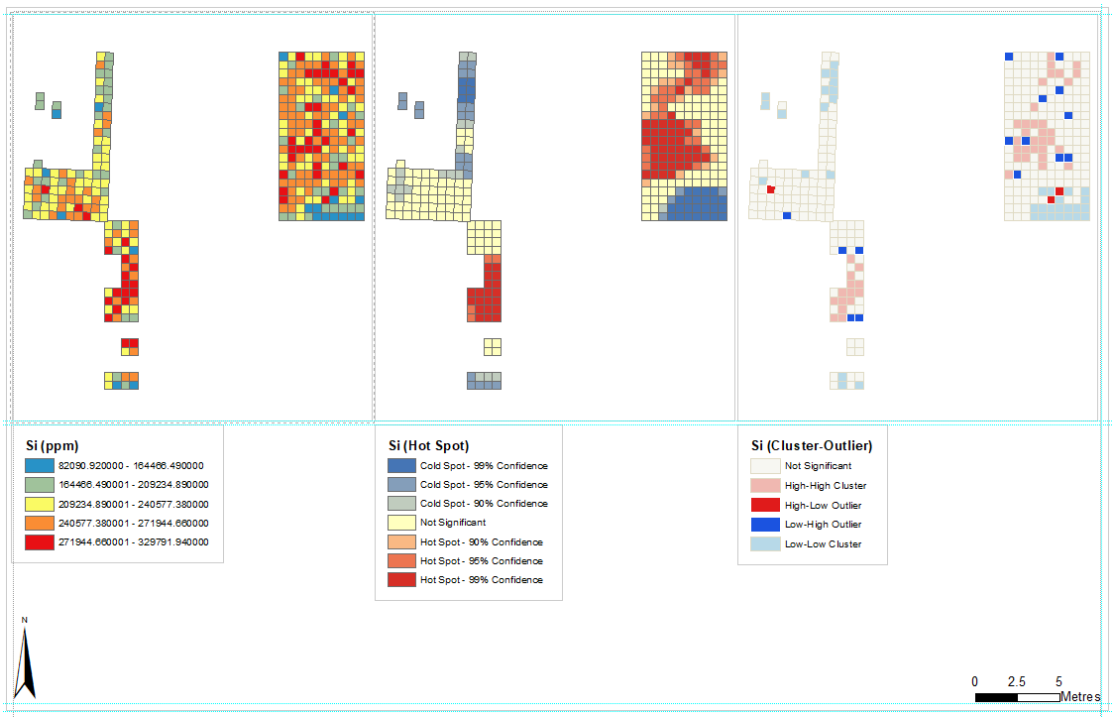

Figure 100. Simple, HSA and C-OA (left to right) plots of readings from pXRF for silicon

The HSA supports the cold spot in the south of trench 11 and additionally statistically identifies a generally hot area across the upper two-thirds of the trench which does not correlate particularly with date of reading. It also flags up three cold spots (in the north of trench 15, halfway down the eastern edge of that trench, and near the southern circular feature) the low values of which were not particularly noticeable in the basic plot, but it does not identify the potential hot spot along the southern edge as statistically significant. The hot spot covering the central-south area of trench 12 is identified, as is another cold spot in the very south of the trench. These hot and cold spots are supported in more limited forms in the C-O analysis which also flags several outliers within these areas, which may be due to inclusions in the soil / lack of homogeneity in the in-situ samples.

These patterns do suggest some caution needs to be taken: The cold spots in the south of trenches 11 and 12 could be due to different moisture levels. This area of trench 11 was slightly lower and usually a little wetter than the rest of the trench (see Figure 98 above), as was the southern end of trench 12, so it is possible these low readings are caused by that and this cannot be ignored as a potential cause. The southern end of 11 was only the gentle start of the slope however so there was no reason for pooling of water specifically rather than it draining further downslope. In addition, Trench 15 ran across a similar elevation to trench 11 and does not show the same patterning (it did not have as noticeable a dip in any corner though). In terms of wet weather, the low readings in trench 11 correlate with some of the grid squares analysed on the 21st. The 21st was brighter than the following day and so we would expect the readings to be higher instead, as they would less likely being impacted by moisture content. In addition, the readings on the 21st extended across the full trench width east to west, whereas this pattern cuts off midway along the trench. The pattern overlaps the area with plough scarring, but the pattern is not elongated north to south along the direction of the scars which implies while the soils were churned here they were not displaced far. In addition, this was an area of dense lithics as presented in chapter four, so this correlation will be discussed further in chapter seven.

Finally of note, the readings for silicon from the two northern possible features (to recap, as seen in four analysis squares that free float from the main analysis grid) flag up as cold spots in both the HSA and C-OA results yet were read on the same day as many of the high readings in trench 11 so this does seem a legitimate result.

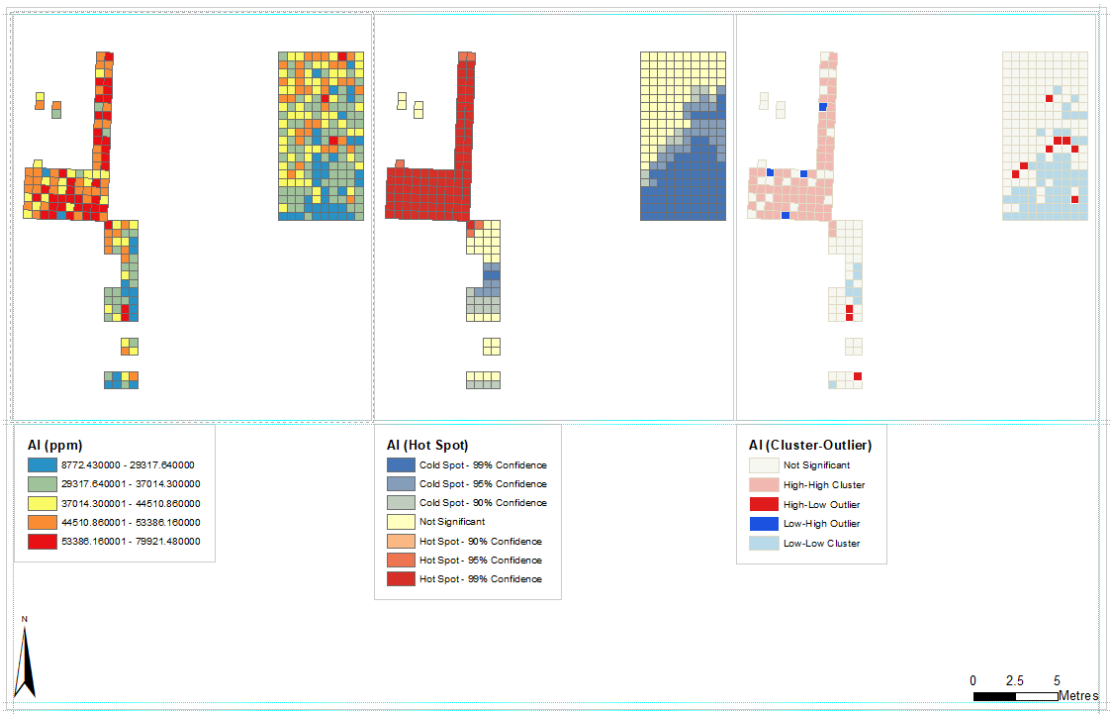

Figure 101. Simple, HSA and C-OA plots of readings from pXRF for aluminium

Similar to the results for silicon, there is a statistically significant cold spot in the south of trench 11 confirmed by the HSA and C-O analysis for aluminium (Figure 101). The lowest values are not just in that southeastern corner but along into the southwestern corner (which did not dip to the same extent). This looks more like it may have been impacted by the ploughing, however, although this is not supported by the iron results either (below).

The trench 15 values for this element are generally all over relatively strongly elevated and the whole area is flagged up as a significant hot spot by HSA and slightly less so by C-OA, reflecting how the values are overall very high and broadly contiguous across the trench. This does include the readings taken on two separate dates and some of which were on the same day as the last of the trench 11 readings so could be a legitimate difference between the trenches and this is supported by the extension of this hot spot in the top corner of trench 12, whose readings were taken the next day. The weather on those days and the preceding day was, however, drier than on the days spent analysing trench 11 so it is possibly due to the drier conditions overall.

Trench 12 again had a statistically significant area in the centre although conversely to the silicon results it was this time flagged as a cold spot, supported by the HSA and C-OA analyses, along with those readings at the southern end of the trench. The feature readings were either average or slightly high but not flagged as statistically significantly different. A few outliers were identified in different locations across the trenches by the C-OA, not all in the same locations as those previously identified for silicon however which could maybe support the inclusions interpretation (as inclusions could be of many different materials of various compositions). The northern trench 15 features do not read significantly high or low in this element.

As with both silicon and aluminium, the cold spot appears at the southern end of trench 11 for iron (supported by HSA and C-OA, see Figure 102). It is covering a broader area though which extends beyond a single date of analysis and moves towards the centre of the trench which is more elevated and nearer the peak of the upland. There is a possible hot spot for iron identified at the northern end of trench 11 by HSA but this seems to be more of an area effect considering it is not significant for C-OA and judging from the basic plot where there are no apparent, clear high values.

In trench 15, there are generally higher values again but two high spots at the northern end and southern end of the trenches allow for statistically significant hot spots to be identified by both statistical methods. Again, the features are not noticeably distinct and there are sporadic outliers.

In trench 12, there are low readings in the southern end, but these are not statistically significant enough to be flagged as a cold spot by HSA or C-OA. However, the northern end

flags as a hot spot, again joining with the hot spot area in the south of trench 15. This hot spot signal overlapping the two trenches seems to be a legitimate candidate for an area where a process aside from the topography/weather is producing a signal.

The northern features do not read significantly high or low in this element.

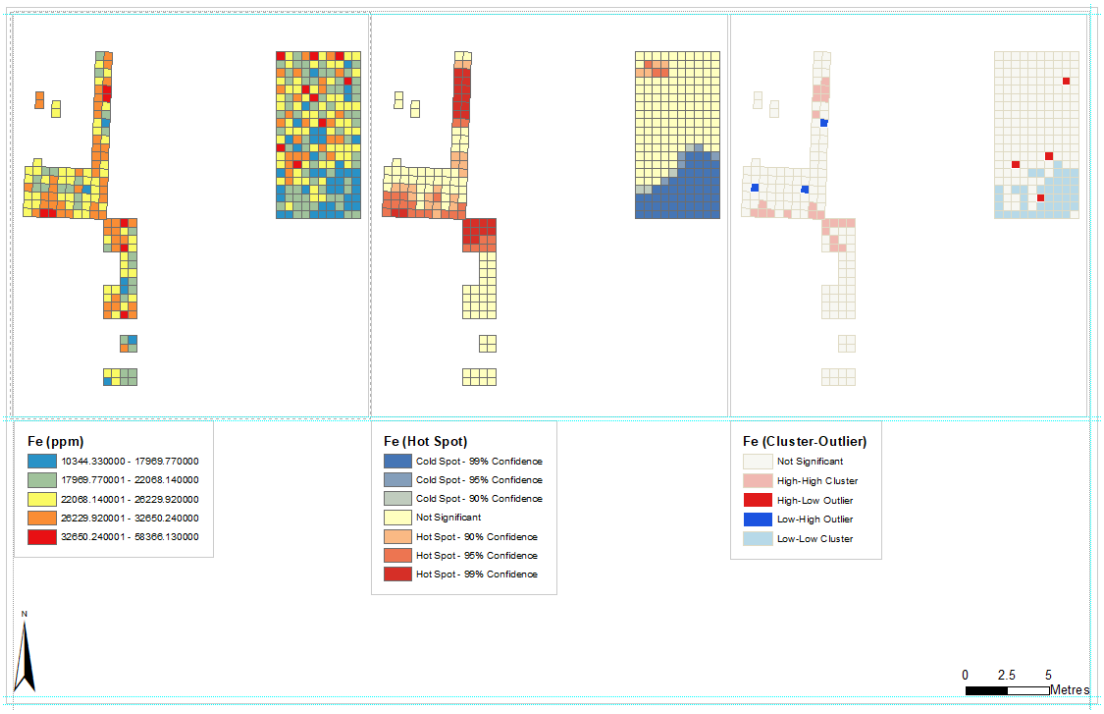

Figure 102. Simple, HSA and C-OA plots of readings from FpXRF for iron

6.5.2.2 Minor elemental contributors (calcium, potassium, titanium, chlorine)

Calcium is very variable across site and is a major contributor in some samples (varying from 1476 up to 17293 ppm, see Figure 103). The calcium plots are particularly interesting given that they reflect relatively high values recorded in the southeast corner of trench 11 and then a cold spot traversing the same trench from northeast to southwest-of-centre. This does not correlate particularly neatly with the measurement dates pattern so does not seem to be an artefact of daily changes. This pattern also broadly fits with the hot spot seen in the same region for silicon. In contrast, there is a cold spot in the northern stem of trench 15, which in this case falls slightly south of a cold spot again also seen in the silicon patterning and also a hot spot in the iron readings. The southwestern corner of trench 15, around the area of the circular feature and burnt flint area, is then identified as a hot spot which for silicon is also flagged as a subtle cold spot with outliers. As such, the relationship between silicon and calcium is not consistent but does support consistent patterning suggesting the soils have maybe undergone alteration by particular, if different, processes in those areas, which is supported by the additional pattern contributed by iron in trench 15.

The northern features do not read significantly high or low in this element.

Figure 103. Simple, HSA and C-OA plots of readings from FpXRF for calcium

Potassium is again a hugely variable element in the samples is a major contributor in some of the samples from trench 15, going up to 10566 ppm maximum (Figure 104). This element again exhibits those low values in the southern ends of trenches 11 and 12, causing statistically significant cold spots with occasional outliers to be identified here by HSA and C-OA. Trenches 11 and 12 immediately look generally lower in values than trench 15, which does not particularly fit with weather patterning. The high values from trench 15 cause much of it to be categorised as a hot spot by HSA but this does seem centred on the southeastern corner, drifting into the northwestern corner of trench 12, and this is supported by the C-OA which centres the hot spot area around that southeastern corner of trench 15 as well. Finally, there is a cold spot in the central zone of trench 12 again as was seen for aluminium, plus as a hot spot for iron and cold outliers for calcium suggesting this may also be an area of interest. The northern features do not read significantly high or low in this element.

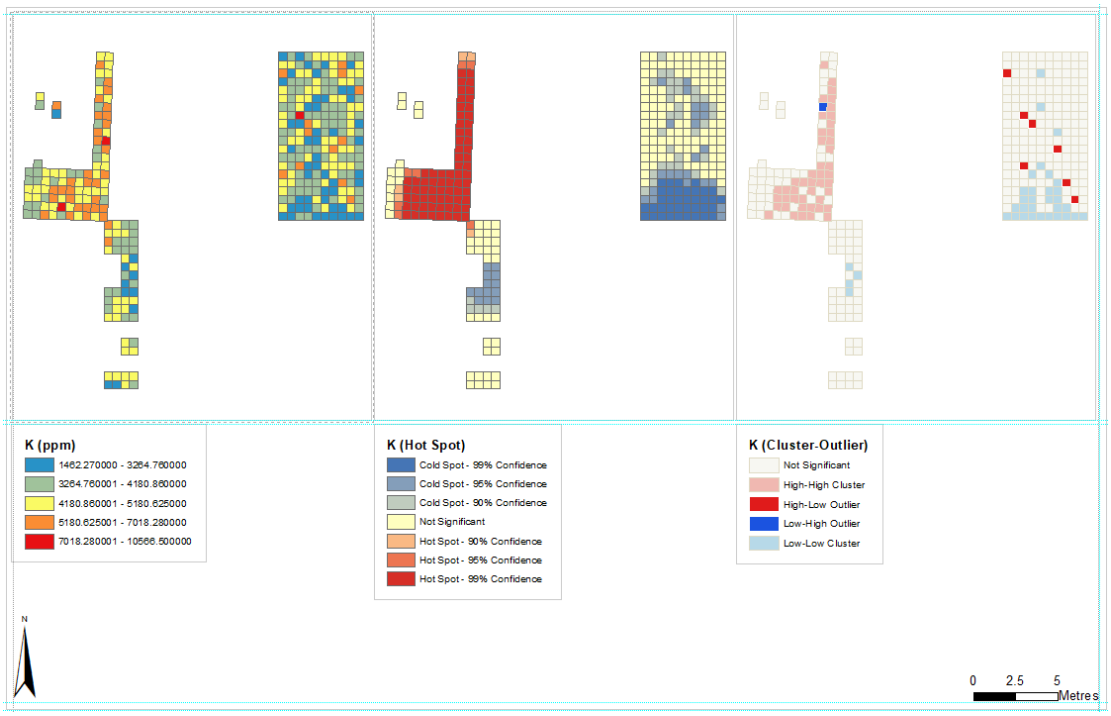

Figure 104. Simple, HSA and C-OA plots of readings from FpXRF for potassium

With titanium, we again see a repetition of some of the previously identified patterning (Figure 105): The low values / cold spot at the southern ends of trenches 11 and 12 (and again being more pronounced in 11); a cold spot north of centre in trench 11 where potassium and calcium have cold spots and silicon has a large hot spot; there is a suggestion of a hot spot in the northern stem of trench 15, though this is slightly south of the other hot/cold spots identified in that area in silicon, iron, and calcium, so not as in keeping; a hotspot in the southeast of trench 15 and northwest of trench 12; a hot spot in the centre of trench 12. While the readings do generally go from low to high with the dates, which fits with progressively drier weather over the days, the fact many of these significant spots overlap with those identified in other elements but they do not all follow the weather patterns does suggest other processes are potentially might be affecting the titanium readings too. The northern features do not read significantly high or low in this element.

As this is just a single reading, the high reading of chlorine is flagged as an outlier (by C-OA, see Figure 106) and does not suggest or support any particular interpretation in terms of specific processes. It is likely a misinterpretation of a peak by the software or a chance pick up of the element from contamination, in solution or bound as an anion with some clay particles or iron / aluminium oxides, as it is a highly mobile element in nature and readily taken up by plants usually. The HSA plot does illustrate how much the underlying statistical algorithm is sensitive to just one high reading and is kept in for reference here. The northern features do not read significantly high or low in this element.

Figure 105. Simple, HSA and C-OA plots of readings from FpXRF for titanium

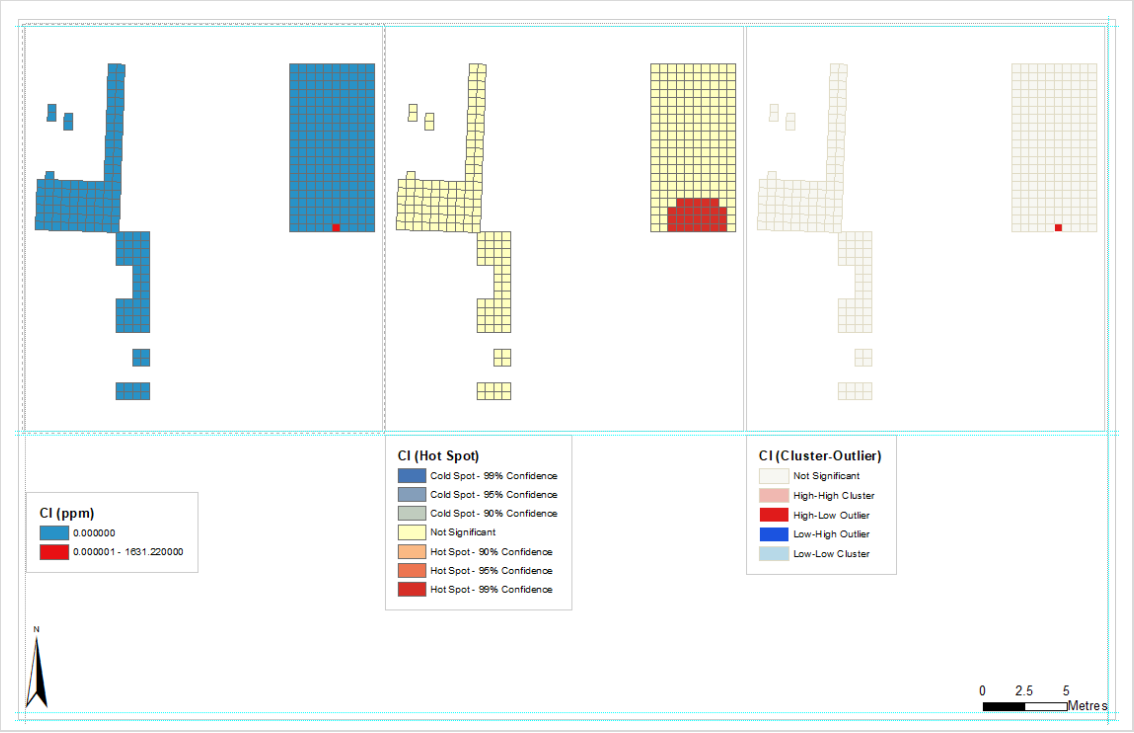

Figure 106. Simple, HSA and C-OA plots of readings from FpXRF for chlorine

As such, the major and minor value plots have suggested a series of areas of potential interest. These are compared with the results for the trace elements in the remainder of this chapter, to see whether these patterns are further reflected in those results as well.

6.5.2.3 Trace elemental contributors (both general and IUPAC, to include sulfur, zirconium, phosphorus, vanadium, manganese, chromium, strontium, zinc, rubidium, tantalum, cadmium, yttrium, silver, nickel, thorium, lead, niobium, copper, mercury, molybdenum, bismuth, arsenic, uranium)

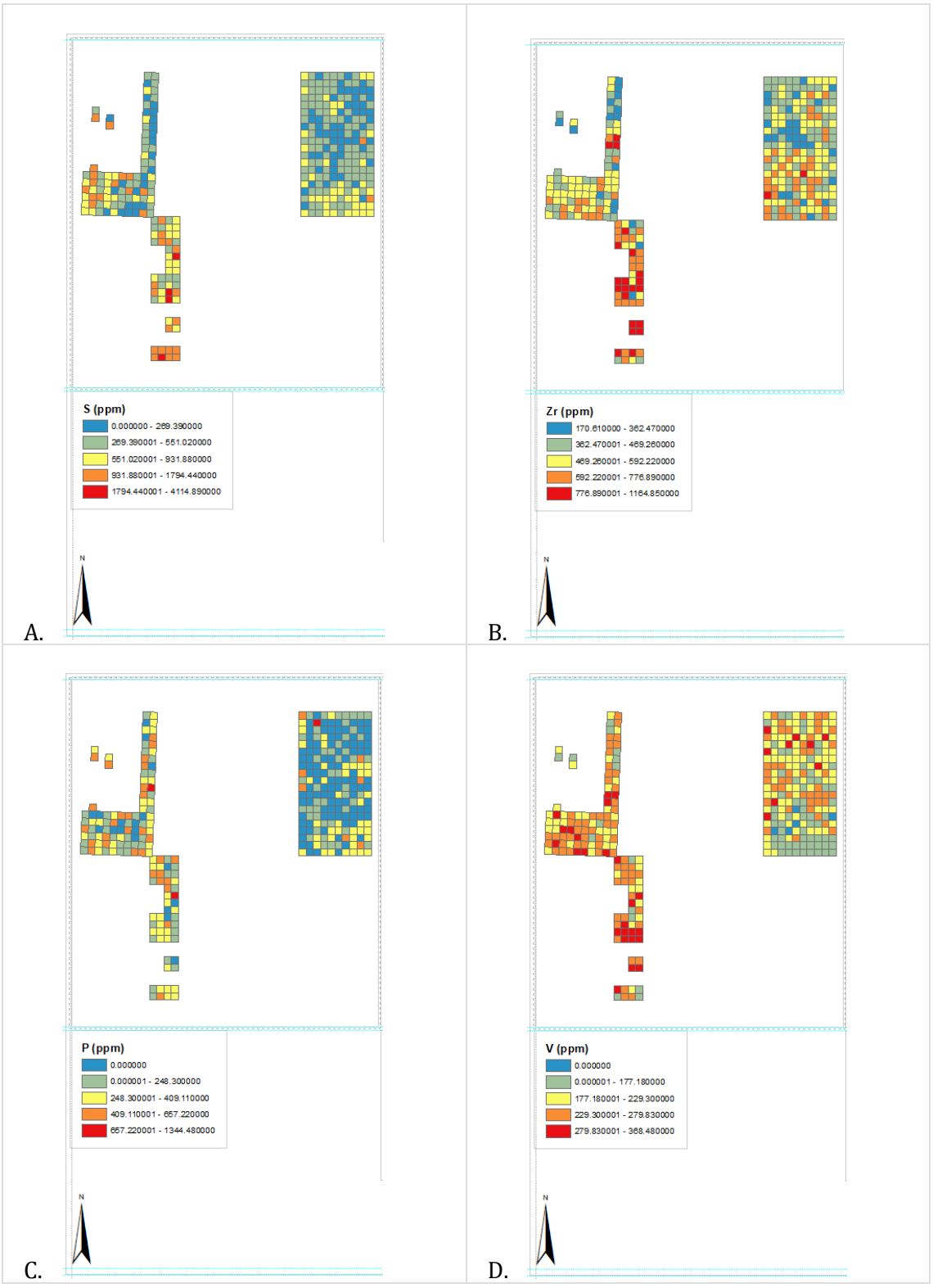

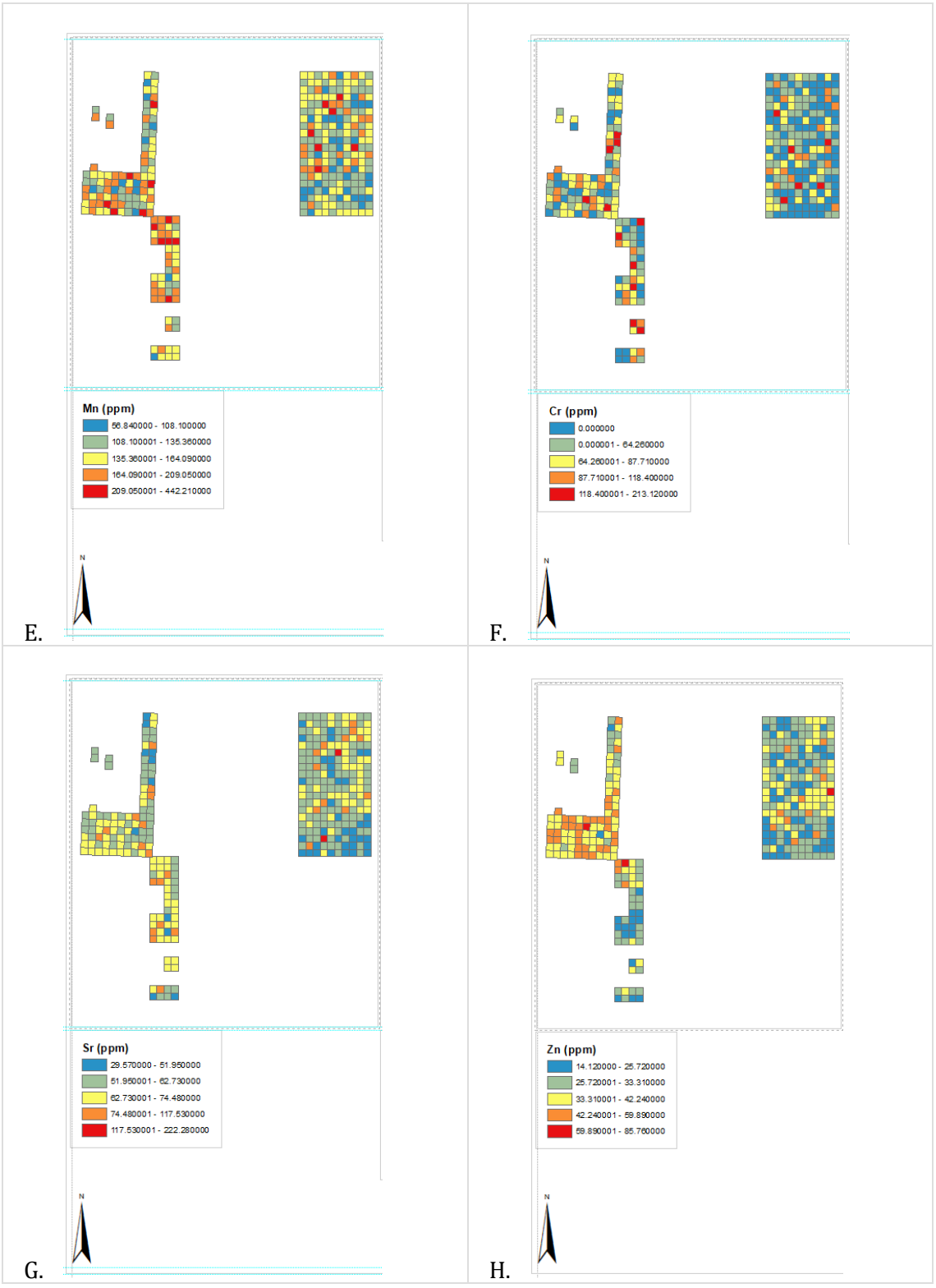
Mn (ppm)
56.840000 - 108.100000
108.100001 - 135.360000
135.360001 - 164.090000
164.090001 - 209.050000
209.050001 - 442.210000
N
E.
Cr (ppm)
0.000000
0.000001 - 64.260000
64.260001 - 87.710000
87.710001 - 118.400000
118.400001 - 213.120000
N
F.
Sr (ppm)
29.570000 - 51.950000
51.950001 - 62.730000
62.730001 - 74.480000
74.480001 - 117.530000
117.530001 - 222.280000
N
G.
Zn (ppm)
14.120000 - 25.720000
25.720001 - 33.310000
33.310001 - 42.240000
42.240001 - 59.890000
59.890001 - 85.760000
N
H.

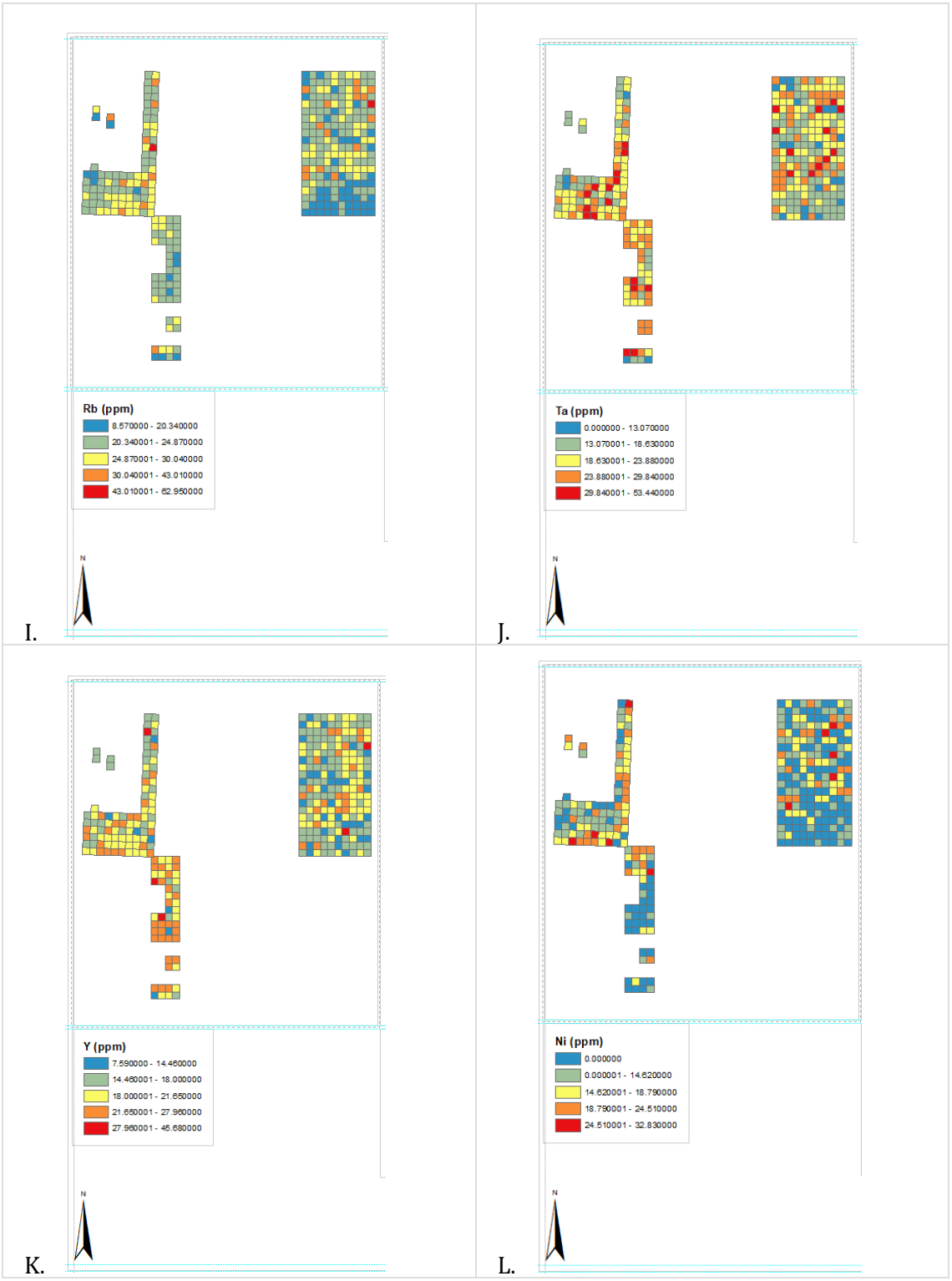
Rb (ppm)
8.570000 - 20.340000
20.340001 - 24.870000
24.870001 - 30.040000
30.040001 - 43.010000
43.010001 - 62.950000
N
Ta (ppm)
0.000000 - 13.070000
13.070001 - 18.630000
18.630001 - 23.880000
23.880001 - 29.840000
29.840001 - 53.440000
N
Y (ppm)
7.590000 - 14.460000
14.460001 - 18.000000
18.000001 - 21.650000
21.650001 - 27.960000
27.960001 - 45.680000
N
Ni (ppm)
0.000000
0.000001 - 14.620000
14.620001 - 18.790000
18.790001 - 24.510000
24.510001 - 32.830000
N

I.

J.

K.

L.

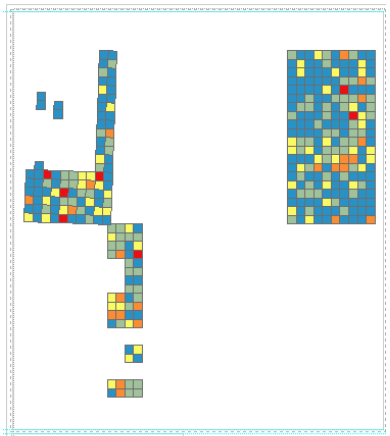
Th (ppm)
0.000000
0.000001 - 14.220000
14.220001 - 21.360000
21.360001 - 31.390000
31.390001 - 54.930000
N

M.

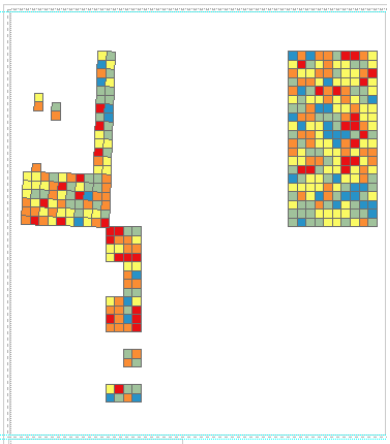
Pb (ppm)
5.380000 - 11.520000
11.520001 - 14.250000
14.250001 - 16.850000
16.850001 - 20.360000
20.360001 - 29.790000
N

N.

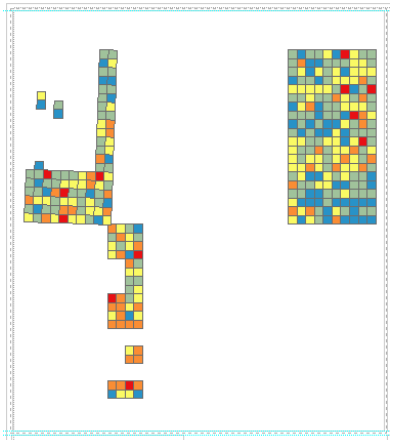
Nb (ppm)
3.860000 - 9.290000
9.290001 - 12.250000
12.250001 - 15.600000
15.600001 - 20.860000
20.860001 - 41.460000
N

O.

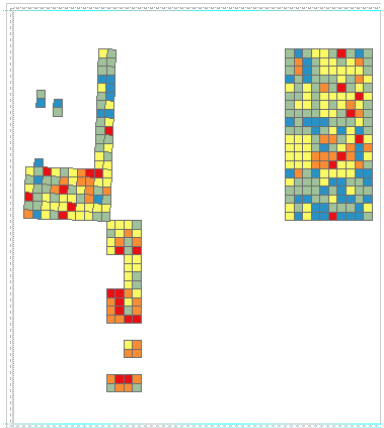
Mo (ppm)
0.000000
0.000001 - 6.940000
6.940001 - 10.870000
10.870001 - 16.480000
16.480001 - 34.350000
N

P.

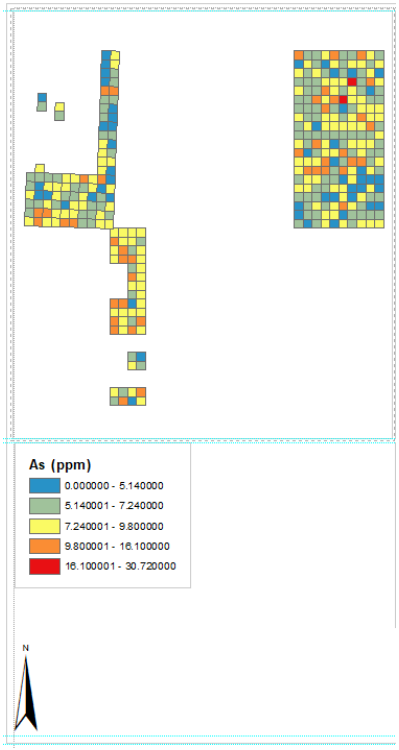
As (ppm)
0.000000 - 5.140000
5.140001 - 7.240000
7.240001 - 9.800000
9.800001 - 16.100000
16.100001 - 30.720000
N

Q.

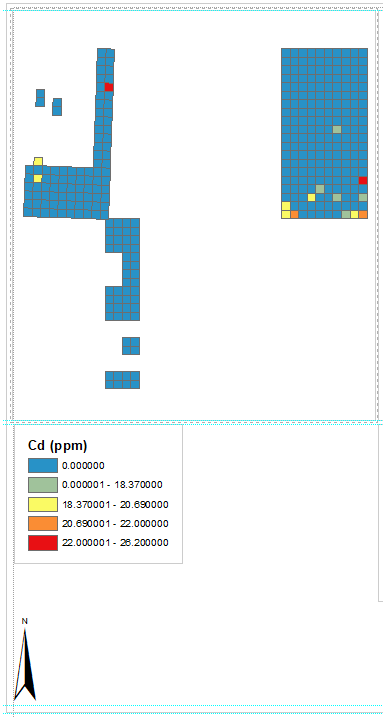
Cd (ppm)
0.000000
0.000001 - 18.370000
18.370001 - 20.690000
20.690001 - 22.000000
22.000001 - 26.200000
N

R.

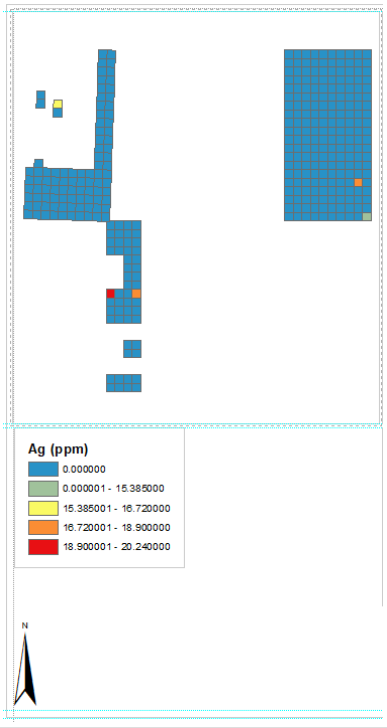
Ag (ppm)
0.000000
0.000001 - 15.385000
15.385001 - 16.720000
16.720001 - 18.900000
18.900001 - 20.240000
N

S.

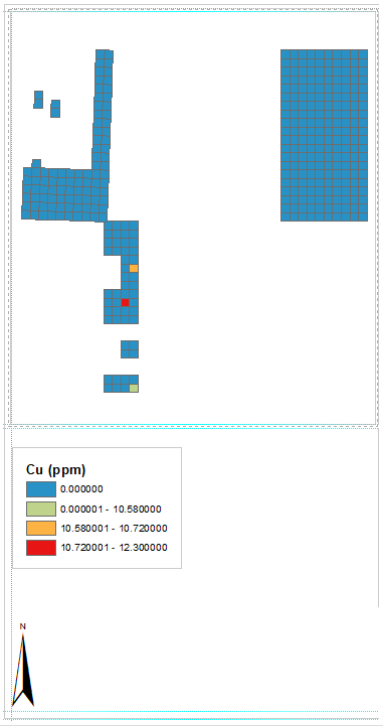
Cu (ppm)
0.000000
0.000001 - 10.580000
10.580001 - 10.720000
10.720001 - 12.300000
N

T.

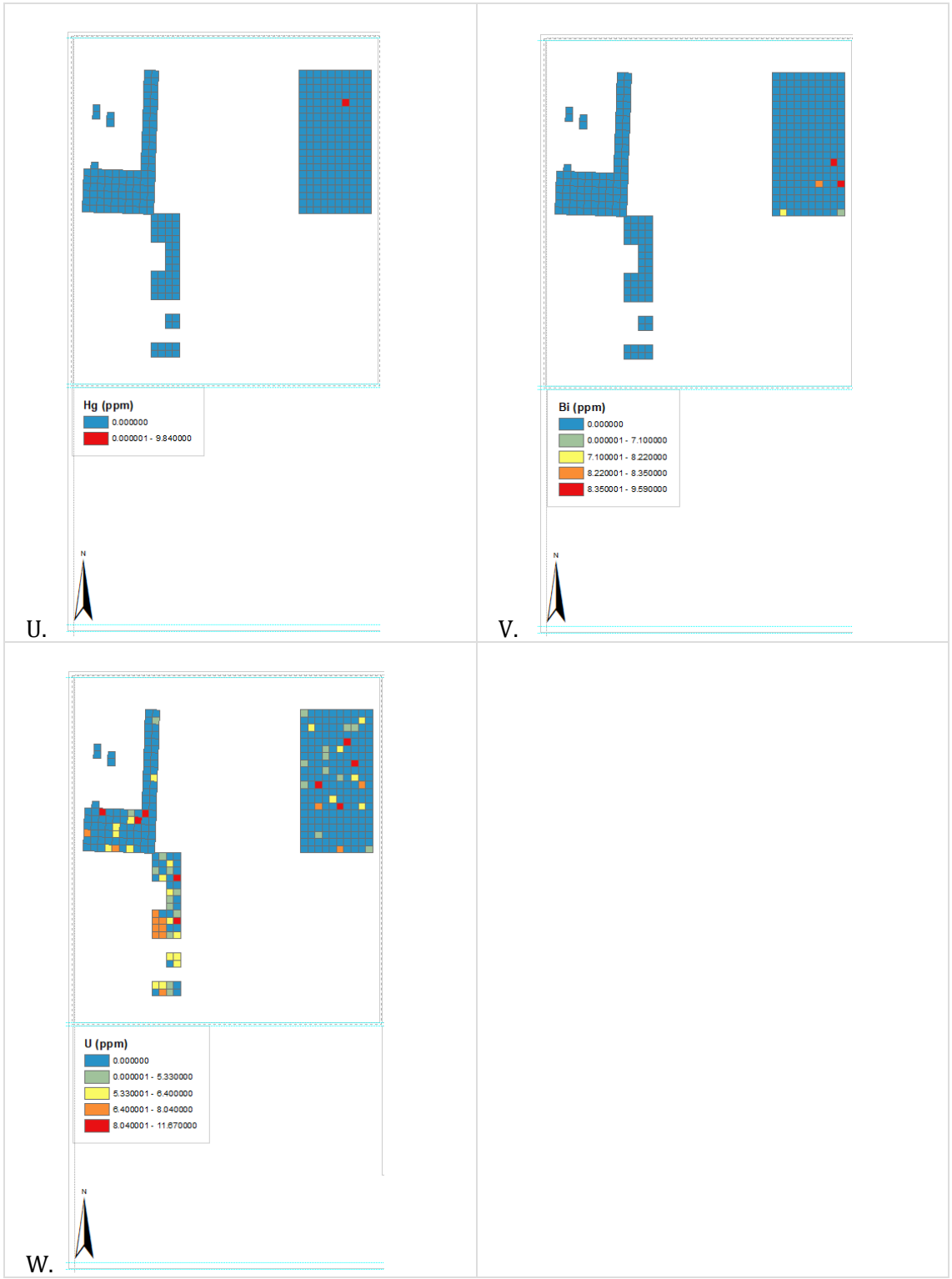

Figure 107 A-W. Basic plots of the values read in ppm from pXRF for the trace elements

The full record of plots for the trace elements is provided in Appendix Six. Cadmium, silver, copper, mercury, bismuth and to a lesser extent uranium (Figure 107 R-W) were clearly majorly affected by the lack of successful measurements above the limit of detection in most samples. The trace elements tend to conform to the patterns with the major and minor elements where the southern ends of trenches 11 and 15 are concerned, in that they are low again for some elements such as rubidium, but in other plots they are the highest readings, such as is the case with sulfur. There is not a consistent inverse to this either, for example

in yttrium the southern end of trench 11 is low while the southern end of trench 12 is above average in the elements, although it must be remembered that this element only varies between 8 to 46 ppm readings.

The area traversing from the northeastern corner of trench 11 to west-of-centre is also a cold spot for sulfur, phosphorus, chromium, and arguably lead; a hot spot for strontium, rubidium, arsenic; while for tantalum, niobium, and molybdenum this area is half hot spot and half cold spot with various outliers so is less clear but still supports there is something interesting going on in this area. Zirconium, zinc, yttrium, thorium, also have significant readings in this general area but more towards the northwest corner of the trench and this perhaps reflects a slightly different process.

Sulfur and arsenic have cold spots while phosphorus, chromium, rubidium, nickel, possibly rubidium have hot spots in the interesting zone along the northern stem of trench 15.

Various elements have hot spots in the southern end of trench 15, either around the feature area (sulfur only), in the centre/centre-south (phosphorus, vanadium, manganese, tantalum, yttrium, lead, molybdenum), or in the southeast corner going into the northwestern corner of trench 12 (chromium, arguably strontium, rubidium, possibly tantalum again, nickel, thorium, lead). These could be part of a general elevation in the area, and zinc is generally high all across the southern area, or instead the results of the influence of more than one process impacting the different regions in the area (which seems more likely given the complementary patterning in the major and minor elements).

Finally, for the area in the centre of trench 12, various elements feature hot spots there: sulfur, zirconium, vanadium, possibly chromium, tantalum, yttrium, silver, thorium, niobium, copper, molybdenum, arsenic, uranium. This is complemented by a smaller number of elements with cold spots in the area: zinc, possibly rubidium, nickel.

Phosphorus is flagged as a hot spot in the northern features area, and seems legitimately enhanced in that vicinity. In addition, silver and nickel are flagged as hot spots, and thorium, niobium, and molybdenum as cold spots by HSA alone which should be considered a lot more cautiously (especially silver as there were such a small sample for consideration there).

As with the ICP-AES results from Trench 4, while the individual elemental results have been presented in this chapter, an integrated model of the groupings of elements and a comparison with the lithics distributions are presented in chapter seven (see section 7.3.3

6.6 Summary of the dryland soils at Flixton Island 2

As such, overall the elemental readings generated by both ICP-AES and field pXRF at Flixton Island 2 produced clear patterns that suggested a number of different processes may be causing some of these signals. How different elements relate to each other and also to the lithics will be investigated through regression and grouping analysis in the integration chapter, chapter seven, which will allow for a better informed consideration of whether the patterning is caused by Mesolithic anthropogenic activities or other processes. The ICP-AES results suggested some statistically significant hot and cold spots to compare with the lithics distributions. The field XRF results do not seem to be entirely dependent on merely changing field conditions and certain areas emerged as having potential.

Activities at Flixton Island: Integrating Scientific Approaches for the Study of Early Mesolithic Living at Ephemeral Sites

Volume two of two

Charlotte Catherine Aneliese Rowley

PhD

University of York

Archaeology

November 2017

List of Contents

Abstract 2

List of Contents 3

List of Tables 10

List of Figures 16

List of Accompanying Material 27

Acknowledgements 28

Author's declaration 29

Chapter 1 Introduction 30

1.1 Project aims and objectives 30

1.1.1 Project Rationale 30

1.1.2 Research aim 31

1.1.3 Objectives 31

1.2 Flixton Island 2 as a persistent place and palimpsest 31

1.2.1 Persistent places and palimpsests in theory 31

1.2.2 Activity areas and multi-elemental soil analysis 32

1.3 The excavations and previous research at Flixton Island 2 35

1.3.1 History of research 35

1.3.2 Recent investigations 38

1.3.3 Postglacial Lake Flixton's formation and the geology of the Vale 40

1.3.4 Soils of the Vale 43

1.3.5 Contexts of the dryland site 44

1.4 Structure of this thesis 45

Chapter 2 The Founding Research into Early Mesolithic Lithics 46

2.1 Introduction 46

2.2 Theoretical approaches to studying lithic artefacts 46

2.2.1 The three main approaches in lithic studies 46

2.2.2 Typology and classification systems 48
2.2.3 Functional studies 49
2.2.4 Technological studies 50
2.3 Considering British Mesolithic lithic assemblages 52
2.3.1 The role of microliths in identifying Mesolithic assemblages 52
2.3.2 Developing typologies and the earliest identification of a British Mesolithic microlithic culture (basally modified Horsham) 55
2.3.3 Defining further microlithic cultures (Star Carr and Deepcar) 59
2.4 Starting to contextualise the Early Mesolithic cultures 64
2.4.1 Branching out from typology 64
2.4.2 Functional approaches to assemblages 65
2.4.3 Early dating of Mesolithic cultures and exploring seasonality 72
2.4.4 Clarke's challenge to oversimplification 81
2.5 Summary 84
Chapter 3 The Dating and Chronology of Early Mesolithic assemblages 86
3.1 Introduction 86
3.2 Roger Jacobi's work on Early Mesolithic Chronologies 86
3.3 Michael Reynier's work on the definitions and chronology of Early Mesolithic cultural groups 90
3.3.1 Background 90
3.3.2 Typological work 90
3.3.3 Chronological work 97
3.4 Recent research on Early Mesolithic Chronologies 104
3.5 Summary 110
Chapter 4 The Lithics Assemblage from Flixton Island 2 112
4.1 Introduction 112
4.2 Methods 113
4.2.1 General methodology 113
4.2.2 Recorded attributes 114

4.2.3 Categories 116
4.2.4 Phasing 117
4.2.5 Issues 119
4.3 The Long Blade Assemblage 121
4.3.1 A possible Federmesser find 125
4.4 The Mesolithic Assemblage 125
4.4.1 Overview 125
4.4.2 Overall Spatial Patterning 130
4.4.3 Burnt and Heated Material 133
4.4.4 Raw materials 135
4.4.5 Technology 142
4.4.6 Knapped tools 153
4.4.7 Core Tools 173
4.4.8 Tool preparation debitage 181
4.5 Summary and discussion 182
Chapter 5 Geoarchaeological and Geochemical Research Methods 184
5.1 Introduction 184
5.2 Micromorphology 185
5.3 Sampling for geoarchaeological testing and elemental analyses in 2012 185
5.4 Basic geoarchaeological assessment 186
5.4.1 Soil colour and texture 187
5.4.2 Estimated carbonate presence 187
5.4.3 pH 187
5.4.4 Estimated phosphorus presence 188
5.4.5 Summary 188
5.5 Portable Energy-Dispersive X-ray Fluorescence (pXRF) 189
5.5.1 Introduction to pXRF 189
5.5.2 pXRF Equipment 189
5.5.3 pXRF analysis strategy in the field at Flixton Island 2 190

5.5.4 Accuracy, precision, quality assurance and controls conducted in the field for pXRF 191
5.5.5 Complementary sampling strategy for supplementary pXRF analysis in the lab at Flixton Island 2 and Star Carr 206
5.5.6 Procedure for pXRF analysis in the laboratory 206
5.5.7 Quality assurance and control readings for lab-based pXRF 207
5.5.8 pXRF results utilised for spatial mapping 210
5.6 Inductively Coupled Plasma Atomic Emission Spectroscopy (ICP-AES) 211
5.6.1 ICP-AES sampling strategy 211
5.6.2 ICP-AES sample preparation 211
5.6.3 ICP-AES analysis 212
5.6.4 ICP-AES outputs 213
5.6.5 Quality assurance and control readings for ICP-AES work 215
5.6.6 ICP-AES results used in spatial mapping 216
5.7 Statistical Analysis Methods 216
5.7.1 Handling data below the limit of detection 217
5.7.2 Descriptive statistics and basic plots 219
5.7.3 Hot Spot Analysis 220
5.7.4 Cluster and Outlier Analysis 221
5.7.5 Grouping Analysis 221
5.7.6 Principal Component Analysis 223
5.8 Summary 223
Chapter 6 Results of Geochemical Analyses on Flixton Island 2 soil samples 224
6.1 Introduction 224
6.2 General physical characterisation of the dryland soils 225
6.3 General elemental characterisation of sediments on site 229
6.4 Results from Trench 4 (2012 excavation) 233
6.4.1 Trench 4 Descriptive and Exploratory Statistics 234

6.4.2 Spatial visualisation of Trench 4 elemental concentrations measured by ICP-AES 252
6.5 Results from pXRF on Trenches 11, 12, and 15 (2014 excavation) 262
6.5.1 Descriptive and exploratory statistics on the dryland trenches excavated in 2014 267
6.5.2 Spatial visualisation of 2014 dryland trench field pXRF results 271
6.6 Summary of the dryland soils at Flixton Island 2 285
Chapter 7 Comparing Patterning in the Flixton Lithics and Soils 311
7.1 Introduction 311
7.2 A deeper exploration of spatial patterning in the Mesolithic lithics 311
7.2.1 Establishing the significance of the clusters 311
7.2.2 Establishing the extent of the clusters using Density Analysis on 3D located lithics data 313
7.2.3 Display of the sieve lithics data 316
7.2.4 Profiles of the lithic scatters 317
7.2.5 Discussion about the scatter profiles 323
7.3 A deeper exploration of spatial patterning in the soils 325
7.3.1 Integrating the elements into one model 325
7.3.2 Results of the Grouping Analysis of Trench 4 ICP-AES Results (from 2012 excavations) 326
7.3.3 Grouping Analysis for Trenches 11, 12 (north), and 15 field pXRF Results (from 2014 excavations) 335
7.4 Discussion 348
Chapter 8 Geochemistry on Structures at Star Carr 349
8.1 Introduction 349
8.2 Introduction to the structures 350
8.3 Potential complications 353
8.4 Individual Elemental Results 354
8.5 Grouping Analysis at Star Carr 359

8.5.1 Grouping analysis on the upper ICP-AES dataset from Star Carr based on major and key element results 359
8.5.2 Ruling out patterning due to proximity alone 362
8.6 Principal Component Analysis 363
8.6.1 Results of PCA on the Star Carr upper dataset 363
8.7 Summary and Comparison with Flixton Island 2 365
Chapter 9 Discussion and Conclusions 366
9.1 The question of activity at Flixton Island 2 366
9.2 Chronology, persistence and palimpsests 368
9.3 The people and activities at Flixton Island 2 372
9.4 Conclusions 375
Appendix 1 Deepcar-type assemblages, as outlined by Radley and Mellars (1964) 377
Appendix 2 Lithics Cataloguing, Definitions, and Typological Classification Notes 382
Categories used on catalogue spreadsheets 382
Appendix 3 Micromorphology notes 395
Taking the sample 395
Thin section processing 396
Microscopic analysis 398
Appendix 4 Field pXRF Quality Assurance and Control 400
Calibration Check Record for Flixton Island 2, 2014 field season 400
Beam Runtime Evaluation 400
Repeat readings from “control” areas 406
Overview 406
Elemental classifications by trench 407
Full data for Flixton Field pXRF 408
Star Carr 425
Appendix 5 Lab-based pXRF Quality Assurance and Control 439
Calibration Check Record 439
Control Readings 439

Systematic experimentation confirming polythene bags interfered with pXRF readings 440
General experiment premise 440
Equipment setup and blank readings 441
Control Sample Analyses 443
Appendix 6 Supplementary Statistical Tables and Graphs for Flixton Island 2 Geochemical Analyses 453
Introduction 453
VP12 ICP-AES Full Dataset 453
VP12 ICP-AES Individual Element Histograms (batches 1 and 4, Trench 4) 453
VP12 ICP-AES Individual Element Spatial Analysis Results (Trench 4) 463
Major 463
Minor 464
Trace 467
IUPAC Trace 473
VP14 FpXRF Full Dataset 490
VP14 FpXRF Individual Element Histograms 490
VP14 FpXRF Individual Element Spatial Analysis Results for Trenches 11, 12 and 15 .506
Major 506
Minor 507
Trace 509
IUPAC Trace 512
Appendix 7 Development of the Grouping Analysis model 521
Abbreviations 522
Glossary 523
Bibliography 527

List of Tables

Table 1. Early Mesolithic radiocarbon dates from Jacobi 1973, p.261. *Site codes obtained from Jacobi 1978. 86

Table 2. Early Mesolithic radiocarbon dates extracted from Jacobi 1976, pp.67–69. 88

Table 3. Early Mesolithic radiocarbon dates from Jacobi 1978, pp.297–301, with various Upper Palaeolithic dates discussed for comparison. 89

Table 4. The frequencies of microliths (blue in chart) and standard tools (orange) included in the study of sites suggested to be characteristically 'Deepcar' by Reynier (2005, 20).... 92

Table 5. Summary of Reynier's proposed typological characteristics for Star Carr, Deepcar and Horsham type assemblages (summarized from Reynier 2005, 18–22). 93

Table 6. Reynier's dates, information, and the calibrated values (dates sourced from Reynier 2005; calibration by C. Rowley) 102

Table 7. Lithic artefact categories employed during this study 116

Table 8. Summary of Long Blade assemblage finds by context groups 118

Table 9. Summary of the Mesolithic assemblage by context groups 119

Table 10. Proportion of burnt material in the Long Blade assemblage 123

Table 11. The Flixton Island 2 Mesolithic assemblage, overall breakdown 127

Table 12. The 'essential' assemblages for Flixton Island 2 and various example sites drawn from Mellars (1976), with the exception of the recent data for Star Carr drawn from Conneller et al. (2018) which she categorises as a Type B site. All Type B sites described by Mellars are provided. The Type A and B1 examples were chosen as being the sites summarised in Mellars with the lowest proportion of microliths (their defining aspect being that their assemblages show a high proportion of microliths), while the Type C example was chosen, similarly, for it being that with the lowest proportion of scrapers (high proportions of scrapers being the defining characteristic of that group). *saws = terminology Mellars uses meaning microdenticulates. 129

Table 13. The burnt and unburnt proportions of the assemblage 133

Table 14. Relative percentages of the source of cores deposited at Flixton Island 2 139

Table 15. Summary of the raw materials used to manufacture different tool categories.. 140

Table 16. Summary of the raw materials used to manufacture key tool types at Flixton Island 2 and Star Carr (data for the former from Conneller et al. 2018) 140

Table 17. Core types in the Mesolithic assemblage....143

Table 18. Comparison of core type assemblages from different Star Carr, Deepcar, and Horsham type sites (Star Carr data reproduced from Conneller et al. (2018) and southern sites derived from Reynier 2005, pp. 32 - 40, with type C cores associated with Reynier's "3 platforms, continuous" category and D and E cores associated with his "other" category 144

Table 19. Complete cores retrieved from sieving....146

Table 20. Summary of the core dimensions....148

Table 21. Summary of the core preparation debitage....149

Table 22. Raw materials of the core preparation debitage artefacts....149

Table 23. Primary and secondary debitage....151

Table 24. Core reduction and general debitage in the Mesolithic assemblage, including tested nodules of raw material ("complete" referring to complete flakes, blades or bladelets) 152

Table 25. Dimensions of measured complete flakes, blades, and bladelets (primary, secondary, or tertiary) in millimetres. 152

Table 26. The microlith assemblage by form. *Pieces described as "interrupted" in the table are those that have generally been retouched into a shape but where the apex of the arc or peak of the triangle is not retouched itself, thus leaving a small shoulder 154

Table 27. Summary of microliths retrieved from sieving, by trench 159

Table 28. Summary of scraper types....165

Table 29. Summary of the frequencies of scrapers retrieved from sieving, by trench....167

Table 30. The burin assemblage....168

Table 31. Relative proportions of the Mesolithic core tool assemblage....173

Table 32. Estimating calcium carbonate....187

Table 33. Eidt and Woods' (1974) phosphate spot test ratings....188

Table 34. Criteria utilised for assessing major, minor, and trace element contributors to samples/readings. *The International Union of Pure and Applied Chemistry (IUPAC) Gold Book defines trace elements as "any element having an average concentration of less than about 100 parts per million atoms (ppma) or less than 100 μg / g" (IUPAC 2009)....192

Table 35. Elements analysed through ICP-AES conducted by ALS Chemex (ME-ICP41), the units results are provided in, and the upper and lower detection limits for specific elements

(modified from Minerals 2009 with amendment received from Louise Clarke, ALS Minerals, pers. comm.) 213

Table 36. Basic geochemical assessment of samples from trench 4 226

Table 37. The results of the readings on topsoil and till controls from Flixton Island 2 by ICP-AES (ordered by highest content in the till sample) 230

Table 38. Descriptive statistics for some of the major and key minor elements analysed in local tills (in ppm). The table includes the results from the seven 'till' controls from Star Carr (values in parts per million), the Flixton Island 2 'till' control results for comparison (all analysed as part of this project by ICP-AES), along with C. Boston's readings in parts per million for tills at Skipsea and Filey on the east coast in Yorkshire, analysed by ICP-MS analysis (reproduced with permission from Boston 2007). All values were rounded to the nearest integer where appropriate 232

Table 39. Descriptive statistics including the number of valid readings (N) and the mean, median, standard deviation, range and maximum and minimum values in ppm from ICP-AES Batch 1 (main trench 4 results). a. Multiple modes exist. The smallest value is shown 235

Table 40. Descriptive statistics including the number of valid readings (N) and the mean, median, standard deviation, range and maximum and minimum values in ppm from ICP-AES Batch 4 (trench 4 expansion). a. Multiple modes exist. The smallest value is shown 237

Table 41. Number of valid readings (N), the mean, median, standard deviation, coefficient of variance, range, maximum and minimum values from lab pXRF analyses on subsample of 10 from trench 4 (units: ppm, where not dimensionless). a. Multiple modes exist. The smallest value is shown 239

Table 42. Statistics relating to skewness and kurtosis of ICP-AES results from trench 4..250

Table 43. Dates of pXRF analysis in the field at Flixton Island 2 as well as notes on conditions made in the field and highlights from the Met Office report for August 2014 (The Met Office 2015) (The Met Office 2015) 264

Table 44. Descriptive statistics for all the elements as measured in the field by pXRF, sorted by descending mean value. a. Multiple modes exist. The smallest value is shown 269

Table 45. Descriptive statistics for the major and key minor elements measured from samples recorded as till at Star Carr (values in parts per million). (Table reproduced from Table 21.2 in Rowley et al. 2018.) 354

Table 46. Ranges of values (ppm) from Star Carr tills compared with Boston's readings on till samples from Skipsea and Filey (reproduced with permission from Boston 2007) 355

Table 47. Plots of the central structure readings for each of the key elements, displayed by Jenks natural breaks in the non-normalized readings (in parts per million). (Reproduced from Rowley et al 2018.) 355

Table 48. ArcMap generated R2 values for each variable from the four different models for nine groupings at Star Carr. They are colour coded from highest values (red) to lowest (blue), with the highest and lowest values in bold font 360

Table 49. Detail of attributes recorded in lithics catalogue 384

Table 50. Calibration checks in the field at Flixton Island 2. *Time settings for analyser had been reset, this is the timestamp as embedded in the datafile. **It is unknown why these times were not recorded by the analyser 400

Table 51. Run time experiment details 401

Table 52. Run time experiment results 401

Table 53. A record of the readings taken in the field at Flixton in August 2014, both for repeats and for new readings, as well as notes on conditions made in the field and highlights from the Met Office report for August 2014 (The Met Office 2015). 406

Table 54. Summary of Field pXRF control reading results for trench 11 407

Table 55. Summary of Field pXRF control reading results for trench 12 408

Table 56. Summary of Field pXRF control reading results for trench 15. There were four different control spots read from the same grid square for Trench 15. This gives an estimation of the variability from within one grid square as well as providing the daily repeats for field conditions 408

Table 57. Trench 11 Field pXRF control readings data (rounded to 2 d.p.) 410

Table 58. Trench 11 Field pXRF control readings descriptive statistics (to 2 d.p.) 412

Table 59. Trench 12 Field pXRF control readings data (to 2 d.p.) 413

Table 60. Trench 12 Field pXRF control readings descriptive statistics (to 2 d.p.) 415

Table 61. Trench 15 Field pXRF control readings data (to 2 d.p.). *n/a = element in another category for this sample 416

Table 62. Trench 15, sample location 1 Field pXRF control readings descriptive statistics (to 2 d.p.) 419

Table 63. Trench 15, sample location 2 Field pXRF control readings descriptive statistics (to 2 d.p.) 420

Table 64. Trench 15, sample location 3 Field pXRF control readings descriptive statistics (to 2 d.p.) 421

Table 65. Trench 15, sample location 4 Field pXRF control readings descriptive statistics (to 2 d.p.) 422

Table 66. Trench 15 Field pXRF control readings descriptive statistics for all four reading locations considered as one set of data (to 2 d.p.) 423

Table 67. Descriptive statistics for all repeat readings across all trenches at Flixton using field pXRF (to 2 d.p.) 424

Table 68. Summary of control field pXRF results for Star Carr's western structure area 425

Table 69. Data for the field pXRF control repeats at Star Carr 425

Table 70. Descriptive statistics for the control field pXRF repeats at Star Carr (2 d.p.) 429

Table 71. Details of standard control repeats taken during the field season at Star Carr 430

Table 72. Standard control repeat results, taken while in the field at Star Carr 431

Table 73. Percent deviation of readings from the expected value of control samples 2710a and 2711a in the field at Star Carr (green: less than +/- 5 % out; light blue 5-20 % low, dark blue more than 20 % below expected values; light red 5-20 % high, dark red greater than 20 % high) 435

Table 74. Descriptive statistics for readings of control samples 2711a in the field at Star Carr, taken 2015 (ppm) 437

Table 75. Descriptive statistics for readings of control samples 2710a in the field at Star Carr, taken 2015 (ppm) 438

Table 76. Calibration check record for lab-based pXRF 439

Table 77. Readings for the five major elements in parts per million (ppm) in the bags. <LOD means below the limit of detection for that element in Geochem mode on this machine. 441

Table 78. Readings for the seven lesser important elements in ppm in the bags. <LOD means below the limit of detection. 442

Table 79. Readings for the five major elements in ppm for single layers of cling film. <LOD means below the limit of detection 442

Table 80. Readings for the seven lesser important elements in ppm in a single layer of cling film. <LOD means below the limit of detection. 442

Table 81. Values in ppm for control sample of soil NIST 2710a. The certified values are in the top row while readings taken on the departmental pXRF are in subsequent rows and have a reading number. <LOD = below limit of detection. 445

Table 82. Values in ppm for control sample of soil NIST 2711a. The certified values are in the top row while readings taken on the departmental pXRF are in subsequent rows and have a reading number. <LOD = below limit of detection. 446

Table 83. Values in ppm for control sample of silicon dioxide. The certified values are in the top row while readings taken on the departmental pXRF are in subsequent rows and have a reading number. <LOD = below limit of detection. 448

Table 84. NIM-GBW07408 certified values of oxides for major elements and ppm for minor elements, all converted to estimate ppm for each central atom of an element plus its bonded oxygen atoms in the oxide form. Numbers in bold and dark red are those provided on the original certification. 450

Table 85. Values in ppm for the major elements in the control sample of NIM-GBW07408, as read by the departmental pXRF 450

Table 86. Values in estimated oxide wt % for the major elements. All except titanium were converted to the oxides listed. Titanium, having been provided in ppm as a minor element in the certified values, was not converted to an oxide but its ppm simply converted 451

List of Figures

Figure 1. Moore's shouldered point (as published as Plate XVI in Clark 1954, p.136, not to scale) 36

Figure 2. Previous excavations at Flixton Island, image reproduced from an internal report by Barry Taylor (POSTGLACIAL Project). Grey trenches indicate Moore's investigation, red trenches were carried out by the VPRT. Site 1 is on the southern part of the island in the vicinity of Moore's large grey trench and site 2 is on the more northerly, dual peaked, part of the island, with the two parts nearly connected by a gravelly ridge. 37

Figure 3. The POSTGLACIAL Excavations, relative to previous excavations in the vicinity (the area delineated in the inset map shows the excavations relative to Figure 2). Contour data was created by Barry Taylor for the POSTGLACIAL project during the environmental coring project that formed his PhD (Taylor 2012) 39

Figure 4. The general areas discussed throughout the text 40

Figure 5. The location of (a) the Vale of Pickering, (b) the uplands enclosing the vale, (c) the underlying geological deposits in the vale, with the orange being lacustrine deposits suggesting the edges of glacial palaeolakes Pickering and Flixton (reproduced from Evans et al. 2017, p.296) 41

Figure 6. The location of the archaeological sites around Palaeolake Flixton, with (a) showing the margins of the British-Irish Ice Sheet and (b) showing the important Palaeolithic and Mesolithic sites on the lake edges (reproduced from Candy et al. 2015, 61) 42

Figure 7. Photomicrograph of aggregated mixture of amorphous iron replaced organic material, humic fine-medium quartz sand and humic clay, sample Flixton VP12/1 (4.5mm = frame width; plane polarized light) (reproduced from internal report by French 2015) ... 44

Figure 8. Callender's Scottish microliths (1927, p. 319) (not to scale) 53

Figure 9. Clark's microlith classifications, showing examples of all major types (A - G). For the geometric forms i.e. type D microliths, subtype 1 are triangles, 2 crescent, 3 lozenge, 4 lanceolate, 5 sub-triangular, 6 trapezoid, 7 rhomboid, 8 trapeze (after Clark 1933, 56–60). Not to scale. 57

Figure 10. Clark's Microlithic 'spectra' (reproduced from Clark 1933, p.64) 58

Figure 11. The microlithic industry from Deepcar, Yorkshire (reproduced from Radley and Mellars 1964, p.10, not to scale) 61

Figure 12. Awls from Deepcar (reproduced from Radley and Mellars 1964, p.17, not to scale)..... 62

Figure 13. Warcock Hill South's awls (reproduced from Radley and Mellars 1964, p.17, not to scale). 64

Figure 14. The Loshult arrow (photograph by Arne Sjöström, reproduced from Larsson and Sjöström 2011a). 67

Figure 15. Microliths and microburins from Thatcham (reproduced from Wymer & King 1962, p.342)..... 71

Figure 16. Jacobi's microlith classification system here based on examples from Mesolithic Wealden. (1-4) Broad blade microliths; (5-9) Narrow Blade microliths; (10) Hollow-based points; (11-13) Inversely retouched points (reproduced from Jacobi 1978b, 16)..... 74

Figure 17. Clarke's examples of hafted microliths as reproduced by Butler (2005, 89)..... 84

Figure 18. Reynier's comparative microlith typology clustered bar chart (2005, p.25). The typologies are: 1 – oblique points; 2 -partially backed points; 3 – triangles; 4 – rhomboids; 5 – trapezoids; 6 – backed points; 7 – transversely based points; 8 – obliquely based points; 9 – hollow based points; 10 – tanged points (2005, p.25) 95

Figure 19. Reynier's box and tail diagram of British Early Mesolithic radiocarbon dates. The dates are uncalibrated, arranged in their chronological order with the tails set at 2 standard deviations (s.d.). The dashed vertical lines indicate the dating plateaux (2005, p.69)..... 99

Figure 20. The dates utilised by Reynier having been calibrated in OxCal v4.2.4, using the IntCal13 atmospheric curve. The site, date identification code, and site types are appended as the labels..... 101

Figure 21. Probability distributions of radiocarbon dates associated with Star Carr-type microlith assemblages (Reproduced from Conneller et al. 2016, p.6.)..... 107

Figure 22. Probability distributions of radiocarbon dates associated with Deepcar-type microliths assemblages (reproduced from Conneller et al. 2016, p.7)..... 108

Figure 23. Probability distributions of radiocarbon dates associated with Basally Modified microliths (reproduced from Conneller et al. 2016, p.8)..... 109

Figure 24. Summary of the use of Early Mesolithic assemblage types as proposed by Conneller et al. The shading reflects the probability that an assemblage type was in use at a particular time (reproduced from Conneller et al. 2016, p.10). 110

Figure 25. All 3D located lithics across the site, symbolised by classification as Long Blade/Federmesser or Mesolithic..... 113

Figure 26. Examples of patinated flint (the centre piece is also burnt). Find numbers, from left to right: <100735>, <107356>, and <100242>. 120

Figure 27. The Long Blade assemblage 121

Figure 28. 3D located Long Blade and Federmesser material 122

Figure 29. Raw materials of the Long Blade assemblage 122

Figure 30. Find <110501> (Photo taken by N. Gevaux) 124

Figure 31. <100213> (Photo taken by N. Gevaux) 124

Figure 32. <106967> (left) and Figure 33. <100242> (photos taken by N. Gevaux) 124

Figure 34. <106591> (Photo taken by N. Gevaux) 125

Figure 35. Overview of the Flixton Island 2 Mesolithic assemblage 126

Figure 36.The complete 3D located Mesolithic assemblage, with finds from categorically gully contexts symbolised separately 130

Figure 37. The 3D located Mesolithic assemblage from the main dryland trenches 131

Figure 38. Zoom on the gully and bar 132

Figure 39. The Mesolithic assemblage from the wetland trenches 132

Figure 40. Examples of burnt or heated material. 133

Figure 41. The burnt Mesolithic material from Flixton highlighted against the unburnt material 134

Figure 42. The burnt Mesolithic tools compared with other burnt material 135

Figure 43. The Flixton Island 2 Mesolithic assemblage in terms of raw material used 137

Figure 44. Photograph of the chert artefacts (photography by N. Gevaux). Find numbers, from left to right: sl/191 and sl/15. 137

Figure 45. Photograph of the possibly limestone artefacts. Find numbers, from left to right: sl/194, sl/192, and sl/193....137

Figure 46. Red-tipped material (photography by N. Gevaux). Find numbers, from left to right: <101285>, <103931>, and <105663>. 138

Figure 47. Raw materials of the Mesolithic cores 139

Figure 48. The Mesolithic core technology, with proportion of the core technology assemblage and artefact count (total count: 192 artefacts) 143

Figure 49. Examples of cores (photography by N. Gevaux). From left to right, top row then bottom: <100617> A2 type in Wolds flint; <101357> B1/irregular core in till flint; and <106899> B1 core in Wolds flint. 145

Figure 50. Distribution of the 3D located complete cores 145

Figure 51. 3D located cores by type (N.B. there was one additional A1 type core in the wetland, not illustrated here) 146

Figure 52. Cores displayed by maximum length as a crude proxy for size 147

Figure 53. The distribution of core preparation debitage and core fragments, alongside the complete core assemblage 150

Figure 54. Photographs of a selection of microlith types from the site (photography by N. Gevaux) 155

Figure 55. Distribution of the microliths and microburins across the site 158

Figure 56. Distributions of the different microlith types across the dryland 159

Figure 57. Examples of the awls/piercers and mèches de foret (photography by N. Gevaux) 162

Figure 58. Distribution of the 3D located awls, piercers and mèches de foret 164

Figure 59. Examples of scrapers (photography by N. Gevaux) 165

Figure 60. The distribution of scrapers and partial scrapers 166

Figure 61. Scrapers by type 167

Figure 62. Examples of the burins (photography by N. Gevaux). 1 is a dihedral burin, 2 is a double angle break burin, and 3 is a possible dihedral burin. 169

Figure 63. Distribution of burins and partial burins 170

Figure 64. The microdenticulates (photography by N. Gevaux) 171

Figure 65. Distribution of the 3D located microdenticulates 172

Figure 66. Distribution of the 3D located core tools across the site 174

Figure 67. Tranchet axe/adze <101854> (photography by N. Gevaux) 175

Figure 68. Preform / broken adze <101636> (photography by N. Gevaux) 176

Figure 69. Photo of small roughout / near complete adze <106735> (photography by N. Gevaux) 177

Figure 70. Roughout <100813> (photography by N. Gevaux) 179

Figure 71. Roughout <104850> (photography by N. Gevaux) 180

Figure 72. Example of a strike-a-light (photography by N. Gevaux).....181

Figure 73. Mesolithic tool preparation debitage assemblage.....182

Figure 74. The sampling strategy for trench 4 (VP12): black dots indicate the full array of samples taken; red triangles are those analysed by ICP-AES to provide general coverage; those in yellow were analysed by ICP-AES, pXRF in the laboratory, and general testing such a pH measurement for more detailed understanding.....186

Figure 75. Sampling in the field in trench 4 (photograph by the POSTGLACIAL project) .186

Figure 76. A reading being taken in trench 11 using the soil foot setup (photograph courtesy of the POSTGLACIAL project).....191

Figure 77. Plan of grid pXRF readings were taken on (one reading per square), in the field at Flixton in 2014 191

Figure 78 A - C. Dot plots of the major element values read from the repeat readings in the same location on different days in the field by pXRF. Note, trench 15's plot depicts 4 pairs of repeats at 4 different 'sample' locations (S1 - 4) in the trench, from within the same grid square.....195

Figure 79 A - C. Minor element values read from repeats on different days in the field by pXRF.....198

Figure 80 A-C. Dot plots of the trace element values read from repeats on different days in the field by pXRF.....200

Figure 81 A-C. Dot plots of the IUPAC trace element values read from repeats on different days in the field by pXRF. If a sample had a successful reading of an element in one repeat but not the other, the reading below the limit of detection is displayed as a point at 1 ppm. If an element was not read at all in any sample, it is not included in any plot 202

Figure 82 A - C. Dot plots of the IUPAC trace element values read from repeats on different days in the field by pXRF: the same results as in Figure 8 but with error bars.....203

Figure 83. Vertical setup for the Olympus Flex Stand, looking down on the stand, with the lid of the chamber lifted to show inside the chamber and the analysis window.....207

Figure 84. The ten samples used in the basic geochemical assessment.....227

Figure 85. Excavations in trench 4 during the 2012 excavation season: this is at the base of the soil, with the yellowish till exposed and only shallow lenses of the mixed soil-till interface (1119) remaining except behind the excavators (photography by the POSTGLACIAL project).....227

Figure 86. A plot of the pH readings from trench 4, ranging from pH 6.83 (slightly acidic) to 7.37 (neutral) 228

Figure 87. Samples analysed from trench 4, labels denoting grid square and with location points symbolised by submission batch (triangle for batch 1 ICP-AES, circle for expansion batch 2 ICP-AES, blue for samples use for the basic assessment and analysed by pXRF). The plans of potential features are also shown (at the western end of the trench) 233

Figure 88 A-E. Comparison of the means for each element as read by ICP-AES (batches 1 and 4) and pXRF in the trench 4 samples. All values in ppm 244

Figure 89. ICP-AES results from all samples in trench 4 (from batches 1 and 4), alongside the results from just batch 1. Visualised using Jenks natural breaks 253

Figure 90. The basic visualisation (Jenks Natural Breaks; top), Hot Spot Analysis (centre), and Cluster-Outlier Analysis (bottom) for iron results (Fixed Band Neighbourhood = 1.85m) 254

Figure 91. The basic visualisation (Jenks; top), Hot Spot Analysis (centre), and Cluster-Outlier Analysis (bottom) for aluminium results (Fixed Band Neighbourhood = 1.85m). 255

Figure 92. The basic visualisation (Jenks; top), Hot Spot Analysis (centre), and Cluster-Outlier Analysis (bottom) for calcium results (Fixed Band Neighbourhood = 1.85m) 256

Figure 93. The basic visualisation (Jenks; top), Hot Spot Analysis (centre), and Cluster-Outlier Analysis (bottom) for magnesium results (Fixed Band Neighbourhood = 1.85m). 257

Figure 94. The basic (Jenks Natural Breaks) visualisation of the results for all detected trace elements. 260

Figure 95. The analysis strategy for field pXRF carried out on the Flixton Island dryland trenches in 2014, with south circular feature illustrated (other two potential features too indistinct and not planned). 262

Figure 96. pXRF analysis grid colour coded by date of analysis 263

Figure 97. An aerial view from the east of the site, with trench 11 in the foreground and the long, thin trench 12 to the south, starting to run down into the lake area to the south (with trench 15 to the northwest of 12 and the wetland trenches to the north of all of these). North is to the left of the picture. Cropped from photograph taken by Paul Howden 265

Figure 98. An elevated photograph facing southeast from the northwest of trench 11, where the slight dip into the southeastern (far) corner can be made out, along with plough marks in the centre-south area of the trench. (Photo taken by the POSTGLACIAL Project.) 265

Figure 99. An elevated side view from the western side of trench 15 (with the northern end of trench 12 to the southeast and trench 11 to the north in the background). (Photo taken by the POSTGLACIAL project.) 266

Figure 100. Simple, HSA and C-OA (left to right) plots of readings from pXRF for silicon 271

Figure 101. Simple, HSA and C-OA plots of readings from pXRF for aluminium 272

Figure 102. Simple, HSA and C-OA plots of readings from FpXRF for iron 274

Figure 103. Simple, HSA and C-OA plots of readings from FpXRF for calcium 275

Figure 104. Simple, HSA and C-OA plots of readings from FpXRF for potassium 276

Figure 105. Simple, HSA and C-OA plots of readings from FpXRF for titanium 277

Figure 106. Simple, HSA and C-OA plots of readings from FpXRF for chlorine 277

Figure 107 A-W. Basic plots of the values read in ppm from pXRF for the trace elements 283

Figure 108. Results of the Average Nearest Neighbour analysis on the main dryland area, which suggests statistically significant clustering based on the 3D located assemblage (autogenerated by the ANN tool, ArcMap). 313

Figure 109. Kernel Density plot of the 3D located Mesolithic assemblage 314

Figure 110. Kernel Density plot of the 3D located Mesolithic assemblage, with the general area polygons superimposed 315

Figure 111. Overlaying the weighted centroids for sieve lithics over the density analysis of the 3D lithics (only sieve material from trenches 4, 9 and 12 could be reliably visualised by grid square as 11 and 15 were impacted by post-excavation errors as discussed in section 4.2.5 317

Figure 112. The density raster across the main dryland area. The outer edge of the layer highlighted red in the density raster was used to define the outer bounds for the three main scatters (southwest, central, and southeast dryland) 318

Figure 113. The 3D located lithics falling within the grid squares identified as the main scatter squares 318

Figure 114. The artefact counts for different lithic categories in the central dryland scatter 320

Figure 115. The artefact proportions for different lithic categories in the central dryland scatter, 3D located data only 320

Figure 116. The artefact proportions for different lithic categories in the central dryland scatter, 3D and sieve data combined....321

Figure 117. The artefact counts for different lithic categories in the southwest dryland scatter, 3D located data only....321

Figure 118. The artefact proportions for different lithic categories in the southwest dryland scatter, 3D located data only....322

Figure 119. The artefact counts for different lithic categories in the southeast dryland scatter, 3D located data only....322

Figure 120. The artefact proportions for different lithic categories in the southeast dryland scatter, 3D located data only....323

Figure 121. The 3D located microlith and scraper distributions superimposed over the density raster....324

Figure 122. Example of a two group run incorporating all major/minor elements....327

Figure 123. The parallel box plot associated with the two group run in the previous figure....327

Figure 124. Example of a five group run incorporating all major/minor elements....328

Figure 125. The parallel box plot associated with the five group run in the previous figure....328

Figure 126. Example of a seven group run incorporating all major/minor elements, with the potential activity areas highlighted. The red outlined areas are those lower in calcium; the blue is those moderately higher in calcium and moderately lower in magnesium....329

Figure 127. The parallel box plot accompanying the seven group analysis in the previous figure....329

Figure 128. An example of the seven group runs incorporating manganese and phosphorus....331

Figure 129. The parallel box plot accompanying the seven group analysis in the previous figure....331

Figure 130. The lithic density raster superimposed on the grouping analysis results (seven-group run example, with key areas highlighted)....332

Figure 131. The ephemeral features plotted in trench 4....333

Figure 132. The features plotted in trench 4, compared with the lithics density raster and the areas of interest identified from the geochemical grouping analysis....334

Figure 133. The features compared with the specific locations of finds and the geochemically identified areas of interest.....334

Figure 134.The reading grid for pXRF analysis in the field (light grey), with the excavated trench outlines illustrated to show the overlap of the northern end of trench 15 excavated and analysed by pXRF in 2014 (teal outline), with trench 4 excavated and sampled.....335

Figure 135. An example two-group run on the combined key elements as measured by pXRF 337

Figure 136. The parallel box plot describing the groups in the previous figure.....337

Figure 137. An example five-group run on the combined key elements as measured by pXRF 338

Figure 138. The parallel box plot describing the groups in the previous figure.....338

Figure 139. An example nine-group run on the combined key elements as measured by pXRF 340

Figure 140. The parallel box plot describing the groups in the previous figure.....340

Figure 141. An example of the five-group runs with key areas discussed in text highlighted. The dark blue outlined areas are characterised by lower silicon and moderately higher calcium. The dark red area has higher silicon while all other elements are slightly or moderately low. The yellow area has moderately higher potassium and aluminium as well as slightly higher iron and titanium in some of the runs. The purple area was tentatively drawn out as an area with slightly higher calcium/higher phosphorus samples in the nine-group runs. The green area was frequently a little different to the rest of trench 12, with values near the global averages. The black area is an area that was often isolated in the nine-group runs but with an inconsistent profile. 341

Figure 142. The grouping analysis model for the pXRF results overlain with the lithics from the associated trenches.....342

Figure 143. The lithics and soils analysis results from trench 11, with A) the five-group soils grouping analysis underlying on the left, and B) the nine-group analysis on the right.....344

Figure 144. The lithics and soils analysis results from trench 15, with the five-group soils grouping analysis underlying on the left, and the nine-group analysis on the right.....345

Figure 145. The lithics and soils analysis results around the plotted feature in K-3, trench 15 346

Figure 146. The lithics (black data points) and five-group soils analysis results from trench 12 347

Figure 147. The general sampling grid across the western structure and the central occupation area, superimposed with plans of the features and symbolised to illustrate the main context variations across the area 351

Figure 148. Sampling over the central structure: the eastern trench edge is at the top of the photo, which is the edge that cuts through the central structure. The structure is in the vicinity, and to the southwest, of the white sample boxes seen near that trench edge. Sampling was taking place across the darker occupation spread areas at the time of the photo. (Kite photograph taken by Sue Storey, reproduced from Rowley et al. 2018.) 351

Figure 149. The grid of soil samples processed for ICP-AES analysis (dark grey). The western structure is the 6 x 4m grid to the west, the rest of the samples are considered to be from the central area. Most of the samples cover the occupation spread and structure (reproduced from Rowley et al. 2018) 352

Figure 150. Ironpan seen at Star Carr, 2015 excavations 354

Figure 151. The western structure and central structure areas, with 9 groupings specified for the complete dataset. (Reproduced from Figure 21.5 in Rowley et al. 2018.) 361

Figure 152. The parallel box plot generated on ArcGIS of the compositions of the different groups identified in Run 1 of the nine group analyses 361

Figure 153. (left) a biplot illustrating the relationships between 1) the five elements (depicted as variable vectors) and their contribution to the components, 2) the individually projected data points for each sample and therefore 3) the relationship between the variable loadings on the components and the elements as shown by their proximity on the graph. Data points are symbolised by area; (right) a plot of the same individually projected sample data points, highlighting the relationship of samples from different areas to the components (made by connecting the most dispersed points of each spread). (Reproduced from Figure 21.6 in Rowley et al. 2018.) 364

Figure 154. The microlithic industry from Deepcar, Yorkshire (reproduced from Radley and Mellars 1964, p.10, not to scale) 378

Figure 155. Awls from Deepcar (reproduced from Radley and Mellars 1964, p.17, not to scale) 380

Figure 156. Acetone vapour exchange setup for drying micromorphology tins from Flixton Island 2 and Star Carr, with a pot of anhydrous calcium chloride as desiccant on right end of the bottom row in the photograph 397

Figure 157. Anhydrous calcium chloride as desiccant, with the fresh powder shown on the left, and the expanded exhausted powder shown on the right 397

Figure 158. The histograms for the data as measured in batch 1 and 4 of the ICP-AES analysis on trench 4 462

Figure 159. The histograms for the data as measured during the field pXRF analysis of trenches 11, 12, and 15 505

Chapter 7 Comparing Patterning in the Flixton Lithics and Soils

7.1 Introduction

The spatial distributions of Mesolithic lithics and individual elemental signatures in the associated soils from the dryland were presented in chapters four and six. This chapter will go on to analyse these data in more depth and holistically. Identified signatures are the result of processes that have been occurring since before the site's first occupation, through the main period of human activity in the Mesolithic, up to the time of excavation and sampling. Both the nature of those signatures and the spatial distributions can inform about what processes might have impacted or influenced the excavated assemblage. Very consciously, there were no predictions or hypotheses made about what patterns might be expected: the aim was for the visualised data to speak for itself as far as possible, given that such an analysis of an Early Mesolithic site has not been attempted previously.

That is not to say there were not subjective influences, which needs acknowledging: some of the main subjective influences on the data presented were in the form of the trench layout decisions, sample selection procedures, and methodological decisions and limitations as outlined in the previous three chapters. Further to this, many statistical analyses are an iterative and intuitive process, being subject to the decision making of the model builder despite being mathematically based: variables are added into models gradually, parameters tweaked, and assessments of the stability and robustness of the model made. As such, analysis must be done in such a way that consciously avoids damaging the legitimacy and veracity of the results, but that does allow exploration of the phenomena in a deeper way to allow for more meaningful and nuanced interpretation if at all possible. This was attempted through the application of various statistical analysis functions available through ArcMap (versions 10.3 - 10.5), as detailed in chapter five.

7.2 A deeper exploration of spatial patterning in the Mesolithic lithics

7.2.1 Establishing the significance of the clusters

In order to consider how well the lithics fitted with the geochemistry, it was decided to perform some simple statistical tests to check the significance and extent of the likely cluster

areas identified in the previous chapter. To establish whether there was genuine clustering exhibited across the 3D located assemblage, the "Average Nearest Neighbor" tool in the Spatial Statistics toolbox on ArcMap was employed. This is a simple tool that calculates the average of all the distances between each input point and compares them to an expected average distance had the point data been randomly distributed across the same area. If the ANN ratio is less than one then it suggests the data is clustered, but the definition of the study area needs careful consideration for the statistic to be meaningful.

The study area can be specified in metres squared or automatically calculated to the smallest rectangle that includes features specified. It should be remembered, however, that only selected areas of the island were excavated and these areas were defined on the basis that we expected material to be present there. The ANN result would have been a truer measure of material clustering across the island's surface had the entirely of the island been excavated and therefore valid to include within the statistical study area. As it was, there were significant stretches of unexcavated ground between some of the trenches and some of the trenches were irregularly shaped. The ANN for the entire 3D located dataset with auto-calculation of the study area to cover all trenches enabled is 0.364 which implies it is highly clustered. However, that generated a single rectangle stretched to include all trenches completely so this would have greatly amplified the impression of clustering, as it included those areas of unexcavated ground. Conversely, finds could have potentially appeared unclustered if finds were generally clustered within one particular region of the excavated trenches and study area auto-calculation was set to the spread of finds only (not the full trenches). Here, the study area would have automatically restricted itself to the area of the cluster itself, so much that there is no sense of known empty excavated trench space around them. As such, the finds would measure as evenly dispersed throughout that overly restricted area which would be misrepresentative.

Overall, therefore, this tool is well purposed for establishing clustering/dispersion where where the auto-generated study area (or a drawn rectangle) would approximate the full extent of the excavated area only. For the wetland and trench 7, an arbitrary study area would have to be defined and as that could not be neatly matched to the excavated trench space (as none of the trenches were regularly shaped) so it was considered inappropriate to apply this analysis in those trenches. However, the clustering of Mesolithic material there is clear. As such, it was decided to apply ANN to the finds from the main central dryland only, i.e. Trenches 4, 9, 11, and 15. The finds were generally well dispersed throughout the excavated areas here and this would establish whether clustering across these combined areas, with the three densely packed areas, was truly statistically significant. This included 5945 out of the 7040 3D located Mesolithic phase finds. The main result report is reproduced below (Figure 108). With an ANN ratio of 0.882, the results were statistically

likely to be clustered. With the z-score of - 17.454, there is a less than 1% likelihood that this clustered pattern could be the result of random chance.

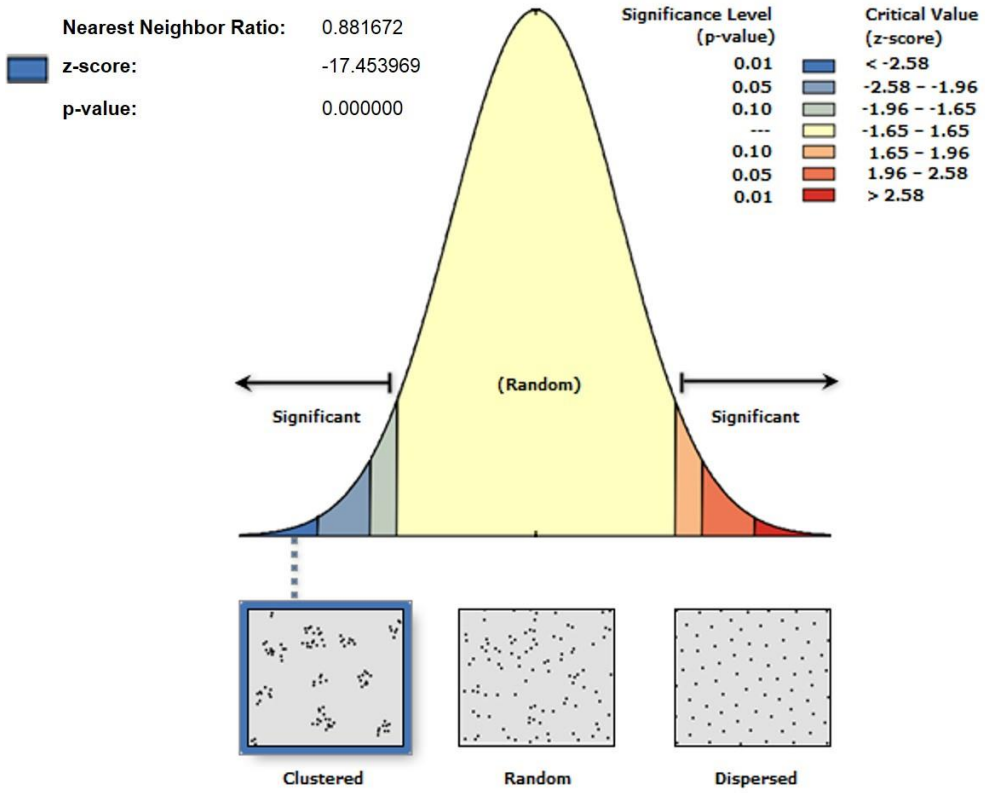

Figure 108. Results of the Average Nearest Neighbour analysis on the main dryland area, which suggests statistically significant clustering based on the 3D located assemblage (autogenerated by the ANN tool, ArcMap).

7.2.2 Establishing the extent of the clusters using Density Analysis on 3D located lithics data

The Kernel Density analysis tool in the Spatial Analyst toolbox on ArcMap calculates a magnitude-per-unit area from the point features of each 3D located artefact. It does this using a mathematical kernel function to fit a smoothly tapered, essentially best-fit, interpolated surface to each data point. Applying this to the Mesolithic lithics assemblage, including material from gully contexts, as well as the unassigned and unknown phases, it highlighted four distinct areas of lithic density (Figure 109 and Figure 110): one on the edge of the wetland, one in trench 3, and two on the main dryland area. The processing extent was matched to the shapefile of the excavated areas, to ensure only empty space in those areas was considered during the construction of the raster.

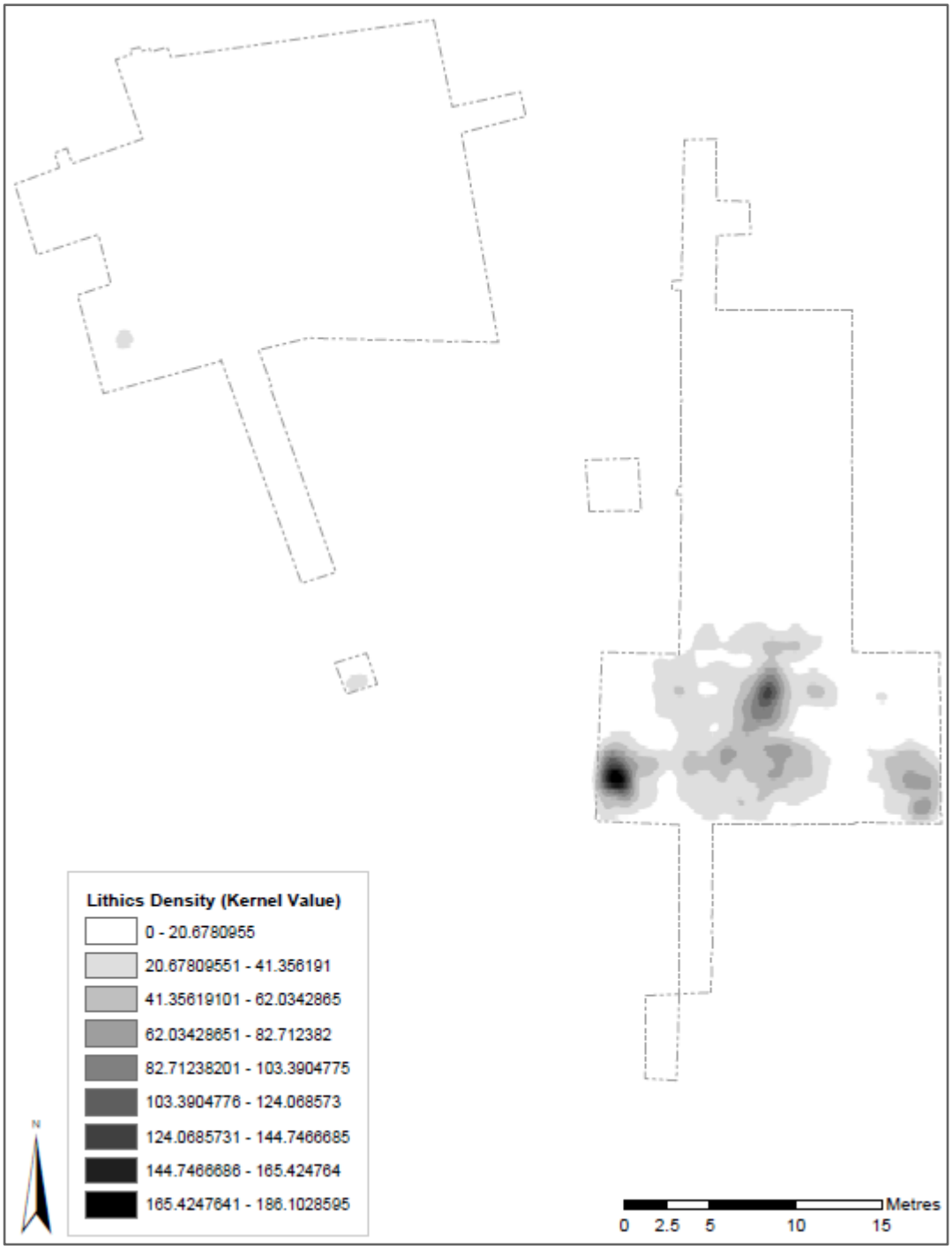

Figure 109. Kernel Density plot of the 3D located Mesolithic assemblage

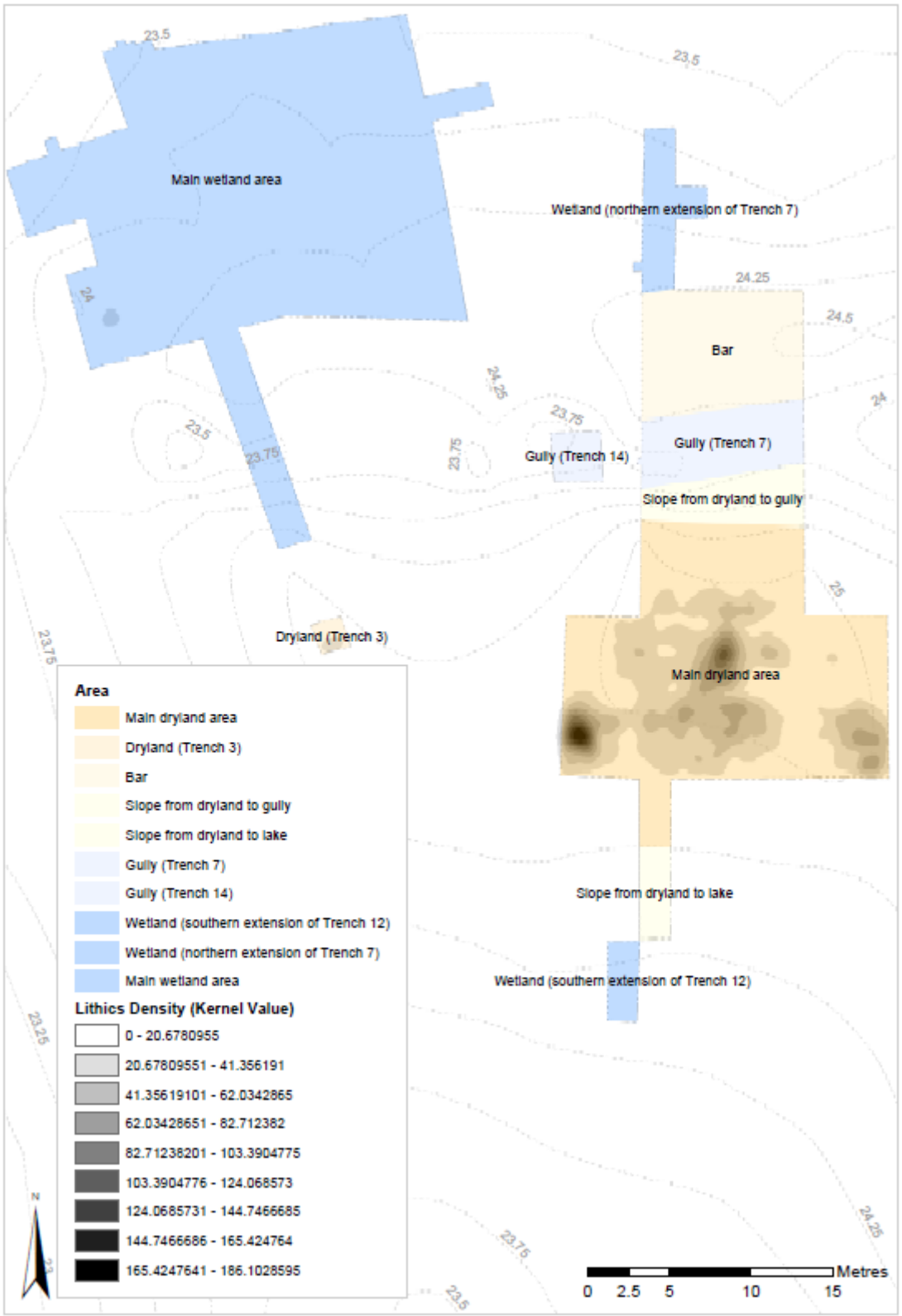

Figure 110. Kernel Density plot of the 3D located Mesolithic assemblage, with the general area polygons superimposed

The clusters on the edge of the wetland area and in trench 3 are quite small relative to the dryland scatters, and in the case of the latter being from such a small trench it is potentially misleading. The remaining areas of lithic density are in the main dryland area. The three

centres of lithic deposition identified from the visual evaluation of the point data are confirmed here: One in the southwest of the main dryland area, one in the southeast, and a broader spread in the centre of the dryland trenches with a peak in the north, on the island's apex.

7.2.3 Display of the sieve lithics data

While lithics retrieved in the sieve were discussed in chapter four on a trench by trench basis for each group, those that have secure grid square data can also be visualised. This is not possible for the sieve lithics in trenches 11 and 15, where the pXRF was conducted and the southwest and southeast dryland scatters are, because of the issue with positive and negative grid numbering (discussed in the same). However, it is possible for trench 4, enabling comparison with the ICP-AES data; trench 12, enabling comparison with pXRF data; and trench 9. From the density analysis, we know the peak of the central cluster is in trenches 4 and 9 so this will improve the information on that specific cluster as well. To do this, the centroids of each polygon representing a square metre of the trench grid were created as points in ArcMap 10.5. Then these points were joined to the sieve lithics catalogue, so the latter could be displayed as separate points in the centre of the grid square (overlapping each other). Finally, the Collect Groups tool, in the Spatial Statistics toolbox, was used to collate the superficial lithics points in each grid square into one point in the centre of the grid square which has the sum of the number of sieve finds located within that square attached as an attribute.

Figure 111 shows the total count of sieve lithics per grid square as weighted centroids, banded into increments of 50 lithic finds. It shows the weighted centroids superimposed over the kernel density raster for the 3D located lithics for comparison. It is immediately clear that the areas where the greatest amounts of sieve lithics are from is within that central cluster area. This is encouraging in terms of considering how horizontally disturbed the lithics from all the dryland contexts are. The sieve lithics in the eastern half of trench 4 and throughout trench 9 display a very similar picture to the 3D located lithics distribution. The sieve lithics in the western half of trench 4 are generally similar to the 3D located distribution as well, but some of the squares with moderate values of sieve lithics were low in 3D recorded lithics, particularly in the northernmost row. Either these squares were more turbated post-deposition, and lithics were carried up into the more heavily sieved contexts, or more artefacts were missed and therefore 'caught' in the sieve here. Regardless, while there may be a slightly higher density of artefacts in that area to consider than the first density plot suggests when considering the geochemical results patterning, the central cluster remains significantly more prevalent in the scope of this trench. Finally, while trench

12 was noticeably lacking in 3D located lithics, the sieve data is correspondingly low, and it is possible the trench was not excavated deeply enough to retrieve all finds.

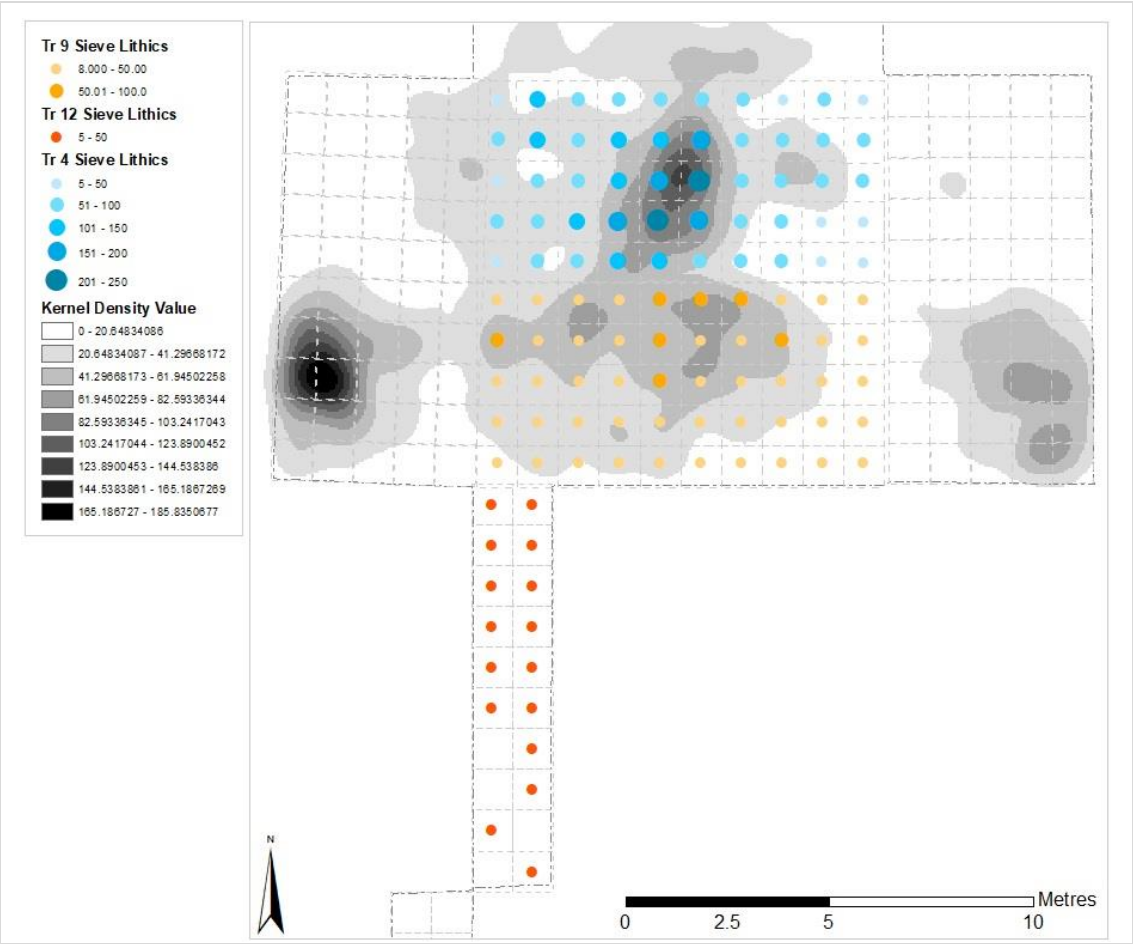

Figure 111. Overlaying the weighted centroids for sieve lithics over the density analysis of the 3D lithics (only sieve material from trenches 4, 9 and 12 could be reliably visualised by grid square as 11 and 15 were impacted by post-excavation errors as discussed in section 4.2.5

7.2.4 Profiles of the lithic scatters

The next logical step was to see what lithic artefacts each scatter consisted of in comparison to each other and the overall Mesolithic assemblage. Figure 112 shows a zoomed perspective of the main dryland area with the grid squares labelled over the kernel density plot based on the 3D located data. One layer of the raster has been highlighted in red. The southeastern scatter was the most ephemeral so it was decided to set the limits of the scatter based on including enough material for characterisation from that scatter. As such, the layer highlighted was chosen as the outermost area of the main body of each scatter and utilised for the scatter lithic composition analysis; any grid square that was more than 25% within the red layer would be considered within the scatter. Using the raster to select grid squares, rather than just counting all artefacts within the appropriate polygonal area defined by the raster, allowed for the incorporation of the sieve data for trenches 4 and 9. Choosing that specific layer of the raster to be the outermost region included the main peaks of all three scatters but excluded some areas that would undeniably be peripheral areas.

However, it also meant that there was a clearer degree of definition between the three main areas considering the next density layer down would bridge between the central and southwestern scatters. The lithic data points included the scatters are shown in Figure 113.

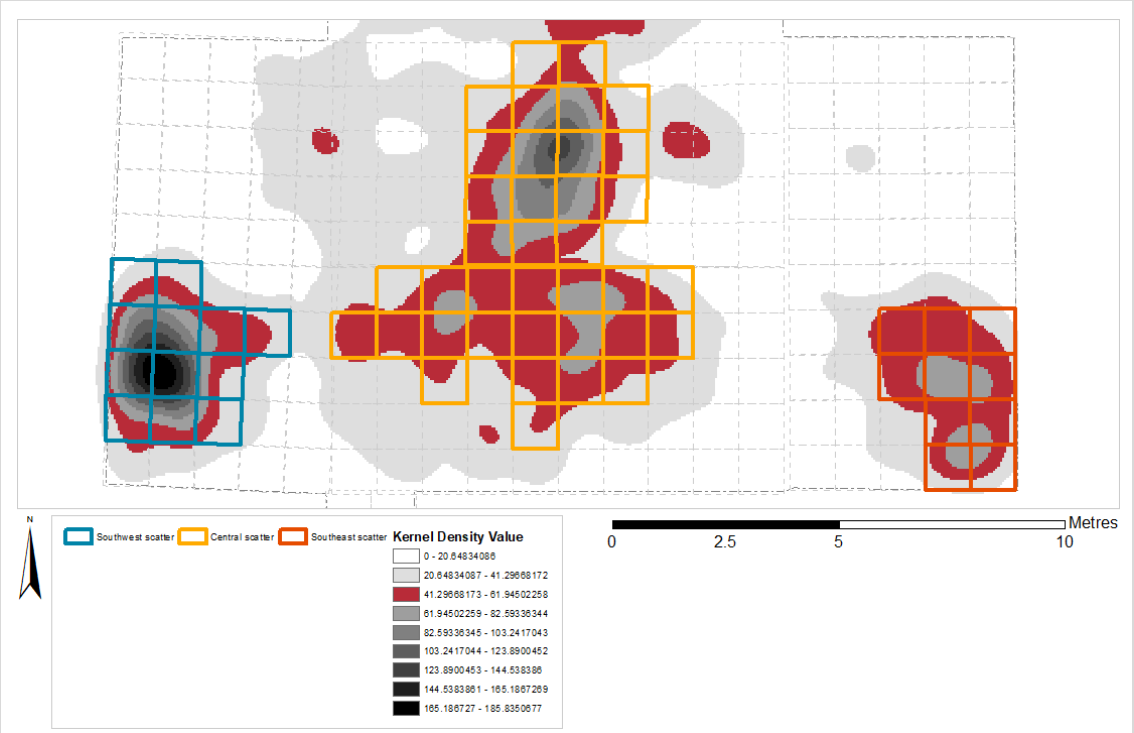

Figure 112. The density raster across the main dryland area. The outer edge of the layer highlighted red in the density raster was used to define the outer bounds for the three main scatters (southwest, central, and southeast dryland)

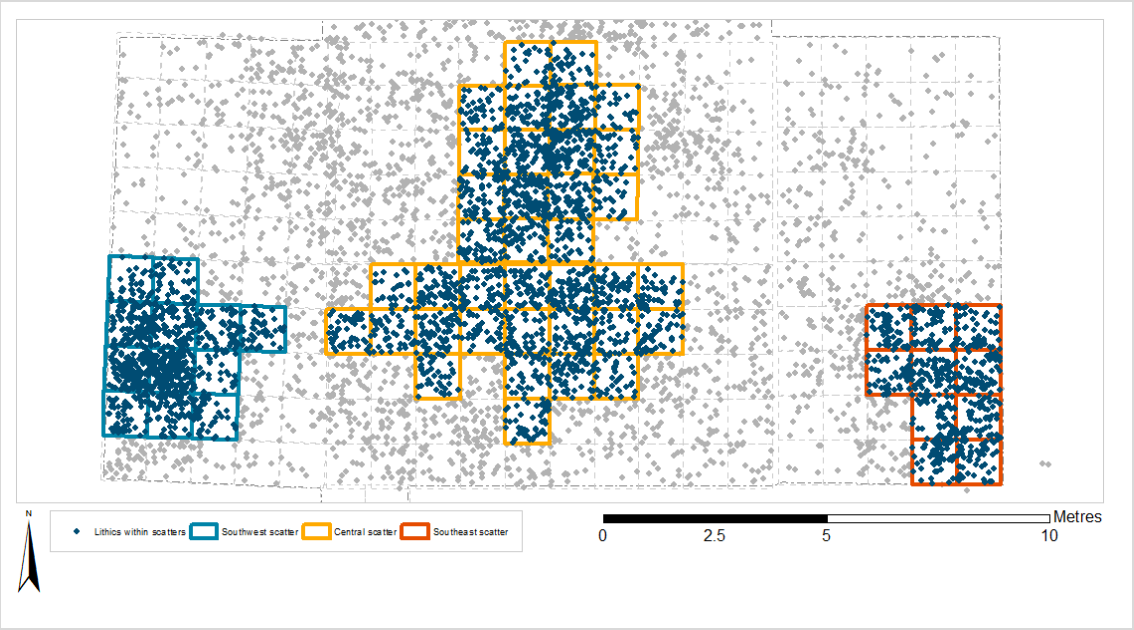

Figure 113. The 3D located lithics falling within the grid squares identified as the main scatter squares

The central dryland scatter was generally taken to spread across trenches 4 and 9. The density plot suggested there were three major peaks of lithic deposition, though with the northern one being more significant than the other two in trench 9. A general 'halo' of thinner artefact deposition spread around the three, which suggested these scatters were

related in some way and as such here they are treated as being within one scatter. There was a slight gap between trenches 4 and 9 which may also account for slightly lower values between the two in the density raster. However, it is possible these peaks represent two or three separate scatters / zones of different activity, though all located across the central dryland area on the apex of the island. There are also three small, separate 'satellite' peaks highlighted red in trench 4 around grid square Y2, trench 15 around grid square G2, and trench 9 in grid square C-4. For the purposes of studying the main profile of the scatter, these peaks were not included in the analysis, however their locations will be considered when comparing the spatial distributions of the geochemical and geophysical results. For the central dryland scatter, the sieve data could be considered by grid square and incorporated alongside the 3D located data.

The southwest dryland scatter was one densely packed, coherent area, which caused it to be noted as a possible feature when it was excavated in the field. Flotation on a bulk sample of the sediment from grid square K-3 yielded further microdebitage, only a small proportion of which was burnt. The southeast scatter was less densely packed than the other two, with two peaks less than a metre apart from each other, encircled with a general 'halo' of material again. Again, these could be peaks from two activities; however, for the purpose of getting a general sense of that area of the trench they are treated together. There was also a small area in grid square U2 in trench 11, that the raster identified as having slightly elevated levels of lithics though not to the same extent. It is not clearly related to any of the main scatters. However, the location of that will be considered in the comparison with the geochemistry. For the southwest and southeast dryland scatters, the sieve lithics could not be confidently attributed to grid square so this data could not be considered in profiling the scatters and the 3D located finds had to be relied upon to be a representative sample.

Figure 114, Figure 115, and Figure 116 show the general profile (by category) of the central dryland scatter. The first pie chart shows just the 3D located material so that it can directly be compared with the data from the other two scatters. There is material from all categories, with a notable tool assemblage, but largely the scatter is made up of tertiary reduction pieces and other generic debitage.

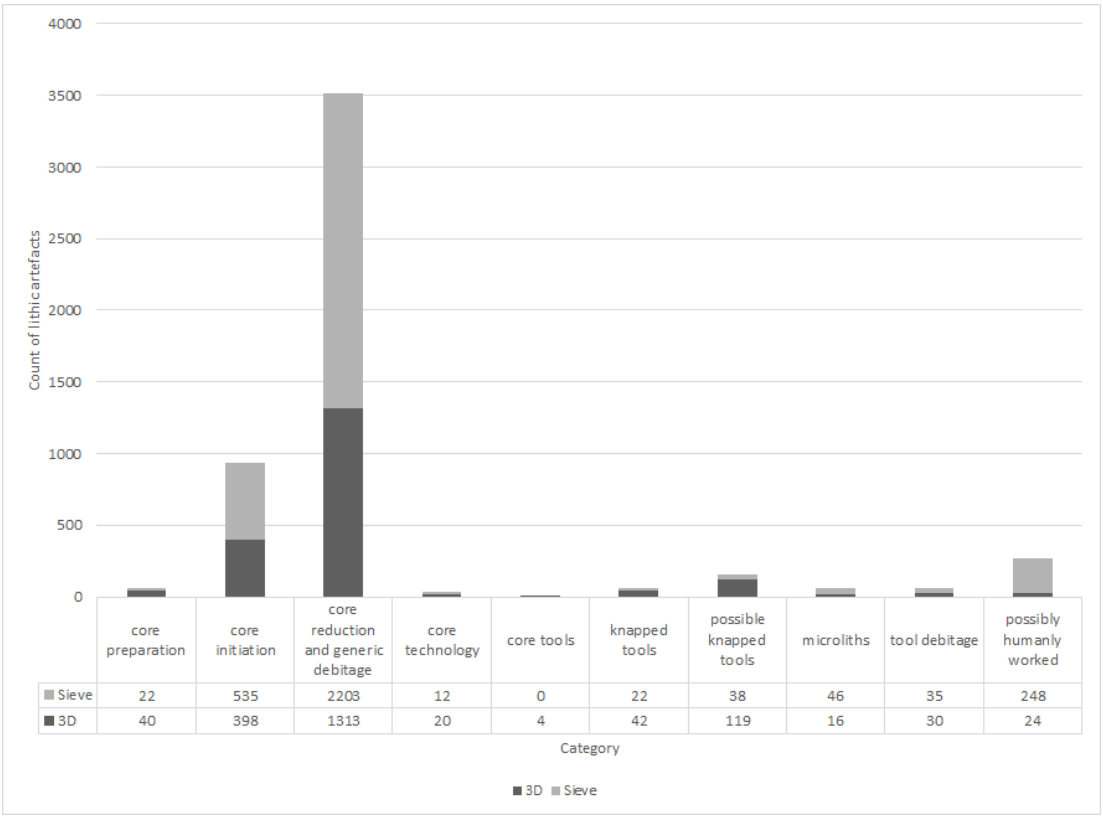

Figure 114. The artefact counts for different lithic categories in the central dryland scatter

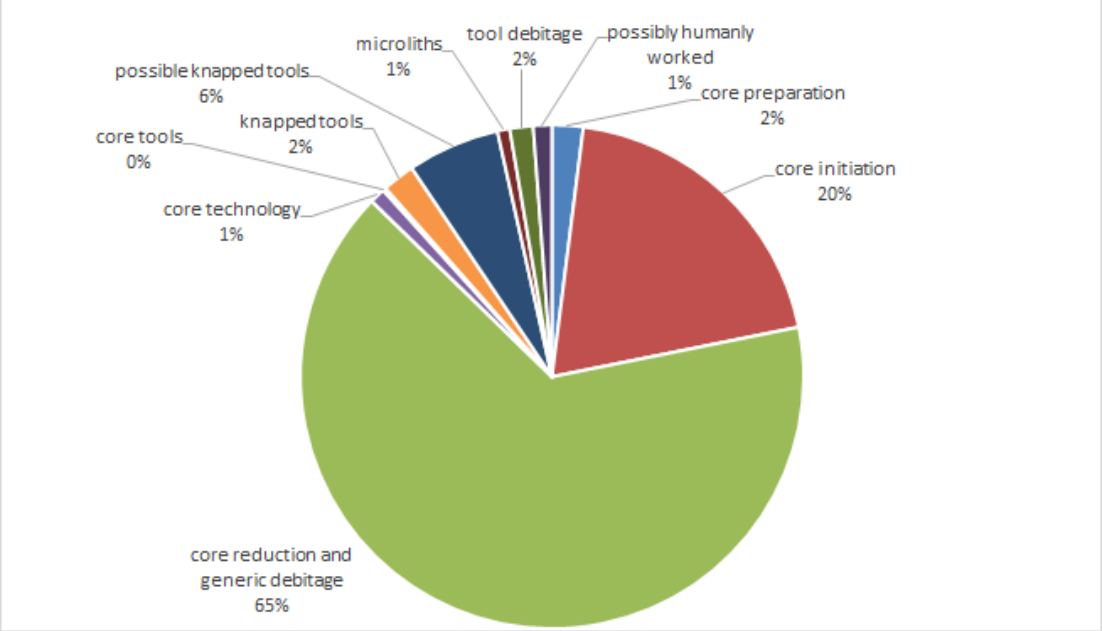

Figure 115. The artefact proportions for different lithic categories in the central dryland scatter, 3D located data only

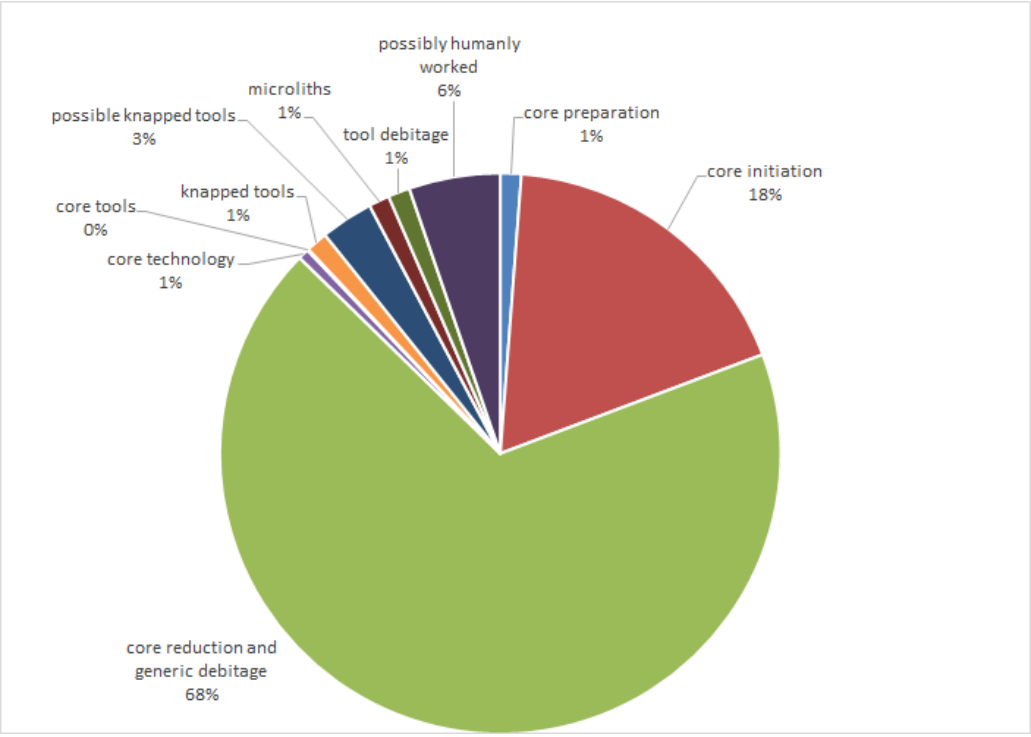

Figure 116. The artefact proportions for different lithic categories in the central dryland scatter, 3D and sieve data combined

Figure 117 and Figure 118 summarise the southwest scatter profile based on the available (3D located) data. Again, the scatter has material from nearly every category except for core tools, and the assemblage here is again dominated by core reduction debitage. However, a higher proportion of the scatter was made up of primary and secondary core initiation debitage.

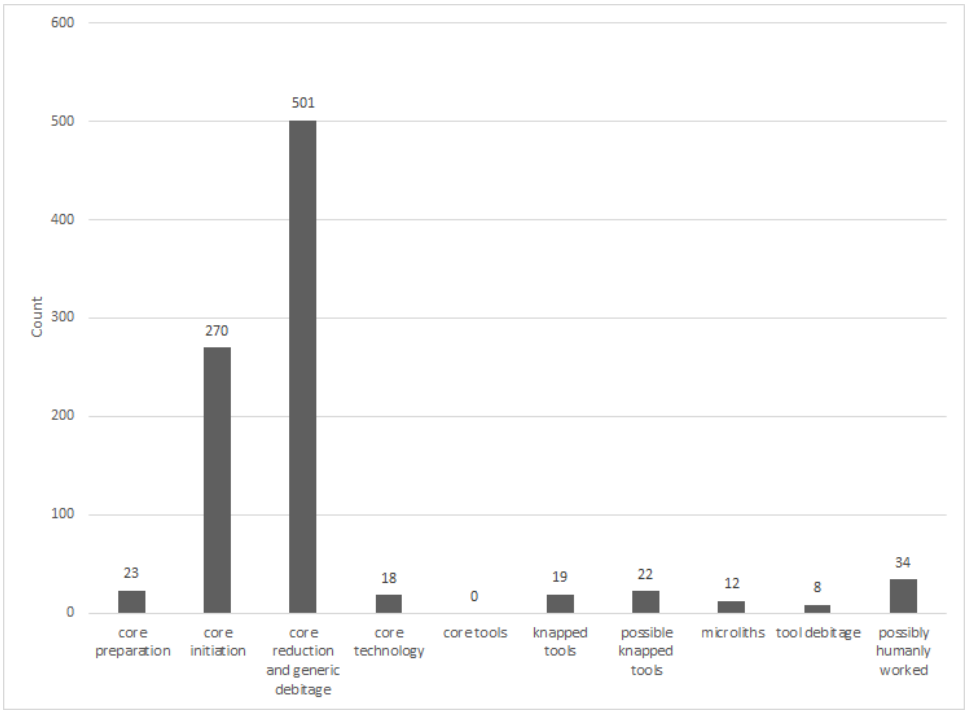

Figure 117. The artefact counts for different lithic categories in the southwest dryland scatter, 3D located data only

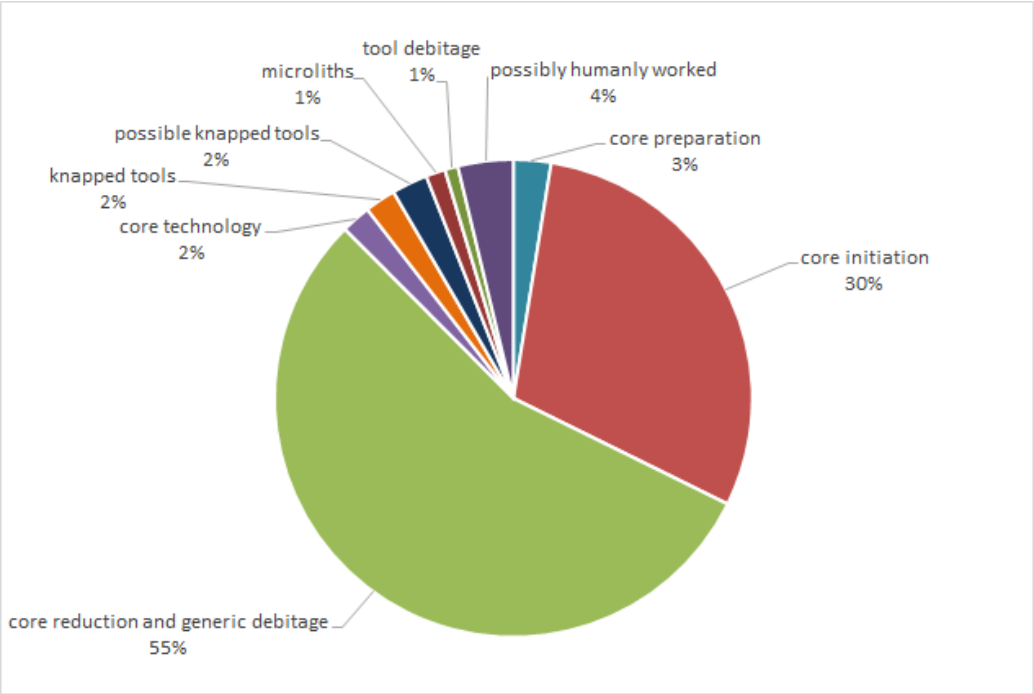

Figure 118. The artefact proportions for different lithic categories in the southwest dryland scatter, 3D located data only

Figure 119 and Figure 120 summarise the southeastern scatter profile. This is a smaller scatter overall than the other two. Again, it is dominated by core reduction and generic debitage. There is a marginally higher amount of core initiation material here proportionately than in the other scatters.

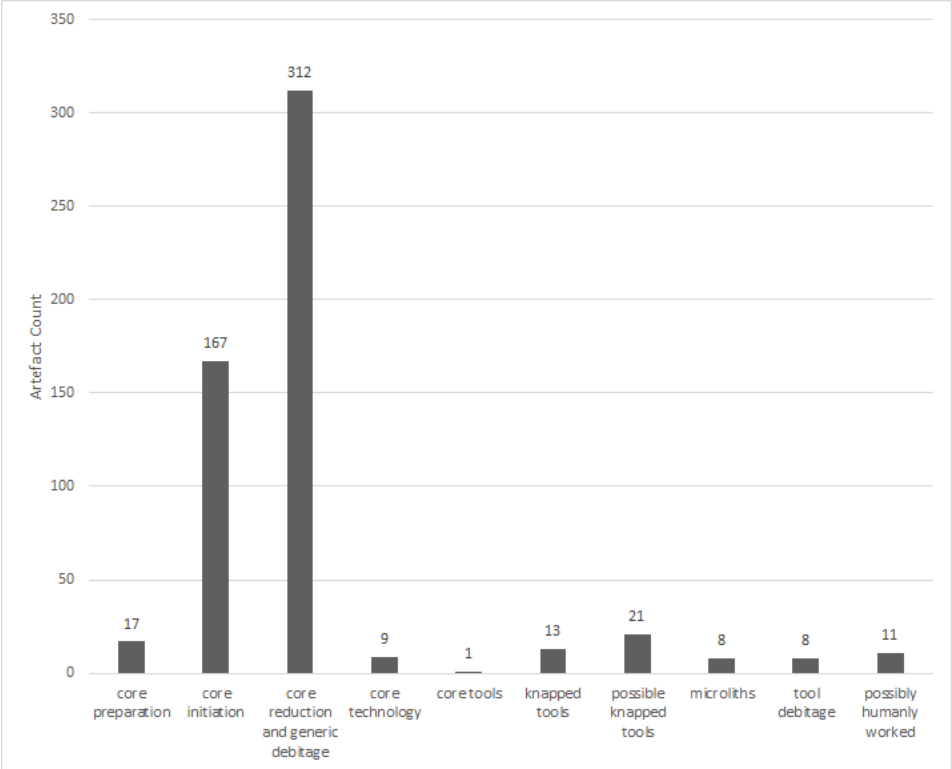

Figure 119. The artefact counts for different lithic categories in the southeast dryland scatter, 3D located data only

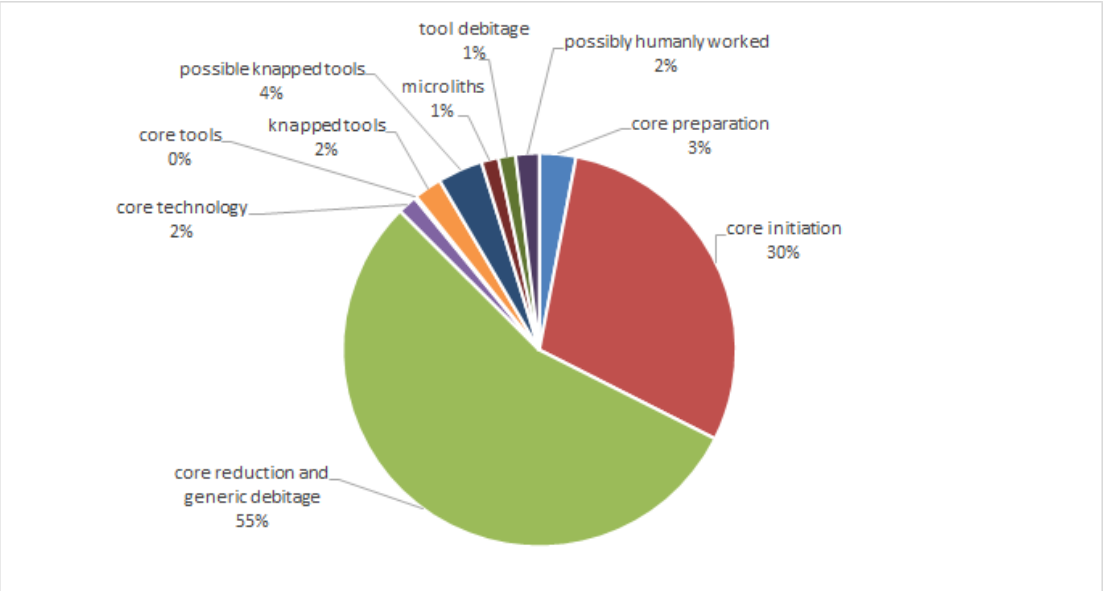

Figure 120. The artefact proportions for different lithic categories in the southeast dryland scatter, 3D located data only

7.2.5 Discussion about the scatter profiles

All three of the scatters are dominated by generic reduction debitage (55-65%, or this increases to 68% for the central scatter when considering the sieve data as well) as well as core initiation (20-30%, reducing to 18% when considering central sieve), core preparation (2-3%, reducing to 1% when considering central sieve), and core technology itself (1-2%, remains the same). The central scatter has more generic debitage and less core initiation relatively, even when just considering the 3D located data, but it seems that a moderate deal of knapping was occurring in all three areas.

The main difference between the scatters is in the raw numbers of knapped tools. In the central dryland scatter there were 42 certain knapped tools just from the 3D located data, compared with 19 and 13 in the southwest and southeast scatters respectively. However, proportionally the number of tools remains the same. If the possible knapped tools are taken into consideration, the difference between the scatters is greatly amplified with 119 of these from the 3D located data for the central scatter, compared with only 22 and 21 for the southwest and southeast scatters respectively.

The second notable difference is that four of the site's 13 core tools came from the central dryland scatter area and most of the others were on its periphery. There was one core scraper found in the southeastern scatter as well, but no core tools in the southwestern scatter. Therefore, the central scatter is the only one associated with the axe/adze technologies.

All three scatters have small numbers of microliths retrieved during excavation, with slightly less from the more ephemeral southeastern scatter. There is a significant additional assemblage of microliths retrieved from the sieve for the central scatter but there is no way

to know if the microliths retrieved from the sieve in trenches 11 and 15 were from the scatter areas so it is difficult to consider this comparatively; all that can be said is that there were a lot of microliths retrieved from the vicinity of the central scatter generally speaking. One thing to note is that while there were microliths throughout the central scatter, and microburins, most of them fell in the trench 9 areas, i.e. to the south of the main peak of this scatter and more in the periphery. There were microliths found in the space between the central and southwestern scatters as well, whereas the area with microliths from the southeastern scatter is distinct. This could reflect that the trench 9 areas of the central scatter are a separate scatter, or an area being drawn upon by both the central scatter users and the southwestern scatter users, or that there was movement between the central and southwest scatters, though it is not possible to investigate any of these hypotheses further at this stage.

The presence of microliths in all three scatters suggests they are all likely Mesolithic (rather than one being part of the Long Blade use phase of the site), but they could be from more than one use period within that. When reconsidering the distributions of microliths in the light of the density raster plot, it is clearer that the microliths tend to cluster in the southwest cluster, the south of the central scatter (in the trench 9 areas), and the north of the southeast scatter (Figure 121). There is also a spread across the northeast corner of the main dryland trenches, outside of the scatter areas. Scrapers, the other dominant formal tool type, on the other hand, are also found in all three scatters but in the central scatter they are denser (and actually exhibit their tightest clustering) in the northern half, and they are also found in the south of the southeast scatter.

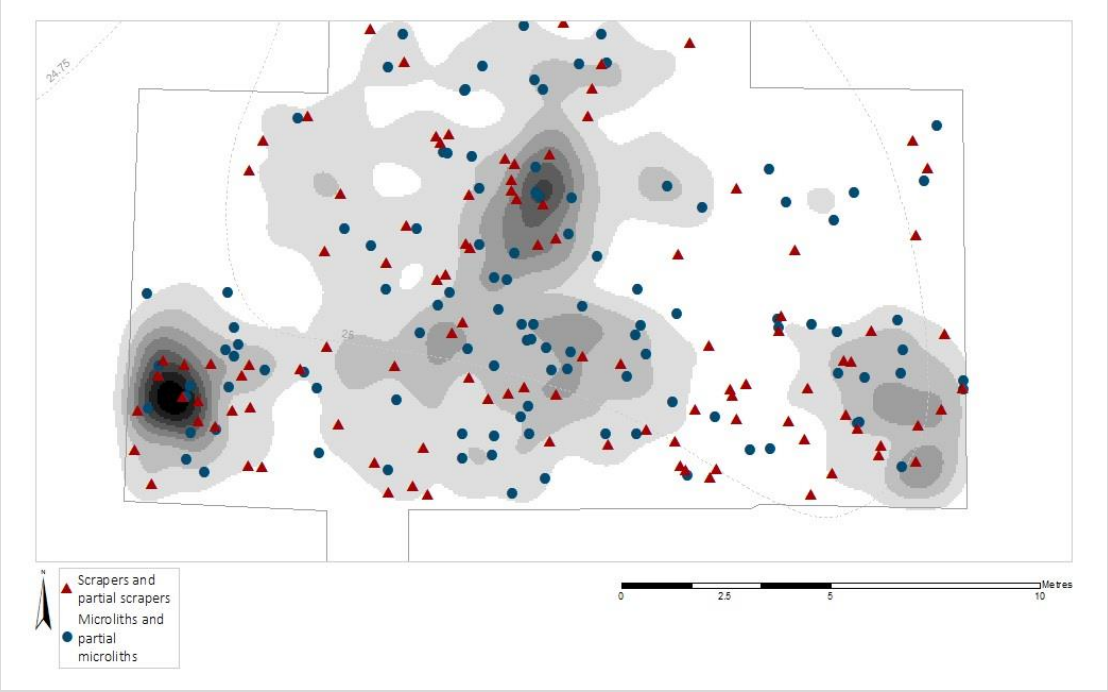

Figure 121. The 3D located microlith and scraper distributions superimposed over the density raster

In general, the scatters are similar in overall composition based on the proportions of knapping debitage to tools. Even if activities were different in each of these scatters, and there is some patterning within them that suggests so, it appears that localised knapping is occurring in the vicinity of each scatter, rather than knapping occurring in one area and then tool use in another. If the geochemical signatures from each of the scatters are both distinct from their surroundings and then either similar or different from each other, then this may inform further about the use or chronology of the scatters.

7.3 A deeper exploration of spatial patterning in the soils

7.3.1 Integrating the elements into one model

The major, minor and trace elemental contributors to the soils at Flixton Island 2 were established based on the ICP-AES and pXRF results in chapter six. It is likely that some of these values are incorrect but consistently so within a given method, i.e. they are inaccurate but precise. For example, an element proposed as being a major contributor is in fact a minor contributor in reality, but that element is just relatively better detected than other elements in the samples by that given method. However, crucially, the relative patterning between samples measured using the same method should not be greatly impacted considering the similarity of the soils and consistency in applying the methods. Choropleth visualisation (using Jenks Natural Breaks to divide the data up into 'natural' groupings), Hot Spot Analysis, and Cluster-Outlier Analysis were used to investigate the spatial patterning of the individual elemental distributions reflected in the soils in the previous chapter. Grouping Analysis, which will be presented here, was the main statistical tool used to explore how these elements interrelate further.

Conducting any cluster or component analysis is an iterative process, requiring repeated application of the tool in order to develop a properly specified, meaningful model. It should not be simply run and accepted at face value. The process takes a long time, with multiple repeat runs of the analysis using different settings, to optimise a model that represents the data in enough detail but at the same time provides a more simplified version of the data than the raw results, which is ultimately the aim. As such, the full documentation of the Grouping Analysis process is documented in Appendix Seven, the methods are described in chapter five, and only the general details of development and the final models are discussed here.

7.3.2 Results of the Grouping Analysis of Trench 4 ICP-AES Results (from 2012 excavations)

7.3.2.1 Overview

Analysis was conducted on the results from the first batch of ICP-AES analysed samples only, i.e. not including the extension results (which were uniformally lower values for all elements regardless of location, as discussed in chapter six also). Initially, a model was developed for the major and minor contributors to the Flixton Island 2 samples: iron, aluminium, calcium, and magnesium. Then, the readings for manganese and phosphorus were incorporated, which were only measured as trace contributors at Flixton Island 2 but had been incorporated into the Grouping Analysis work on the results from Star Carr. This expansion would allow a better comparison of the two sites (in chapter eight) as well as expanding the analysis to test the robustness of the model when incorporating new data. The Star Carr analysis also included potassium but incorporation of that element into the model was unsuccessful due to the lack of variability in the readings (as detailed in the appendix).

7.3.2.2 Major and minor element (Fe, Al, Ca, Mg) grouped model

Firstly, there appears to be trench-wide variations particularly in the iron and aluminium in the soils, and that generally the samples are usually either higher on average in all four elements or lower on average in all four (considering the pXRF model results later, this is quite likely due to variable silicon content that could not be measured by this method). Because of this, the natural split into just two groups (Figure 122 and Figure 123) was simply between those higher in all elements and those lower in all elements, but particularly higher or lower in iron and aluminium. Samples of both groups are present in all areas of the trench, albeit in diagonal strips across the full trench, and there is no reason to suppose all elements are being read lower in certain samples due to a methodological difference in processing. No clear areas were isolated as if by a localised activity on the two group run, and as such there were no enhancements or depletions of elements so significant as to overcome this seemingly general, background trend. There were two parallel groups similar to these groups in all later runs, but as additional groups were separated out, the averages of the parallel strands represented got closer to the global average, and samples retained in these parallel groups were generally mixed throughout the trench between those samples grouped into the more polarised profiles.

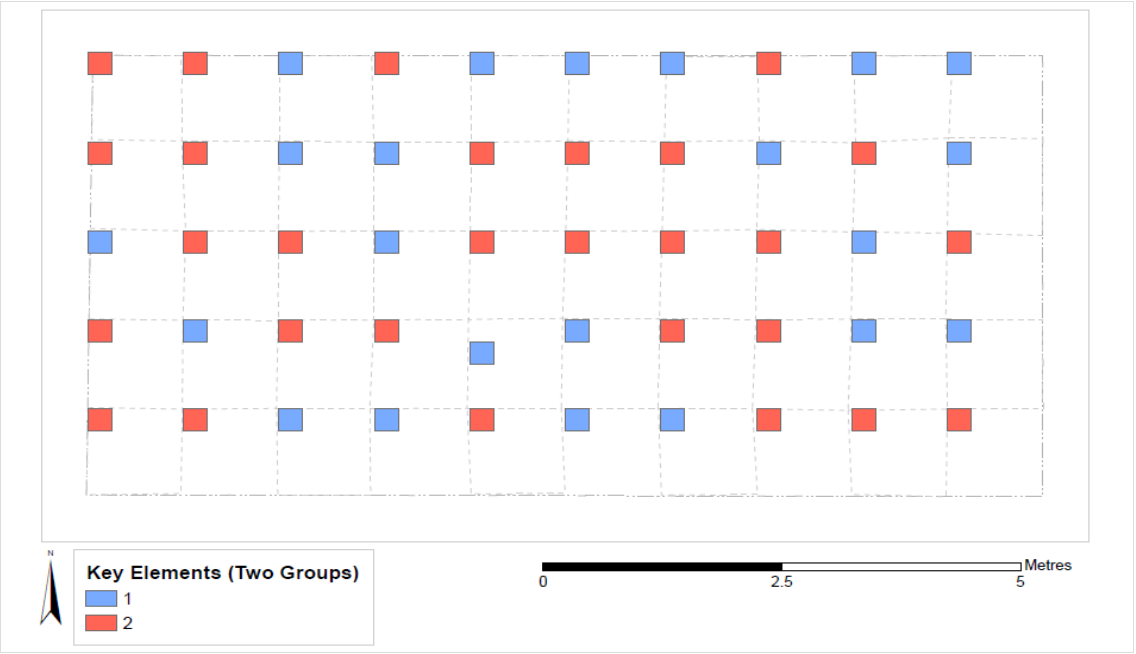

Figure 122. Example of a two group run incorporating all major/minor elements

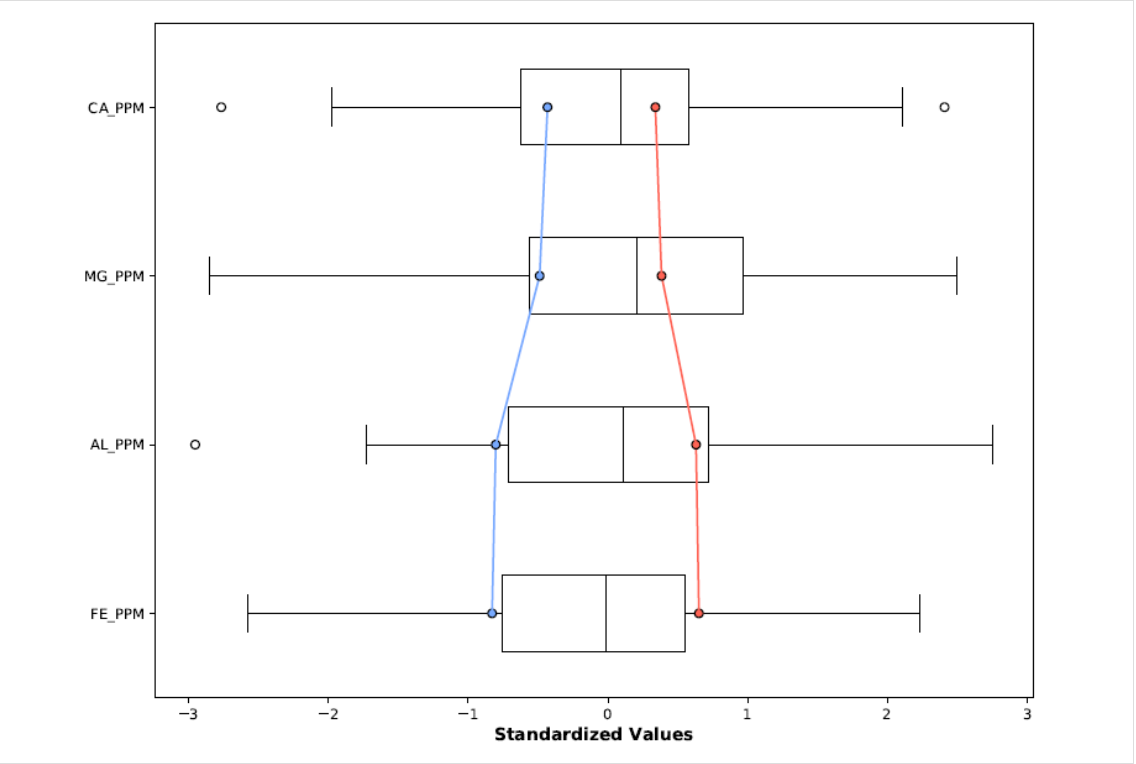

Figure 123. The parallel box plot associated with the two group run in the previous figure

However, allowing more groups to develop allowed for the influences of calcium and magnesium to be identified, which in turn isolated potential areas of specific localised processes, anthropogenic or otherwise (Figure 124 and Figure 125). Areas lower on average in calcium were the first, and therefore strongest, localised trend to be identified in the three-group repeats. These tended to fall around grid squares B2 and C2, just to the west of the centre of the trench, and grid squares X0 and Y1. The five group repeats amplified this effect, with there being one group particularly low in calcium in all repeat runs with other readings usually within the box area of the plot so only slightly higher or lower, or

sometimes this group was less significantly lower in calcium but joined by a second group also low in calcium with average readings notably higher than the global average for the other three elements but particularly iron (depending on where the random seeds generated). The areas were broadly consistent in this, being around those same grid squares as in the three-group runs.

Figure 124. Example of a five group run incorporating all major/minor elements

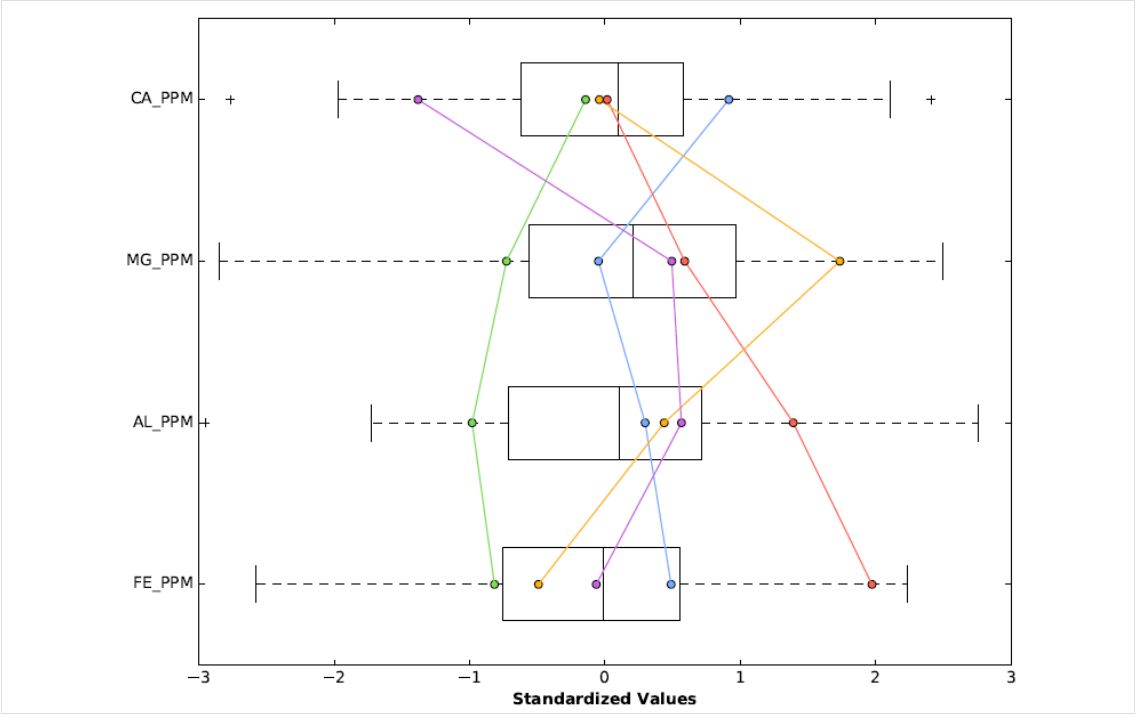

Figure 125. The parallel box plot associated with the five group run in the previous figure

The seven group runs confirmed this trend for lower calcium levels in these areas (Figure 126 and Figure 127). As such, this will be an area highlighted for comparison with the other evidence as it is potentially due to a localised process this has occurred, and could therefore

indicate an activity area. The seven group runs also drew out another area that was potentially characterised by being relatively higher in calcium and lower in magnesium: This did not appear on two of the repeat runs or any of the lower group runs because the enhancements/depletions were subtle but it appears the combination of these two attributes allowed these samples to form as groups in these two runs. As such, this is also an area that will be compared with the other evidence.

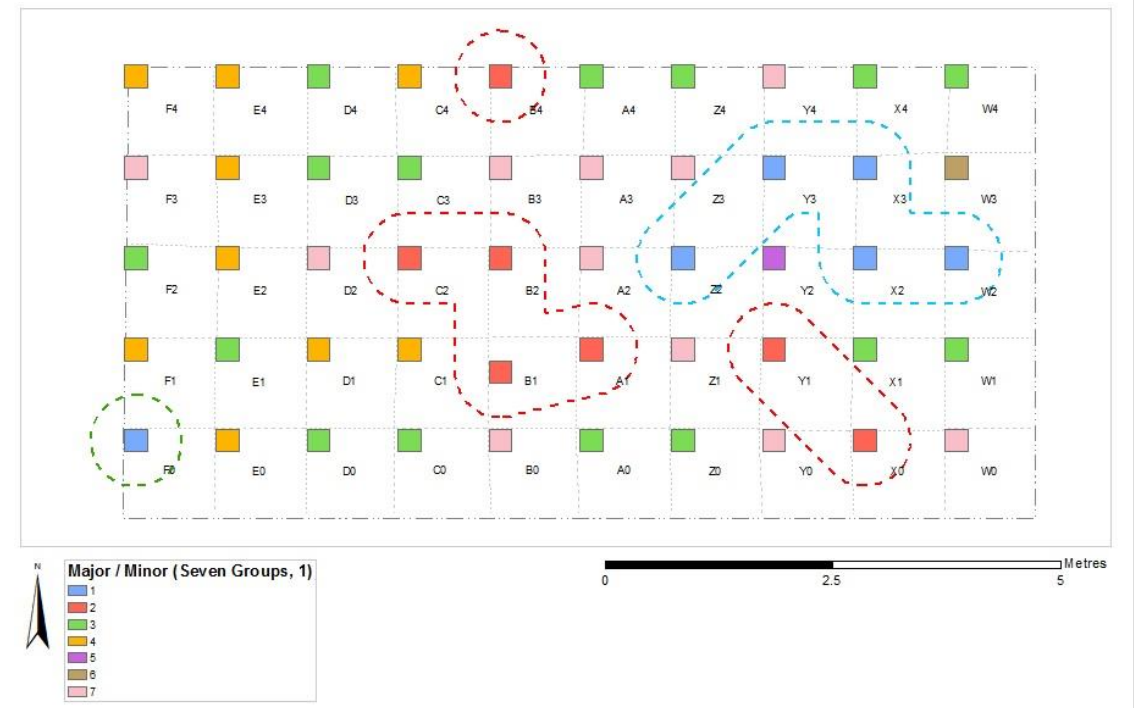

Figure 126. Example of a seven group run incorporating all major/minor elements, with the potential activity areas highlighted. The red outlined areas are those lower in calcium; the blue is those moderately higher in calcium and moderately lower in magnesium

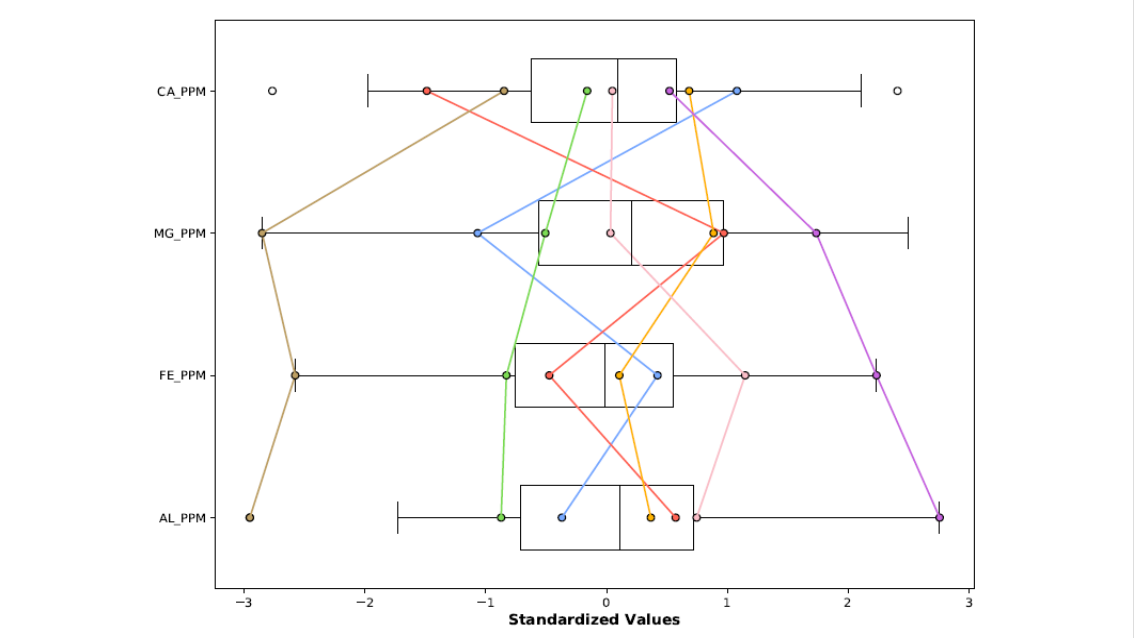

Figure 127. The parallel box plot accompanying the seven group analysis in the previous figure

7.3.2.3 Expanded key elements (Fe, Al, Ca, Mg, Mn, P) grouped optimal model

After these areas had been established based on the major and minor elements identified from the ICP-AES readings, manganese and phosphorus were also considered individually and then incorporated into the model through a series of seven-group runs (Figure 128 Figure 129. Their additions both strengthened the patterning argued for in the existing model but also reinforced that the southwest corner of the trench, that had been grouped with the higher calcium samples previously and therefore highlighted for that purpose was actually the area with notable phosphorus enhancement (now highlighted green). In this model, samples in and near this high phosphorus area are no longer grouped as being with a low magnesium group as in the first model as they are better characterised by this profile (separating it out from the area highlighted blue).

Incorporating the new elements into the model reinforced the areas around B2 and Y1 being areas of interest. These were areas with general relative depletion of calcium, manganese, and phosphorus (with slightly lower iron, and slightly/moderately higher magnesium and aluminium) and this grouping broadly came up in every repeat run of the tool. The incorporation of phosphorus also caused the area in the southwestern corner of the trench to be grouped as an area of notably high phosphorus in three of the runs (as well as manganese and iron, slightly elevated magnesium, and near average/slightly low aluminium and iron). This had been an area flagged up as slightly high in calcium and low in magnesium before, with the group mainly formed of the samples around the anomalous sample in W3. Now, the blue-highlighted samples (yellow, purple, and blue groupings) follow the same profile shape with higher calcium, and to a lesser extent manganese and phosphorus, balanced against lower magnesium, aluminium, and to a lesser extent iron, but calcium is not always above average relative to the global dataset. The anomalous sample from W3 stood out as a sole member of a 'group' in one of the expansion runs, but was also sometimes grouped with one or two other samples instead.

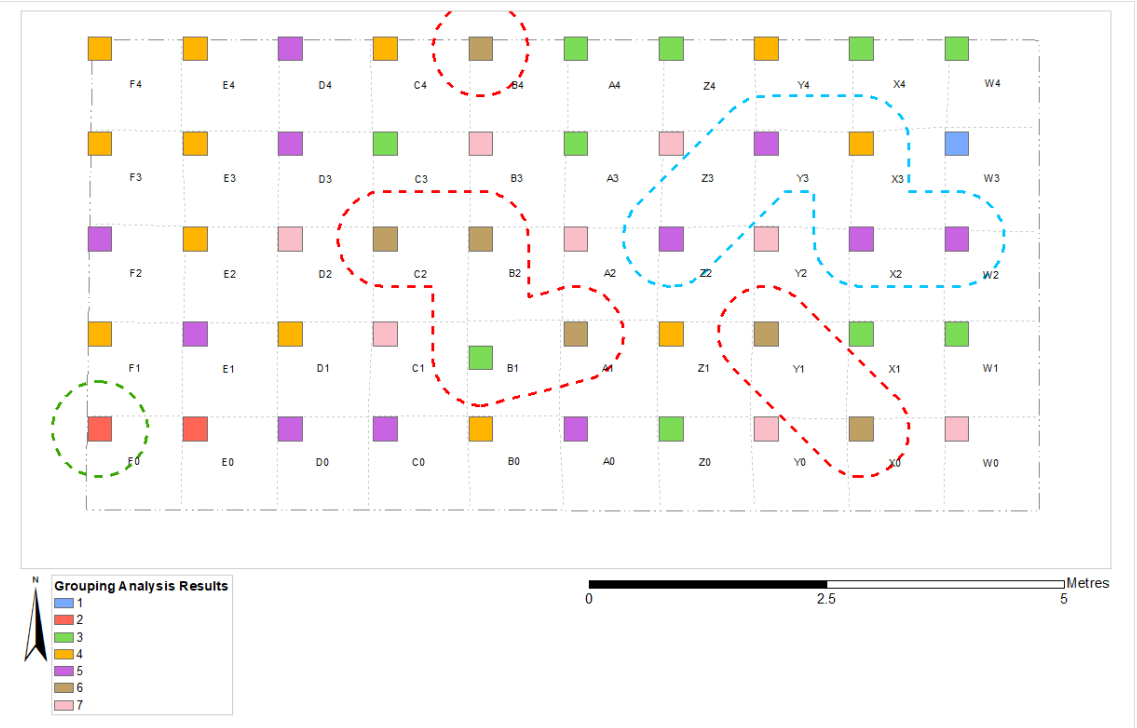

Figure 128. An example of the seven group runs incorporating manganese and phosphorus

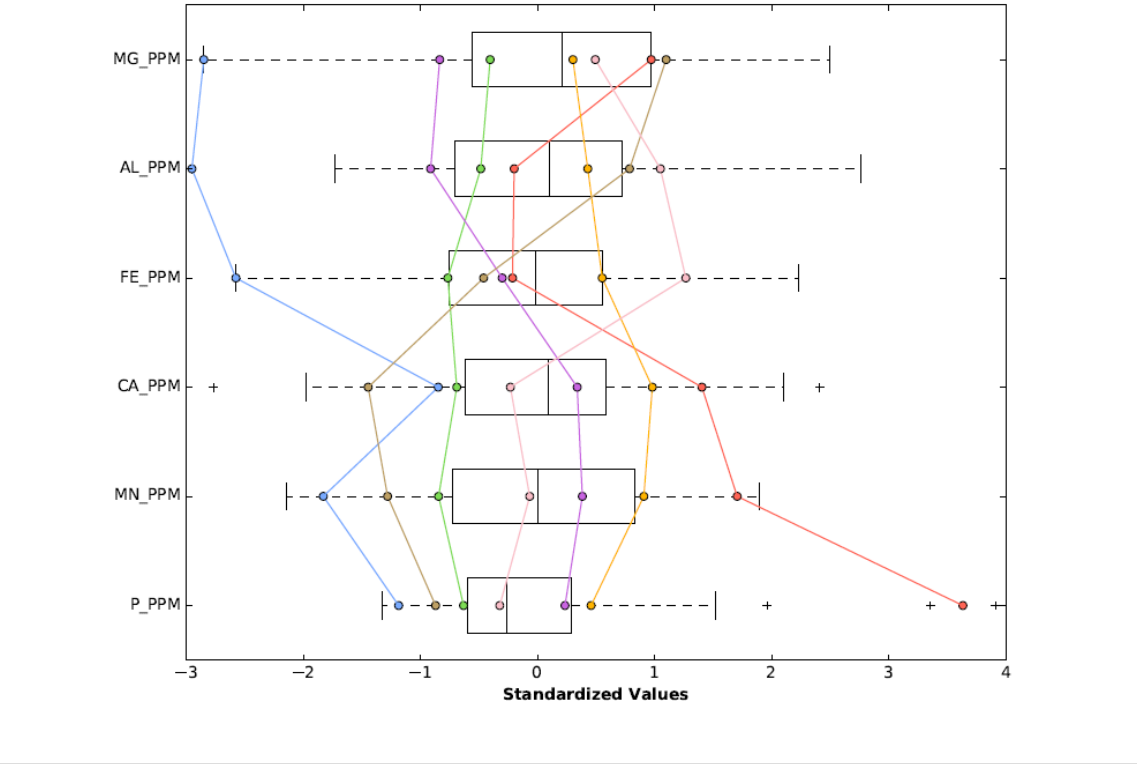

Figure 129. The parallel box plot accompanying the seven group analysis in the previous figure

7.3.2.4 Comparison with lithics data

The areas with clearer and most consistent geochemical groupings, again outlined in red, blue and green, tend to be associated with different areas of the central lithic scatter (Figure 130). The main red-outlined area, in the vicinity of grid square B2 (made up mainly of samples from the brown group mostly in the figure below), is just to the west and south of the peak of the lithic densities. The other red-outlined samples are not associated with areas

with dense lithics, but on the periphery only, however as the main and most consistent identification of this grouping was in and around B2, this is arguably a signature associated with the lithics scatter itself or perhaps from an activity taking place immediately adjacent to it. The trench was topographically nearly flat and there is no reason to suggest this area would be significantly different from the other areas of the trench. It could be the impact of a modern process, but it being so localised and also being so closely associated with the scatter supports that this is either an archaeological signature associated with the use or deposition processes impacting the lithics, or that it is resulting from a post-deposition process that impacted both the geochemistry and the distribution of the lithics. It is hard to think of a process that would result in these patterns of concentrations in both those strands of evidence, however.

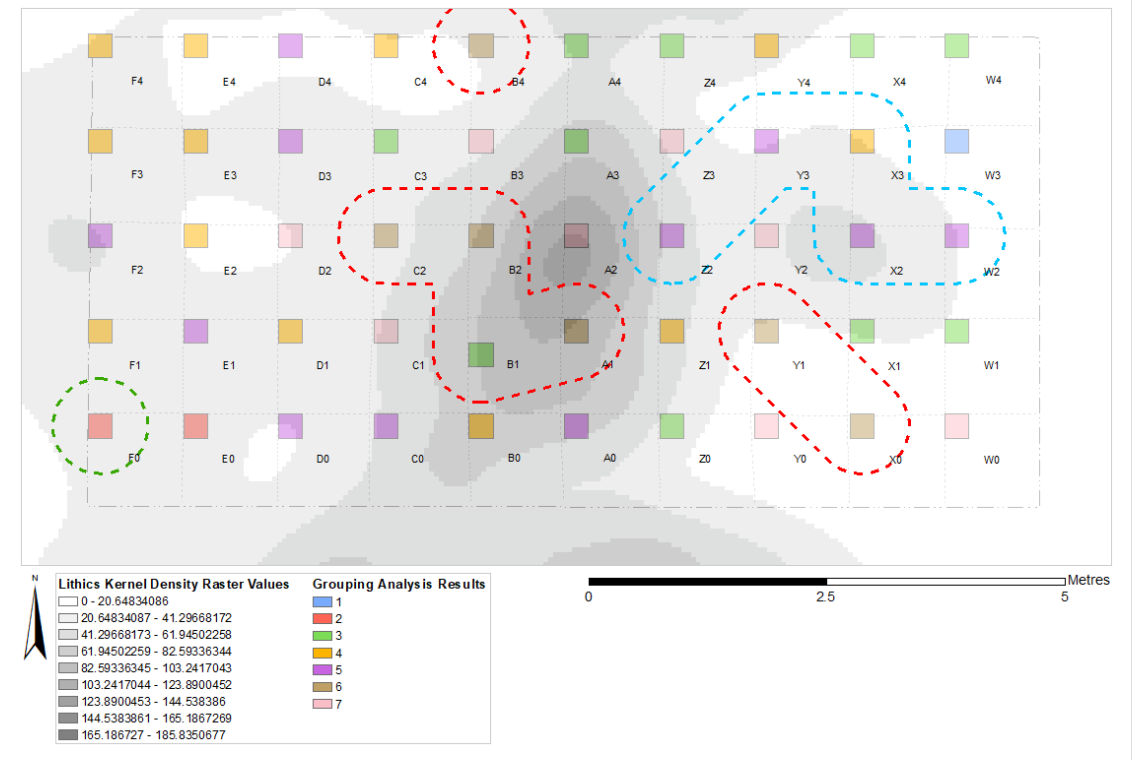

Figure 130. The lithic density raster superimposed on the grouping analysis results (seven-group run example, with key areas highlighted)

The blue-outlined area of interest seems to be associated with the smaller peak to the east of the main central dryland scatter. Again, it is not centred on the peak itself but overlaps and curves around it so again, if legitimately associated, then it could be a signal from an activity taking place nearby. The high-phosphorus area was not associated with any areas of high lithic density particularly. Future analysis will consider the distributions of actual types of lithics in relation to these potential activity areas.

7.3.2.5 Integration of known plotted potential features

There were a number of shallow, irregular, and slightly elongated depressions found in trench 4, as shown in Figure 131, that were recorded as potential features. These were very

ephemeral and it was unclear if these were natural or anthropogenic in nature, and whether archaeological or modern. They were not obviously postholes because they were so shallow, but they may have been post supports, or else had been heavily truncated. Being all in the western end of the trench, they respect the main distribution of the scatter in the centre and east of the trench, but they do not form an obvious spatial pattern in relation to it either such as surrounding it. They are generally distributed between the red-outlined area and the green-outlined area of interest, with several of them on the edges of that area with higher phosphorus levels (Figure 132). The geochemical groupings do not suggest anything further about these features: The samples from the same grid squares are assigned to many different groups. Considering the specific location of finds, there were finds within, directly above and around the features (Figure 133).

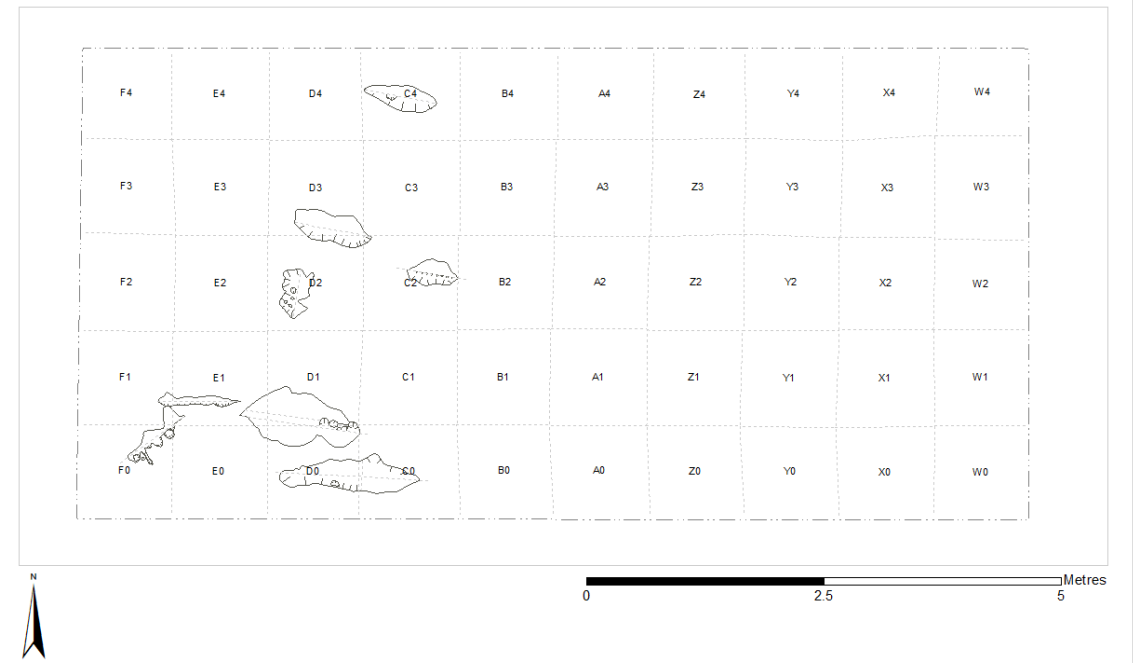

Figure 131. The ephemeral features plotted in trench 4

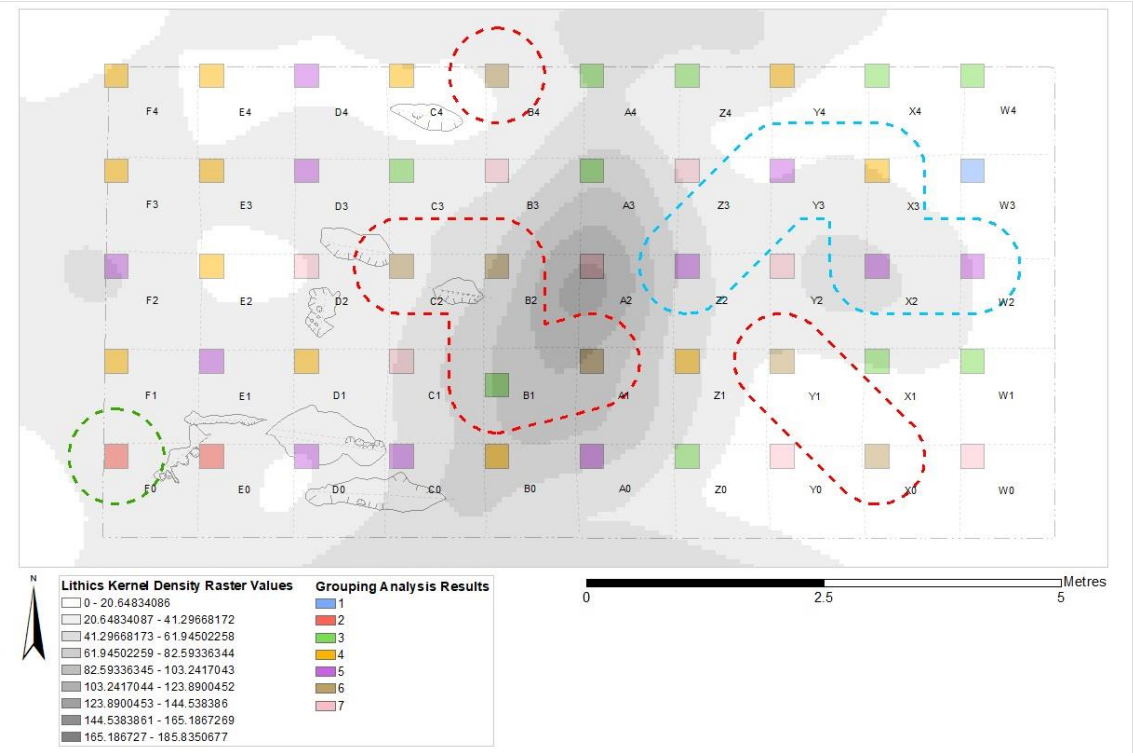

Figure 132. The features plotted in trench 4, compared with the lithics density raster and the areas of interest identified from the geochemical grouping analysis

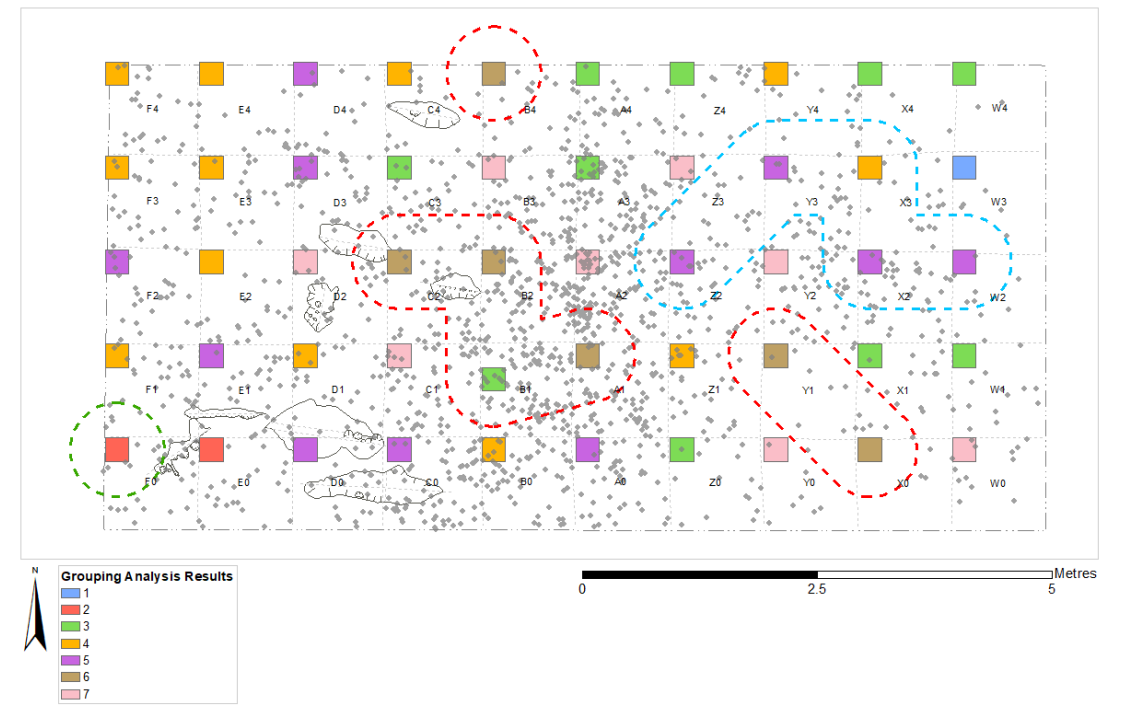

Figure 133. The features compared with the specific locations of finds and the geochemically identified areas of interest

7.3.3 Grouping Analysis for Trenches 11, 12 (north), and 15 field pXRF Results (from 2014 excavations)

7.3.3.1 Overview

Analysis was conducted on the results from pXRF in the field during the 2014 field season. As with the ICP-AES results, the major and minor elements, as measured by this method at Flixton Island 2, were evaluated individually. In addition, manganese and phosphorus were also considered. This was not to facilitate direct comparison with the outputs of the Star Carr and Flixton Island 2 ICP-AES Grouping Analyses particularly as, being measured by different methods, the outputs are not reliably comparable. However, this had proved a useful expansion to those models in strengthening the model as well as when considering both activity areas and the soil environment. Magnesium could not be incorporated as it was below the limit of detection using this method.

There was some overlap of trench 15 with the area that had been previously excavated as part of trench 4 (Figure 134). This was not distinguished in the field and, as such, pXRF readings were taken in this area. This impacted the northern transect of readings in trench 15, along the eastern edge. These samples did not stand out as being notably different from those of the rest of the trench and are still discussed here, but this must be kept in mind.

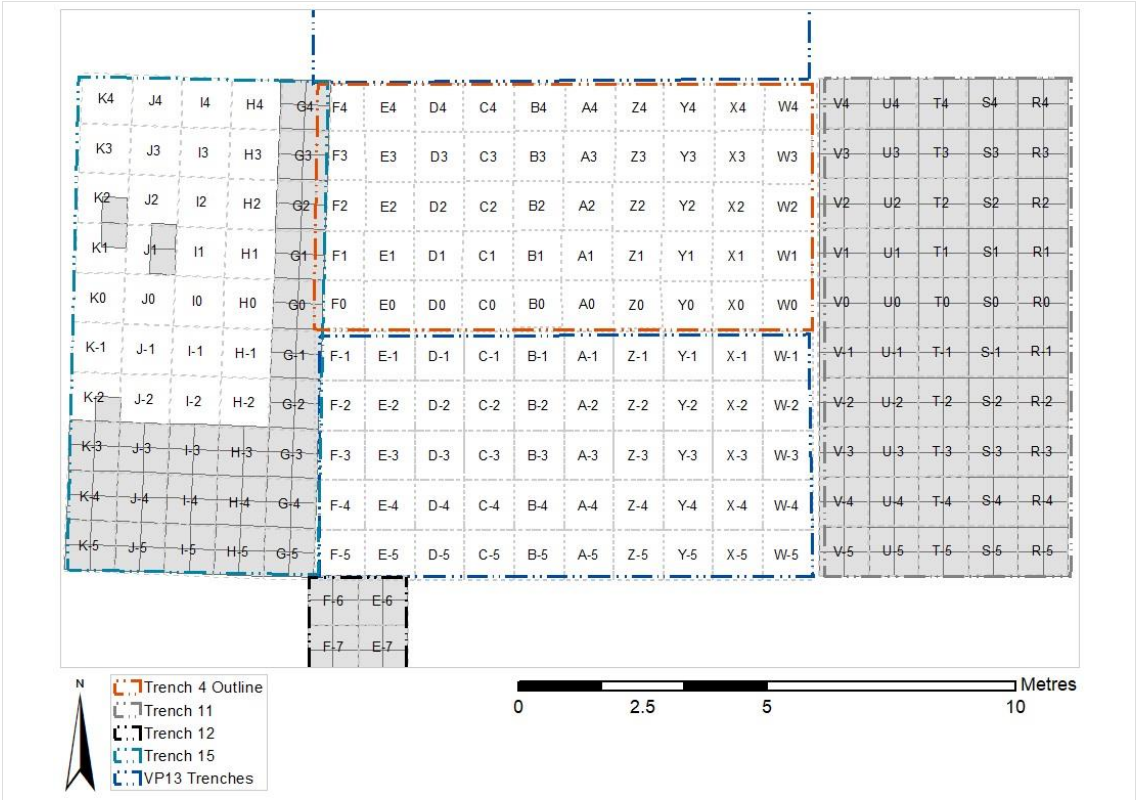

Figure 134.The reading grid for pXRF analysis in the field (light grey), with the excavated trench outlines illustrated to show the overlap of the northern end of trench 15 excavated and analysed by pXRF in 2014 (teal outline), with trench 4 excavated and sampled

Overall, the individual elemental plots were not as encouraging, and the combined model was more difficult to establish coherent areas within. The readings were generally more mixed than the ICP-AES, although this is partly a deception on account of the samples here being examined across a wider area but actually being more closely spaced to each other, and the 0.25 m^2 gridded surface they represented was processed as if continuous, rather than with spacing between them.

7.3.3.2 Expanded key elements (Si, Al, Fe, Ca, K, Ti, Mn, P) optimal model

The five grouping runs highlighted the importance of running at a greater number of groups, even though the tool suggest two was the optimal number in this instance. The samples were divided into two groups on the two-group run; one with higher silicon on average and lower averages for all the other elements incorporated, and the other group the inverse to this, with lower silicon on average and higher averages for all other elements (Figure 135 and Figure 136). However, the lower silicon samples in the blue group in the five-group run below (Figure 137 and Figure 138) were consistently grouped into the higher silicon group in the two group run. This is counter-intuitive but not unexplainable. The averages for silicon in the two groups in the two-group run were close together, presumably being drawn closer together by the interaction of the low silicon samples in trench 11 on the statistical spread of the apparently high silicon group. The samples from trench 11 must have on average, across all the elements, been more similar to each other than to the samples placed in the group with lower silicon (which mainly came from other trenches). This resulted in the samples in the low silicon group of samples, blue in the five-group run, originally being placed into the higher silicon group when only two groupings were generated.

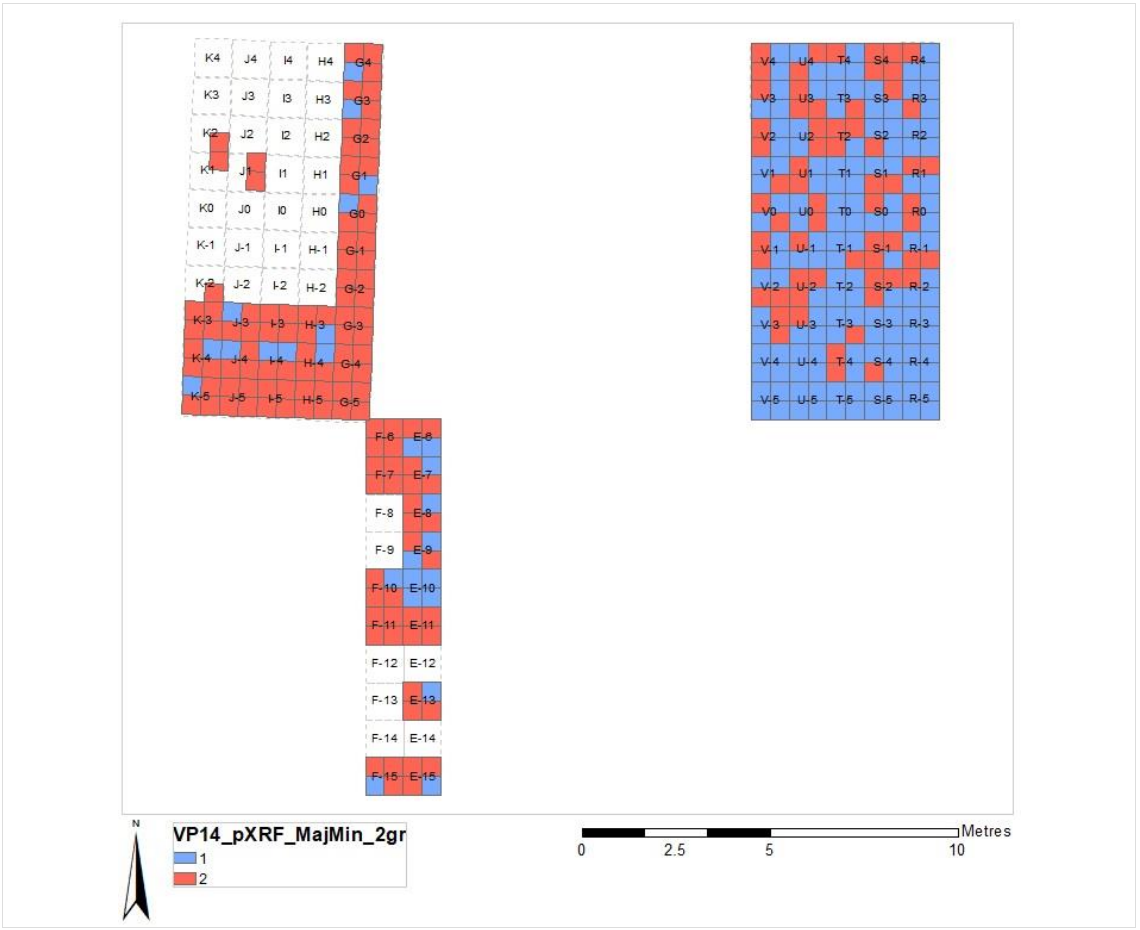

Figure 135. An example two-group run on the combined key elements as measured by pXRF

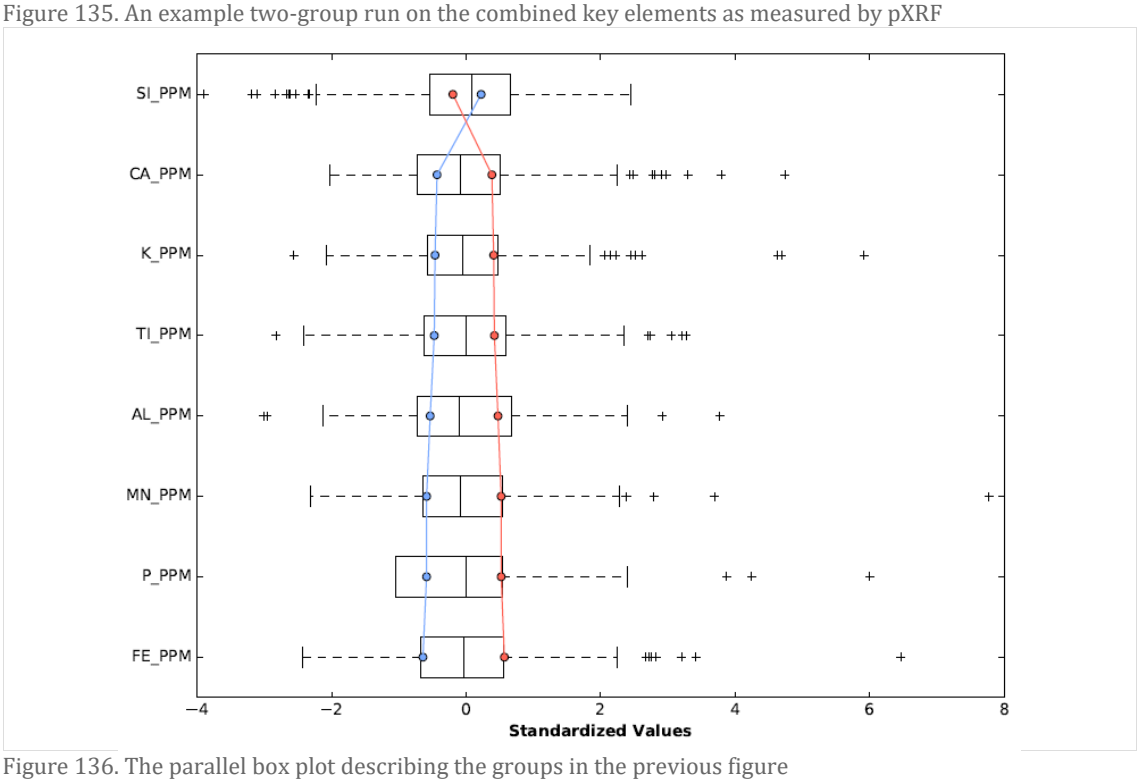

Figure 136. The parallel box plot describing the groups in the previous figure

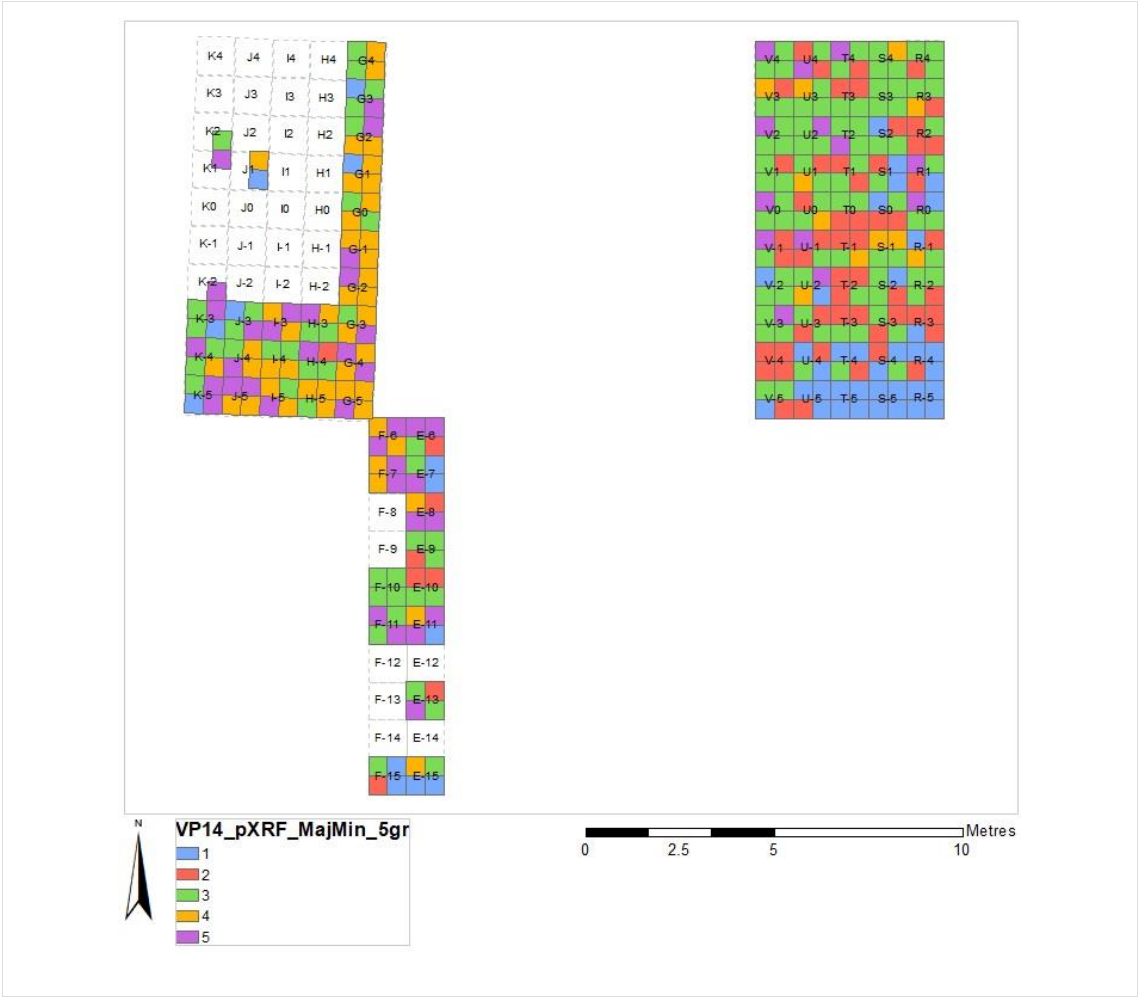

Figure 137. An example five-group run on the combined key elements as measured by pXRF

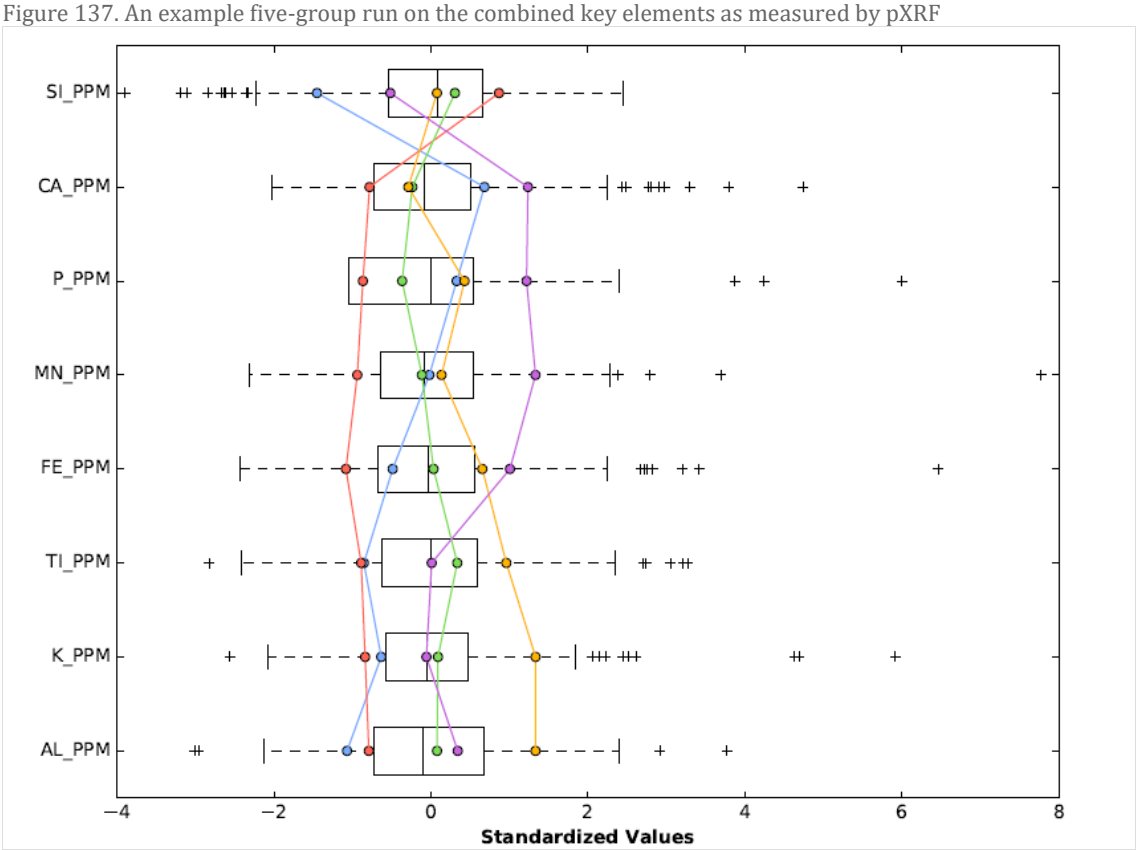

Figure 138. The parallel box plot describing the groups in the previous figure

Looking at this blue group in further detail, the southeastern corner of trench 11 grouped into this noticeable lower silicon grouping in both the five- (Figure 137 and Figure 138) and nine-(Figure 139 and Figure 140) group runs, also characterised by moderately or slightly lower aluminium, potassium, and titanium compared to the global average, near average (slightly lower or higher) iron, manganese and phosphorus, and moderately higher calcium. There is a second, smaller pocket of similarly grouped samples midway up the trench around grid square R1. This is generally confirmed in the repeat runs.

Immediately to the north of the blue group area, there is an area more in keeping with the originally suggested trend for higher silicon on average in this trench: this group of samples, red in Figure 137 and Figure 138, are the highest in average silicon, and lower than average in the other elements. The northern half of the trench meanwhile is generally assigned to a group characterised by being near-global average in all elements (green group in the five-group run). Much of the trench 15 samples are placed into a grouping characterised by particularly high potassium and aluminium, but also moderately or slightly high iron and titanium on average (yellow group in the five-group run). There is one sample that is occasionally placed into a single-sample grouping for being anomalously high in potassium and phosphorus but in most runs this was subsumed into the general groups of the trench, and it does not seem to have a great bearing on the profile of that main group when it is incorporated.

In the nine-group runs (Figure 139 and Figure 140), a pocket of samples is identified in the southeastern corner of the trench as being in similar groupings (red and purple grouped samples in the nine-group example) but this output was not consistent in spread or chemical profile. It may be further enhanced by integration of other elements but for now it is disregarded as too tenuous. The southwestern corner of trench 15 is also generally a little different to the rest of trench 15, being mixed but there were usually slightly more samples here that were frequently grouped into a group defined by slightly or moderately higher calcium, phosphorus, manganese and iron (purple group) but other samples in this group were scattered in the south of trench 15 more generally and in the northern end of trench 12(N). Trench 12(N) is generally mixed. The southern end of it features several samples grouped into the low silicon group and was always similar to the southeastern corner of trench 1. There are samples in the vicinity grouped into the high silicon group and other groups also though. These key areas are highlighted in Figure 141.

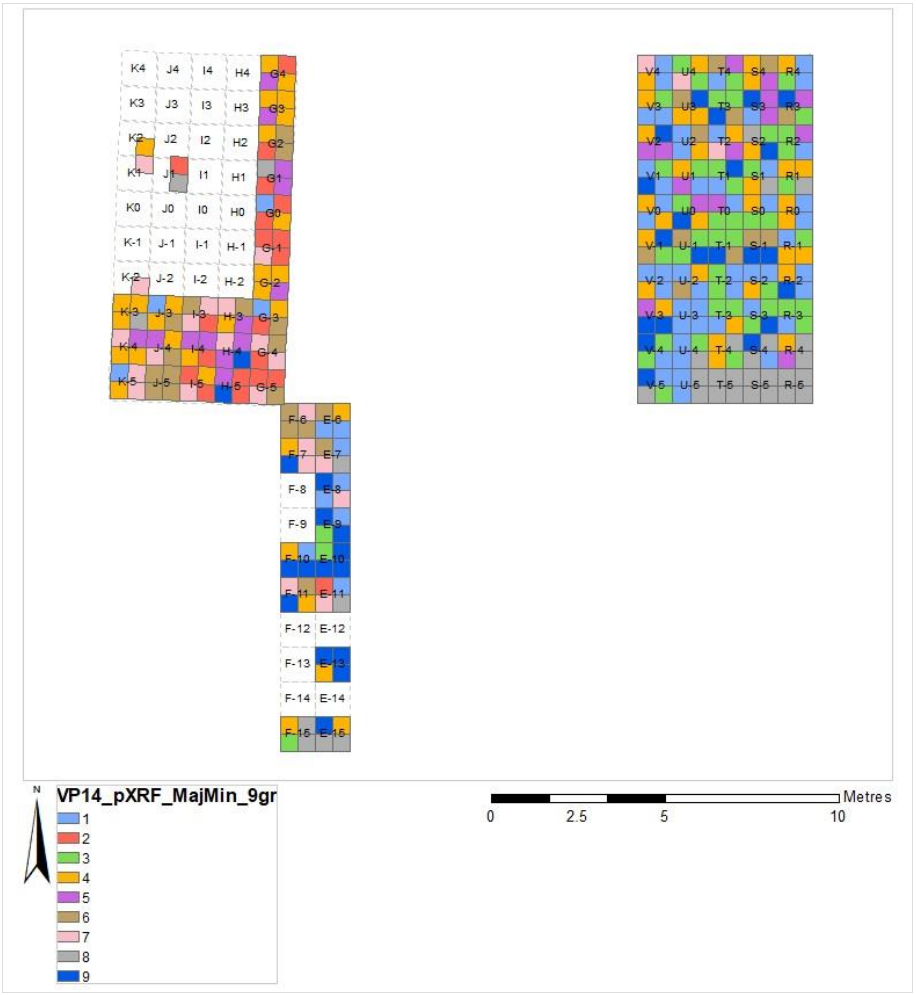

Figure 139. An example nine-group run on the combined key elements as measured by pXRF

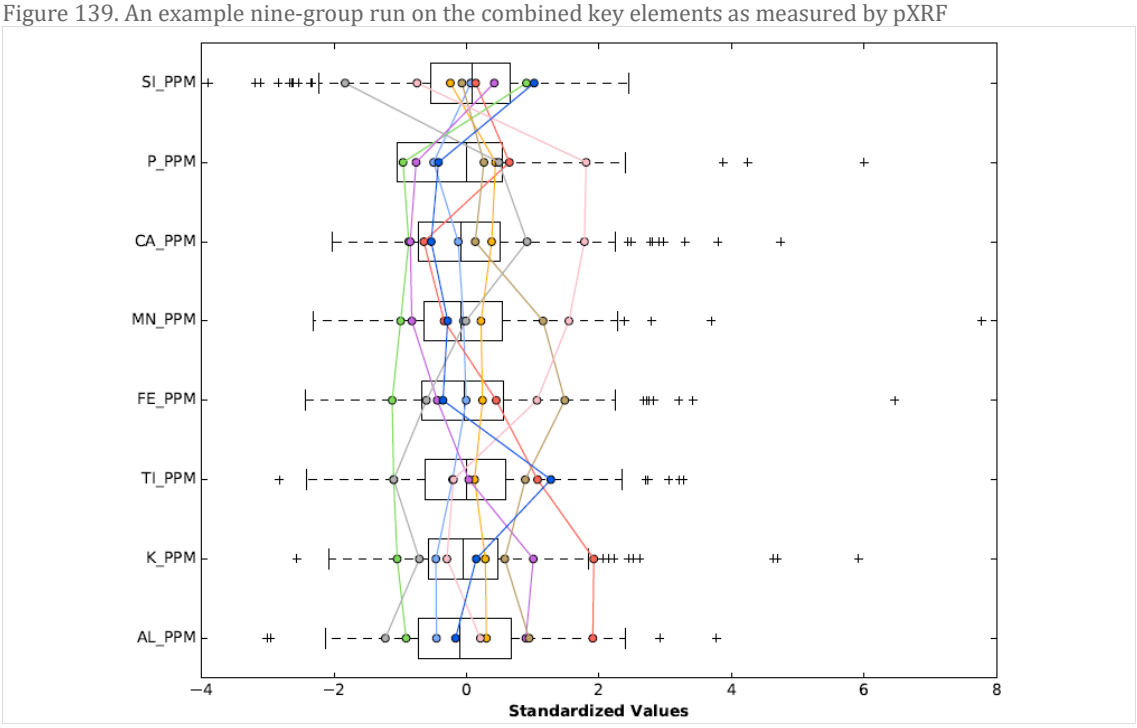

Figure 140. The parallel box plot describing the groups in the previous figure

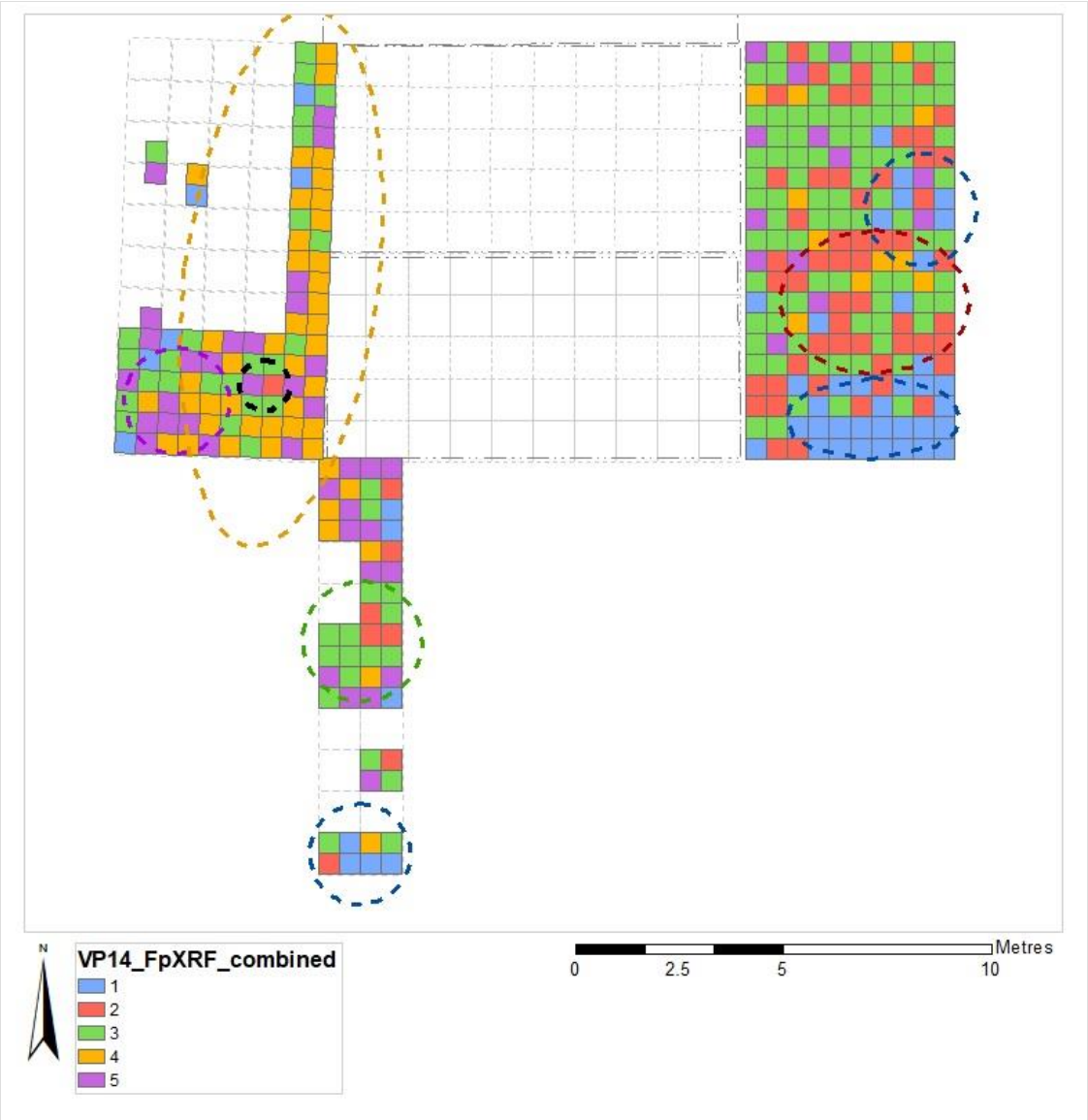

Figure 141. An example of the five-group runs with key areas discussed in text highlighted. The dark blue outlined areas are characterised by lower silicon and moderately higher calcium. The dark red area has higher silicon while all other elements are slightly or moderately low. The yellow area has moderately higher potassium and aluminium as well as slightly higher iron and titanium in some of the runs. The purple area was tentatively drawn out as an area with slightly higher calcium/higher phosphorus samples in the nine-group runs. The green area was frequently a little different to the rest of trench 12, with values near the global averages. The black area is an area that was often isolated in the nine-group runs but with an inconsistent profile.

7.3.3.3 Comparison with lithics data and the K-3 'feature' plot

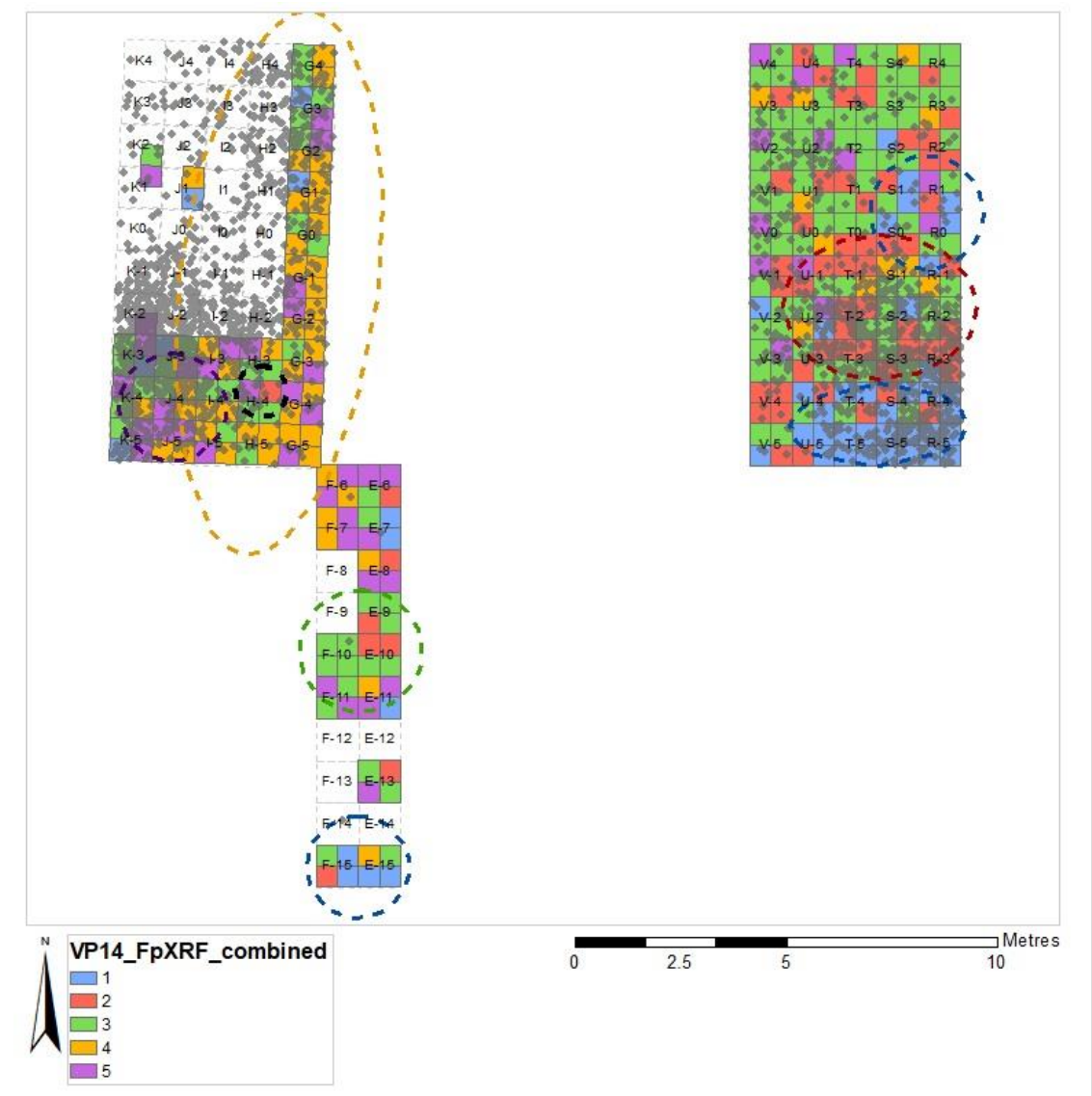

Figure 142. The grouping analysis model for the pXRF results overlain with the lithics from the associated trenches

The soil analysis areas overlap with the areas the southeastern and southwestern scatters are located (Figure 142). The clearest area in terms of the pXRF groupings had been the southeastern corner of trench 11, in the vicinity of the southeastern dryland scatter. This was the slightly lower, and generally wetter, end of the trench and it is possible that the blue-outlined group (coded light blue or grey in the five- and nine-group runs respectively) geochemical signature here was caused by moisture, as the readings there were also taken at the start of a run of dry days. However, that would not explain the presence of the scatter material being here as well; it was not the base of the slope so it is not an area where the water would have naturally pooled and remained over the rest of the trench, though it dried out comparatively slower. There is a small area with some blue-group samples at the southern end of trench 12 which was also wetter relative to the rest of the trench, but in contrast there is a third area of blue-grouped samples to the north of the red-group area

back in trench 11 which were not in a particularly wet area. Neither of those areas were particularly associated with lithics either though.

The southeast scatter spreads across both the blue- and red-outlined areas which were chemically profiled quite differently (Figure 143 A and B). However, given the presence of the lithics, it is proposed that despite the groups providing a different signal, these groups could both be related to the scatter's use or deposition. The blue-outlined group's measurements were perhaps more impacted by the moisture levels and this could be why the area is divided (both being signatures associated with the scatter but just one being impacted by moisture more). Alternatively, they could also be two signals associated with two different activities occurring in the vicinity of this scatter and this is actually supported by the dual peaks presented in the lithics density raster.

The other thing to note is that while the blue-outlined group was generally lower in silicon than the other groups, the main constituent of flint is silicon dioxide: As such, it would be logical to expect silicon to be higher in areas there had been scatters excavated, especially if there had been knapping and microdebitage in this area that may have left small fragments that were impossible to retrieve.

Despite the southeast and southwest scatters having similar profiles, they are not associated with the same dominant geochemical signatures. However, there is a tenuous connection. The areas in trench 15 containing lithics are those that had readings around the global average (green and blue group), those that were slightly higher in calcium, phosphorus, and manganese (the purple group), and importantly, two of the blue/grey group samples. The blue/grey group samples are not the dominant signal here as with the other scatter and are found occasionally elsewhere in the trench, but they are found right where the lithics are most densely packed (Figure 143 and Figure 144) and also where the plotted, ephemeral feature in grid square K-3 was located (Figure 145). The purple-outlined group (purple samples in the five group run, pink and brown samples in the nine group run), which had only been weakly established from the Grouping Analysis work, was most densely identified in the vicinity of the southwestern dryland scatter which strengthened the idea of it being a genuine area of interest geochemically relating to anthropogenic activity. This has ramifications in comparison with the southeast dryland scatter as while the southwestern scatter was more noticeable in the field, the geochemical signature associated with the southeastern scatter (if it is related to anthropogenic processes) is more homogeneous. Despite these scatters having similar profiles, they are not associated with the same dominant geochemical signatures, but there is a small number of blue samples in the region of the southwestern scatter.

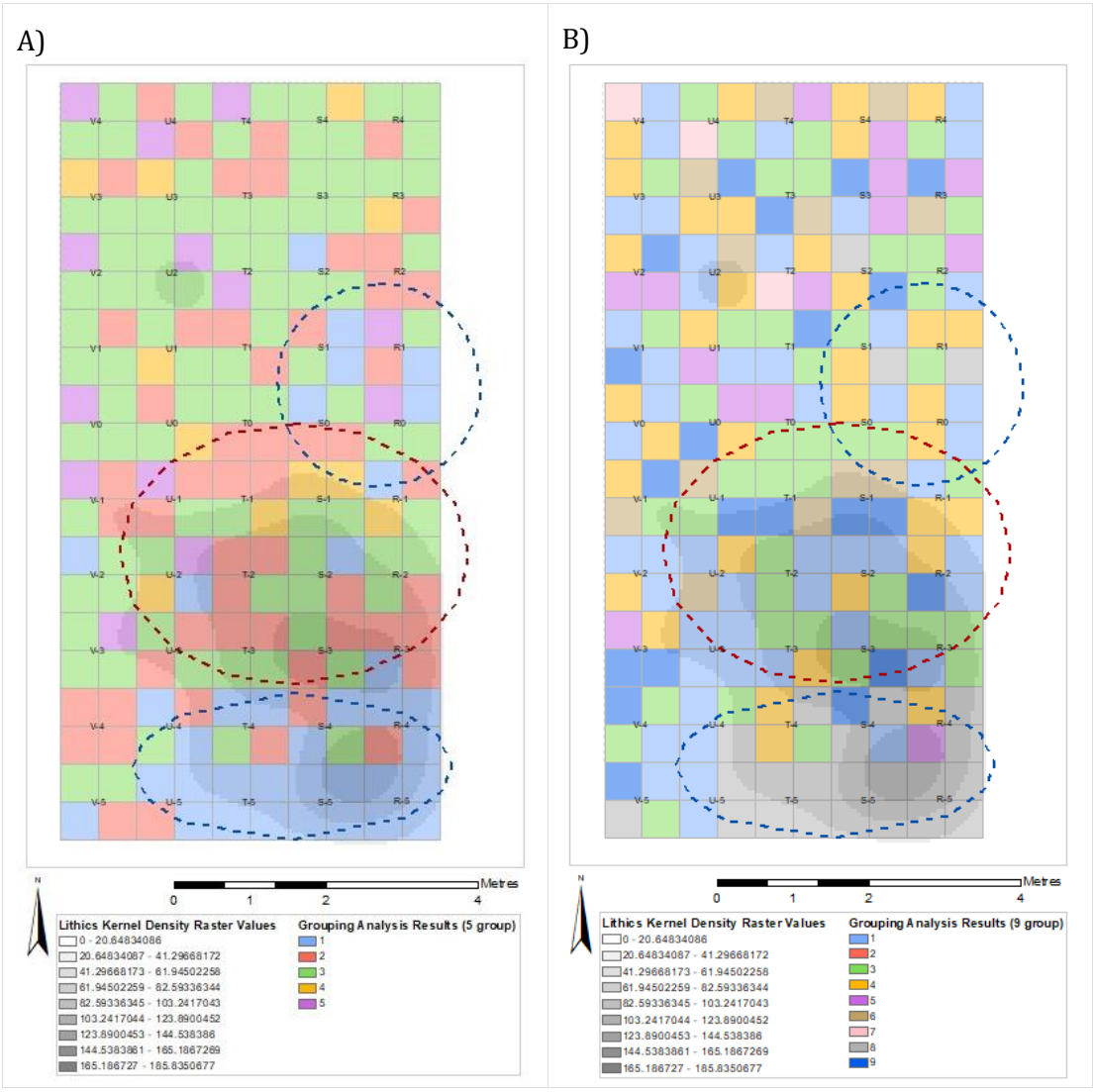

Figure 143. The lithics and soils analysis results from trench 11, with A) the five-group soils grouping analysis underlying on the left, and B) the nine-group analysis on the right

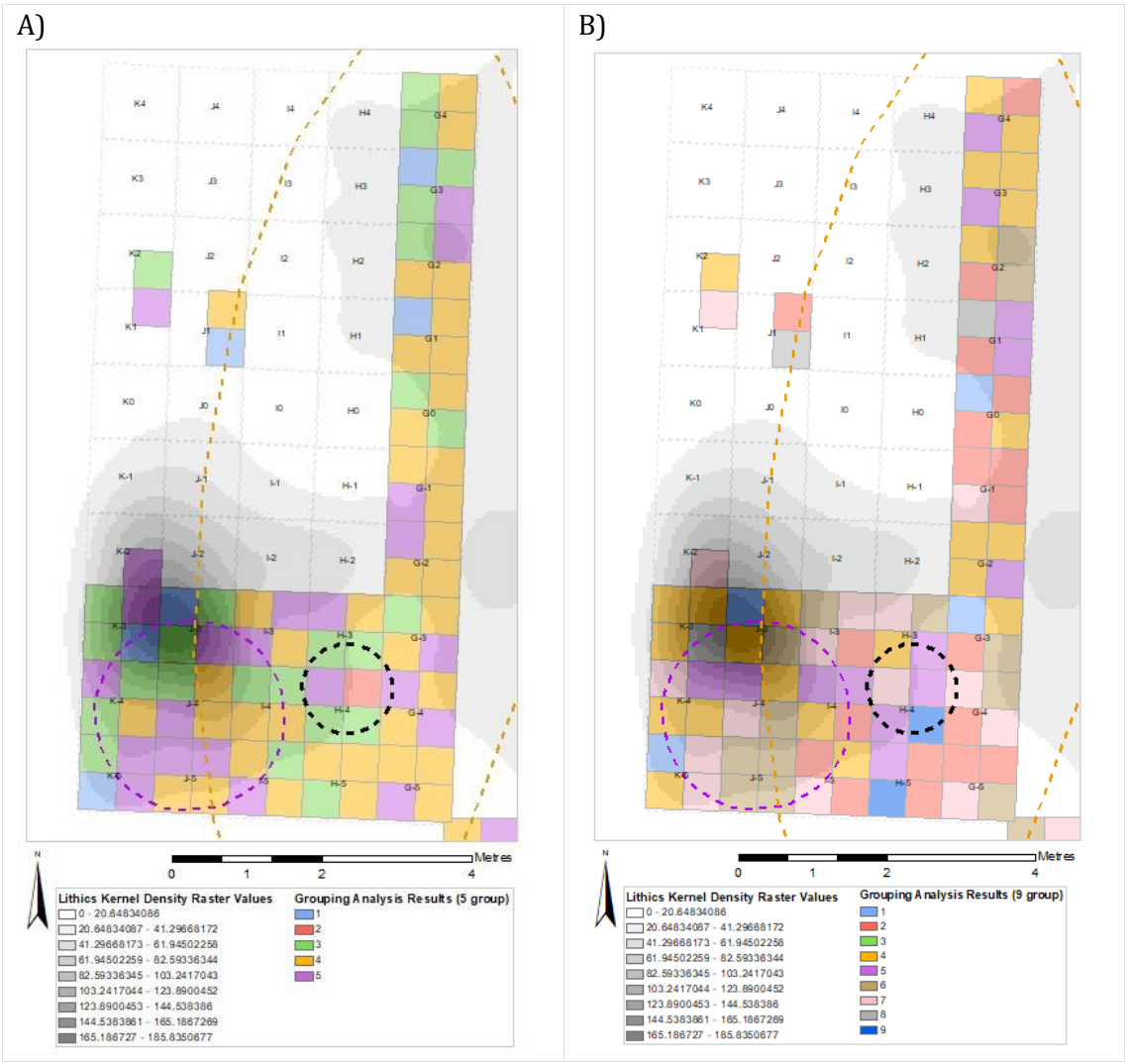

Figure 144. The lithics and soils analysis results from trench 15, with the five-group soils grouping analysis underlying on the left, and the nine-group analysis on the right

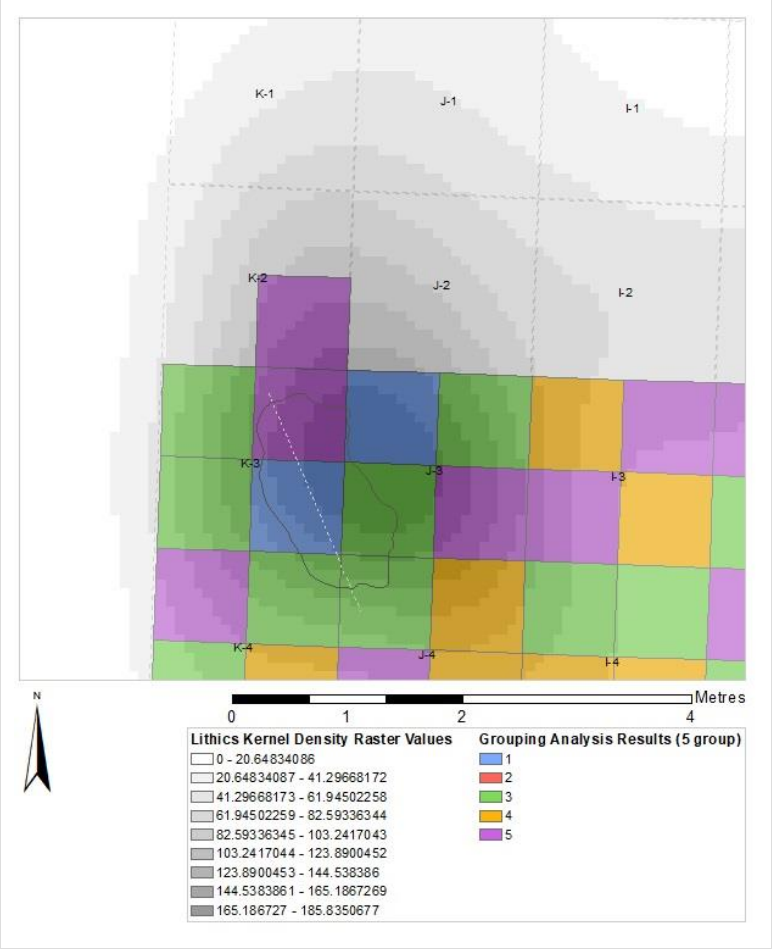

Figure 145. The lithics and soils analysis results around the plotted feature in K-3, trench 15

Much of the northern transect readings were in the yellow-outlined group associated with the yellow group established by grouping analysis, and it must be remembered that some of these grid squares had been partially excavated before. However, in the area of the transect that is nearer to the peak on the edge of the central cluster area i.e. in and around grid square G2, there are more green, blue, and purple grouped samples again. If we consider the areas in both trenches 11 and 15 that are lower in lithics, the areas in trench 15 are dominated by the yellow group samples in the five group run, while those in 11 are dominated by green group samples in the five group run. The small peak in the north of trench 11 is actually near to two purple grouped samples again, although there are other purple samples throughout the trench so this is very tenuous. It could be that the sediments from the trenches were subtly different and therefore just had a different general background. However, as the trenches are only 10 m apart at their closest edges, there was no noticeable difference in the sediments visually, texturally, or in topographical positioning, and there were slightly more lithics associated with the yellow group samples, it is possible that the yellow group represents a signature associated with the the thinner occupation spread of lithics between the southwestern and central scatters. However, without analysis from the rest of trench 15 and trench 9, this cannot not be more confidently established or dismissed.

Finally, there are very few 3D located lithics to consider for trench 12 and there was a small number of sieve lithics obtained from every grid square so there was no obvious patterning in that material either. Geochemically, the northern end also seems to match the signature from the southeastern corner of trench 15, implying this trench should have been a continuation. Regardless of the reason, there are barely any lithics to compare with the pXRF results. In the five-group run, there are three approximate areas to the trench: an area dominated by purple samples in the north, an area dominated by green samples in the centre, an area dominated by blue samples in the south (Figure 146). All areas are mixed though and if the very small assemblage from this trench is considered, there are lithics within or nearby to all three areas. As such, little can be said about this trench at this stage.

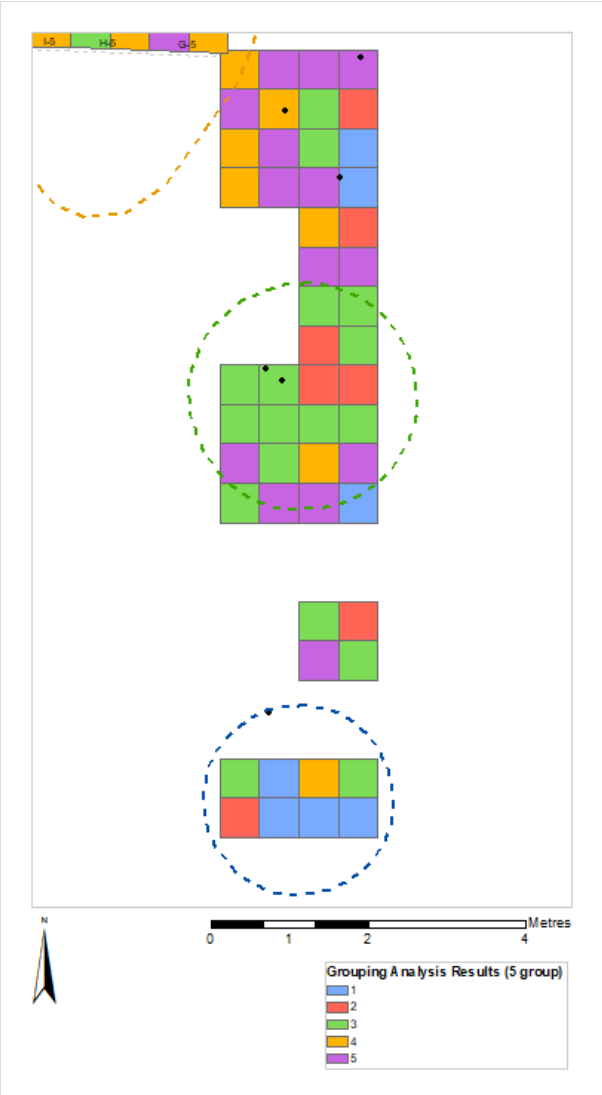

Figure 146. The lithics (black data points) and five-group soils analysis results from trench 12

Overall, patterns were not clear cut in association with the scatters but this is not unreasonable. The deposits are shallow and subject to runoff, and the field they are in is open grassland so while not being affected by roots, the area is not sheltered in any way as deposits in a cave might be. Given the fact that pXRF is sensitive to moisture levels and that the readings may also be imprecise to +/- 10% in several of the major and minor elements

(more so for iron, as discussed in chapter five), a degree of more mixed signatures even from areas homogeneously affected by specific processes such as an anthropogenic activity in the past, is not surprising. However, there do seem to be general trends in the geochemistry as identified through the grouping analysis that appeared to be in association with the major lithic scatters: the dark blue outlined area in the southeast of trench 11 associated with the southern peak in the scatter there, characterised by lower silicon and moderately higher calcium, with perhaps geochemically similar samples in the densest area of the southwest scatter. The dark red outlined area in trench 11 that has higher silicon while all other elements are slightly or moderately low seemed to be associated with the second peak in the southeast scatter. There also seemed to be a background signature that was perhaps subtly different in areas between the southwest and central scatters that caused the identification of the yellow outlined area in trench 15, though the sample coverage was not adequate to explore this further. The fact that there is any homogeneity in the samples associated with the scatters was a surprising result.

7.4 Discussion

There were encouraging results from this holistic integration of the lithics dataset and the geochemical datasets from both ICP-AES in the laboratory and pXRF in the field. It is difficult to say if one method was better than the other, due to the samples being differently spaced out and requiring slightly different visualisation. However, both revealed signatures that seemed to be associated with the scatters. Further to this, the ICP-AES revealed two potential areas of interest that were associated with two different peaks in the central scatter and similarly the pXRF results generated two potential areas of interest that spatially coincided with the two peaks in the southeastern scatter. The pXRF on trench 15 also added support to status of the ephemeral, possible feature in K-3 as being a likely genuine archaeological feature given the different geochemical signature there as well as the associated lithic densities. Future work will include a careful consideration of the elemental composition and what this might mean for specific activities, as is demonstrated in the next chapter for the model developed for Star Carr.

Chapter 8 Geochemistry on Structures at Star Carr

8.1 Introduction

During the POSTGLACIAL Project excavation seasons 2013 to 2015, two or possibly three potential structures were observed on the dryland areas at Star Carr, becoming known as the central structure(s) which had an associated occupation area and the western structure (Milner et al. 2018). Geochemical sampling was undertaken in these areas to see whether 1) geochemical patterning would confirm the contextual changes proposed and 2) whether the geochemical patterning would suggest any identified areas being used for specific activities. As such, the hypotheses considered for the statistical analyses are:

- Samples from within features will differ in their elemental composition, distinctly from the till.
- Samples from within features will differ in their elemental composition, distinctly from each other.
- The elemental composition identified within features will suggest differentiation in activity (based on evidence proposed from known sites and experimental reproductions) that correlates with the activities suggested from the artefactual evidence.

This would also provide a highly complementary, comparative study to the geochemical work at Flixton Island 2. At Flixton, there were no features around which to base the research questions and hypotheses, and as such a very general approach was deliberately taken to avoid any interpretative presuppositions about the data. At Star Carr, the areas within proposed features could be directly compared to those outside features. As such, this was an opportunity to compare the geochemical signatures from not only a different Early Mesolithic site in the same landscape, featuring similar geology and soils on the dryland areas, but one that already had some spatial differentiation unlike Flixton. The activities on the two sites could have functionally overlapped or been different (given their very different natures in extent, chronological use span, and the artefactual evidence, see Milner, Conneller and Taylor (Eds) 2018) so it was not anticipated that a similar signal would be produced necessarily, even allowing for their analysis in separate batches. Rather, any successful identification of spatial geochemical differentiation at Star Carr, particularly in alignment with the features or artefactual evidence, would strengthen the argument that that identifying activity area markers on Mesolithic sites was viable. Any proposed activity areas on both sites might give a sense of the types of signals to expect from Mesolithic sites as well.

Soil samples from both areas at Star Carr were analysed using inductively coupled plasma atomic emission spectroscopy (ICP-AES) and portable x-ray fluorescence (pXRF) in the laboratory. The western structure was also analysed by pXRF in the field in 2015, though as the structure had been first identified in 2014, the field and laboratory sampling from this area was 10 cm below the anticipated Mesolithic occupation level itself.

This chapter is based on a book chapter co-authored with Charles French and Nicky Milner for the Star Carr monograph (2018). The work at Star Carr was initially undertaken with the intention of being a small, supplementary study to see how well the methodology worked on a site where there were more easily distinguishable structures than Flixton Island 2. The results were very encouraging, and it was decided to expand that into a larger project. The ICP-AES results for seven major and key minor elements from the general soil samples have been presented as a model thus far.

8.2 Introduction to the structures

The interpretation of the structures was largely based on the spread of postholes, visually identified changes of context within structural areas which were sometimes associated with a shallow hollowing in the ground or outside spreads in potential occupation areas (see Figure 147), and the density of artefacts generally in those regions. The main central structure was the clearest, with part of a shallow hollow floor encircled by postholes and a number of pits (some of which may form a second structure in this area, although this had been partially excavated as a test pit and not identified prior to these excavations). Around this was a visually identifiable spread that transitions from dark to light, possibly relating to occupation. The structure, the spread, and to a lesser extent the area to the southwest of the structure were the focus of one of lithic scatters identified by Conneller et al. (2018). The western structure was different in nature, featuring a smaller area with several small posthole-like features, with no very clear broader contextual changes but being covered with a significant amount of burnt lithic debitage.

The central and western structure contexts and surroundings were sampled using the same method of sampling as at Flixton Island 2 in 2012 (see chapter five). The sampling took place in 2014 while excavating the central structure and surrounding occupation spread, and 2015 while excavating the western structure (Figure 148). A total of 505 samples were taken from these areas, in spits on a 0.5 m x 0.5 m grid (aligned with the 1 m^2 site grid), supplemented with additional samples taken from the postholes and pits.

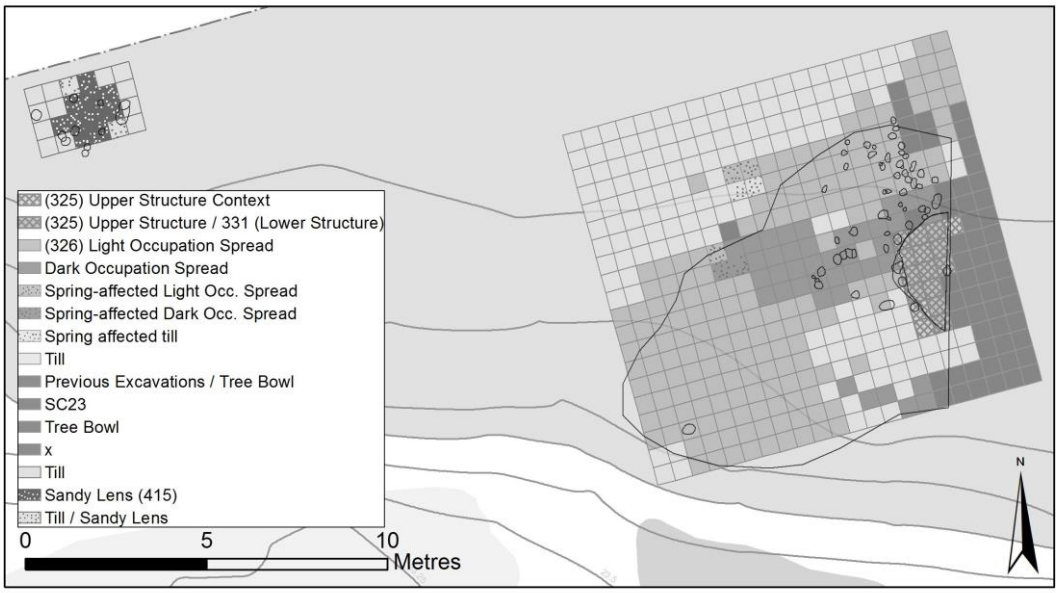

Figure 147. The general sampling grid across the western structure and the central occupation area, superimposed with plans of the features and symbolised to illustrate the main context variations across the area

Figure 148. Sampling over the central structure: the eastern trench edge is at the top of the photo, which is the edge that cuts through the central structure. The structure is in the vicinity, and to the southwest, of the white sample boxes seen near that trench edge. Sampling was taking place across the darker occupation spread areas at the time of the photo. (Kite photograph taken by Sue Storey, reproduced from Rowley et al. 2018.)

189 samples were selected from around the central occupation area for analysis, including seven control samples taken from the generally archaeologically 'sterile' till clay outside the main occupation, context (308) (see Figure 149). The results from the small posthole features are not presented here, only those from 172 samples taken as general coverage of the main sediments within and without the main central structure itself, due to time constraints (the posthole results will be presented in a future publication). Two sets of samples were taken from both the top of the central structure (hereafter termed the upper sample set) and from lower down in the context, towards the base (lower). The remaining samples were from a single layer across the occupation spread contexts or from fills of smaller features. 24 samples were also taken from the western structure area at the level where the potential postholes had been confirmed, which was about 10 cm below the interface between the peat and the till where occupation was anticipated based on artefact distributions and the micromorphology (302: Mid grey peat/till interface layer) (Milner et al. 2018).

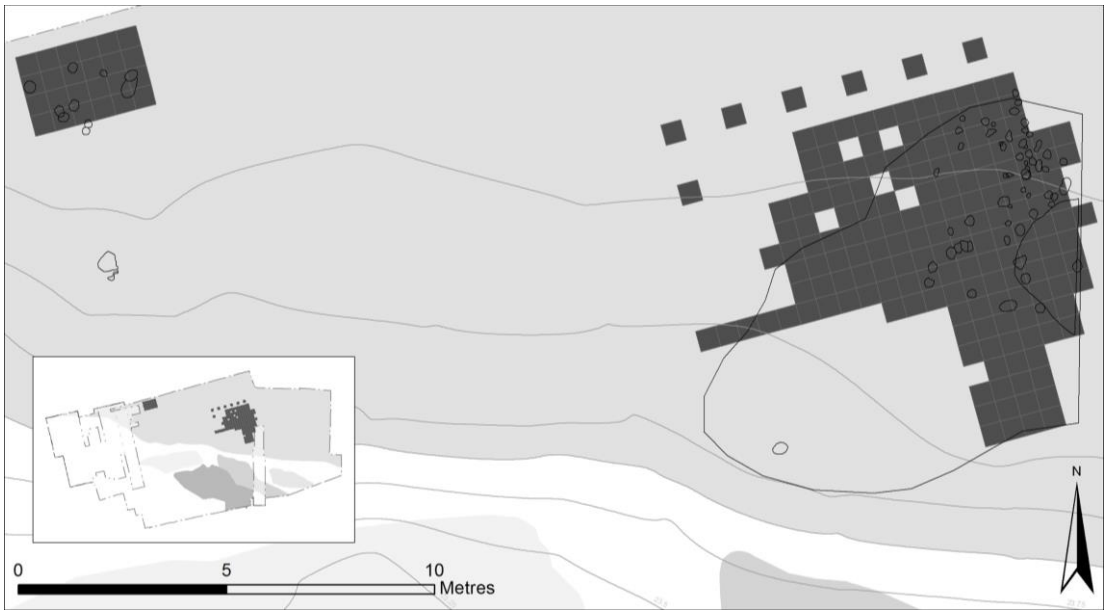

Figure 149. The grid of soil samples processed for ICP-AES analysis (dark grey). The western structure is the 6 x 4m grid to the west, the rest of the samples are considered to be from the central area. Most of the samples cover the occupation spread and structure (reproduced from Rowley et al. 2018)

The elemental compositions of the soils in the associated contexts were analysed using ICP-AES and pXRF as described in chapter five. A pilot study of 29 samples from across both structures was first submitted for ICP-AES to test whether there would be any differentiation in the results. The results suggested potential for geochemical differentiation between inside the structure and out so the study was expanded to a total of 218 samples which were also by analysed by ICP-AES in 2016. Again, due to time constraints, the results of the pXRF work will be presented in a future publication. It is the results of the ICP-AES analyses that are presented here.

Grouping Analysis, utilising a k-means++ algorithm, was conducted on the ArcGIS ArcMap (10.4.1 and 10.5) and Principal Component Analysis was conducted on SPSS 24 and OriginPro 2016. From the ICP-AES results, thus providing readings for 36 elements in each sample, seven elements were selected for the initial statistical study published in the monograph: aluminium (Al), calcium (Ca), iron (Fe), potassium (K), magnesium (Mg), and phosphorus (P) as they made the highest contributions to the composition of the samples and manganese (Mn) which showed a high degree of variability across site (from 17 ppm up to 700 ppm). These are all standard elements considered in other soil analysis applications. Other elements available, such as sulfur, were minor or trace contributors to the samples.

8.3 Potential complications

As mentioned in the monograph, the soils at Star Carr are complex given the palaeolakeshore location, local historic peat drainage and agricultural procedures in more recent times, subsequent acidification of the soils and sediments, and the variable underlying chemical composition of the till and marls. Supplementary micromorphology was undertaken within the central structure by French and, in summary, his results suggested that while the sediments contained anthropogenic debris that had possibly been within the structure, they were disturbed and mixed. Furthermore, bone fragments present in the slides had evidently been affected by the acidity and groundwater fluctuations (see C. French's section in Rowley, French and Milner 2018).

Aluminium, iron and manganese are all naturally occurring in mineral and oxide accumulations in the soils at Star Carr (see Figure 150), and particularly in subsoils on top of the clayey till substrate resulting from the gradual weathering due to the erratic water levels at the locale. As the structures are on the dryland area of the site, they are better drained but they will still have been saturated from time to time and subject to groundwater fluctuations post-occupation. As such, these elements and possibly, in addition, calcium potentially derived from the substrate below the site may have been enriched as a result of these natural processes occurring on site.

Another potential issue during the Grouping Analysis is that the samples might be grouped because they are close together and are therefore on naturally similar substrates. In order to test this, repeat runs of the tool looking at the seven key elements were conducted on the data from the contiguous samples from both structures, but not the till. Similarly, further repeat runs were conducted on the contiguous samples from just the central occupation area. The group patterning seen in the analyses for the complete sample for these elements was maintained across the repeat runs and therefore the general variance in different areas does not appear to have been influential in the formation of the groups for those elements.

Figure 150. Ironpan seen at Star Carr, 2015 excavations

8.4 Individual Elemental Results

The descriptive statistics from the Star Carr till samples excavated more than 1 m from the recorded occupation spread contexts are provided in Table 45. This gives a sense of the general geochemical composition of the local till. Table 46 illustrates the range of the Star Carr till results compared with Boston's results from Filey and Skipsea (see chapter six, Table 38, for full data comparison): as can be seen, while the Star Carr ranges show high variability in the sample readings, the tills were even more variable particularly at Skipsea but also at Filey. This is unsurprising given the mixed nature of such glacially deposited sediments.

Table 45. Descriptive statistics for the major and key minor elements measured from samples recorded as till at Star Carr (values in parts per million). (Table reproduced from Table 21.2 in Rowley et al. 2018.)

Value (ppm)	**Al**	**Ca**	**Fe**	**K**	**Mg**	**Mn**	**P**
Minimum	3500	1300	7100	200	700	17	90
Maximum	31200	20000	46500	1700	6100	703	4750
Range	27700	18700	39400	1500	5400	686	4660
Mean	11320	3990	18907	646	3180	125	735
Median	11500	3600	18000	500	3300	94	580
Mode	11100	3500	17500	500	3500	88	550
Std. deviation (popul.)	3978	1892	5665	363	965	98	622

Table 46. Ranges of values (ppm) from Star Carr tills compared with Boston's readings on till samples from Skipsea and Filey (reproduced with permission from Boston 2007)

Range (ppm)	**Al**	**Ca**	**Fe**	**K**	**Mg**	**Mn**	**P**
Star Carr	27700	18700	39400	1500	5400	686	4660
Skipsea	63377	129697	32252	15539	10095	852	10826
Filey	24765	82603	23947	13958	10906	269	1309

Table 47 is a direct reproduction of the individual elemental plots and the discussion as presented in Figure 21.4 in the Star Carr monograph, with additional comments in square brackets added for clarification. The structure outline is plotted over the symbolised results, with the small, near semi-circular outline of the suggested structure itself on the eastern edge of the sampling area, surrounded by scattered postholes and pits, almost all of which are contained within a wider plotted area that was the suggested extent of the darker occupation spread contexts (there was not a neat edge to this to be plotted definitively). The terms 'enhancement' and 'depletion' were used to discuss values relatively higher (red) or lower (blue) than the average (yellow), but this does not necessarily indicate actual enhancement or depletion through either a natural or cultural process (e.g. all the 'low' values could in fact be the unmodified sediment value reading, so all those higher could have been actively enhanced in some way).

Table 47. Plots of the central structure readings for each of the key elements, displayed by Jenks natural breaks in the non-normalized readings (in parts per million). (Reproduced from Rowley et al 2018.)

Values in ppm, displayed grouped by natural breaks (in the local dataset only)	**Analysis**
Aluminium 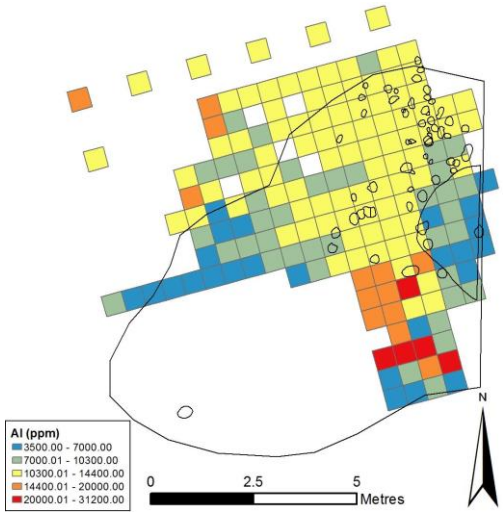	There are three main areas which show fairly widespread evidence of aluminium depletion (shown in blue): the central structure hollow, the area to the west of the occupation spread and the southernmost squares. The area to the north (part of the occupation spread) has average readings (yellow). It has long been established that clay consists of aluminium silicates with impurities (cf. Weems 1903; Kerr 1952; Brindley 1952), and the patterning which clearly delimits the structure may suggest less clay in the sediment within the hollow. In contrast, there is a strong peak (red) next to pit/posthole [336] (to the southwest of the central structure) the fill of which contained an interesting collection of flint including some burnt pieces (Chapter 8 [Star Carr Monograph]) and 26 pieces of bone, the vast majority of which had been heat affected (Chapter 7 [Star Carr Monograph]).

Values in ppm, displayed grouped by natural breaks (in the local dataset only)	Analysis
Calcium 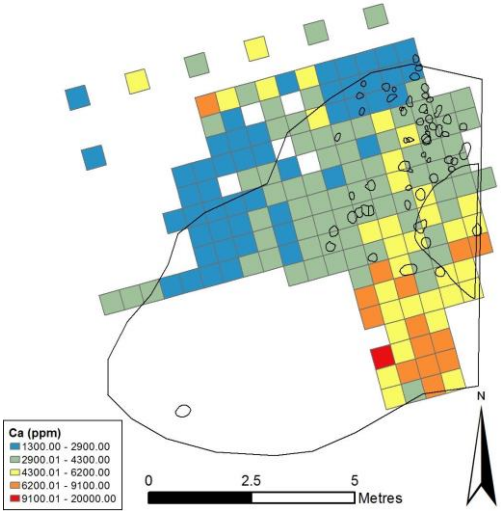 	Calcium can be enhanced by bone (and tooth) refuse and therefore has been found enhanced on agricultural sites where these are consistently incorporated into soil enrichment practices (e.g. Entwistle,Abrahams and Dodgshon 2000). Therefore, it is possible in a Mesolithic context that enhancement could suggest activities involving bone processing of some sort, dependent on intensity and preservation. Here the readings for the central structure and its environs are average or slightly depleted. The area to the northwest is generally depleted but there are patches of higher readings in the area to the southwest of the structure. It has been noted from the micromorphology that some fragments of bone exist within the structure and this may account for the average and slightly elevated readings for this element in that area. In addition, calcium, along with phosphorus and potassium, was found to be elevated in the vicinity of a wood fired oven in a modern earthen floored house studied by (Middleton,Price and Price 1996). Therefore, these readings might relate to the burnt material in pit/posthole [336]. There is also one square to the north which has higher than average readings.
Iron 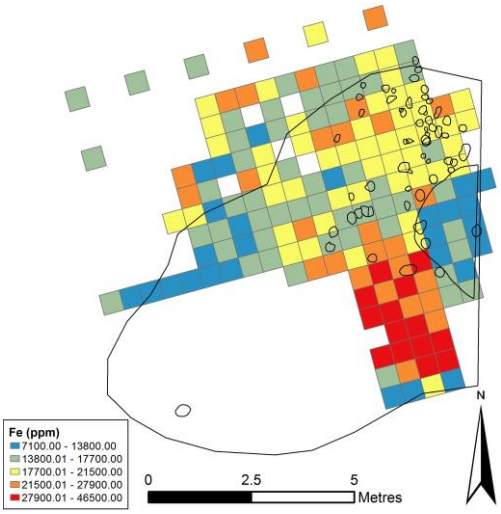 	Iron differences in soil tend to result from redox processes causing it to go into solution as Fe II compounds and then redeposit as insoluble Fe III. It is shown from the micromorphology results that iron had precipitated in the structure. In fact, orange powder was visible in areas of the dryland and probably results from the oxidation of pyrite (see Chapter 22 [Star Carr Monograph]). Nevertheless, in this plot, the central structure is defined by relative depletion of the deposits, as is the area to the west of the spread. The area to the north is mixed. The area to the southwest of the structure shows higher than average readings. Homsey and Capo (2006) found that iron increased with clay content and thus it is possible that the sediments within the structure are relatively depleted because there is a lower clay content here.

Values in ppm, displayed grouped by natural breaks (in the local dataset only)	Analysis
Potassium 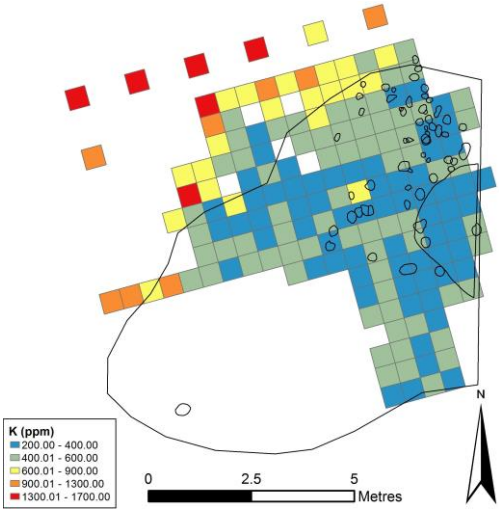	The presence of potassium can generally be enhanced by activities involving plants and has been associated with occupation areas (Middleton and Price 1996; Entwistle,McCaffrey and Dodgshon 2007). This could be from deposition of residual wood ash as seen sometimes, but inconsistently, in modern wood burning contexts (Scotter 1963). Potassium salts are highly soluble so would likely disappear through leaching within a short period after the fires that deposited them but they could potentially fix in the clay content of the soil and till (Stanford 1947; Oonk,Slomp and Huisman 2009). In this case, most of the occupation area, particularly the central structure, are relatively depleted; whereas the till and the edge of the occupation area appears to be relatively enhanced. This is either related to the nature of the soils (the enhanced area is generally more clayey and the occupation spread is more of a sandy/clayey loam) or there is some depletion due to the nature of the occupation.
Magnesium 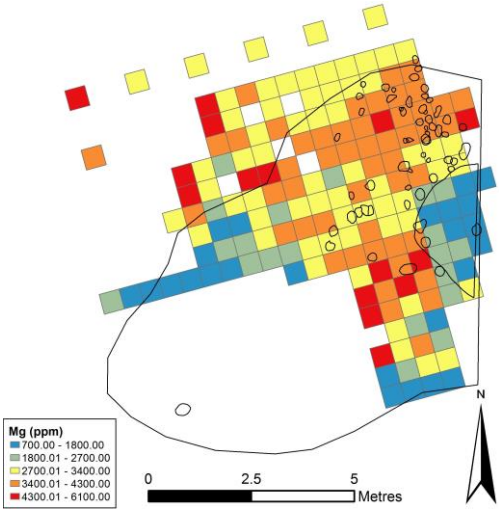	Magnesium can correlate with potassium, and is also generally thought be associated with plant nutrients, wood ash, and wood burning (see Scotter's 1963 work on forest fires, Middleton and Price 1996, Oonk et al. 2009). Again, the salts are soluble but might fix in the clays given suitable conditions (Oonk et al. 2009). The patterning for this element shows depletion within the central structure and some to the area to the west, as well as to the south of the structure. High readings to the southwest of the structure surround pit/posthole [336] containing burnt material. The pattern is dissimilar to potassium in that the rest of the occupation spread shows average and higher than average readings. Although ash was found within the micromorphology samples from the structure, its presence was so small and relatively infrequent that it was unlikely to increase the elements noticeably, explaining the discrepancy with these results.

Values in ppm, displayed grouped by natural breaks (in the local dataset only)	Analysis
Manganese 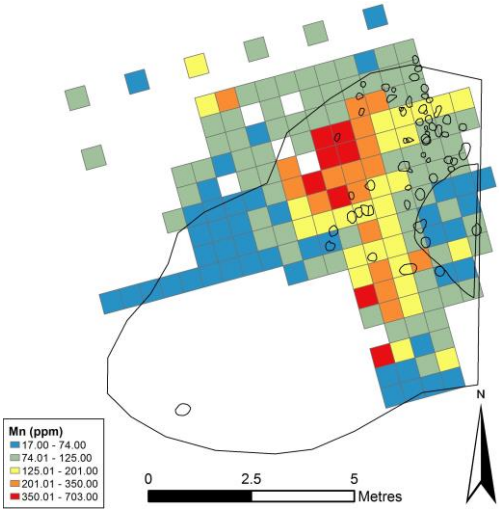 	Manganese tends to be associated with iron as both are frequently found in redox induced deposits (Lindbo,Stolt and Vepraskas 2010). This mineral is mainly depleted across the area except for the central part of the occupation spread which has no obvious relationship to any archaeological features or any patterns from other elements. This would suggest this is a natural phenomenon, and indeed manganese oxide is found to occur in delimited areas across the site.
Phosphorus 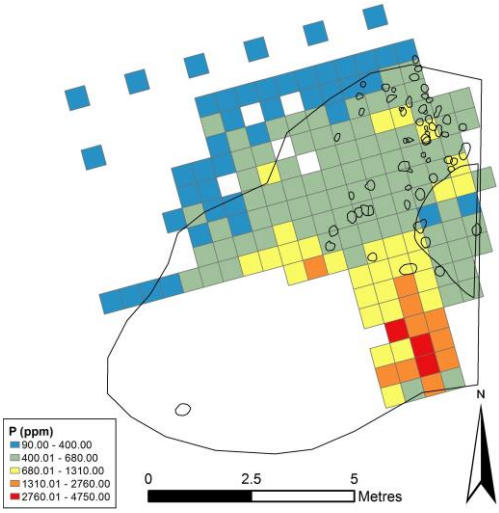 	Phosphorus is the most well established elemental indicator of anthropogenic enhancement in soils (Entwistle,McCaffrey and Dodgshon 2007; Oonk et al. 2009). It is often enhanced by middening, food processing, and other depositions of excrement, animal remains and plant nutrients. It is chemically relatively stable and therefore persistent in most soils (though note, as such, it will move with the soils if they are physically moved). There is clear patterning with this element, with the northern area of the sampled area being depleted and the area to the southwest of the central structure being enriched.

It can be seen the central structure samples stand out on several of the plots as distinct from their immediate surroundings particularly concerning aluminium, magnesium, iron, and manganese. As discussed in the monograph, we explained that all of these can be affected by groundwater and therefore could be caused by differential drainage in the area. Middleton and Price (1996) found that aluminium, iron and magnesium all correlated well in an ethnographic study of a modern earthen floored residence and its surroundings and argued this was best explained by natural geochemical processes. Looking at the correlations between these elements, the statistically strongest correlations in the dataset were between aluminium and iron and aluminium and magnesium (with Pearson correlation coefficients above 0.7 i.e. above 70% correlation). This did not explain exactly why these elements were so much lower inside the structure relative to the immediate environs, however. It could be that the anthropogenic processes that took place within the

structure impacted the natural geochemical processes occurring and this is a signature from the prevention of a natural process being interrupted i.e. we are not seeing a signature from an activity, but prevention of a process. Alternatively, there may be an enhanced level of some elements within the structure that cannot be measured by ICP-AES but which is altering the detection of the elements that can be measured. Finally, Wilson (pers. comm.) noted that the areas with high readings external to the structure were being enhanced in some way through cultural activities that occurred in the occupation vicinity but not within the structures themselves.

In addition, phosphorus is often considered an indicator of human activity, though it can be an indicator of a wide range of processes. It is relatively elevated to the southwest of the structure, but average/depleted in the structure itself and the rest of the occupation spread area, and then more strongly depleted outside the occupation area. This perhaps suggests that the structure interior was kept relatively clean of waste from activities or at least treated differentially, with the area to the southwest of the structure being where refuse may have been deposited, either deliberately or accidentally, or otherwise influenced by the use of the large pit/posthole located just to the southwest of the structure (Star Carr feature cut [336]).

8.5 Grouping Analysis at Star Carr

8.5.1 Grouping analysis on the upper ICP-AES dataset from Star Carr based on major and key element results

The optimal number of groups established by repeat runs of the algorithm on the key element results for the upper dataset suggested between six and 10 groups (results: 6, 10, 9, 9, 10, 9, 10) but more likely at the higher end of that range (nine or 10). Four repeat runs of the tool set to identify nine statistical groups in the upper dataset identified several reasonably consistent groupings and an example of this was discussed in the monograph (see further detail below). For the lower dataset, the suggested optimal numbers were between seven and 12 (results: 12, 11, 12, 7, 11, 10, 7, 9, 8, 10, 11, 8, 10, 8, 8), but eight was most commonly generated and again produced reasonably consistent groupings. These ranges suggest that the patterning of the elements in the samples is complex but the consistency of groupings both between repeat runs on the same dataset and when comparing the upper and lower datasets of the central structure supports the identification of robust groupings. This is unsurprising given the interplay of many natural processes affecting the soils at Star Carr, as well as any potentially compounding influences from anthropogenic processes.

The samples that were grouped together by the analysis as having similar geochemistry suggested patterning that further built on the results from the individual elements. ArcGIS generates R^2 values for each variable which can be used to suggest how good that variable is in discriminating between different features. The larger the R^2 value, which ranges from zero to one, the better that variable at discriminating. Table 48 shows the R^2 values for the models produced by the four runs for nine groupings by major element readings. As can be seen, the scores produced for all elements are actually quite high. The highest values (in bold on red) come from potassium, aluminium or iron depending on the run while lowest values (in bold on blue) come from phosphorus or calcium. While the maximum and minimum values do not consistently come from the same variable, potassium, aluminium and iron are always the top three discriminating variables while the remaining four elements (further including magnesium and manganese) are less influential.

Table 48. ArcMap generated R2 values for each variable from the four different models for nine groupings at Star Carr. They are colour coded from highest values (red) to lowest (blue), with the highest and lowest values in bold font

Element	*Run 1*	*Run 2*	*Run 3*	*Run 4*
K	**0.7872**	0.7857	0.785	0.7878
Al	0.7629	**0.794**	**0.8542**	0.7935
Fe	0.737	0.7792	0.7701	**0.821**
Mg	0.6924	0.7082	0.7059	0.7379
Ca	0.6111	**0.656**	**0.6042**	**0.6462**
Mn	0.5622	0.7301	0.7334	0.7667
P	**0.5502**	0.6622	0.6944	0.7007

Figure 151, reproduced from the monograph, is an an example of the results when the analysis was set to produce a nine group output on the upper dataset. The areas with samples grouped together were: The central structure combined with the western area of the central occupation spread (purple); the majority of samples from the central occupation area, forming a rough ring pattern (red); a small number of samples from the central occupation area, which are in the centre of the red ring pattern and which aligns with some of the posthole placements, supplemented with another group of samples from the south of the central occupation area (green); finally, the till samples and the majority of the western structure, which suggests that perhaps the main signature from the western structure was for the natural till because of it being too far below the genuine occupation layer (grey).

Figure 151. The western structure and central structure areas, with 9 groupings specified for the complete dataset. (Reproduced from Figure 21.5 in Rowley et al. 2018.)

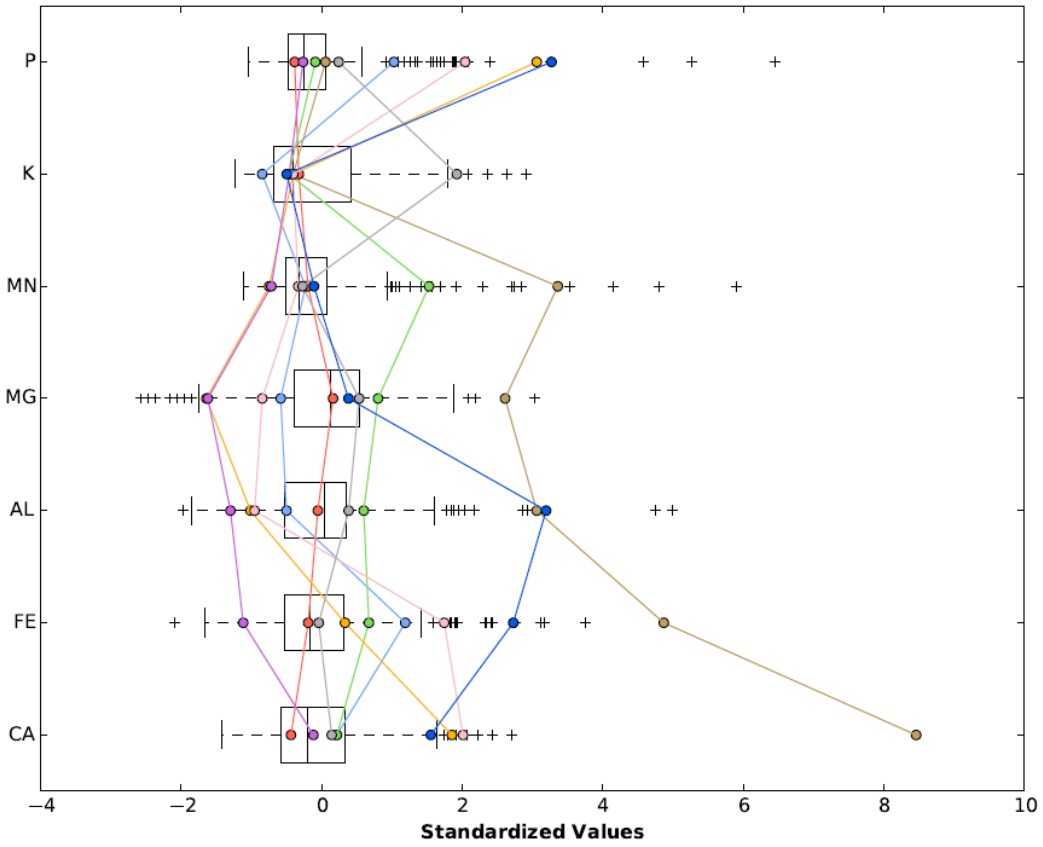

Figure 152. The parallel box plot generated on ArcGIS of the compositions of the different groups identified in Run 1 of the nine group analyses

The purple/central structure group was relatively depleted in most of the elements and it was suggested this may have been from the fill of the hollowed out structure coming from material carried in or even covered with a natural material flooring, or due to a clearing out process, in contrast to more clayey samples based on the till from outside the structure. However, the purple grouping also included samples from elsewhere in the occupation spread that did not come from areas showing clear hollows or features, which is not as easily explained. One possibility is that there had been other structures that were not visible

archaeologically. Another is that similar material working or activities were taking place in those regions independent of structure presence. They do not exhibit chemical signatures traditionally associated with hearths. Topographically, they are on a gentle slope and not in a position where all the purple-coded samples would experience similar water drainage or pooling different to the other samples from the central area.

The red and green/occupation spread areas are not particularly clear when examining the individual elements except perhaps for manganese and if this is a natural elevation of this element, as manganese oxide is frequently found in the soils in the vale as a black solid, it may be just a natural enhancement being reflected in the grouping analysis. This would explain the visible darkness of the sediment in these areas too. However, these occupied area samples were still geochemically distinct from the till samples from unoccupied areas regardless of whether this related to a natural phenomenon or a direct anthropogenic enhancement.

The area to the southwest of the structure yielded less homogeneous chemical signature patterning. It seems to be largely because of the complexity of this area that around nine groupings were suggested as optimal statistically by the analysis tool. Phosphorus and aluminium were relatively enhanced in this area generally. All of the readings for phosphorus above 2000 parts per million were from samples in this region (n = 7 samples). While not high enough to suggest intensive, sustained middening practices, this may have reflected a localised signature for smaller scale, potentially anthropogenic, organic waste disposal. The distributions of lithic artefacts suggested that the entrance to the central structure may have been here so the patchwork of signatures here may be connected to that (Conneller, Little and Birchenall 2018).

8.5.2 Ruling out patterning due to proximity alone

One issue that might have been problematic with any of these groupings was that the proximity of samples may have been having an influence on groupings. As the occupation area samples were less spread out than the till samples, their being contiguous unlike the subsample of till samples that were selected every three grid squares, it is possible they were being grouped purely because their proximity made them much more similar to each other in underlying composition. This was unlikely given that the samples had delineated the central structure so clearly but still needed to be tested. In order to address this, three, six, nine and twelve group runs of the major element datasets were conducted on just the upper samples from the Central Structure area, central occupation spread and Western Structure area to the exclusion of the spread out till samples and similarly again just on the contiguous samples from the Central Structure area and local occupation spread alone. Within these analyses the groups identified from the complete sample set were maintained.

8.6 Principal Component Analysis

It was possible to conduct Principal Component Analysis (PCA) on the ICP-AES results from Star Carr, given the greater number of samples analysed relative to Flixton Island 2. This was conducted in OriginPro 2016 and with no rotation applied in SPSS. The Kaiser–Meyer–Olkin measure verified the sampling adequacy for the analysis (KMO = 0.702, rating 'good' and all KMO values for individual variables were > 0.5, the acceptable limit, according to Field 2009). Bartlett's test of sphericity χ^2 (10) = 437.189, p < .001, indicated that correlations between items were sufficiently large for PCA. Preliminary evaluation of intercorrelation between variables led to the exclusion of certain elements available in the ICP-AES dataset to improve robustness of the model. As such, five of the seven elements were incorporated into the established robust final statistical model: aluminium (Al), calcium (Ca), iron (Fe), magnesium (Mg), and manganese (Mn). Phosphorus and potassium had to be excluded on the grounds they generally did not correlate well with any of the other five elements or each other and therefore could not be included confidently in the linear components identified.

One component had an eigenvalue over Kaiser's criterion of 1 which would explain just 58.96% of the variance in the global dataset if extracted on its own. By Joliffe's criterion of 0.7 we could extract three variables. The scree plot showed a point of inflexion that would justify retaining three components, although values still dropped off further after the inflexion. All communality values were above the recommended threshold of 0.7 after extraction, which indicates that the amount of variance in each variable is adequately explained by the retained factors. Given the small (yet theoretically adequate) sample size, the communality values generated, the convergence of the scree plot and Joliffe's criterion on three components, the number of components on the final analysis was taken as three. This explained 91.95% of the variance in the samples.

8.6.1 Results of PCA on the Star Carr upper dataset

Principal Component Analysis based on five elements (Al, Ca, Fe, Mg, Mn) supported the interpretation there was consistent depletion in the values of these elements from the central structure and occupation area relative to the till; the principal linear combinations of the variables separated out clear clusters from the structure samples and occupation spread contexts compared to the more varied (less well clustered) till samples. The samples from the structure and occupation area formed localised groupings within statistical regions based on the readings of the five elements that could be incorporated into the model. The projected scores are displayed plotted as points on both graphs in Figure 153 against axes that represent the two most significant components i.e. the directions of

greatest variation (PC1, which would also be the line of best fit for the data should one be projected) and second greatest variation (PC2) in the dataset.

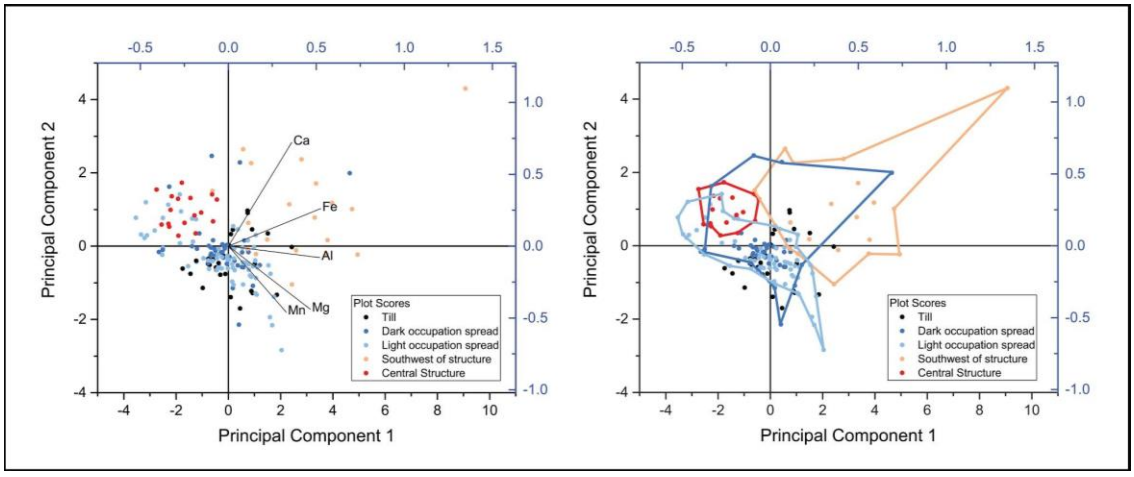

Figure 153. (left) a biplot illustrating the relationships between 1) the five elements (depicted as variable vectors) and their contribution to the components, 2) the individually projected data points for each sample and therefore 3) the relationship between the variable loadings on the components and the elements as shown by their proximity on the graph. Data points are symbolised by area; (right) a plot of the same individually projected sample data points, highlighting the relationship of samples from different areas to the components (made by connecting the most dispersed points of each spread). (Reproduced from Figure 21.6 in Rowley et al. 2018.)

The biplot (on the left of Figure 153) illustrates the relationships identified between the five variables (the vectors) and also the individually projected data (the scatter plot) in the space of the first two components (i.e. the most significant components). Loading vectors that are close to one another indicate closely correlated variables. In addition, the closer to the axes, the more that element loads on the component represented by that axis. The loading vectors show that aluminium heavily loads on PC1, which is the most important component. Aluminium is in the same graph quadrant as magnesium and manganese. Magnesium and manganese are most strongly correlated to each other, but the other elements are less closely correlated to both them and one another.

The projected scores show that those readings from the central structure (in red) group closely together (outlined on the right in Figure 153). They plot closest to the calcium vector, suggesting they are slightly more influenced by calcium than the other elements. However, the graph illustrates how these samples are relatively depleted in all elements relative to most of the other samples (particularly manganese), considering their position on the left hand side of the graph, opposite to the direction of the variable vectors. The structure readings do not overlap with the till sample score cluster (in black) at all, and only overlap or come close to some of the light and dark occupation spread (light and dark blue respectively) and southwest of structure (orange) sample scores. The southwest of structure sample scores are most disperse in how they load onto these two components, which is unsurprising given their variable nature. They mainly overlap with till and dark

occupation spread samples but they are generally dispersed quite differently, mostly being in the upper right quadrant of the plot i.e. with positive loading scores on both components. This suggests they are also quite different in nature, and this seems to relate to their iron and calcium content.

8.7 Summary and Comparison with Flixton Island 2

As such, despite a complex situation regarding the soils and sediments at Star Carr, the central structure and occupation spread area was successfully identified. This was not on the basis of one single element but from the combination of a multi-elemental analysis and then statistical integration, considered alongside the artefact patterning to confirm. While the results from Flixton were not as clear cut, they showed promise, and Star Carr suggests the viability of such techniques for successfully identifying Mesolithic activity areas on occupation sites.

Chapter 9 Discussion and Conclusions

9.1 The question of activity at Flixton Island 2

This thesis provides the first presentation of the significant Early Mesolithic lithic assemblage from Flixton Island 2. With the dryland site not being clearly associated with organic remains or clear features, the stratigraphy being relatively shallow, and considering the sheer number of finds in such a small area, the Flixton Island 2 Mesolithic site provides a challenge for interpretation.

The typological lithic analysis revealed a site that did not conform with the standard type classifications that have been proposed for the Early Mesolithic, and raised further questions about the validity of those categories themselves. It shows the need for site-specific approaches and potentially more regional nuance to be recognised and considered. Broader frameworks can provide a very useful starting point but they are ultimately a simplification of the data and in the case of Early Mesolithic sites, the framework has too often been based on a small number of sites from specific areas of the UK, often in the south of England. There may be some common attributes shared by different sites but at the moment these connections have not been rigorously explored with respect to the different landscapes and situations found across Britain, as while statistical analyses have been conducted, the underlying issues with sampling have inherent biases. The insular location of Flixton Island 2 is likely a key factor in why it is being used, and how it is used, and as such it is not surprising that it does not conform to these types of site as they have never been established based on island site profiles.

One part of a site-specific approach is investigating what different avenues of evidence are viable there. High resolution spatial recording of all artefactual materials and high proportions of sieving are more time consuming but proved valuable here for the amount of information retrieved that enhanced the understanding of this ephemeral site. Furthermore, exploring the geochemical signatures at high resolution as a method to investigate for potential activity area markers is something that should be considered for all sites where possible: even in the light of the mixed results at Flixton Island 2, it was felt to be profitable at both sites for either exploring the known features and the associated occupation area (Star Carr) or resolving clearer patterning in finds deposited with little stratigraphy or clear horizontal patterning (Flixton). Even if specific activity areas are not defined, the geochemical analysis increases understanding of the sedimentological contexts that may be impacting the assemblage in a number of ways.

The results at Star Carr provided the clearest results and demonstrated how this method is viable even in areas with more complex soil geochemistry. The Flixton Island 2 results did not yield as clean a signal, but this was understandable: the soils were in shallower stratigraphy in sandier soils, more subject to leaching; there were no signs of structures that might have confined and therefore intensified the signals received or even possibly protected them for a time after abandonment; the pXRF analysis in the field particularly involves analysing samples that are of varying moisture levels, potentially with pebbles interfering with the signal.

In terms of the ICP-AES, in the case of Flixton the aim to process 800 samples was too ambitious within the restrictions of the project but 50 samples spaced a metre apart were not quite enough of a subsample in retrospect. Samples from the full extent of trench four (up to every edge) submitted as one batch would have improved the analysis as it would have permitted surface extrapolation to visualise the results. However, even so, readings 1 m apart is a very coarse scale to try to identify activities that are not occurring on an agricultural or industrial scale but may have been small tasks handled by one or two individuals potentially in a tightly localised area. The pXRF strategy of a reading from every 0.25 m^2, and the similar resolution grid of samples analysed from Star Carr, was an improvement on this and allowed for more confidence in the potential to pick up small-scale activities better. In addition, it is certainly recommended that for ICP-AES, multiple solvents are used on samples to evaluate the different outcomes of the analyses rather than relying on a signal solvent type entirely from the outset. A further improvement would have been to apply two different elemental analysis methods (or more) consistently across datasets and to complement the results with more extensive micromorphological sampling which proved useful at Star Carr.

Despite all these factors, there were still areas of potential activity identified that were consistent with the statistical clustering of the lithics on the dryland. The lithics had been so densely spread across the dryland that the scatters were not identified during excavation, but the geochemical analyses combined with the spatial statistical analyses highlighted their location. In addition, nuances concerning differentiation within the clusters themselves were supported based on the spatial patterning in the geochemistry for the central and southeastern scatters. As such, multi-elemental geochemical analysis added another weapon in the arsenal for drawing out more information from both sites even when soil conditions were far from the ideals presented by porous, frequently resurfaced floors or clearly delineated features often studied in the wider (global, multi-period) literature.

9.2 Chronology, persistence and palimpsests

There are two questions that relate to the chronology of the site of Flixton Island 2: Firstly, was the material deposited at one time, or was it deposited over decades or even centuries as has been found to be the case at Star Carr (Conneller et al. 2016) so, in other words, what was the duration of the site? Secondly, at what point in the Early Mesolithic was this site in use, and can we position it relative to the other sites in the Vale with the evidence available?

We immediately know that the site was at the very least returned to over longer time periods because of the adjacency of the Long Blade/Palaeolithic material with the Early Mesolithic material. The material assigned to the Long Blade occupation from Flixton Island 2 is distinct either stratigraphically or clearly morphologically; there is a stratigraphic sequence demonstrating a break in occupation between the phases in the wetland. While the dates built into the model developed by Conneller et al. (2016) show that Long Blade cultures can overlap with both Star Carr and indeed the earliest of Deepcar type Early Mesolithic sites, Long Blade cultural material appears much earlier in the British archaeological record generally. At Flixton Island 2, it is associated with horse remains which also links it with being from an earlier time period, at the end of the last stadial or earlier in the start of the Holocene. This contrasts with the wooded environment associated with the Vale's Mesolithic sites and at Flixton Island 2 this is implied by the shift to dominance in deer remains, lacking horse, in the faunal assemblage associated with higher stratigraphy in the wetland and also from the gully. The possible Federmesser piece would lengthen the complete timespan of the use of the place even more, though with intervening hiatuses, this is not to argue there was continuity between the sites.

While the stratigraphy in the wetland allows for reasonably clear phasing of the material, on the dryland this is not the case. While sediments, in the forms of marl, gyttja, and peat, were developing from the start of the Holocene in the wetland areas, it is unknown how sheltered the dryland was and over the time of occupation it is possible that erosion from natural exposure and even footfall depleted the sediments between occupations. With the four pieces of Long Blade material from the dryland, we know that the island itself overall exhibits a palimpsest of material across the longer time frames represented. However, the majority of the material from the dryland does seem to be either generic or Early Mesolithic in nature.

The dryland area is so densely packed with lithic material, there are many possible interpretations. Firstly, would be that the dryland deposit was the result of being a dumping ground for material from elsewhere on the island and as such could be across short periods of time or very long ones. There are no features, no clear hearths, the overall character of the scatters is similar, and the burnt material is scattered throughout the dryland trenches,

clustering with unburnt material alike. However, why deposit the material at the apex of the hillock in an area so disassociated with any centres of main activity that they would have to be outside the area of the excavations? As such, while this interpretation is possible, it seems unlikely.

The dryland scatters, and all the material spread horizontally between them, could represent activity areas during one occupation or at least very closely spaced occupations. As one area got saturated with lithic debris, activity could have been displaced to the next area, and then the next. The preliminary consideration of the general nature of the scatters is similar, with the balance between tools, cores, and knapping debris similar in each one, which might also support this interpretation. There is also potential movement between the scatters, particularly the central and southwestern scatter based on the material spread between the two foci of the scatters. However, the central scatter is much larger and more spread out than the other two even if its two southern peaks are considered separately.

The ICP-AES suggested different geochemical signals adjacent to two peaks in the northern end of the central scatter. The pXRF revealed different geochemical signals from the southwest scatter, the northern peak of the southeast scatter and, and the southern peak in the southeast scatter. The multipartite nature of the central and southeast scatters both in terms of their multiple peaks in lithics and in varying profiles geochemically associated with those peaks are particularly compelling in suggesting that at least some of the scatters represent slightly different activities despite the similarity of the overall lithics profiles of the three and difficulties in interpreting specific processes represented geochemically. These activities could have been contemporary or at different times, and material could have been moving between the three. There is less sharing of material between the southeast scatter and the other two, if the generally scarcer spread of material between that scatter and the other two can be considered an indicator. A future, more in-depth consideration of the tool assemblage composition from the scatters and the different regions of the scatters may help to disentangle this more.

It is possible the scatters represent different periods of occupation, perhaps spread over thousands of years, as has been found to be the case at Star Carr (Conneller et al. 2016, Milner et al. 2018). This raises the idea of durability and reuse of the materials present. We are lacking the concealed, deliberate caches, of lithic raw material and cores, that are found at other sites across the Vale (that are often small pockets of good quality flint seemingly deliberately gathered and buried). However, it is possible that the whole site being within a known, insular location was operating almost as a large lithic cache in itself. People were bringing material here, not from vast distances as even the coast is only a couple of hours walk away as the crow flies (and that is excluding the possibility of using water craft to travel on the lake most of the way east), but still consciously transporting material to the

island for performing knapping and other activities here. With the density of material both in cores and debitage but even tools at Flixton Island 2, if they were returning here they would also have known that the material was likely to still be here year after year even if some of the material had been removed or utilised by other groups operating in the area. As such, that might explain why the site went out of use when there were still viable materials here to exploit, and tools abandoned halfway through manufacture like the axe/adze roughouts. It could be simply that any caches on the island were not yet recovered as they were in areas of the island unexcavated. But, if there really were no caches on Flixton Island, this means that something about the location, perhaps its insularity, was actually causing or allowing people to interact differently with the lithic raw materials: to be less protective and possessive of them, perhaps to deliberately leave materials to be shared between the island's users, or at the very least to not worry about having to relocate viable material.

As such, it is clear that Flixton Island 2 is a tangled palimpsest and even with further analysis, it may not be possible to say more about its chronology. Moore (1950) was similarly unsure of whether the two clusters at Flixton Island 1 were two separate occupations or not. However, Flixton Island 2's very nature as a palimpsest reflects something about the relevance of this site in the landscape, the relevance of its location as an island, and how it may have been a place of people connecting both with each other and with the recent past of their own time. If this was used by one person, with the density of the material it must have been a persistent, anchored place in the landscape for them (there is too much material and such a variety of tools manufactured that this is not a simple, single knapping episode). If it was used by several people, which seems more likely given the amount of material (though this cannot truly be tested), it was a place of coming together for a purpose and potentially sharing materials, even if they did not gather there at the same time. From the amount of cores and nodules there, and the variety of artefacts found there, it seems that people were consciously travelling to the site with forethought to transport material there and perform certain activities and wilfully leaving material there, this is not an accumulation from entirely random excursions.

The Flixton assemblage does raise the question of the relationship between Long Blade assemblages and non-Star Carr type Early Mesolithic assemblages though. Briefly turning to Moore's Early Mesolithic site at Flixton Island 1, on the southern island, in terms of the microliths it did have a slightly different nature to Flixton Island 2 which is of relevance if the microlith types do associate with site type and/or chronology in some way. First of all he retrieved 78 microliths so a lower count, but this was proportionally the same as Flixton Island 2 in forming 1% of the entire assemblage he retrieved (Moore 1950). His microlith assemblage was dominated by obliquely blunted points again but joined by 19 isosceles

triangles (24% of his microlith assemblage), 5 scalenes, and 3 crescents; therefore, it was very generally speaking more in keeping with a Star Carr type assemblage. He argued the presence of scalenes and crescents in one of the two clusters he identified might even suggest that scatter was later than the other one. The Flixton Island 2 assemblage presented here, with a predominance of scalene triangles, is of a different nature. This is possibly because it is from a slightly later time, or because there were two activities occurring on the two islands.

This returns us to the question of the validity and proposed chronologies of Early Mesolithic site types. Flixton Island 2 did not conform to the Early Mesolithic site types and demonstrated that it is not always easy to pigeonhole sites into these categories. This is exacerbated by the fact that lithics analysis is not an objective process, as it is sometimes presented, but involves decision making on the part of the analyst. In defining his site categories (as discussed in chapters two and four), Mellars opted to select formal tools that were less subjective in interpretation to make his classifications of sites. In doing so, he ignored certain attributes of the assemblage that may have had a significant bearing on what activities were actually occurring on these sites, not least of which was the fact that informal tools such as utilised flakes were completely eliminated from consideration. When we then consider that many Mesolithic sites do run the risk of being both turbated and may be undetected palimpsests, you end up with the issue that the categories have not only been based on small sample sizes from certain locations in Britain, and that they maybe selective in the tool types they consider valid to include, but also that they may themselves be based on composite assemblages presenting as one site.

Setting this aside, Long Blade assemblages do seem to precede Star Carr assemblages, and these in turn precede other Early Mesolithic assemblages, and this is supported stratigraphically at Flixton Island 2. However, when we consider the overlapping of dates presented modelled by Conneller et al. (2016), the end of the use of Long Blade type sites does seem to overlap with the appearance of Star Carr type sites significantly but only just overlaps with the Deepcar type and possibly other later Early Mesolithic type assemblages, though this is only based on the dates from two Long Blade sites. If we continue to accept the use of the traditional categories of sites for the present, there is a possibility that, functionally speaking (using functional in its broadest sense), Deepcar type sites might take the place or fill the niche left by Long Blade type sites while Star Carr type sites performed a different, complementary, function/role to the two. In which case, the Flixton Island sites together may represent an interaction between the two islands, one with a Star Carr type signature, the other with a Long Blade then later different Early Mesolithic complementary signature.

9.3 The people and activities at Flixton Island 2

Even if the people that used the site in association with the Long Blade and Mesolithic cultures were wholly unrelated to each other, the island was still drawing people to it to be used for whatever purpose in different climatic circumstances. Knight et al. (forthcoming) explore the faunal remains from Flixton Island 2 that are associated with the Long Blade material and that evidence suggests that Palaeolithic Flixton Island 2 was a horse butchery site. The Early Mesolithic site was not being used in this way, and could not be: with the shift from tundra to maritime temperate landscape, the emphasis shifted from horse to woodland animals like deer, and the small amount of faunal remains considered associated with the Mesolithic phases of the site from the wetland and gully are not complete animals but haunches. Meat and other animal parts are being brought to the site already having been killed and with at least preliminary butchery elsewhere, as is ethnographically seen with modern hunters today. As a result, the Mesolithic site does not appear to be a butchery site based on the remains that are available (though what, if any, remains were lost on the dryland site is of course unknown).

In terms of what the lithics reflect about activities on the site, one thing that is certainly happening is that people seem to be knapping here. The cores seem to reflect a range of ability, or expediency, in knapping, with many hinge and step terminations cutting into the material, rather than the clean, feathered terminations of a well-aimed strike to remove a flake. This was even the case on large cores (smaller ones perhaps being worked at a difficult size purely to make the most of the material, thus running a higher risk of being mis-knapped by even skilled knappers). In contrast, there are some examples of particularly delicate working also demonstrated, for example in the production of some of the microdenticulates. There appear to be some tools that are well knapped on poorer quality material (such as the chert microliths) and others that are badly knapped on better quality material. This also seems to confirm that there was a range of people on site and possibly of different experience or even ages, if skill can be considered a proxy for these. There were also possible aesthetic/style choices being reflected in the assemblage, for example with the unusually large piercer being manufactured on a notably patterned piece of striped flint. I also like to think that the small, irregular and broken axe/adze could have been discarded into the fire in anger once it went awry, but these points are highly speculative.

The dominant tools of the assemblage were microliths (270 including partials), scrapers (194 including partials), and potentially utilised debitage like flakes (209), in terms of raw count. It must be remembered that microliths can represent a much lower number of tools, if multiples were hafted to form one composite artefact, as has been found at other Mesolithic sites. Of the microliths found at Flixton Island 2, some had broken tips or other

forms of likely macrowear but others were seemingly unused. The crucial benefit to the original users, and bane for archaeologists, is that in being small, generalised elements of composite tools they were therefore highly versatile and could have been used for a very broad range of tasks. Without microwear or residues confirming what they were used on, if they were used, there is little that can be said confidently about what they represent in terms of the site's activities. The majority of evidence in the Mesolithic based on those hafted are for their use as projectile points on arrow or harpoon type constructs, such as that found at Loshult, but they could have been used for plant processing and a host of other tasks (as discussed in chapter four).

Scrapers were the most dominant non-microlith tool on site by a significant margin. As these are tools that have been deliberately retouched into thicker working edges, these are usually considered to be for gradual reducing of material such as hide, bone, wood and plants, and possibly even pebbles of iron oxide for ochreous powder production (as discussed in chapter four), as opposed to being for slicing, crushing, or smashing for example. As such, this is another versatile tool group that could have been used for processing many materials on the site. The integration shows there may have been some interplay between the areas of the scatters that had microliths and those that had scrapers.

Again, a very similar issue of versatility arises for utilised debitage. It has often been the case that possibly utilised informal tools, i.e. expedient, unmodified debitage that shows signs of use, is overlooked in the analysis of sites. Indeed, in Mellars' (1976) and later Reynier's (2005) work, unmodified but utilised flake proportions are barely discussed in assigning site types. This is partly because even if microwear studies are conducted, they cannot necessarily confirm use, and the recording of what constitutes a potentially utilised piece of debitage is even more subjective than the recording of formal stone tools with classical attributes to identify them. However, these are often a significant part of stone tool assemblages as they are at Flixton Island 2, and here these would have been a very versatile resource on hand not only for those during the occupation in which they were knapped but also potentially later returning individuals, available for them from the very moment of arrival and setting up camp. If so, this would be akin to modern hikers today using shared cabins in the boreal forest, where they are expected to leave a match ready for striking with cold fingers; this would generate a sense of community or connection with past dwellers, as well as responsibility perhaps to leave viable material for future users.

At various times, researchers have attempted to interrogate stone tool assemblages for gender markers, or have placed assumptions on the interpretation of tools that they consider "male" or "female" domain (and very occasionally non-binary interpretations, but

these have usually been interpreted as shamanic or elite/special individuals). Microliths and their interpretation of being projectile points has often resulted in them being implicitly associated with 'man the hunter'. Meanwhile, scrapers have been argued to be associated with the domestic sphere and therefore women. Flixton Island 2 of course has plenty of both tools, and even possibly a binary relationship between the spatial zoning of these tool types, but even if there were a predominance of one of these tool types or another that has been gender-loaded, there is simply no way of knowing what stone tools were made and utilised by men, women or people of other gender(s) in the prehistoric Vale of Pickering.

There are no reasons (biological, ethnographic, experimental, or otherwise) that people of any sex and/or gender can automatically be ruled out of the gathering of resources or manufacture or use of certain tool types (Gero 1991). People may have been excluded from doing so for socio-cultural reasons but we have no clear way of reconstructing those at this stage, with the current evidence available. Often associations of people of certain biological sexes with particular material culture in death has been taken to indicate their gendered association with those tools in life. This has inherent problems associated with it (grave goods are placed there by the living and reflect their choices as much as the deceased's) but regardless, there have been no human remains located associated with the sites in the Vale of Pickering that could provide a local, nuanced discussion of this. Mesolithic interpretations have also been plagued with attempted reconstructions of family units, with even multifamily households presented as nuclear families sharing space (e.g. Grøn 2003). These are huge and unevidenced assumptions and while these papers have opened up discussion on these topics, they are often lacking adequate evidence. Finally, there is very little consideration of biologically intersex individuals and non-binary genders in the archaeological literature, despite these being ethnographically reported in hunter-gatherer societies globally and growing awareness of these more generally. With the evidence from Flixton Island 2 presented here, it is too difficult to consider further what demographics of people may have utilised the site without falling into the same kinds of traps, at least without having a great deal more time to carefully interrogate the detail needed to make such suggestions appropriately (as has been seen in the work of Nyree Finlay). There is no clear reason for the island to have been considered the domain of any particular demographic at this stage.

The island would have provided a convenient, confined space in the lowland landscape for physical social separation/segregation and it is possible this was part of its persistent use and appeal in some way, though this in itself is highly speculative. The insularity could have been a place of retreat or safety, or isolation.

9.4 Conclusions

Flixton Island 2, particularly the dryland, was an enigmatic challenge from the outset for interpretation. Deliberately adopting a multi-method approach, grounded in high resolution recording and sampling, alongside the application of scientific analytical methods, allowed for additional information about the dryland to be extracted that otherwise would have been lost. In defying the traditional categories of Early Mesolithic sites, this site has demonstrated the need for such categorisations to be challenged and further developed. It certainly shows that more can be done with geochemical analyses than is usually conducted on British Mesolithic sites. Several patterns in the lithics only became apparent when being explored both with more robust spatial statistical methods and also when comparing the geochemistry to the lithics distributions. As more work is done on other sites, the more we will be able to consider what different geochemical signals might mean though with the caveat that even when using the same overall method (such as ICP-AES), the results are not necessarily directly equivalent.

As with all archaeological sites, the more strands of evidence there are to compare, the better supported the patterns are and this is the case at every level: multi-elemental analysis is preferable over single element studies, multi-method analysis is preferable over single-method analysis, and exploiting all the strands of evidence available i.e. not neglecting the soil science that could be utilised, regardless of how variable the material culture assemblage is, all result in more robust modelling and more nuanced interpretations of the sites. Based on the work here, field analysis techniques can be good but the signals are not as clean, and conducting multi-elemental analysis using more than one method would have allowed for deeper critique of the results. At the same time, laboratory-based techniques should not automatically be assumed to be better as the variance between the batches of ICP-AES analysed data from Flixton Island 2 demonstrated.

This work has focussed on looking at the broader intra-site patterning at the scale that considered the lithics assemblage in relation to the geochemistry. There is certainly scope to take the Flixton assemblage further by considering the chaîne opératoire and object biographies of the lithics through with more extensive refitting studies (already piloted by undergraduate Bethany Nash at the University of York with encouraging results) and technological analysis which were not possible in the timeframe of this project, and further comparative work on the geochemical samples incorporating new methods as well as phytolith analysis. All of these in addition to detailed micromorphological analysis would be complementary methods here and at other Mesolithic sites that would allow a rich interpretation for each to be developed.

All in all, considered applications of both geochemical analysis and spatial statistics, provided adequate sample sizes are used and robust models are developed, can certainly enhance our understanding of lithic assemblages and ephemeral sites, such as the palimpsest on the dryland at Flixton Island 2. The more detailed an understanding we can develop, even if for at least a sample of Mesolithic sites, the better we will be able to challenge overgeneralization of the spectrum of sites there are and also develop better regional understandings of why different microlithic cultures come into and out of use.

Appendices

Appendix 1 Deepcar-type assemblages, as outlined by Radley and Mellars (1964)

The Warcock Hill North, Lominot and Windy Hill assemblages were all similarly constituted to Radley and Mellars' Deepcar assemblage and predominantly made of the opaque grey or white flint that Buckley had noted as well. The Lominot sites excavated in 1924 and interpreted to be one collective site divided into two round emplacements were on high ground immediately to the south of an important geometric/Narrow Blade site, March Hill. Windy Hill site 3 is located to the north of the main hill, in a densely distributed assemblage at the summit of a shale spur, and had been excavated by Buckley in 1922.

Radley and Mellars outlined the character of these assemblages utilising Clark's classification system. In terms of the microliths (Radley and Mellars 1964, 9–10 & 15), the industries at Warcock Hill North, Lominot and Windy Hill were dominated by obliquely blunted points, with the retouch usually featuring on the left-hand side. Sometimes these featured additional leading edge retouch and of these a relatively large number of pieces had been initially blunted down the right-hand side instead. Alternatively, fairly frequently, pieces showed blunting down the whole of one side (what would later come to be termed "backed") which were mostly still relatively broad although a few were narrower and more rod like. Rare but still present are also several examples of large isosceles triangles. Figure 11 illustrates the different forms found at Deepcar.

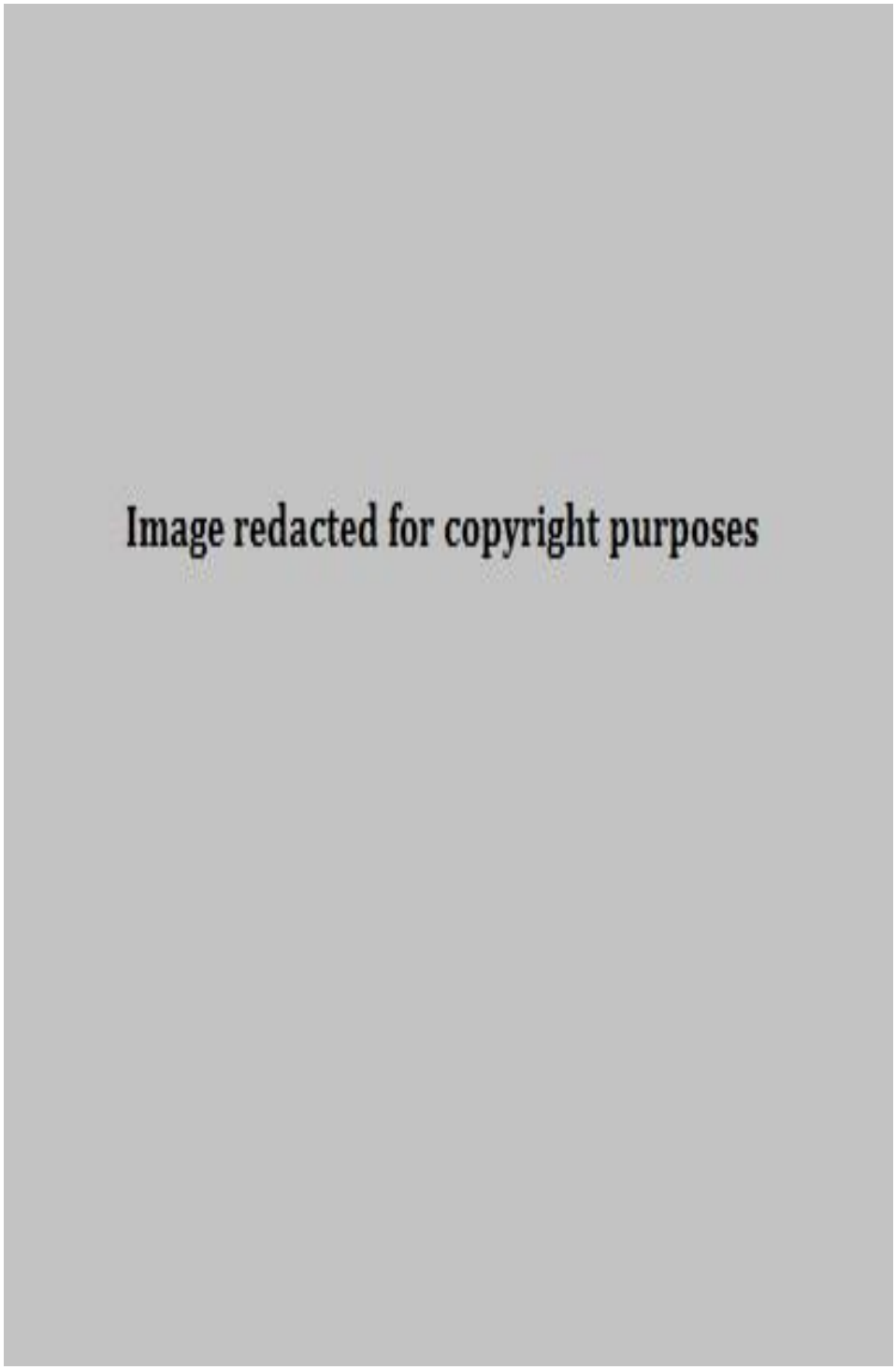

Figure 154. The microlithic industry from Deepcar, Yorkshire (reproduced from Radley and Mellars 1964, p.10, not to scale)

The non-microlithic assemblages were also similarly composed between these sites. Of the microburins, 87 out of 102 at Deepcar featured a notch on the right-hand side and consisted of the removed proximal end (the end with the bulb) of the flake (Radley and Mellars 1964, 9). Of the remaining 15, there were five right-hand-side notched distal tips and three left-hand-side notched butts, one double-ended microburin and six miss-hits or unfinished forms. On typical sites, microliths outnumber microburins but at Deepcar this trend was reversed: Radley and Mellars attribute this to differences in retrieval practice as these

pieces are often less than 1cm in diameter and therefore easily missed (p.9). On the other sites, microburins are common but only numbering from 17 to 27, the majority of which are retouched on the right-hand-side (pp.18 & 24) although at Warcock Hill South, there is more of a balance with left-hand-side modified pieces only numbering one less than the eight right-hand-side ones. In addition to this collection, there were also nine small pieces with microburin facets from Deepcar that appeared to be the detached tips of microburin facets, similar to some at Thatcham (p.9).

End scrapers, formed by abrupt or semi-abrupt retouch around the end of flakes or blades, are frequent at Deepcar and the other sites (Radley and Mellars 1964, 15). Double-ended and rounded scrapers (blunted around the complete diameter) are present but occasional on all (*ibid*.). They also identified some notched pieces including possible hollow scrapers at Deepcar (p.12). Of the 37 clearly identified scrapers from Deepcar, 13 did not exhibit bulbs so they were possibly broken and the lengths varied from 12mm – 51mm for complete examples (*ibid*.). Burins were difficult to categorise and much less common than scrapers on all the sites (p.15). At Deepcar they were infrequent, totalling eight convincing burins and several spalls, and cut into chunky pieces of white flint (p.12).

At Deepcar only 17 cores were found, which Radley and Mellars considered to be a product of the lack of local raw material sources, which is backed up by 111 artefacts of core rejuvenation/preparation that would have extended the cores' lifespans (Radley and Mellars 1964, 8 & 9). The cores range from 9 to 85 grams, averaging 36 grams. They were mostly single platform with only part of the perimeter worked (9 type A1 cores in nomenclature also developed by Clark), the next common being three platform cores (3 type C1s) as well as low numbers of whole perimeter worked single platform (1 A2 type) and two-platform cores (2 B1s and 2 B2s). Of the core rejuvenation flakes, most were intended to renew heavily utilised striking platforms which particularly makes sense if most of the cores were single platform types. While they did complete the Clark classification for these, they found they were sometimes making arbitrary decisions about which category to place them into. Nevertheless, 58 of the specimens were struck obliquely to the platform (type C), while the other well-represented types were struck from the same plane as the platform (type A) and at a right angle to the platform (type B). Regarding the other sites, cores are rare, ranging from 9 to 34 in number (combining the chert and flint finds from Windy Hill), and their average weights similar, ranging from 18 to 38g.

Two pieces were categorised by Radley and Mellars as awls although they are quite different from each other (Radley & Mellars 1964, pp.11–12 and see Figure 5). This classification was based on their function rather than morphological similarity, the only commonality being that they had been retouched to produce a point. In this case it can be seen that one artefact is steeply retouched all along its edges so that it comes to a fairly think point at the tip. The

other is neatly retouched with two small, adjacent (opposed) notches to produce a slightly protruding point off the side of the piece. This reflects the important issue with any nomenclature being based on an implicit assumption about use: Objects will not always be categorised separately even if they are significantly different physically and therefore potentially would have a different methodology in the practice of using them.

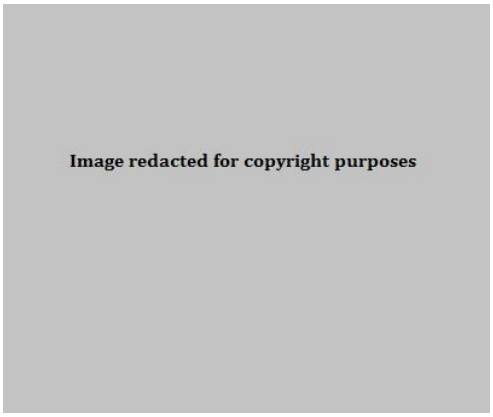

Figure 155. Awls from Deepcar (reproduced from Radley and Mellars 1964, p.17, not to scale).

Regarding other occasional finds, at Deepcar and the other sites there was also a small number (five at Deepcar itself) of short blades retrieved with one end truncated with steep blunting, either transversely, concavely or obliquely, with one double obliquely truncated piece from Lominot (Radley and Mellars 1964, 12 & 18). Deepcar also produced one small possible tranchet axe which had been badly damaged by fire but no resharpening flakes were located implying that axes may not even have been used in the area except in material reuse and no axes or resharpening flakes were found in the other locations (Radley & Mellars 1964, pp.12 & 18). In addition, there were two 'saw' flakes identified at Deepcar, one with fine the other with coarser dentitions, with two similar pieces to the finer one being found at Warcock Hill (Radley & Mellars 1964, pp.12 & 18). A number of the flakes, normally counted within the debitage, showed heavy use-wear at Deepcar (Radley & Mellars 1964, p.12).

The main difference between Deepcar and the other sites is that the Marsden sites all feature a very small number of the minute geometric forms heavily utilised in the 'Narrow Blade' industries elsewhere in the Pennines. However, Radley and Mellars do also comment that all of these sites are in close proximity to true 'Narrow Blade' sites or the geometric microliths in question were found in very discrete areas or higher up in the stratigraphy than the 'Broad Blade' assemblage elements (Radley & Mellars 1964, p.18). This, however, might be taken to suggest that Deepcar and similar sites are perhaps related to Narrow Blade assemblages chronologically and/or typologically – an idea which takes root more firmly in later research on Early Mesolithic typologies.

Thus it was that Radley and Mellars would outline the Deepcar assemblage type based on these Pennine assemblages. They expanded their discussion to include excavations in south and east England at Shapwick, Middlezoy, Dozmare Pool, Broxbourne, Colne Valley and Thatcham; all sites considered to be within the similar Maglemosian tradition (Radley & Mellars 1964, p.19). Despite the limited size of these assemblages, Radley and Mellars deemed them to also be very similar to the Pennine assemblages with two differences (Radley & Mellars 1964, p.20). Firstly, they note that the microlith form with blunting down the full length of both edges is absent on the northern sites but present on most in the south, for which there is no obvious explanation. Secondly, they note that the non-Pennine sites are characterised by tranchet axes, unlike those in the Pennines (*ibid*.). In addition to this, there is the presence of the single characteristic Horsham point at Thatcham although this was located during fieldwalking of the site and as such was technically unstratified (Wymer & King 1962 as cited in Radley & Mellars 1964). However, Mellars and Radley discuss that this may be an attribute of being a difference between upland and lowland sites, with the latter likely being more heavily wooded and, if an axe is interpreted as being for tree felling then it would be needed more in such a context (Radley & Mellars 1964, p.20). They also bring in the example of Pike Low as being a Pennine site which also has the markers of a Deepcar-type site which also has a clearly identifiable axe-resharpening flake, as well as two tranchet axes found through fieldwalking on the moors (Radley & Mellars 1964, p.20 but also cf. Davies & Rankine 1960; Radley & Marshall 1963).

Appendix 2 Lithics Cataloguing, Definitions, and Typological Classification Notes

Categories used on catalogue spreadsheets

- General information
  - Find number
    - All unique numbers, no letters
    - General format
  - Location data (x, y, z)
    - "#N/A" for absent data, which was separated out before integration into ArcGIS and treated like sieve material
  - Site code
    - VP12/13/14
  - Trench
    - "#N/A" for non-applicable data.
    - "Unknown" used if not recorded on bag.
    - N.B. In older records for Flixton, trench codes were prefixed with "F" (for Flixton, to differentiate from Star Carr) but this was later deemed unnecessary.
  - Context
    - If recorded as two contexts on the bag (as on the interface of the two), then was recorded as the upper context with an added note appended.
    - If context had suffixes e.g. a, b, c, then that was put in a note as well, but only the number was included in the context column.
    - "Molehill" for mole hill finds.
    - "Spoilheap" for spoil heap finds.
  - Grid square (grid_sq)
    - "#N/A" when grid squares not applicable e.g. for mole hill finds.
    - "Unknown" when should have a grid square but has not been recorded on the bag.
    - N.B. As explained in the lithics chapter, positive and negative grid square numbers were not consistently recorded. From 2013, all grid squares in trench 9 were labelled with negative numbers (even if marked up differently, that is an error). All others from the main trenches on site were positive numbers and should be treated as such. However, in 2014, trenches 11 and 15 had both positive and negative numbered grid squares and there was confusion both on site and during post-excavation processing that meant the material was guaranteedly mislabelled in an unquantifiable number of cases. As such, ex-situ material retrieved from the sieve from those trenches (or in-situ for which the EDM recording failed) could be from either the positive or negative grid squares.
  - Material
    - "Lithic" for knapped material (originally "flint" was utilised but this was changed by CCAR).
    - "Stone" for coarse, unknapped stone finds.
    - Other categories of material were passed on to the appropriate specialist(s).
  - Basic notes (basic_notes)
    - Notes from in the field or initial cataloguing.

    - Storage Location
        - KM_box#: Storage box at Kings Manor, University of York, containing finds sorted in numerical order.
        - Enviro_AL or Enviro_SC: With specialists at BioArCh, University of York.
        - KM_specials: Finds pulled out of general storage as of particular interest for ease of access. Stored at Kings Manor.
        - KM_microliths: All microliths and a selection of microburins retrieved from general storage for ease of access. Stored at Kings Manor.
        - Unknown: If artefact lost.
        - Discarded: If discarded as non-artefact. (Finds from all periods were retained and passed on to specialists or stored, only natural material was removed.)
- Quantity
    - If two or more refitting pieces were bagged together as from the exact same location, they were treated as one find, with one unique find number, and recorded as a combined piece. The quantity number would reflect the number of refitting pieces in any such bags.
    - If non-refitting finds were bagged together, they were assigned new unique find numbers, separated into a new bag, and entered as a new catalogue entry using the 3D location data for the original numbered point. Original numbers were recorded in the notes.
- Completion
    - Proximal
    - Proximal-medial (prox-med)
    - Medial
    - Medial-distal (med-dist)
    - Distal
    - Edge (a complete or near complete length but divided parallel to the axis of the piece, so as not to be considered near complete)
    - Near complete (when measurements taken on the piece are thought to be still very close to complete and therefore approximately valid)
    - Complete
    - "#N/A" used for natural; debitage chunks, chips and spalls; and nodule chunks
- General type (type_general) and specific subtype (type_specific). Fully detailed in Table 49.

Table 49. Detail of attributes recorded in lithics catalogue

General type	Specific type	Notes
Axe/adze	Tranchet (where applicable)	Unless use as one or the other was confirmed by a usewear or residues specialist, it was decided to record these as axe/adze.
Axe/adze preform	Roughout Unfinished (when completed except for tranchet / unused suggesting may have been unfinished) Attempted tranchet (where attempted to remove the tranchet spall but was unsuccessful on a preform)	
Axe/adze resharpening flake		Difficult to identify without refitting. Likely underestimated numbers.
Backed bladelet Backed bladelet segment		Bladelet with blunting retouch straight down one side to form a back for utilising the opposite side, but if forms a point then counted as a microlith.
Blade Blade segment		A blade is 12 mm or greater in width following Butler (2005), and at least two times greater in length than width.
Bladelet Bladelet segment Blade / bladelet segment (when ambiguous from fragment available)		A bladelet is less than 12 mm following Butler (2005), and at least two times greater in length than width.
Burin	Break, single angle	Removal of burin spall from edge of broken blade or flake.

General type	Specific type	Notes
Partial burin	Break, double angle	Same as above but with two removals from the same break.
	Break, alternate angle	Same as above but with two removals from either end of the piece on two breaks.
	Truncation, single	Spall removed from rtd concave / convex / oblique truncation at one or both ends of flake / blade.
	Truncation, double	Same as above but with two burin spall removals from same truncation.
	Truncation, alternate angle	Same as above but with two burin spall removals two truncations at either end of the piece.
	Dihedral	Spall(s) removed from a piece to form a point, could be manufactured on a previous single burin facet (normally un-retouched), on a break, or on a natural facet.
	Irregular (transverse, other)	Other pieces seemingly featuring burin facets but not of a standard form.
	Attempted break / irregular etc.	When attempted but not successfully produced.
Burin spall Burin spall segment	Resharpening Transverse Oblique Unknown	Burin spalls suggested by length, termination and triangular cross-section, however further refitting work needed to confirm many of these. Could also appear to have signs of platform preparation or retouch that prepared the original piece for the spall removal.
Combination Partial combination		Used when a tool features two tool modifications e.g. a scraper and a burin on one blade.

General type	Specific type	Notes
Core Core fragment Core fragment / irregular core (if could be complete but uncertain)	A1: Single platform with flakes and blades removed all the way round the core. A2: Single platform core with flakes and blades removed part of the way round the core. B1: Core with two parallel platforms. B2: Two platforms, with one at an oblique angle. B3: Two platforms at right-angles. C: Three or more platforms. D: With flakes struck from either side of a ridge. E: As D, but with one platform or more.	
Core tablet Core tablet segment		
Core tool	Core type and tentatively suggested use from macrodamage e.g. "Type E core used between surfaces as a wedge or splitter" for fine number 100801.	Used when not an identifiable classic core tool type but is a core that appears to have been modified and/or utilised in some irregular way
Debitage Chip (<1 cm diameter) Debitage Chunk (>1 cm diameter) Debitage Spall (long and thin debitage)	Burin spall (where applicable) Possible burin spall (where applicable) Heat spall (where applicable) Possible heat spall (where applicable)	Used for debitage not identifiably flakes, blades or other specific types. Usually irregular shapes (particularly the chunks) but show signs of being humanly knapped regardless.

General type	Specific type	Notes
Denticulate		Piece featuring large denticulations producing a serrated edge.
Flake Flake fragment Flake / blade fragment (when not diagnostic fragment retrieved) Flake / bladelet fragment (when fragment can be identified to being a possible bladelet rather than a blade but not diagnostic as to whether squatter or longer than necessary for classification between the two)		A flake is any complete piece of debitage less than two times long as it is wide.
Flanc de nucléus Flanc de nucléus fragment		Can be difficult to differentiate from regular flakes but here considered to be thicker flakes that remove areas heavily knapped already.
Microburin Partial microburin Microburin / notched blade Partial microburin / notched blade(let) fragment	Attempted (when has been struck but not broken at notch point) Intermediate (when has been notched but not broken)	Microburin / notched blade used when width > 12 mm
Microdenticulate		Piece featuring small denticulations producing a finely serrated edge.

General type	Specific type	Notes
Microlith Partial microlith Backed bladelet / microlith	For full typology see below. Unidentifiable	Potential microliths / piercers were catalogued as microliths (with notes added)
Natural Natural / debitage chip, chunk, flake, spall, or other (if uncertain)		
Nodule chunk Nodule chunk / core fragment (if uncertain)		
Awl / piercer (sometimes separated where can tell use or distinctive retouch) Awl / piercer tip Awl / piercer segment Mèche de foret	Single edge Double edge Alternate edge	

Scraper Partial scraper	Double: Semi-abrupt / abrupt retouch at both ends. End, short: Semi-abrupt / abrupt retouch at one end (usu. distal), less than two times as long as wide. End, long: Same as above but greater than two times as long as wide. End, unknown: Same as above but when broken so do not know the complete length. Hollow: When the retouch forms a concave hollow, rather than being convex. This is in addition to the other subtype classifications. Usually on end scrapers but can be on side scrapers (when use suggests scraper use rather than production of a notch). Nosed: End scrapers on longer blades coming to a narrow, pointed end (can look like blunted / broken piercers but can be distinguished as deliberate blunting retouch, rather than creating a sharp point.) Side: Semi-abrupt / abrupt retouch along one lateral edge (sometimes both), normally slightly convex but could be straight, often has retained an edge with cortex (possibly to provide a grip or handhold). Side and end: A piece retouched at the end and also along one or both sides, either continuously or not. Round: Retouched all the way around. Irregular: If does not fall into the above categories.	

General type	Specific type	Notes
Strike-a-light		
Truncated piece Partial truncated piece		
All tool types	Attempted	When seems to be malformed or featuring failed modifications
	Possible	When suggestive of a specific type but some doubt
For debitage types	Long Blade Possible Long Blade	If shows signs of being part of the Long Blade assemblage.
	Platform rejuvenation	Debitage from removing a platform / section of platform from a core to provide a fresh surface
	Platform preparation	Debitage from shaping a platform before removal
	Proxy	When a blade or bladelet in dimensions but does not have nicely parallel sides or truly classic form
	Tool resharpening	

- Whether core initiation debitage i.e. pieces removed for cortex removal from a nodule for use as a core (or a tool manufactured on a core initiation piece). This includes primary and secondary debitage, and counted as "possibly core initiation" if could be secondary or tertiary.
- Modifications (if not creating a specific tool type)
    - Backed
    - Burinated (when spall removed but does not seem to be a formal burin)
    - Crested
    - Denticulated
    - Faceted
    - Heat treated
    - Possibly utilised
    - Retouched
    - Truncated
- Category
    - If falls into two categories, then counted as category listed first.
    - Core tool: axes, adzes, preforms, strike-a-lights, other core tools
    - Microliths are divided into the following cultural groupings:
        - Star Carr
        - Deepcar
        - Palaeolithic (backed bladelets)
        - Undiagnostic
    - Removed tools: Most formal tool types and partials thereof, along with retouched or truncated debitage pieces, excluding microliths and excluding possibly utilised or possibly modified debitage (which are just considered as core reduction or debitage).
    - Microburins
    - Tool production debitage: Axe sharpening or resharpening flakes, burin spalls (N.B. many of these are difficult to identify with certainty, especially without a comprehensive refitting program as is the case as of September 2017)
    - Core preparation: Platform rejuvenation pieces, core tablets, flancs de nucléus
    - Core initiation: Primary and secondary debitage, "possibly" if possible secondary or tertiary
    - Core technology: Cores, core fragments
    - Possibly utilised debitage.
    - Crested / possibly crested.
    - Possibly burinated.
    - Core reduction: unused or possibly utilised but unmodified tertiary blades, flakes, and bladelets, along with debitage of unknown stage.
    - Debitage: indefinable chips, chunks, spall, and tips.
    - Possible debitage: Material classified as "natural / debitage…." as uncertain but looks potentially knapped, as well as nodule chunks (or possible nodule chunks)
    - Natural
- Length and width for complete pieces, plus thickness for cores and unusual tools (if noticeably thick)

    - These were taken from the maximum length at a right angle to the platform and width at a right angle to the length.
    - Thickness would be maximum thickness from ventral to dorsal face for tools.
    - For cores, length was length from centre of platform face to longest point; width was widest breadth; thickness was maximum thickness at right angle to maximum width orientation (or as close as possible).
    - All pieces were measured using a plastic tipped digital caliper, in millimetres to 1 decimal point.
- Retouch
    - Abrupt
    - Semi-abrupt
    - Fine (abrupt or semi-abrupt)
    - Invasive
- Retouch side (rt_side)
    - Both: both ends
    - Distal / proximal: One end
    - Rhs / lhs: right hand side or left hand side of tip or midside of piece
    - Concave
    - Either: One end but unclear whether proximal or distal as bulb absent and ripples unclear)
    - Rhs base / lhs base: retouch on that side but near the base, not further towards the tip
    - Leading edge: If one side is partially or completely blunted and then just the opposite edge tip is also blunted then the main side is recorded as rhs / lhs plus leading edge retouch.
    - "Unidentifiable" if has retouch but not obviously within any of the above categories
- Macroscopic wear, damage, or possible use markers
    - All recorded as 0 for not applicable or 1 for applicable
        - Edge damage / wear (N.B. this could still be modern and has not been confirmed with microscopic analysis)
        - Polish or gloss (polish_gloss) (N.B. this could be natural)
        - Macroresidue (N.B. this could be natural)
- Whether burnt or heated (Heating_Burning)
    - 0 for no, 1 for yes
- Cortical extent
    - On a scale of 0 to 5, with 1 being up to 20% cortified, 2 being up to 40% cortified and so on.
    - 0 - 1 suggests a very small amount of cortex is present.
- Reduction stage
    - 1: primary (core testing or initiation)
    - 2: secondary (core initiation)
    - 3: tertiary (core reduction)
    - 1 - 2 / 2 - 3: could be either category
    - Core
    - 2 / Core: Possible core or secondary chunk
    - 3 / Core: Possible core or tertiary chunk

    - Unknown: Could be from 1 - 3 (usually for very small pieces technically with high cortex but actually only a small fragment of original piece)
    - n/a: If a debitage piece that is not from a clear stage of the knapping process
- Termination:
    - Recorded for the distal end of all pieces except complete tools where the non-retouched end is recorded (to provide additional information)
        - Abraded
        - Broken / snap
        - Modern break
        - Core terminations
            - Conical (flat platform with removals from all sides coming to a point)
            - Cylindrical (parallel sides but flat base and top as one or two platforms)
            - Globular (removals from all sides forming a globe)
            - Disc feather (when removals form a flat face backed by the convex, round pebble surface; shaped like a hemisphere)
            - Ridge (removal on both sides forming a ridge edge)
            - Irregular polygon
        - Feather
        - Hinge
        - Step
        - Overshoot (feathered but curving around what would have been the core)
        - Platform (if recording the non utilised end of the tool
        - Break (snap)
        - Thick feather (where feathers but not as smoothly to as thin an end as a normal feathered piece)
- Raw material source
    - Till
    - Wolds
    - Unknown (N.B. grew less common as became more familiar with material therefore more dominant in VP12 assemblage record yet this is misleading and should be treated with caution)
    - Pat / unpat: Patinated or unpatinated
- Raw material
    - Flint
    - Chert
    - Quartzite
    - Quartz
    - Oolitic limestone
    - Unknown
- Colour (two colours plus colours of inclusions or speckling)
    - Two colours would record the dominant colours of the matrix material
    - Abbreviations:
        - Lt = light
        - Dk = dark
        - Med = medium darkness
        - Bw = brown

        - Blk = black
        - Gy = grey
        - Grn = green
        - Or = orange
        - Wht = white
        - Yell = yellow
        - Might also record as burnt if the colour is thought to be as a result of the burning.
    - Inclusions could have more than one colour, lightest colours recorded first
- Translucency:
    - Op: opaque (no light could come through)
    - Semi: semi-opaque (light could come through edges but not centre when held to light)
    - Op / semi: When a little light could get through around the edges.
    - Tlucent: Translucent (when light could come through entire piece).
    - Semi / tlucent: When light can get through most of piece but not quite all.
- Additional patination:
    - Wht: An opaque white patination that could be lightly developed, making the piece look 'cloudy' rather than opaque, up to fully opaque
    - Or lines: Fine orange lines of iron deposition in a crazed pattern across the surface usually.
    - Red or or: Red or orange patination, more so than regularly so (pieces are marked as "unpat" if not stained orange or brown in some capacity, pieces marked with this suggests an additionally intense staining or some areas stained on generally unstained / unpatinated pieces)
- Microcracking: Used to record fine lines or spalls that have developed from heating of the piece
- Post-depositional: Modern damage or trowelling damage are present on the piece
- Weathered: If sharpness of edges have been worn down by weathering or water rolling, seemingly natural rather than from use.
- Refits: Refit information indicating finds that refit or potentially refit with this piece.
- Date catalogues: This is to give a sense of time depth to the record (as recording improved with my experience with the material so VP12 material was catalogued first and is the most likely to contain errors or underestimations of certain tool types like burins)
- Additional notes.
- For natural pieces, only the source and material were completed. All other details were ignored.

Appendix 3 Micromorphology notes

Micromorphology facilitates the analysis of samples that are undisturbed and unconsolidated by the excavation process. The samples are processed into resin blocks in a manner to preserve their structure and composition as they were in-situ in the soil so that the formation, disturbance and modification processes that have affected those deposits can be assessed as thin sections with transmitted light microscopy.

The aim of the micromorphology undertaken on the dryland at Flixton Island 2 was carried out in order to assess the taphonomic and sedimentary processes. It was hoped the micromorphology would be able to provide information about:

- General composition of the deposit
- Movement of sediments
- Weathering
- Bioturbation
- Effects of grazing and ploughing
- Changing water levels and drainage effects, with a potential for causing redox or rubefaction
- Evidence for burning or plant clearance (ash, charcoal, phytoliths)
- The degree of free iron and other significant minerals (which may therefore impact other chemical analyses)
- Evidence for phosphate minerals (confirming readings from the general testing)
- The presence of calcium carbonate

Taking the sample

One discrete aluminium Kubiena tin (sample number 2012) was taken in the field from an undisturbed section in trench 4 on 18th September 2012 by Dr H. Williams. The block was 2.5 x 6 x 3.5cm. The aim of taking this sample was to facilitate assessment of bioturbation and land surface in the Mesolithic dryland area. The trench was reasonably shallow and the above-till deposits mostly consisted of topsoil (context 1000). The sample was deemed to contain topsoil only from the thin section. One tin (sample 1010) was also taken from trench 3 covering topsoil (context 1000) transitioning into the till (context 1059). The block was 3.5 x 8 x 5cm. The orientation of the sample and sample details were marked up on the outside of the block in permanent marker and maintained throughout processing and samples. Sample 1012 from trench 4 on the dryland was stored at room temperature from September 2012 until 2nd January 2014 after which it was processed. Sample 1010 was

stored at room temperature until 2nd January 2014 and then refrigerated until 26th January 2015.

Thin section processing

The samples were processed in the Mary Cudworth laboratory at the University of York using standard procedures developed by the University of Stirling Thin Section and Micromorphology labs (MacLeod 2008). Samples need to be dried before resin impregnation due to the hydrophobic nature of the resin. Samples were dried by the acetone vapour exchange method developed by the Stirling labs (*ibid*.). The water in the soil block is very gradually replaced with acetone through water evaporating out of the sample and the sample absorbing acetone vapour in its place. This method avoids the development of cracks that can occur during air, heat or freeze drying and the sediment disturbance caused by direct immersion in acetone (Lang 2014). For this process, both lids of the Kubiena tin were removed, with the base lid being replaced with a perforated lid. The soil sample was then placed on a raised, perforated platform in a resealable plastic container, with approx. 1cm depth Fisher Scientific analytical reagent grade acetone under the platform (see Figure 156). A small container of Fisher Scientific anhydrous calcium chloride was also placed on the platform to speed the drying process as it acts as a desiccant, drawing water from the sample. The desiccant was replaced as necessary with it transitioning from solid, white powder granules to expanded granules and even breaking down into a liquid in the early stages of processing for some blocks (see Figure 157).

Figure 156. Acetone vapour exchange setup for drying micromorphology tins from Flixton Island 2 and Star Carr, with a pot of anhydrous calcium chloride as desiccant on right end of the bottom row in the photograph.

Figure 157. Anhydrous calcium chloride as desiccant, with the fresh powder shown on the left, and the expanded exhausted powder shown on the right

Using this method, some of the water evaporating from the sample condenses onto the sides of the container and mixes with the acetone in the base, diluting it. Fresh acetone was replaced for the diluted mix of acetone and water 1 – 2 times per week. As the sample dries, there is less water in the acetone-water mix at the end of each cycle. Samples were measured for dryness by the MacLeod densiometric method, using a hydrometer to monitor the levels of water in the acetone-water mix at the end of exchange cycles until the water content is equal to or less than 0.5% (MacLeod 2008). The degree of dissolution of the desiccant also gave a general visual indicator of when the sample was approaching dryness. The hydrometer measurement for specific gravity was then checked against the calibration curve produced by Stirling Micromorphology labs (*ibid*.) to evaluate the percentage of the mixture that is water. Sample 1012 was in the exchange for six months, sample 1010 for 18 months.

The blocks were placed into aluminium formers for resin impregnation. A suitably sized sheet of aluminium was placed on top of the open side of the sample which was then flipped over carefully so as not to disturb the sediment (taking note of the orientation of the sample so that its relative orientation when in the ground was still known). The sheet was then folded into a former around the tin, removing the perforated base once the sides of the sample were supported. The orientation and sample details were then marked up on the outside of the new former in permanent marker as well as being recorded on paper and photographed to ensure this information was not lost during impregnation. The formers were all placed into an aluminium tray in a known orientation so that they could be moved around the lab, and so that any resin overflows during impregnation are contained within the tray.

The blocks were impregnated with the ABL Stevens / Reichhold polyester based Polylite® 32032-00 Clear Casting resin hardened with ABL Stevens / United Initiators Curox® M-312 methyl ethyl ketone peroxide (MEKP) catalyst. To 350ml of casting resin was added 0.2ml of MEKP, this mixture was then diluted to 400ml volume with acetone. The thoroughly mixed resin was then poured along the glass rod into a corner of the former, resting on the edge of the Kubiena tin to minimise the disturbance of the sample sediments. The resin was poured into the blocks until a consistent layer of resin formed over the upper surface of the block. After the first impregnation, the sample tray was placed into a vacuum desiccator and the chamber evacuated and kept sealed for 24 hours to draw any air bubbles out of the resin. The resin was further topped up every two days, with samples air drying in a fume hood, until the sample was saturated. Samples were left to cure for 8 - 12 weeks with the final week in an oven at under 40°C to complete polymerisation.

The impregnated blocks were sliced in the plane parallel to the section using a Petrocut abrasive cutter and ground down to a flat, uniform surface on a Logitech LP50 lapping plate. The slice was then mounted onto a glass slide using a thin layer of epoxy resin. The slides were clamped to the slices during setting using a spring mounted pressure jig. The excess slice was then cut from the slide with care using the abrasive cutter. The slide was then lapped down to 30µm of sample (excluding slide thickness), with 15µm calcined aluminium oxide as the grinding medium on a Logitech LP50 lapping machine. Finally, the slides were polished on a Logitech CL-40 Polishing Plate utilising 30µm diamond oil suspension.

Microscopic analysis

Slides were evaluated both by the author and also Prof. Charles French at the University of Cambridge, Division of Archaeology. In York, they were analysed on a Zeiss Axio Scope A1 setup with an AxioCam MRc5 camera, electronically controlled stage and an X-Cite 120 Q fluorescence excitation light source as well as an Axio Lab A1 with the ERc 5s camera, set

up with the rotating stage. Zeiss AxioVision software was used for processing the images from both microscopes.

Appendix 4 Field pXRF Quality Assurance and Control

This appendix contains the calibration check record; the details of and results from the beam runtime assessment; and the raw data tables of field repeats and control readings taken in the field by pXRF

Calibration Check Record for Flixton Island 2, 2014 field season

The calibration check assesses and compensates for drift as the machine is calibrated against a known metal alloy. The machine will not proceed to take readings if it fails the calibration check. These checks were conducted at the start of every working day, and repeated if there was a significant break in work during that day.

Table 50. Calibration checks in the field at Flixton Island 2. *Time settings for analyser had been reset, this is the timestamp as embedded in the datafile. **It is unknown why these times were not recorded by the analyser.

Date	Time	Reading	Mode	Elapsed Time Total
20/08/2014	10:05:39	#1	Cal Check	14.89
21/08/2014	05:13:34*	#1	Cal Check	not recorded**
23/08/2014	09:43:03	#1	Cal Check	14.88
24/08/2014	09:07:46	#1	Cal Check	not recorded**
25/08/2014	09:21:21	#1	Cal Check	14.89
	14:25:49	#11	Cal Check	14.84
26/08/2014	09:14:54	#1	Cal Check	14.87
27/08/2014	09:08:00	#1	Cal Check	14.86

Beam Runtime Evaluation

Both the high and low energy beams emitting x-radiation can be run for varying lengths of time. This allows more time for x-rays to interact with the substrate being analysed and also rarer elements within the sample are more likely to be detected over longer runtimes as there is a greater probability of an x-ray interacting with them and then returning to the detector. However, this has to be balanced against the time available to conduct the study, field excavation constraints and so on (as running a sample for five minutes rather than one can make a vast difference in the total study time needed when analysing hundreds of samples). Initially, in the field, repeat readings were taken at two locations to establish whether a 30 second beam reading was altered by increasing the duration to 60 second runtime, and whether a 60 second beam reading was improved by a 90 second beam time.

The details and results are provided in Table 51 and Table 52 respectively. Results were highlighted using a basic scheme:

- Reading on scale of tens of ppm: variation if machine detects / doesn't detect
- Scale of 100s: >20 ppm different
- Scale of 1000s: >200 ppm different
- Scale of 10,000s and above: >500 ppm different

Table 51. Run time experiment details

	Date	20/08/2014	20/08/2014		**Date**	20/08/2014	20/08/2014	
	Trench	12	12		**Trench**	12	12	
	Description	30 sec beams	60 sec beams		**Description**	60 sec beams	90 sec beams	
	Sample #	1870	1870		**Sample #**	1872	1872	
	Time	11:16:33	11:19:23		**Time**	11:29:32	11:34:03	
	Reading	#5	#6		**Reading**	#7	#8	
	Mode	Geochem	Geochem		**Mode**	Geochem	Geochem	

Table 52. Run time experiment results

Result type	**Category**	**Criteria to flag up (diff in ppm)**	**Element**	**20/08/2014 Reading #5**	**20/08/2014 Reading #6**	**Difference**	**Element**	**20/08/2014 Reading #7**	**20/08/2014 Reading #8**	**Difference**
Estimate		n/a	**Light Elements (LE)**	826874.19	827265.66		**Light Elements (LE)**	759575.1	759988.81	
Readings	Major (>10,000 ppm)	>500	**Si**	113393.51	112627.11	766.4	**Si**	166665.05	166589.64	75.41
			Al	24989.37	25367.66	-378.29	**Al**	36641.26	36458.31	182.95
			Fe	18082.93	18024.52	58.41	**Fe**	20084.91	19861.7	223.21
	Minor (1000 -	>200	**Ca**	9221.4	9379.37	-157.97	**Ca**	7892.75	7864.95	27.8

Result type	Category	Criteria to flag up (diff in ppm)	Element	20/08/2014 Reading #5	20/08/2014 Reading #6	Difference	Element	20/08/2014 Reading #7	20/08/2014 Reading #8	Difference
	10,000 ppm)		**K**	3325.17	3308.86	16.31	**K**	4375.04	4321.66	53.38
			Ti	2296.03	2228.19	67.84	**Ti**	2411.93	2510.62	-98.69
			S	946.79	969.99	-23.2	**S**	1046.96	1042.8	4.16
	Trace (100 – 1000 ppm)	>20	**Zr**	385.91	386.5	-0.59	**Zr**	522.85	515.12	7.73
			P	217.12	175.33	41.79	**P**	322.01	313.95	8.06
			Mn	127.12	130.34	-3.22	**Mn**	118.27	122.84	-4.57
	IUPAC Trace (<100 ppm)	detects?	**Sr**	52	50.7	1.3	**Sr**	53.77	53.28	0.49
			Zn	20.67	21.13	-0.46	**Zn**	21.94	22.52	-0.58
			Rb	16.17	16.36	-0.19	**Rb**	19.26	19.85	-0.59
			Pb	15.4	9.47	5.93	**Pb**	10.95	8.8	2.15
			Y	14.47	14.36	0.11	**Y**	17.09	15.91	1.18
			Nb	5.9	5.22	0.68	**Nb**	5.28	4.91	0.37
			U	5.9	<LOD		**U**	<LOD	<LOD	
			As	5.24	9.25	-4.01	**As**	5.03	5.88	-0.85
			Mo	4.68	<LOD		**Mo**	<LOD	<LOD	
			Ag	<LOD	<LOD		**Ag**	<LOD	<LOD	
			Bi	<LOD	<LOD		**Bi**	8.77	7.22	1.55
			Cd	<LOD	<LOD		**Cd**	<LOD	15.11	
			Cl	<LOD	<LOD		**Cl**	<LOD	<LOD	
			Co	<LOD	<LOD		**Co**	<LOD	<LOD	

Result type	Category	Criteria to flag up (diff in ppm)	Element	20/08/2014 Reading #5	20/08/2014 Reading #6	Difference	Element	20/08/2014 Reading #7	20/08/2014 Reading #8	Difference
			Cr	<LOD	<LOD		**Cr**	<LOD	33.9	
			Cu	<LOD	<LOD		**Cu**	<LOD	<LOD	
			Hg	<LOD	<LOD		**Hg**	<LOD	<LOD	
			Mg	<LOD	<LOD		**Mg**	<LOD	<LOD	
			Ni	<LOD	<LOD		**Ni**	11.78	8.24	3.54
			Sb	<LOD	<LOD		**Sb**	<LOD	<LOD	
			Se	<LOD	<LOD		**Se**	<LOD	<LOD	
			Sn	<LOD	<LOD		**Sn**	<LOD	<LOD	
			Ta	<LOD	9.99		**Ta**	10.09	13.89	-3.80
			Th	<LOD	<LOD		**Th**	<LOD	<LOD	
			V	<LOD	<LOD		**V**	179.91	200.1	-20.19
			W	<LOD	<LOD		**W**	<LOD	<LOD	
Errors			**Ag +/-**	916.69	647.05		**Ag +/-**	627.75	509.7	
			Al +/-	724.69	512.68		**Al +/-**	523.5	423.54	
			As +/-	1.32	0.91		**As +/-**	0.87	0.69	
			Bi +/-	363.93	259.56		**Bi +/-**	2.36	1.91	
			Ca +/-	60.67	43.57		**Ca +/-**	38.31	30.97	
			Cd +/-	1104.66	782.8		**Cd +/-**	763.91	4.17	
			Cl +/-	3056.11	2176.28		**Cl +/-**	1536.68	1243.87	
			Co +/-	302.04	212.12		**Co +/-**	213.79	173.45	

Result type	Category	Criteria to flag up (diff in ppm)	Element	20/08/2014 Reading #5	20/08/2014 Reading #6	Difference	Element	20/08/2014 Reading #7	20/08/2014 Reading #8	Difference
			Cr +/-	171.03	121.2		**Cr +/-**	119.96	10.09	
			Cu +/-	68.4	48.85		**Cu +/-**	45.98	38.48	
			Fe +/-	124.18	87.61		**Fe +/-**	89.14	71.75	
			Hg +/-	152.87	109.91		**Hg +/-**	105.66	82.99	
			K +/-	42.68	30.16		**K +/-**	33.05	26.61	
			LE +/-	1077.6	760.86		**LE +/-**	846.6	685.43	
			Mg +/-	34999.79	24708.23		**Mg +/-**	15897.44	12947.71	
			Mn +/-	15.39	10.96		**Mn +/-**	10.62	8.7	
			Mo +/-	1.26	93.67		**Mo +/-**	92.37	74.76	
			Nb +/-	1.3	0.91		**Nb +/-**	0.89	0.72	
			Ni +/-	66.68	48.19		**Ni +/-**	3.11	2.47	
			P +/-	48.01	33.52		**P +/-**	34.1	27.52	
			Pb +/-	1.79	1.18		**Pb +/-**	1.17	0.92	
			Rb +/-	0.83	0.58		**Rb +/-**	0.59	0.48	
			S +/-	34.46	24.43		**S +/-**	23.98	19.35	
			Sb +/-	2319.41	1646.04		**Sb +/-**	1621.19	1315.45	
			Se +/-	22.87	15.33		**Se +/-**	14.24	11.77	
			Si +/-	692.88	487.41		**Si +/-**	585.41	474.42	
			Sn +/-	1834.23	1294.37		**Sn +/-**	1273.27	1033.9	
			Sr +/-	1.13	0.79		**Sr +/-**	0.79	0.64	

Result type	Category	Criteria to flag up (diff in ppm)	Element	20/08/2014 Reading #5	20/08/2014 Reading #6	Difference	Element	20/08/2014 Reading #7	20/08/2014 Reading #8	Difference
			Ta +/-	213.46	2.66		**Ta +/-**	2.65	2.22	
			Th +/-	552.17	393.51		**Th +/-**	374.12	304.14	
			Ti +/-	104.24	73.12		**Ti +/-**	73.49	60.27	
			U +/-	1.87	204.37		**U +/-**	193.16	159.35	
			V +/-	348.13	244.5		**V +/-**	29.67	24.37	
			W +/-	255.75	180.13		**W +/-**	173.99	144.52	
			Y +/-	1.02	0.72		**Y +/-**	0.73	0.59	
			Zn +/-	2.19	1.56		**Zn +/-**	1.54	1.26	
			Zr +/-	3.04	2.15		**Zr +/-**	2.45	1.97	

In terms of the trace elements, molybdenum (Mo) and uranium (U) were only detected in the shortest 30 second beam and not in the comparative 60 second beam, again in tiny amounts (9.99 and 5.90 ppm respectively); this could have been purely down to chance statistics that they were able to be picked up or because the peak was misinterpreted by the machine. As such, this suggested caution against using the shorter beam runtime, even though these are not particularly crucial elements for human activity identification in this scenario. Increasing to 60 s beam, allowed for the identification of tantalum (Ta) at 9.99 ppm. Increasing to 90 second beam additionally allowed for the detection of cadmium (Cd) and chromium (Cr) at 12 and 24 ppm. It was decided that detecting these elements was interesting but not crucial, and at such low levels could hardly be used to justify activity area detection (as the research goal). If a reading came out higher than it would likely be enough to say we were getting readings in certain areas of the trench versus readings being below the limits of detection of the machine.

Silicon (Si) varied by more than 500 ppm between the 30 second and 60 second runtime readings, yet varied by less than 200ppm between the 60 and 90 second runtime readings. This major element appeared in concentrations in the tens and hundreds of thousands respectively so reducing the difference drastically was deemed a benefit worth maintaining

for the reading of this element. Similarly, phosphorus (P) varied by 41.79 ppm between the 30 and 60 second runtimes but only by 8.06 ppm between the 60 and 90 second runtimes.

As such, overall it was decided that 60 second runtimes would be the best use of time, providing sufficient results for the purpose while maximising the time available to take readings while trenches were open and available for analysis.

Repeat readings from "control" areas

Overview

At the start of every day involving field pXRF at Flixton, repeat readings were taken to compare readings from the same location on site (in the approximate centre of a 0.25 m^2 sample area).

Due to how excavations proceeded at Flixton, it was not possible for a single location to be maintained across the full period at Flixton as trenches were excavated further down to the till once readings from the proposed Mesolithic layers had been taken on the pXRF. As such, a location was maintained for each trench to act as a control area for repeat readings while that trench was being systematically scanned by pXRF (which usually took more than a single day). In trenches 11 and 12, this was the southeasternmost sample square in those trenches. For trench 15, this was the northeasternmost sample square in that trench. When transitioning between two trenches, readings from the older, first trenches' control areas were taken on the same day as readings from the new trench that were used as controls. These repeat readings give a sense of the precision of field pXRF readings taken using this method, both based on daily variance caused by changing field conditions and also measurement error (see Table 53, Table 54, Table 55 and Table 56). As most readings were taken in the morning, they were likely influenced by the previous day and night's conditions.

Table 53. A record of the readings taken in the field at Flixton in August 2014, both for repeats and for new readings, as well as notes on conditions made in the field and highlights from the Met Office report for August 2014 (The Met Office 2015).

Date	***Field pXRF readings taken***	***Field conditions as noted***	***Field conditions from Met Office report for August 2014***
20	Trench 12 four initial test readings	Not noted.	The 19th and 20th were cooler with sunshine and more isolated, light showers but otherwise dry.

Date	*Field pXRF readings taken*	*Field conditions as noted*	*Field conditions from Met Office report for August 2014*
21	Trench 12 repeat; Trench 11 readings	Rain (gradually increasing during day).	The 21st started mainly bright with isolated showers but a band of rain spread from the northwest during the afternoon, reaching the southeast during the evening.
23	Trench 11 repeat + continued readings	Had rained overnight and during previous day (the day off). This repeat reading was in the wettest corner of the trench (so should reflect any significant alteration).	The showers were more widespread and frequent on the 23rd with the heaviest ones again in the east.
24	Trench 11 repeat + continued readings	Had rained overnight. Sunny, clear day.	A bright but chilly start on the 24th with areas in Dorset falling to 3°C but it was a bright day for many although rain edged into the far southwest during the late afternoon.
25	Trench 11 repeat + continued readings; Trench 15 readings	Cloudy and misty in the morning but ground not apparently that wet.	The country was split on the 25th with the northern half mainly dry and bright and southern half being wet for much of the day with areas of Kent and London recording over 35 mm of rain.
26	Trench 15 repeat + continued readings (to completion)	Not noted.	An area of rain affected southern areas for much of the 26th with other areas dry but mainly cloudy; remaining cool in a northwest wind.
27	Trench 12 repeat + readings	Fairly dry night. Warm, sunny morning.	The 27th was generally dry and bright but rain spread into the southwest during the afternoon.

Elemental classifications by trench

Table 54. Summary of Field pXRF control reading results for trench 11

Category	**ppm**	**For trench 11:**
Major	>10000	Al, Ca, Fe, Si
Minor	1000 - 10000	K, S, Ti

Trace	100 - 1000	Mn, P, V, Zr
IUPAC Trace	<100	Ag, As, Bi, Cd, Cr, Mo, Nb, Pb, Rb, Sr, Ta, Th, U, Y, Zn
<LOD		Cl, Co, Cu, Hg, Mg, Ni, Sb, Se, Sn, W

Table 55. Summary of Field pXRF control reading results for trench 12

Category	**ppm**	**For trench 12:**
Major	>10000	Si, Al, Fe, Ca
Minor	1000 - 10000	K, Ti, S
Trace	100 - 1000	Zr, P, Mn, V
IUPAC Trace	<100	Sr, Zn, Rb, Y, Ta, Pb, As, Nb, Cr, Co, Mo, Th
<LOD		Mg, Cl, Co, Ni, Se, Ag, Cd, Sn, Sb, W, Hg, Bi, U

Table 56. Summary of Field pXRF control reading results for trench 15. There were four different control spots read from the same grid square for Trench 15. This gives an estimation of the variability from within one grid square as well as providing the daily repeats for field conditions

Categories	**ppm**	**For trench 15:**
Major	>10000	Al, Fe, Si
Minor	1000 - 10000	Ca, K, Ti
Trace	100 - 1000	Mn, P (not for control 4*), S (not for control 4), V, Zr
IUPAC Trace	<100	As, Cr, Mo, Nb, Ni (not for control 2), Pb, Rb, S (only for control 4), Sr, Ta, Th (only for control 3), U (only for control 3), Y, Zn
<LOD		Ag, Bi, Cd, Cl, Co, Cu, Hg, Mg, Ni (only for control 2), P (only for control 4), Sb, Se, Sn, Th (not for control 3), U (not for control 3), W

Full data for Flixton Field pXRF

The next few pages are the complete data tables for all the Flixton trench repeat control Field pXRF readings, tabulated by trench, followed by the related descriptive statistics tables. At the end of each site's data, there is a descriptive statistical summary of all the results considered together as one.

Table 57 and Table 58 provide the data and the descriptive statistics for that data for trench 11.

Table 59 and Table 60 provide the data and the descriptive statistics for that data for trench 12.

Table 61 to Table 66 provide the data and the descriptive statistics for trench 15. The trench 15 readings were repeated on four spots in the northeasternmost grid squares of the trench to allow comparison. As such, results are presented for all four reading locations.

Table 67 provides the descriptive statistics for all repeat readings across all trenches at Flixton Island 2, to give a sense of the variability across the entire dataset for the controls.

Table 57. Trench 11 Field pXRF control readings data (rounded to 2 d.p.)

Trench 11	23/08/2014 #2 Reading (ppm)	Error (+/-) or estimated LOD (ppm)	24/08/2014 #2 Reading (ppm)	Error (+/-) or estimated LOD (ppm)	25/08/2014 #2 Reading (ppm)	Error (+/-) or estimated LOD (ppm)
Light Elements						
LE	777700.75	833.29	755472.03	830.08	848189.21	828.81
Major						
Al	38929.54	545.57	25686.4	477.07	22362.51	587.06
Ca	11653.69	48.4	8886.48	40.29	13383.02	64.01
Fe	22871.59	98.4	16170.68	76.2	22995.27	119.71
Si	140565.57	531.97	186381.11	624.58	86052.68	475.12
Minor						
K	3277.55	29.5	2943.76	29.29	2507.92	31.91
S	1090.71	23.92	813.62	23.5	1072.02	29.6
Ti	2484.04	72.75	2423.84	73.55	2155.69	80.28
Trace						
Mn	146.13	11.01	122.65	10.66	175.87	13.22
P	378.25	34.67	369.97	35.86	413.64	42.81
V	157.71	29.12	111.46	29.63	135.63	32.96
Zr	502.6	2.44	390.39	2.01	340.21	2.33
IUPAC Trace						
Ag	12.44	4.1	<LOD	LOD: 627.88	<LOD	LOD: 744.84
As	7.56	0.91	6.03	0.87	10.02	1.13
Bi	<LOD	LOD: 249.34	7.1	2.3	<LOD	LOD: 304.07
Cd	17.96	5.11	19.44	5.03	<LOD	LOD: 900.87
Cr	47.6	12.45	70.26	13.04	<LOD	LOD: 151.89
Mo	3.9	0.91	<LOD	LOD: 89.24	11.48	1.04
Nb	7.07	0.9	4.8	0.87	15.37	1.12
Pb	11.43	1.19	11.55	1.15	16.26	1.5

Trench 11	23/08/2014 #2 Reading (ppm)	Error (+/-) or estimated LOD (ppm)	24/08/2014 #2 Reading (ppm)	Error (+/-) or estimated LOD (ppm)	25/08/2014 #2 Reading (ppm)	Error (+/-) or estimated LOD (ppm)
Rb	16.61	0.57	14.34	0.54	15.61	0.67
Sr	50.09	0.77	46.33	0.73	52.94	0.93
Ta	15.35	2.77	12.67	2.67	17.35	3.23
Th	<LOD	LOD: 377.87	<LOD	LOD: 372.51	22.21	3.16
U	<LOD	LOD: 196.87	<LOD	LOD: 194.99	5.02	1.54
Y	13.54	0.71	13.33	0.68	17.17	0.85
Zn	38.29	1.79	21.76	1.51	32.9	2.03
Not detected in any samples						
Cl	<LOD	LOD: 1661.31	<LOD	LOD: 1375.25	<LOD	LOD: 2828.76
Co	<LOD	LOD: 228.18	<LOD	LOD: 189.86	<LOD	LOD: 273.11
Cu	<LOD	LOD: 47.16	<LOD	LOD: 46.23	<LOD	LOD: 56.96
Hg	<LOD	LOD: 97.72	<LOD	LOD: 105.51	<LOD	LOD: 125.8
Mg	<LOD	LOD: 17072.8	<LOD	LOD: 14831.22	<LOD	LOD: 34210.86
Ni	<LOD	LOD: 47.25	<LOD	LOD: 45.97	<LOD	LOD: 58.81
Sb	<LOD	LOD: 1574.27	<LOD	LOD: 1600.32	<LOD	LOD: 1899.42
Se	<LOD	LOD: 14.43	<LOD	LOD: 14.62	<LOD	LOD: 18.56
Sn	<LOD	LOD: 1239.37	<LOD	LOD: 1260.38	<LOD	LOD: 1497.32
W	<LOD	LOD: 170.52	<LOD	LOD: 181.55	<LOD	LOD: 214.87

Table 58. Trench 11 Field pXRF control readings descriptive statistics (to 2 d.p.)

Trench 11 controls (ppm)	*N*	Range	Minimum	Maximum	Mean	Std. Deviation
LE	3	92717.18	755472.03	848189.21	793787.33	48406.64
Al	3	16567.03	22362.51	38929.54	28992.82	8764.47
Ca	3	4496.54	8886.48	13383.02	11307.73	2268.15
Fe	3	6824.59	16170.68	22995.27	20679.18	3904.97
Si	3	100328.43	86052.68	186381.11	137666.45	50227.01
K	3	769.63	2507.92	3277.55	2909.74	385.94
S	3	277.09	813.62	1090.71	992.12	154.87
Ti	3	328.35	2155.69	2484.04	2354.52	174.81
Mn	3	53.22	122.65	175.87	148.22	26.67
P	3	43.67	369.97	413.64	387.29	23.20
V	3	46.25	111.46	157.71	134.93	23.13
Zr	3	162.39	340.21	502.60	411.07	83.15
Ag	1	0	12	12	12.44	
As	3	3.99	6.03	10.02	7.87	2.01
Bi	1	0	7	7	7.10	
Cd	2	1	18	19	18.70	1.047
Cr	2	23	48	70	58.93	16.02
Mo	2	8	4	11	7.69	5.36
Nb	3	10.57	4.80	15.37	9.08	5.56
Pb	3	4.83	11.43	16.26	13.08	2.76
Rb	3	2.27	14.34	16.61	15.52	1.14
Sr	3	6.61	46.33	52.94	49.79	3.32
Ta	3	4.68	12.67	17.35	15.12	2.35
Th	1	0	22	22	22.21	
U	1	0	5	5	5.02	
Y	3	3.84	13.33	17.17	14.68	2.16
Zn	3	16.53	21.76	38.29	30.98	8.43

Table 59. Trench 12 Field pXRF control readings data (to 2 d.p.)

Trench 12	20/08/2014 #6 Reading (ppm)	Error (+/-) or estimated LOD (ppm)	21/08/2014 #2 Reading (ppm)	Error (+/-) or estimated LOD (ppm)	21/08/2014 #3 Reading (ppm)	Error (+/-) or estimated LOD (ppm)	27/08/2014 #2 Reading (ppm)	Error (+/-) or estimated LOD (ppm)
Light Elements								
LE	827265.66	760.86	779231.74	972.03	782930.88	938.99	850001.28	696.65
Major								
Al	25367.66	512.68	36113.82	640.52	35532.82	618.61	18712.79	472.72
Ca	9379.37	43.57	6430.79	40.36	6329.85	39.28	18475.66	72.03
Fe	18024.52	87.61	18169.42	97.89	18047.49	95.1	23044.64	105.11
Si	112627.11	487.41	151615.61	654.67	148848.85	631.24	81073.52	396.06
Minor								
K	3308.86	30.16	4393.24	40.45	4237.5	38.67	2599.97	26.03
S	969.99	24.43	587.45	29.14	563.83	27.72	2262.54	28.06
Ti	2228.19	73.12	2338.45	85.57	2416.15	83.94	2243.42	70.9
Trace								
Mn	130.34	10.96	136.94	12.81	103.18	11.95	204.99	11.89
P	175.33	33.52	148.92	41.99	130.93	39.87	588.97	36.33
V	<LOD	LOD: 244.5	159.37	35.18	143.76	33.94	183.42	29.05
Zr	386.5	2.15	497.36	2.8	509.77	2.77	391.15	2.21
IUPAC Trace								
As	9.25	0.91	6.62	1.03	8.34	0.99	8.58	0.93
Cr	<LOD	LOD: 121.2	<LOD	LOD: 140.92	49.01	14.6	44.57	12.4
Cu	<LOD	LOD: 48.85	<LOD	LOD: 56.47	10.58	3.13	<LOD	LOD: 49.66
Mo	<LOD	LOD: 93.67	7.67	1.06	5.05	1.05	3.14	0.92
Nb	5.22	0.91	7.35	1.05	7.5	1.02	11.53	0.96
Ni	<LOD	LOD: 48.19	12.37	3.7	<LOD	LOD: 54.98	<LOD	LOD: 49.25
Pb	9.47	1.18	11.64	1.39	8.54	1.29	10.73	1.22
Rb	16.36	0.58	20.55	0.7	20.04	0.67	18.94	0.61

Trench 12	20/08/2014 #6 Reading (ppm)	Error (+/-) or estimated LOD (ppm)	21/08/2014 #2 Reading (ppm)	Error (+/-) or estimated LOD (ppm)	21/08/2014 #3 Reading (ppm)	Error (+/-) or estimated LOD (ppm)	27/08/2014 #2 Reading (ppm)	Error (+/-) or estimated LOD (ppm)
Sr	50.7	0.79	45.96	0.87	46.21	0.84	50.26	0.8
Ta	9.99	2.66	11.82	3.07	11.63	3.01	18.02	2.9
Th	<LOD	LOD: 393.51	10.9	3.05	<LOD	LOD: 437.95	<LOD	LOD: 388.98
Y	14.36	0.72	16.81	0.85	15.67	0.82	22.09	0.78
Zn	21.13	1.56	25.21	1.87	22.42	1.77	29.82	1.7
Not detected in any samples								
Ag	<LOD	LOD: 647.05	<LOD	LOD: 757.33	<LOD	LOD: 731.75	<LOD	LOD: 650.16
Bi	<LOD	LOD: 259.56	<LOD	LOD: 299.14	<LOD	LOD: 288.92	<LOD	LOD: 256.61
Cd	<LOD	LOD: 782.8	<LOD	LOD: 921.45	<LOD	LOD: 887.09	<LOD	LOD: 785.74
Cl	<LOD	LOD: 2176.28	<LOD	LOD: 2159.08	<LOD	LOD: 2088.05	<LOD	LOD: 1999.55
Co	<LOD	LOD: 212.12	<LOD	LOD: 236.19	<LOD	LOD: 229.89	<LOD	LOD: 237.86
Hg	<LOD	LOD: 109.91	<LOD	LOD: 127.21	<LOD	LOD: 122.44	<LOD	LOD: 112.56
Mg	<LOD	LOD: 24708.23	<LOD	LOD: 24176.7	<LOD	LOD: 24630.12	<LOD	LOD: 25028.16
Sb	<LOD	LOD: 1646.04	<LOD	LOD: 1955.79	<LOD	LOD: 1882.81	<LOD	LOD: 1681.36
Se	<LOD	LOD: 15.33	<LOD	LOD: 17.5	<LOD	LOD: 17.54	<LOD	LOD: 15.75
Sn	<LOD	LOD: 1294.37	<LOD	LOD: 1535.85	<LOD	LOD: 1479.93	<LOD	LOD: 1320.96
U	<LOD	LOD: 204.37	<LOD	LOD: 236.87	<LOD	LOD: 221.45	<LOD	LOD: 202.33
W	<LOD	LOD: 180.13	<LOD	LOD: 215.91	<LOD	LOD: 206.7	<LOD	LOD: 188.77

Table 60. Trench 12 Field pXRF control readings descriptive statistics (to 2 d.p.)

Trench 12 controls (ppm)	*N*	Range	Minimum	Maximum	Mean	Std. Deviation
LE	4	70769.54	779231.74	850001.28	809857.39	34532.82
Al	4	17401.03	18712.79	36113.82	28931.77	8412.02
Ca	4	12145.81	6329.85	18475.66	10153.92	5725.28
Fe	4	5020.12	18024.52	23044.64	19321.52	2482.90
Si	4	70542.09	81073.52	151615.61	123541.27	33422.90
K	4	1793.27	2599.97	4393.24	3634.89	839.76
S	4	1698.71	563.83	2262.54	1095.95	799.69
Ti	4	187.96	2228.19	2416.15	2306.55	87.85
Mn	4	101.81	103.18	204.99	143.86	43.29
P	4	458.04	130.93	588.97	261.04	219.38
V	3	39.66	143.76	183.42	162.18	19.98
Zr	4	123.27	386.50	509.77	446.20	66.47
As	4	2.63	6.62	9.25	8.20	1.12
Cr	2	4.44	44.57	49.01	46.79	3.14
Cu	1	0.00	10.58	10.58	10.58	
Mo	3	4.53	3.14	7.67	5.29	2.27
Nb	4	6.31	5.22	11.53	7.90	2.64
Ni	1	0.00	12.37	12.37	12.37	
Pb	4	3.10	8.54	11.64	10.10	1.37
Rb	4	4.19	16.36	20.55	18.97	1.87
Sr	4	4.74	45.96	50.70	48.28	2.55
Ta	4	8.03	9.99	18.02	12.87	3.53
Th	1	0.0	10.9	10.9	10.90	
Y	4	7.73	14.36	22.09	17.23	3.39
Zn	4	8.69	21.13	29.82	24.65	3.85

Table 61. Trench 15 Field pXRF control readings data (to 2 d.p.). *n/a = element in another category for this sample

Tr15 Sample 1	S1 25/08/2014 #17 Reading (ppm)	Error (+/-) / estimated LOD (ppm)	S1 26/08/2014 #2 Reading (ppm)	Error (+/-) / estimated LOD (ppm)	Tr15 Sample 2	S2 25/08/2014 #18 Reading (ppm)	Error (+/-) / estimated LOD (ppm)	S2 26/08/2014 #3 Reading (ppm)	Error (+/-) / estimated LOD (ppm)	Tr15 Sample 3	S3 25/08/2014 #19 Reading (ppm)	Error (+/-) / estimated LOD (ppm)	S3 26/08/2014 #4 Reading (ppm)	Error (+/-) / estimated LOD (ppm)	Tr15 Sample 4	S4 25/08/2014 #20 Reading (ppm)	Error (+/-) / estimated LOD (ppm)	S4 26/08/2014 #5 Reading (ppm)	Error (+/-) / estimated LOD (ppm)
Light Elements					**Light Elements**					**Light Elements**					**Light Elements**				
LE	697653.29	1109.07	713189.96	1039.82	**LE**	696750.97	1045.6	699209.05	1139.13	**LE**	724561.24	992.79	708796.73	1083.7	**LE**	675187.33	1059.65	661054.41	1076.3
Major					**Major**					**Major**					**Major**				
Al	62698.09	701.57	51792.65	640.18	**Al**	44069.81	604.45	45731.51	672.54	**Al**	50120.6	617.46	50328.12	651.75	**Al**	49763.36	599.22	49855.18	616.76
Fe	27027.86	124.86	29543.56	128.7	**Fe**	19192.93	95.94	22306.51	114.7	**Fe**	24735.34	111.19	31461.84	139.68	**Fe**	30707.35	127.91	15619.7	83.19
Si	200276.82	749.43	189066.25	700	**Si**	224879.53	778.31	217166.56	828.37	**Si**	184987.26	674.53	193109.37	734.55	**Si**	232648.27	773.43	260691.25	833.29
Minor					**Minor**					**Minor**					**Minor**				
Ca	2093.31	31.29	6310.73	39.02	**Ca**	4653.37	36.32	5708.06	42.22	**Ca**	5546.83	36.18	4930.27	36.45	**Ca**	2478.78	30.25	2566.75	33.49
K	5500.34	45.11	4329.65	38.56	**K**	5125.6	42.69	4530.22	45.26	**K**	5016.87	39.41	5344.38	43.09	**K**	5106.91	40.98	5504.34	45.28
Ti	3829.49	98.52	4025.89	94.82	**Ti**	3658.67	96.71	3579.95	103.01	**Ti**	3439.49	88.97	4397.79	101.17	**Ti**	3147.85	87.5	3647.88	98.58
Trace					**Trace**					**Trace**					**Trace**				
Mn	113.54	12.7	149.24	12.69	**Mn**	139.76	12.89	146.46	14.07	**Mn**	136.39	12.17	172.83	13.61	**Mn**	106.52	11.93	94.87	12.3
P	<LOD	LOD: 350.76	363.01	40.94	**P**	207.05	42.01	203.85	47.74	**P**	311.41	38.71	370.18	42.55	**n/a***				
S	<LOD	LOD: 300.15	416.59	25.89	**S**	325.73	27.01	566.57	32.18	**S**	307.28	24.37	260.92	26.53	**n/a**				
V	250.08	37.71	247.05	35.5	**V**	238.29	37.5	160.12	39.09	**V**	223.02	34.33	238.72	37.29	**V**	196.3	33.98	134.47	37.29
Zr	296	2.06	270.98	1.91	**Zr**	512.56	2.68	456.66	2.72	**Zr**	323.08	2.03	252.45	1.93	**Zr**	496.39	2.6	516.4	2.63
IUPAC Trace					**IUPAC Trace**					**IUPAC Trace**					**IUPAC Trace**				
As	10.11	1.12	5.4	1.04	**As**	4.37	1.11	4.78	1.08	**As**	7.86	1.06	7.74	1.1	**As**	5.98	0.99	3.6	0.97
Cr	<LOD	LOD:	81.22	14.79	**Cr**	69.06	15.56	67.64	16.61	**Cr**	65	14.33	62.59	15.24	**Cr**	<LOD	LOD:	69.85	15.84

		151.17															142.28		
Mo	4.6	1.03	<LOD	LOD: 94.4	**Mo**	5.56	1.04	11.16	1.13	**Mo**	<LOD	LOD: 95.3	6.74	1	**Mo**	<LOD	LOD: 98.86	4.86	1.02
Nb	11.37	1.09	8.65	1.03	**Nb**	11.41	1.04	10.86	1.13	**Nb**	16.66	1.04	13.81	1.12	**Nb**	8.33	1.02	9.73	1.03
Ni	37.55	4.26	16.83	3.74	**n/a**					**Ni**	16.14	3.58	24.24	4.06	**Ni**	14.12	3.67	<LOD	LOD: 56.47
Pb	12.96	1.46	13.71	1.41	**Pb**	21.89	1.52	11.28	1.48	**Pb**	16.51	1.4	12.18	1.47	**Pb**	9.83	1.34	11.25	1.34
Rb	26.82	0.78	24.22	0.72	**Rb**	24.92	0.72	20.39	0.74	**Rb**	33.8	0.78	27.31	0.79	**Rb**	20.97	0.68	22.19	0.69
n/a					**n/a**					**n/a**					**S**	<LOD	LOD: 240.38	84.29	27.05
Sr	69.19	1.03	67.26	0.99	**Sr**	55.98	0.91	45.67	0.91	**Sr**	67.39	0.95	70.8	1.05	**Sr**	48.3	0.86	50.5	0.86
Ta	23.77	3.57	21.45	3.37	**Ta**	9.83	3.05	20.88	3.54	**Ta**	19.45	3.21	22.38	3.55	**Ta**	16.59	3.18	12.38	3.05
n/a					**n/a**					**Th**	<LOD	LOD: 410.02	11.77	3.11	**n/a**				
n/a					**n/a**					**U**	<LOD	LOD: 218.05	4.92	1.57	**n/a**				
Y	17.58	0.87	16.46	0.82	**Y**	16.55	0.84	16.02	0.9	**Y**	15.73	0.81	21.99	0.9	**Y**	14.14	0.81	18.8	0.84
Zn	47.23	2.31	39.26	2.07	**Zn**	26.17	1.86	25.78	1.99	**Zn**	32.64	1.92	49.93	2.36	**Zn**	22.69	1.79	27.29	1.86
Not detected in any samples					**Not detected in any samples**					**Not detected in any samples**					**Not detected in any samples**				
Ag	<LOD	LOD: 750.84	<LOD	LOD: 702.07	**Ag**	<LOD	LOD: 735.96	<LOD	LOD: 798.57	**Ag**	<LOD	LOD: 695.22	<LOD	LOD: 737.32	**Ag**	<LOD	LOD: 696.23	<LOD	LOD: 747.83
Bi	<LOD	LOD: 291.25	<LOD	LOD: 271.36	**Bi**	<LOD	LOD: 289.06	<LOD	LOD: 311.31	**Bi**	<LOD	LOD: 271.83	<LOD	LOD: 287.48	**Bi**	<LOD	LOD: 269.81	<LOD	LOD: 291.44
Cd	<LOD	LOD: 909.41	<LOD	LOD: 849.66	**Cd**	<LOD	LOD: 890.6	<LOD	LOD: 968.31	**Cd**	<LOD	LOD: 840.17	<LOD	LOD: 895.82	**Cd**	<LOD	LOD: 842.31	<LOD	LOD: 901.11
Cl	<LOD	LOD: 1748.81	<LOD	LOD: 1620.43	**Cl**	<LOD	LOD: 1460.43	<LOD	LOD: 1690.87	**Cl**	<LOD	LOD: 1612.01	<LOD	LOD: 1679.31	**Cl**	<LOD	LOD: 1377.66	<LOD	LOD: 1300.82
Co	<LOD	LOD: 289.34	<LOD	LOD: 289.56	**Co**	<LOD	LOD: 232.68	<LOD	LOD: 268.52	**Co**	<LOD	LOD: 256.6	<LOD	LOD: 310.05	**Co**	<LOD	LOD: 287.38	<LOD	LOD: 205.84
Cu	<LOD	LOD:	<LOD	LOD:	**Cu**	<LOD	LOD:	<LOD	LOD: 58.8	**Cu**	<LOD	LOD:	<LOD	LOD:	**Cu**	<LOD	LOD:	<LOD	LOD:

		59.69		53.28			54.47					53.33		58.44			51.36		54.52
Hg	<LOD	LOD: 131.4	<LOD	LOD: 118.61	**Hg**	<LOD	LOD: 125.44	<LOD	LOD: 132.16	**Hg**	<LOD	LOD: 120.85	<LOD	LOD: 125.69	**Hg**	<LOD	LOD: 118.89	<LOD	LOD: 124.81
Mg	<LOD	LOD: 17337.92	<LOD	LOD: 16389.68	**Mg**	<LOD	LOD: 15385.86	<LOD	LOD: 17937.18	**Mg**	<LOD	LOD: 16780.97	<LOD	LOD: 17713.21	**Mg**	<LOD	LOD: 13630.97	<LOD	LOD: 13056.12
n/a					**Ni**	<LOD	LOD: 56.62	<LOD	LOD: 60.24	**n/a**					**n/a**				
n/a					**n/a**					**n/a**					**P**	<LOD	LOD: 292.34	<LOD	LOD: 278.94
Sb	<LOD	LOD: 1952.96	<LOD	LOD: 1800.33	**Sb**	<LOD	LOD: 1893.64	<LOD	LOD: 2076.23	**Sb**	<LOD	LOD: 1800.4	<LOD	LOD: 1904.08	**Sb**	<LOD	LOD: 1797.49	<LOD	LOD: 1919.75
Se	<LOD	LOD: 17.17	<LOD	LOD: 16.68	**Se**	<LOD	LOD: 17.85	<LOD	LOD: 18.41	**Se**	<LOD	LOD: 16.46	<LOD	LOD: 17.65	**Se**	<LOD	LOD: 17.13	<LOD	LOD: 17.46
Sn	<LOD	LOD: 1520.33	<LOD	LOD: 1413.89	**Sn**	<LOD	LOD: 1490.48	<LOD	LOD: 1628.31	**Sn**	<LOD	LOD: 1415.35	<LOD	LOD: 1491.44	**Sn**	<LOD	LOD: 1413.64	<LOD	LOD: 1510.62
Th	<LOD	LOD: 440.37	<LOD	LOD: 409.83	**Th**	<LOD	LOD: 436.69	<LOD	LOD: 471.97	**n/a**					**Th**	<LOD	LOD: 408.81	<LOD	LOD: 441.57
U	<LOD	LOD: 232.53	<LOD	LOD: 213.72	**U**	<LOD	LOD: 227.59	<LOD	LOD: 243.61	**n/a**					**U**	<LOD	LOD: 209.15	<LOD	LOD: 231.66
W	<LOD	LOD: 230.44	<LOD	LOD: 201.23	**W**	<LOD	LOD: 212.76	<LOD	LOD: 219.43	**W**	<LOD	LOD: 206.99	<LOD	LOD: 218.98	**W**	<LOD	LOD: 200.34	<LOD	LOD: 211.08

Table 62. Trench 15, sample location 1 Field pXRF control readings descriptive statistics (to 2 d.p.)

Trench 15, control 1 (ppm)	N	Range	Minimum	Maximum	Mean
Light Elements					
LE	2	15536.67	697653.29	713189.96	705421.63
Major					
Al	2	10905.44	51792.65	62698.09	57245.37
Fe	2	2515.70	27027.86	29543.56	28285.71
Si	2	11210.57	189066.25	200276.82	194671.54
Minor					
Ca	2	4217.42	2093.31	6310.73	4202.02
K	2	1170.69	4329.65	5500.34	4915.00
Ti	2	196.40	3829.49	4025.89	3927.69
Trace					
Mn	2	35.70	113.54	149.24	131.39
P	1	0.00	363.01	363.01	363.01
S	1	0.00	416.59	416.59	416.59
V	2	3.03	247.05	250.08	248.57
Zr	2	25.02	270.98	296.00	283.49
IUPAC Trace					
As	2	4.71	5.40	10.11	7.76
Cr	1	0.00	81.22	81.22	81.22
Mo	1	0.0	4.6	4.6	4.60
Nb	2	2.72	8.65	11.37	10.01
Ni	2	20.72	16.83	37.55	27.19
Pb	2	0.75	12.96	13.71	13.34
Rb	2	2.60	24.22	26.82	25.52
Sr	2	1.93	67.26	69.19	68.23
Ta	2	2.32	21.45	23.77	22.61
Y	2	1.12	16.46	17.58	17.02
Zn	2	7.97	39.26	47.23	43.25

Table 63. Trench 15, sample location 2 Field pXRF control readings descriptive statistics (to 2 d.p.)

Trench 15, control 2 (ppm)	N	Range	Minimum	Maximum	Mean	Std. Deviation
Light Elements						
LE	2	2458.08	696750.97	699209.05	697980.01	1738.13
Major						
Al	2	1661.70	44069.81	45731.51	44900.66	1175.00
Fe	2	3113.58	19192.93	22306.51	20749.72	2201.63
Si	2	7712.97	217166.56	224879.53	221023.05	5453.89
Minor						
Ca	2	1054.69	4653.37	5708.06	5180.72	745.78
K	2	595.38	4530.22	5125.60	4827.91	421.00
Ti	2	78.72	3579.95	3658.67	3619.31	55.66
Trace						
Mn	2	6.70	139.76	146.46	143.11	4.74
P	2	3.20	203.85	207.05	205.45	2.26
S	2	240.84	325.73	566.57	446.15	170.30
V	2	78.17	160.12	238.29	199.21	55.28
Zr	2	55.90	456.66	512.56	484.61	39.53
IUPAC Trace						
As	2	0.41	4.37	4.78	4.58	0.29
Cr	2	1.42	67.64	69.06	68.35	1.00
Mo	2	5.60	5.56	11.16	8.36	3.96
Nb	2	0.55	10.86	11.41	11.14	0.39
Pb	2	10.61	11.28	21.89	16.59	7.50
Rb	2	4.53	20.39	24.92	22.66	3.20
Sr	2	10.31	45.67	55.98	50.83	7.29
Ta	2	11.05	9.83	20.88	15.36	7.81
Y	2	0.53	16.02	16.55	16.29	0.38
Zn	2	0.39	25.78	26.17	25.98	0.28

Table 64. Trench 15, sample location 3 Field pXRF control readings descriptive statistics (to 2 d.p.)

Trench 15, control 3 (ppm)	N	Range	Minimum	Maximum	Mean	Std. Deviation
Light Elements						
LE	2	15764.51	708796.73	724561.24	716678.99	11147.19
Major						
Al	2	207.52	50120.60	50328.12	50224.36	146.74
Fe	2	6726.50	24735.34	31461.84	28098.59	4756.35
Si	2	8122.11	184987.26	193109.37	189048.32	5743.20
Minor						
Ca	2	616.56	4930.27	5546.83	5238.55	435.97
K	2	327.51	5016.87	5344.38	5180.63	231.59
Ti	2	958.30	3439.49	4397.79	3918.64	677.62
Trace						
Mn	2	36.44	136.39	172.83	154.61	25.77
P	2	58.77	311.41	370.18	340.80	41.56
S	2	46.36	260.92	307.28	284.10	32.78
V	2	15.70	223.02	238.72	230.87	11.10
Zr	2	70.63	252.45	323.08	287.77	49.94
IUPAC Trace						
As	2	0.12	7.74	7.86	7.80	0.09
Cr	2	2.41	62.59	65.00	63.80	1.70
Mo	1	0.00	6.74	6.74	6.74	
Nb	2	2.85	13.81	16.66	15.24	2.02
Ni	2	8.10	16.14	24.24	20.19	5.73
Pb	2	4.33	12.18	16.51	14.35	3.06
Rb	2	6.49	27.31	33.80	30.56	4.59
Sr	2	3.41	67.39	70.80	69.10	2.41
Ta	2	2.93	19.45	22.38	20.92	2.07
Th	1	0.00	11.77	11.77	11.77	
U	1	0.00	4.92	4.92	4.92	
Y	2	6.26	15.73	21.99	18.86	4.43
Zn	2	17.29	32.64	49.93	41.29	12.23

Table 65. Trench 15, sample location 4 Field pXRF control readings descriptive statistics (to 2 d.p.)

Trench 15, control 4 (ppm)	N	Range	Minimum	Maximum	Mean	Std. Deviation
Light Elements						
LE	2	14132.92	661054.41	675187.33	668120.87	9993.48
Major						
Al	2	91.82	49763.36	49855.18	49809.27	64.93
Fe	2	15087.65	15619.70	30707.35	23163.53	10668.58
Si	2	28042.98	232648.27	260691.25	246669.76	19829.38
Minor						
Ca	2	87.97	2478.78	2566.75	2522.77	62.20
K	2	397.43	5106.91	5504.34	5305.63	281.03
Ti	2	500.03	3147.85	3647.88	3397.87	353.58
Trace						
Mn	2	11.65	94.87	106.52	100.70	8.24
V	2	61.83	134.47	196.30	165.39	43.72
Zr	2	20.01	496.39	516.40	506.40	14.15
IUPAC Trace						
As	2	2.38	3.60	5.98	4.79	1.68
Cr	1	0.00	69.85	69.85	69.85	
Mo	1	0.00	4.86	4.86	4.86	
Nb	2	1.40	8.33	9.73	9.03	0.99
Ni	1	0.00	14.12	14.12	14.12	
Pb	2	1.42	9.83	11.25	10.54	1.00
Rb	2	1.22	20.97	22.19	21.58	0.86
S	1	0.00	84.29	84.29	84.29	
Sr	2	2.2	48.3	50.5	49.40	1.56
Ta	2	4.21	12.38	16.59	14.49	2.98
Y	2	4.66	14.14	18.80	16.47	3.30
Zn	2	4.60	22.69	27.29	24.99	3.25

Table 66. Trench 15 Field pXRF control readings descriptive statistics for all four reading locations considered as one set of data (to 2 d.p.)

Trench 15, all controls (ppm)	N	Range	Minimum	Maximum	Mean	Std. Deviation
Light Elements						
LE	8	63506.83	661054.41	724561.24	697050.37	20473.42
Major						
Al	8	18628.28	44069.81	62698.09	50544.92	5550.62
Fe	8	15842.14	15619.70	31461.84	25074.39	5708.12
Si	8	75703.99	184987.26	260691.25	212853.16	26005.15
Minor						
Ca	8	4217.42	2093.31	6310.73	4286.01	1660.09
K	8	1174.69	4329.65	5504.34	5057.29	430.05
Ti	8	1249.94	3147.85	4397.79	3715.88	377.86
Trace						
Mn	8	77.96	94.87	172.83	132.45	25.69
P	5	166.33	203.85	370.18	291.10	81.42
S	6	482.28	84.29	566.57	326.90	160.68
V	8	115.61	134.47	250.08	211.01	43.34
Zr	8	263.95	252.45	516.40	390.57	115.36
IUPAC Trace						
As	8	6.51	3.60	10.11	6.23	2.18
Cr	6	19	63	81	69.23	6.46
Mo	5	7	5	11	6.58	2.69
Nb	8	8.33	8.33	16.66	11.35	2.77
Ni	5	23	14	38	21.78	9.61
Pb	8	12.06	9.83	21.89	13.70	3.87
Rb	8	13.41	20.39	33.80	25.08	4.34
Sr	8	25.13	45.67	70.80	59.39	10.38
Ta	8	13.94	9.83	23.77	18.34	4.99
Th	1	0	12	12	11.77	
U	1	0	5	5	4.92	
Y	8	7.85	14.14	21.99	17.16	2.38
Zn	8	27.24	22.69	49.93	33.87	10.42

Table 67. Descriptive statistics for all repeat readings across all trenches at Flixton using field pXRF (to 2 d.p.)

All trenches, all controls (ppm)	N	Range	Minimum	Maximum	Mean	Std. Deviation
LE	15	188946.87	661054.41	850001.28	746479.63	61832.21
Ag	1	0	12	12	12.44	
Al	15	43985.30	18712.79	62698.09	40471.00	12876.65
As	15	6.51	3.60	10.11	7.08	2.03
Bi	1	0	7	7	7.10	
Ca	15	16382.35	2093.31	18475.66	7255.13	4482.70
Cd	2	1	18	19	18.70	1.05
Cl	0					
Co	0					
Cr	10	37	45	81	62.68	11.86
Cu	1	0	11	11	10.58	
Fe	15	15842.14	15619.70	31461.84	22661.25	5210.27
Hg	0					
K	15	2996.42	2507.92	5504.34	4248.47	1063.15
Mg	0					
Mn	15	110.12	94.87	204.99	138.65	29.71
Mo	10	8	3	11	6.42	2.89
Nb	15	11.86	4.80	16.66	9.98	3.50
Ni	6	25	12	38	20.21	9.42
P	12	458	131	589	305.13	135.17
Pb	15	13.35	8.54	21.89	12.62	3.39
Rb	15	19.46	14.34	33.80	21.54	5.21
S	13	2178	84	2263	717.04	563.48
Sb	0					
Se	0					
Si	15	179617.73	81073.52	260691.25	173999.32	53017.46
Sn	0					
Sr	15	25.13	45.67	70.80	54.51	9.29
Ta	15	13.94	9.83	23.77	16.24	4.69
Th	3	11	11	22	14.96	6.29
Ti	15	2242.10	2155.69	4397.79	3067.79	769.42
U	2	0	5	5	4.97	0.07
V	14	139	111	250	184.24	47.64
W	0					
Y	15	8.76	13.33	22.09	16.69	2.65
Zn	15	28.80	21.13	49.93	30.84	9.16
Zr	15	263.95	252.45	516.40	409.50	95.81

Star Carr

pXRF took place in the environs of the Western Structure at Star Carr and while the results are not presented in this thesis, the accuracy and precision of the readings at this site are informative. Readings were taken across three days and the position in the southwest quadrant of grid square E31 was repeatedly analysed. In addition to the repeat field readings, two controls were also analysed at the start and end of every session.

Elemental classifications for repeat field readings

A summary of the repeat field pXRF reading results is provided in Table 68Table 68. Star Carr had more elements in the major elements category, as measured by pXRF, than Flixton's controls. The data and descriptive statistics are provided in Table 69 and Table 70 respectively.

Table 68. Summary of control field pXRF results for Star Carr's western structure area

Category	**ppm**	**Star Carr Western Structure Area**
Major	>10000	Si Al Fe Ca K S
Minor	1000 - 10000	Ti
Trace	100 - 1000	P Zr V Mn Sr
IUPAC Trace	<100	Rb Zn Cr Ta Y Pb Ni Nb As U Th Mo
<LOD		Ag Bi Cd Cl Co Cu Hg Mg Sb Se Sn W

Table 69. Data for the field pXRF control repeats at Star Carr

Element / Error (+/-)	**28/04/2015 #5 Reading / error estimation (ppm)**	**28/04/2015 #40 Reading / error estimation (ppm)**	**29/04/2015 #5 Reading / error estimation (ppm)**	**29/04/2015 #62 Reading / error estimation (ppm)**	**07/05/2015 #5 Reading / error estimation (ppm)**	**07/05/2015 #27 Reading / error estimation (ppm)**	**07/05/2015 #30 Reading / error estimation (ppm)**
Ag	<LOD	<LOD	<LOD	<LOD	<LOD	<LOD	<LOD
Ag +/-	697.21	726.96	661.32	685.28	656.31	680.89	684.69
Al	71616.78	73745.06	56280.71	80355.64	77815.26	81806.7	83529.16
Al +/-	689.54	696.15	616.42	661.6	656.36	669.93	698.52
As	7.86	7.26	8.37	8.37	9.23	7.91	7.51
As +/-	1.2	1.26	1.05	1.18	1.06	1.08	1.08
Bi	<LOD	<LOD	<LOD	<LOD	<LOD	<LOD	<LOD

Element / Error (+/-)	28/04/2015 #5 Reading / error estimation (ppm)	28/04/2015 #40 Reading / error estimation (ppm)	29/04/2015 #5 Reading / error estimation (ppm)	29/04/2015 #62 Reading / error estimation (ppm)	07/05/2015 #5 Reading / error estimation (ppm)	07/05/2015 #27 Reading / error estimation (ppm)	07/05/2015 #30 Reading / error estimation (ppm)
Bi	278.88	289.49	265.53	270	265.33	270.6	273.38
+/-							
Ca	13707.47	9191.01	4845.3	16314.49	1888.83	1648.09	4056.58
Ca	60.19	50.9	36.48	66.52	34.48	34.72	37.4
+/-							
Cd	<LOD	<LOD	<LOD	<LOD	<LOD	<LOD	<LOD
Cd	844.24	879.96	800.68	829.79	793.45	821.01	824.86
+/-							
Cl	<LOD	<LOD	<LOD	<LOD	<LOD	<LOD	<LOD
Cl	1203.48	1233.28	1329.8	1062.34	1182.68	1320.98	1275.63
+/-							
Co	<LOD	<LOD	<LOD	<LOD	<LOD	<LOD	<LOD
Co	311.18	321.24	267.97	349.92	272.34	266.43	268.76
+/-							
Cr	51.67	68.63	<LOD	67.67	77.77	71.67	76.72
Cr	15.1	15.9	133.09	15.35	14.7	14.83	14.98
+/-							
Cu	<LOD	<LOD	<LOD	<LOD	<LOD	<LOD	<LOD
Cu	60.17	62.21	53.3	58.23	54.53	55.75	56.86
+/-							
Fe	34093.09	34764.35	28327.24	43111.43	29708.42	27438.05	27942.16
Fe	137.35	142.04	116.57	156.82	116.89	113.66	115.36
+/-							
Hg	<LOD	<LOD	<LOD	<LOD	<LOD	<LOD	<LOD
Hg	126.1	128.3	107.99	124.19	116.27	119.79	118.47
+/-							
K	13685.9	14089.44	11484.95	14035.21	15420.9	15307.71	14637.24
K +/-	63.82	67.29	56.52	64.18	66.61	67.94	65.38
Mg	<LOD	<LOD	<LOD	<LOD	<LOD	<LOD	<LOD
Mg	11210.8	11848.94	12967.41	9897.63	10511.55	11641.74	11403.7
+/-							
Mn	216.48	258.95	154.7	176	161.81	144.54	163.51

Element / Error (+/-)	28/04/2015 #5 Reading / error estimation (ppm)	28/04/2015 #40 Reading / error estimation (ppm)	29/04/2015 #5 Reading / error estimation (ppm)	29/04/2015 #62 Reading / error estimation (ppm)	07/05/2015 #5 Reading / error estimation (ppm)	07/05/2015 #27 Reading / error estimation (ppm)	07/05/2015 #30 Reading / error estimation (ppm)
Mn	13.83	14.97	12.02	13.49	12.45	12.36	12.69
+/-							
Mo	<LOD	7.03	3.45	<LOD	<LOD	<LOD	<LOD
Mo	96.36	1.04	0.93	94.98	90.72	93.79	94.34
+/-							
Nb	22.92	18.74	13.63	15.41	15.71	16.89	15.24
Nb	1.13	1.14	1.01	1.1	1.02	1.04	1.04
+/-							
Ni	23.17	21.13	<LOD	22.13	23.7	20	23.63
Ni	3.9	4.02	51.75	3.97	3.66	3.65	3.71
+/-							
P	486.87	585.58	693.22	869.35	431.33	572.64	666.04
P +/-	43.88	46.54	40.83	47.41	40.15	40.92	43.17
Pb	23.39	25.4	16.77	19.07	14.97	17.77	17.47
Pb	1.62	1.71	1.4	1.59	1.39	1.45	1.45
+/-							
Rb	87	78.12	62.13	81.96	74.16	76.68	73.72
Rb	1.19	1.17	0.96	1.17	1.04	1.07	1.06
+/-							
S	11020.89	7165.39	1951.13	19021.01	877.62	1421.49	3430.55
S +/-	61.86	51.9	30.22	82.45	27.67	30.03	37.18
Sb	<LOD	<LOD	<LOD	<LOD	<LOD	<LOD	<LOD
Sb	1801.65	1876.09	1700.95	1787.46	1691.72	1747.28	1768.04
+/-							
Se	<LOD	<LOD	<LOD	<LOD	<LOD	<LOD	<LOD
Se	17.26	18.3	15.24	16.86	15.59	16.38	16.79
+/-							
Si	212771.85	240558.24	213350.24	252881.26	255339	235999.97	230119.72
Si	712.59	783.44	703.2	751.35	753.43	732.97	724.27
+/-							
Sn	<LOD	<LOD	<LOD	<LOD	<LOD	<LOD	<LOD

Element / Error (+/-)	28/04/2015 #5 Reading / error estimation (ppm)	28/04/2015 #40 Reading / error estimation (ppm)	29/04/2015 #5 Reading / error estimation (ppm)	29/04/2015 #62 Reading / error estimation (ppm)	07/05/2015 #5 Reading / error estimation (ppm)	07/05/2015 #27 Reading / error estimation (ppm)	07/05/2015 #30 Reading / error estimation (ppm)
Sn	1409.86	1475.68	1334.75	1396.14	1325.01	1375.37	1383.3
+/-							
Sr	100.64	93.88	72.24	92.75	79.41	77.09	81.08
Sr	1.18	1.18	0.96	1.15	1	1	1.03
+/-							
Ta	42.42	41.36	31.47	41.75	34.75	32.43	36.41
Ta	3.94	4.07	3.39	4	3.56	3.56	3.62
+/-							
Th	<LOD	9.83	<LOD	<LOD	<LOD	<LOD	<LOD
Th	416.75	3.13	399.45	403.04	396.57	405.68	409.96
+/-							
Ti	5766.75	4919.47	3313.24	5509.85	4696.74	4741.1	4627.43
Ti	108.12	106.78	84.89	107.38	96.56	98.55	99.18
+/-							
U	5.22	6.89	<LOD	<LOD	<LOD	<LOD	6.06
U +/-	1.61	1.68	219.09	229.88	222.23	225.91	1.52
V	335.79	304.22	164.86	315.93	253.92	237.79	233.5
V +/-	39.16	39.47	32.92	38.73	36.05	36.64	36.38
W	<LOD	<LOD	<LOD	<LOD	<LOD	<LOD	<LOD
W	212.28	222.18	195.24	210.1	200.15	211.88	203.26
+/-							
Y	26.37	23.49	16.74	22.55	20.74	19.23	20.25
Y +/-	0.98	0.99	0.83	0.97	0.87	0.88	0.88
Zn	70.08	70.53	45.34	62.43	69.09	63.37	60.96
Zn	2.54	2.63	2.04	2.47	2.38	2.35	2.32
+/-							
Zr	374.04	393.7	290.24	391.78	304.65	317.44	359.43
Zr	2.25	2.37	1.86	2.29	1.89	1.96	2.1
+/-							
LE	635463.38	613552.3	678874.04	566583.98	612681.97	629961.44	629815.64
LE	1134.97	1180.79	1023.33	1176.19	1082.68	1088.31	1099.1
+/-							

Table 70. Descriptive statistics for the control field pXRF repeats at Star Carr (2 d.p.)

Star Carr Western Structure (ppm)	N	Range	Minimum	Maximum	Mean	Std. Deviation
Light Elements						
LE	7	112290.06	566583.98	678874.04	623847.54	33530.13
Major						
Al	7	27248.45	56280.71	83529.16	75021.33	9301.58
Ca	7	14666.40	1648.09	16314.49	7378.82	5825.51
Fe	7	15673.38	27438.05	43111.43	32197.82	5645.51
K	7	3935.95	11484.95	15420.90	14094.48	1323.26
S	7	18143.39	877.62	19021.01	6412.58	6647.30
Si	7	42567.15	212771.85	255339.00	234431.47	17076.62
Minor						
Ti	7	2453.51	3313.24	5766.75	4796.37	786.03
Trace						
Mn	7	114.41	144.54	258.95	182.28	40.91
P	7	438.02	431.33	869.35	615.00	145.05
Sr	7	28.40	72.24	100.64	85.30	10.45
V	7	170.93	164.86	335.79	263.72	59.18
Zr	7	103.46	290.24	393.70	347.33	42.74
IUPAC Trace						
As	7	1.97	7.26	9.23	8.07	0.65
Cr	6	26.10	51.67	77.77	69.02	9.44
Mo	2	3.58	3.45	7.03	5.24	2.53
Nb	7	9.29	13.63	22.92	16.93	3.07
Ni	6	3.70	20.00	23.70	22.29	1.50
Pb	7	10.43	14.97	25.40	19.26	3.76
Rb	7	24.87	62.13	87.00	76.25	7.77
Ta	7	10.95	31.47	42.42	37.23	4.61
Th	1	0.00	9.83	9.83	9.83	
U	3	1.67	5.22	6.89	6.06	0.84
Y	7	9.63	16.74	26.37	21.34	3.12
Zn	7	25.19	45.34	70.53	63.11	8.76

Data tables for readings of control samples 2710a and 2711a in the field

In addition to the field readings, control readings were taken. They were taken on NIST soil standards in pXRF pots with Prolene windows. They were read whilst out in the field before a session, after a break in the session, and at the end of a session where possible. These will not be affected by field soil conditions, as those in the ground may be, but will be affected by systematic variations of the machine, say temperature of the internal components or any contamination of the Prolene window. Table 71 provides the details of the readings. Table 72 presents the control repeat data, highlighted if they are within +/- 20 % of the mean value (green), greater than that (red), or lower than that (blue). Table 73 shows the percent deviation of readings from the expected value of control samples 2710a and 2711a in the field. Table 74 and Table 75 show the descriptive statistics for the results for each control.

Table 71. Details of standard control repeats taken during the field season at Star Carr

NIST 2711a	Reading	Time	Mode	Elapsed Time 1	Elapsed Time 2	Elapsed Time Total
	28/04 /2015 #3	10:38:48	Geochem	59.2	59.68	118.88
	28/04 /2015 #38	13:25:13	Geochem	59.19	59.67	118.86
	29/04 /2015 #4	10:08:47	Geochem	59.19	59.68	118.88
	29/04 /2015 #65	16:26:35	Geochem	59.2	59.68	118.88
	07/05 /2015 #4	11:58:49	Geochem	59.19	59.67	118.86
	07/05 /2015 #32	16:06:23	Geochem	59.27	59.72	118.98

NIST 2710a	Reading	Time	Mode	Elapsed Time 1	Elapsed Time 2	Elapsed Time Total
	28/04/2015 #3	10:42:44	Geochem	59.2	59.63	118.83
	28/04/2015 #38	13:28:01	Geochem	59.18	59.6	118.78
	29/04/2015 #4	10:11:49	Geochem	59.18	59.61	118.79
	29/04/2015 #65	16:29:18	Geochem	59.23	59.63	118.86
	07/05/2015 #4	12:01:35	Geochem	59.19	59.62	118.81
	07/05/2015 #32	16:03:41	Geochem	59.19	59.62	118.81

Table 72. Standard control repeat results, taken while in the field at Star Carr

NIST 2711a	Cert. Value	-20%	20%	28/04/2015 #3 Reading (ppm)	28/04/2015 #38 Reading (ppm)	29/04/2015 #4 Reading (ppm)	29/04/2015 #65 Reading (ppm)	07/05/2015 #4 Reading (ppm)	07/05/2015 #32 Reading (ppm)	NIST 2710a	Cert. Value	-20%	20%	28/04/2015 #3 Reading (ppm)	28/04/2015 #38 Reading (ppm)	29/04/2015 #4 Reading (ppm)	29/04/2015 #65 Reading (ppm)	07/05/2015 #4 Reading (ppm)	07/05/2015 #32 Reading (ppm)
Ag	**6**	4.8	7.2	<LOD	<LOD	<LOD	<LOD	<LOD	<LOD	Ag	**40**	32	48	28.2	33.65	37.34	32.32	41.86	36.94
Ag +/-				739.9	729.84	736.56	738.62	732.58	779.82	Ag +/-				6.63	6.39	6.47	6.82	6.48	6.58
Al	**67200**	53760	80640	63241.68	63882.11	60930.83	59970.79	62330.84	55539.14	Al	**59500**	47600	71400	55878.33	62141.66	62638.25	56993.91	61507.8	57541.12
Al +/-				724.92	695.86	693.18	682.79	688.31	713.6	Al +/-				700.44	683.32	688.56	689.94	684.81	676.95
As	**107**	85.6	128.4	84.73	74.23	82.4	64.58	85.7	80.23	As	**1540**	1232	1848	1465.82	1429.19	1400.84	1467.73	1424.78	1503
As +/-				6.96	6.94	6.92	6.93	6.93	7.43	As +/-				16.16	15.56	15.64	16.52	15.75	16.29
Bi	**Not**			<LOD	<LOD	<LOD	<LOD	<LOD	<LOD	Bi	**Not**			<LOD	<LOD	<LOD	<LOD	<LOD	<LOD
Bi +/-				337.47	331.74	333.07	333.72	332.41	359.96	Bi +/-				347.75	338.9	342.35	356.01	347.69	343.42
Ca	**24200**	19360	29040	25452.03	25562.32	25569.66	24422.35	25878.31	23948.67	Ca	**9640**	7712	11568	6370.06	6350.33	6625.46	6535.23	6735.64	6121.56
Ca +/-				98.6	97.76	99.15	96.05	99.38	100.8	Ca +/-				47.4	47.96	50.34	49.61	50.45	46.63
Cd	**54.1**	43.28	64.92	47.71	55	46.4	45.1	54.37	52.36	Cd	**12.3**	9.84	14.76	<LOD	<LOD	<LOD	<LOD	<LOD	<LOD
Cd +/-				6.78	6.73	6.78	6.79	6.73	7.3	Cd +/-				739.83	732.4	741.02	764.27	743.54	732.17
Cl	**Not**			<LOD	<LOD	<LOD	<LOD	<LOD	<LOD	Cl	**Not**			<LOD	<LOD	<LOD	<LOD	<LOD	<LOD
Cl +/-				1115.27	1108.63	1133.73	1165.51	1128.19	1316	Cl +/-				1264.21	1174.36	1171.4	1299.29	1208.8	1271.16
Co	**9.89**	7.912	11.868	<LOD	<LOD	<LOD	<LOD	<LOD	<LOD	Co	**5.99**	4.792	7.188	<LOD	<LOD	<LOD	<LOD	<LOD	<LOD
Co +/-				333.71	334.08	331.35	333.97	332.79	355.57	Co +/-				388.98	375.36	381.35	396.7	383.29	386.47
Cr	**52.3**	41.84	62.76	<LOD	<LOD	<LOD	<LOD	<LOD	<LOD	Cr	**23**	18.4	27.6	<LOD	<LOD	<LOD	<LOD	<LOD	<LOD
Cr +/-				160.17	155.22	158.25	152.59	157.42	174.61	Cr +/-				148.78	148.07	146.56	152.99	149.66	153.05

Cu	**140**	112	168	154.89	152.5	158.01	154.05	143.27	138.93
Cu +/-				6.44	6.31	6.5	6.38	6.4	6.8
Fe	**28200**	22560	33840	34771.86	35880.67	35162.6	35289.92	35428.09	36307.61
Fe +/-				150.08	152.1	151.08	152.9	150.8	166.52
Hg	**7.42**	5.936	8.904	12.85	13.23	12.09	13.3	10.53	13.02
Hg +/-				2.38	2.41	2.36	2.43	2.33	2.55
K	**25300**	20240	30360	22909.65	23189.88	22783.91	21805.03	23118.65	21584.94
K +/-				95.08	94.72	95.09	92.06	95.38	97.47
Mg	**10700**	8560	12840	<LOD	<LOD	<LOD	<LOD	<LOD	<LOD
Mg				11124.91	11003.23	11337.63	11722.53	11109.4	13601.73
Mn	**675**	540	810	710.93	724.19	725.46	706.14	719.34	726.76
Mn				21.75	21.64	21.7	21.44	21.57	22.87
Mo	**Not**			5.66	8.12	5.74	7.57	5.58	10.58
Mo				1.12	1.1	1.09	1.11	1.09	1.18
Nb	**Not**			24.14	27.37	26.87	27.74	25.77	28.03
Nb				1.28	1.29	1.29	1.3	1.28	1.38
Ni	**21.7**	17.36	26.04	23.79	24.63	14.77	16.27	16.83	14.31
Ni +/-				4.39	4.38	4.19	4.25	4.23	4.48
P	**842**	673.6	1010.4	656.84	697.24	664.24	696.11	776.5	572.64
P +/-				53.23	51.94	51.46	50.93	51.68	52.59
Pb	**1400**	1120	1680	1552.09	1575.73	1551.51	1565.1	1569.54	1615.05
Pb +/-				10.5	10.49	10.44	10.56	10.46	11.42

Cu	**3420**	2736	4104	3858.33	3683.73	3780.48	3835.16	3718.61	3936.5
Cu +/-				26.84	25.47	25.89	27.32	25.85	27.03
Fe	**43200**	34560	51840	52341.44	52398.48	52361.94	53325.36	52068.23	54405.73
Fe +/-				213.45	203.96	203.8	219.73	205.21	218.31
Hg	**9.88**	7.904	11.856	28.97	20.77	20.67	34.2	29.26	20.6
Hg +/-				5.01	4.74	4.88	5.17	4.83	5.01
K	**21700**	17360	26040	20555.74	21585.42	22714.04	21235.97	22182.17	20644.31
K +/-				93.08	92.98	97.51	96.73	96.72	92.5
Mg	**7340**	5872	8808	<LOD	<LOD	<LOD	<LOD	<LOD	<LOD
Mg				13041.52	11558.47	11373.83	13404.62	11797.44	12994.94
Mn	**2140**	1712	2568	2176.82	2115.35	2120.91	2138.13	2114.3	2265.81
Mn				33.39	32.58	32.92	33.87	32.97	33.79
Mo	**Not**			14.91	10.21	9.49	16.23	10.55	12.82
Mo				1.25	1.17	1.18	1.25	1.19	1.21
Nb	**Not**			22.67	18.93	20.29	22.86	16.99	22.15
Nb				1.4	1.34	1.36	1.43	1.35	1.39
Ni	**8**	6.4	9.6	<LOD	<LOD	<LOD	<LOD	<LOD	<LOD
Ni +/-				57.29	55.64	56.78	58.84	56.54	55.72
P	**1050**	840	1260	904.94	1041.82	1031.19	1027.13	1098.11	967.78
P +/-				49.99	50.59	51.21	51.44	51.16	48.94
Pb	**5520**	4416	6624	5823.25	5656.1	5680.52	5827.53	5689.5	5934.69
Pb +/-				27.37	25.62	25.72	27.76	26	27.55

Rb	**120**	96	144	118.6	120.21	115.68	116.84	118.39	121.87
Rb +/-				1.54	1.54	1.52	1.53	1.53	1.66
S	**Not present**			879.56	946.06	814.45	886.04	976.91	959.43
S +/-				31.77	31.13	30.5	30.49	31.78	32.88
Sb	**23.8**	19.04	28.56	40.35	64.91	52.19	<LOD	<LOD	<LOD
Sb +/-				12.25	12.15	12.18	1898.03	1878.86	2006.84
Se	**2**	1.6	2.4	<LOD	2.92	<LOD	<LOD	<LOD	<LOD
Se +/-				29.72	0.9	28.07	28.93	29.32	31.15
Si	**31400**	25120	37680	245266.8	247765.7	244020.4	235185.4	245231.7	218733.8
Si +/-				837.56	827.17	829.92	814.59	824.76	831.7
Sn	**Not present**			<LOD	<LOD	<LOD	<LOD	<LOD	<LOD
Sn +/-				1483.61	1465.15	1471.58	1478.12	1468.26	1564.81
Sr	**242**	193.6	290.4	233	239.36	235.17	233.29	234.6	238.17
Sr +/-				1.97	1.99	1.97	1.98	1.96	2.12
Ta	**1**	0.8	1.2	26.66	<LOD	34.49	23.24	41.31	44.82
Ta +/-				6.64	320.33	6.73	6.63	6.82	7.34
Th	**15**	12	18	23.75	19.74	16.47	16.22	22.48	36.3
Th +/-				3.54	3.5	3.48	3.49	3.51	3.82
Ti	**3170**	2536	3804	3294.2	3203.07	3424.79	3297.49	3156.9	3351.94

Rb	**117**	93.6	140.4	108.5	106.09	108.04	109.43	107.53	110.84
Rb +/-				1.7	1.64	1.67	1.75	1.67	1.72
S	**Not present**			16235.94	17643.83	17933.82	16803.83	18222.29	16394.66
S +/-				85.87	87.4	88.58	88.51	90.96	84.93
Sb	**52.5**	42	63	42.81	61.33	56.26	<LOD	54.06	41.02
Sb +/-				13.59	13.16	13.25	1618.98	13.36	13.59
Se	**1**	0.8	1.2	7.99	4.87	<LOD	<LOD	<LOD	5.26
Se +/-				1.67	1.59	42.2	43.94	42.36	1.66
Si	**31100**	24880	37320	231429.8	254099.2	261126.0	237736.4	253469.4	233365.6
Si +/-				863.29	872.09	889.68	884.14	881.4	854.69
Sn	**Not present**			<LOD	<LOD	<LOD	<LOD	<LOD	<LOD
Sn +/-				1233.96	1216.02	1223.56	1264.78	1233.45	1213.09
Sr	**255**	204	306	251.39	248.35	245.34	248.47	243.28	251.27
Sr +/-				2.27	2.2	2.19	2.31	2.2	2.27
Ta	**0.9**	0.72	1.08	46.05	72.65	<LOD	72.01	63.27	<LOD
Ta +/-				14.73	14.48	591.86	15.29	14.55	602.36
Th	**18.1**	14.48	21.72	31.81	27.7	24.33	36.86	34.03	30.52
Th +/-				3.91	3.79	3.79	4.03	3.86	3.89
Ti	**3110**	2488	3732	2927.58	2910.96	2873.08	3051.71	2946.42	2849.11

Ti +/-				99.72	98.84	99.85	99.67	96.95	104.75
U	**3.01**	2.408	3.612	<LOD	<LOD	<LOD	7.6	<LOD	8.89
U +/-				278.3	277.91	278.74	2.07	277.72	2.23
V	**80.7**	64.56	96.84	264.42	323.84	366.97	278.29	306.14	323.56
V +/-				40.32	40.53	41.4	40	40.33	42.86
W	**Not present**			<LOD	<LOD	<LOD	<LOD	<LOD	<LOD
W +/-				336.45	340.45	331.77	344.91	335.82	360.57
Y	**Not present**			37.82	36.27	37.76	35.43	38.75	38.18
Y +/-				1.47	1.46	1.46	1.45	1.46	1.56
Zn	**414**	331.2	496.8	434.78	441.28	427.9	423.84	444.19	456.54
Zn +/-				6.28	6.28	6.2	6.2	6.28	6.81
Zr	**Not present**			299.52	295.48	302.22	314.74	304.13	301.64
Zr +/-				2.28	2.24	2.27	2.33	2.28	2.44
LE				599431.6	594673.8	602416.9	614397.5	598961.0	634752.5
LE +/-				1274.13	1259.86	1258.74	1250.04	1253.88	1302.22

Ti +/-				92.29	92.49	92.08	96.55	92.75	91.76
U	**9.11**	7.288	10.932	8.99	<LOD	11.56	10.84	9.81	9.6
U +/-				2.48	248.73	2.44	2.58	2.45	2.49
V	**82**	65.6	98.4	293.11	261.64	317.47	322.45	186.09	280.56
V +/-				37.72	37.21	38.33	39.38	37.01	37.21
W	**190**	152	228	184.93	171.78	211.67	177.73	151.62	211.3
W +/-				17.69	17.02	17.41	18.08	16.99	18.02
Y	**Not present**			21.95	26.61	22.49	18.11	26.34	21.34
Y +/-				2.17	2.12	2.12	2.21	2.14	2.18
Zn	**4180**	3344	5016	4308.61	4167.64	4181.86	4292.64	4153.55	4503.78
Zn +/-				24.08	22.74	22.89	24.43	22.93	24.75
Zr	**200**	160	240	218.63	216.92	211.76	207.51	206.74	209.74
Zr +/-				2.24	2.16	2.15	2.24	2.16	2.2
LE				594412.4	563494.8	554234.8	584420.2	563487.7	588302.3
LE +/-				1400.85	1384.09	1398.61	1432.53	1399.03	1395.8

Table 73. Percent deviation of readings from the expected value of control samples 2710a and 2711a in the field at Star Carr (green: less than +/- 5 % out; light blue 5-20 % low, dark blue more than 20 % below expected values; light red 5-20 % high, dark red greater than 20 % high)

Element	NIST 2711a Cert. Value	Category	28/04/2015 #2 (% from certified value)	28/04/2015 #37 (% from certified value)	29/04/2015 #3 (% from certified value)	29/04/2015 #64 (% from certified value)	07/05/2015 #3 (% from certified value)	07/05/2015 #33 (% from certified value)	Range (ppm)	Standard Deviation
Ag	**6**	IUPAC	<LOD	<LOD	<LOD	<LOD	<LOD	<LOD		
Al	**672**	maior	-5.89	-4.94	-9.33	-10.76	-7.25	-17.35	8342	3032.6
As	**107**	trace	-20.81	-30.63	-22.99	-39.64	-19.91	-25.02	21.1	8.01
Bi	**N/A**	minor	<LOD	<LOD	<LOD	<LOD	<LOD	<LOD		
Ca	**242**	maior	5.17	5.63	5.66	0.92	6.94	-1.04	1929	766.77
Cd	**54.1**	IUPAC	-11.81	1.66	-14.23	-16.64	0.50	-3.22	9.90	4.28
Cl	**N/A**	minor	<LOD	<LOD	<LOD	<LOD	<LOD	<LOD		
Co	**9.89**	IUPAC	<LOD	<LOD	<LOD	<LOD	<LOD	<LOD		
Cr	**52.3**	IUPAC	<LOD	<LOD	<LOD	<LOD	<LOD	<LOD		
Cu	**140**	trace	10.64	8.93	12.86	10.04	2.34	-0.76	19.0	7.46
Fe	**282**	maior	23.30	27.24	24.69	25.14	25.63	28.75	1535	545.21
Hg	**7.42**	IUPAC	73.18	78.30	62.94	79.25	41.91	75.47	2.77	1.06
K	**253**	maior	-9.45	-8.34	-9.95	-13.81	-8.62	-14.68	1604	693.08
Mg	**107**	maior	<LOD	<LOD	<LOD	<LOD	<LOD	<LOD		
Mn	**675**	trace	5.32	7.29	7.48	4.61	6.57	7.67	20.6	8.48
Mo	**N/A**	trace	5.66	8.12	5.74	7.57	5.58	10.58	5.00	1.98

Element	NIST 2710a Cert. Value (ppm)	Category	28/04/2015 #3 (% from certified value)	28/04/2015 #38 (% from certified value)	29/04/2015 #4 (% from certified value)	29/04/2015 #65 (% from certified value)	07/05/2015 #4 (% from certified value)	07/05/2015 #32 (% from certified value)	Range (ppm)	Standard Deviation
Ag	**40**	IUPAC	-29.50	-15.88	-6.65	-19.20	4.65	-7.65	13.6	4.72
Al	**595**	maior	-6.09	4.44	5.27	-4.21	3.37	-3.29	6759	2969.0
As	**154**	minor	-4.82	-7.20	-9.04	-4.69	-7.48	-2.40	102.	37.01
Bi	**N/A**	trace	<LOD	<LOD	<LOD	<LOD	<LOD	<LOD		
Ca	**964**	minor	-33.92	-34.13	-31.27	-32.21	-30.13	-36.50	614.	220.72
Cd	**12.3**	IUPAC	<LOD	<LOD	<LOD	<LOD	<LOD	<LOD		
Cl	**N/A**	trace	<LOD	<LOD	<LOD	<LOD	<LOD	<LOD		
Co	**5.99**	IUPAC	<LOD	<LOD	<LOD	<LOD	<LOD	<LOD		
Cr	**23**	IUPAC	<LOD	<LOD	<LOD	<LOD	<LOD	<LOD		
Cu	**342**	minor	12.82	7.71	10.54	12.14	8.73	15.10	252.	93.56
Fe	**432**	maior	21.16	21.29	21.21	23.44	20.53	25.94	2337	888.99
Hg	**9.88**	IUPAC	193.22	110.22	109.21	246.15	196.15	108.50	13.6	5.85
K	**217**	maior	-5.27	-0.53	4.67	-2.14	2.22	-4.86	2158	853.11
Mg	**734**	minor	<LOD	<LOD	<LOD	<LOD	<LOD	<LOD		
Mn	**214**	minor	1.72	-1.15	-0.89	-0.09	-1.20	5.88	151.	59.04
Mo	**N/A**	trace	14.91	10.21	9.49	16.23	10.55	12.82	6.74	2.75

Nb	**N/A**	trace	24.14	27.37	26.87	27.74	25.77	28.03	3.89	1.47	**Nb**	**N/A**	trace	22.67	18.93	20.29	22.86	16.99	22.15	5.87	2.35
Ni	**21.7**	IUPAC	9.63	13.50	-31.94	-25.02	-22.44	-34.06	10.3	4.58	**Ni**	**8**	IUPAC	<LOD	<LOD	<LOD	<LOD	<LOD	<LOD		
P	**842**	trace	-21.99	-17.19	-21.11	-17.33	-7.78	-31.99	203.	66.54	**P**	**105**	minor	-13.82	-0.78	-1.79	-2.18	4.58	-7.83	193.	66.81
Pb	**140**	minor	10.86	12.55	10.82	11.79	12.11	15.36	63.5	23.39	**Pb**	**552**	minor	5.49	2.47	2.91	5.57	3.07	7.51	278.	110.20
Rb	**120**	trace	-1.17	0.18	-3.60	-2.63	-1.34	1.56	6.19	2.23	**Rb**	**117**	trace	-7.26	-9.32	-7.66	-6.47	-8.09	-5.26	4.75	1.63
S	**N/A**	minor	879.56	946.06	814.45	886.04	976.91	959.43	162.	61.40	**S**	**N/A**	trace	16235.9	17643.8	17933.8	16803.8	18222.2	16394.6	1986	838.49
Sb	**23.8**	IUPAC	69.54	172.73	119.29	<LOD	<LOD	<LOD	24.5	12.28	**Sb**	**52.5**	IUPAC	-18.46	16.82	7.16	<LOD	2.97	-21.87	20.3	8.81
Se	**2**	IUPAC	<LOD	46	<LOD	<LOD	<LOD	<LOD	0		**Se**	**1**	IUPAC	699.00	387.00	<LOD	<LOD	<LOD	426.00	3.12	1.70
Si	**314**	maior	-21.89	-21.09	-22.29	-25.10	-21.90	-30.34	2903	10996.	**Si**	**311**	maior	-25.59	-18.30	-16.04	-23.56	-18.50	-24.96	2969	12542.
Sn	**N/A**	minor	<LOD	<LOD	<LOD	<LOD	<LOD	<LOD			**Sn**	**N/A**	trace	<LOD	<LOD	<LOD	<LOD	<LOD	<LOD		
Sr	**242**	trace	-3.72	-1.09	-2.82	-3.60	-3.06	-1.58	6.36	2.61	**Sr**	**255**	trace	-1.42	-2.61	-3.79	-2.56	-4.60	-1.46	8.11	3.22
Ta	**1**	IUPAC	2566.00	<LOD	3349.00	2224.00	4031.00	4382.00	21.5	9.22	**Ta**	**0.9**	IUPAC	5016.67	7972.22	<LOD	7901.11	6930.00	<LOD	26.6	12.39
Th	**15**	IUPAC	58.33	31.60	9.80	8.13	49.87	142.00	20.0	7.42	**Th**	**18.1**	IUPAC	75.75	53.04	34.42	103.65	88.01	68.62	12.5	4.47
Ti	**317**	minor	3.92	1.04	8.04	4.02	-0.41	5.74	267.	97.29	**Ti**	**311**	minor	-5.87	-6.40	-7.62	-1.87	-5.26	-8.39	202.	70.94
U	**3.01**	IUPAC	<LOD	<LOD	<LOD	152.49	<LOD	195.35	1.29	0.91	**U**	**9.11**	IUPAC	-1.32	<LOD	26.89	18.99	7.68	5.38	2.57	1.03
V	**80.7**	IUPAC	227.66	301.29	354.73	244.85	279.36	300.94	102.	36.65	**V**	**82**	IUPAC	257.45	219.07	287.16	293.23	126.94	242.15	136.	49.95
W	**N/A**	minor	<LOD	<LOD	<LOD	<LOD	<LOD	<LOD			**W**	**190**	trace	-2.67	-9.59	11.41	-6.46	-20.20	11.21	60.0	23.43
Y	**N/A**	minor	37.82	36.27	37.76	35.43	38.75	38.18	3.32	1.26	**Y**	**N/A**	trace	21.95	26.61	22.49	18.11	26.34	21.34	8.50	3.22
Zn	**414**	trace	5.02	6.59	3.36	2.38	7.29	10.28	32.7	11.88	**Zn**	**418**	minor	3.08	-0.30	0.04	2.69	-0.63	7.75	350.	133.00
Zr	**N/A**	minor	299.52	295.48	302.22	314.74	304.13	301.64	19.2	6.48	**Zr**	**200**	trace	9.32	8.46	5.88	3.76	3.37	4.87	11.8	4.92

Table 74. Descriptive statistics for readings of control samples 2711a in the field at Star Carr, taken 2015 (ppm)

	N	Range	Minimum	Maximum	Mean	Std. Deviation
LE	6	40078.73	594673.85	634752.58	607438.9333	14957.38390
Ag	0					
Al	6	8342.97	55539.14	63882.11	60982.5650	3032.69016
As	6	21.12	64.58	85.70	78.6450	8.00911
Bi	0					
Ca	6	1929.64	23948.67	25878.31	25138.8900	766.77344
Cd	6	9.90	45.10	55.00	50.1567	4.28330
Cl	0					
Co	0					
Cr	0					
Cu	6	19.08	138.93	158.01	150.2750	7.45800
Fe	6	1535.75	34771.86	36307.61	35473.4583	545.20603
Hg	6	2.77	10.53	13.30	12.5033	1.05969
K	6	1604.94	21584.94	23189.88	22565.3433	693.07717
Mg	0					
Mn	6	20.62	706.14	726.76	718.8033	8.47671
Mo	6	5.00	5.58	10.58	7.2083	1.97661
Nb	6	3.89	24.14	28.03	26.6533	1.46518
Ni	6	10.32	14.31	24.63	18.4333	4.57745
P	6	203.86	572.64	776.50	677.2617	66.53562
Pb	6	63.54	1551.51	1615.05	1571.5033	23.39079
Rb	6	6.19	115.68	121.87	118.5983	2.23397
S	6	162.46	814.45	976.91	910.4083	61.40045
Sb	3	25	40	65	52.48	12.283
Se	1	0	3	3	2.92	
Si	6	29031.94	218733.83	247765.77	239367.3550	10996.47018
Sn	0					
Sr	6	6.36	233.00	239.36	235.5983	2.60858
Ta	5	22	23	45	34.10	9.224
Th	6	20.08	16.22	36.30	22.4933	7.42185
Ti	6	267.89	3156.90	3424.79	3288.0650	97.29195
U	2	1	8	9	8.25	0.912
V	6	102.55	264.42	366.97	310.5367	36.65305
W	0					
Y	6	3.32	35.43	38.75	37.3683	1.25608
Zn	6	32.70	423.84	456.54	438.0883	11.87976
Zr	6	19.26	295.48	314.74	302.9550	6.48400

Table 75. Descriptive statistics for readings of control samples 2710a in the field at Star Carr, taken 2015 (ppm)

	N	Range	Minimum	Maximum	Mean	Std. Deviation
LE	6	40177.57	554234.83	594412.40	574725.3817	16359.55761
Ag	6	13.66	28.20	41.86	35.0517	4.72287
Al	6	6759.92	55878.33	62638.25	59450.1783	2969.09211
As	6	102.16	1400.84	1503.00	1448.5600	37.00539
Bi	0					
Ca	6	614.08	6121.56	6735.64	6456.3800	220.72322
Cd	0					
Cl	0					
Co	0					
Cr	0					
Cu	6	252.77	3683.73	3936.50	3802.1350	93.56024
Fe	6	2337.50	52068.23	54405.73	52816.8633	888.99327
Hg	6	13.60	20.60	34.20	25.7450	5.85184
K	6	2158.30	20555.74	22714.04	21486.2750	853.10721
Mg	0					
Mn	6	151.51	2114.30	2265.81	2155.2200	59.04238
Mo	6	6.74	9.49	16.23	12.3683	2.75049
Nb	6	5.87	16.99	22.86	20.6483	2.35364
Ni	0					
P	6	193.17	904.94	1098.11	1011.8283	66.81080
Pb	6	278.59	5656.10	5934.69	5768.5983	110.19655
Rb	6	4.75	106.09	110.84	108.4050	1.62769
S	6	1986.35	16235.94	18222.29	17205.7283	838.48574
Sb	5	20	41	61	51.10	8.809
Se	3	3	5	8	6.04	1.700
Si	6	29696.24	231429.82	261126.06	245204.4417	12542.67077
Sn	0					
Sr	6	8.11	243.28	251.39	248.0167	3.22120
Ta	4	27	46	73	63.50	12.392
Th	6	12.53	24.33	36.86	30.8750	4.46525
Ti	6	202.60	2849.11	3051.71	2926.4767	70.93647
U	5	3	9	12	10.16	1.028
V	6	136.36	186.09	322.45	276.8867	49.95240
W	6	60.05	151.62	211.67	184.8383	23.42935
Y	6	8.50	18.11	26.61	22.8067	3.22471
Zn	6	350.23	4153.55	4503.78	4268.0133	132.99590
Zr	6	11.89	206.74	218.63	211.8833	4.92086

Appendix 5 Lab-based pXRF Quality Assurance and Control

Calibration Check Record

Table 76 is the complete calibration check record for all lab-based pXRF conducted.

Table 76. Calibration check record for lab-based pXRF

Date	Time	Reading	Mode	Elapsed Time Total
15/08/2016	05:12:58	#1	Cal Check	14.89
15/08/2016	10:34:39	#2	Cal Check	14.9
15/08/2016	15:05:17	#14	Cal Check	14.97
16/08/2016	11:17:30	#1	Cal Check	14.94
16/08/2016	15:01:27	#16	Cal Check	14.96
17/08/2016	09:43:06	#1	Cal Check	14.98
17/08/2016	13:06:23	#13	Cal Check	14.89
18/08/2016	09:54:40	#1	Cal Check	14.97
18/08/2016	09:58:07	#2	Cal Check	14.92
19/08/2016	10:15:42	#1	Cal Check	14.94
22/08/2016	10:43:22	#1	Cal Check	14.93
23/08/2016	09:43:11	#1	Cal Check	15.19
24/08/2016	10:12:09	#1	Cal Check	15.42
25/08/2016	09:35:05	#1	Cal Check	14.98
26/08/2016	10:14:44	#1	Cal Check	14.94
29/08/2016	13:15:02	#1	Cal Check	14.97
30/08/2016	09:51:38	#1	Cal Check	14.96
31/08/2016	11:09:22	#1	Cal Check	14.87

Control Readings

Control readings using 60 second beam times were taken at the start of every session, and every 20 readings. Due to issues with the machine overheating, controls were taken at the end of every session for preference, but this was not always possible (i.e. unless work was stopped by the operating temperature getting too high).

The data tables could not be formatted for print out in a useable format, so they are provided in digital form on the accompanying digital media.

Systematic experimentation confirming polythene bags interfered with pXRF readings

General experiment premise

Initial readings in the laboratory of soils analysed in situ in the field being reanalysed as prepared samples in sample bags (a standard method) suggested that something methodological was influencing the laboratory based readings. In order to check whether the sample bags may be interfering with readings of soils, these experiments were devised with specialist guidance from Gianni Gallello, MATRIX Project, Department of Archaeology, University of York.

We focused on investigating the impact of the bags on key elements making up soil compositions, i.e. aluminium, calcium, iron, silicon, and titanium. We also looked at a selection of other important elements in characterising soils: copper (Cu), manganese (Mn), nickel (Ni), potassium (K), strontium (Sr), zinc (Zn), and zirconium (Zr). As alternatives to bags, we investigated using supermarket bought cling film and spare Prolene® (polypropylene) film discs as loose soil mounting substrates. The following samples were analysed and compared:

- NIST 2710a - internationally recognised control Montana soil with independently verified certified values utilising multiple methods (NIST Certificate issued: 7 April 2009), provided by Olympus
- NIST 2711a - internationally recognised control Montana soil with independently verified certified values utilising multiple methods (NIST Certificate issued: 22 May 2009), provided by Olympus
- Silicon Dioxide (SiO_2) fine powder - internationally recognised control material with independently verified certified values for this batch, utilising multiple methods, provided by Sigma Aldrich (certification date: 20th October 2014)
- NIM GBW07408 - internationally recognised control Chinese soil with independently verified certified values utilising alternative methods, provided by Gianni Gallello (certified values provided as pers. comm.)

Equipment setup and blank readings

The artefacts were scanned within the Flex Stand's test chamber, up against the window of the analyzer. Initially the pXRF stand was set up in a horizontal position but later it was altered to a vertical position (so that the samples weight directly down on the analyser window). In the vertical position, the readings should be more consistent theoretically, with the sample better pressed against the window of the analyser.

Results were downloaded in parts per million. Including the light elements calculation (generated by the software), all readings summed to 1,000,000 parts out of 1,000,000 with the exception of the two readings taken on cling film with no sample, which summed to 999999.4 parts out of 1,000,000. This is possibly due to the readings on this material being weak and giving false peaks.

Empty polythene easy-seal bags

Readings taken on 01.03.16 by CCAR on new, empty bags, showed that the bags were picked up by the XRF, if in small amounts. These elements do not necessarily reflect the composition of the bags but false readings of other elemental components that are not factored into the algorithm of the machine in Geochem mode and can therefore give false readings when analysing soil or suggest the material is too thick for accurate readings of the soil to be obtained through. When CCAR attempted to read the empty chamber, the machine recorded a proximity error, suggesting that the chamber itself would not be being picked up by the machine if the sample did not cover the window fully and that in this case the bags were being read.

Readings for the five major elements in parts per million are presented in Table 77. The readings for seven less important elements are presented in Table 78: Copper, manganese, nickel, and zinc were not detected in any of the bag readings.

Table 77. Readings for the five major elements in parts per million (ppm) in the bags. <LOD means below the limit of detection for that element in Geochem mode on this machine.

Sample	Al	Ca	Fe	Si	Ti
1.3.16 #12	16125.66	3638.27	136.63	5179.78	20184.13
1.3.16 #14	<LOD	3068.95	<LOD	6254.67	<LOD
1.3.16 #15	<LOD	3312.64	<LOD	7106.15	<LOD

Table 78. Readings for the seven lesser important elements in ppm in the bags. <LOD means below the limit of detection.

Sample	Cu	Mn	Ni	K	Sr	Zn	Zr
1.3.16 #12	<LOD	<LOD	<LOD	821.24	11.77	<LOD	21.6
1.3.16 #14	<LOD	<LOD	<LOD	3001.11	11.49	<LOD	19.15
1.3.16 #15	<LOD	<LOD	<LOD	3475.91	11.24	<LOD	19.39

Single and folded samples of cling film

As a cheap, readily available alternative, GG suggested investigating the feasibility of using supermarket cling film as an alternative to polygrip bags. As such, we scanned a single layer of cling film to see if it would produce a result on its own. It did, but the parts did not sum fully to 1,000,000 including the light element calculations so the machine evidently struggled with reading this material.

Readings for the five major elements in parts per million are presented in Table 79. The readings for seven lesser important elements are presented in Table 80. Al, Ca, Si, Ti, Mn, Ni, K, Sr, Zr were not detected in any of the bag readings.

Table 79. Readings for the five major elements in ppm for single layers of cling film. <LOD means below the limit of detection.

Sample description	Al	Ca	Fe	Si	Ti
Single layer cling film, no soil sample	<LOD	<LOD	10.36	<LOD	<LOD
Single layer cling film, no soil sample	<LOD	<LOD	9.38	<LOD	<LOD

Table 80. Readings for the seven lesser important elements in ppm in a single layer of cling film. <LOD means below the limit of detection.

Sample description	Cu	Mn	Ni	K	Sr	Zn	Zr
Single layer cling film, no soil sample	3.54	<LOD	<LOD	<LOD	<LOD	11.48	<LOD
Single layer cling film, no soil sample	2.43	<LOD	<LOD	<LOD	<LOD	11.57	<LOD

Prolene® (polypropylene) film

Two readings were attempted with just discs of clean Prolene® film in place over the analyser window in the vertical stand position. Both readings failed due to a "proximity abort" meaning the machine aborted for safety as it did not register any material to read was covering the analyser window, which was encouraging in selecting this material as a potential substrate for analyses.

Control Sample Analyses

The control samples provided by Olympus with the machine come in plastic sample pots with a clear film end which is the end placed against the analyser window for readings. The clear film is made of Prolene® which is a thin 4.0 µm thick polypropylene film with high transmittance values (cf. http://www.chemplex.com/thin-film/rolls-pre-cut-circles-48/spectrocertified-thin-film-sample-support-windows-in-continuous-rolls-pre-perforated-rolls-and-precut-circles). The samples we hold departmentally are two Montana soils (internationally recognised controls for soils) NIST 2710a and NIST 2711a sourced from Olympus with the machine, and a fine dry powder >99.999% pure silicon dioxide sourced from Sigma Aldrich (which was used to replace a damaged sample of the same originally provided by Olympus). These samples were provided with certified values of their constituent elements, as measured by several different methods, from the manufacturers. GG also had a loose soil sample of internationally recognised NIM GBW07408, a Chinese soil, for further comparison.

NIST 2710a

All readings presented here for the control sample of Montana II Soil NIST 2710a were taken with the stand set up in the horizontal position on 23rd June 2016. The readings in the bags were taken with the transparent side of the bag in front of the analyser window. The certified values were those provided by Olympus with the control sample.

In

Table 81 below, the certified values measured independently for the certification are displayed in the top row, italicised in dark red font. Readings taken on the pXRF have a reading number and are listed in subsequent rows. Measurements are displayed in ppm.

Table 81. Values in ppm for control sample of soil NIST 2710a. The certified values are in the top row while readings taken on the departmental pXRF are in subsequent rows and have a reading number. <LOD = below limit of detection.

Sample	Al	Ca	Fe	Si	Ti
NIST 2710a certified values	*59500*	*9640*	*43200*	*311000*	*3110*
NIST 2710a control – without bag (reading 5.1)	56016.94	<LOD	60376.35	270761.61	2896.56
% difference from certified value	*-5.85388*	*n/a*	*39.76007*	*-12.93839*	*-6.863*
NIST 2710a control – without bag (5.2)	56579.81	<LOD	59771.14	269948.96	2762.61
% difference from certified value	*-4.90788*	*n/a*	*38.35912*	*-13.19969*	*-11.17*
NIST 2710a control - in bag (6.1)	10354.05	5528.99	49482.18	75308.34	2331.86
% difference from certified value	*-82.5982*	*-42.6453*	*14.54208*	*-75.7851*	*-25.021*
NIST 2710a control - in bag (6.2)	10650.56	5572.77	49719.29	75721.16	2271.7
% difference from certified value	*-82.0999*	*-42.1912*	*15.09095*	*-75.65236*	*-26.955*

Of the values taken without the bag, for readings where values could be detected (i.e. not less than the limit of detection), aluminium, silicon, and titanium were all reading slightly lower than the certified values but on the same scale numerically. However, iron was reading around 40% higher than the expected values. Calcium was below the limit of detection for this element on this machine and with an expected value of 9640 ppm that is not surprising. As the pXRF manual suggests that readings out by +/- 20% are acceptable for this machine, all readings without the bags would pass this test with the exception of the readings for iron.

In comparison, in readings taken with the bag in addition, aluminium, silicon, and titanium were all reading greatly lower than the expected values (between 42 to 82% lower than

expected). In this case, calcium was detected but also apparently reading lower than expected at 42.19% lower: however, as calcium was not detected without the bag, it is entirely possible that this is actually a completely false peak generated as a computational error by misinterpretation of a different element in the bag material. Iron was still reading higher by 14.5 – 15.1%, suggesting that this is the reading of a signal being detected as incorrectly higher from the material but that enhanced signal is then being "dampened" by the bag's physical interference.

NIST 2711a

All readings presented here for the control sample of Montana II Soil NIST 2711a were taken with the stand set up in the horizontal position on 23rd June 2016. The readings in the bags were taken with the transparent side of the bag in front of the analyser window. The certified values were those provided by Olympus with the control sample.

In Table 82 below, the certified values measured independently for the certification are displayed in the top row, italicised in dark red font. Readings taken on the pXRF have a reading number and are listed in subsequent rows. Measurements are displayed in ppm.

Table 82. Values in ppm for control sample of soil NIST 2711a. The certified values are in the top row while readings taken on the departmental pXRF are in subsequent rows and have a reading number. <LOD = below limit of detection.

Sample	**Al**	**Ca**	**Fe**	**Si**	**Ti**
NIST 2711a certified values	*67200*	*24200*	*28200*	*314000*	*3170*
NIST 2711a control – without bag (reading 7.1)	61408.72	20162.87	39885.12	291162.54	3321.08
% difference from certified value	*-8.61798*	*-16.6824*	*41.4366*	*-7.273076*	*4.76593*
NIST 2711a control – without bag (7.2)	62141.55	19777.04	39814.77	290212.93	3218.12
% difference from certified value	*-7.52746*	*-18.2767*	*41.18713*	*-7.5755*	*1.51798*
NIST 2711a control - in bag (8.1)	7770.08	19775.06	33135.33	59140.4	2368.52
% difference from certified value	*-88.4374*	*-18.2849*	*17.50117*	*-81.16548*	*-25.283*

NIST 2711a control - in bag (8.2)	6736.73	19846.03	33182.68	58721.73	2604.35
% difference from certified value	*-89.9751*	*-17.9916*	*17.66908*	*-81.29881*	*-17.844*

Of the values taken without the bag, aluminium and silicon were all reading slightly lower than the certified values but on the same scale numerically. Calcium was also on the same scale but more significantly reduced, at 17 and 18% lower for the two readings. However, iron again was reading around 41% higher than the expected values in both readings. Titanium was also reading slightly higher than the certified values in this case (2 and 5% in the two readings) but on the same scale numerically. Again, therefore, as per the suggested acceptable variance in the machine manual of +/- 20%, all readings without the bags would pass this test with the exception of the readings for iron.

In comparison, the values taken with the bag in addition for aluminium, silicon, and titanium all were reading greatly lower than the expected values (between 25 to 88% lower than expected). In this case, calcium was still reading significantly lower but by the same percentage as without the bag (around 18% for both readings). Iron was still reading higher but by reduced figures of around 18%, similar to the trend seen in the NIST 2710a readings.

Silicon Dioxide (SiO_2)

All readings presented here for the control sample of silicon dioxide were taken on 23rd June 2016. Readings were taken in both the horizontal and vertical stand positions to enable comparison of the effect of that. The readings in the bags were taken with the side of the bag with inked white stripes in front of the analyser window. The certified values were those provided by Sigma Aldrich with the control sample.

In Table 83 below, the certified values measured independently for the certification are displayed in the top row, italicised in dark red font. Readings taken on the pXRF have a reading number and are listed in subsequent rows. Measurements are displayed in ppm. Measurements highlighted in bold illustrate readings for values which should not exist at these levels within the sample itself as is it is meant to be silicon dioxide of >99.99% purity (so other elements should measure 0.01% or less in total).

Table 83. Values in ppm for control sample of silicon dioxide. The certified values are in the top row while readings taken on the departmental pXRF are in subsequent rows and have a reading number. <LOD = below limit of detection.

23.06.16	Sample	Al	Ca	Fe	Si	Ti
	SiO2 certified values				*468991*	
2.1	SiO2 control (horizontal stand)	<LOD	<LOD	<LOD	420091.11	<LOD
	% difference from certified value				*-10.42662*	
2.2	SiO2 control (horizontal stand)	<LOD	<LOD	<LOD	419214.06	<LOD
	% difference from certified value				*-10.61362*	
14.1	SiO2 control (vertical stand)	<LOD	<LOD	<LOD	431593.22	<LOD
	% difference from certified value				*-7.974093*	
14.2	SiO2 control (vertical stand)	<LOD	<LOD	<LOD	430733.02	<LOD
	% difference from certified value				*-8.157508*	
3.1	SiO2 control in bag	**2867.64**	<LOD	<LOD	75000.24	**2955.02**
	% difference from certified value				*-84.00817*	
3.2	SiO2 control in bag	**2570.83**	<LOD	<LOD	74879.93	**2913.3**
	% difference from certified value				*-84.03382*	
13.1	SiO2 control with cling film	<LOD	<LOD	<LOD	116101.14	<LOD
	% difference from certified value				*-75.24448*	
13.2	SiO2 control with cling film	<LOD	<LOD	<LOD	116419.55	<LOD
	% difference from certified value				*-75.17659*	

Of the values taken without the bag in the horizontal stand position, silicon readings were 10 and 11% lower than the expected value. Taking readings in the vertical position seemed to improve readings slightly, with readings now only around 8% lower than the expected

value. Both sets of readings are within the +/-20% Olympus recommended allowances, of course.

As can be seen, of the values taken within the bag there are several erroneous readings, albeit in small amounts, of aluminium and titanium. However the readability of silicon in the sample is greatly decreased, with samples reading around 84% lower than the certified values. In the controls read within cling film, as an alternative, the erroneous readings were not present but the ability to read the silicon present was still greatly reduced by around 75% of what it should be.

NIM GBW07408

The sample of NIM-GBW07408 was provided as a loose soil by GG. The soil was placed within a bag, then within cling film, then on top of a Prolene sheet in the analyser chamber covering the window, all in the vertical stand orientation. Readings 12.1 and 12.2 in cling flim were repeats of readings in cling film as they were rearranged for better sample depth and with a weight on top to see if this would improve readings.

The machine generates ppm or percent of individual elements but not oxides (though it does suggest a bulk figure for all light element components like oxygen). Oxide components can be estimated through applying mathematical transformations but this requires significant treatment of the raw data to be statistically valid. To convert to the oxides, the coordination number of the cation (the number of other atoms to which the central atom being measured is bonded) needs to be known. As such there is uncertainty for elements where the coordination number can be variable e.g. Fe+2 or Fe+3.

The NIM-GBW07408 certified values were provided, however, as oxide wt % for major elements (in this case excluding titanium) and ppm for trace elements. Therefore, in order to compare the reading from the departmental pXRF machine, a conversion must be made. Table 84 below provides the certified values for the sample. The values actually provided on the certification are in light red. It was decided to calculate the ppm for both the central atoms and their bonded atoms summed (i.e. to convert from weight % directly to ppm of that oxide supposedly in the sample). As can be seen, there are two different iron oxides estimated to be present (FeO and Fe_2O_3) (i.e. the iron has varying coordination numbers) so in order to estimate how much iron and oxygen combined is certified being in the sample, both were converted and then summed. As such, the final figures in the table, in dark red and bold on the final row, represent the number of ppm of both the central atoms *and* their bonded oxygen atoms.

Table 84. NIM-GBW07408 certified values of oxides for major elements and ppm for minor elements, all converted to estimate ppm for each central atom of an element plus its bonded oxygen atoms in the oxide form. Numbers in bold and dark red are those provided on the original certification.

NIM-GBW07408 certified values (provided as oxide weight % or in ppm)	**Al_2O_3**	**CaO**	**FeO**	**Fe2O3**	**SiO_2**	**Ti**
Oxide wt % certified value	11.92%	8.27%	1.22%	4.48%	58.61%	
Trace element in ppm certified						3800
Conversion to ppm from oxide wt %	119200	82700	12200	44800	586100	3800
Sum ppm for each element or its oxides	***119200***	***82700***	***57000***		***586100***	***3800***

Table 85 below provides the unmodified values in ppm as read on GG's sample by the departmental machine. In order to calculate a conversion from a reading in ppm of a single element to the oxide percent weight we do the following calculation:

Central atom element ppm x ((atomic mass of element in ppm x number of atoms of this in oxide) + (atomic mass of oxygen x number of oxygen atoms in oxide)) / atomic mass of element in ppm.

This calculation was used to estimate the oxide weight % for Al, Ca, Fe, and Si from the readings taken by the departmental machine. In the case of iron, the oxide form was assumed to be FeO, although this could be in error. The value for titanium was not converted to an oxide as it was provided in ppm on the certified values table – instead this is simply directly converted from ppm to element wt % for easy comparison with the other elements. These values are presented in Table 86.

Table 85. Values in ppm for the major elements in the control sample of NIM-GBW07408, as read by the departmental pXRF

PPM	**Sample**	**Al**	**Ca**	**Fe**	**Si**	**Ti**
9.1	NIM GBW07408 - in bag	5531.55	47552.57	37539.93	45458.94	2913.52

PPM	Sample	Al	Ca	Fe	Si	Ti
9.2	NIM GBW07408 - in bag	4734.69	47147.22	37716.22	44670.97	2839.48
11.1	NIM GBW07408 - in cling film	19201.33	22962.18	32073.83	88578.67	2388.32
11.2	NIM GBW07408 - in cling film	18260.57	22753.17	32063.62	87678.72	2469.57
12.1	NIM GBW07408 - in cling film	18405.32	21553.96	32195.72	82966.62	2374.57
12.2	NIM GBW07408 - in cling film	17870.08	21640.72	32113.96	82410.9	2399.7
17.1	NIM GBW07408 - on Prolene	59666.5	61475.04	46015.13	256027.5	3685.78
17.2	NIM GBW07408 - on Prolene	60559.57	59147.5	45666.73	253270.1	3617.5

Table 86. Values in estimated oxide wt % for the major elements. All except titanium were converted to the oxides listed. Titanium, having been provided in ppm as a minor element in the certified values, was not converted to an oxide but its ppm simply converted

PERCENTAGES OF CONVERTED OXIDES		Al_2O_3	CaO	Iron Oxides	SiO_2	Ti
NIM GBW07408 certified values (SUM %)		*11.92%*	*8.27%*	*5.70%*	*58.61%*	*0.38%*
9.1	NIM GBW07408 - in bag	1.045146	6.653539	4.829472	9.725154	0.291352
9.2	NIM GBW07408 - in bag	0.894585	6.596823	4.852152	9.556581	0.283948
11.1	NIM GBW07408 - in cling film	3.62795	3.21286	4.126264	18.94987	0.238832
11.2	NIM GBW07408 - in cling film	3.4502	3.183616	4.124951	18.75735	0.246957
12.1	NIM GBW07408 - in cling film	3.47755	3.015823	4.141945	17.74927	0.237457
12.2	NIM GBW07408 - in cling film	3.37642	3.027962	4.131427	17.63039	0.23997
17.1	NIM GBW07408 - on Prolene	11.27355	8.601566	5.919798	54.77265	0.368578
17.2	NIM GBW07408 - on Prolene	11.44228	8.275898	5.874976	54.18276	0.36175

As can be seen, the readings taken in the bags are all below the values they should be reading. Particularly for silicon, readings that should be around 59% are only reading around 10%. Next heavily affected are the readings for aluminium that should be around 12% but are only around 1%. Although for iron (reading around 5% when should be around 6%), titanium (reading around 0.3% when should be around 0.4%), and calcium (reading around 7% when should be around 8%) this effect is reduced, in all elements the accuracy is improved when readings are taken on Prolene film in comparison.

While cling film slightly improved the readings for aluminium and silicon, it actually slightly worsened the readings for calcium, iron and titanium which all read even lower than simply in the bags.

The values from readings taken on the Prolene seem to more closely meet with the certified values: aluminium oxide 11.92% (12% rounded up) certified to 11.27 and 11.44% (11% rounded up) measured; calcium oxide 8.27% (8%) certified to 8.60 and 8.28% (9 and 8%) measured; iron oxides (N.B. only calculated here as FeO remember) 5.70% (6%) certified to 5.92 and 5.88% (6%) measured, which in fact seem slightly raised which fits with the slightly elevated readings taken on the other control samples; silicon oxide 58.61% (59%) certified to 54.77 and 54.18% (55% and 54%) measured; and finally percent titanium certified to be 0.38% was measured to be 0.37 and 0.36%. As such, silicon is the only value out by >1% (measured value) and even then it is out by <5% (measured value).

Conclusions

From the readings taken on the four control samples (SIO2, NIST 2710a, NIST 2711a, and NIM GBW07408), using normal grip-seal bags and cling film seem to affect the results to potentially inconsistent degrees. Most importantly, they seem to affect different elements to differing degrees, making the results less reliable in terms of considering the proportions of certain elements against one another. Using a single layer of Prolene however gave us good results for at least the major elements Al, Ca, Ti, Fe, and Si based on three soil control samples (Montana soils NIST 2710a and NIST 2711a as well as Chinese soil NIM-GBW07408). We seem to be able to measure Al, Ca, and Ti within 10000 ppm of the certified values, and Si and Fe to be within 50000 ppm. To correct for the high Fe and low Si readings, the machine was submitted for a full service and recalibration as this was considered to be a potential machine error rather but this did not improve the readings (see work on controls utilised during lab-based pXRF analyses).

Appendix 6 Supplementary Statistical Tables and Graphs for Flixton Island 2 Geochemical Analyses

Introduction

This appendix provides the full datasets and all the supplementary statistical tables and graphs relating to the geochemical results from Flixton Island 2.

VP12 ICP-AES Full Dataset

This data could not be formatted appropriately for printing, therefore it is provided in digital format on the associated media.

VP12 ICP-AES Individual Element Histograms (batches 1 and 4, Trench 4)

The following, in Figure 158, are the histograms for the data as measured in batch 1 and 4 of the ICP-AES analysis on trench 4. The table background is colour-coded so that red indicates a minor contributor, yellow is for minor contributors, blue is for trace contributors and white is for IUPAC-trace contributors. Entries marked n/a are because that element could not be measured in that batch but was in the other batch. All other elements that were below the LODs in both batches are not included in the table at all.

	Batch 1 Result	Batch 4 Result
Fe	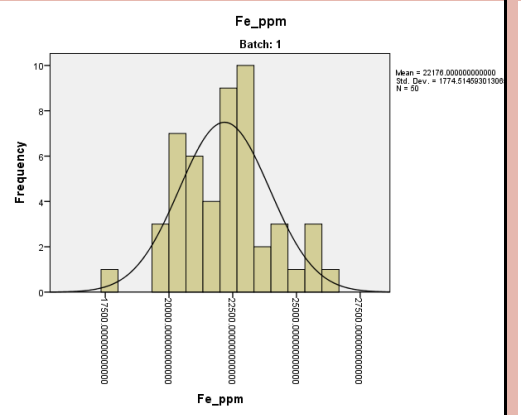	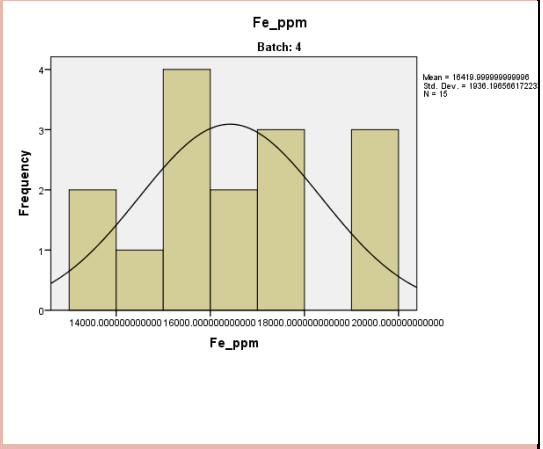

Al	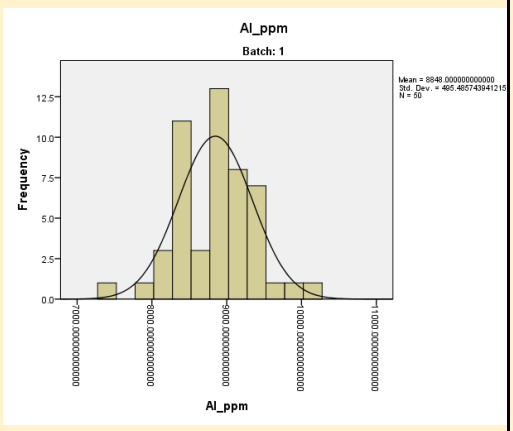 Al_ppm Batch: 1 Mean = 8848.000000000000 Std. Dev. = 485.465743941215 N = 50 Frequency Al_ppm	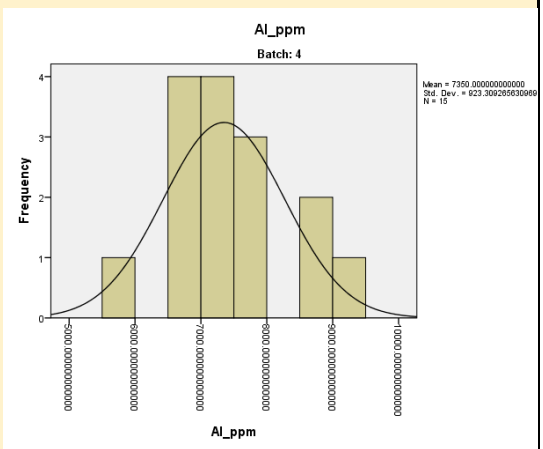 Al_ppm Batch: 4 Mean = 7350.000000000000 Std. Dev. = 923.309265630969 N = 15 Frequency Al_ppm
Ca	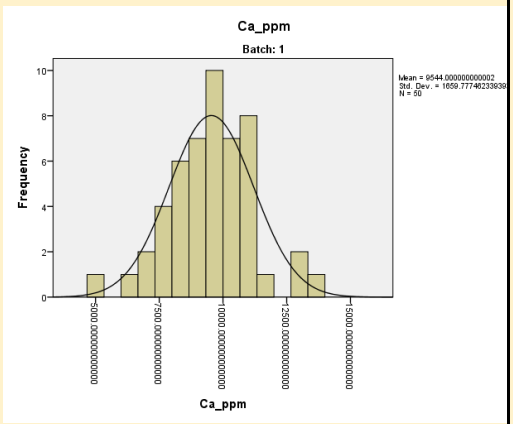 Ca_ppm Batch: 1 Mean = 9544.000000000002 Std. Dev. = 1659.777462339391 N = 50 Frequency Ca_ppm	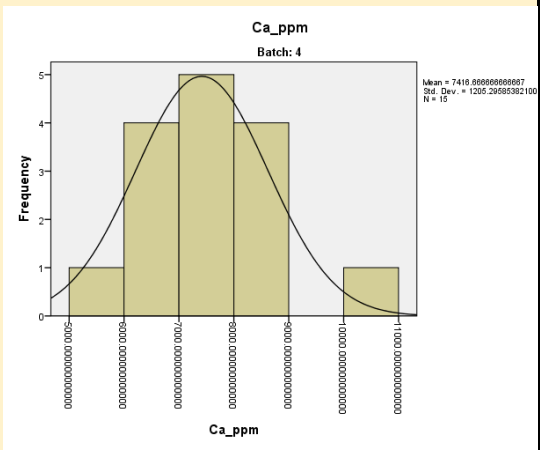 Ca_ppm Batch: 4 Mean = 7418.666666666667 Std. Dev. = 1205.295853821000 N = 15 Frequency Ca_ppm
Mg	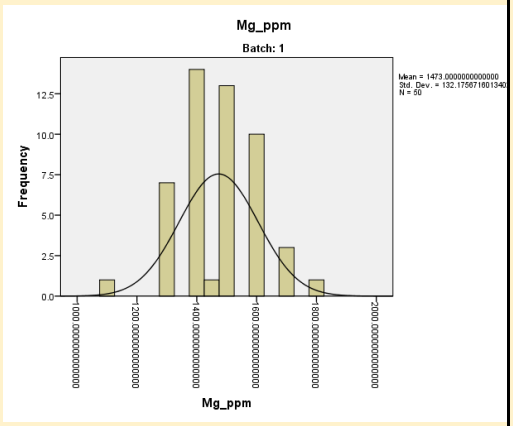 Mg_ppm Batch: 1 Mean = 1473.000000000000 Std. Dev. = 132.175671001340 N = 50 Frequency Mg_ppm	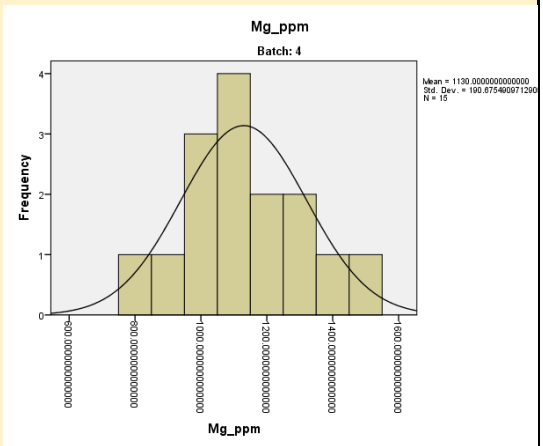 Mg_ppm Batch: 4 Mean = 1130.000000000000 Std. Dev. = 190.675409971290 N = 15 Frequency Mg_ppm

Ba	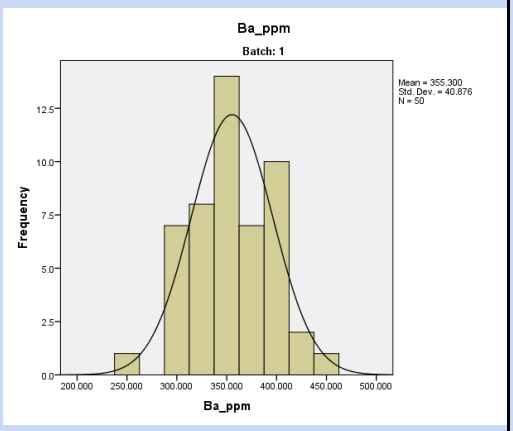 Ba_ppm Batch: 1 Mean = 355.300 Std. Dev. = 40.876 N = 50 Frequency Ba_ppm	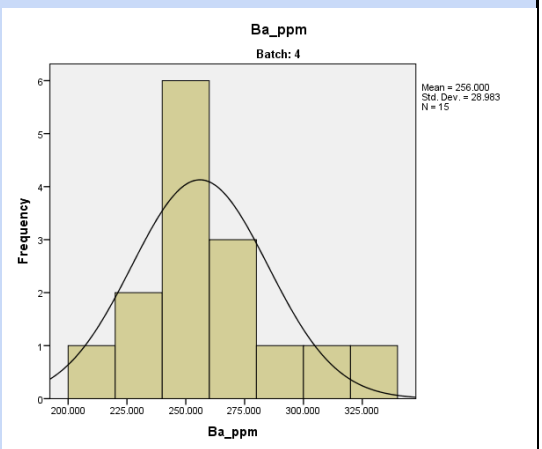 Ba_ppm Batch: 4 Mean = 256.000 Std. Dev. = 28.983 N = 15 Frequency Ba_ppm
K	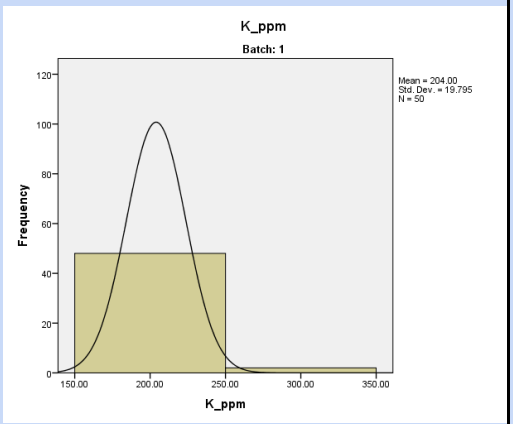 K_ppm Batch: 1 Mean = 204.00 Std. Dev. = 19.795 N = 50 Frequency K_ppm	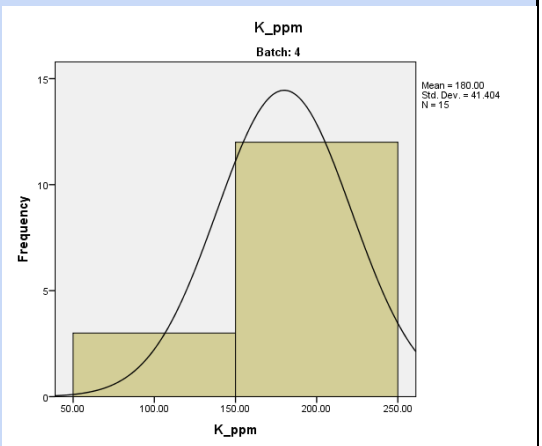 K_ppm Batch: 4 Mean = 180.00 Std. Dev. = 41.404 N = 15 Frequency K_ppm
Mn	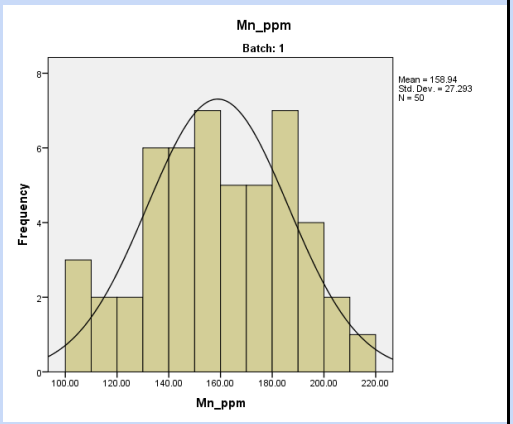 Mn_ppm Batch: 1 Mean = 158.94 Std. Dev. = 27.293 N = 50 Frequency Mn_ppm	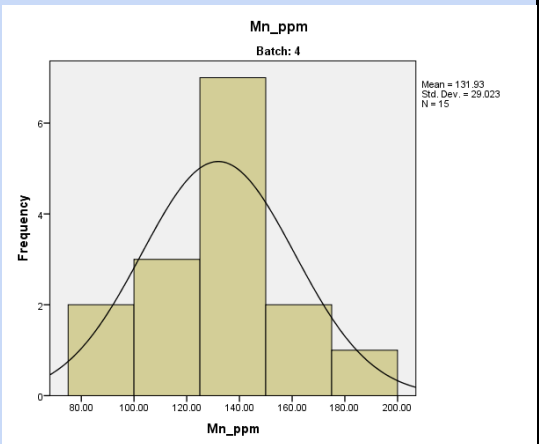 Mn_ppm Batch: 4 Mean = 131.93 Std. Dev. = 29.023 N = 15 Frequency Mn_ppm

Na	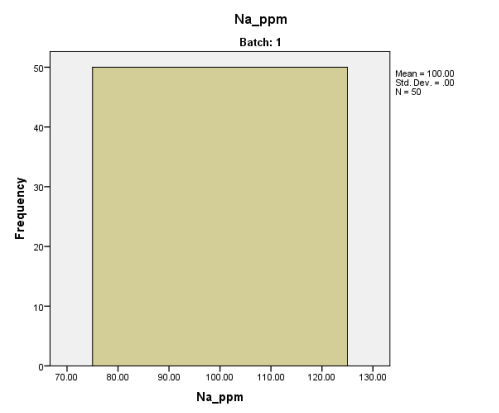 Na_ppm Batch: 1 Mean = 100.00 Std. Dev. = .00 N = 50 Frequency Na_ppm	**n/a**
P	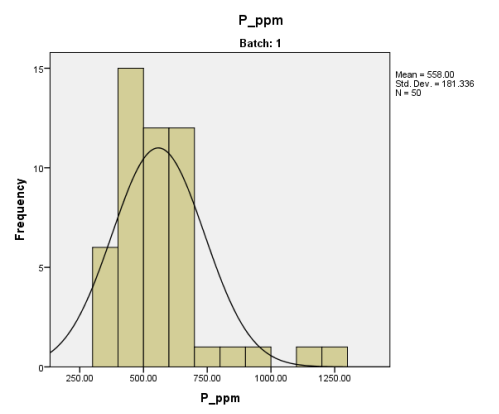 P_ppm Batch: 1 Mean = 558.00 Std. Dev. = 181.336 N = 50 Frequency P_ppm	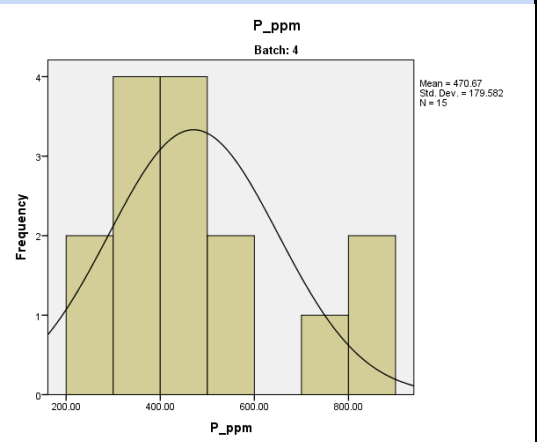 P_ppm Batch: 4 Mean = 470.67 Std. Dev. = 179.582 N = 15 Frequency P_ppm
S	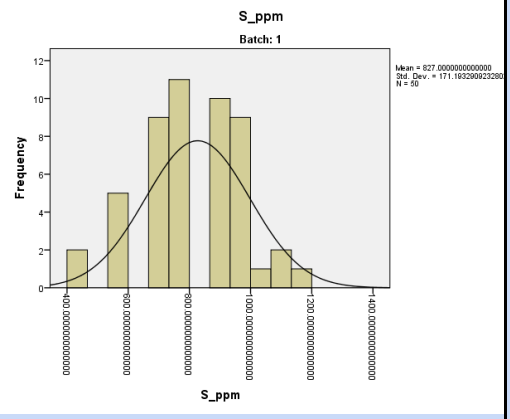 S_ppm Batch: 1 Frequency S_ppm	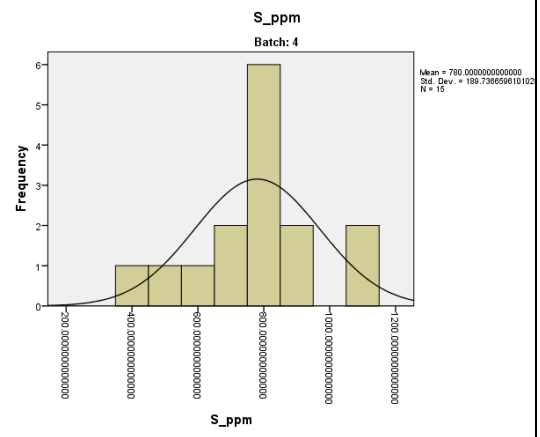 S_ppm Batch: 4 Mean = 780.0000000000000 N = 15 Frequency S_ppm

Ti	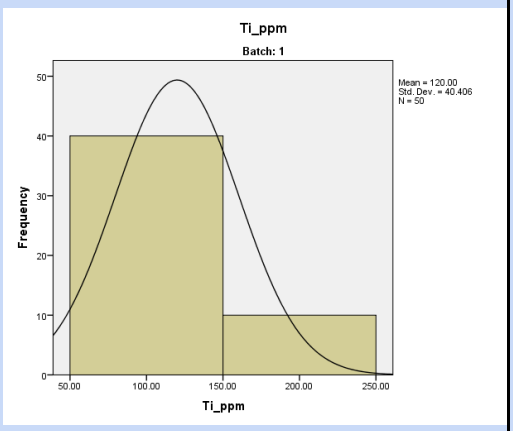 Ti_ppm Batch: 1 Mean = 120.00 Std. Dev. = 40.406 N = 50 Frequency Ti_ppm	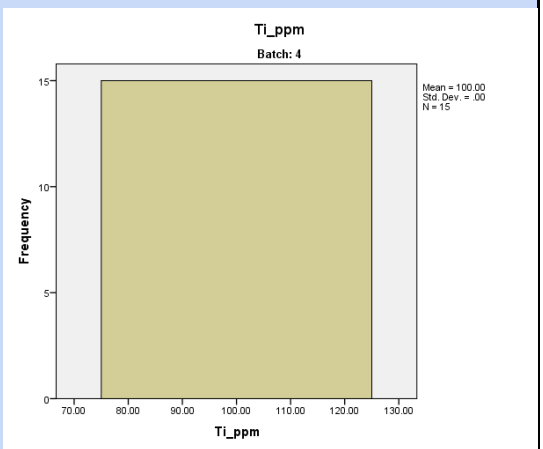 Ti_ppm Batch: 4 Mean = 100.00 Std. Dev. = .00 N = 15 Frequency Ti_ppm
Ag	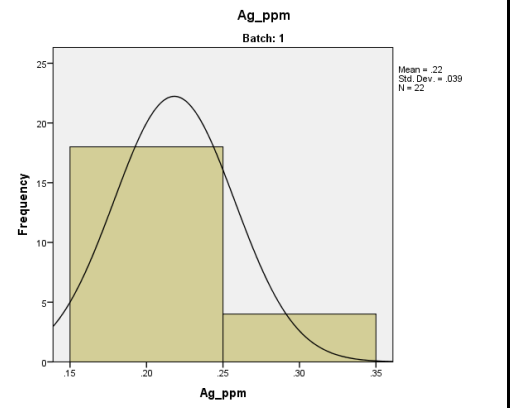 Ag_ppm Batch: 1 Mean = .22 Std. Dev. = .039 N = 22 Frequency Ag_ppm	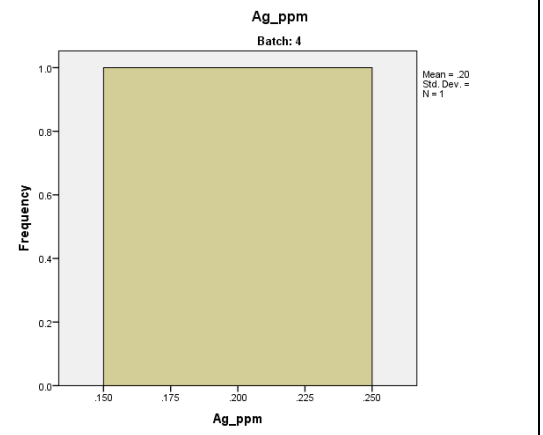 Ag_ppm Batch: 4 Mean = .20 Std. Dev. = N = 1 Frequency Ag_ppm
As	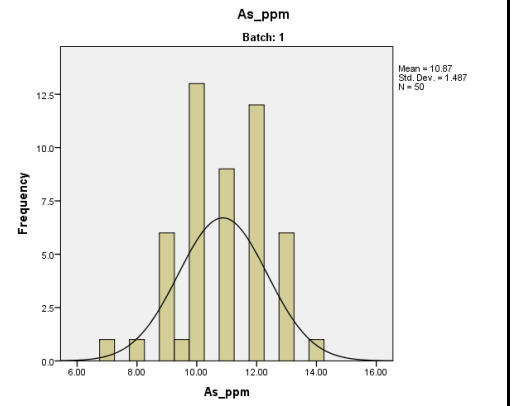 As_ppm Batch: 1 Mean = 10.87 Std. Dev. = 1.487 N = 50 Frequency As_ppm	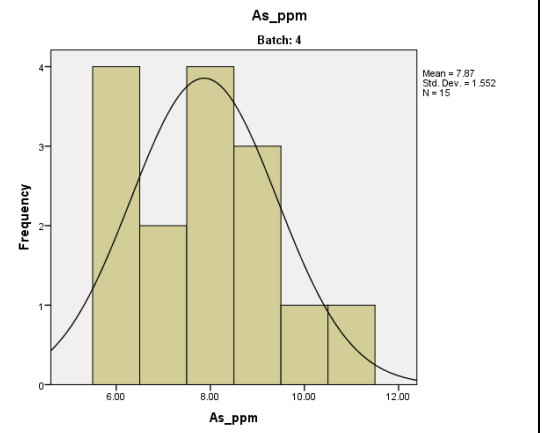 As_ppm Batch: 4 Mean = 7.87 Std. Dev. = 1.552 N = 15 Frequency As_ppm

B	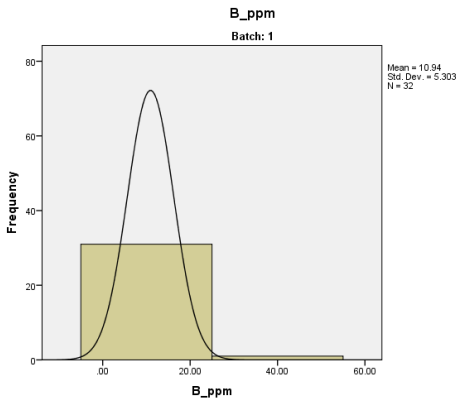 B_ppm Batch: 1 Mean = 10.94 Std. Dev. = 5.303 N = 32 Frequency B_ppm	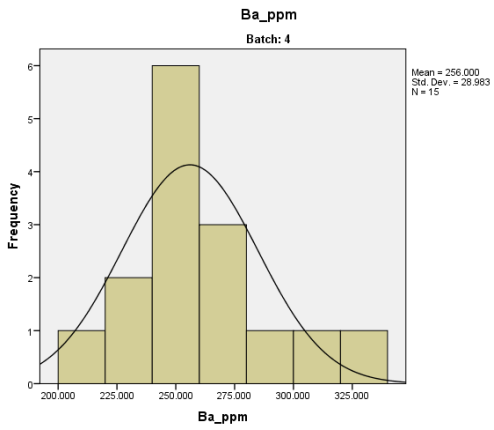 Ba_ppm Batch: 4 Mean = 256.000 Std. Dev. = 28.983 N = 15 Frequency Ba_ppm
Be	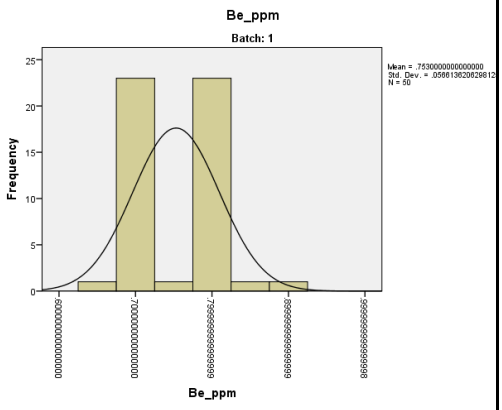 Be_ppm Batch: 1 Frequency Be_ppm	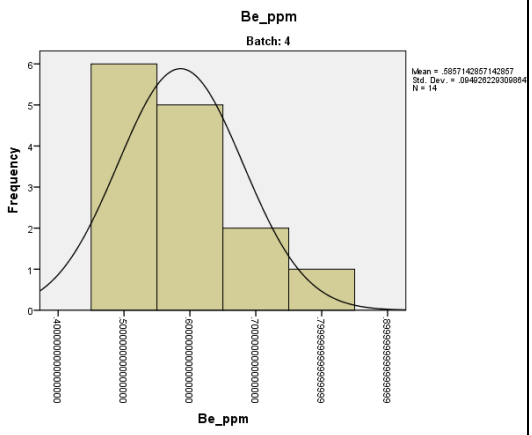 Be_ppm Batch: 4 Frequency Be_ppm
Co	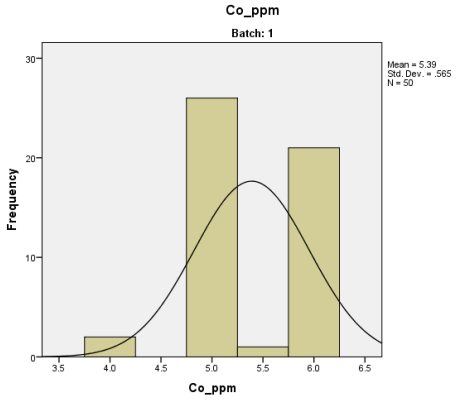 Co_ppm Batch: 1 Mean = 5.39 Std. Dev. = .565 N = 50 Frequency Co_ppm	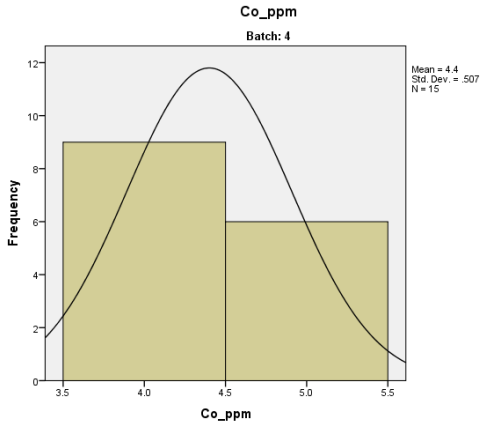 Co_ppm Batch: 4 Mean = 4.4 Std. Dev. = .507 N = 15 Frequency Co_ppm

Cr	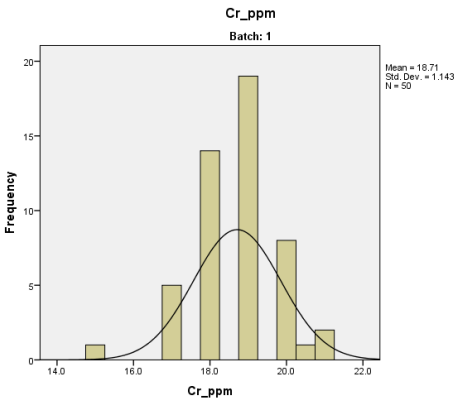 Cr_ppm Batch: 1 Mean = 18.71 Std. Dev. = 1.143 N = 50 Frequency Cr_ppm	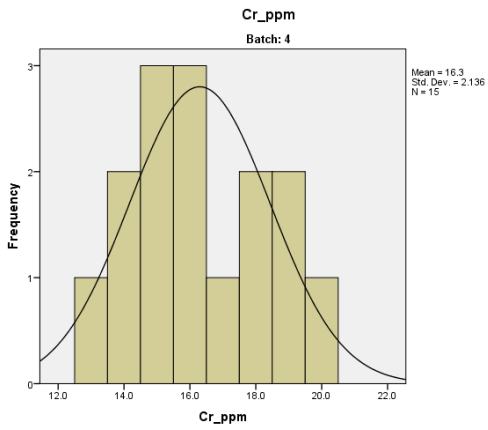 Cr_ppm Batch: 4 Mean = 16.3 Std. Dev. = 2.136 N = 15 Frequency Cr_ppm
Cu	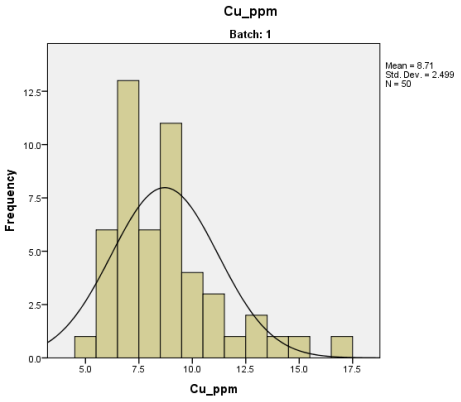 Cu_ppm Batch: 1 Mean = 8.71 Std. Dev. = 2.499 N = 50 Frequency Cu_ppm	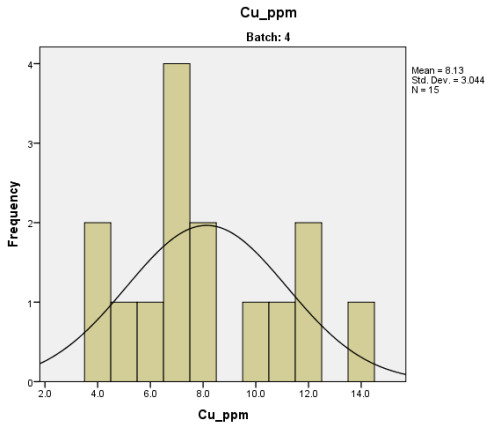 Cu_ppm Batch: 4 Mean = 8.13 Std. Dev. = 3.044 N = 15 Frequency Cu_ppm
Hg	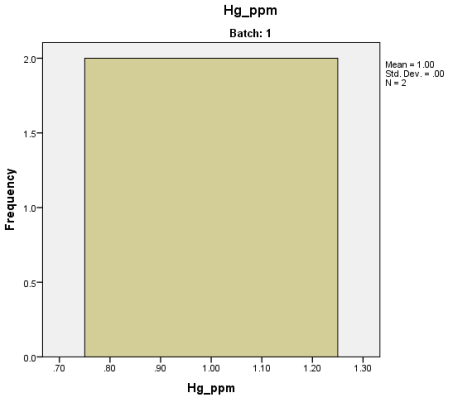 Hg_ppm Batch: 1 Mean = 1.00 Std. Dev. = .00 N = 2 Frequency Hg_ppm	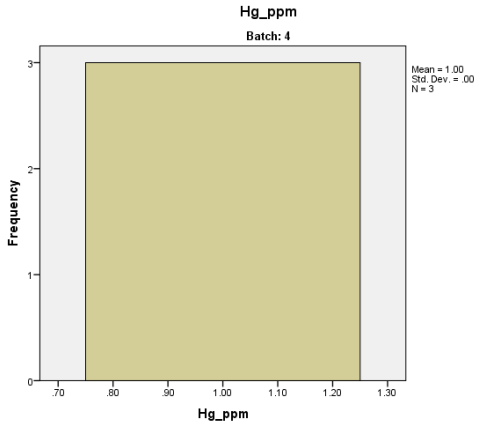 Hg_ppm Batch: 4 Mean = 1.00 Std. Dev. = .00 N = 3 Frequency Hg_ppm

La	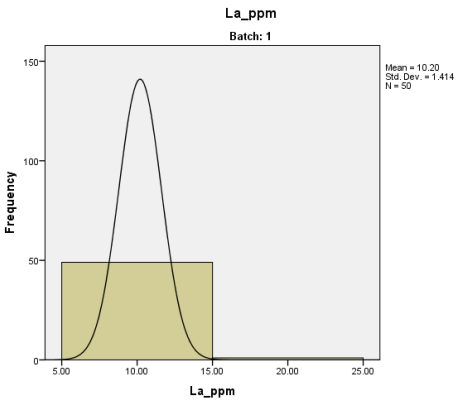 La_ppm Batch: 1 Mean = 10.20 Std. Dev. = 1.414 N = 50 Frequency La_ppm	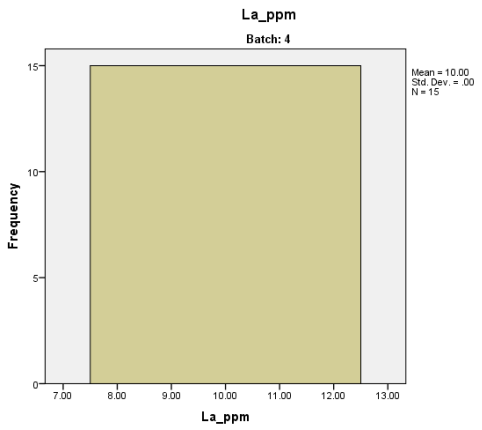 La_ppm Batch: 4 Mean = 10.00 Std. Dev. = .00 N = 15 Frequency La_ppm
Mo	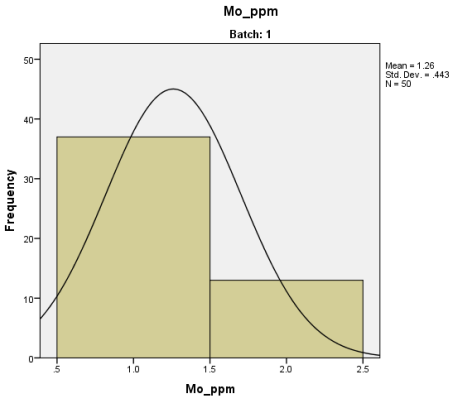 Mo_ppm Batch: 1 Mean = 1.26 Std. Dev. = .443 N = 50 Frequency Mo_ppm	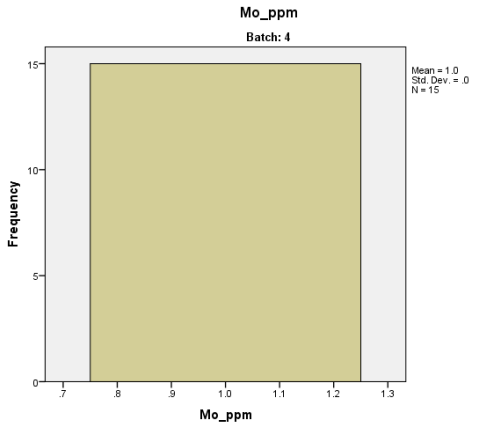 Mo_ppm Batch: 4 Mean = 1.0 Std. Dev. = .0 N = 15 Frequency Mo_ppm
Ni	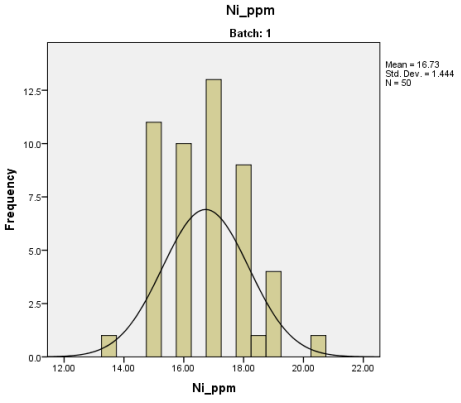 Ni_ppm Batch: 1 Mean = 16.73 Std. Dev. = 1.444 N = 50 Frequency Ni_ppm	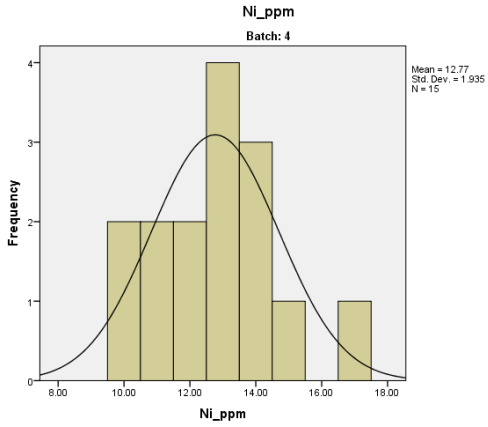 Ni_ppm Batch: 4 Mean = 12.77 Std. Dev. = 1.935 N = 15 Frequency Ni_ppm

Pb	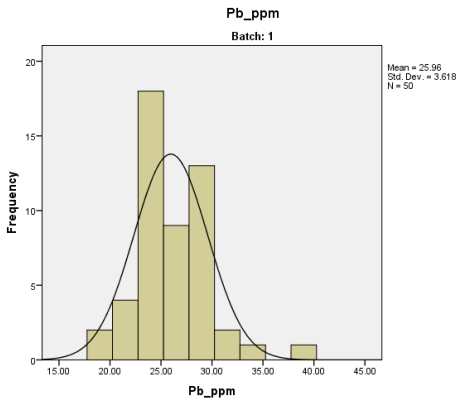 Pb_ppm Batch: 1 Mean = 25.96 Std. Dev. = 3.618 N = 50 Frequency Pb_ppm	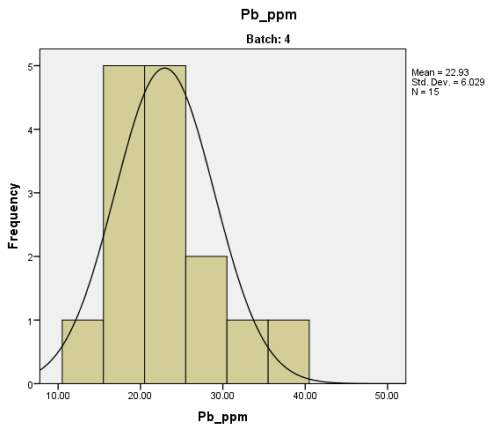 Pb_ppm Batch: 4 Mean = 22.93 Std. Dev. = 6.029 N = 15 Frequency Pb_ppm
Sb	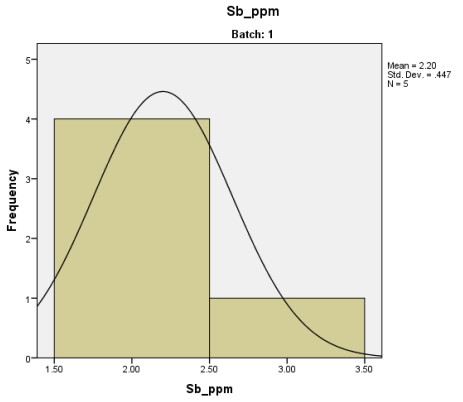 Sb_ppm Batch: 1 Mean = 2.20 Std. Dev. = .447 N = 5 Frequency Sb_ppm	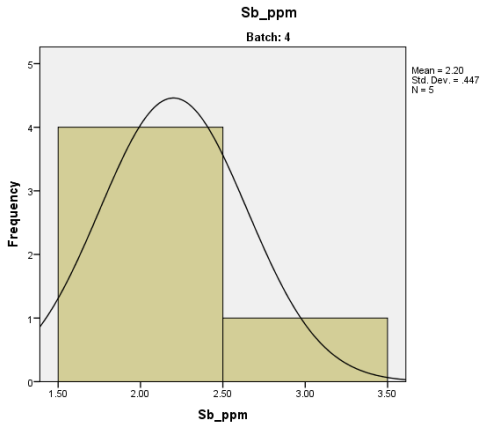 Sb_ppm Batch: 4 Mean = 2.20 Std. Dev. = .447 N = 5 Frequency Sb_ppm
Sc	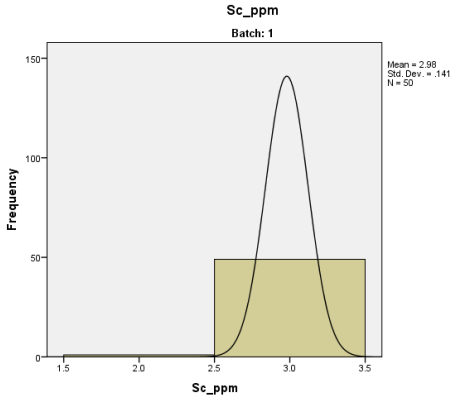 Sc_ppm Batch: 1 Mean = 2.98 Std. Dev. = .141 N = 50 Frequency Sc_ppm	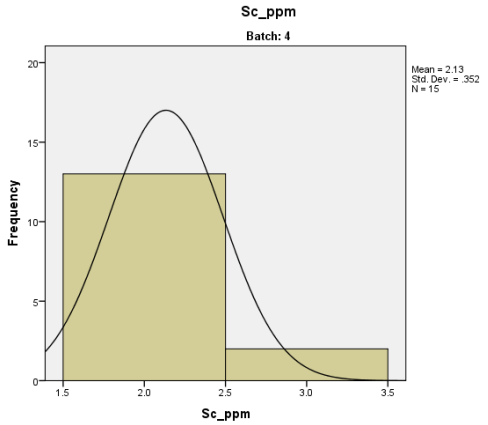 Sc_ppm Batch: 4 Mean = 2.13 Std. Dev. = .352 N = 15 Frequency Sc_ppm

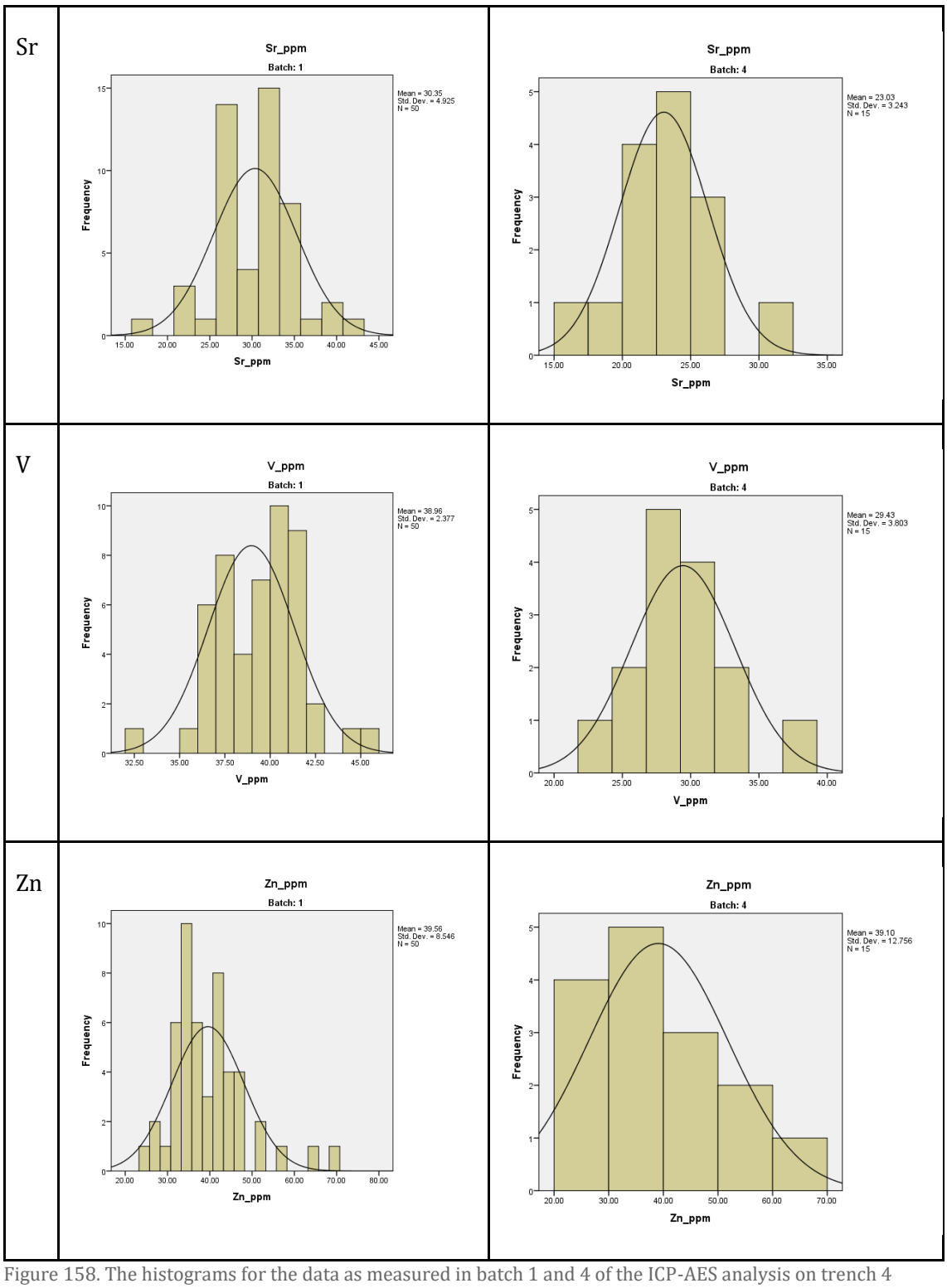

Figure 158. The histograms for the data as measured in batch 1 and 4 of the ICP-AES analysis on trench 4

VP12 ICP-AES Individual Element Spatial Analysis Results (Trench 4)

Major

Iron

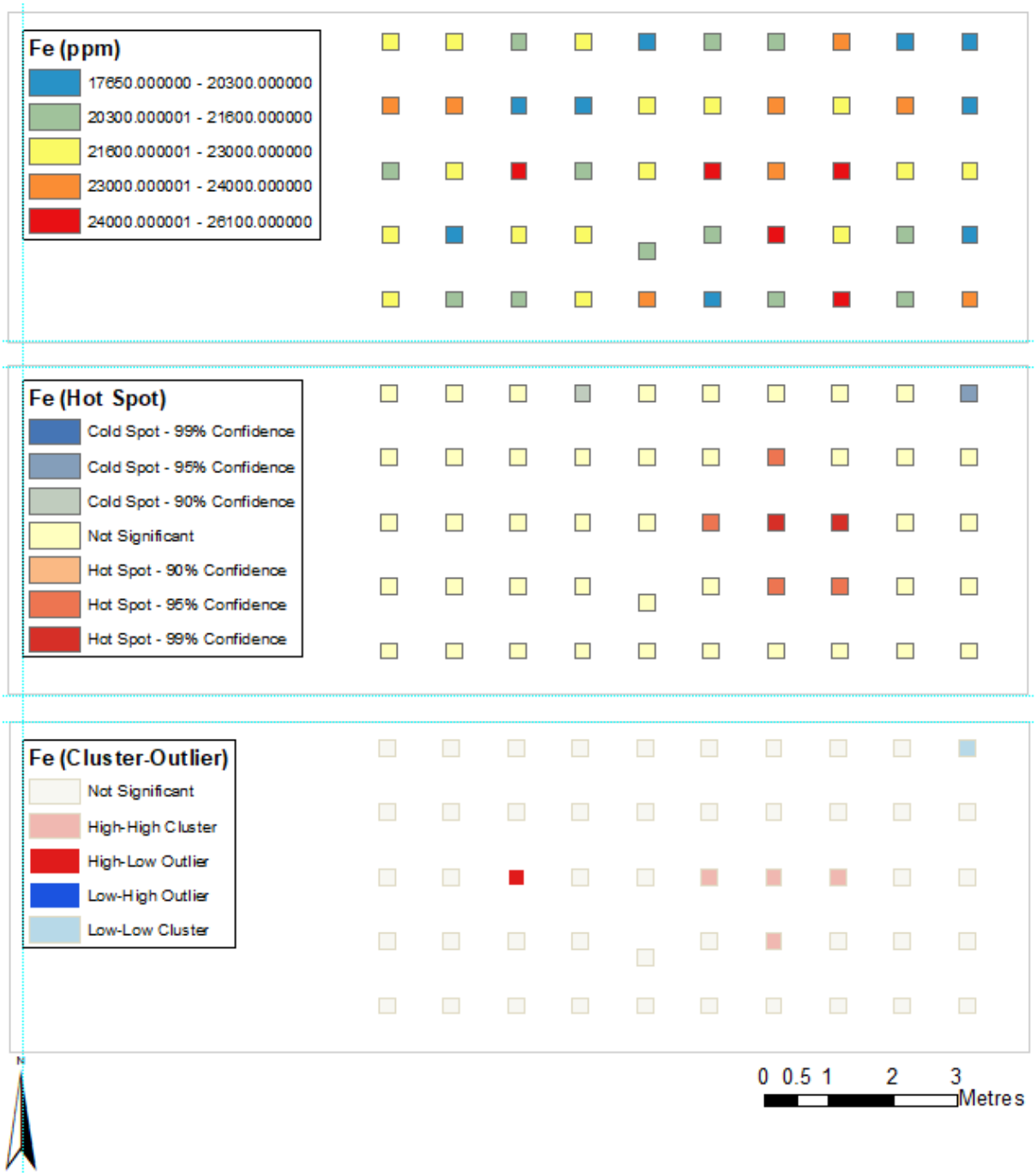

Minor

Aluminium

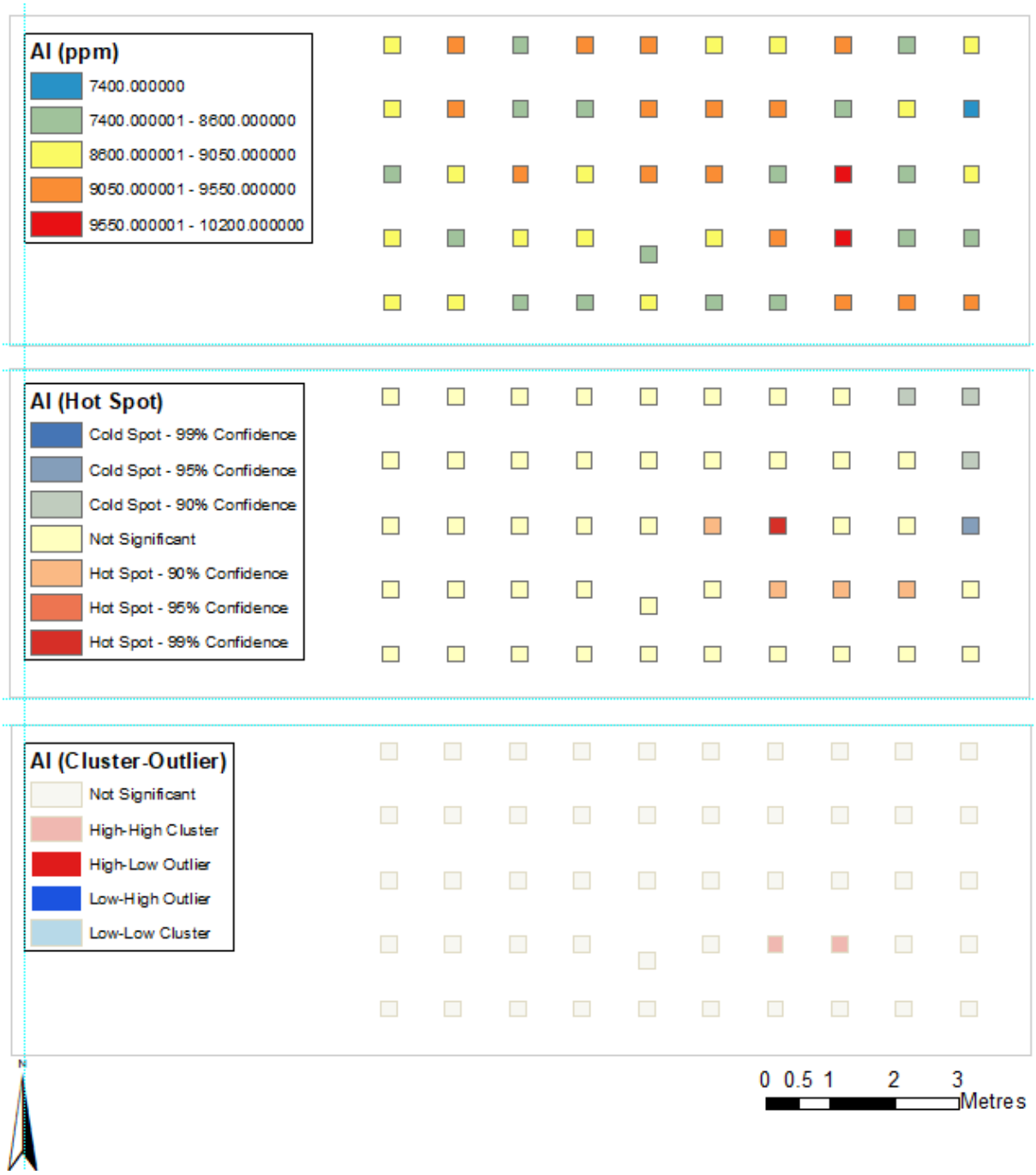

Calcium

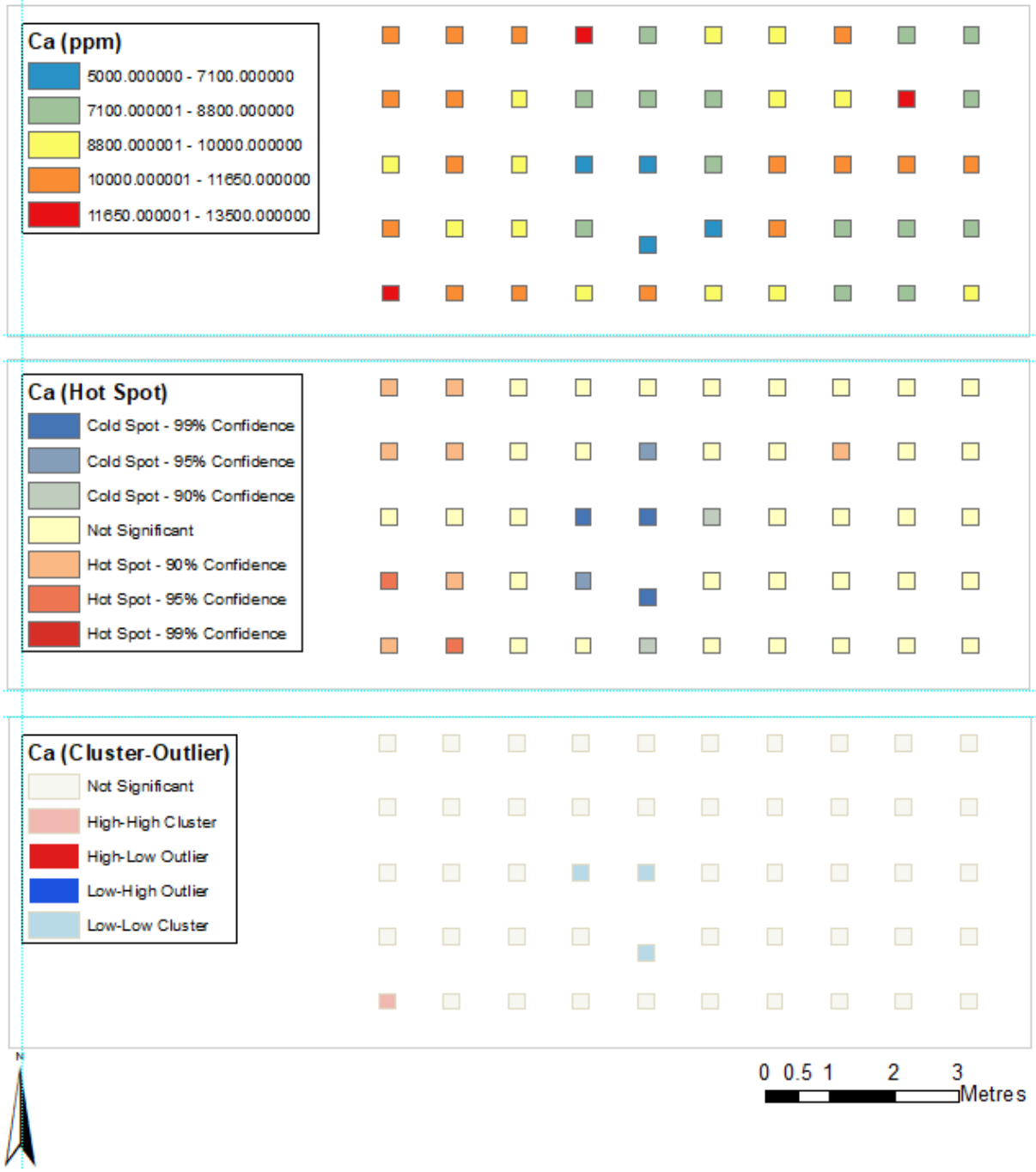
Ca (ppm)
5000.000000 - 7100.000000
7100.000001 - 8800.000000
8800.000001 - 10000.000000
10000.000001 - 11650.000000
11650.000001 - 13500.000000
Ca (Hot Spot)
Cold Spot - 99% Confidence
Cold Spot - 95% Confidence
Cold Spot - 90% Confidence
Not Significant
Hot Spot - 90% Confidence
Hot Spot - 95% Confidence
Hot Spot - 99% Confidence
Ca (Cluster-Outlier)
Not Significant
High-High Cluster
High-Low Outlier
Low-High Outlier
Low-Low Cluster
N
0 0.5 1 2 3
Metres

Magnesium

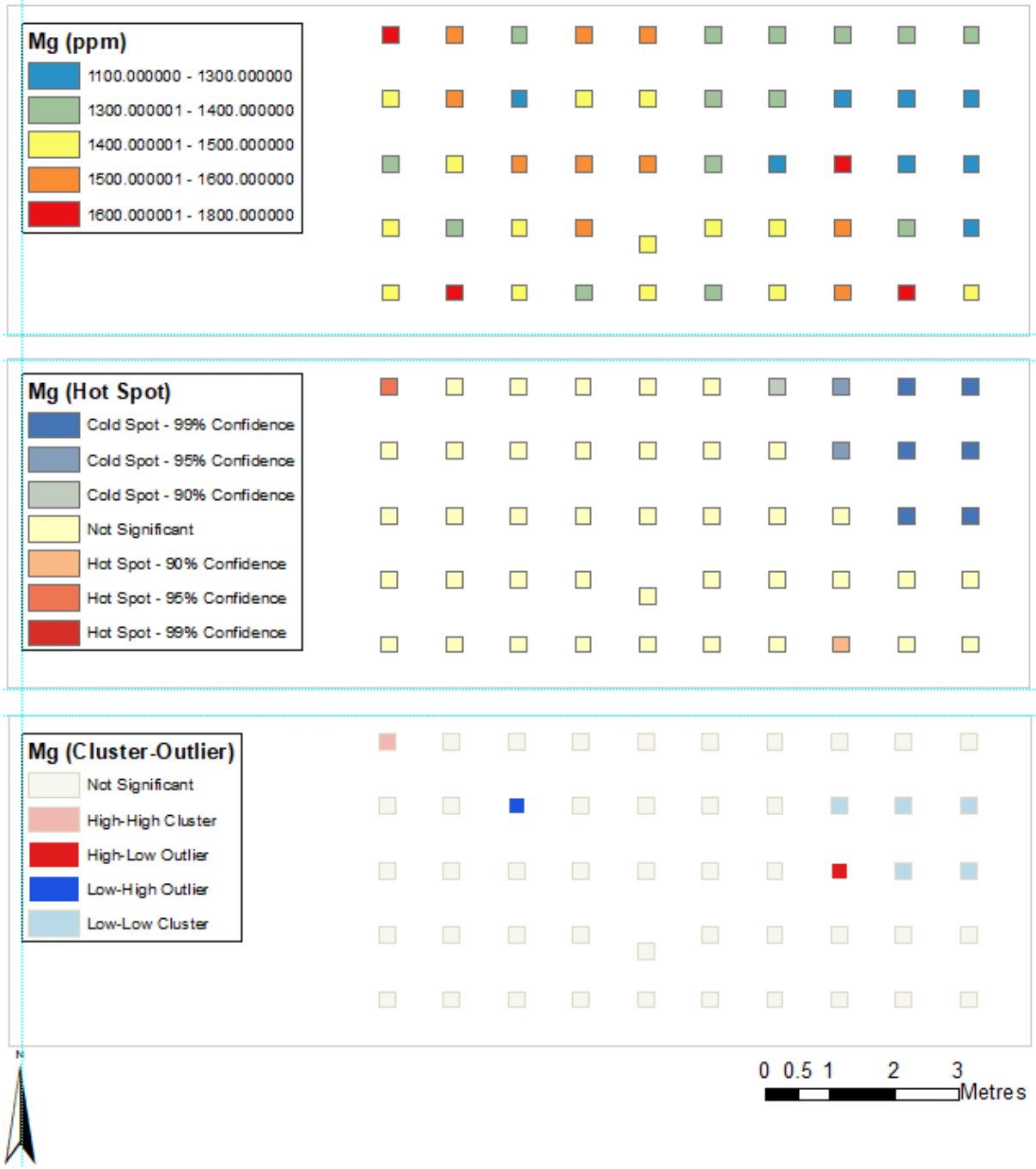
Mg (ppm)
1100.000000 - 1300.000000
1300.000001 - 1400.000000
1400.000001 - 1500.000000
1500.000001 - 1600.000000
1600.000001 - 1800.000000
Mg (Hot Spot)
Cold Spot - 99% Confidence
Cold Spot - 95% Confidence
Cold Spot - 90% Confidence
Not Significant
Hot Spot - 90% Confidence
Hot Spot - 95% Confidence
Hot Spot - 99% Confidence
Mg (Cluster-Outlier)
Not Significant
High-High Cluster
High-Low Outlier
Low-High Outlier
Low-Low Cluster
N
0 0.5 1 2 3
Metres

Trace

Barium

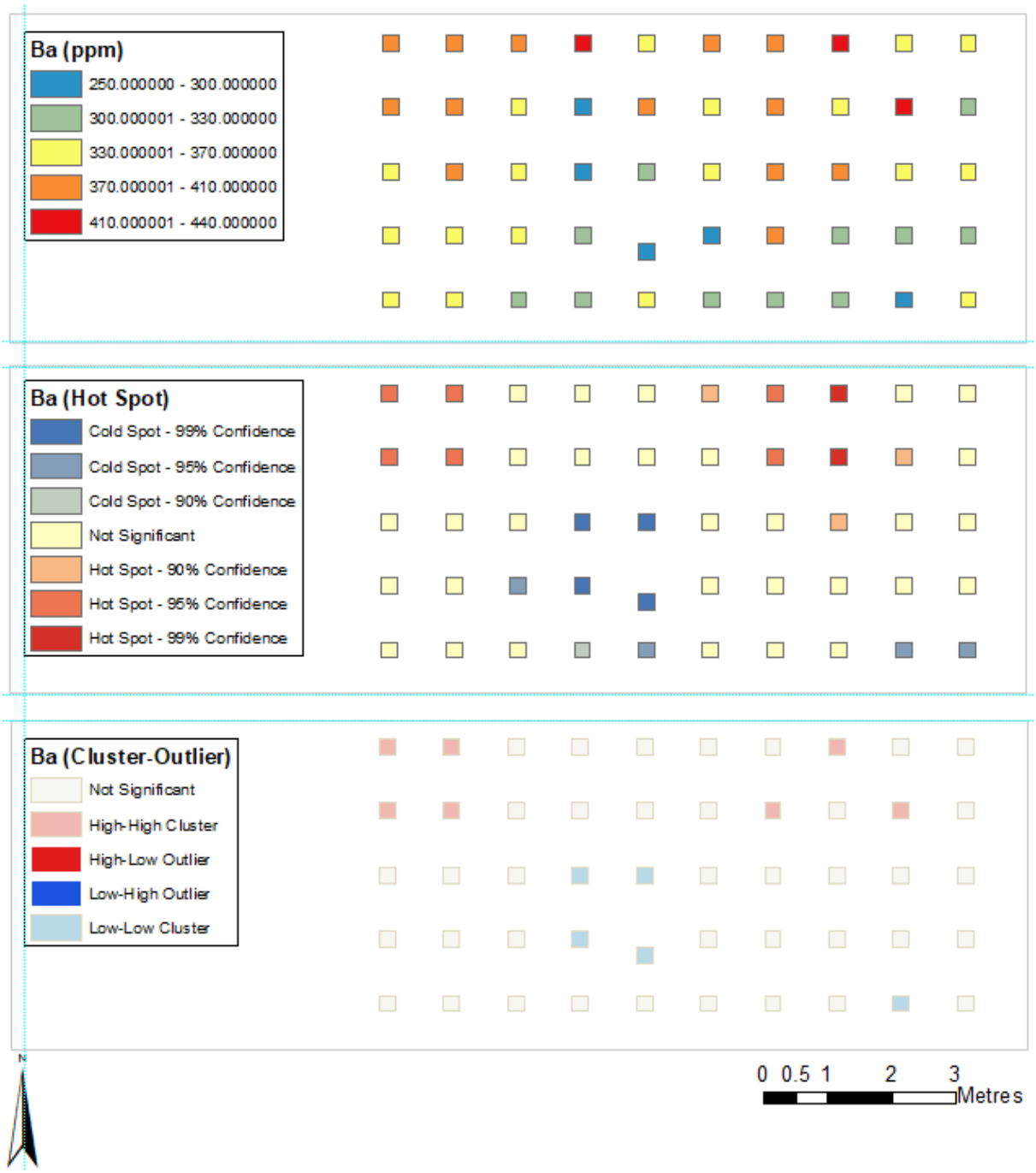

Potassium

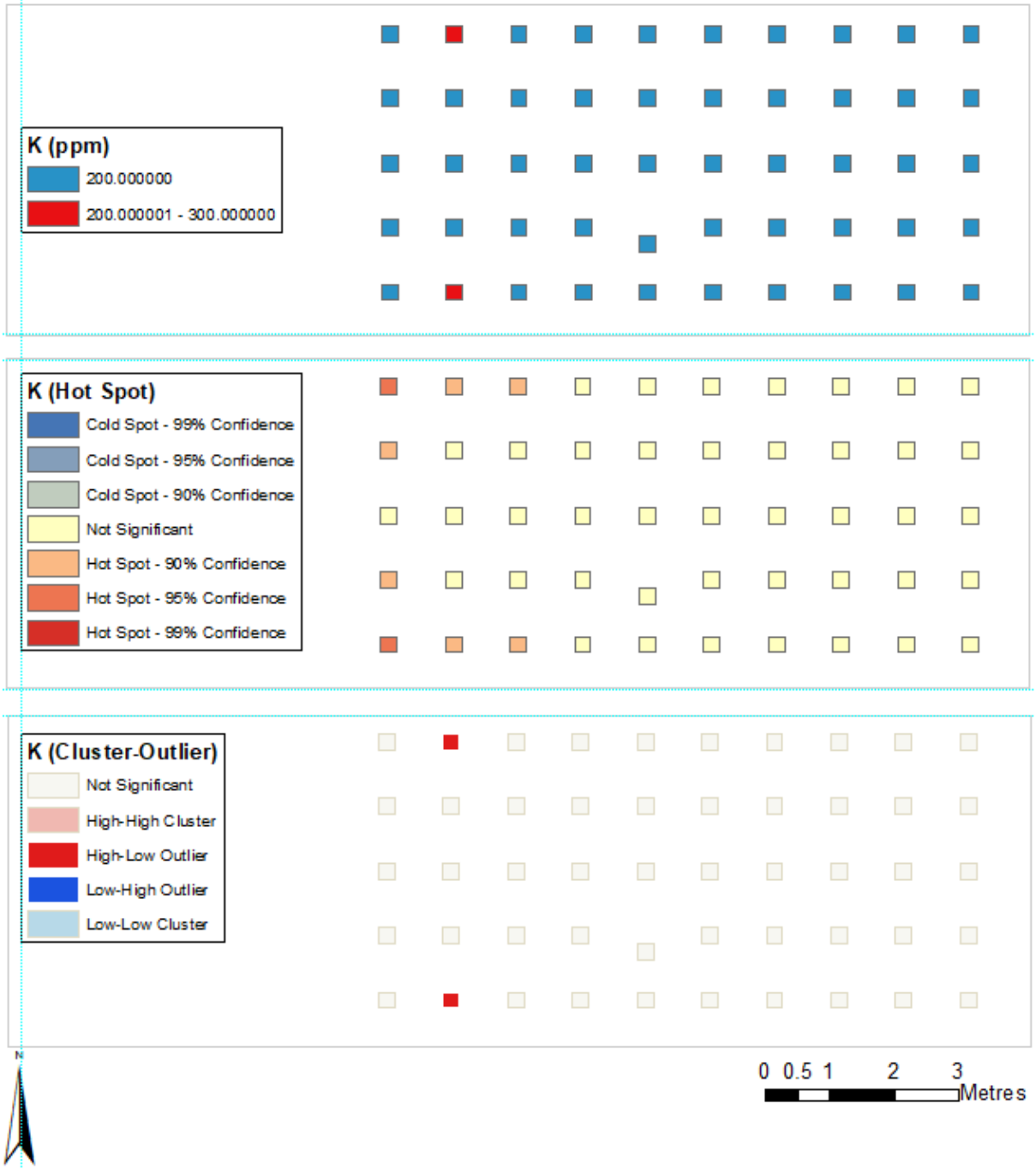
K (ppm)
200.000000
200.000001 - 300.000000
K (Hot Spot)
Cold Spot - 99% Confidence
Cold Spot - 95% Confidence
Cold Spot - 90% Confidence
Not Significant
Hot Spot - 90% Confidence
Hot Spot - 95% Confidence
Hot Spot - 99% Confidence
K (Cluster-Outlier)
Not Significant
High-High Cluster
High-Low Outlier
Low-High Outlier
Low-Low Cluster
N
0 0.5 1 2 3
Metres

Manganese

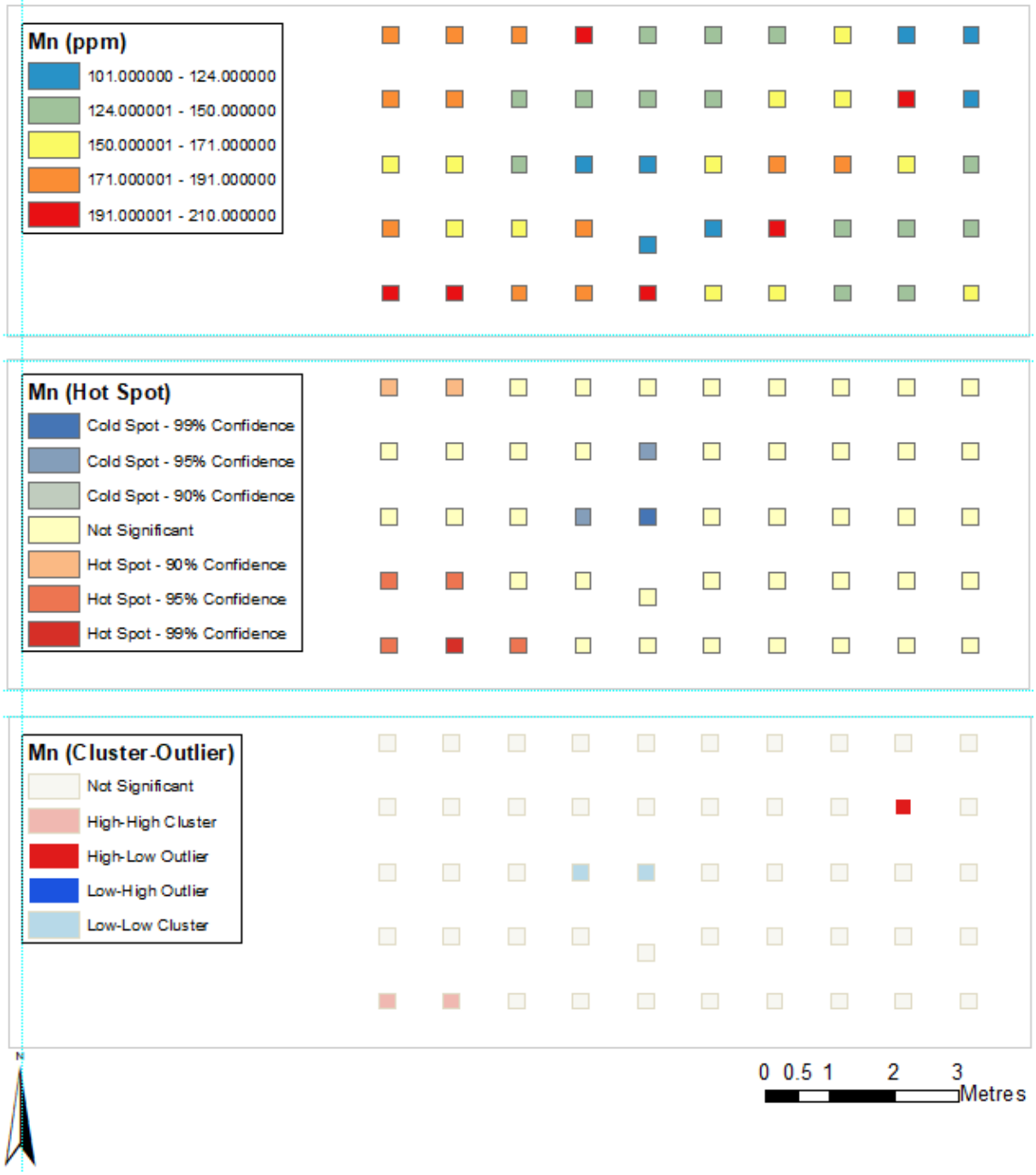
Mn (ppm)
101.000000 - 124.000000
124.000001 - 150.000000
150.000001 - 171.000000
171.000001 - 191.000000
191.000001 - 210.000000
Mn (Hot Spot)
Cold Spot - 99% Confidence
Cold Spot - 95% Confidence
Cold Spot - 90% Confidence
Not Significant
Hot Spot - 90% Confidence
Hot Spot - 95% Confidence
Hot Spot - 99% Confidence
Mn (Cluster-Outlier)
Not Significant
High-High Cluster
High-Low Outlier
Low-High Outlier
Low-Low Cluster
N
0 0.5 1 2 3
Metres

Phosphorus

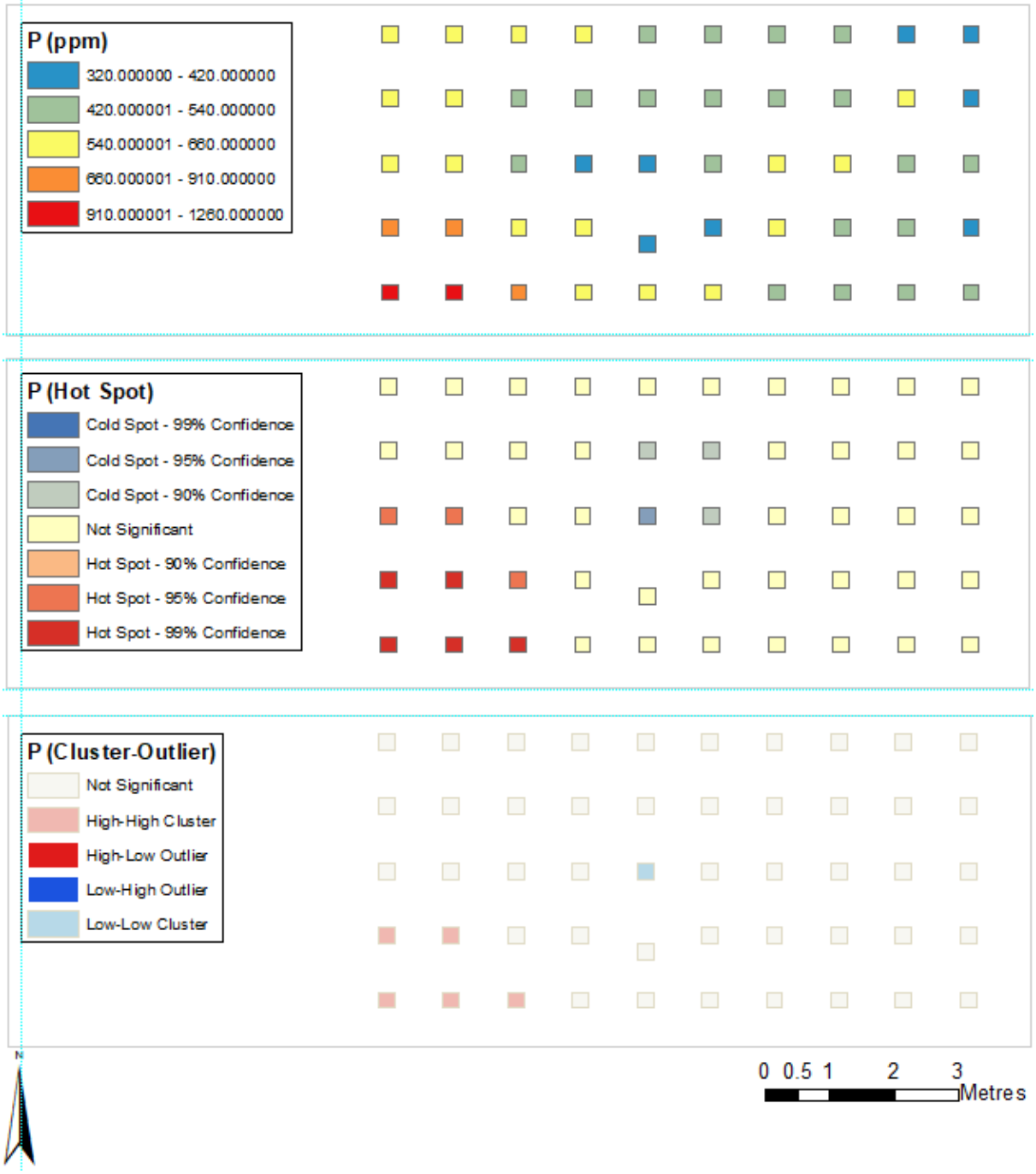
P (ppm)
320.000000 - 420.000000
420.000001 - 540.000000
540.000001 - 660.000000
660.000001 - 910.000000
910.000001 - 1260.000000
P (Hot Spot)
Cold Spot - 99% Confidence
Cold Spot - 95% Confidence
Cold Spot - 90% Confidence
Not Significant
Hot Spot - 90% Confidence
Hot Spot - 95% Confidence
Hot Spot - 99% Confidence
P (Cluster-Outlier)
Not Significant
High-High Cluster
High-Low Outlier
Low-High Outlier
Low-Low Cluster
N
0 0.5 1 2 3
Metres

Sulfur

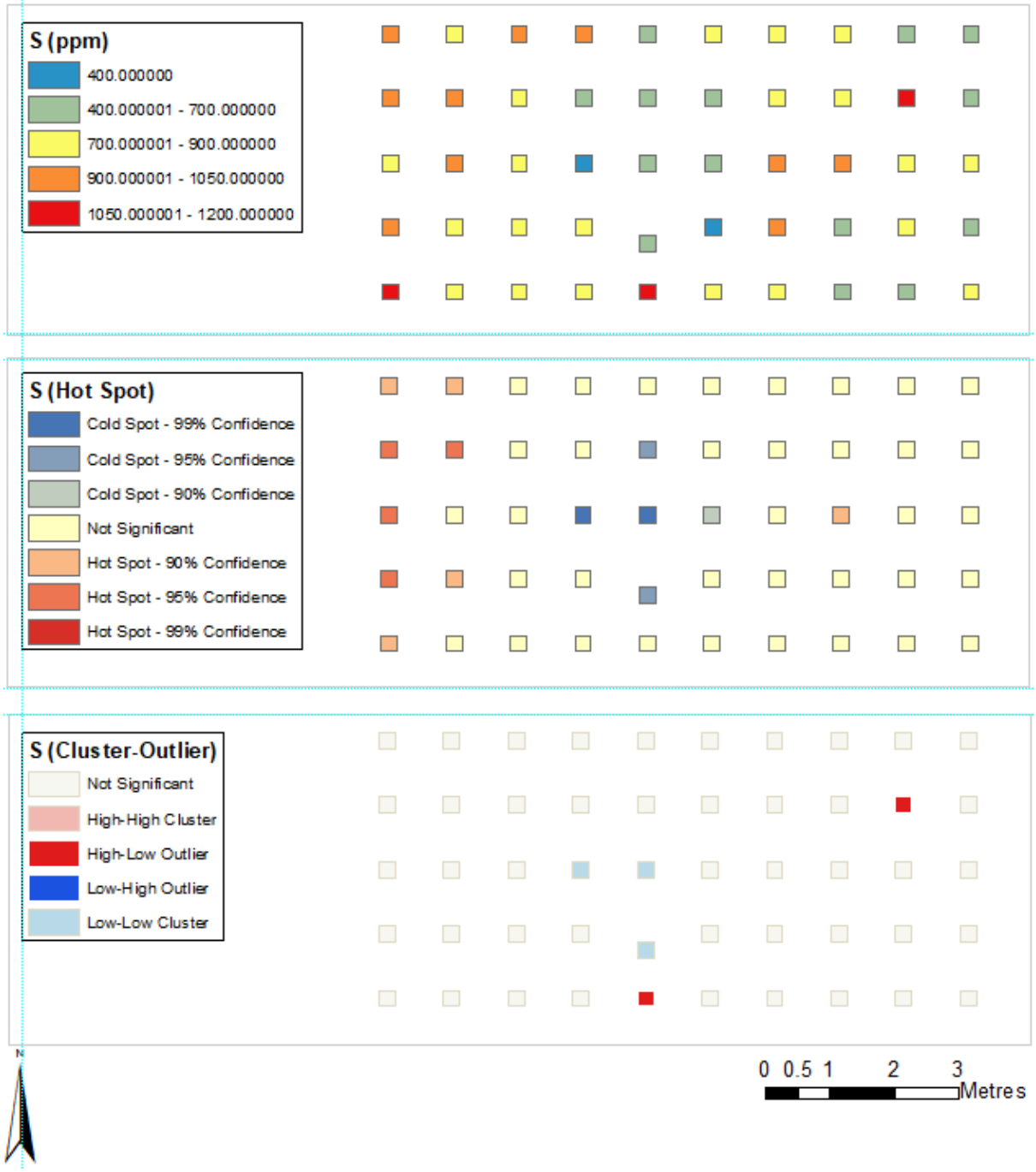
S (ppm)
400.000000
400.000001 - 700.000000
700.000001 - 900.000000
900.000001 - 1050.000000
1050.000001 - 1200.000000
S (Hot Spot)
Cold Spot - 99% Confidence
Cold Spot - 95% Confidence
Cold Spot - 90% Confidence
Not Significant
Hot Spot - 90% Confidence
Hot Spot - 95% Confidence
Hot Spot - 99% Confidence
S (Cluster-Outlier)
Not Significant
High-High Cluster
High-Low Outlier
Low-High Outlier
Low-Low Cluster
N
0 0.5 1 2 3
Metres

Titanium

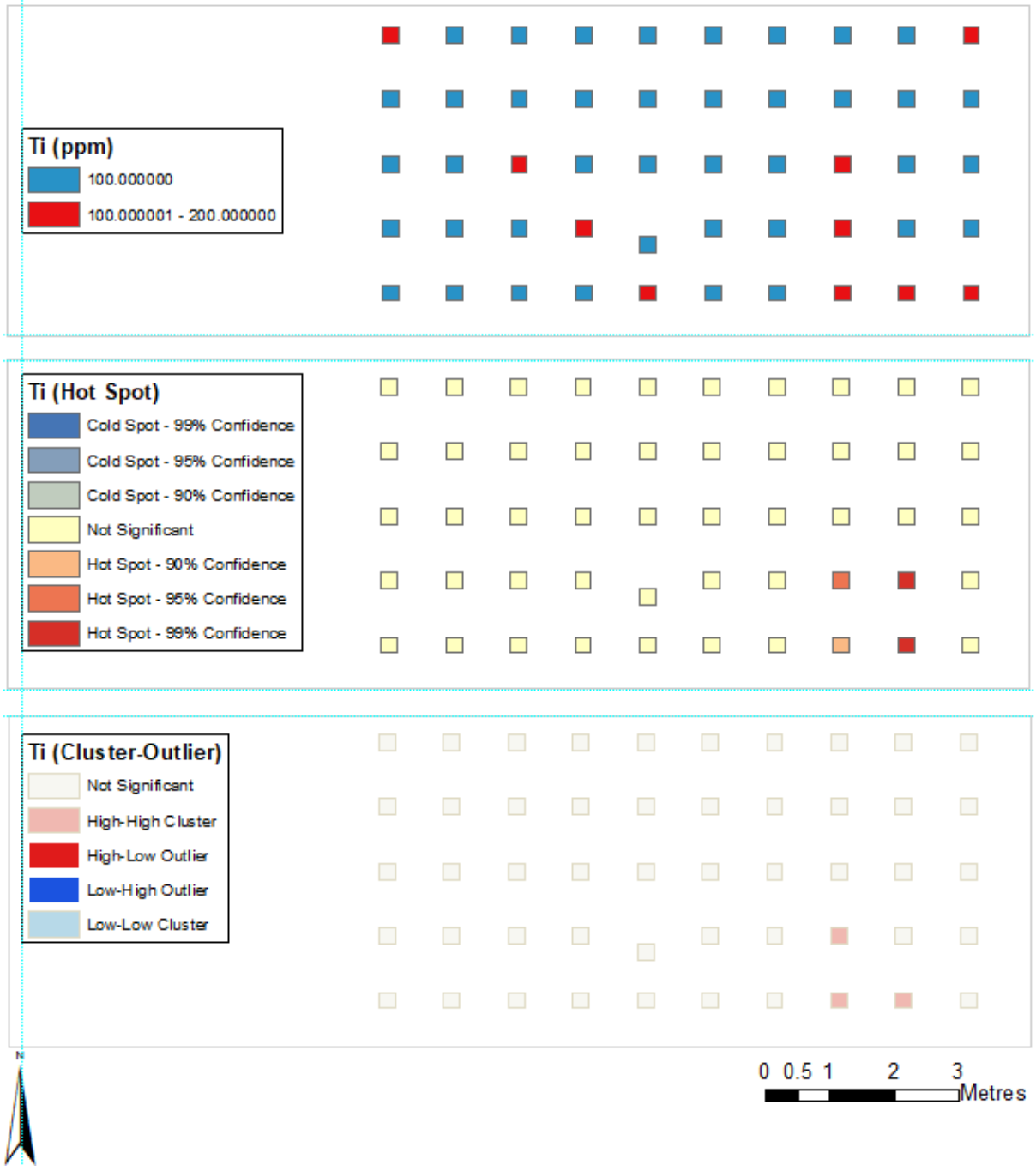
Ti (ppm)
100.000000
100.000001 - 200.000000
Ti (Hot Spot)
Cold Spot - 99% Confidence
Cold Spot - 95% Confidence
Cold Spot - 90% Confidence
Not Significant
Hot Spot - 90% Confidence
Hot Spot - 95% Confidence
Hot Spot - 99% Confidence
Ti (Cluster-Outlier)
Not Significant
High-High Cluster
High-Low Outlier
Low-High Outlier
Low-Low Cluster
N
0 0.5 1 2 3
Metres

Silver

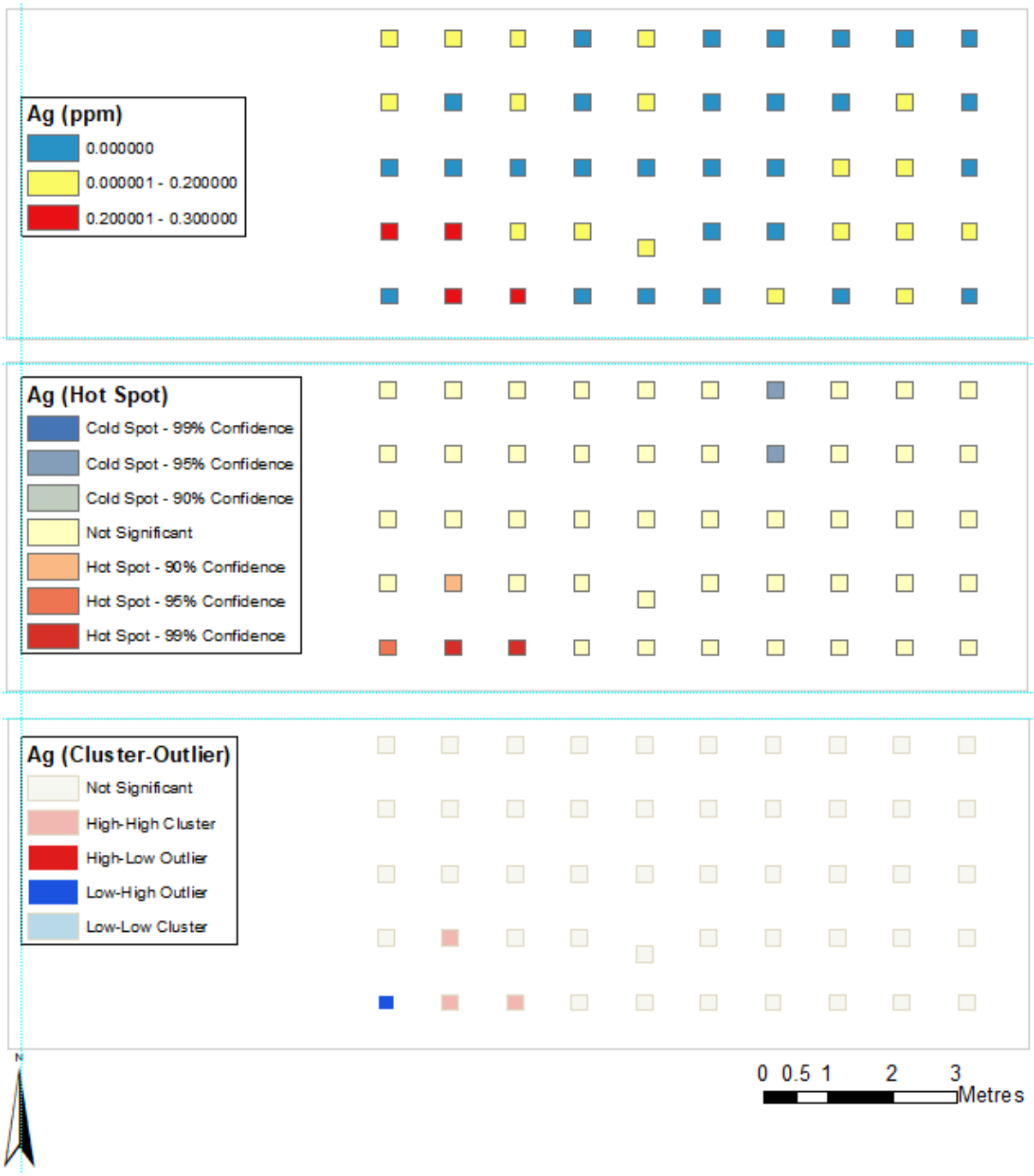
Ag (ppm)
0.000000
0.000001 - 0.200000
0.200001 - 0.300000
Ag (Hot Spot)
Cold Spot - 99% Confidence
Cold Spot - 95% Confidence
Cold Spot - 90% Confidence
Not Significant
Hot Spot - 90% Confidence
Hot Spot - 95% Confidence
Hot Spot - 99% Confidence
Ag (Cluster-Outlier)
Not Significant
High-High Cluster
High-Low Outlier
Low-High Outlier
Low-Low Cluster
N
0 0.5 1 2 3
Metres

Arsenic

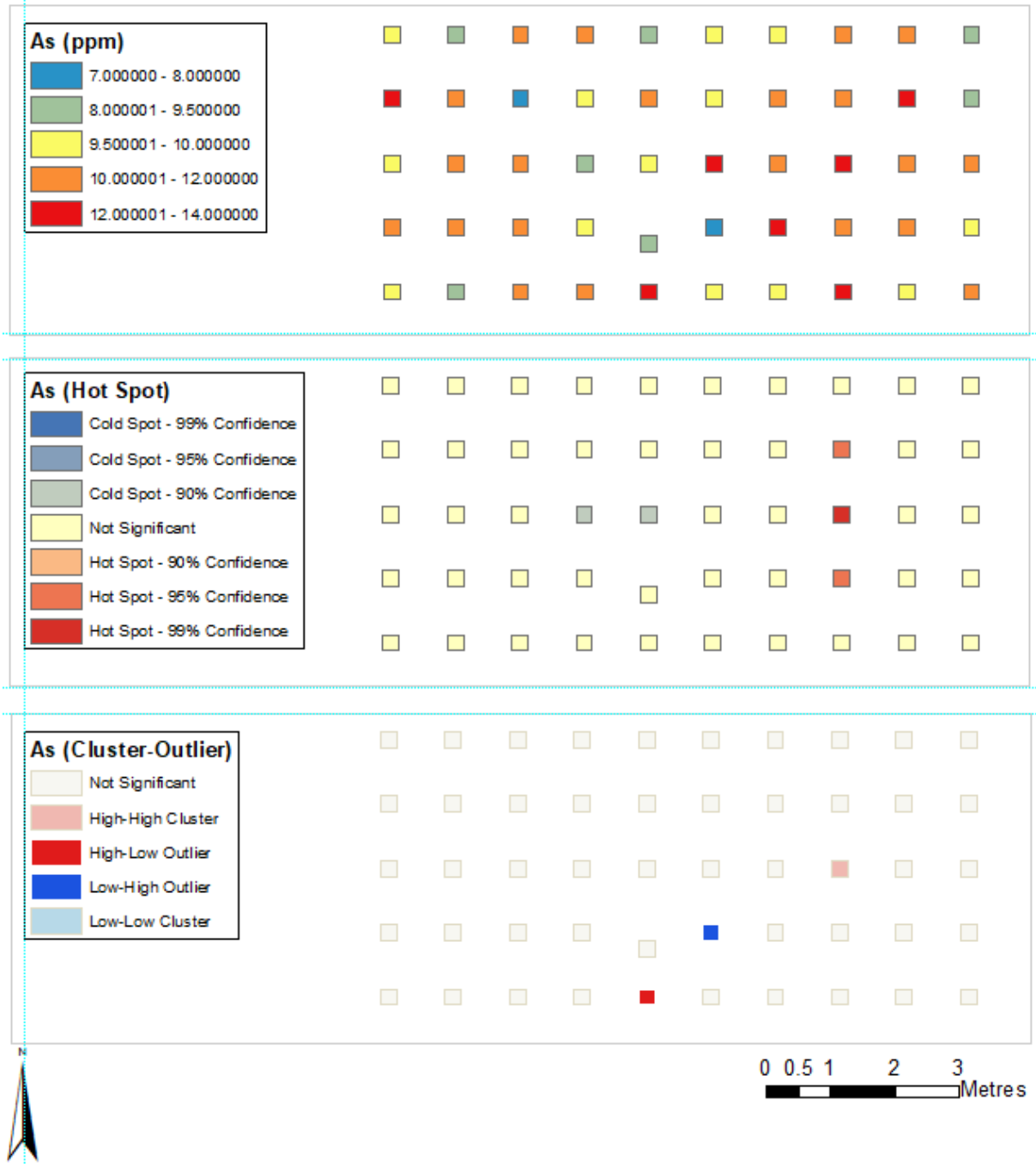
As (ppm)
7.000000 - 8.000000
8.000001 - 9.500000
9.500001 - 10.000000
10.000001 - 12.000000
12.000001 - 14.000000
As (Hot Spot)
Cold Spot - 99% Confidence
Cold Spot - 95% Confidence
Cold Spot - 90% Confidence
Not Significant
Hot Spot - 90% Confidence
Hot Spot - 95% Confidence
Hot Spot - 99% Confidence
As (Cluster-Outlier)
Not Significant
High-High Cluster
High-Low Outlier
Low-High Outlier
Low-Low Cluster
N
0 0.5 1 2 3
Metres

Boron

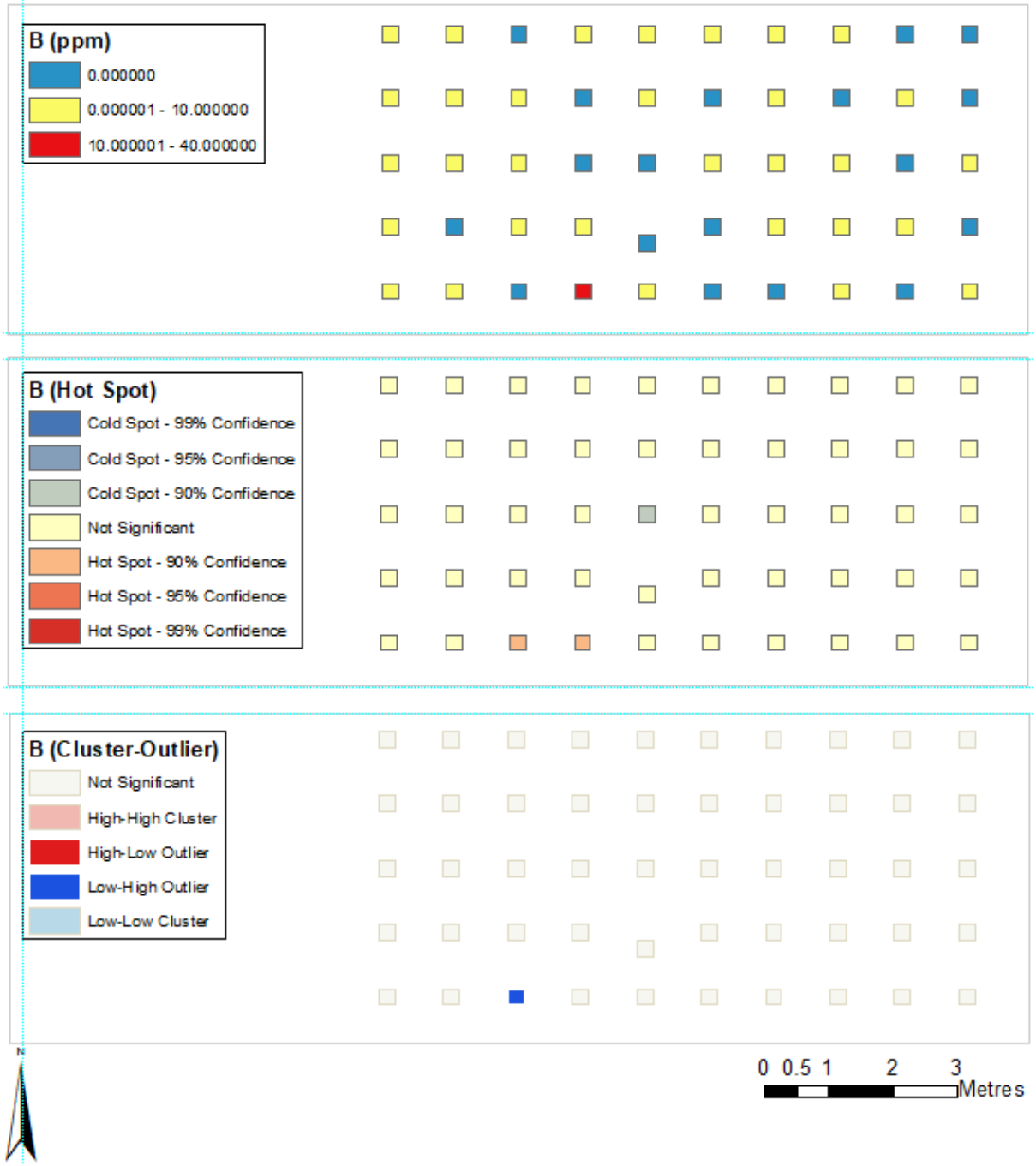
B (ppm)
0.000000
0.000001 - 10.000000
10.000001 - 40.000000
B (Hot Spot)
Cold Spot - 99% Confidence
Cold Spot - 95% Confidence
Cold Spot - 90% Confidence
Not Significant
Hot Spot - 90% Confidence
Hot Spot - 95% Confidence
Hot Spot - 99% Confidence
B (Cluster-Outlier)
Not Significant
High-High Cluster
High-Low Outlier
Low-High Outlier
Low-Low Cluster
N
0 0.5 1 2 3
Metres

Beryllium

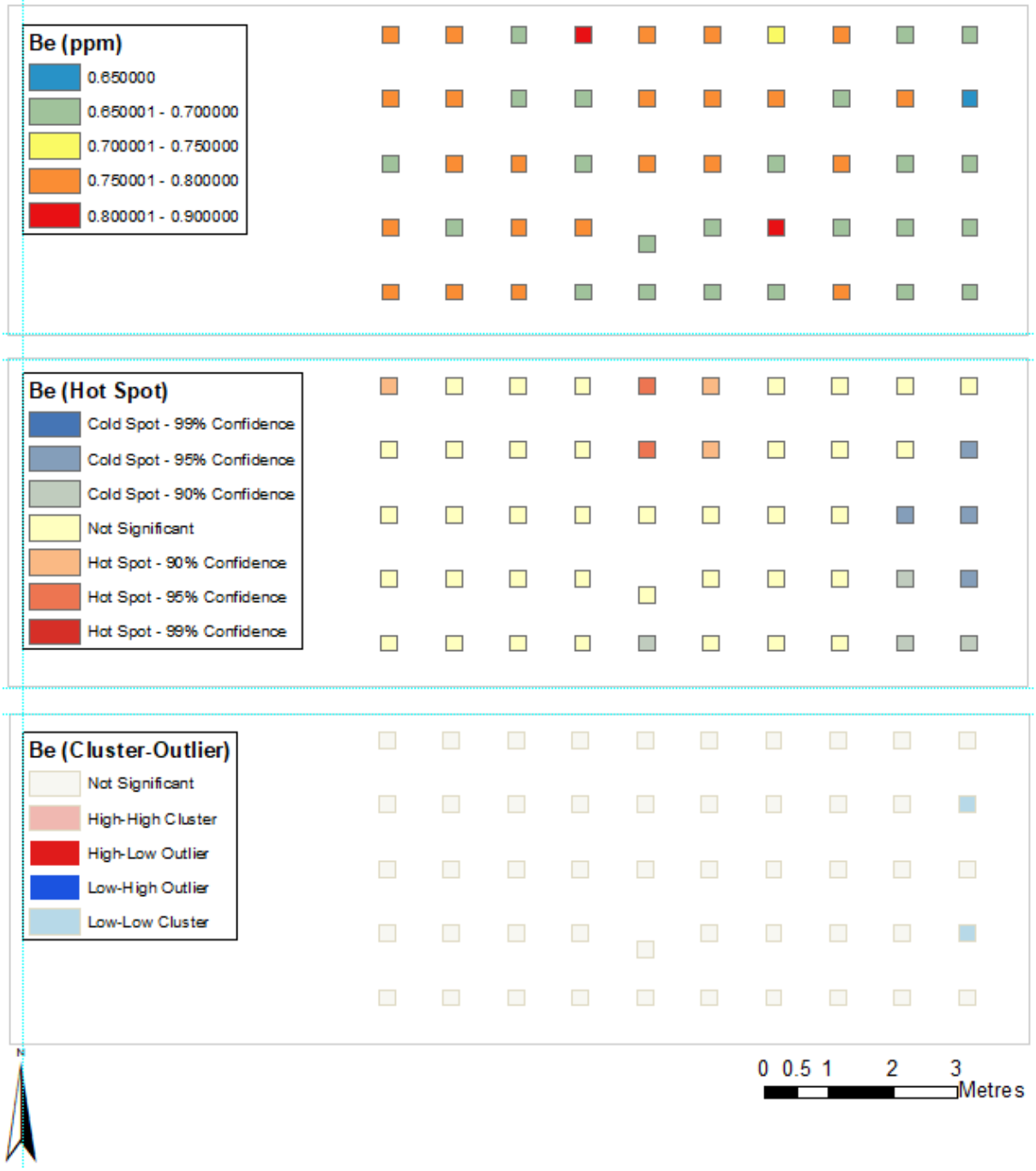
Be (ppm)
0.650000
0.650001 - 0.700000
0.700001 - 0.750000
0.750001 - 0.800000
0.800001 - 0.900000
Be (Hot Spot)
Cold Spot - 99% Confidence
Cold Spot - 95% Confidence
Cold Spot - 90% Confidence
Not Significant
Hot Spot - 90% Confidence
Hot Spot - 95% Confidence
Hot Spot - 99% Confidence
Be (Cluster-Outlier)
Not Significant
High-High Cluster
High-Low Outlier
Low-High Outlier
Low-Low Cluster
N
0 0.5 1 2 3
Metres

Cobalt

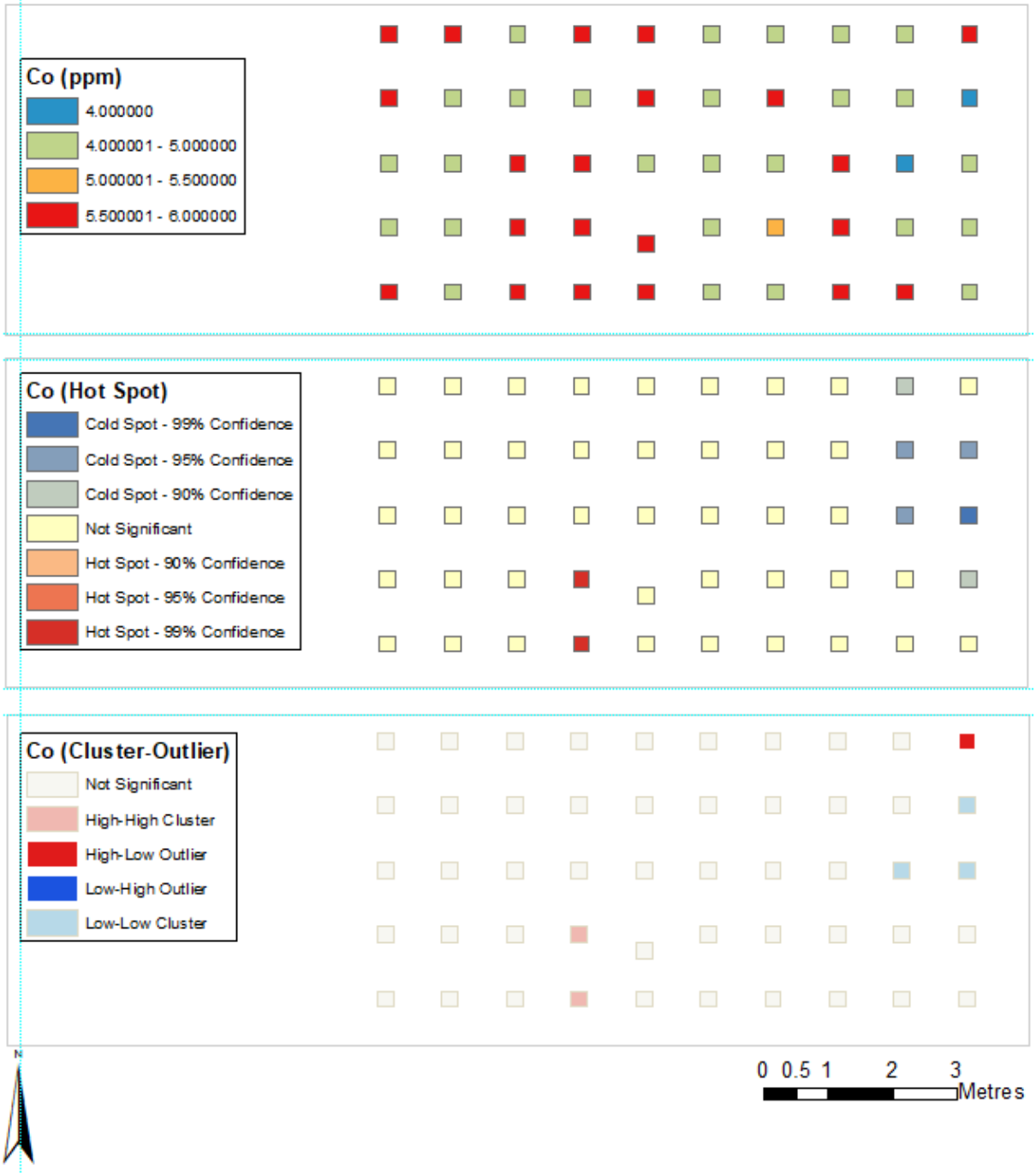
Co (ppm)
4.000000
4.000001 - 5.000000
5.000001 - 5.500000
5.500001 - 6.000000
Co (Hot Spot)
Cold Spot - 99% Confidence
Cold Spot - 95% Confidence
Cold Spot - 90% Confidence
Not Significant
Hot Spot - 90% Confidence
Hot Spot - 95% Confidence
Hot Spot - 99% Confidence
Co (Cluster-Outlier)
Not Significant
High-High Cluster
High-Low Outlier
Low-High Outlier
Low-Low Cluster
N
0 0.5 1 2 3
Metres

Chromium

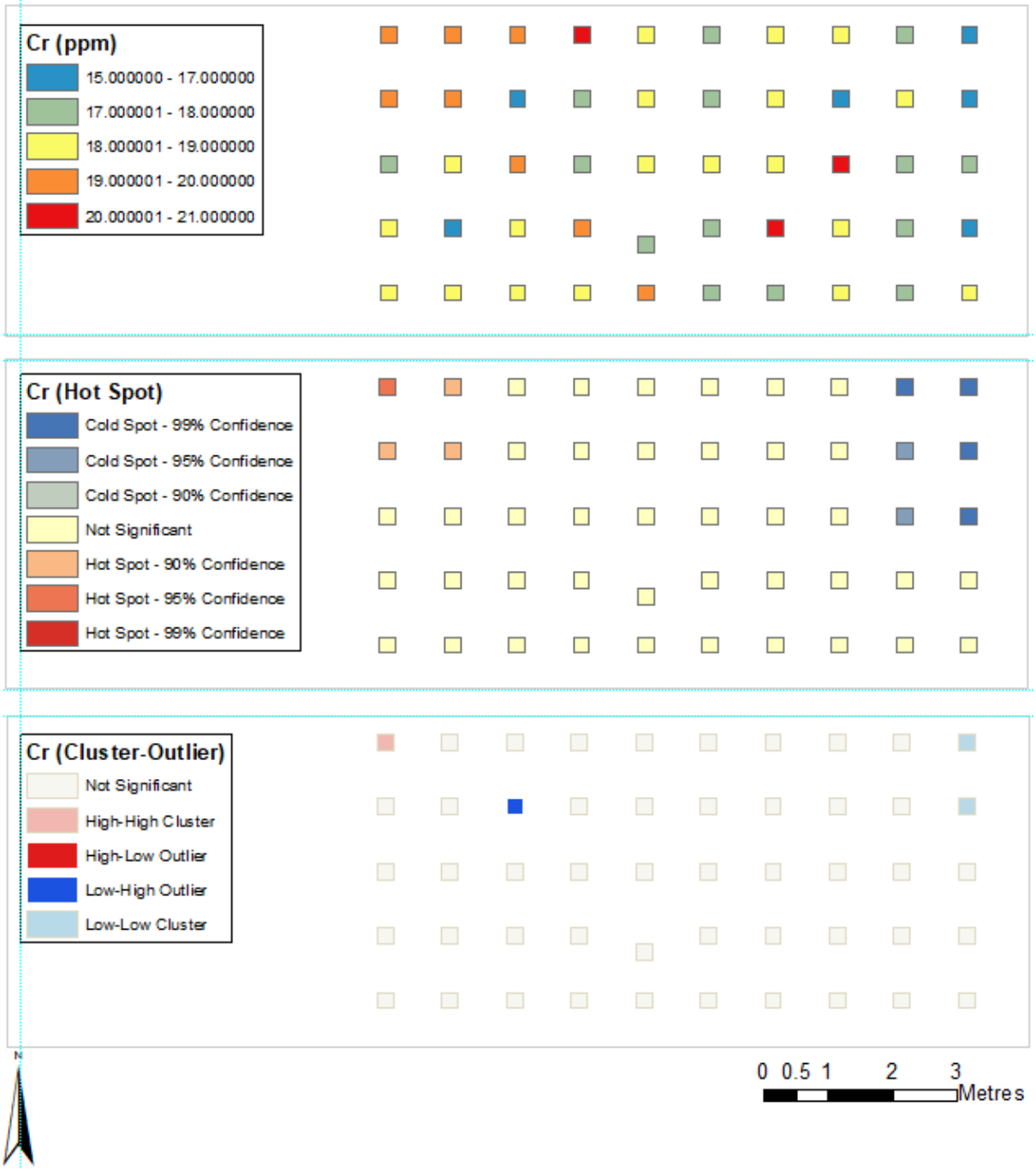
Cr (ppm)
15.000000 - 17.000000
17.000001 - 18.000000
18.000001 - 19.000000
19.000001 - 20.000000
20.000001 - 21.000000
Cr (Hot Spot)
Cold Spot - 99% Confidence
Cold Spot - 95% Confidence
Cold Spot - 90% Confidence
Not Significant
Hot Spot - 90% Confidence
Hot Spot - 95% Confidence
Hot Spot - 99% Confidence
Cr (Cluster-Outlier)
Not Significant
High-High Cluster
High-Low Outlier
Low-High Outlier
Low-Low Cluster
N
0 0.5 1 2 3
Metres

Copper

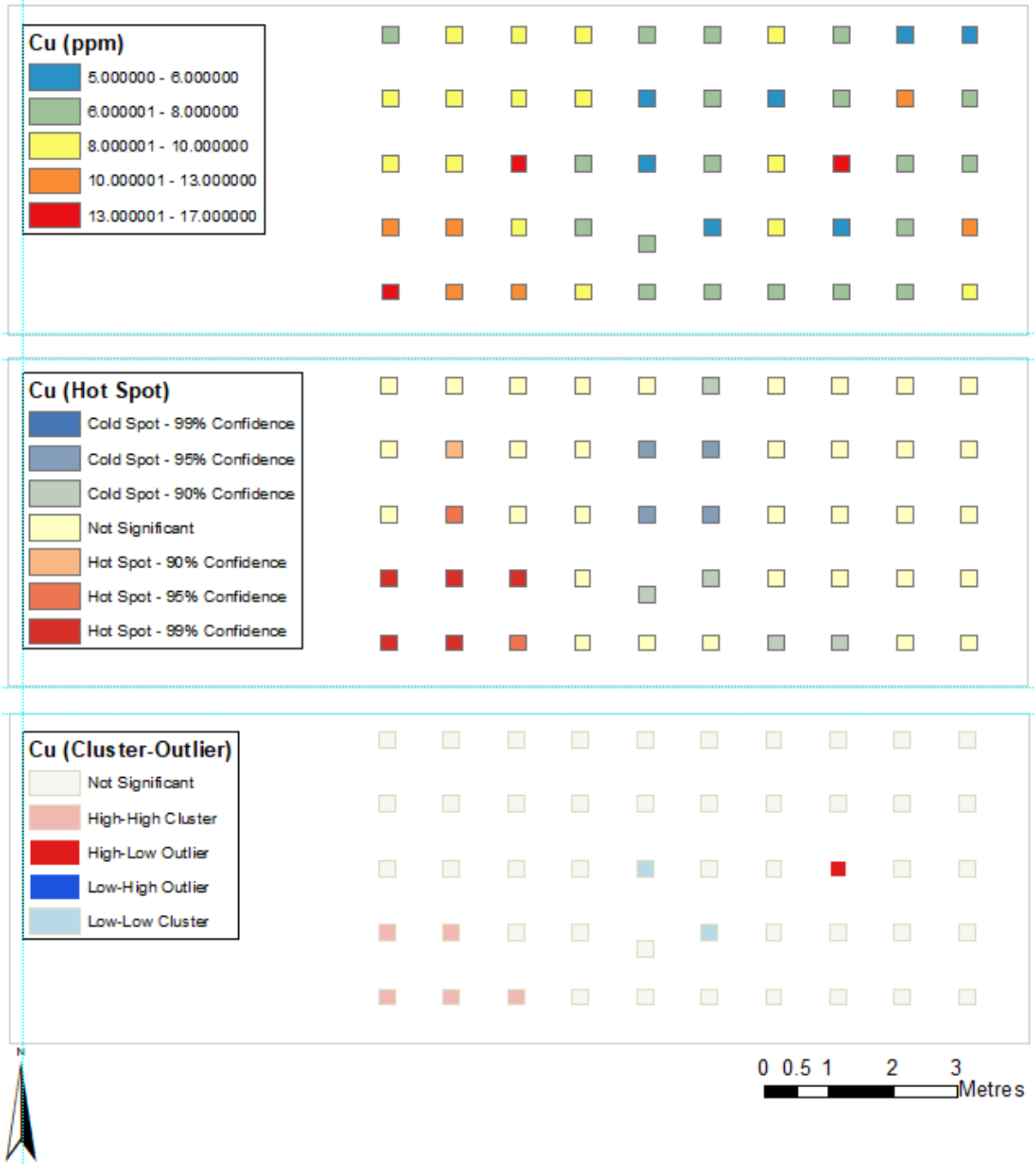
Cu (ppm)
5.000000 - 6.000000
6.000001 - 8.000000
8.000001 - 10.000000
10.000001 - 13.000000
13.000001 - 17.000000
Cu (Hot Spot)
Cold Spot - 99% Confidence
Cold Spot - 95% Confidence
Cold Spot - 90% Confidence
Not Significant
Hot Spot - 90% Confidence
Hot Spot - 95% Confidence
Hot Spot - 99% Confidence
Cu (Cluster-Outlier)
Not Significant
High-High Cluster
High-Low Outlier
Low-High Outlier
Low-Low Cluster
N
0 0.5 1 2 3
Metres

Mercury

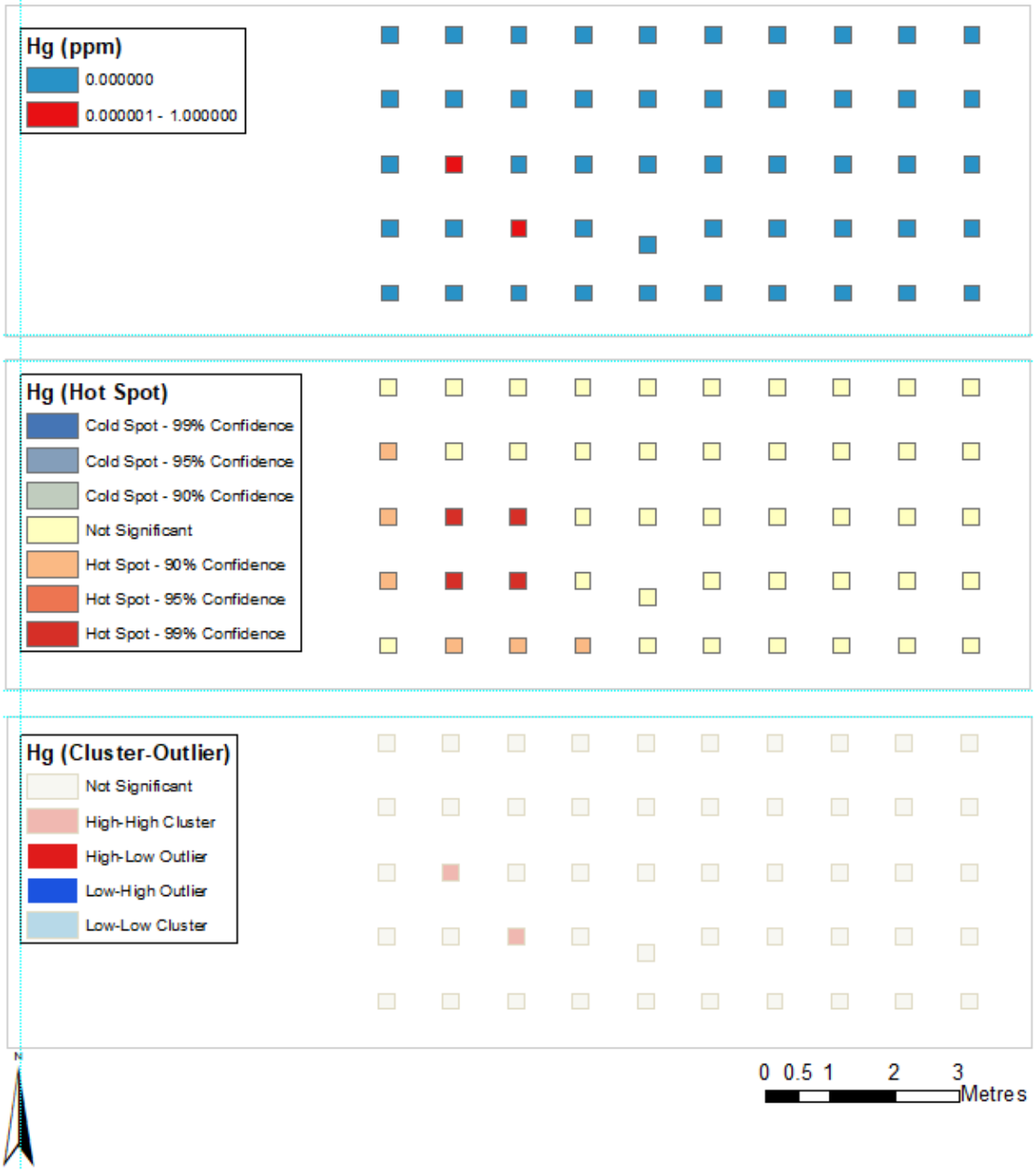
Hg (ppm)
0.000000
0.000001 - 1.000000
Hg (Hot Spot)
Cold Spot - 99% Confidence
Cold Spot - 95% Confidence
Cold Spot - 90% Confidence
Not Significant
Hot Spot - 90% Confidence
Hot Spot - 95% Confidence
Hot Spot - 99% Confidence
Hg (Cluster-Outlier)
Not Significant
High-High Cluster
High-Low Outlier
Low-High Outlier
Low-Low Cluster
N
0 0.5 1 2 3
Metres

Lanthanum

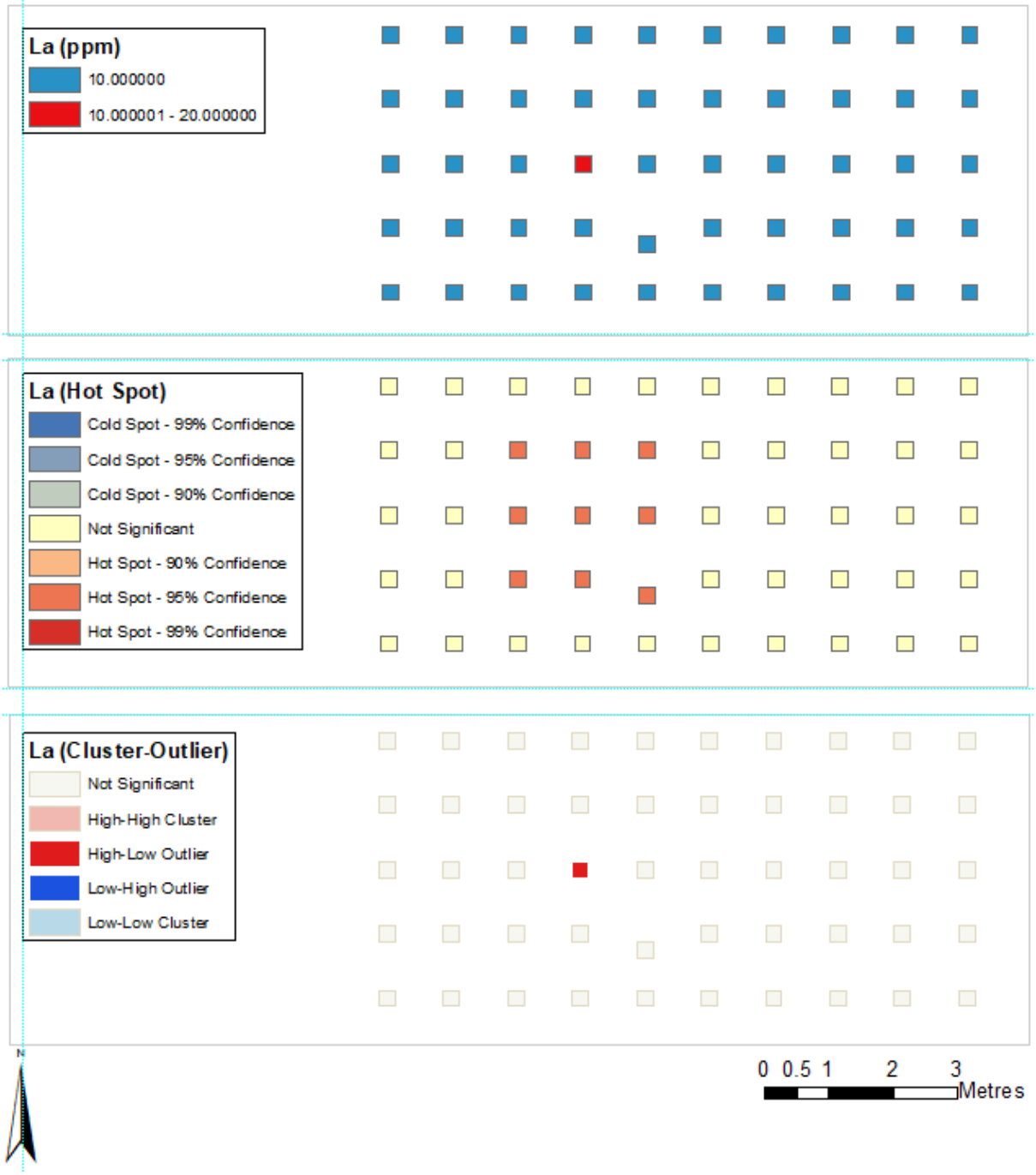
La (ppm)
10.000000
10.000001 - 20.000000
La (Hot Spot)
Cold Spot - 99% Confidence
Cold Spot - 95% Confidence
Cold Spot - 90% Confidence
Not Significant
Hot Spot - 90% Confidence
Hot Spot - 95% Confidence
Hot Spot - 99% Confidence
La (Cluster-Outlier)
Not Significant
High-High Cluster
High-Low Outlier
Low-High Outlier
Low-Low Cluster
N
0 0.5 1 2 3
Metres

Molybdenum

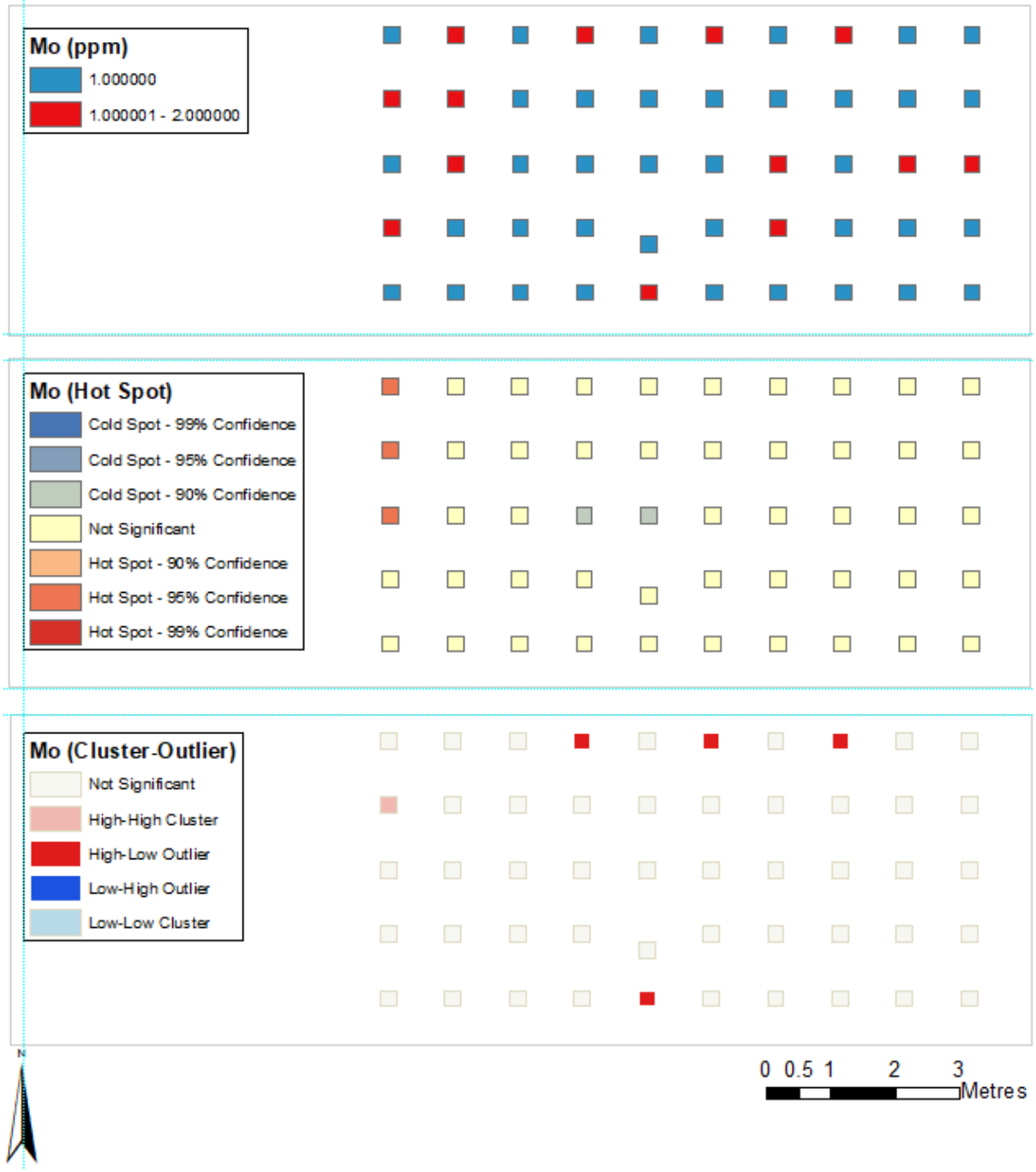
Mo (ppm)
1.000000
1.000001 - 2.000000
Mo (Hot Spot)
Cold Spot - 99% Confidence
Cold Spot - 95% Confidence
Cold Spot - 90% Confidence
Not Significant
Hot Spot - 90% Confidence
Hot Spot - 95% Confidence
Hot Spot - 99% Confidence
Mo (Cluster-Outlier)
Not Significant
High-High Cluster
High-Low Outlier
Low-High Outlier
Low-Low Cluster
N
0 0.5 1 2 3
Metres

Nickel

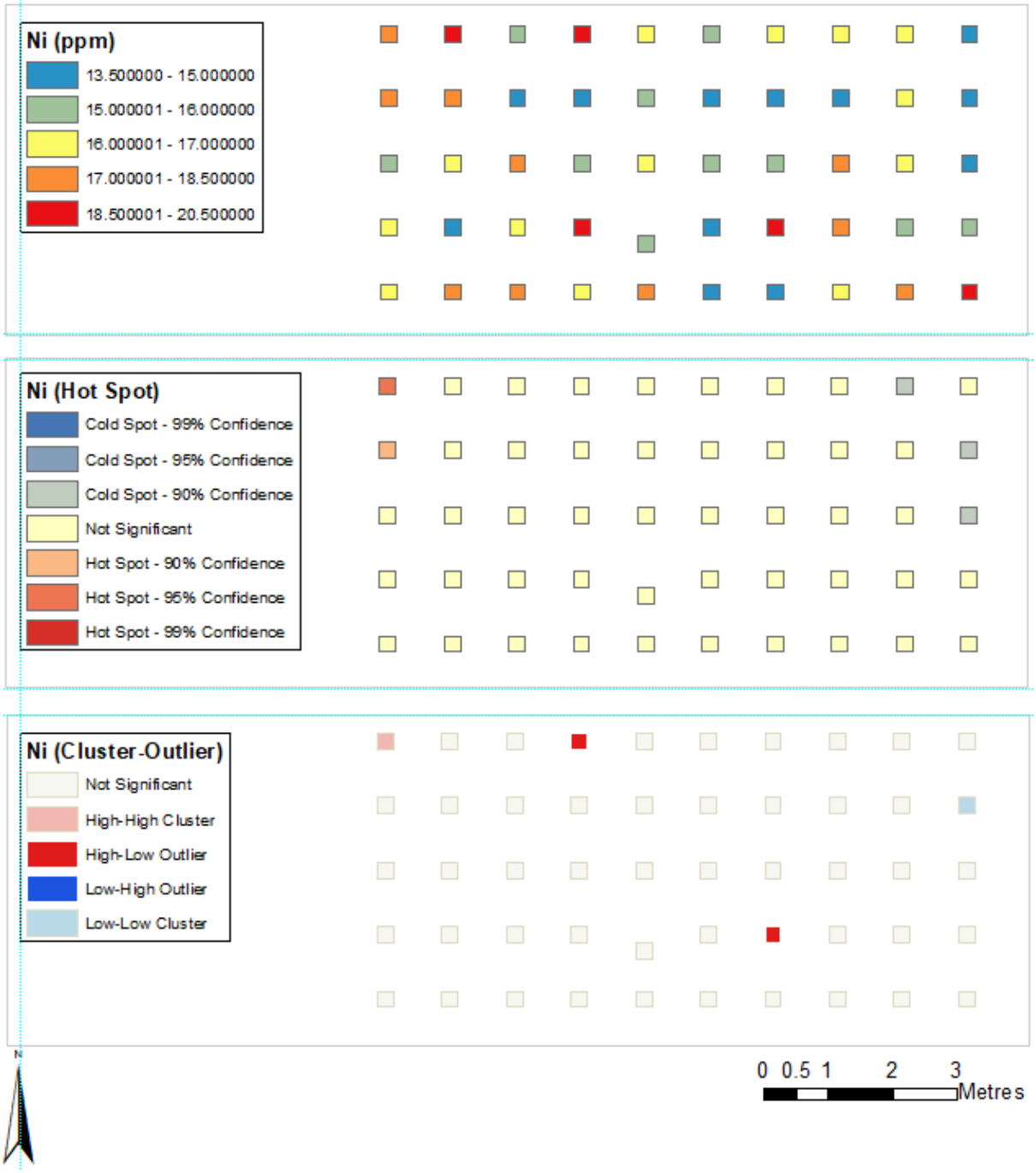
Ni (ppm)
13.500000 - 15.000000
15.000001 - 16.000000
16.000001 - 17.000000
17.000001 - 18.500000
18.500001 - 20.500000
Ni (Hot Spot)
Cold Spot - 99% Confidence
Cold Spot - 95% Confidence
Cold Spot - 90% Confidence
Not Significant
Hot Spot - 90% Confidence
Hot Spot - 95% Confidence
Hot Spot - 99% Confidence
Ni (Cluster-Outlier)
Not Significant
High-High Cluster
High-Low Outlier
Low-High Outlier
Low-Low Cluster
N
0 0.5 1 2 3
Metres

Lead

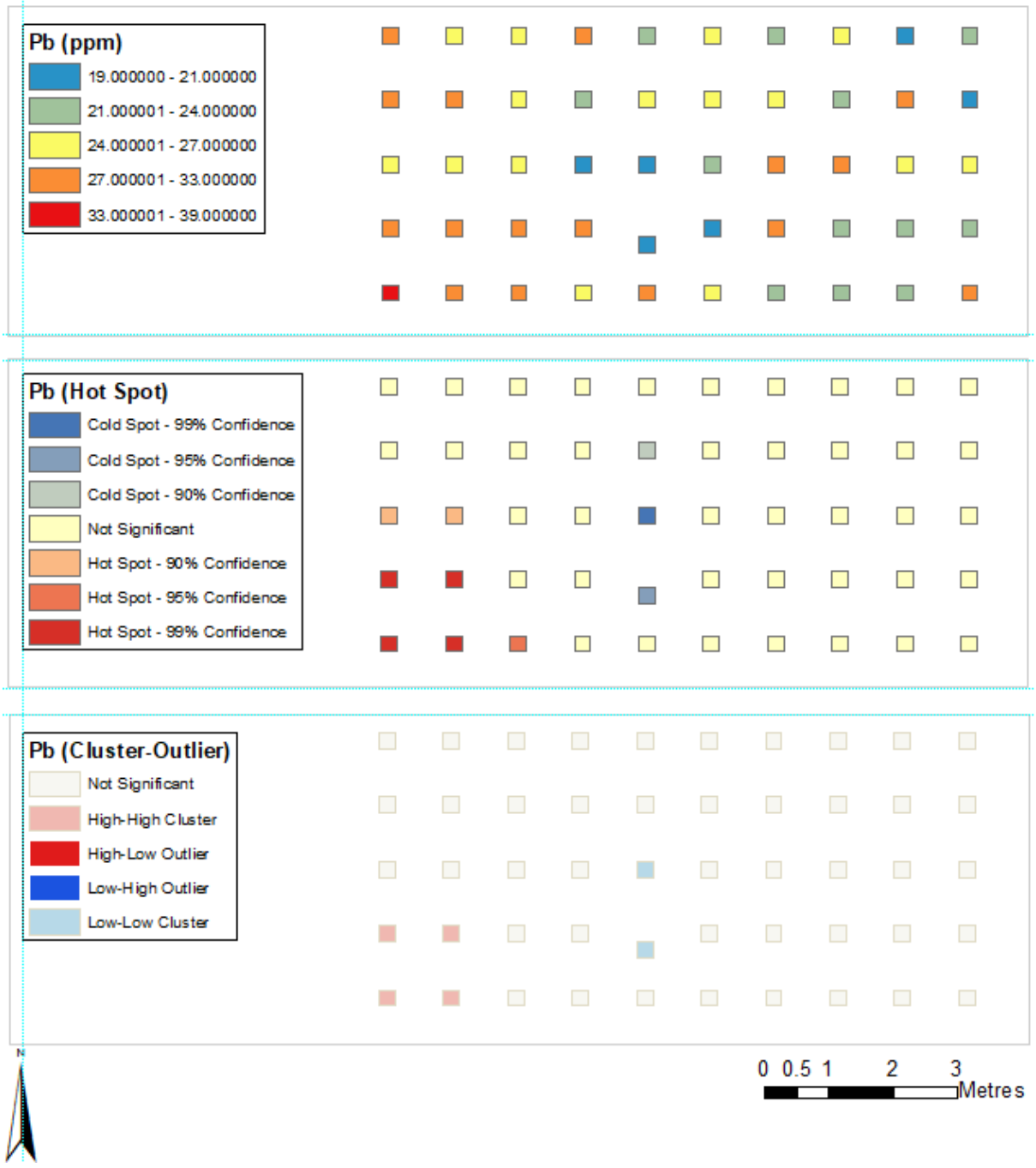
Pb (ppm)
19.000000 - 21.000000
21.000001 - 24.000000
24.000001 - 27.000000
27.000001 - 33.000000
33.000001 - 39.000000
Pb (Hot Spot)
Cold Spot - 99% Confidence
Cold Spot - 95% Confidence
Cold Spot - 90% Confidence
Not Significant
Hot Spot - 90% Confidence
Hot Spot - 95% Confidence
Hot Spot - 99% Confidence
Pb (Cluster-Outlier)
Not Significant
High-High Cluster
High-Low Outlier
Low-High Outlier
Low-Low Cluster
N
0 0.5 1 2 3
Metres

Tin

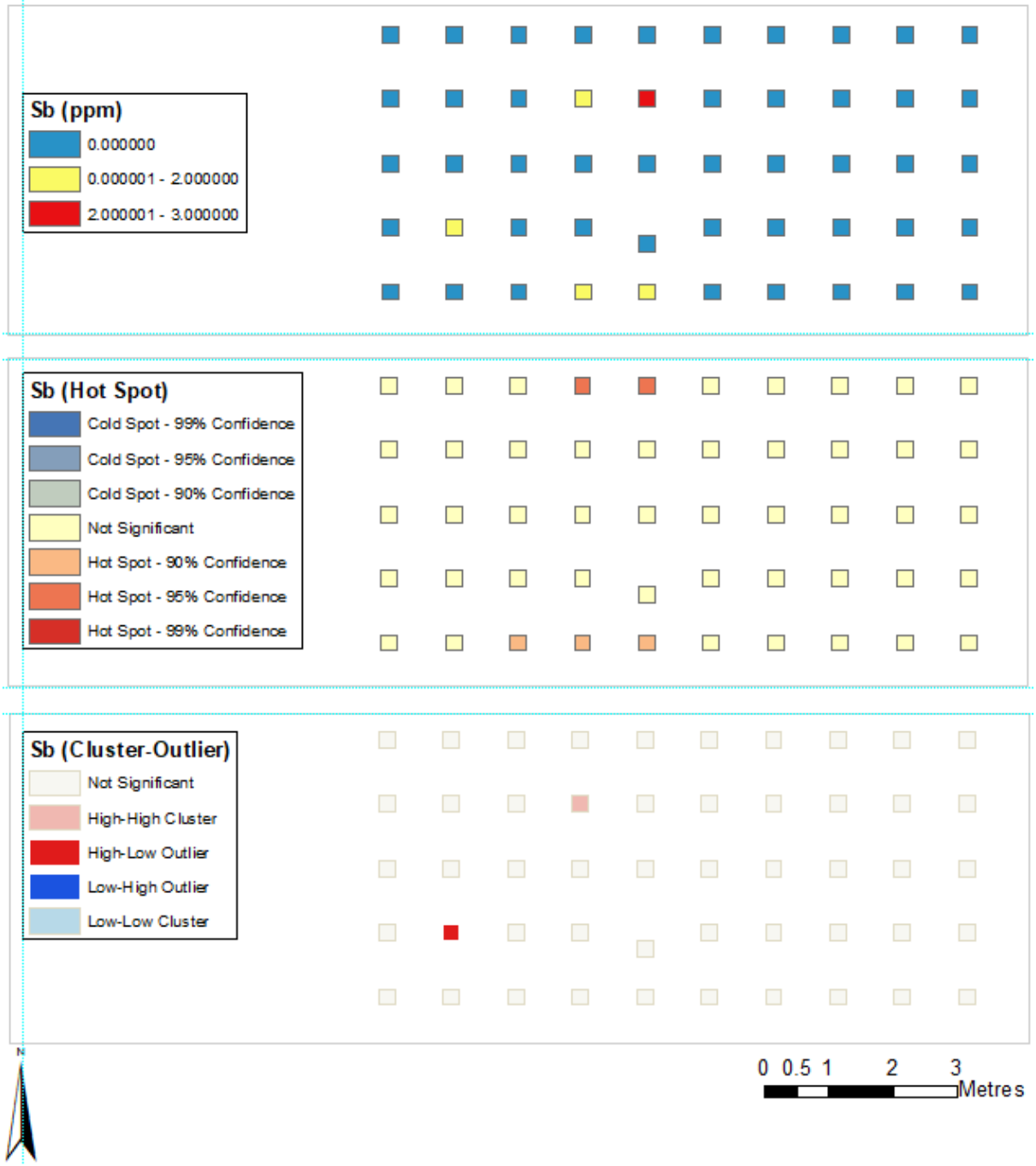
Sb (ppm)
0.000000
0.000001 - 2.000000
2.000001 - 3.000000
Sb (Hot Spot)
Cold Spot - 99% Confidence
Cold Spot - 95% Confidence
Cold Spot - 90% Confidence
Not Significant
Hot Spot - 90% Confidence
Hot Spot - 95% Confidence
Hot Spot - 99% Confidence
Sb (Cluster-Outlier)
Not Significant
High-High Cluster
High-Low Outlier
Low-High Outlier
Low-Low Cluster
N
0 0.5 1 2 3
Metres

Scandium

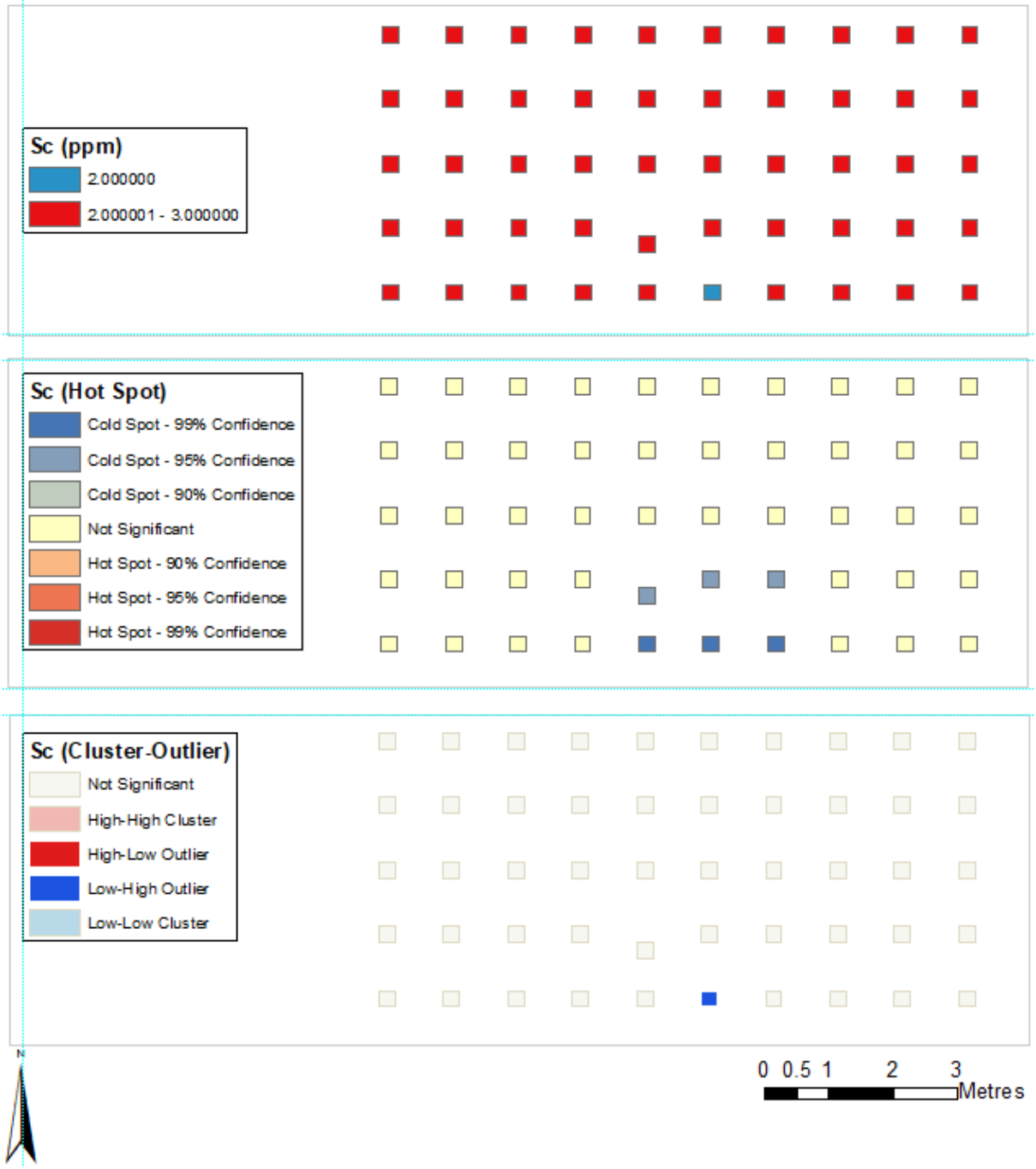
Sc (ppm)
2.000000
2.000001 - 3.000000
Sc (Hot Spot)
Cold Spot - 99% Confidence
Cold Spot - 95% Confidence
Cold Spot - 90% Confidence
Not Significant
Hot Spot - 90% Confidence
Hot Spot - 95% Confidence
Hot Spot - 99% Confidence
Sc (Cluster-Outlier)
Not Significant
High-High Cluster
High-Low Outlier
Low-High Outlier
Low-Low Cluster
N
0 0.5 1 2 3
Metres

Strontium

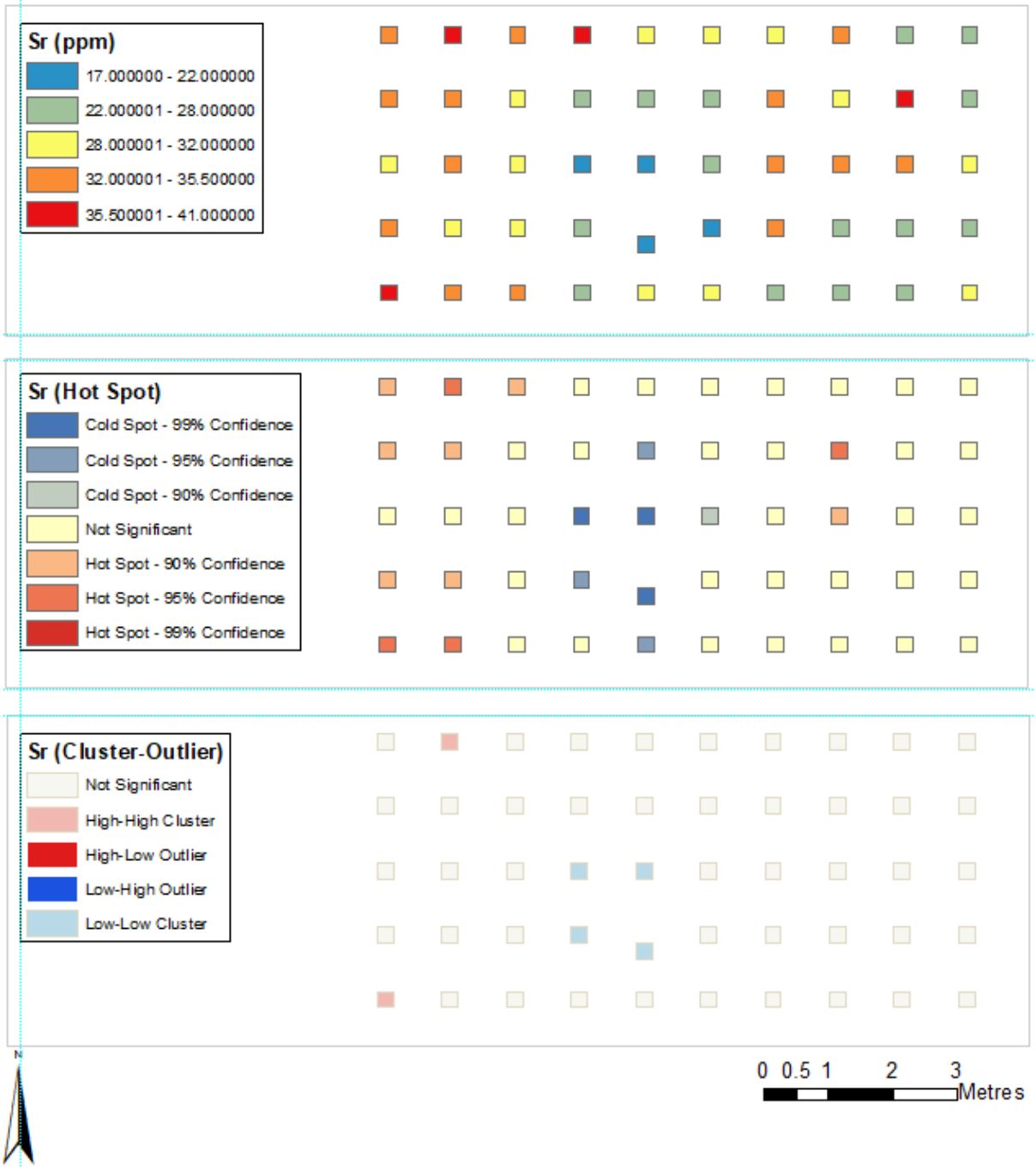
Sr (ppm)
17.000000 - 22.000000
22.000001 - 28.000000
28.000001 - 32.000000
32.000001 - 35.500000
35.500001 - 41.000000
Sr (Hot Spot)
Cold Spot - 99% Confidence
Cold Spot - 95% Confidence
Cold Spot - 90% Confidence
Not Significant
Hot Spot - 90% Confidence
Hot Spot - 95% Confidence
Hot Spot - 99% Confidence
Sr (Cluster-Outlier)
Not Significant
High-High Cluster
High-Low Outlier
Low-High Outlier
Low-Low Cluster
N
0 0.5 1 2 3
Metres

Vanadium

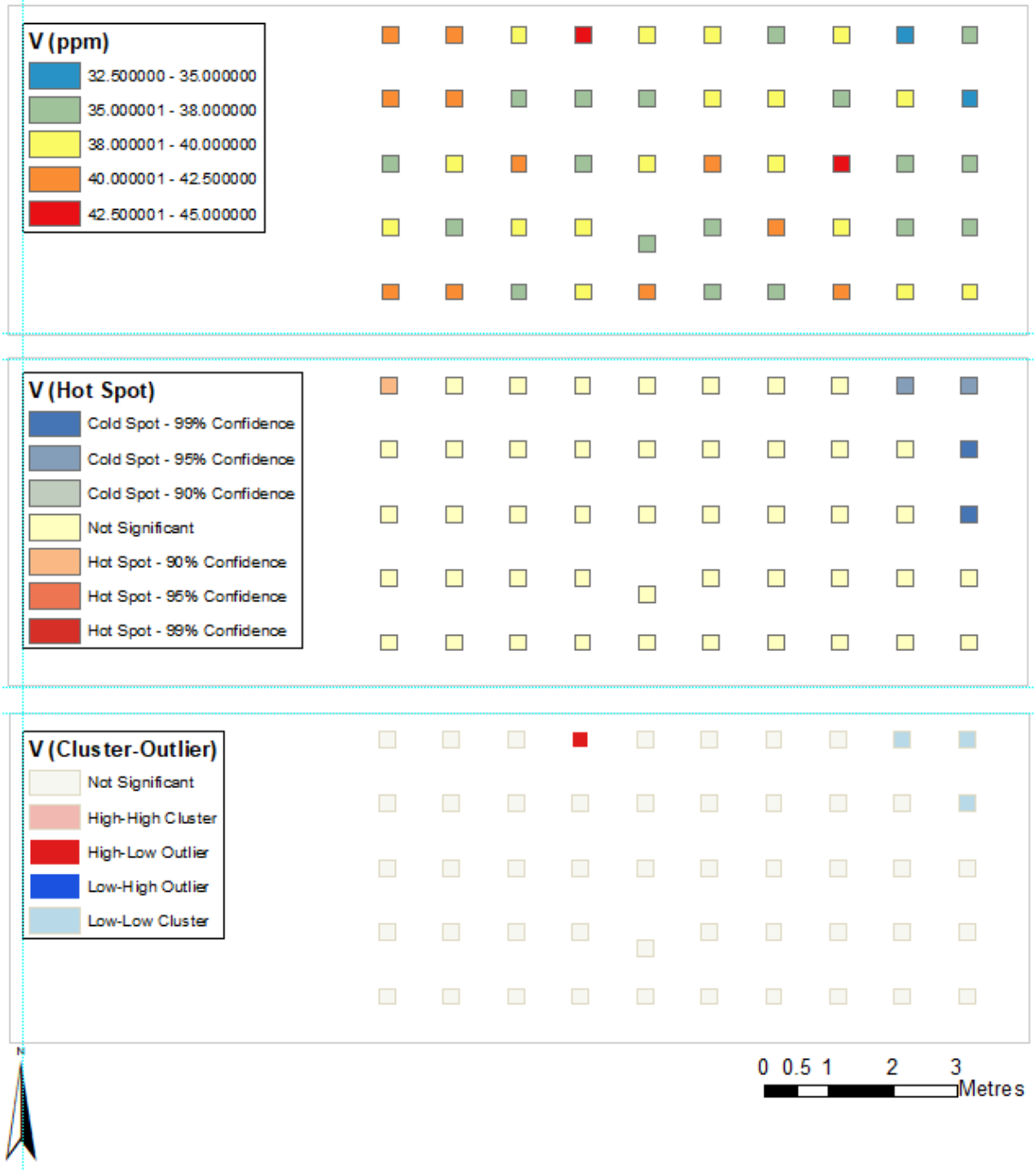
V (ppm)
32.500000 - 35.000000
35.000001 - 38.000000
38.000001 - 40.000000
40.000001 - 42.500000
42.500001 - 45.000000
V (Hot Spot)
Cold Spot - 99% Confidence
Cold Spot - 95% Confidence
Cold Spot - 90% Confidence
Not Significant
Hot Spot - 90% Confidence
Hot Spot - 95% Confidence
Hot Spot - 99% Confidence
V (Cluster-Outlier)
Not Significant
High-High Cluster
High-Low Outlier
Low-High Outlier
Low-Low Cluster
N
0 0.5 1 2 3
Metres

Zinc

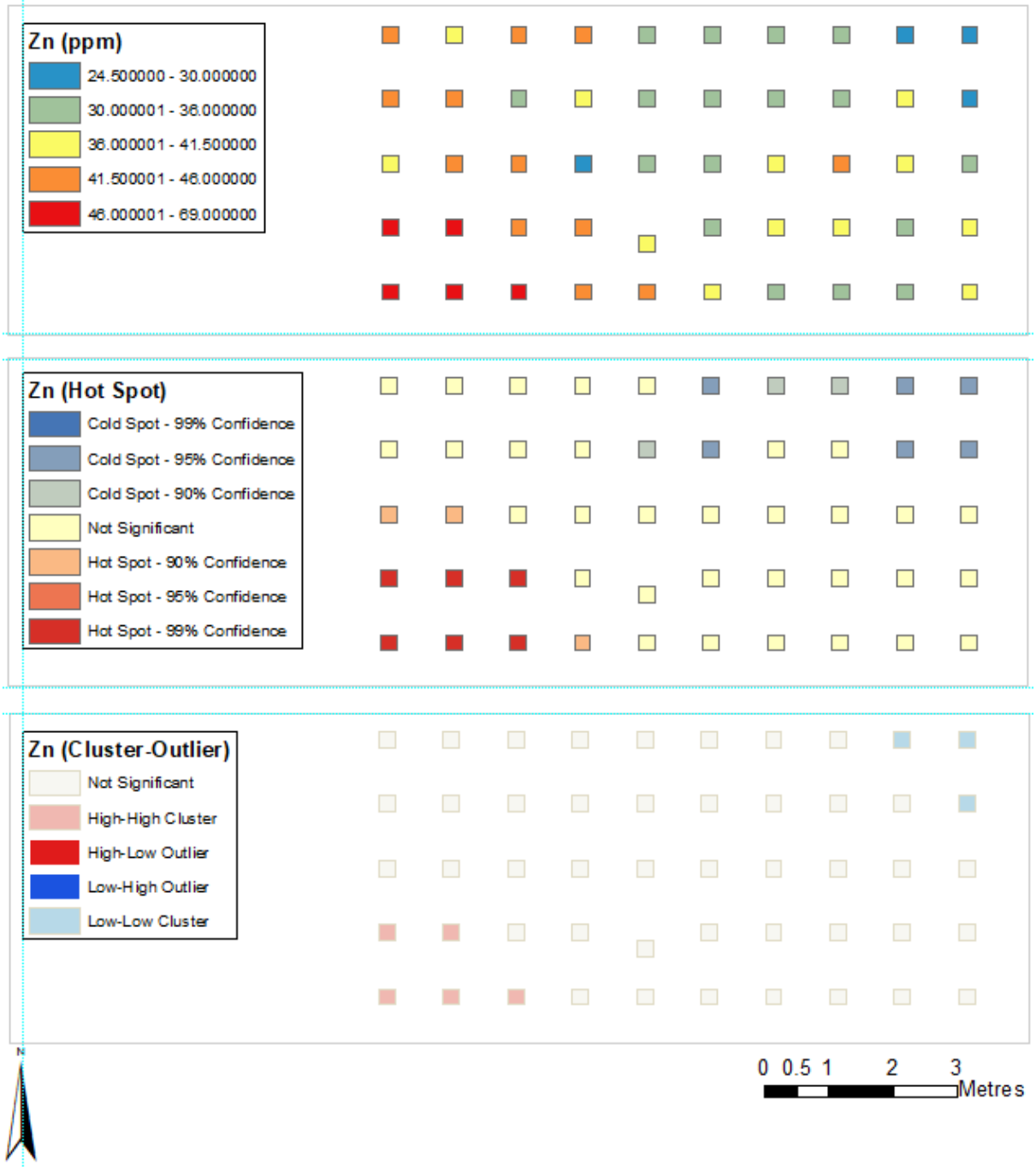
Zn (ppm)
24.500000 - 30.000000
30.000001 - 36.000000
36.000001 - 41.500000
41.500001 - 46.000000
46.000001 - 69.000000
Zn (Hot Spot)
Cold Spot - 99% Confidence
Cold Spot - 95% Confidence
Cold Spot - 90% Confidence
Not Significant
Hot Spot - 90% Confidence
Hot Spot - 95% Confidence
Hot Spot - 99% Confidence
Zn (Cluster-Outlier)
Not Significant
High-High Cluster
High-Low Outlier
Low-High Outlier
Low-Low Cluster
N
0 0.5 1 2 3
Metres

VP14 FpXRF Full Dataset

This is provided in digital format on the associated media.

VP14 FpXRF Individual Element Histograms

The following, in Figure 159, are the histograms for the data as measured in situ for trenches 11, 12, and 15 in the 2014 excavation season. The classification column background is colour-coded so that red indicates a minor contributor, yellow is for minor contributors, blue is for trace contributors and white is for IUPAC-trace contributors. All other elements that were below the LODs are not included in the table at all.

Class based on mean	**Element**	**Histogram**
Major	Si_ppm	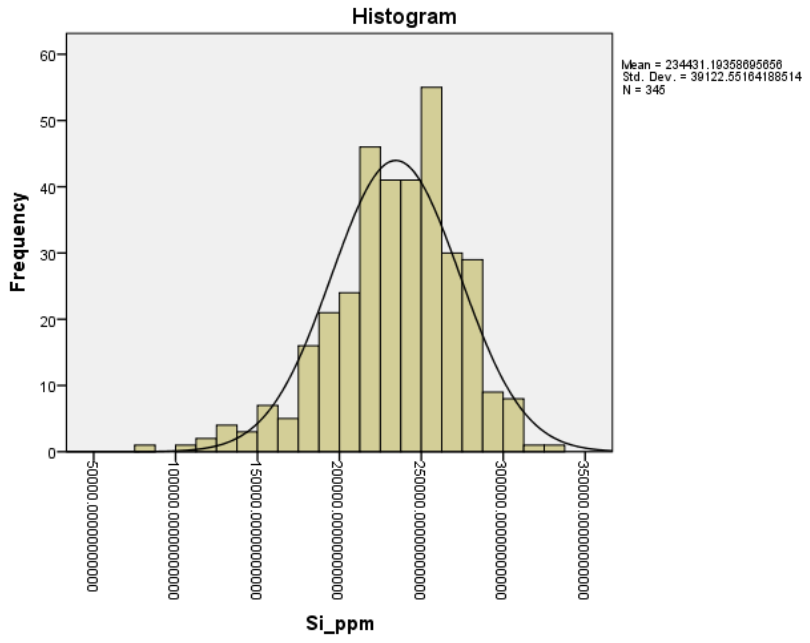

Class based on mean	Element	Histogram
	Al_ppm	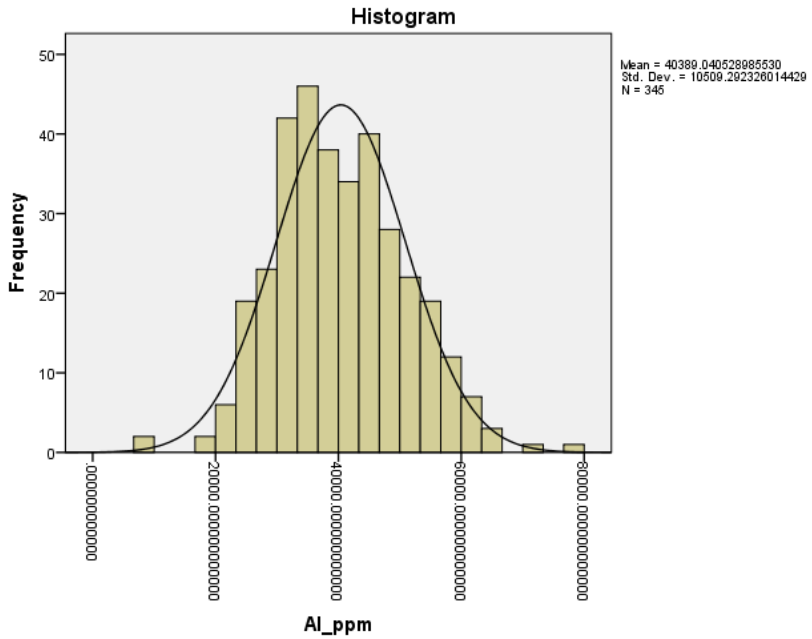
	Fe_ppm	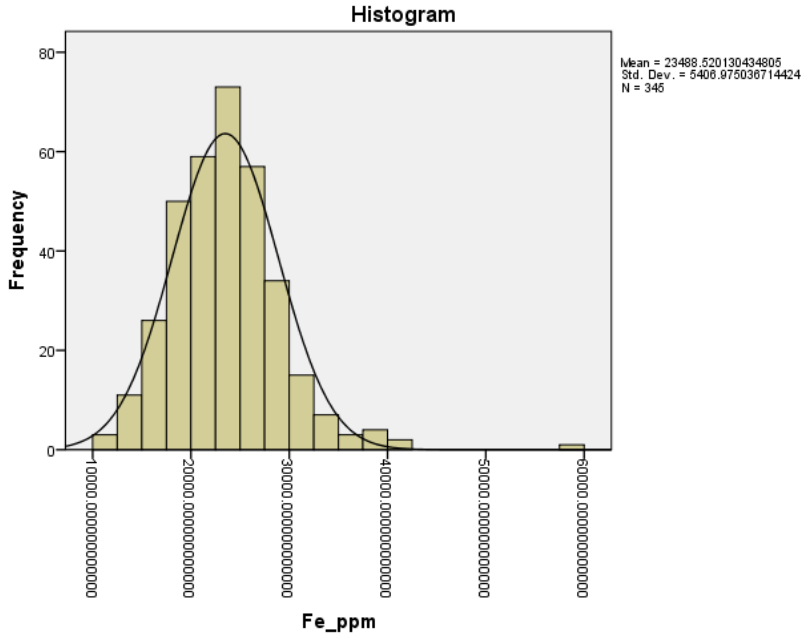

Class based on mean	Element	Histogram
Minor	Ca_ppm	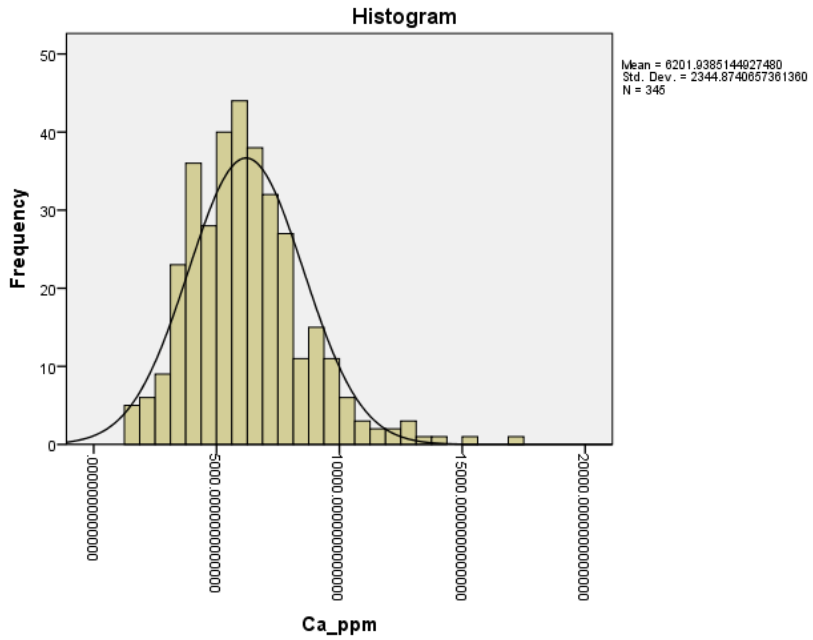
	K_ppm	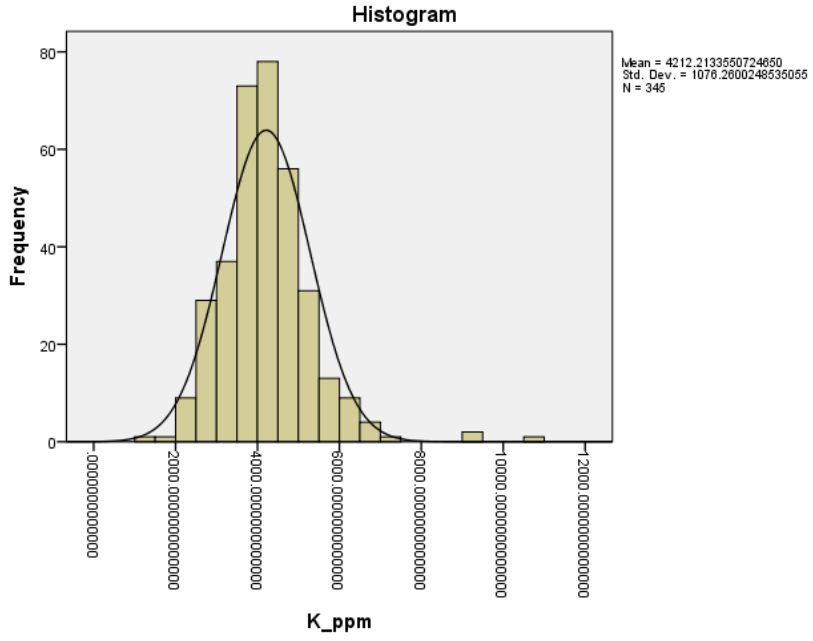

Class based on mean	Element	Histogram
	Ti_ppm	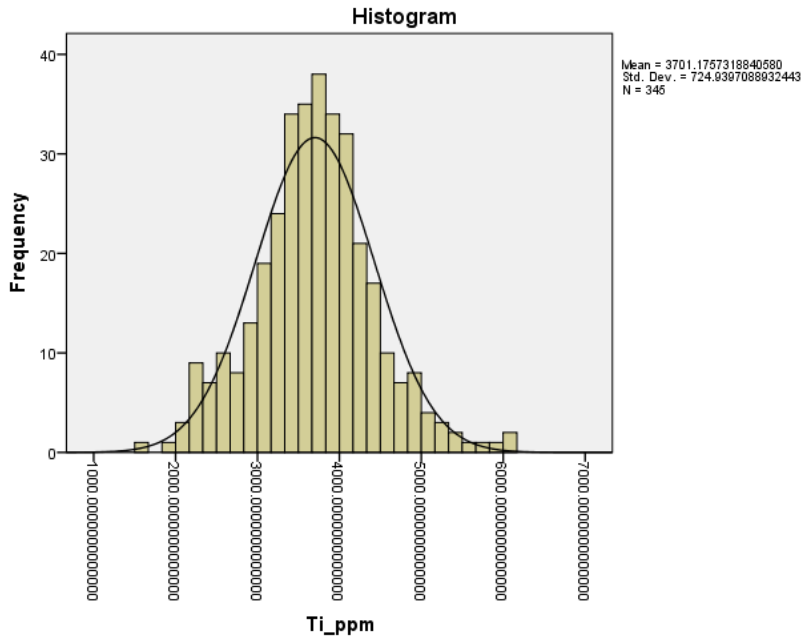
	Cl_ppm	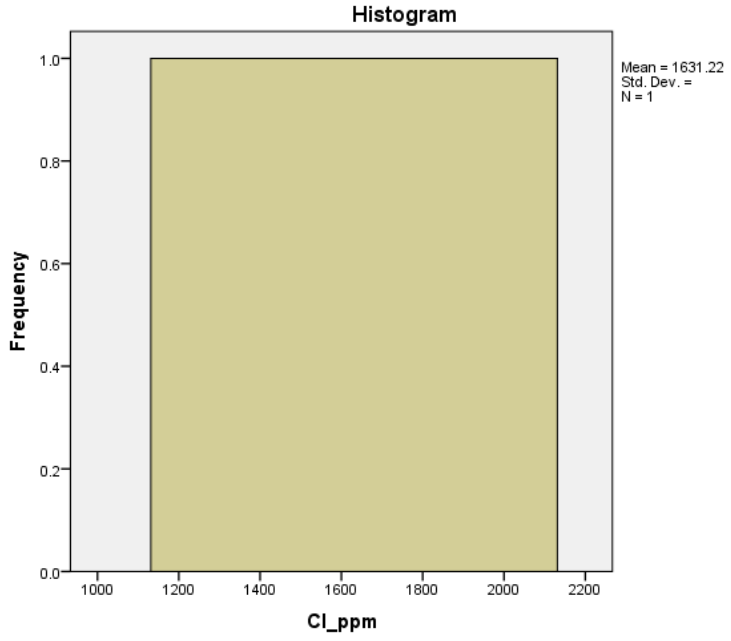

Class based on mean	Element	Histogram
Trace	S_ppm	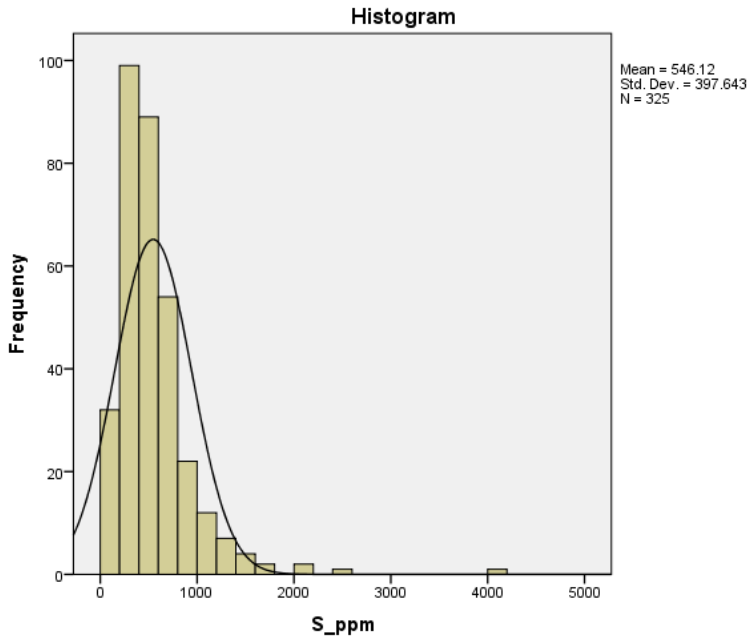
	Zr_ppm	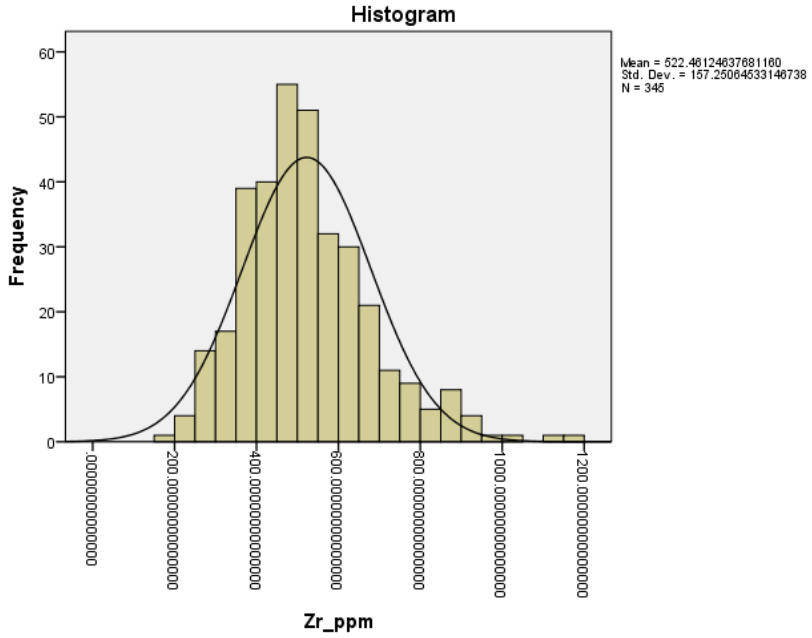

Class based on mean	Element	Histogram
	P_ppm	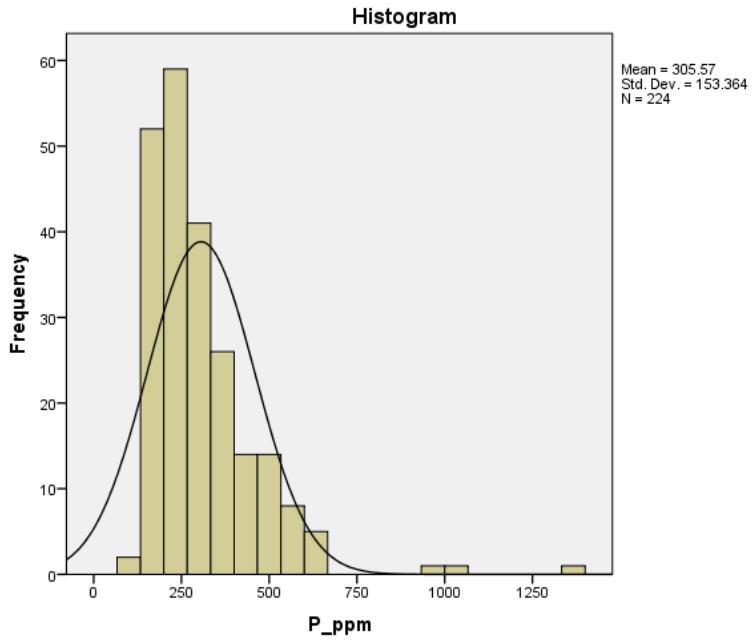
	V_ppm	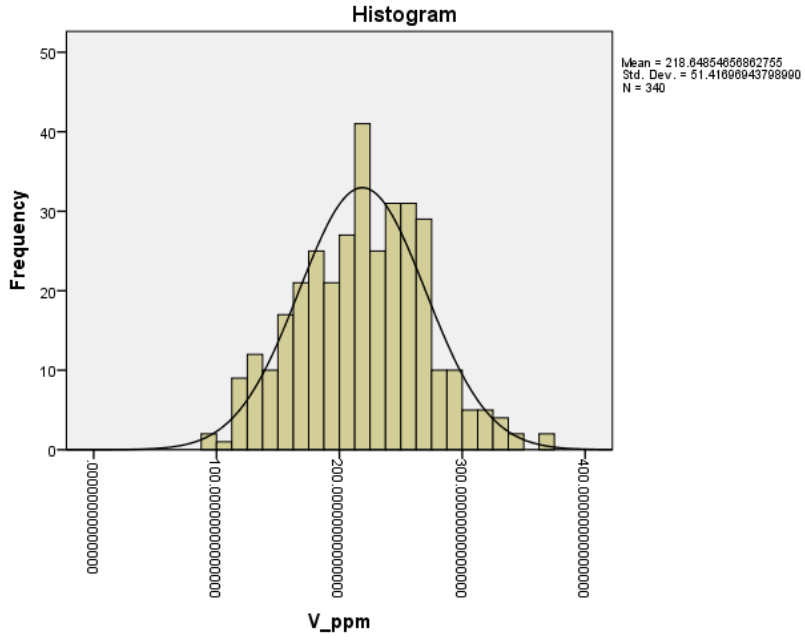

Class based on mean	Element	Histogram
	Mn_ppm	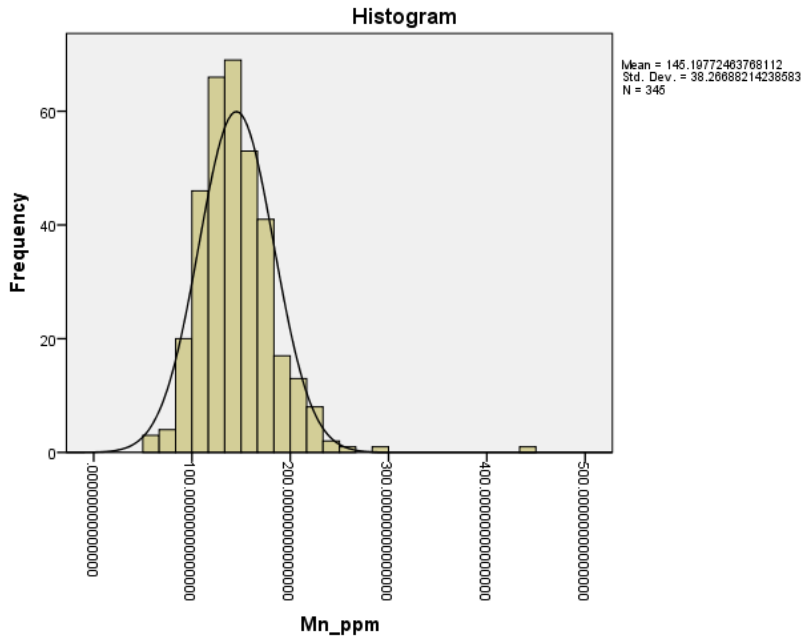
IUPAC-Trace	Cr_ppm	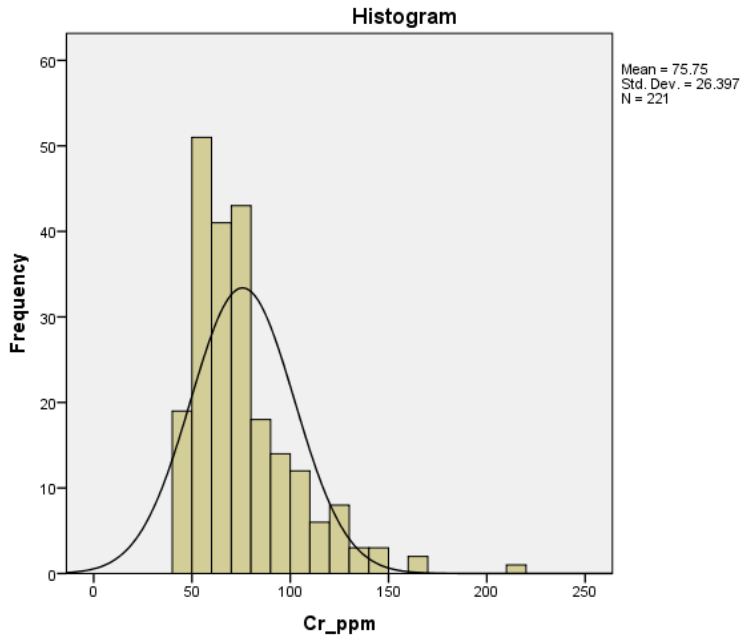

Class based on mean	Element	Histogram
	Sr_ppm	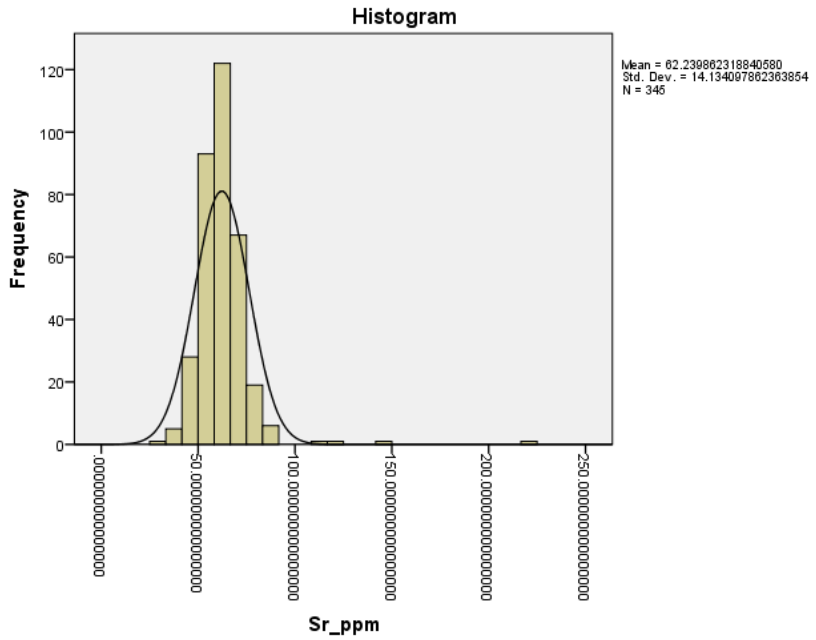
	Zn_ppm	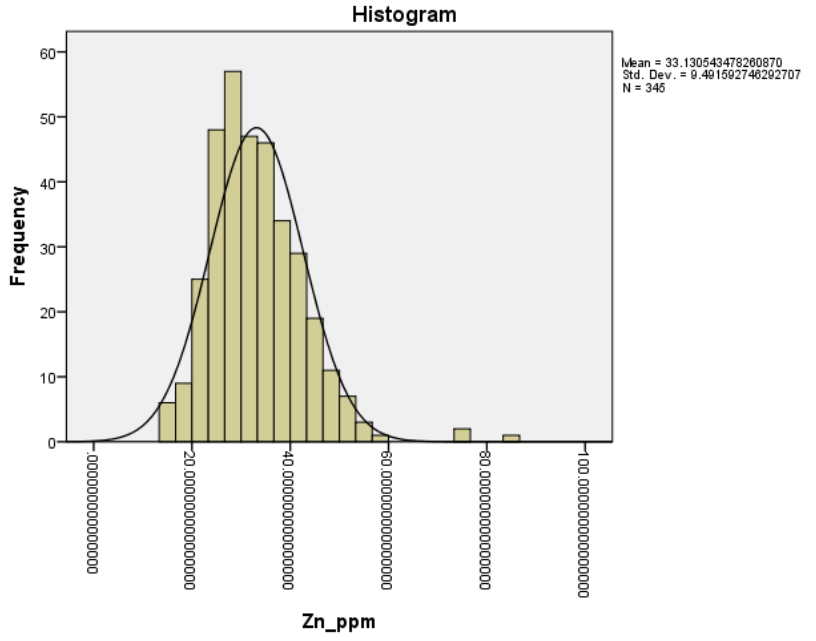

Class based on mean	Element	Histogram
	Rb_ppm	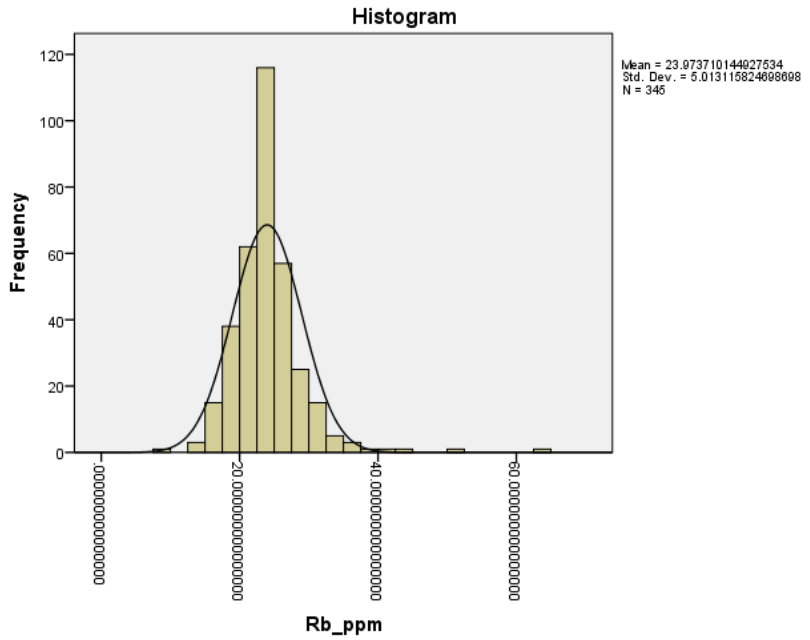
	Ta_ppm	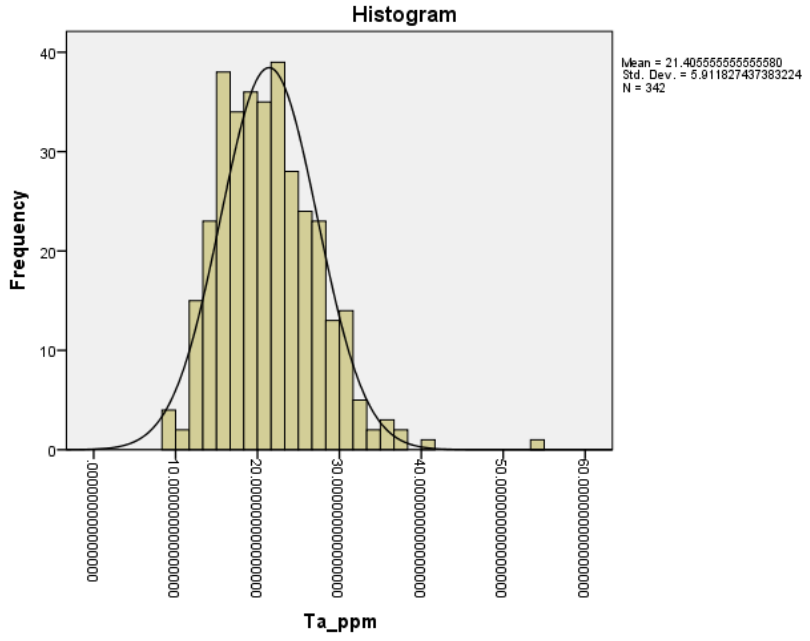

Class based on mean	Element	Histogram
	Cd_ppm	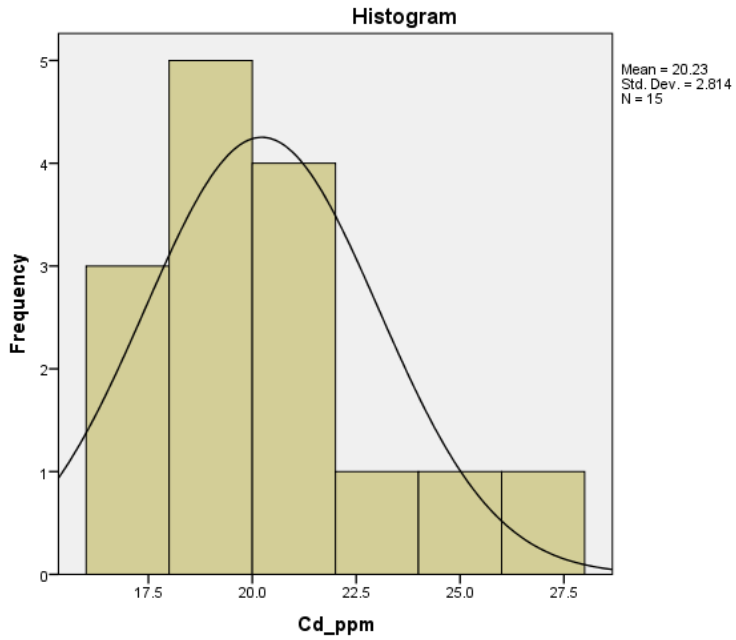
	Y_ppm	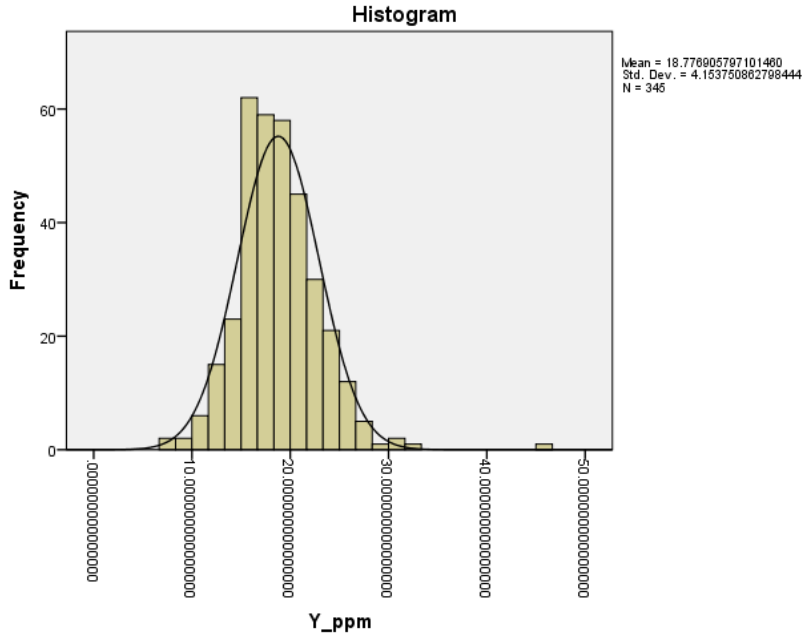

Class based on mean	Element	Histogram
	Ag_ppm	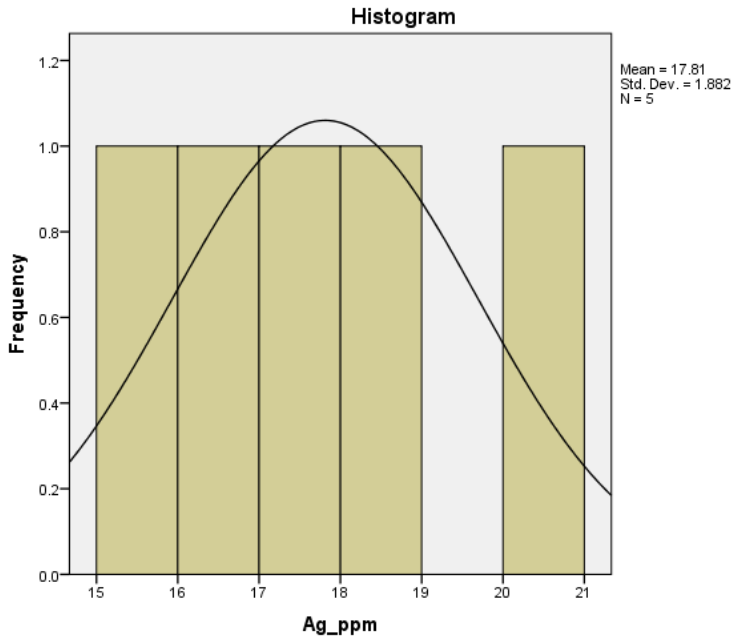
	Ni_ppm	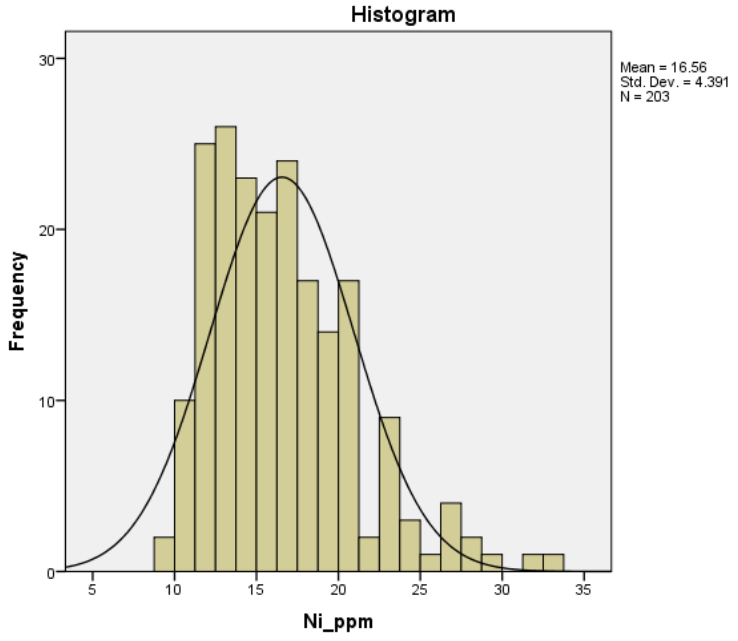

Class based on mean	Element	Histogram
	Th_ppm	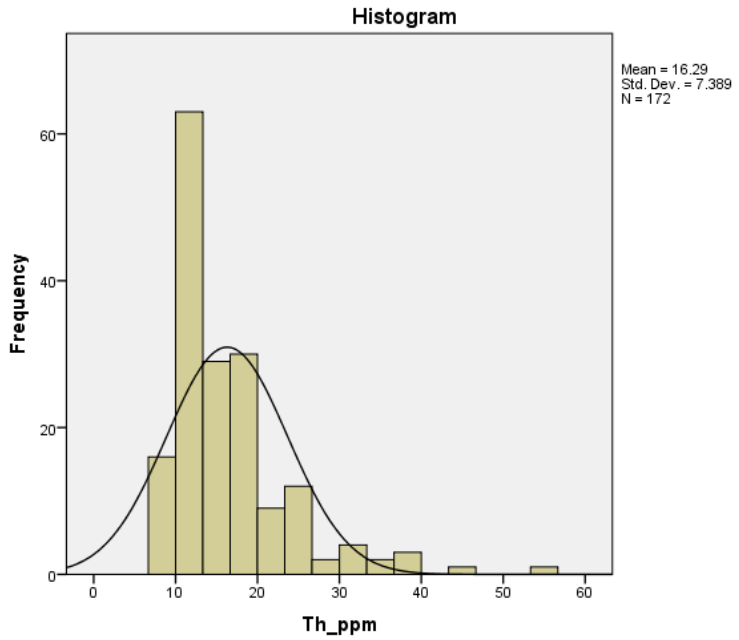
	Pb_ppm	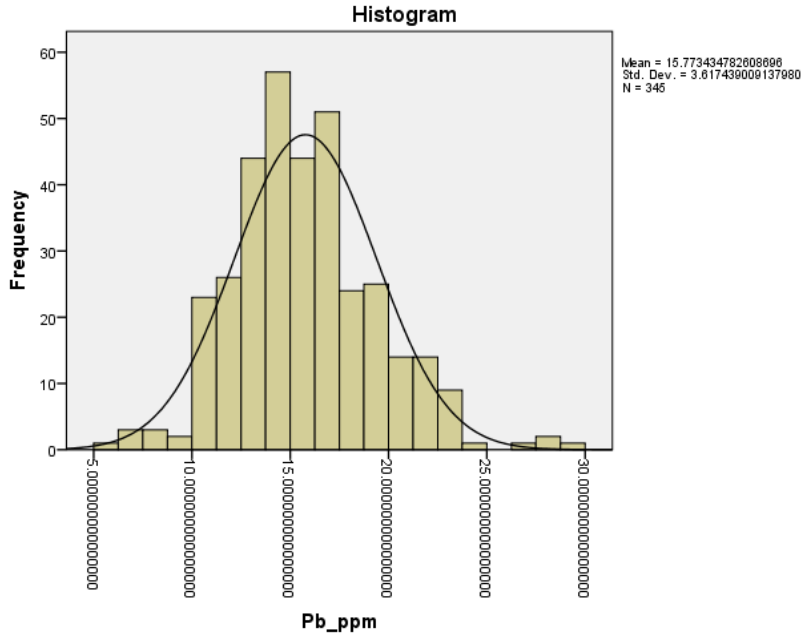

Class based on mean	Element	Histogram
	Nb_ppm	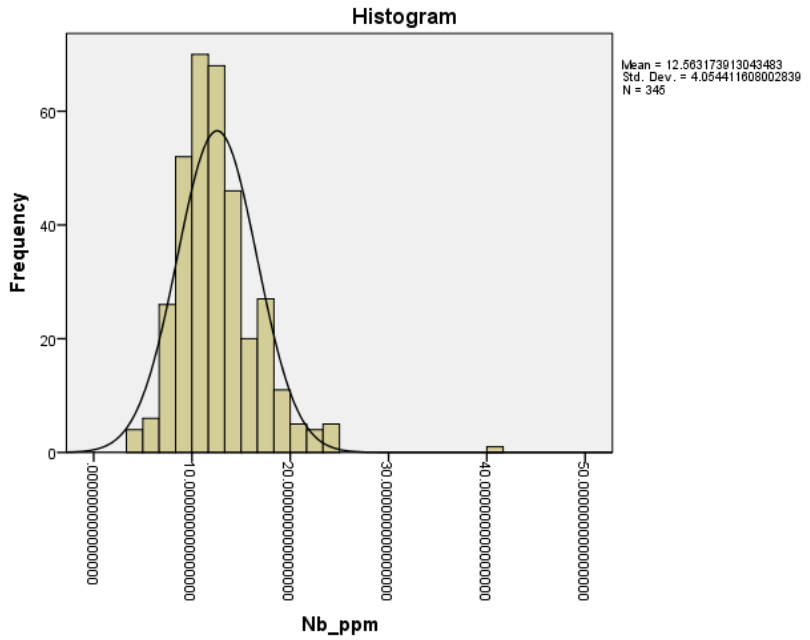
	Cu_ppm	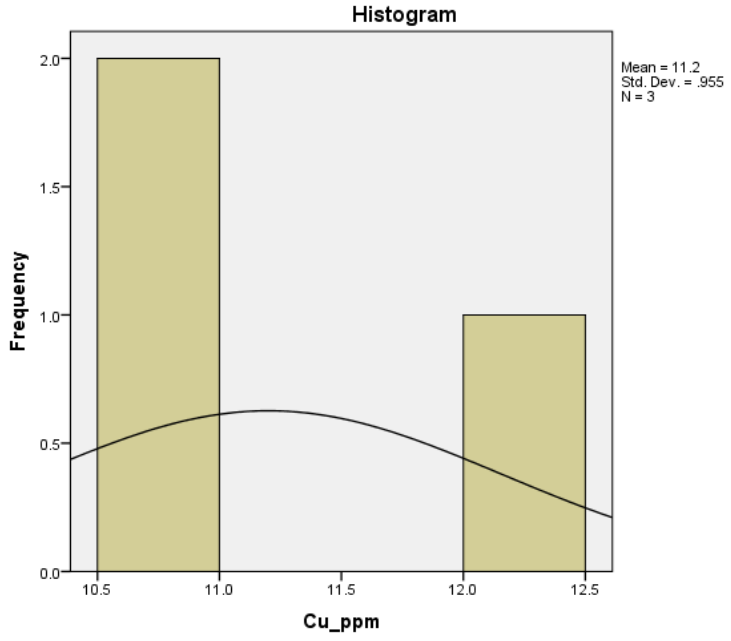

Class based on mean	Element	Histogram
	Hg_ppm	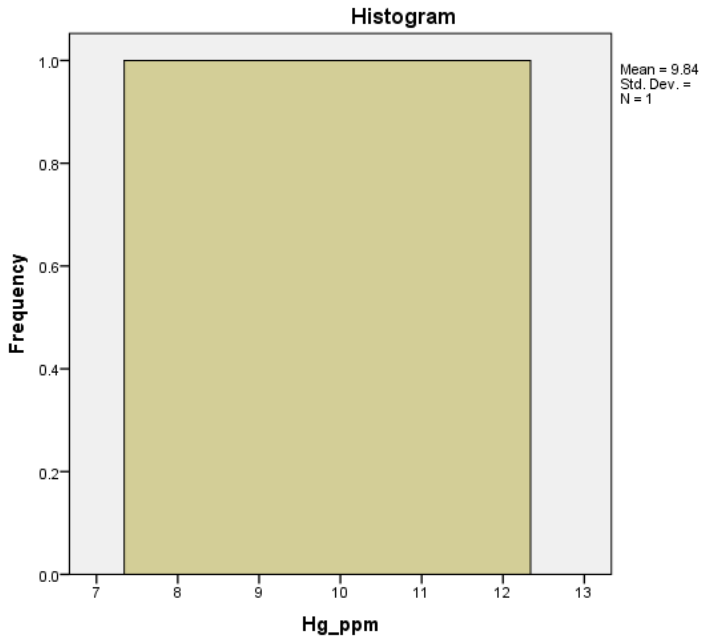
	Mo_ppm	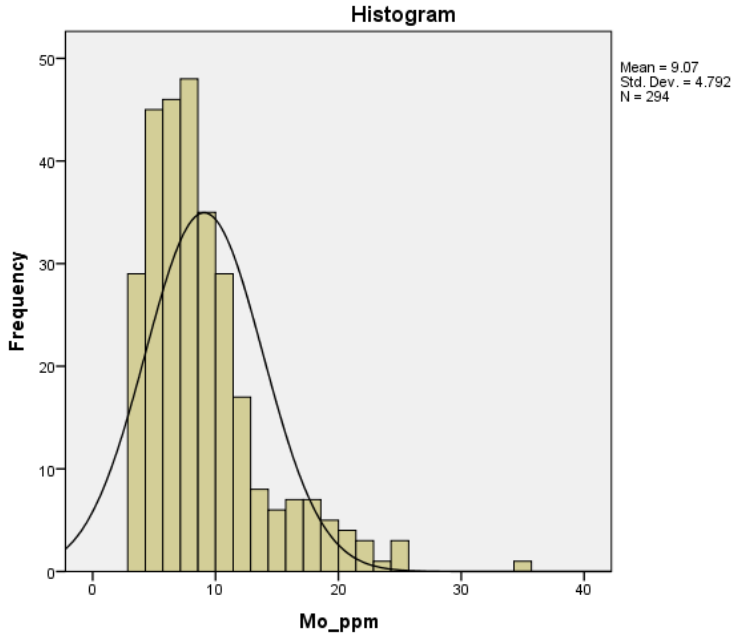

Class based on mean	Element	Histogram
	Bi_ppm	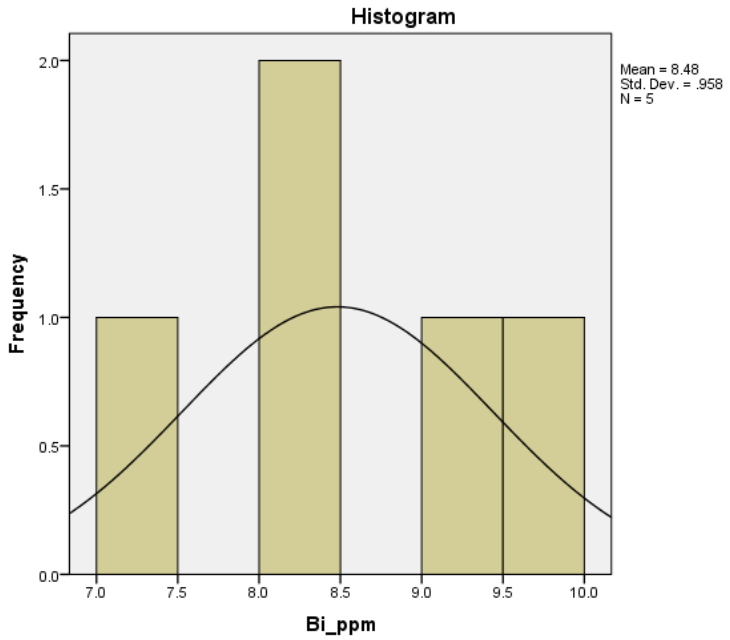
	As_ppm	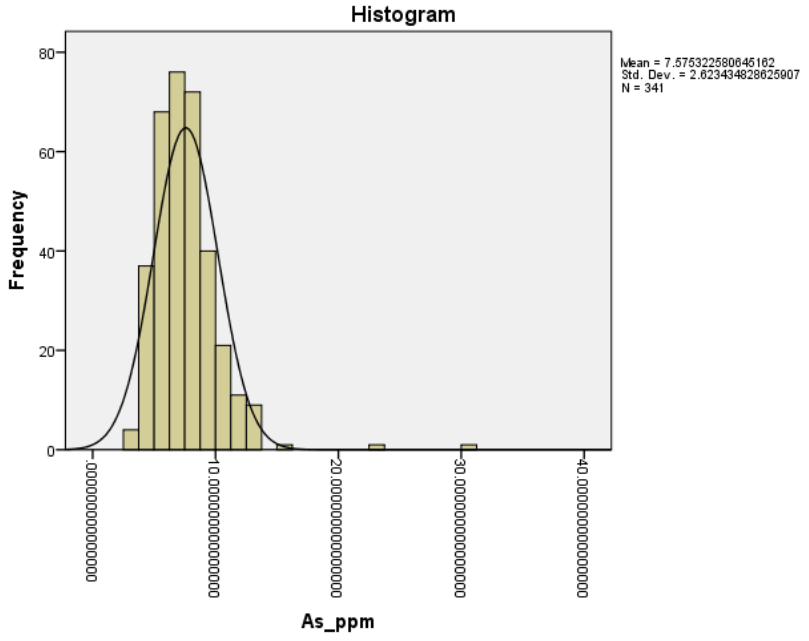

Class based on mean	Element	Histogram
	U_ppm	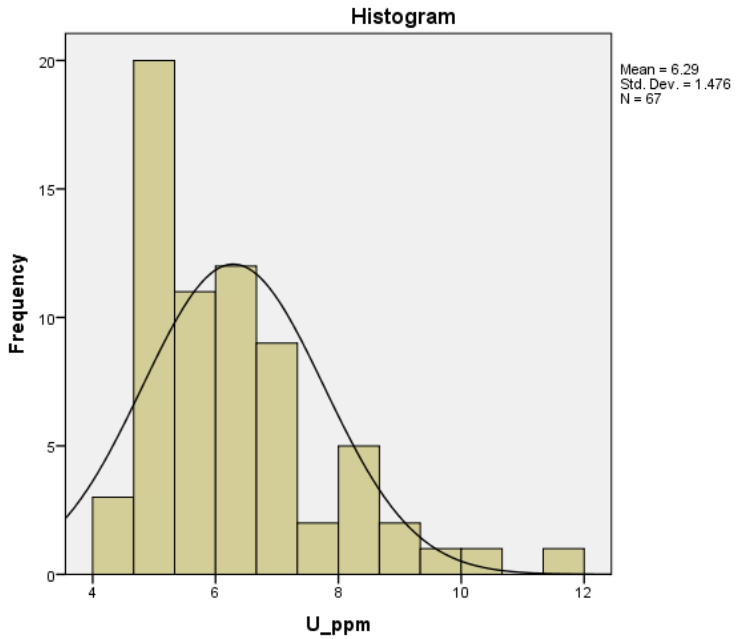

Figure 159. The histograms for the data as measured during the field pXRF analysis of trenches 11, 12, and 15

VP14 FpXRF Individual Element Spatial Analysis Results for Trenches 11, 12 and 15

Major

Silicon

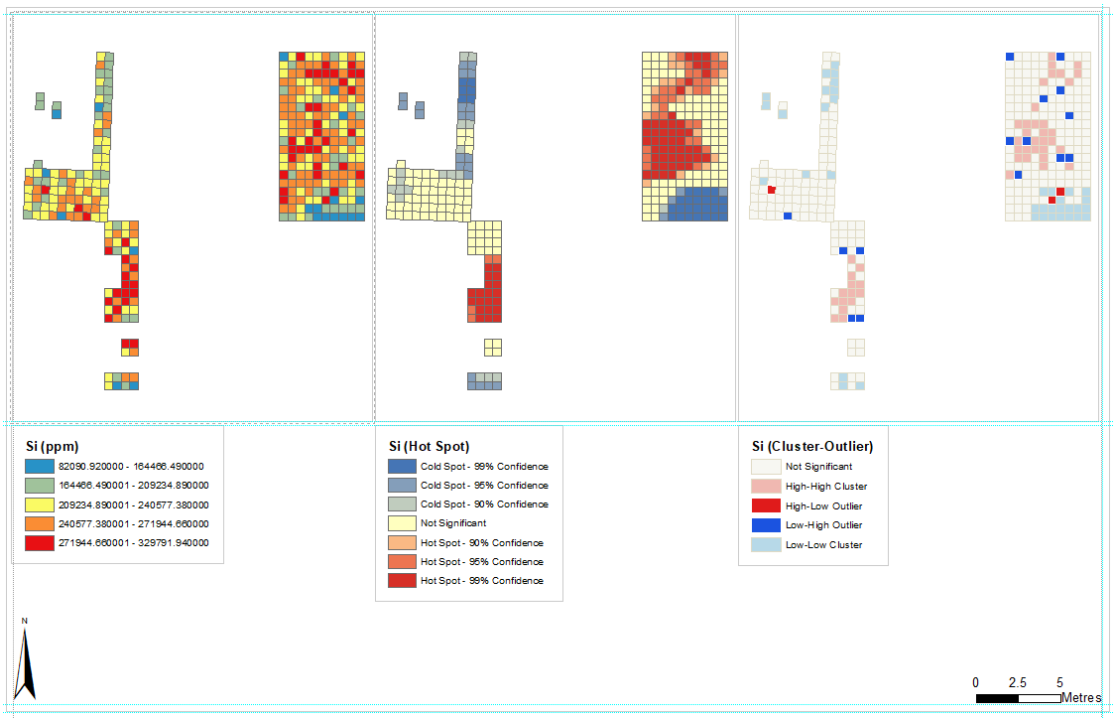

Aluminium

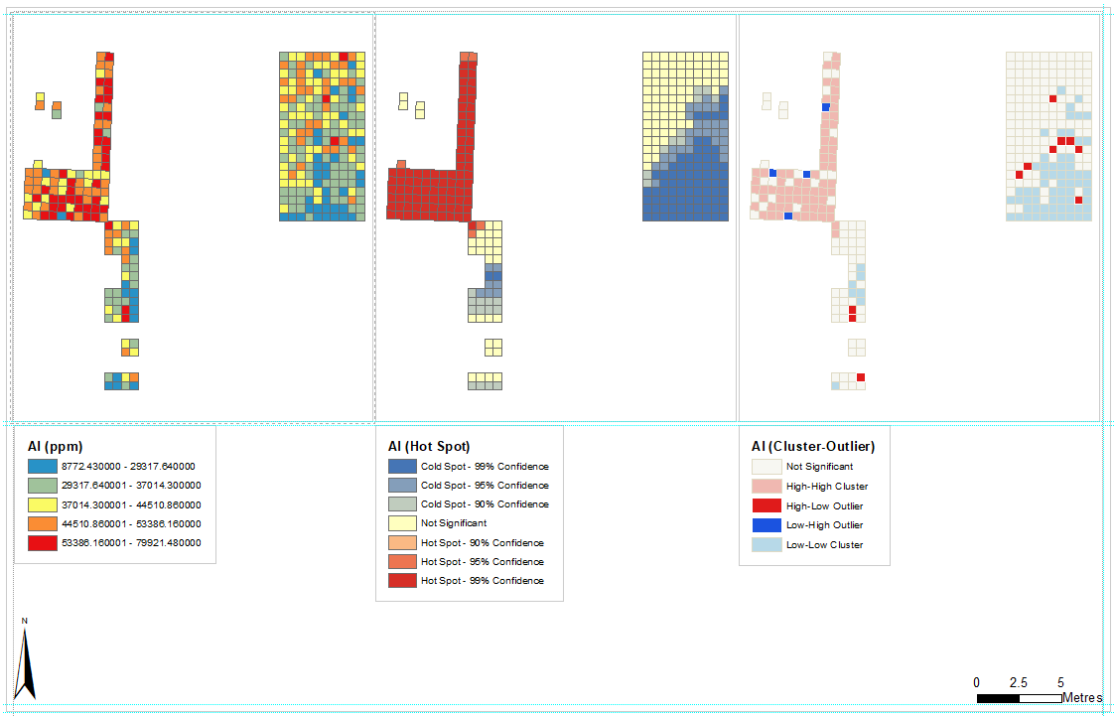

Iron

Minor

Calcium

Potassium

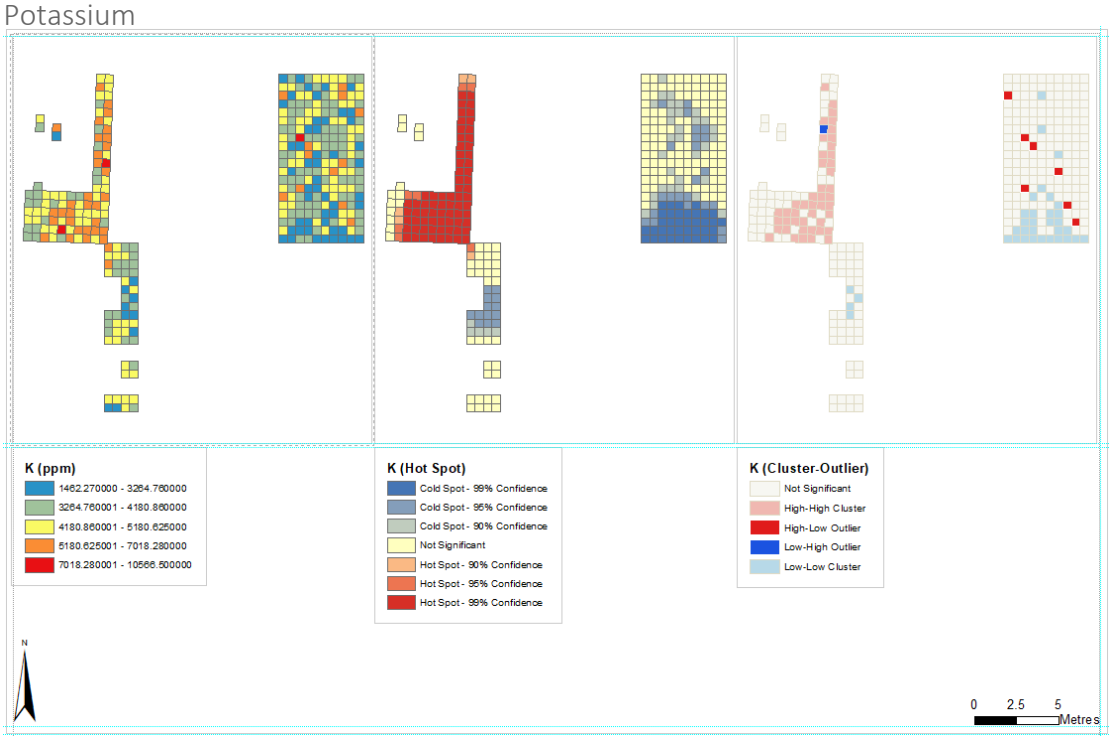

Titanium

Chlorine

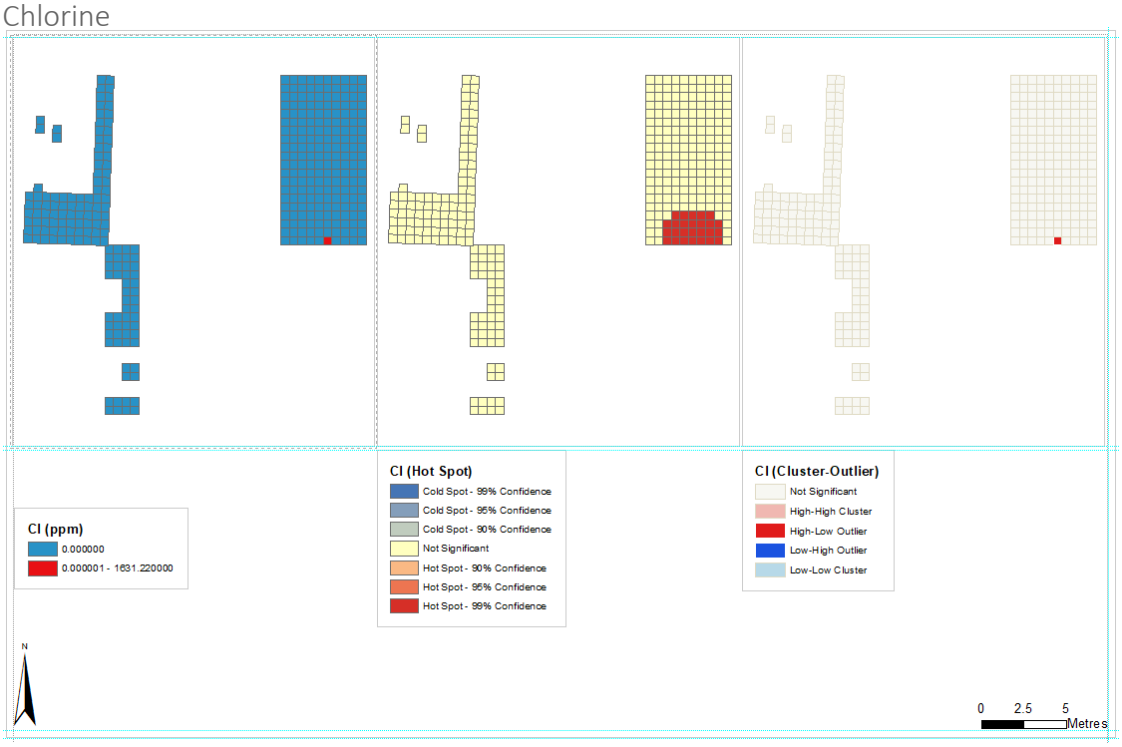

Trace

Sulfur

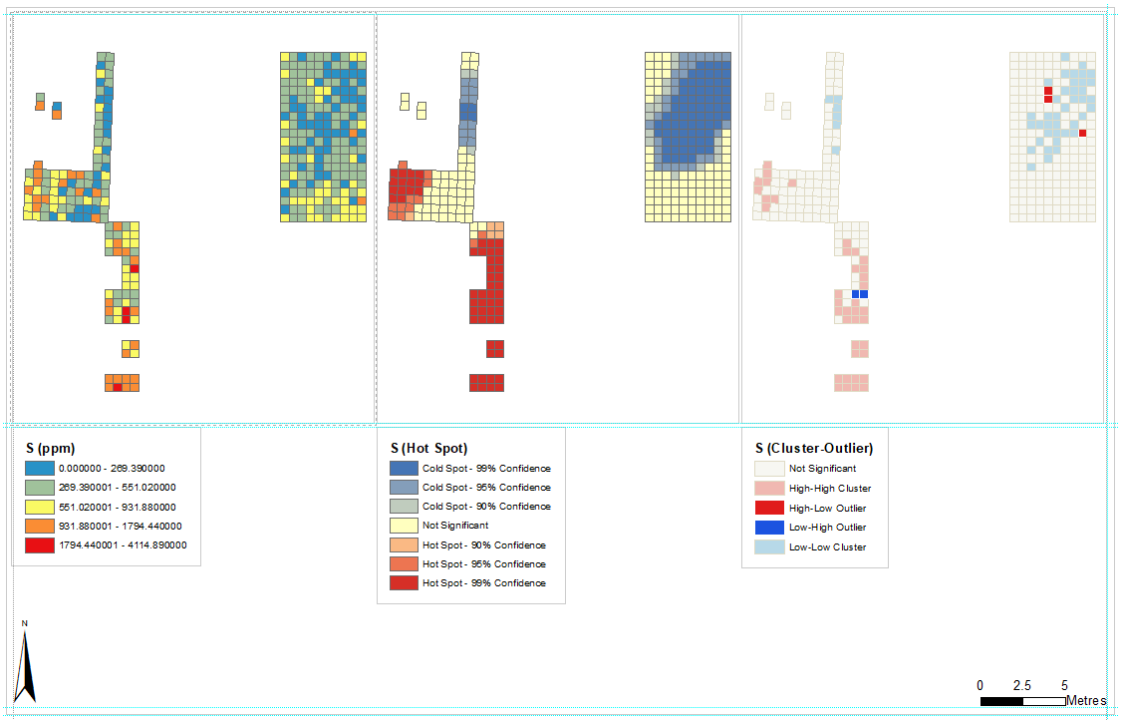

Zirconium

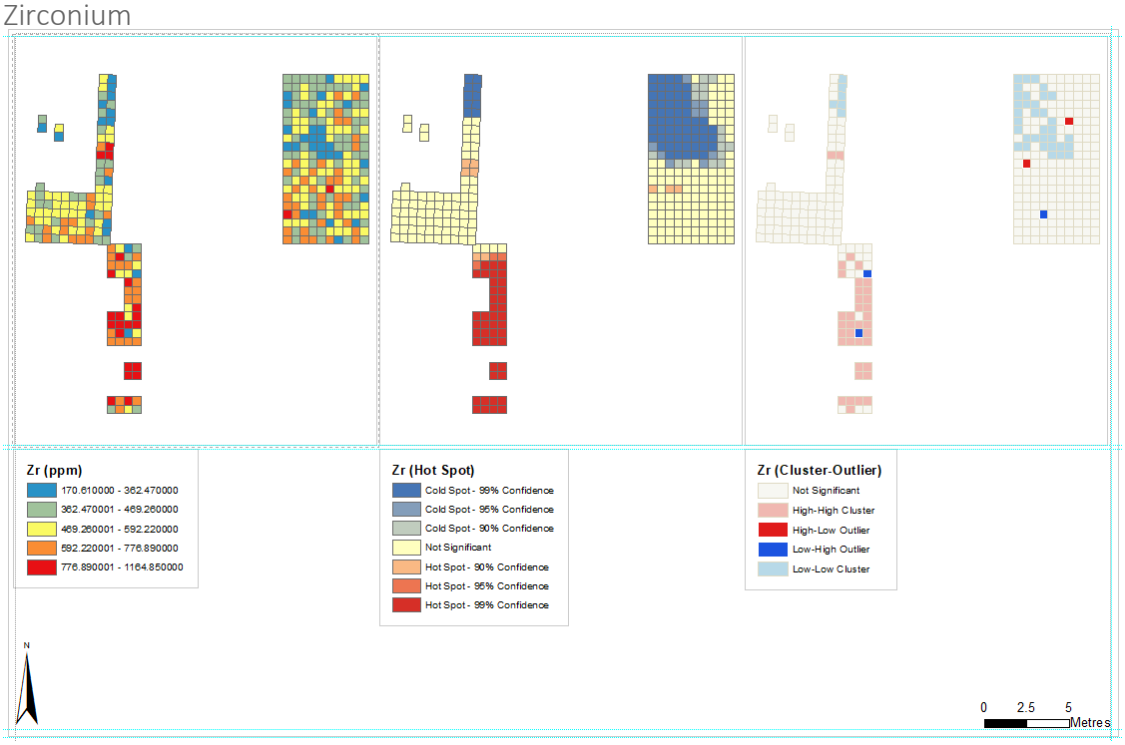

Phosphorus

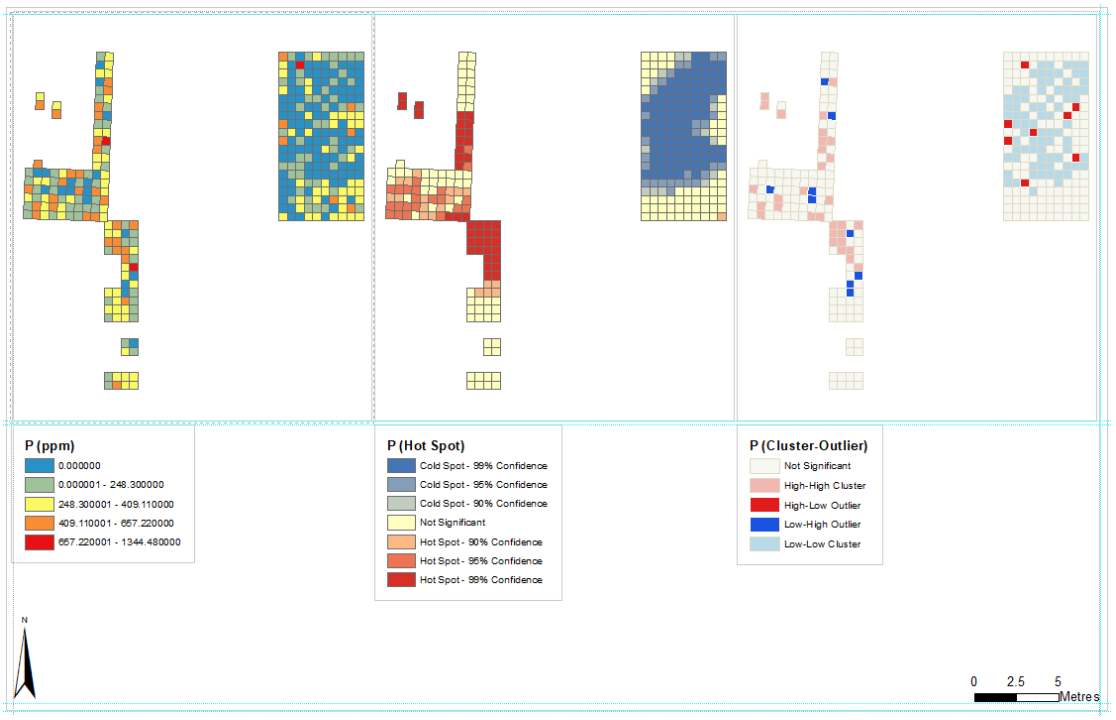

Vanadium

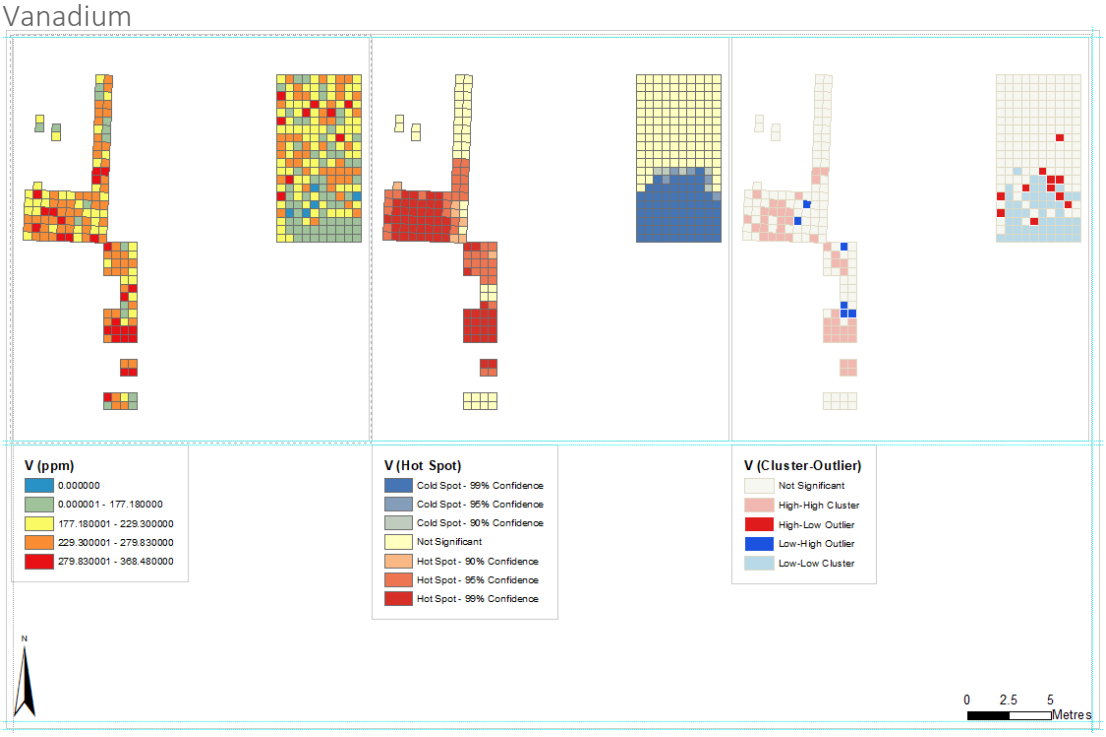

Manganese

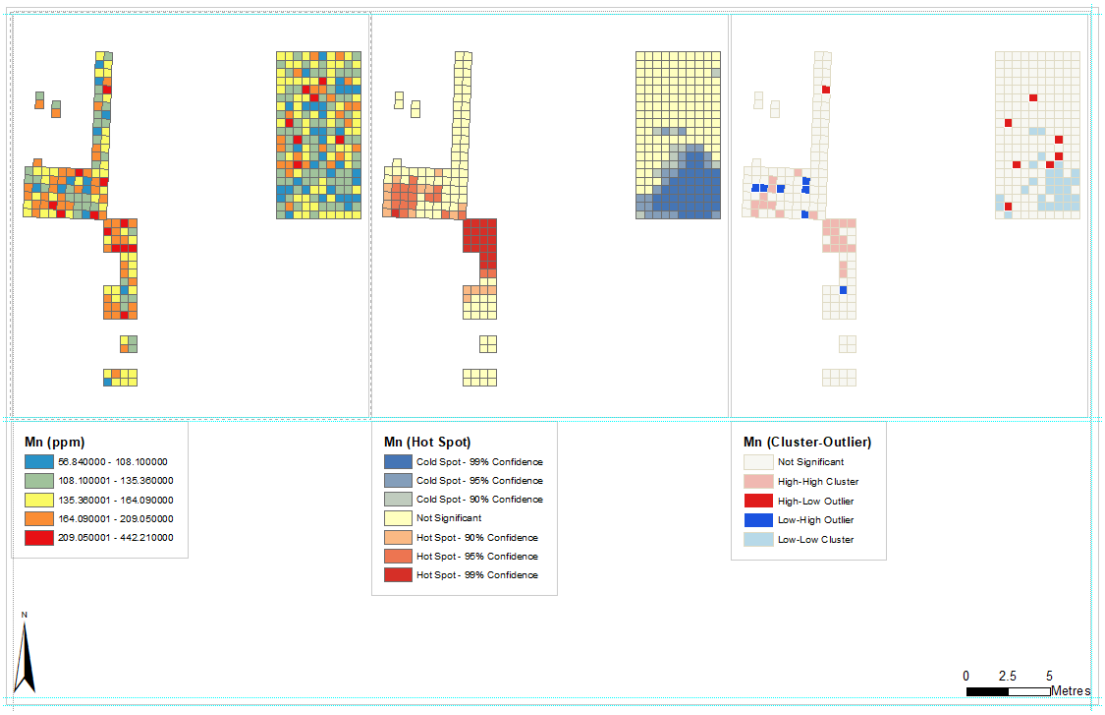

IUPAC Trace

Chromium

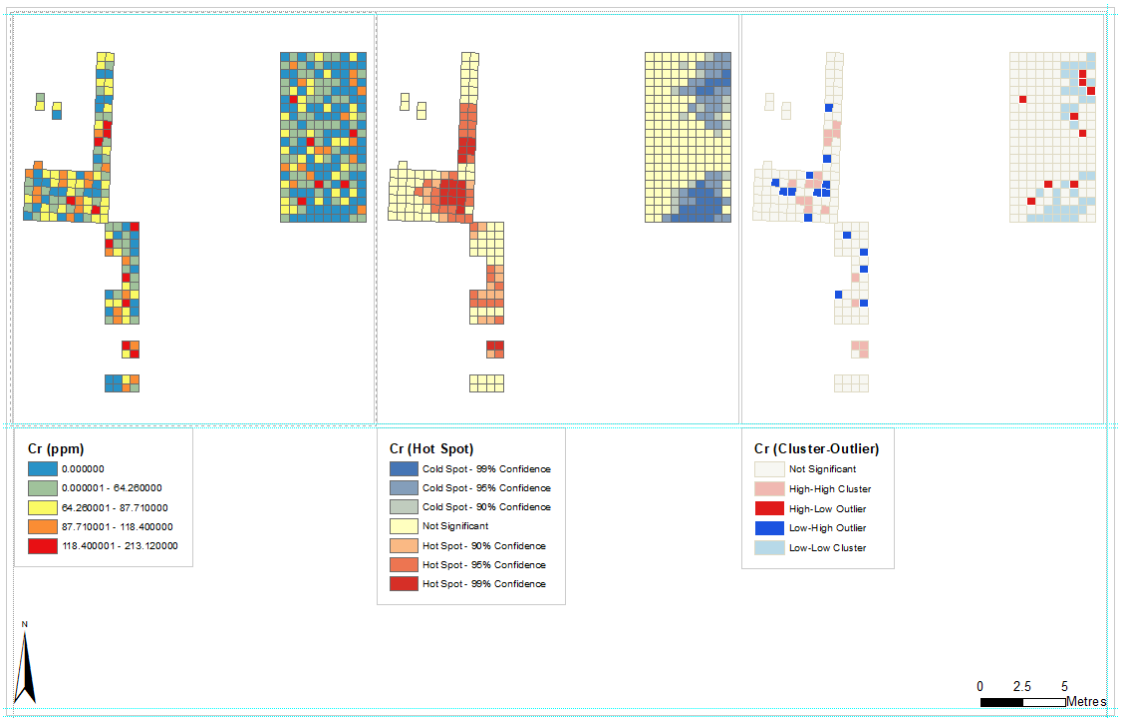

Strontium

Zinc

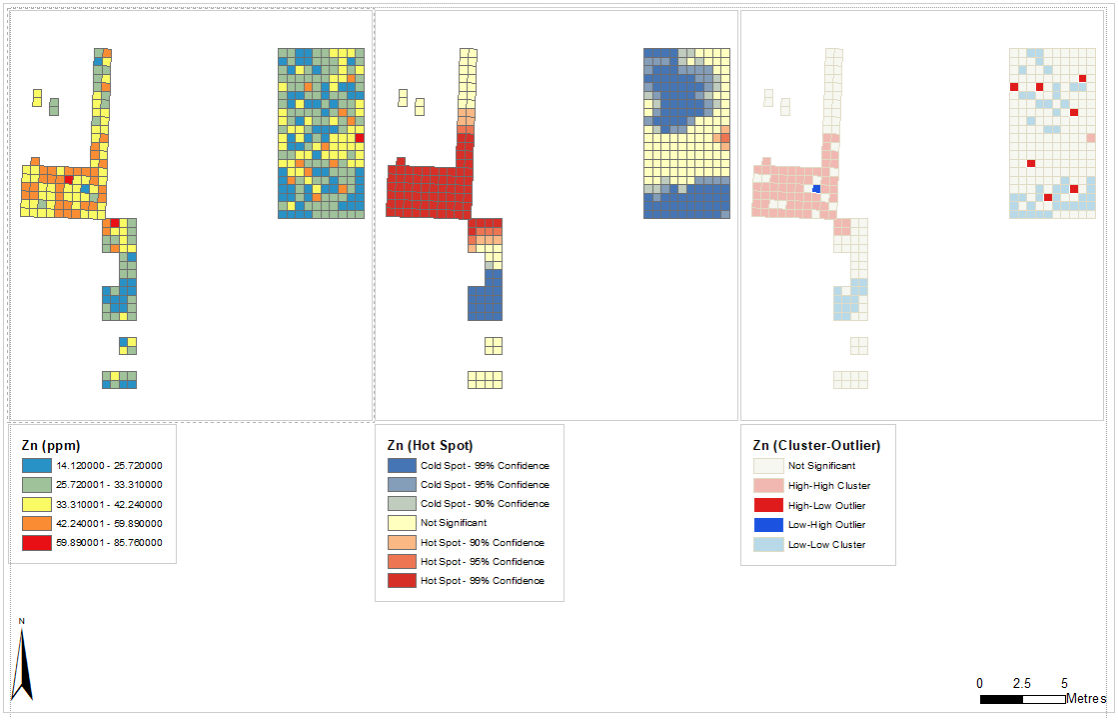

Rubidium

Tantalum

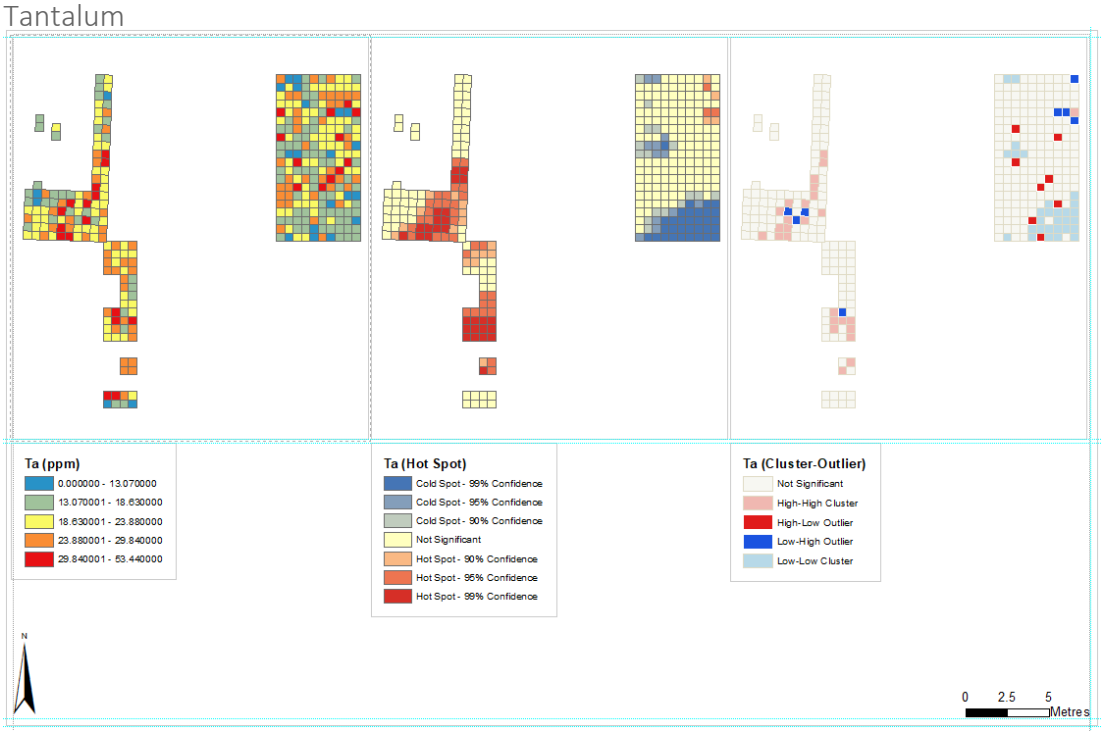

Cadmium

Yttrium

Silver

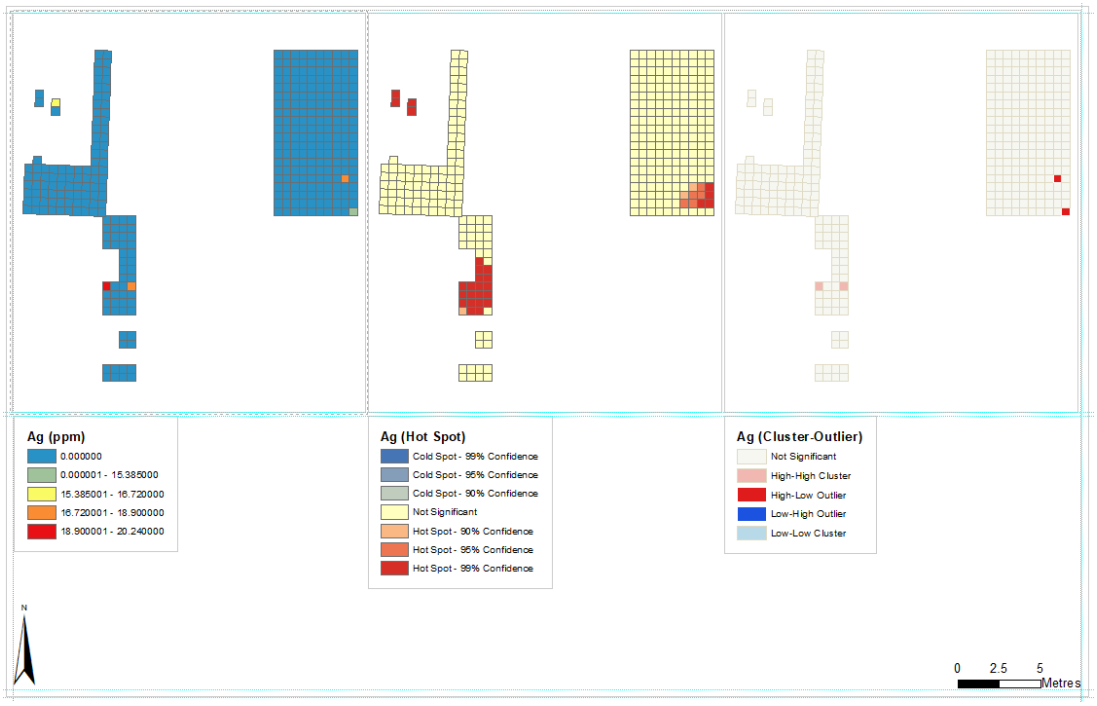

Nickel

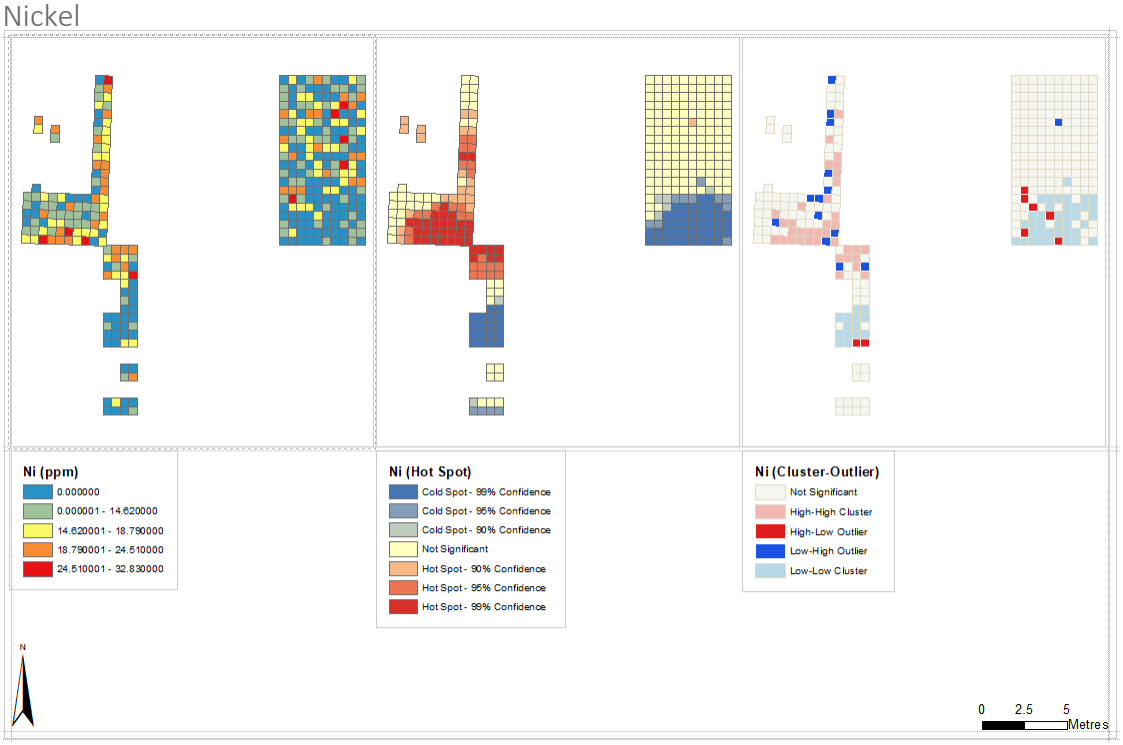

Thorium

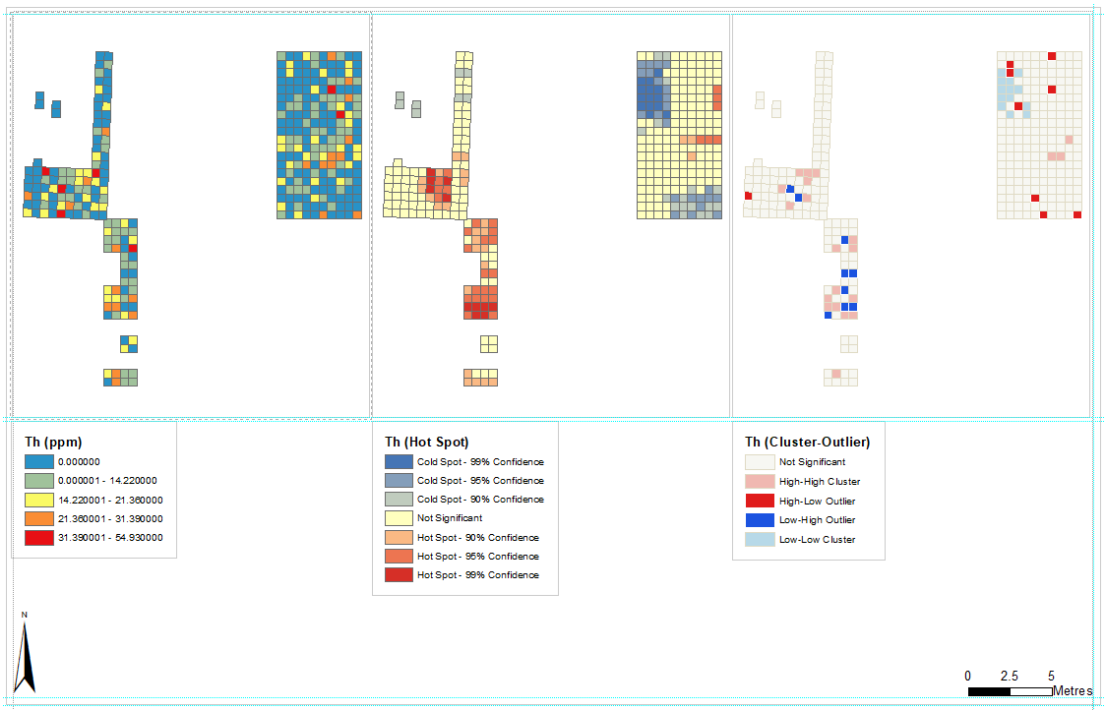

Lead

Niobium

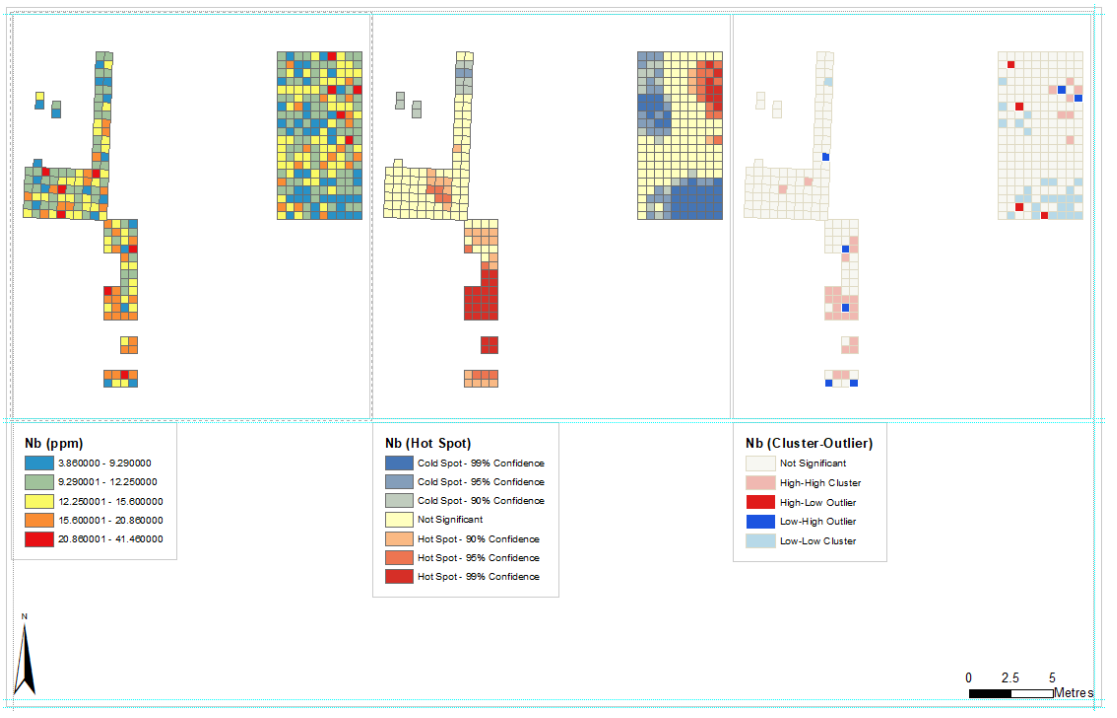

Copper

Mercury

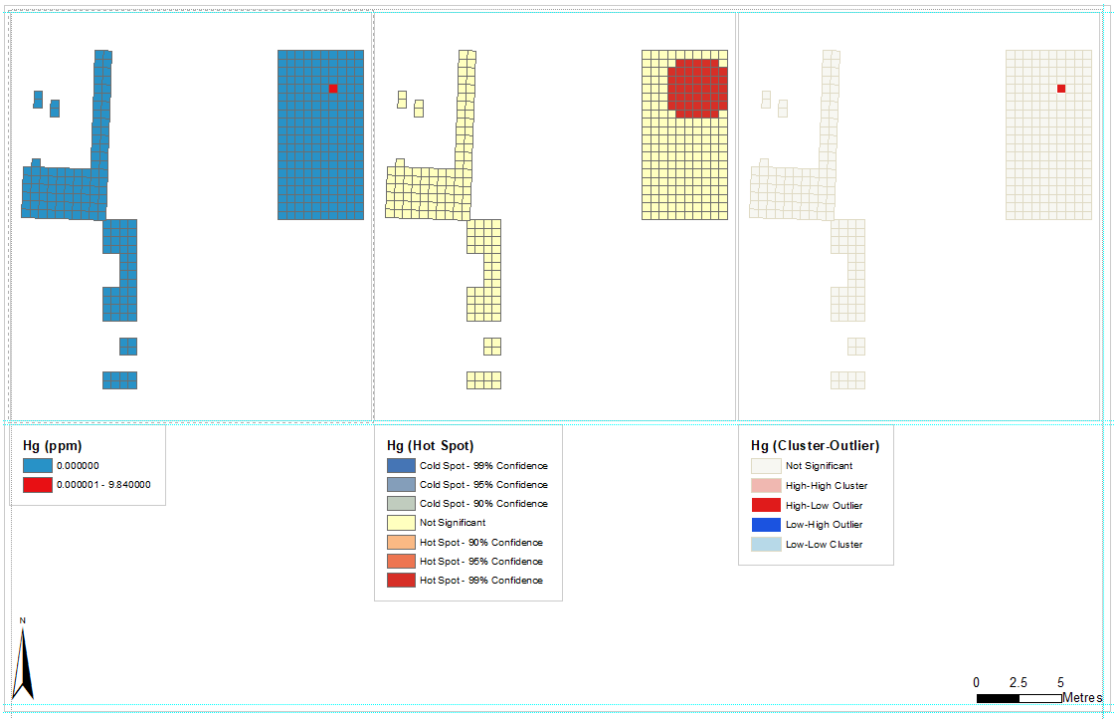

Molybdenum

Bismuth

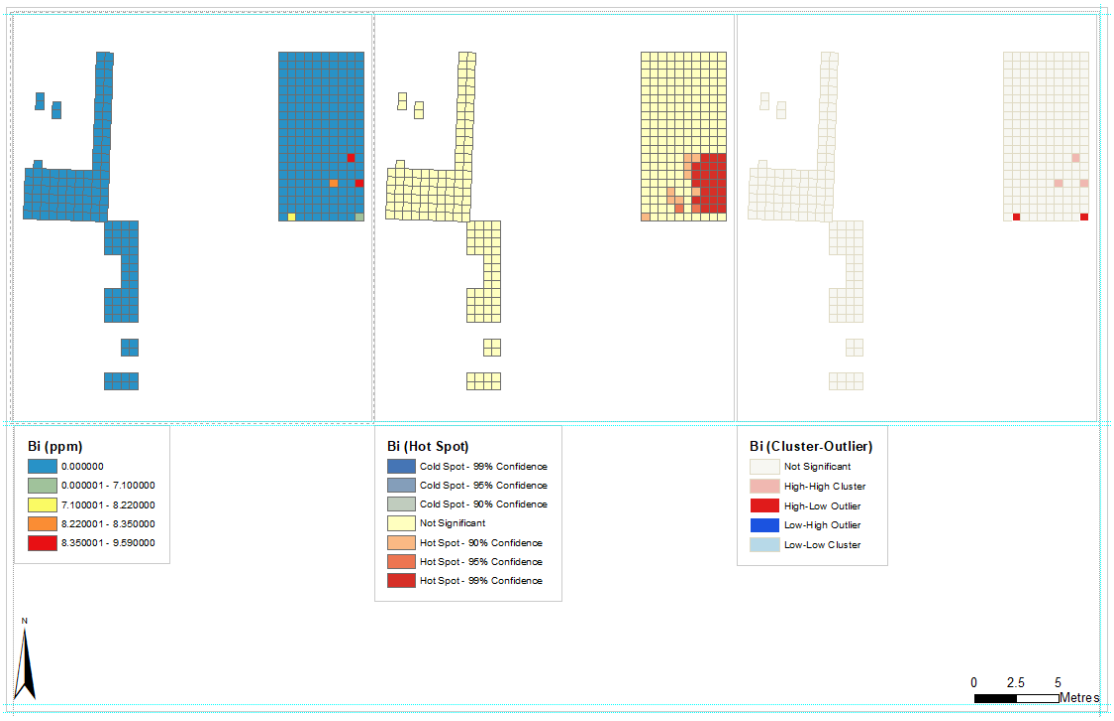

Arsenic

Uranium

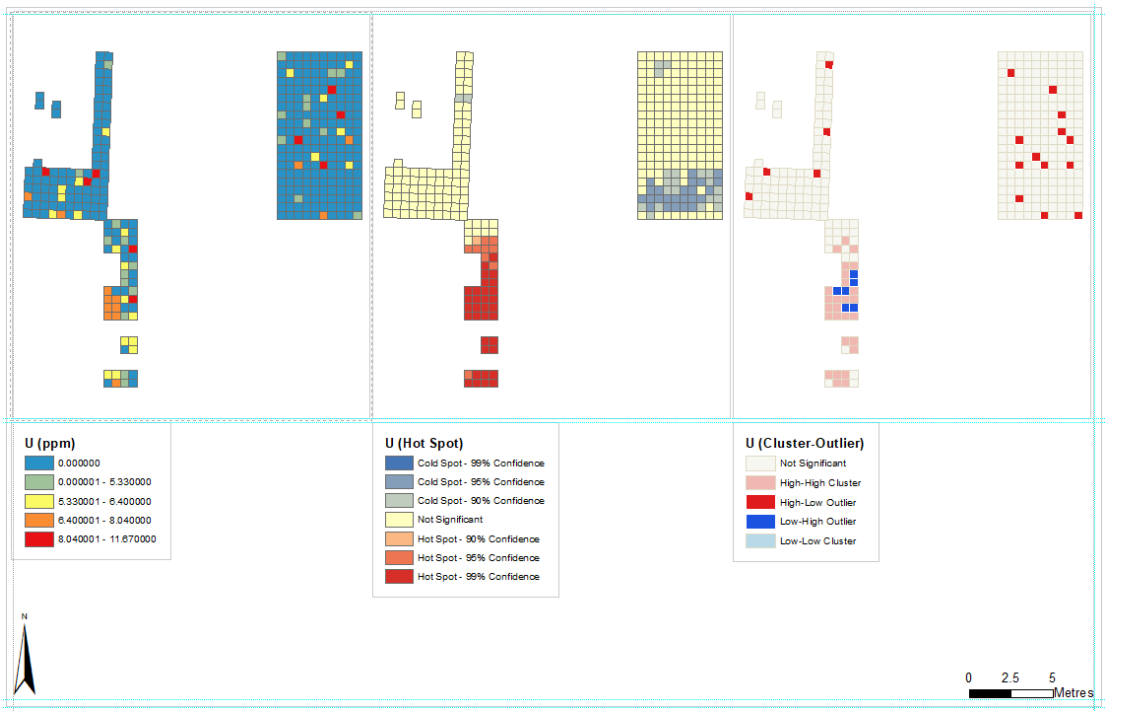

Appendix 7 Development of the Grouping Analysis model

As a statistical model developed using the Grouping Analysis tool on ArcMap is an iterative process, there are many outputs to record. As such, once compiled, the record for producing the models at Flixton generated a document over 140 pages long. It was thought necessary to provide a copy of these results as they can never be 100% replicated due to the random seed generation that initiates group formation for each run. The results are provided in PDF form on the accompanying media.

Abbreviations

ANN	Average Nearest Neighbour
C-OA	Cluster-Outlier Analysis (non-standard abbreviation)
FpXRF	Field portable x-ray fluorescence.
GA	Grouping Analysis (non-standard abbreviation)
HSA	Hot Spot Analysis (non-standard abbreviation)
ICP-AES	Inductively coupled plasma atomic emission spectroscopy.
IUPAC	International Union of Pure and Applied Chemistry
LE	Light Elements (grouped reading provided in pXRF outputs)
LOD	Limit of detection
ppm	Parts per million
pXRF	Portable X-ray fluorescence.
PCA	Principal Component Analysis
VPRT	Vale of Pickering Research Trust
XRF	X-ray fluorescence.

BP	Before present (1950 CE), calibrated.
bp	Before present, uncalibrated.
BC	Before Christ/Common Era, calibrated.
bc	Before Christ/Common Era, uncalibrated.

VP12	Site code for excavations at Flixton Island 2 in 2012
VP13	Site code for excavations at Flixton Island 2 in 2013
VP14	Site code for excavations at Flixton Island 2 in 2014
N.B. In the literature,sites Flixton Island 1 and 2 have also been referred to as Flixton 1 and 2. As Flixton School House and Flixton School Field are also known site locations, POSTGLACIAL standardised to using the full title to avoid confusion.	

Major	>10000 ppm
Minor	1000 - 10000 ppm
Trace	100 - 1000 ppm
IUPAC Trace	<100 ppm: The International Union of Pure and Applied Chemistry (IUPAC) Gold Book defines trace elements as “any element having an average concentration of less than about 100 parts per million atoms (ppma) or less than 100 μg/g (IUPAC 2009).

Glossary

Aqua regia	A mixture of nitric acid and hydrochloric acid, used as a solvent here.
Awl	These are blades or flakes with retouch along one or both edges leading to the tip or an artificial point, that form usually sturdy, squared off points or apices. The difference between a piercer and an awl is generally considered to be in the rotational direction of use which is can be confirmed by usewear examination.
Axe and adze	A core tool usually shaped on both facies, with further retouch refining the shape of the edges, that is thought to be used end on for striking. An axe is used with the blade orientated upright/vertical/parallel, while an adze is used with the blade flat/horizontal/perpendicular to the direction of movement.
Backed	Blunting down the whole of one side.
Backed pieces	When retouched along one edge to form a (usually flat) blunt back to a piece so pressure can be applied to the opposite edge or it can be hafted.
Blade	A piece of knapped lithic material that is equal to or more than two times longer than it is wide, and 12 mm or wider at its widest point.
Bladelet	A piece of knapped lithic material that is equal to or more than two times longer than it is wide, but less than 12 mm wide at its widest point.
Bulb of percussion	A bulge of lithic material on an artefact, where the initial impact of knapping percussion to remove the piece from the core was struck. This leaves a matching negative scar in the material it was removed from.
Burin	flakes or blades with removals perpendicular to the flat axis of the piece, thus forming a sharp corner on the piece
Burin Spall	The spall produced when initially creating or resharpening a burin.
Butt	See platform.
Chalk	A form of limestone mainly made of the mineral calcite.
Chemical	Materials that are chemically bonded with either ionic or covalent bonds.
Chip	Debitage of an undiagnostic type (usually a shatter piece) that is <1 cm diameter.
Chunk	Debitage of an undiagnostic type (usually a shatter piece) that is >1 cm diameter.
Clay	Loose rock and mineral fragments of the finest grade (more than gravel, sand, or silt). Clayey soils are the finest grained type of soil. In UK soil science, this is set to fragments less than 4 micrometres in diameter (Goldberg and Macphail 2006).
Combination	When a lithic artefacts performs two or more functions e.g. a scraper and a burin on the same piece.
Core	A nodule of lithic material from which material has been knapped repeatedly.
Core tablet	A removal taking off the entire knapping platform of a core (not just the edge of the platform) to rejuvenate it for further use.
Debitage	Flakes, blades and bladelets that may be waste products from knapping but also have the potential to be unmodified tools. They are the unmodified byproduct of knapping.
Denticulate	A blade or occasionally a flake that has been retouched so that it has a series of teeth along one edge. See also microdenticulate.

Distal	The termination end of a lithic artefact.
Epipalaeolithic	A term used to encompass material from the very end of the Upper Palaeolithic moving into the Early Mesolithic (although sometimes, it is used to mean the Mesolithic as a whole).
Expedient tool	A tool made from a generic piece of debitage (a flake or blade usually) without carefully shaping it into a formal tool type but using it unmodified or barely modified.
Flake	A piece of knapped lithic material that is less than two times longer than it is wide.
Flanc de nucléus	Pieces removed from a core to rejuvenate the outer surface of the knapping faces themselves.
Formal tool	A stone tool made intentionally for a specific purpose e.g. a scraper.
Gley	Soils which have developed due to poor drainage (either due to surface drainage, groundwater levels, or brackish flooding), resulting in the reduction of iron and other elements in the soils and causing the soils to take on a grey/blue colour (NSRI staff 2011).
Gravel	Loose rock and mineral fragments of the coarsest grade (more than sand, silt, or clay). Gravelly soils are the coarsest grade of soil. In UK soil science, this is set to fragments 2 mm upwards (Goldberg and Macphail 2006).
Graver	See burin.
Gyttja	See nekron mud.
Hafting	When a piece of material is mounted or bound onto another piece to form a tool, for example onto a handle or projectile shaft.
Histosols	A soil consisting primarily of organic soil materials.
Humus	Organic matter that has formed from the decay of floral material.
Knapping	When raw material is struck, either directly or indirectly through another material, to remove a piece of that material. Usually with reference to nodules of flint.
Leaching	Where soluble materials are washed down the soil profile by water (NSRI staff 2011).
Leading edge retouch	When a microlith has retouch down one side and then also along the edge of the opposite side at the tip i.e. at the leading edge.
Limestone	Sedimentary rocks mainly formed of calcium carbonate based minerals (particularly calcite and aragonite). Mainly formed from skeletal remains of marine organisms.
Loam	Loam is a soil that is not predominantly sand, silt, or clay, usually with some organic content.
Marl	Calcareous clay that is 30 - 60 % calcium carbonate (NSRI Staff 2011).
Mèches de foret	A particular type of awl/piercer that has retouch around the full circumference i.e. including the base, forming a lanceolate or teardrop shaped piercer with a sturdy point.
Medial	The middle section of a lithic artefact.
Microburin	The resulting debitage from the formation of a notch on a complete bladelet using fine retouch, at which point the bladelet is snapped off at the notch to shorten it for production into a microlith through further retouching (a process known as the microburin technique).
Microdenticulate	A bladelet,or occasionally a thin blade or flake, that has been retouched so that it has a very fine-toothed edge.
Microlith	A bladelet that has been retouched into a small tool, generally considered to be designed for hafting onto a composite tool such as providing the tip and barbs on an arrow.

Mineral and mineraloid	A naturally occurring chemical compound of one chemical composition. They are classified based on their chemical composition and crystal structure. These include silicates, sulfides, sulfates, oxides, halides, carbonates, and phosphates. Mineraloids are the same but do not demonstrate crystallinity. Polymorphs of minerals are those made of the same compounds but with different crystal structures e.g. calcite and aragonite.
Molecules	Two or more atoms (of the same or different elements) bonded together.
Nekron mud	Mud formed from the decay of peat in wetland contexts
Nodule chunk	Raw material that appears to be a manuport but has not been knapped.
Oblique blunting	Blunting across the width of the piece at an oblique angle.
Organic soil materials	Materials with an organic carbon content by weight of 12 to 18 percent (varying depending on the clay content). Peat (fibric soil material) is an example of an organic soil material.
Organosols	See histosols.
Pan	A well-defined layer interrupting soils, that can sometimes inhibit or impact drainage. This can be the formation of chemical deposits such as 'iron pan' which is an accumulation of iron oxides in acid gley soils or compaction (for example, from repeated ploughing) (NSRI Staff 2011).
Peat	An accumulation of partially decayed vegetation or organic matter. It is the main constituent of histosol type soils.
Pedolith	See soil.
Piercer	See awl.
Platform	The surface that is struck by a hammer for the removal of a piece during knapping.
Platform rejuvenation piece	A piece removing the very edge of a platform to rejuvenate it.
Preform	When the shape of an adze/axe has been roughed out and then further retouched on the edges to form a cleaner shape so completed except for tranchet blow.
Proximal	End of a lithic artefact with the striking platform and bulb, i.e. the end the piece was struck at to remove it.
Retouch	The removal of small flakes with an aim to reshape or blunt a piece. Retouch can be abrupt, semi-abrupt, or invasive and it is sometimes finer when used on small pieces like microliths.
Rock	An aggregate or one or more minerals.
Roughout	When the shape of an adze/axe has been roughed out but no further shaping has taken place e.g. along the edges to produce a cleaner outline, and the piece has not been finished off with a tranchet blow or utilised without it.
Sand	Loose rock and mineral particles finer than gravel but coarser than silt. Sandy soils are coarse grained, and the second coarsest grade of soil. In UK soil science, this is set to fragments between 63 micrometres up to 2 mm (Goldberg and Macphail 2006).
Sandy soil	Soil containing more than 85% sand-sized particles.
Saw	See microdenticulate.
Scraper	Flakes or blades retouched to form a thick edge face on the end or edge.
Sediment	This is naturally occurring, disaggregated material broken down by weathering or erosion. Glacial till is an example of a sediment.

Silt	Loose rock and mineral fragments of the second finest grade (between clay and sand in coarseness). In UK soil science, this is set to fragments less than 63 micrometres, but more than 4 micrometres (Goldberg and Macphail 2006).
Soil	This is a mixture of organic matter and minerals and rocks (the matrix), gases (the soil atmosphere), liquids (the soil solution), and organisms. Histosols are an example of a type of soil, in this case consisting mainly of peat.
Solute	The substance dissolved in a solvent to produce a solution.
Solution	A homogeneous mixture of two or more substances.
Solvent	Substance that dissolves another substance (the solute) into a solution.
Spall	Pieces of very small debitage that come off during retouching, or from use or damage. Here pieces catalogued as "debitage spall" are longer than they are wide, in differentiation to debitage chips.
Stone	See rock.
Test nodule	A nodule of lithic material from which material has been knapped only once or twice, seemingly to test whether the nodule is viable for knapping, before being discarded or lost.
Till (glacial)	Sediment dragged and/or deposited by a glacier, and as such is a mixture of different rocks, minerals, and material.
Tranchet removal	A removal transversely or obliquely across the width of a core tool, to produce a sharp edge.
Transverse blunting	Blunting perpendicular to the main axis of the piece, i.e. cutting across the width of the piece in a straight line.
Truncation	Pieces that are blunted either transversely or obliquely across an end.
Typology	Assigning into classification groups, with an aim to simplify the dataset for consideration.

Bibliography

Andrefsky, W. (1998). *Lithics : macroscopic approaches to analysis*. Cambridge: Cambridge University Press.

Antweiler, R. C. and Taylor, H. E. (2008). Evaluation of Statistical Treatments of Left-Censored Environmental Data using Coincident Uncensored Data Sets: I. Summary Statistics. *Environmental Science & Technology*, 42 (10), American Chemical Society., pp.3732–3738.

Arrhenius, O. (1929). Die phosphatfräge. *Zeitschrift für Pflanzenernährung, Dungung, und Bodenkund*, 10, pp.185–194.

Arthur, D. and Vassilvitskii, S. (2007). k-means ++ : The Advantages of Careful Seeding. In: *SODA '07 Proceedings of the eighteenth annual ACM-SIAM symposium on Discrete algorithms*. January 2007. Philadelphia : Society for Industrial and Applied Mathematics. pp.1027–1035.

Baales, M. (2006). Environnement et archéologie durant le Paléolithique final dans la région du Rhin moyen (Rhénanie, Allemagne) : conclusions des 15 dernières années de recherches. *L'Anthropologie*, 110, pp.418–444.

Bailey, G. and Galanidou, N. (2009). Caves, palimpsests and dwelling spaces: examples from the Upper Palaeolithic of south-east Europe. *World Archaeology*, 41 (2), Routledge ., pp.215–241.

Barba, L. (2007). Chemical residues in lime-plastered archaeological floors. *Geoarchaeology*, 22 (4), pp.439–452.

Barton, R. (1992). *Hengistbury Head, Dorset, Volume 2: The Late Upper Palaeolithic and Early Mesolithic Sites*. Monograph. Oxford : Oxford University Committee for Archaeology.

Bayliss, A. (2015). Quality in Bayesian chronological models in archaeology. *World Archaeology*, 47 (4), Oxford: Routledge., pp.677–700.

Becker, B. (1993). An 11,000-Year German Oak and Pine Dendrochronology for Radiocarbon Calibration. *Radiocarbon*, 35 (1), pp.201–213.

Becker, B., Kromer, B. and Trimborn, P. (1991). A stable-isotope tree-ring timescale of the late Glacial/Holocene boundary. *Nature (Letters)*, 353, pp.648–649.

Bennett, L. and Vale, F. (2014). Spatial Statistics: Simple Ways to Do More with Your Data. *ESRI, Technical Workshop*. [Online]. Available at: http://video.esri.com/watch/4003/spatial-statistics-simple-ways-to-do-more-with-your-data.

Binford, L. (1978). *Nunamiut Ethnoarchaeology*. New York : Academic Press.

Binford, L. (1980). Willow Smoke and Dogs' Tails Hunter Gatherer Settlement Systems and Archaeological Site Formation. *American Antiquity*, 45 (1), pp.4–20.

Binford, L. (1983). *In Pursuit of the Past: Decoding the Archaeological Record*.

Binford, L. R. and Binford, S. R. (1966). A Preliminary Analysis of Functional Variability in the Mousterian of Levallois Facies. *American Anthropologist*, 68 (2), pp.238–295.

Bordes, F. (1961). *Typologie du Paléolithique ancien et moyen*. Bordeaux : Impr. Delmas.

Bordes, F. and Sonneville-Bordes, D. De. (1970). The Significance of Variability in Palaeolithic Assemblages. *World Archaeology*, 2 (1), pp.61–73.

Boston, C. M. (2007). *An examination of the Geochemical properties of late devensian glacigenic sediments in Eastern England*. University of Durham. [Online]. Available at: http://etheses.dur.ac.uk/2609.

Brindley, G. W. (1952). Structural Mineralogy of Clays. *Clays and Clay Minerals*, 1 (1), pp.33–43.

British Geological Survey. *The BGS Lexicon of Named Rock Units - Speeton Clay Formation*. [Online]. Available at: http://www.bgs.ac.uk/Lexicon/lexicon.cfm?pub=SPC.

Buckley, F. (1921). *A microlithic industry, Marsden, Yorkshire*. Yorkshire : Privately Published.

Buckley, F. (1924). *A microlithic industry of the Pennine Chain, related to the Tardenois of Belgium*. Yorkshire : Privately Published.

Butler, C. (2005). *Prehistoric Flintwork*. 3rd ed. Stroud : The History Press.

Callander, J. G. (1927). A Collection of Tardenoisian Implements from Berwickshire. *Proceedings of the Society of the Antiquaries of Scotland*, pp.318–327.

Candy, I. et al. (2015). The evolution of Palaeolake Flixton and the environmental context of Star Carr: An oxygen and carbon isotopic record of environmental change for the early Holocene. *Proceedings of the Geologists' Association*, 126 (1), The Geologists' Association., pp.60–71.

Childe, V. G. (1947). The Economy of the Forest Period. In: *Prehistoric Communities of the British Isles*. 2nd ed. London : W & R Chambers Ltd. pp.16–30.

Clark, G. (1972). *Star Carr: A Case Study in Bioarchaeology*. Reading : Addison-Wesley.

Clark, G. (1975). *The earlier Stone Age settlement of Scandinavia*. Cambridge: Cambridge University Press.

Clark, J. G. D. (1932). *The Mesolithic Age in Britain*. Cambridge : Cambridge University Press.

Clark, J. G. D. (1933). The Classification of a Microlithic Culture: The Tardenoisian of Horsham. *The Archaeological Journal*, 90 (1), Oxford: Routledge., pp.52–77.

Clark, J. G. D. (1954). *Excavations at Star Carr: an early mesolithic site at Seamer near Scarborough, Yorkshire*. Cambridge: Cambridge University Press.

Clarke, D. (1968). *Analytical Archaeology*. London : Methuen.

Clarke, D. (1973). Archaeology: the loss of innocence. *Antiquity*, 47 (January), pp.6–18.

Clarke, D. (1976). Mesolithic Europe: the economic basis. In: Sieveking, G. de G., Longworth, I. H. and Wilson, K. E. (Eds). *Problems in Economic and Social Archaeology*. London : Duckworth. pp.449–481.

Cloutman, E. W. (1988). Palaeoenvironments in the Vale of Pickering. Part I: Stratigraphy and Palaeogeography of Seamer Carr, Star Carr and Flixton Carr. *Proceedings of the Prehistoric Society*, 54, Cambridge University Press., pp.1–19.

Conneller, C. (2000). *Space, time and technology: the early Mesolithic of the Vale of Pickering, North Yorkshire*. University of Cambridge PhD Thesis.

Conneller, C. et al. (2016). The Resettlement of the British Landscape: Towards a chronology of Early Mesolithic lithic assemblage types. *Internet Archaeology*, (42). [Online]. Available at: doi:10.11141/ia.42.11.

Conneller, C. et al. (2018). Chapter 35: Worked Flint. In: *Star Carr, Volume 2: studies in technology, subsistence and environment*. York : White Rose University Press.

Conneller, C. C. et al. (2012). Substantial settlement in the European Early Mesolithic : new research at Star Carr. *Antiquity*, 86, pp.1004–1020.

Conneller, C. and Higham, T. (2015). Dating the Early Mesolithic: new results from Thatcham and Seamer Carr. In: *No Stone Unturned: Papers in honour of Roger Jacobi*. Oxford : Oxbow Books.

Conneller, C. J. and Rowley, C. C. A. The Long Blade Assemblage from Flixton Island 2. In: Milner, N., Conneller, C. and Taylor, B. (Eds). *Flixton Island II*.

Conneller, C., Little, A. and Birchenall, J. (2018). Chapter 8: Spatial Analysis of the Flint. In: Milner, N., Conneller, C. and Taylor, B. (Eds). *Star Carr, Volume 1: a persistent place in a changing landscape*. York : White Rose University Press.

Conneller, C. and Schadla-Hall, T. (2003). Beyond Star Carr: The Vale of Pickering in the 10th Millennium BP. *Proceedings of the Prehistoric Society*, 69, pp.85–105.

Cooper, L. P. et al. (2017). Making and Breaking Microliths: A Middle Mesolithic Site at Asfordby, Leicestershire. *Proceedings of the Prehistoric Society*, 83, pp.43–96.

Crawford, O. G. S. (1922). A Flint Factory at Thatcham, part II: The Flint Implements and Flakes. *Proceedings of the Prehistoric Society of East Anglia*, 3 (4), pp.500–514.

Croft, S. (2017). *Lithic residue analysis at Star Carr*. University of York PhD Thesis.

Croghan, C. and Egeghy, P. P. (2003). Methods of Dealing with Values below the Limit of Detection using SAS. In: *Southeastern SAS User Group, St. Petersburg, FL, September 22-24, 2003*. USA: EPA Science Inventory.

Crombé, P. et al. (2001). Wear analysis on early Mesolithic microliths from the Verrebroek site, East Flanders, Belgium. *Journal of Field Archaeology*, 28 (3–4), pp.253–269.

Davies, J. and Rankine, W. F. (1960). Mesolithic Flint Axes from the West Riding of Yorkshire. *Yorkshire Archaeological Journal*, XL, pp.209–214.

Day, S. P. (1996). Dogs, Deer and Diet at Star Carr: a Reconsideration of C-isotope Evidence from Early Mesolithic Dog Remains from the vale of Pickering, Yorkshire, England. *Journal of Archaeological Science*, 23 (5), pp.783–787.

Dibble, H. L. (1991). Mousterian Assemblage Variability on an Interregional Scale. *Journal of Anthropological Research*, 47 (2), pp.239–257.

Ding, C. and He, X. (2004). K-means clustering via principal component analysis. *Proceedings of the twenty-first international conference on Machine learning*, Cl (2000), p.29.

Dore, C. D. and López Varela, S. L. (2010). Kaleidoscopes, Palimpsests, and Clay: Realities and Complexities in Human Activities and Soil Chemical/Residue Analysis. *Journal of Archaeological Method and Theory*, 17 (3), pp.279–302.

Eidt, R. C. and Woods, W. I. (1974). *Abandoned Settlement Analysis: Theory and Practice*. Wisconsin : Field Test Association.

Elston, R. G. et al. (2002). *Thinking small : global perspectives on microlithization*. Arlington: American Anthropological Association.

Entwistle, J. A. and Abrahams, P. W. (1997). Multi-Element Analysis of Soils and Sediments from Scottish Historical Sites. The Potential of Inductively Coupled Plasma-Mass Spectrometry for Rapid Site Investigation. *Journal of Archaeological Science*, 24, pp.407–416.

Entwistle, J. A., Abrahams, P. W. and Dodgshon, R. A. (2000). The Geoarchaeological Significance and Spatial Variability of a Range of Physical and Chemical Soil Properties from a Former Habitation Site, Isle of Skye. *Journal of Archaeological Science*, 27, pp.287–303.

Entwistle, J. A., McCaffrey, K. J. W. and Dodgshon, R. A. (2007). Geostatistical and multi-elemental analysis of soils to interpret land-use history in the Hebrides, Scotland.

Geoarchaeology, 22 (4), pp.391–415.

ESRI. *How Grouping Analysis works*. [Online]. Available at: http://pro.arcgis.com/en/pro-app/tool-reference/spatial-statistics/how-grouping-analysis-works.htm [Accessed 1 November 2016].

Evans, D. J. A., Bateman, M. D., Roberts, D. H., Medialdea, A., Hayes, L., Duller, G. A. T., Fabel, D., and Clark, C. D. (2017). Glacial Lake Pickering: stratigraphy and chronology of a proglacial lake dammed by the North Sea Lobe of the British–Irish Ice Sheet. *Journal of Quaternary Science*, 32 (2), pp.295–310.

Field, A. (2009). *Discovering Statistics using SPSS*. 3rd ed. London : SAGE.

Flynn, M. R. (2009). Analysis of censored exposure data by constrained maximization of the Shapiro–Wilk W statistic. *The Annals of Occupational Hygiene*, 54 (3), Oxford University Press., pp.263–271.

French, C. A. I. (2015a). *A handbook of geoarchaeological approaches for investigating landscapes and settlement sites*. Oxford : Oxbow Books.

French, C. A. I. (2015b). *Star Carr 2013 and 2013 (and Flixton Island 2012) Internal Report: Micromorphology*.

Friesem, D. E. and Lavi, N. (2017). Foragers, tropical forests and the formation of archaeological evidences: An ethnoarchaeological view from South India. *Quaternary International*, 448, Elsevier Ltd., pp.117–128.

Gasser, J. K. R. and Bloomfield, C. (1955). The Mobilization of Phosphate in Waterlogged Soils. *Journal of Soil Science*, 6 (2), pp.219–232.

Gatty, R. A. (1901). Notes on a Collection of Very Minute Flint Implements From. *Proceedings of The Society of Antiquaries of Scotland*, 35 (1900–1901), pp.98–108.

Gero, J. M. (1991). Genderlithics: Women's Roles in Stone Tool Production. *Engendering Archaeology: Women and Prehistory*, pp.163–193.

Grace, R. (2012). *Stone Age Reference Collection: A guide to the typology, technology and study methods of the stone age*. Ikarus Books.

Grøn, O. (2003). Mesolithic dwelling places in south Scandinavia: their definition and social interpretation. *Antiquity*, 77 (298), Cambridge University Press., pp.685–708.

Healy, F. (1988). *The Anglo-Saxon Cemetery at Spong Hill, North Elmham, Part VI: Occupation during the 7th–2nd millennia BC, Volume 39 (1988) - Contents*. EAA Volume. Norfolk : Norfolk Museums Service. [Online]. Available at: http://archaeologydataservice.ac.uk/archives/view/eaa/contents.cfm?volume_id=1162

[Accessed 23 November 2017].

Helsel, D. (2010). Much Ado About Next to Nothing: Incorporating Nondetects in Science. *Annals of Occupational Hygiene*, 54 (3), Oxford University Press., pp.257–262.

Helsel, D. R. and Cohn, T. A. (1988). Estimation of descriptive statistics for multiply censored water quality data. *Water Resources Research*, 24 (12), pp.1997–2004..

Henson, D. (1982). *Flint as a raw material in prehistory*. University of Sheffield Unpublished Masters Dissertation.

Hewett, P. and Ganser, G. H. (2007). A Comparison of Several Methods for Analyzing Censored Data. *The Annals of Occupational Hygiene*, 51 (7), Oxford University Press., pp.611–632.

High, K. (2014). *Fading Star: Understanding Accelerated Decay of Organic Remains at Star Carr*. University of York PhD Thesis.

Högberg, A. (1994). Microdenticulates of the Funnel Beaker Culture. *Acta Archaeologica*, pp.11–32.

Holliday, V. T. (2004). *Soils in Archaeological Research*. Oxford : Oxford University Press.

Homsey, L. K. and Capo, R. C. (2006). *Integrating Geochemistry and Micromorphology to Interpret Feature Use at Dust Cave , a Paleo-Indian Through Middle-Archaic Site in Northwest Alabama*. 21 (3), pp.237–269.

Honywood, T. (1877). Discovery of Flint Implements near Horsham, in St. Leonard's Forest. *Sussex Archaeological Collections*, 27, pp.177–182.

Howard, C. D. (2002). The Gloss Patination of Flint Artifacts. *Plains Anthropologist*, 47 (182), pp.283–287.

Hurst, V. J. and Kelly, A. R. (1961). Patination of Cultural Flints. *Science (New York, N.Y.)*, 134 (3474), pp.251–256.

Ingold, T. (2000). Society, Nature, and the Concept of Technology. In: Ingold, T. (Ed). *The Perception of the Environment: Essays on livelihood, dwelling and skill*. London : Routledge. pp.312–322.

Inizan, M.-L. et al. (1999). *Technology and terminology of Knapped Stone : followed by a multilingual vocabulary Arabic, English, French, German, Greek, Italian, Portuguese, Spanish*. Nanterre : Cercle de Recherches et d'Etudes Préhistoriques.

Inizan, M.-L., Roche, H. and Tixier, J. (1992). *Technology of knapped stone. Prehistoire de la Pierre Taillee, Tome 3*. Meudon : Cercle de Recherches et d'Etudes Préhistoriques.

IUPAC. (2009). *IUPAC Compendium of Chemical Terminology*. Nič, M. et al. (Eds). Research

Triagle Park, NC/Oxford : IUPAC/ Blackwell Scientific. [Online]. Available at: doi:10.1351/goldbook [Accessed 4 June 2017].

Iyamuremye, F. and Dick, R. P. (1996). Organic amendments and phosphorus sorption by soils. *Advances in Agronomy*, 56, pp.139–185.

Jacobi, R. (1973). Aspects of the 'Mesolithic Age' in Great Britain. In: Kozłowski, S. K. (Ed). *The Mesolithic in Europe (papers read at the international archaeological symposium in Europe, Warsaw, May 7-12 1973)*. Warsaw : Warsaw University Press.

Jacobi, R. (1976). Britain Inside and Outside Mesolithic Europe. *Proceedings of the Prehistoric Society*, 42, pp.67–84.

Jacobi, R. (1978a). Northern England in the eighth millennium BC: an essay. In: Mellars, P. (Ed). *The Early Post-Glacial Settlement of Northern Europe: an Ecological Perspective*. London : Duckworth. pp.295–332.

Jacobi, R. (1978b). The Mesolithic of Sussex. In: Drewett, P. L. (Ed). *Archaeology in Sussex to AD 1500, CBA Research Report*. 29. London .

Jacobi, R. M. (1981). The last hunters in Hampshire. In: Shennan, S. J. and Schadla-Hall, R. T. (Eds). *The Archaeology of Hampshire*. Winchester : Hampshire Field Club and Archaeological Society. pp.10–25.

Jenks, G. F. (1967). The Data Model Concept in Statistical Mapping. *International Yearbook of Cartography*, 7, pp.186–190.

Johansson, P. (2014). *Returning to Vuollerim : Geoarchaeological study of Soil Samples from a Stone Age Settlement*. Umeå University PhD Thesis.

Karlin, C. and Julien, M. (1994). Prehistoric technology: a cognitive science? In: Renfrew, C. and Zubrow, E. B. W. (Eds). *The ancient mind*. Cambridge : Cambridge University Press. pp.152–164.

Kerr, P. F. (1952). Formation and Occurrence of Clay Minerals. *Clays and Clay Minerals*, 1 (1), pp.19–32.

Knight, B. The Faunal Remains from Flixton Island II. In: Milner, N., Conneller, C. and Taylor, B. (Eds). *Flixton Island II*.

Knudson, K. J. et al. (2004). Chemical characterization of Arctic soils: Activity area analysis in contemporary Yup'ik fish camps using ICP-AES. *Journal of Archaeological Science*, 31 (8), pp.443–456.

Kromer, B. and Becker, B. (1993). German oak and pine 14C calibration, 7200-9439 BC. *Radiocarbon*, 35 (1), pp.125–135.

Kuhn, S. L. and Stiner, M. C. (2001). The Antiquity of Hunter-gatherers. *Hunter-Gatherers: Interdisciplinary Perspectives*, pp.99–142.

Lahr, J., Kahn, B. and Morton, S. (2007). Radioanalytical Chemistry Principles and Practices. In: Kahn, B. (Ed). *Radioanalytical Chemistry*. 1st ed. New York : Springer. pp.64–76.

Lajunen, L. H. J. and Perämäki, P. (2004). Sample preparation. In: Lajunen, L. H. J. and Perämäki, P. (Eds). *Spectrochemical Analysis by Atomic Absorption and Emission*. 2nd ed. London: The Royal Society of Chemistry. pp.286–313.

Lancelotti C, Negre J, Alcaina-Mateos J, Carrer F. (2017). Intra-site Spatial Analysis in Ethnoarchaeology. *Environmental Archaeology*, 22 (4), Routledge., pp.354–364.

Lancelotti, C., Pecci, A. and Zurro, D. (2017). Anthropic Activity Markers: Archaeology and Ethnoarchaeology. *Environmental Archaeology*, 22 (4), Taylor & Francis., pp.339–342.

Lang, C. (2014). *The hidden archive of historical human inhumations locked within burial soils*, University of York PhD Thesis.

Larsson. L. (1990). Mesolithic of Southern Scandinavia. *Journal of World Prehistory* (1990) pp.4-257.

Larsson, L. and Sjöström, A. (2011). Early Mesolithic flint-tipped arrows from Sweden. *Antiquity*. [Online]. Available at: http://www.antiquity.ac.uk/projgall/larsson330/ [Accessed 17 July 2014].

Legge, A. J. and Rowley-Conwy, P. (1988). *Star Carr Revisited: a Re-analysis of the Large Mammals*. London : Birkbeck.

Lindbo, D. L., Stolt, M. H. and Vepraskas, M. . (2010). Redoximorphic features. In: Stoops, G., Marcelino, V. and Mees, F. (Eds). *Interpretation of Micromorphological features in soils and regoliths*. Oxford : Elsevier. pp.129–147.

Linderholm, J. (2010). *The soil as a source material in archaeology. Theoretical considerations and pragmatic applications.* Umeå University PhD Thesis.

MacLeod, G. (2008). *Thin Section & Micromorphology methods: drying*. [Online]. Available at: http://www.thin.stir.ac.uk/2008/06/03/methods-drying/ [Accessed 25 November 2017].

Marreiros, J., Bicho, N. and Gibaja, J. F. (2014). *International conference on use-wear analysis : use-wear 2012*. Marreiros, J., Bicho, N. and Gibaja, J. F. (Eds). Newcastle upon Tyne UK : Cambridge Scholars Publishing.

McFadyen, L. (2007). Mobile Spaces of Mesolithic Britain. *Home Cultures*, 4 (2), pp.117–128.

Mellars, P. (1976). Settlement patterns and industrial variability in the British Mesolithic. In: Sieveking, G. de G., Longworth, I. H. and Wilson, K. E. (Eds). *Problems in Economic and*

Social Archaeology. London : Duckworth. pp.375–400.

Mellars, P. and Dark, P. (1998). *Star Carr in Context*. Cambridge : McDonald Institute for Archaeological Research.

Middleton, W. D. (2004). Identifying Chemical Activity Residues on Prehistoric House Floors: a methodology and rationale for multi-elemental characterization of a mild acide extract of anthropogenic sediments. *Archaeometry*, 46 (1), pp.47–65.

Middleton, W. D., Price, D. T. and Price, T. D. (1996). Identification of Activity Areas by Multi-element Characterization of Sediments from Modern and Archaeological House Floors Using Inductively Coupled Plasma-atomic Emission Spectroscopy. *Journal of Archaeological Science*, 23 (5), pp.673–687.

Middleton, W. D. and Price, T. D. (1996). Identification of Activity Areas by Multi-element Characterization of Sediments from Modern and Archaeological House Floors Using Inductively Couple Plasma-atomic Emission Spectroscopy. *Journal of Archaeological Research*, 23, pp.673–687.

Mikołajczyk, Ł. and Milek, K. (2016). Geostatistical approach to spatial, multi-elemental dataset from an archaeological site in Vatnsfjörður, Iceland. *Journal of Archaeological Science: Reports*, 9, pp.577–585.

Mikołajczyk, Ł. and Schofield, J. E. (2017). A Geochemical Signal from a Mesolithic Intertidal Archaeological Site: A Proof-of-Concept Study from Clachan Harbor, Scotland. *Geoarchaeology*, 32 (3), pp.400–413.

Milner, N. et al. (2013). *Star Carr: Life in Britain after the Ice Age*. York : Council for British Archaeology.

Milner, N. et al. (2016). A Unique Engraved Shale Pendant from the Site of Star Carr: the oldest Mesolithic art in Britain. *Internet Archaeology*, (40), Internet Archaeology. [Online]. Available at: doi:10.11141/ia.40.8 [Accessed 23 November 2017].

Milner, N. et al. (2018). Sediments and Stratigraphy. In: Milner, N., Conneller, C. J. and Taylor, B. (Eds). *Star Carr, Volume 2: studies in technology, subsistence and environment*. York : White Rose University Press.

Milner, N., Conneller, C. and Taylor, B. (Eds). (2018). *Star Carr Volume I: A Persistent Place in a Changing World*. York : White Rose University Press. [Online]. Available at: doi:10.22599/book1.

Minerals, A. (2009). *ALS Minerals Geochemical Procedure Description: ME-ICP41 Trace LevelMethods using Conventional ICP-AES Analysis*.

Moore, J. W. (1950). Mesolithic Sites in the Neighbourhood of Flixton, North-east Yorkshire.

Proceedings of the Prehistoric Society, 16, Cambridge: Cambridge University Press., pp.101–108.

Moore, J. W. (1954). Excavations at Flixton, Site 2 (as Appendix). In: Clark, J. G. D. (Ed). *Excavations at Star Carr: An Early Mesolithic Site at Seamer, near Scarborough, Yorkshire*. Cambridge : Cambridge University Press. pp.192–194.

Myers, A. (1989). Reliable and mantainable technological strategies in the Mesolithic of mainland Britain. In: Torrence, R. (Ed). *Time, energy and stone tools: New directions in Archaeology*. Cambridge : Cambridge University Press. pp.78–91.

Myers, A. M. (1987). All Shot to Pieces? Inter-assemblage variability, lithic analysis and Mesolithic assemblage 'types'; some preliminary observations. *Lithic Analysis and Later British Prehistory: Some problems and approaches,* (January 1987).

Noe-Nygaard, N. (1975). Two shoulder blades with healed lesions from Star Carr. *Proceedings of the Prehistoric Society*, 41, pp.10–16.

Noe-Nygaard, N. (1977). Butchering and marrow Fracturing as a Taphonomic Factor in Archaeological Deposits. *Paleobiology*, 3, pp.218–257.

Noe-Nygaard, N. (1983). A new Find of Brown bear (Ursus arctos) at Star Carr and Other Finds in the Late Glacial and Post Glacial of Britain and Denmark. *Journal of Archaeological Science*, 10, pp.317–325.

Nomura, C. S. and Oliveira, P. V. (2007). Micro Sampling for Solid and Slurries Analytical Methods. In: Arruda, M. A. Z. (Ed). *Trends in Sample Preparation*. pp.1–27.

Ogden, T. L. (2010). Handling results below the level of detection. *The Annals of Occupational Hygiene*, 54 (3), Oxford University Press., pp.255–256.

Olympus. (2014a). *Handheld XRF Analyzers, Limits of Detection*. pp.1–2. [Online]. Available at: http://www.olympus-ims.com/en/.downloads/download/?file=285213158&fl=en_US.

Olympus. (2014b). *Olympus DELTA Family Handheld XRF Analyzer User Manual (International Edition)*. (February), Waltham : Olympus NDT.

Oonk, S. et al. (2009). Effects of site lithology on geochemical signatures of human occupation in archaeological house plans in the Netherlands. *Journal of Archaeological Science*, 36 (6), Elsevier Ltd., pp.1215–1228.

Oonk, S., Slomp, C. P. and Huisman, D. J. (2009). *Geochemistry as an Aid in Archaeological Prospection and Site Interpretation : Current Issues and Research Directions*. 51 (August 2008), pp.35–51.

Palmer, A. P. et al. (2015). The evolution of Palaeolake Flixton and the environmental

context of Star Carr, NE. Yorkshire: Stratigraphy and sedimentology of the Last Glacial-Interglacial Transition (LGIT) lacustrine sequences. *Proceedings of the Geologists' Association*, 126 (1), The Geologists' Association., pp.50–59.

Pastor, A. et al. (2016). Mineral soil composition interfacing archaeology and chemistry. *TrAC Trends in Analytical Chemistry*, 78, pp.48–59.

Paterson, H. M. L. (1913). Pygmy Flints in the Dee Valley. *Royal Anthropological Institute of Great Britain and Ireland*, 13, pp.103–105.

Peake, H. (1922). A Flint Factory at Thatcham, Berks, part I: Report of Site and Excavations. *Proceedings of the Prehistoric Society of East Anglia*, 3 (4), pp.499–500.

Pecci, A., Barba, L. and Ortiz, A. (2017). Chemical Residues as Anthropic Activity Markers. Ethnoarchaeology, Experimental Archaeology and Archaeology of Food Production and Consumption. *Environmental Archaeology*, 22 (4), Taylor & Francis., pp.343–353.

Pelegrin, J. (1990). Prehistoric lithic technology : Some aspects of the research. *Archaeological Review from Cambridge*, 9 (1), pp.116–127.

Pettitt, P. (2009). François Bordes. *Great Prehistorians: 150 Years of Palaeolithic Research, 1859–2009 (Special Volume 30 of Lithics: The Journal of the Lithic Studies Society)*, pp.201–212.

Pitts, M. W. (1979). Hides and antlers: a new look at the gatherer-hunter site at Star Carr, North Yorkshire, England. *World Archaeology*, 11, pp.32–42.

Pollard, A. M. and Heron, C. (1996). *Archaeological Chemistry*. Cambridge : Royal Society of Chemistry.

Radley, J. and Marshall, G. (1963). Mesolithic Sites in South-west Yorkshire. *Yorkshire Archaeological Journal1*, XLI, pp.81–97.

Radley, J. and Mellars, P. (1964). A Mesolithic Structure at Deepcar, Yorkshire, England, and the Affinities of its associated Flint Industries. *Proceedings of the Prehistoric Society*, 30 (I), pp.1–24.

Reimer, P. et al. (2013). IntCal13 and Marine13 Radiocarbon Age Calibration Curves 0–50,000 Years cal BP. *Radiocarbon*, 55 (4), pp.1869–1887.

Reynier, M. (2005). *Early Mesolithic Britain: Origins, development and directions. British Archaeological Report 393.* Oxford : Hadrian Books Ltd.

Rolland, N. and Dibble, H. L. (1990). A New Synthesis of Middle Paleolithic Variability. *American Antiquity*, 55 (3), pp.480–499.

Rondelli, B., Lancelotti, C., Madella, M., Pecci, A., Balbo, A., Ruiz Perez, J., Inserra, F., Gadekar,

C., Angel Cau Ontiveros, M., and Ajithprasad, P. (2014). Anthropic activity markers and spatial variability : an ethnoarchaeological experiment in a domestic unit of Northern Gujarat (India). *Journal of Archaeological Science*, 41, Elsevier Ltd., pp.482–492.

Rose, S., Spinks, N. and Canhoto, A. I. (2015). Tests for the assumption that a variable is normally distributed (Supplementary Note). In: Rose, S., Spinks, N. and Canhoto, A. I. (Eds). *Management Research: Applying the Principles*. Abingdon : Routledge. pp.1–4.

Rowley, C. C. A., French, C. A. I. and Milner, N. (2018). Geochemistry of the Central and Western Structures. In: Milner, N., Conneller, C. and Taylor, B. (Eds). *Star Carr, Volume 2: studies in technology, subsistence and environment*. York : White Rose University Press.

Sarauw, G. F. L. (1903). En stenalderboplads i Maglemose ved Mullerup: Sammenholdt med beslaegtede Fund. *Aarbfger for Nordisk Oldkyndighed og Historie*, pp.148–315.

Saville, A. (1981a). Honey Hill, Elkington: A Northamptonshire Mesolithic Site. *Northamptonshire Archaeology*, 16, pp.1–13.

Saville, A. (1981b). Mesolithic Industries in Central England: an exploratory investigation using microlith typology. *Archaeological Journal*, 138 (1), Routledge., pp.49–71.

Schlanger, N. (1994). Mindful technology: unleashing the chaîine opératoire for an archaeology of mind BT - The ancient mind: Elements of cognitive archaeology. *The ancient mind: Elements of cognitive archaeology*, pp.143–151.

Schmalz, R. F. (1960). Flint and the Patination of Flint Artifacts. *Proceedings of the Prehistoric Society (New Series)*, 26 (3), pp.44–49.

Scotter, G. . (1963). Effects of forest fires on soil properties in northern Saskatchewan. *The Forestry Chronicle*, (39), pp.412–421.

Sellet, F. (1993). Chaîne Opératoire; the concept and its applications. *Lithic Technology*, 18 (1/2), Taylor & Francis, Ltd., pp.106–112.

Shackley, M. S. (2011). *X-Ray fluorescence spectrometry (XRF) in geoarchaeology*. New York : Springer.

Sparrow, L. A., Peverill, K. I. (Kenneth I. and Reuter, D. J. (Douglas J. . (1999). *Soil analysis : an interpretation manual*. Australia: CSIRO.

Stanford, G. (1947). Fixation of potassium in soils under moist conditions and on drying in relation to type of clay mineral. *Soil Science Society of America Journal*, 12, pp.167–171.

Switsur, V. R. and Jacobi, R. M. (1975). Radiocarbon Dates for the Pennine Mesolithic. *Nature*, 256 (July), pp.32–34.

Taylor, B. (2012). *The occupation of wetland landscapes during the British Mesolithic: case*

studies from the Vale of Pickering. University of Manchester PhD Thesis.

Taylor, B. et al. (2018). Chapter Four: Climate, environment and Lake Flixton. In: Milner, N., Conneller, C. and Taylor, B. (Eds). *Star Carr, Volume 1: a persistent place in a changing landscape*. York : White Rose University Press.

Terry, R. E., Fernandez, F. G., Parnell, J. J., and Inomata, T. (2004). The story in the floors: Chemical signatures of ancient and modern Maya activities at Aguateca, Guatemala. *Journal of Archaeological Science*, 31 (9), pp.1237–1250..

The Met Office. (2015). *August 2014 - Weather Report*. [Online]. Available at: https://www.metoffice.gov.uk/climate/uk/summaries/2014/august [Accessed 26 November 2017].

Torrence, R. (2002). Thinking big about small tools. *Archeological Papers of the American Anthropological Association.* 12 (1), pp.179–189.

Valdeyron, N. (2008). The Mesolithic in France. In: Bailey, G. and Spikins, P. (Eds). *Mesolithic Europe*. Cambridge : Cambridge University Press. pp.182–202.

Vyncke, K. Degryse, P., Vassilieva, E. and Waelkens, M. (2011). Identifying domestic functional areas. Chemical analysis of floor sediments at the Classical-Hellenistic settlement at Düzen Tepe (SW Turkey). *Journal of Archaeological Science*, 38 (9), pp.2274–2292.

Weems, J. B. (1903). *Chemistry of Clays*. Iowa Geological Survey Annual Report, 14, pp.319-346.

Wells, E. C. (2004). Investigating activity patterns in prehispanic plazas: weak acid-extraction ICP-AES analysis of anthrosols at Classic period El Coyote, Northwestern Honduras. *Archaeometry*, 46 (1), pp.67–84.

Weninger, B., Schulting, R., Bradtmöller, M., Clare, L., Collard, M., Edinborough, K., Hilpert, J., Jöris, O., Niekus, M., Rohling, E. J., Wagner, B. (2008). *The catastrophic final flooding of Doggerland by the Storegga Slide tsunami*. Documenta Praehistorica. Volume 35 (2008).

Wheeler, A. (1978). Why were there no fish remains at Star Carr? *Journal of Archaeological Science*, 5, pp.85–90.

Wilson, C. A., Davidson, D. A. and Cresser, M. S. (2008). Multi-element soil analysis: an assessment of its potential as an aid to archaeological interpretation. *Journal of Archaeological Science*, 35 (2), pp.412–424.

Wymer, J. and King, J. (1962). Excavations at the Maglemosian Sites at Thatcham, Berkshire, England. *Proceedings of the Prehistoric Society*, 28, pp.329–361.

LandIS Soilscapes Map Viewer. [Online]. Available at: http://www.landis.org.uk/soilscapes/ [Accessed 20 July 2011].